UNIVERSITÀ DI PARMA

UNIVERSITA' DEGLI STUDI DI PARMA

DOTTORATO DI RICERCA IN
"Scienze Chimiche"

CICLO XXXVII

Iron-catalyzed C−H activations with unsaturated hydrocarbons: a sustainable tool for molecular complexity using pharmacologically relevant triazoles

Coordinatore:
Chiar.mo Prof. Giovanni Maestri

Tutore:
Chiar.mo Prof. Gianpiero Cera

Dottoranda: Silvia Cattani

Anni Accademici 2021/2022–2023/2024

Abstract

Transition metal-catalyzed C–H functionalizations stands out as one of the most powerful and efficient tools in synthetic organic chemistry. This approach minimizes lengthy synthetic processes and reduces waste by activating inert C–H bonds directly, thus providing new environmentally-benign and economically-attractive alternatives to traditional synthetic methods. Recently, precious 4d and 5d metals have been extensively studied for their ability to form unprecedented C–C and C–Het bonds. However, their high cost and toxicity limit their use in the agrochemical and pharmaceutical industries. A greener and more cost-effective approach uses less toxic, naturally abundant 3d transition metals. Among these, iron stands out due to its abundance in the Earth's crust, low cost, low toxicity, and catalytic versatility, making it an ideal candidate for developing efficient catalyst systems for sustainable C–H activation strategies. In particular, the introduction of bidentate directing groups such as 8-aminoquinoline and 1,2,3-triazoles, paved the way for broader applications of iron catalyzed C−H functionalizations. The research described in this thesis is aimed at developing new iron-catalyzed C−H activation methods for the direct hydroarylation of unsaturated compounds that leverage the assistance of triazole-based directing groups.

In the introduction, the most representative achievements in iron-catalyzed C–H functionalizations will be discussed, starting from early reports of organometallic C–H activations to more recent examples that exploits the power of iron catalysts.

In the first project we present a new strategy for iron-catalyzed C–H alkylations of benzamide substrates with olefins enabled by *N*-triazole assistance. We disclosed a complementary reactivity with respect to the use of 8-aminoquinoline, which enabled the synthesis of both linear and branched alkylation products, depending on the type of olefin, using the same catalytic system.

The second project was aimed at discovering new reaction pathways in iron-catalyzed C–H activations. We envisioned to employ 2-vinyl benzofurans as effective substrates for iron-catalyzed C–H functionalizations with triazole-functionalized benzamides. Notably, the iron catalysis facilitated an unprecedented cascade reaction that resulted in the formation of complex isoquinolone derivatives produced through a challenging *β*–O elimination from a C(sp^2)–O bond for the ring-opening of the benzofuran ring. Both computational and experimental studies were conducted to identify the working mode of the iron catalyst.

In the third project we considered the potential of utilizing readily available allenes to investigate *Z*-selective, iron-catalyzed C−H alkylations. Our goal was to control the stereochemistry of the iron catalysis by leveraging the geometric constraints provided by the triazole directing group and the orthogonal cumulative π bonds of allenes, aiming for the synthesis of internal, disubstituted olefins. The newly developed protocol was found effective in the C−H alkylations with both

monosubtituted and 1,1-disubstituted allenes, providing the desired product with excellent levels of *Z*-selectivity.

The first research project conducted in Ackermann's group aimed to synthesize a family of iron(0) complexes with NHC ligands and test their catalytic activity in the imine-directed indole C–H alkylation with olefins under mild conditions, without Grignard reagent and additional additives. The regioselectivity of the C–H alkylation is affected by the nature of the alkene substrate (styrenes or vinylsilanes), resulting in alkylated indoles with Markovnikov or anti-Markovnikov selectivity. Moreover, this approach was also beneficial in terms of the applicability of the method, as sensitive and potentially reactive functional groups were tolerated.

The last project presented in this thesis details a nickel-catalyzed C−H method developed in Ackermann's group about the atroposelective C−H alkylation of benzimidazole substrates with olefins for the construction of C−N axially chiral compounds. In this project, the design of new heteroatom-substituted secondary phosphine oxide (HASPO) as highly effective chiral preligands was crucial for achieving C−N axially chiral benzimidazole derivatives with high enantioselectivities utilizing a Ni–Al bimetallic system.

Table of Contents

1. Introduction

1.1 General Introduction

Organic synthesis plays a crucial role for molecular construction, with significant applications in material sciences, natural product synthesis, and active pharmaceuticals ingredients.[1] Extensive efforts have been directed towards developing innovative methods for chemical synthesis, leading to diverse applications that offer numerous advantages for the society.[2] However, despite undeniable advancements, organic synthesis continues to be viewed as a polluting discipline due to issues such as waste generation, resource and energy consumption, and the use of toxic chemicals.[3] In 1988, Paul T. Anastas and John C. Warner identified catalysis as one of the "12 Principles of Green Chemistry."[4] Over the past century, catalysis has become a cornerstone of the chemical industry, achieving significant progress in creating economically, environmentally, and technologically beneficial transformations.[5]

1.2 Transition Metal-Catalyzed C–H Functionalizations

Transition metal catalysis stands out as one of the most powerful and efficient methods in organic synthesis, in particular for the formation of challenging arene structures, as aromatic rings are present in nearly 80% of all marketed active pharmaceutical ingredients.[6] In this regard, cross-coupling reactions have emerged as a fundamental technology across various research fields due to their ease of use and versatility. A variety of methods were developed for the targeted creation of carbon-carbon (C–C) and carbon-heteroatom (C–Het) bonds under mild conditions, mainly utilizing precious palladium as the transition metal.[7] The significant influence and progress achieved by this branch of chemistry were recognized when Richard F. Heck, Eiichi Negishi, and Akira Suzuki were awarded the Nobel Prize in Chemistry in 2010.[8] Nevertheless, despite the undeniable advancements, cross-coupling reactions still face considerable limitations. These challenges arise, among other factors, from the necessity for pre-functionalized substrates and organometallic compounds, which notably hinder user-friendliness, sustainability, and overall efficiency.

a) Traditional cross-coupling reactions

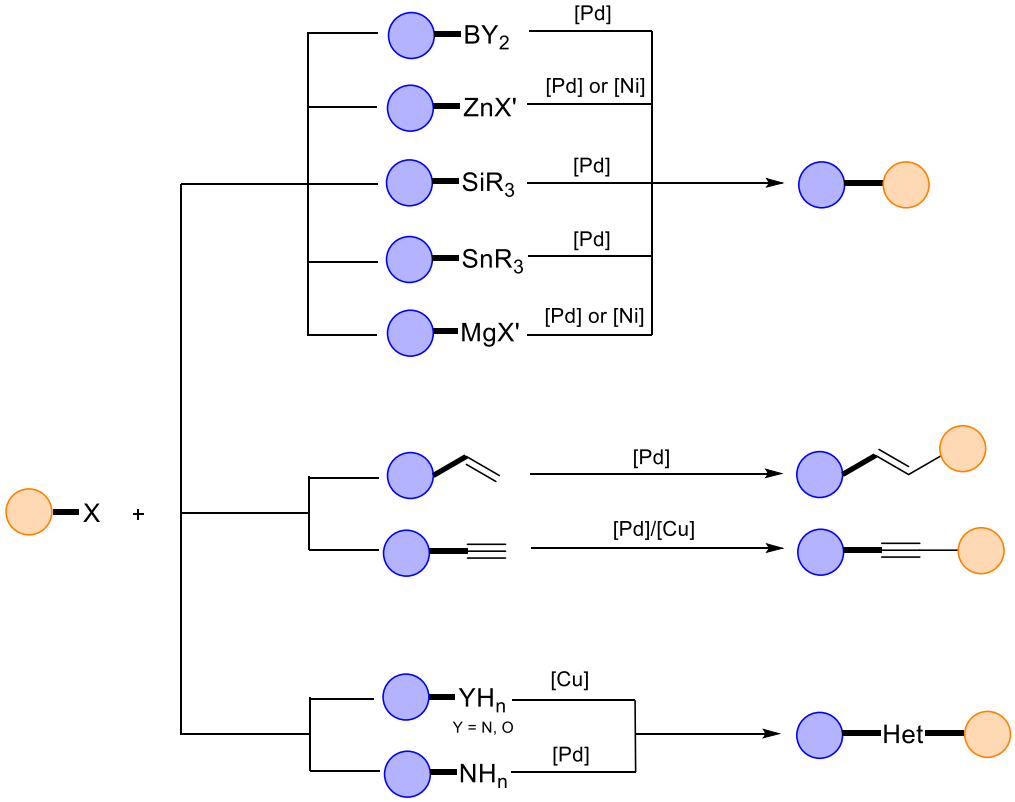

a) C–H functionalizations

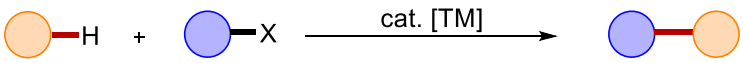

Scheme 1.1 Comparison of classical cross-coupling chemistry with catalytic C–H activations.

A notable advancement in organic synthesis has been the direct functionalization of ubiquitous C–H bonds.[9] This approach minimizes lengthy synthetic processes and reduces waste by activating inert C–H bonds directly, rather than relying on pre-functionalized substrates, thus providing new environmentally-benign and economically-attractive alternatives.[10]

A mechanistic understanding of the C–H cleavage step is necessary to design more efficient catalytic systems, thus extensive research has been conducted to uncover the different modes of C–H activation. Apart from radical-type outer-sphere mechanisms,[11] five distinct mechanistic pathways are recognized for organometallic C–H activation and this are strictly related to the chosen transition metal and its oxidation state but also to the ligand that is involved in the transformation.[12]

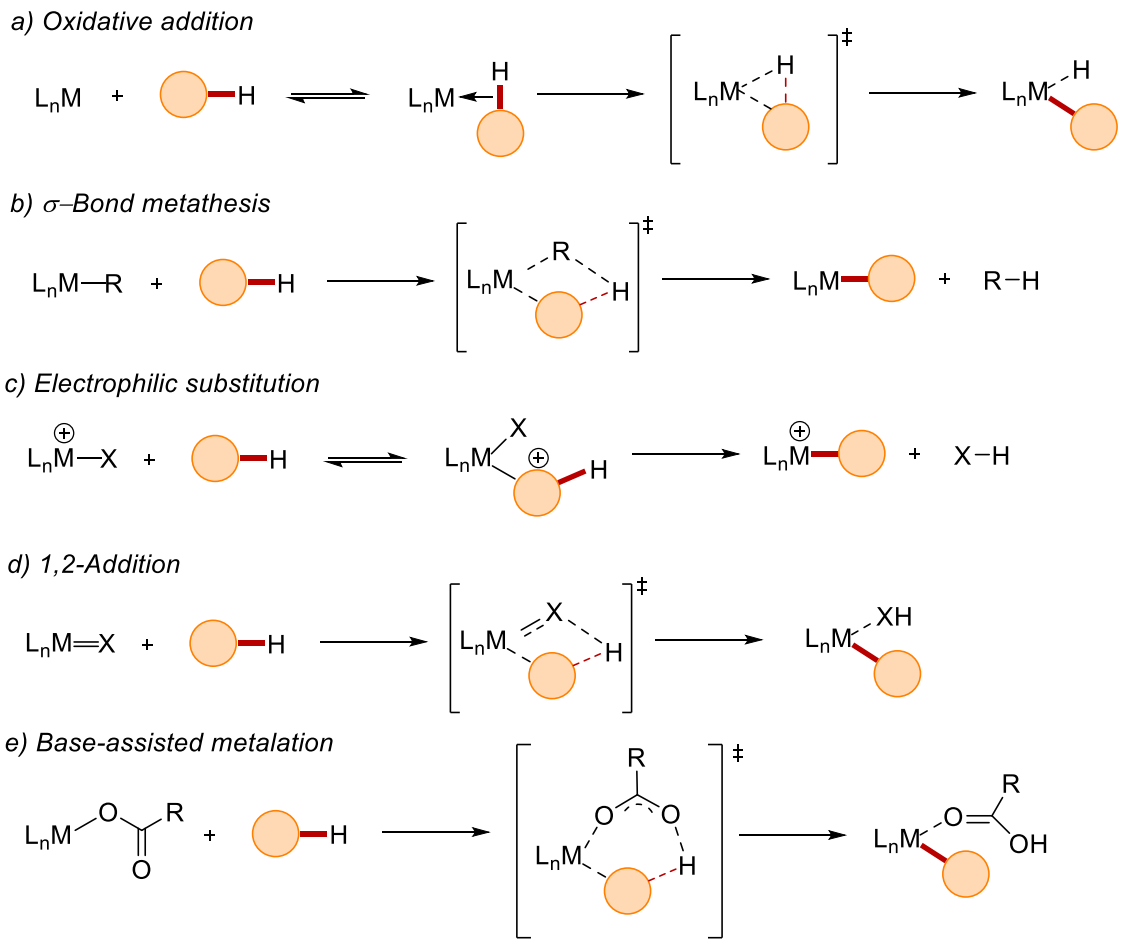

Scheme 1.2 Mechanistic pathways for C–H cleavage step.

The oxidative addition manifold is generally at play with electron-rich, low-valent complexes of late transition metals. Here an energetically high lying filled orbital of the transition-metal interacts with the anti-bonding σ*-orbital of the C–H bond. After the insertion of the metal center, its oxidation state is increased by +2 (Scheme 1.2, a).[13] High-valent early transition-metals lack of suitable filled orbitals and therefore can't interact with the anti-bonding σ*-orbital of the C–H bond. In this case the C–H activation step occurs via σ-bond metathesis, which has been considered for alkyl- or hydride-metal complex, (Scheme 1.2, b) without observing a change in the metal oxidation state.[14] Instead, late transition metals with higher oxidation states preferentially react through the electrophilic substitution pathway via electrophilic attack of the transition metal center to the carbon of the C–H bond of interest (Scheme 1.2, c).[15] The 1,2-addition pathway is usually preferred with complexes that contain unsaturated M=X bonds, such as group IV and V metal imido, oxo and alkylidene complexes (Scheme 1.2, d).[16] When carbonate or carboxylate ligands are involved in the catalytic process, the C–H activation step occurs *via* a base-assisted metalation step. The cleavage of the C–H bond occurs simultaneously

with the formation of the C–M bond. This mode of action is observed for complexes bearing a coordinated base, e.g. ruthenium (II)-carboxylate complexes, and proceeds through an electrophilic attack of the metal and deprotonation by carboxylate (Scheme 1.2, e).[17]

This latter mechanism can be further subdivided; over the past few years, several transition states have been proposed based on their structure and the accumulation of partial charges. Sakaki initially described a deprotonative transition state,[18] which Fagnou later referred to as a concerted metalation-deprotonation (CMD).[19] This manifold describes the synergistic interaction between the metal, the ligand and the C–H bond via a six-membered transition state. A similar transition state has been proposed for the ambiphilic metal-ligand activation (AMLA),[20] in which there is an additional agostic interaction between the metal center and the C–H bond (Scheme 1.3, a). Both these mechanisms generally take place with electron-deficient substrates with significant kinetic C–H acidity. Conversely, Ackermann introduced the base-assisted internal electrophilic substitution (BIES) mechanism (Scheme1.3, b), which is particularly effective for activating electron-rich and electron-neutral arenes and proceeds *via* an electrophilic substitution-like pathway.[21]

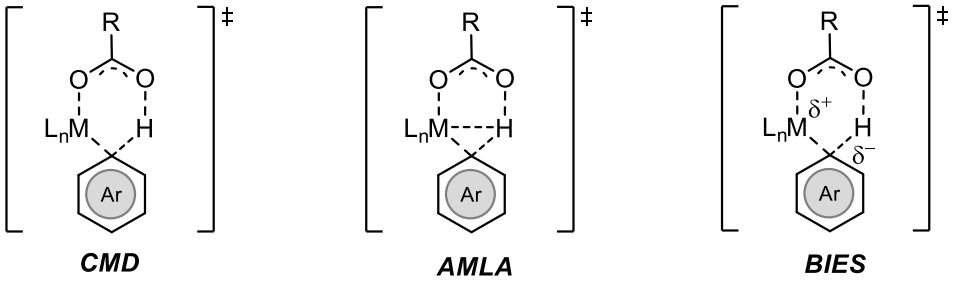

Scheme 1.3 Proposed transition states for base-assisted C–H activation.

In the past decades, much progress has been accomplished in the construction of molecular complexity *via* C–H activation methodologies. However, site-selectivity is still one of the major challenges associated with this approach because of the number of ubiquitous C–H bonds found in organic molecules, with often similar bond dissociation energies (BDEs) and acidities.[22] Nevertheless, different strategies can be adopted to get past the selectivity issues. Site-selectivity in C–H functionalizations can be achieved by exploiting the inherent properties of the target molecule. In fact, certain C–H bonds in heteroaromatic compounds show inherently higher kinetic acidities and lower bond dissociation energies (Scheme 1.4, a).[23] Additionally, bulky substituents in the substrate can prevent the access to nearby C–H bonds, forcing the activation to occur at the sterically least hindered site in the molecule (Scheme 1.4, b).[24] Since these approaches, based on electronic and steric biases, highly depend on the nature of the substrates, they are typically limited in terms of number of applications. In sharp contrast, a far more general strategy exploits

the coordination of a heteroatom-containing, Lewis-basic directing group (DG) that coordinates the Lewis-acidic metal center, bringing it near to a specific C–H bond (Scheme 1.4, c).

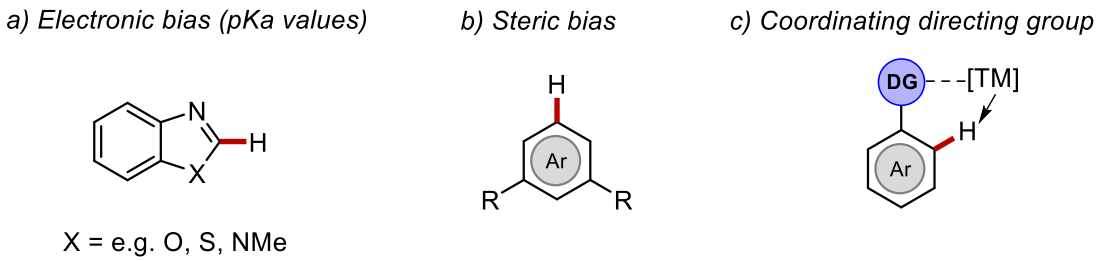

Scheme 1.4 Strategies for site-selective C–H activation.

Over the years, various directing groups have been investigated for different substrate classes, enabling site-selective functionalization of arenes.[25] Particular focus has been directed towards monodentate and bidentate directing groups for assistance. Overall, bidentate directing groups are more widely utilized than monodentate ones due to their easier metal coordination and adjustable coordinating properties.[26]

1.3 Iron-Catalyzed C–H Functionalizations

The construction of new bonds is the fundamental process to produce all synthetic organic molecules commonly employed in material science, biochemistry, agrochemicals, pharmaceuticals, and many other industries. A more sustainable method involves the direct functionalization of otherwise inert C–H bonds. Recently, precious 4d and 5d metals like palladium,[27] ruthenium,[28] iridium[29] and rhodium[30] have been extensively studied for their ability to form unprecedented C–C and C–Het bonds. However, their high cost and toxicity limit their use in the agrochemical and pharmaceutical industries, making them less viable alternatives to traditional cross-coupling reactions. A greener and more cost-effective approach uses less toxic, naturally abundant 3d transition metals.[31] Among these, iron stands out due to its abundance in the Earth's crust, low cost, low toxicity, and catalytic versatility, making it an ideal candidate for sustainable organic synthesis.[32] Unlike late transition metals, iron can exhibit a range of oxidation states from –2 to +6 and different spin states. This versatility allows iron catalysis to facilitate various reactions through different elementary pathways by adjusting its oxidation states with appropriate ligands. In this context, iron catalysis serves as an effective platform not only as a Lewis acid or in oxidation and hydrogenation reactions,[33] but also in the realm of C–H functionalizations. Like other transition metal-catalyzed C–H functionalizations, the reactivity of iron catalysts can be divided into two main categories. The first involves an outer-sphere activation mode, while the second operates through an inner-sphere, or organometallic, mechanism which will be discussed in this introduction. Inspired by early reports from Kochi on iron-catalyzed cross-coupling reactions,[34] the scientific community has concentrated its efforts on developing efficient iron catalyst systems for sustainable C–H activation strategies.

1.3.1 Early Findings on Iron-Catalyzed C–H Activation

It's important to highlight that Miyake's 1968 report was one of the earliest examples of stoichiometric organometallic C–H activation promoted by iron catalyst.[35] It was demonstrated that iron complexes can promote stoichiometric C–H activations, leading to the formation of well-defined, cyclometalated iron species. The synthesis of hydride ferracycle complex **2** was achieved by irradiating the $[Fe(dppe)_2C_2H_4]$ complex **1** with UV-light through oxidative addition of an *ortho* C–H bond (Scheme 1.5).

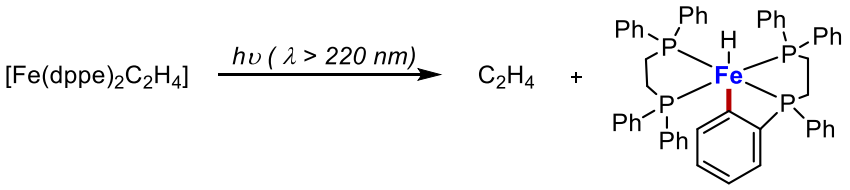

Scheme 1.5 Stoichiometric organometallic C–H activation.

Later studies confirmed that iron complexes can effectively promote the stoichiometric activation of C–H bonds.[36] For example, Klein and colleagues showed that low-valent iron complexes, like iron(0) complex $Fe(PMe_3)_4$ or iron(II) complex $FeMe_2(PMe_3)_4$, are suitable for the stoichiometric *ortho*-selective metalation of ketimines **3** (Scheme 1.6).[37]

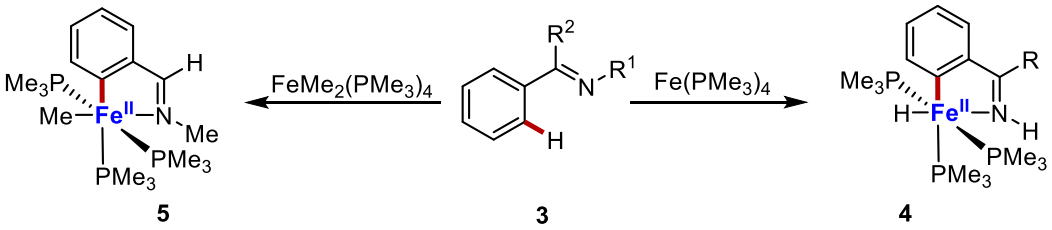

Scheme 1.6 Stoichiometric *ortho*-C–H metalation of ketimines **3** by iron complexes.

Specifically, they reported that an iron(0) trimethyl-phosphine complex reacts with an aromatic imine *via* oxidative addition of the *ortho* C−H bond to the iron(0) center to deliver complex **4**. Also complex $FeMe_2(PMe_3)_4$ can react with imine **3** to generate the *ortho*-methylated iron(II) complex **5**. The reaction proceeds by *ortho* C–H activation *via* σ-bond metathesis to generate an iron(II) ferracycle and methane without addition to the imine's double bond.

These groundbreaking studies inspired different research groups to develop catalytic C–H functionalizations using readily available iron catalysts. Early efforts by Jones et al. to develop iron-catalyzed C–H bond activations were not pursued for synthetic applications due to low reaction efficiency.[38] A breakthrough in catalytic iron C–H functionalizations is represented by

the unexpected discovery made by Nakamura, Yoshikai and coworkers in 2006. During the optimization of the cross-coupling reaction between 2-bromopyridine **6** and an *in situ* generated diphenylzinc reagent, they discovered a ternary coupling product **8** which was formed in an 8% yield (Scheme 1.7).

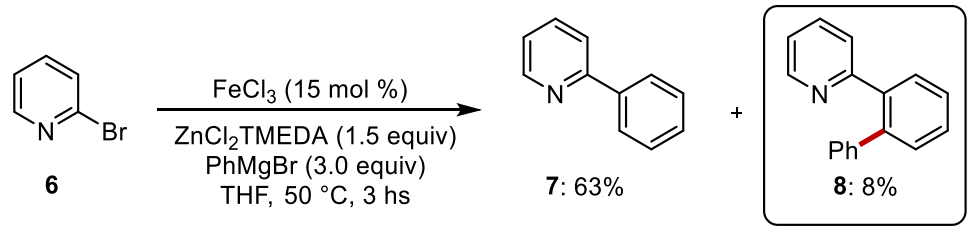

Scheme 1.7 Iron-catalyzed cross-coupling of 2-bromopyridine **6** with C–H arylation of 2-phenylpyridine.

Product **8** was suggested to be formed by the iron-catalyzed C–H arylation of the initially formed 2-phenylpyridine. It was later understood that this side reaction was promoted by oxygen that had unintentionally penetrated the reaction vessel and by 1,1'-bipyridine, a byproduct of the homocoupling of 2-bromopyridine.[39]

This finding, along with thorough optimization studies of the crucial reaction parameters, resulted in the development of an efficient (low-valent) iron-catalyzed C–H arylation process that was reported in 2008 by Nakamura (Scheme 1.8).[40] The arylation occurs exclusively at the 10 position of substrate **9** due to the directing effect of the nitrogen, which coordinates with the iron and allows for the selective activation of the C–H bond, leading to the formation of the cyclometallated intermediate. The use of an organozinc as a coupling partner, generated *in situ* by reaction of Ph_2Zn from PhMgBr and $ZnCl_2$TMEDA, was found to be essential for promoting the desired C–H transformation. A suitable dichloroalkane oxidant, DCIB, and the identification of a bidentate nitrogen ligand (1,10-phenantroline) to stabilize the iron intermediate were pivotal findings that enabled the organoiron species to complete the catalytic cycle.

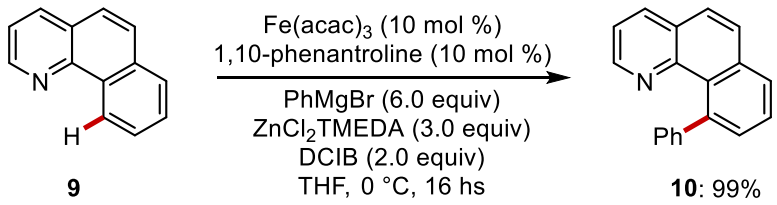

Scheme 1.8 Iron-catalyzed directed C–H arylation of α-benzoquinoline.

Only a few years later Shaik, Chen and colleagues conducted theoretical calculations, based on density functional theory, to clarify the mechanism behind nitrogen-directed low-valent iron-catalyzed C–H arylation.[41] Based on the mechanistic experiments by Nakamura et al.,[40] Chen's

calculations identified a two-state reactivity scenario (TSR) for iron catalyzed C−H bond activation. In particular, the authors propose a catalytic cycle in which iron can have three oxidation states: Fe(II), Fe(III), and Fe(I) (Scheme 1.9). The calculations suggested a spin acceleration effect during the crucial C−H activation step, in which the high-spin ground state of Fe(II) or Fe(III) is crossed over by both the low-spin singlet and doublet state. Compared with Fe(II) and Fe(III), this C–H activation is energetically less favourable for iron in the Fe(0) or Fe(I) oxidation state. In the proposed reaction mechanism, the first step of the reaction is the activation of the C–H bond *via* σ-bond metathesis (**II**). This is followed by a transmetalation reaction, mediated by diphenylzinc, where the chloride coordinated to the iron is exchanged with a phenyl group to afford **III**. Subsequently, oxidation occurs through a single electron transfer (SET) mechanism, where 1,2-dichloroisobutane oxidizes the Fe(II) center to Fe(III) **IV**. The Fe(III) species is prone to undergo a reductive elimination reaction, enabling the C−C coupling between the phenyl group and the carbon of α-benzoquinoline **9**, forming an Fe(I) species **V**. A new α-benzoquinoline then replaces the arylated product, followed by a second SET oxidation that converts Fe(I) back to Fe(II) (**VI**). The Fe(II) species undergoes another transmetalation mediated by diphenylzinc, regenerating the initial active catalytic species **I**. The direct oxidative addition alternative pathway of the dichloroalkane is not favoured for Fe(I) oxidation compared with the SET pathway.

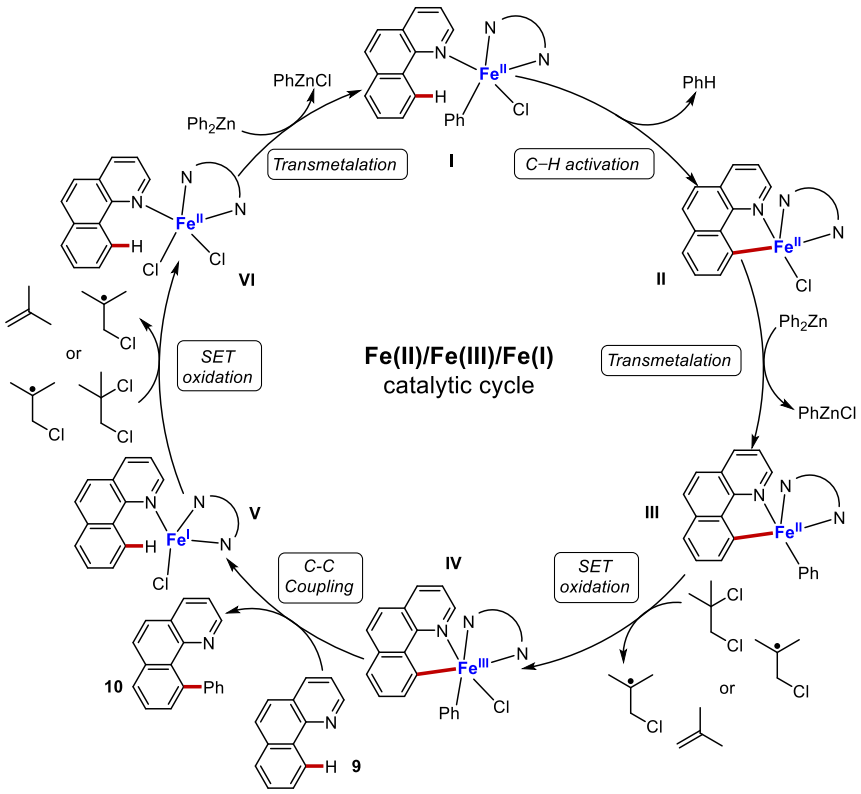

Scheme 1.9 Proposed Fe(II)/Fe(III)/Fe(I) mechanism pathway based on density functional theory studies.

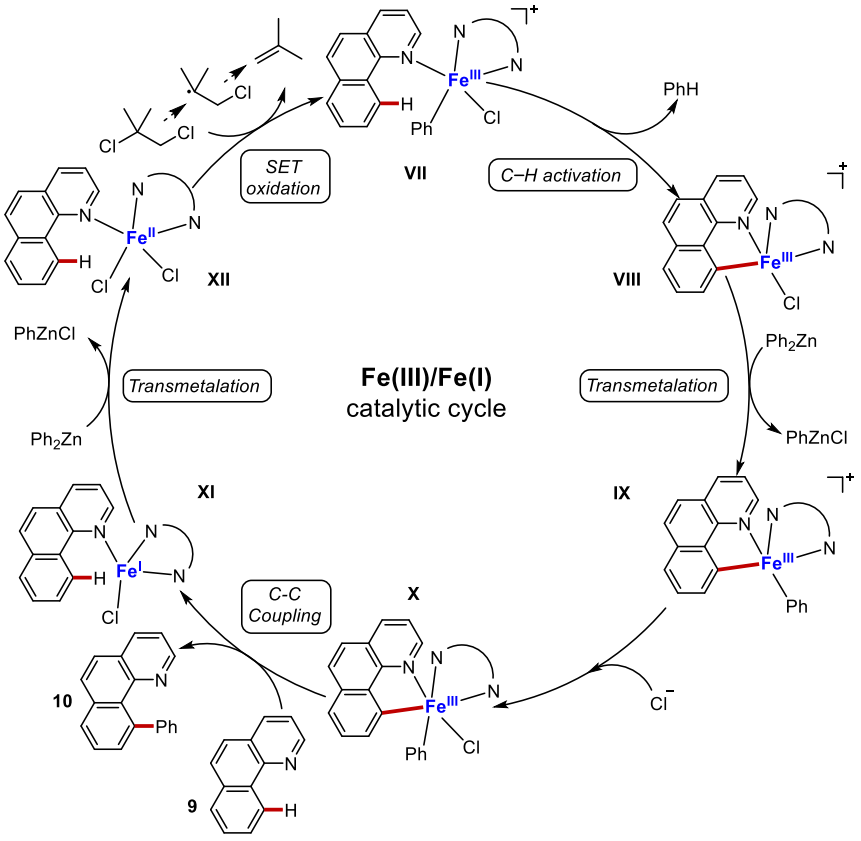

Scheme 1.10 Proposed Fe(III)/Fe(I) mechanism pathway based on density functional theory studies.

Further theoretical studies by the authors highlighted the importance of the ligand sphere of iron in stabilizing the reactive low-spin state, which is essential for C−H activation in the TSR mechanism. On the basis of all the DFT studies, the authors proposed that, during the catalytic cycle, the oxidation state evolves in either Fe(II)/Fe(III)/Fe(I) (Scheme 1.9) or Fe(III)/Fe(I) (Scheme 1.10).

Regarding catalytic C–H functionalizations, two potential reaction pathways can be considered. Firstly, C–H transformations might occur using organometallic reagents and an external oxidant, which would enable an oxidation-induced reductive elimination (Scheme 1.11, a). Alternatively, C–H activation reactions can proceed through the reaction of organic electrophiles with the nucleophilic metallacycle (Scheme 1.11, b).

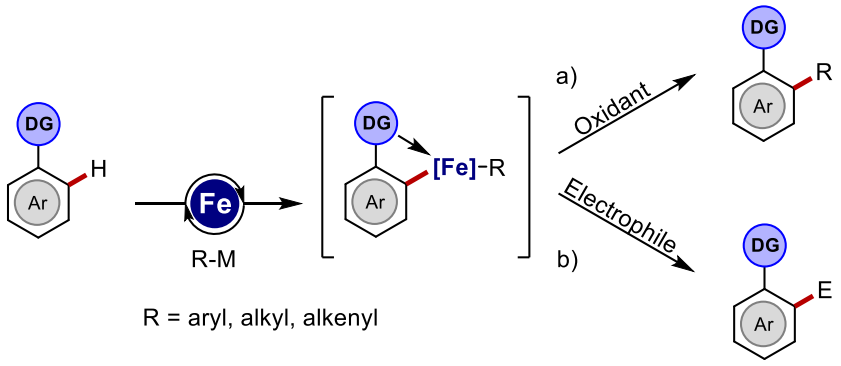

Scheme 1.11 Organometallic iron catalyzed C–H functionalizations pathways.

Nakamura's pioneering work paved the way for the development of several new iron-catalyzed C(sp^2)–H arylations and alkylations methods with the assistance of monodentate directing groups (e.g., imines, amides, ketones).[42] A notable breakthrough in iron-catalyzed C–H functionalization was achieved with the use of bidentate directing groups.[43] These groups not only enabled unprecedented C(sp^3)–H activations but also greatly expanded the range of possible transformations. Significant progress in bidentate directing group-assisted iron-catalyzed C–H functionalizations was made by Nakamura with the 8-aminoquinoline (Q) group[44] and by Ackermann with the readily available triazolyldimethylmethyl (TAM) group.[45]

1.3.2 Iron-Catalyzed C−H Functionalizations with Organometallic Reagents

The first example of C–H bond activation directed by Lewis-basic functional groups such as arylimines was reported by Nakamura in 2009.[46] Interestingly, the reaction showed high chemo-selectivity as aryl triflates and tosylates were fully tolerated, without any cross-coupling products being formed, enabling the *ortho* selective functionalization of the target substrate (Scheme 1.12).

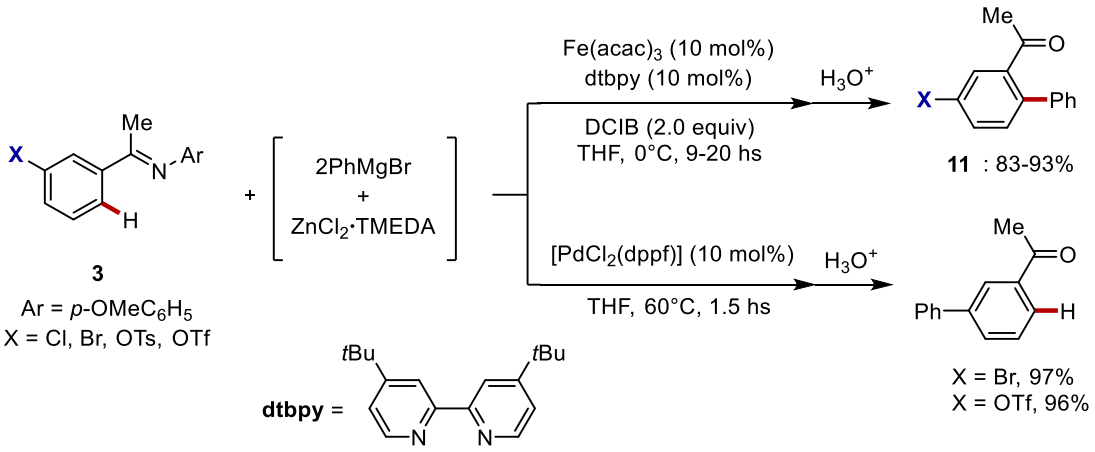

Scheme 1.12 Iron-catalyzed *ortho* C−H arylation of arylimines with Grignard reagent.

Similarly, benzamides were found to be effective substrates for iron-catalyzed C–H *ortho* monoarylation with organozinc reagents under oxidative conditions (Scheme 1.13).[47] The lack of reactivity for a tertiary *N*,*N*-dimethyl benzamide (**12c**) to undergo C–H arylation indicates the necessity of the N–H acidic functionality and that the deprotonated amide serves as directing group for the transformation.

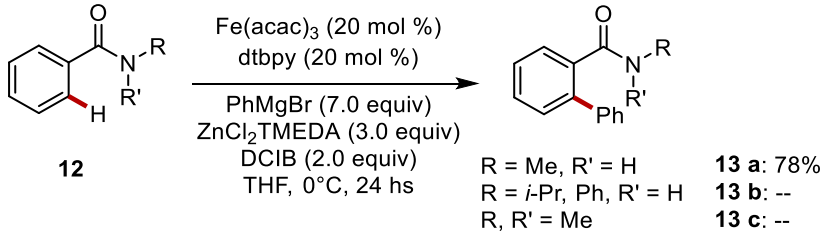

Scheme 1.13 Iron catalyzed *ortho* mono C−H arylation of benzamides.

An early example of bidentate directing group-assisted C−H functionalization was reported by Nakamura and coworkers.[48] The efficacy of 8-aminoquinoline (Q) as a robust directing group was originally demonstrated by Daugulis for palladium-catalyzed functionalizations of unactivated C(sp^3)–H bonds.[44] In his study, Nakamura further demonstarted that the

quinolinamide group acts as an exceptionally effective directing group for iron catalyzed C(sp^3)–H bond activation for the *β*-arylation of 2,2-disubstituted carboxamides **14**.

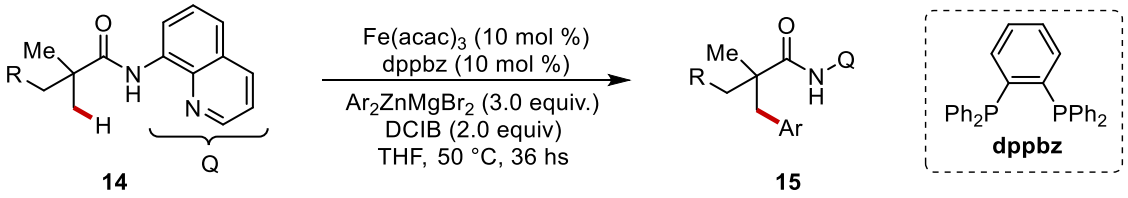

Scheme 1.14 Iron-catalyzed C(sp^3)–H arylation of quinolinamides **14**.

In addition, the same group reported the 8-aminoquinoline assisted iron catalyzed C(sp^2)−H bond functionalization with organoboron-based reagents under mild oxidative conditions (Scheme 1.15).[49] The preliminary activation of the organoboron compound to an organoborate using *n*BuLi generates the transmetalating agent. A zinc salt is required to facilitate the transfer of the organic group from boron to iron, while the use of 1,2-dichloroisobutane (DCIB) promotes the formation of the C−C bond as previously discussed. It is important to note that the organoborate is not a strong reducing agent; therefore, iron remains in its oxidation state (III), which is the active species in the catalytic cycle.

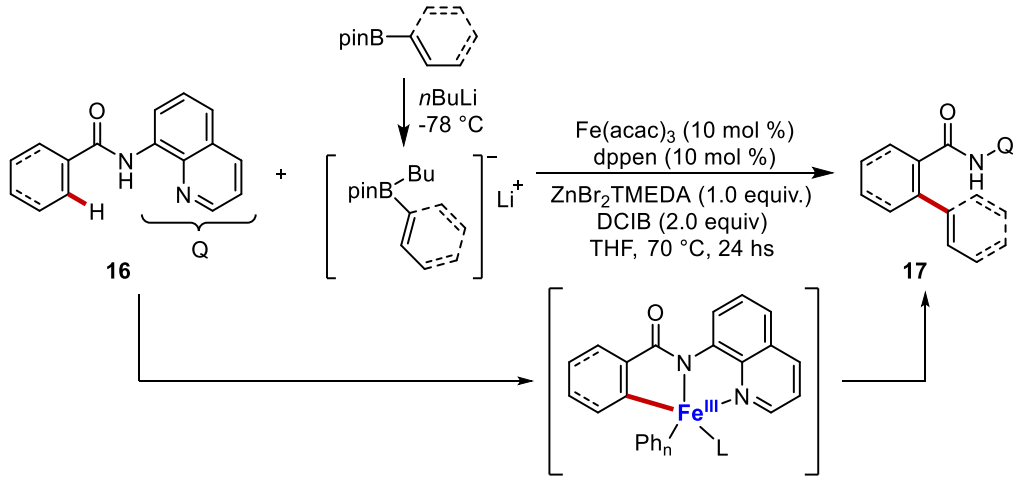

Scheme 1.15 Iron catalyzed alkenylation and arylation with organoboron compounds assisted by Q.

Despite its indisputable advantages, the Q auxiliary has some drawbacks, including the difficulty of accessing it in a modular fashion and the requirement of harsh reaction conditions for its removal. Additionally, it can sometimes engage in side-reactions, leading to undesired by-products that could complicate the purification process and reduce the overall yield of the desired product.[50] Consequently, a significant advancement in iron-catalyzed C–H activation was achieved with the introduction of a modular family of readily accessible triazole-based directing

groups. In 2014, Ackermann and coworkers identified the 1,2,3-triazole as a key motif in bidentate directing groups for iron-catalyzed C(sp^2)–H and C(sp^3)–H arylations.[51]

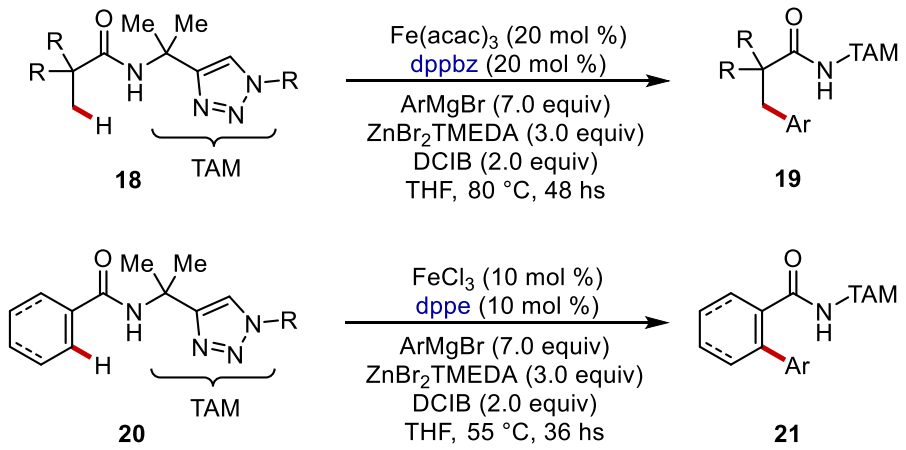

Scheme 1.16 Iron-catalyzed C(sp^3)–H and C(sp^2)–H arylation of TAM-carboxamides.

The oxidative functionalization manifold using organometallic reagents could be extended also to challenging alkylation of the C(sp^2)–H bond with an alkyl metal compound. This process is more difficult due to the possibility of fast β-hydride elimination compared to C–H bond arylation. Direct *ortho*-selective C–H alkylations were successfully accomplished by generating alkylzinc reagents *in situ*, through bidentate chelation assistance with the Q auxiliary.[52]

Significant progress in iron-catalyzed C–H functionalizations has been achieved through the development of protocols for the site selective C–H methylation of C(sp^2)–H and C(sp^3)–H bonds. In 2015, Nakamura reported an effective methylation protocol that utilizes the commercially available $AlMe_3$ or its air-stable derivative, DABCO-2$AlMe_3$, as an efficient methyl donor in the presence of 2,3-dichlorobutane as the oxidant.[53] This reaction is compatible with a range of amide substrates bearing a picolinyl or 8-aminoquinolyl directing group, enabling the methylation of various (hetero)aryl, alkenyl, and alkyl amides (Scheme 1.17).

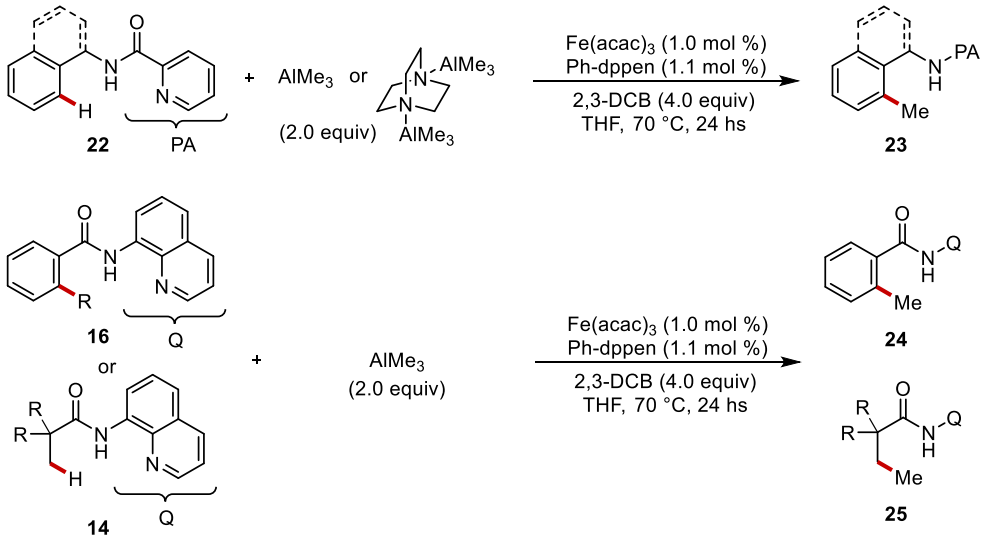

Scheme 1.17 Iron-catalyzed directed C(sp^2)–H and C(sp^3)–H functionalization with trimethylaluminum.

In the same year Ackermann and coworkers developed a versatile iron-catalyzed methylation method for C(sp^2)–H and C(sp^3)–H bonds, utilizing TAM assistance, which facilitated site-selective C–H functionalizations on both arenes and heteroarenes.[54] The optimized catalytic system exhibited high diastereoselectivities in the (*Z*)-functionalization of alkenes and even enabled challenging C(sp^3)–H functionalizations on alkanes, all utilizing the same catalytic system.

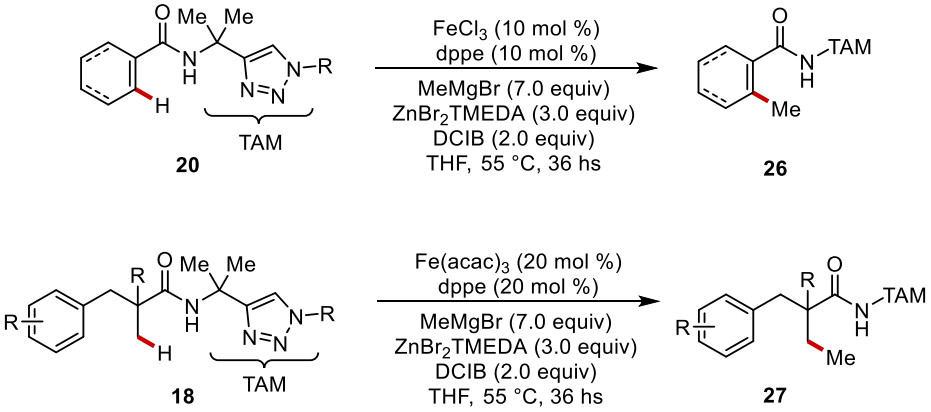

Scheme 1.18 Iron-catalyzed directed C(sp^2)–H and C(sp^3)–H methylations by triazole assistance.

Similarly, the introduction of TST (tri-substituted triazole) directing groups enabled the iron catalyzed C–H arylations of geometrically flexible, electron-rich benzylamide derivatives.[55] In this context, a phosphine with a rigid backbone, like *cis*-1,2-bis(diphenylphosphino)ethene (dppen), was crucial for efficiently functionalizing benzylamides in the presence of 1,2-DCIB as a mild oxidant. The protocol was found viable for the iron-catalyzed C–H methylation, alkylation and arylation of benzyl and arylamines with ample scope.

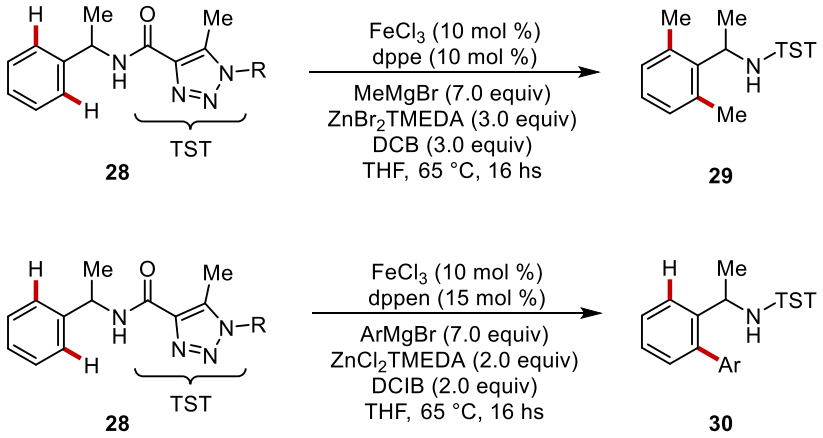

Scheme 1.19 Iron-catalyzed directed C(sp^2)−H methylations and arylations with tri-substituted triazole.

Recent mechanistic studies have enabled the identification and isolation of the key cyclometallated iron(II) species proposed as intermediate in C–H bond activation reactions, featuring an *ortho*-directing triazolylmethyl (TAM) group **20a**.[56] The use of ^{57}Fe Mössbauer spectroscopy on reaction mixtures frozen at 80K, along with magnetic circular dichroism (MCD), enabled the identification of the Fe complexes postulated in the mechanism and the characterization of their spin state, coordination number, and oxidation state. The first intermediate was identified by analyzing the reaction mixture from a stoichiometric experiment were substrate **1a** was treated with one equivalent of Ar_2Zn reagent in the presence of $Fe(acac)_3$ and 1,2-bis(diphenylphosphino)benzene (dppbz), resulting in the predominant formation of a high-spin iron(II) species. Further studies using magnetic circular dichroism identified this species as a distorted, tetrahedral complex of type **XIII** where the bidentate phosphine ligand dppbz does not coordinate to iron.

When the reaction was performed with three equivalents of organozinc reagent, intermediate **XIII** was consumed, forming two new low-spin iron species. The major species was identified as a cyclometallated iron(II) dimer [(**20a**)(dppbz)(THF)Fe]$_2$(μ-MgX_2) **XV** via X-ray spectroscopy, where a magnesium salt bridges two neutral monomers. The minor species was identified as the five-coordinate, non-THF-ligated analogue **XIV**. In contrast to **XIII**, formation of **XIV** and **XV** requires dppbz to be present.

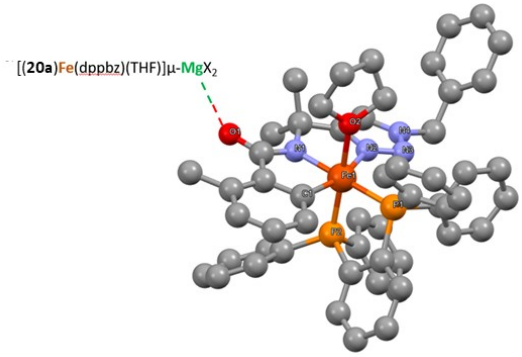

Figure 1.1 Single-crystal X-ray dimeric structure of cyclometallated complex **XV**.

The addition of two more equivalents of Ar_2Zn to a THF solution of **XIV**/**XV** formed a new species identified as a cyclometallated low-spin iron(II)−phenyl dimer, [(**20a**)-(dppz)(Ph)Fe]$_2$(μ-Mg(THF)$_3$) **XVI**. This intermediate was competent for C–C bond formation, with its consumption to produce the *ortho*-arylated product by stoichiometric reaction with DCIB. Along **XVI**, the Mössbauer analysis showed the formation of another species **XVII** (7% of all iron) which is more similar to Fe(0) complexes like Fe(η^6-biphenyl)(dppbz); therefore, it is reasonable to assign it the structure of Fe(η^6-biaryl)(dppz), generated by the reduction of Fe(II). The dichloroalkane plays a crucial role initially by oxidizing off-cycle reduced iron(0) species, like **XVII**, and transient on-cycle iron(I) species, which then re-enter the catalytic cycle. Since **XVI** does not react without an oxidant, it is improbable that the catalytic cycle involves the reductive elimination of Fe(II) to produce Fe(0). Instead, stoichiometric reactions indicate that the catalytic cycle follows an Fe(II)/Fe(III)/Fe(I) pathway, as previously suggested by detailed DFT mechanistic studies.[41] In this scenario, DCIB promotes the oxidation of **XVI** via a single-electron transfer (SET) mechanism to a putative iron(III) intermediate, which then undergoes reductive elimination to yield the *ortho*-functionalized arylated product and lower-valent iron(I) species. These species re-enter the catalytic cycle after oxidation by a second equivalent of dihaloalkane. Although the exact mechanism of this initial oxidation to Fe(III) is unclear, the authors claims that it might occur through outer-sphere oxidation or the displacement of a phosphine ligand.

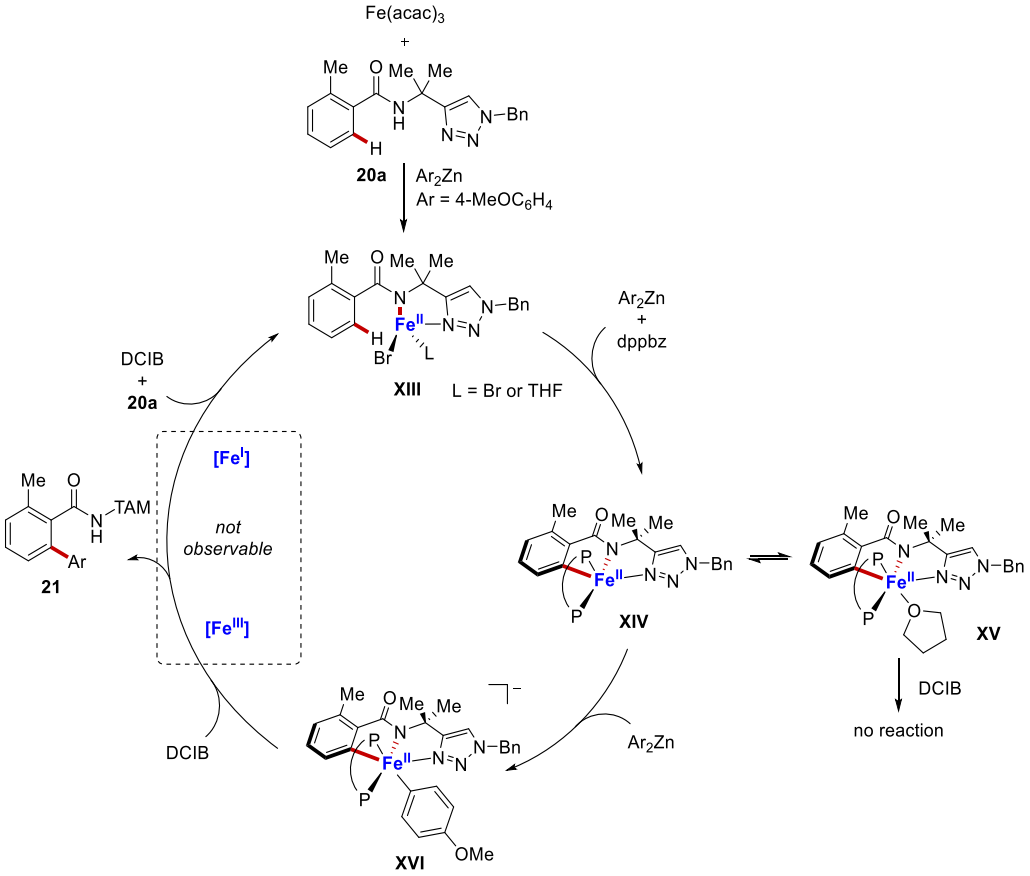

Scheme 1.20 Proposed mechanism for iron-catalyzed C(sp^2)–H bond arylation with TAM assistance.

Very recently iron-catalyzed C−H functionalization with organometallic reagent were extended by Nakamura to a twofold C–H activation/cross-coupling of (hetero)arenes based on chelate assistance of 8-amoniquinoline under oxidative conditions.[57] This approach enables the efficient production of C−C heterocoupling products by exploiting the transient connection of the two reactants through the Q auxiliary. The employment of Me_3SiCH_2MgCl as the organometallic base was essential, as simple Grignard reagents like MeMgBr or PhMgBr led to *ortho* C–H methylation and arylation of the carboxamide substrate.

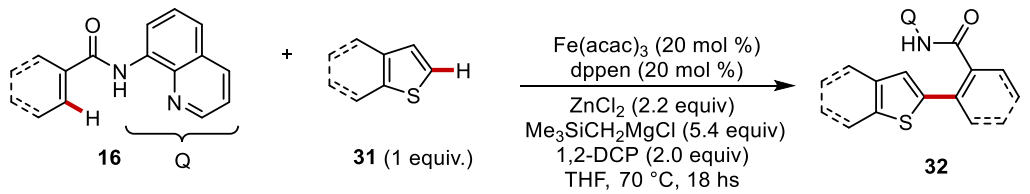

Scheme 1.21 Iron-catalyzed twofold C–H activation/cross-coupling of heteroarenes.

Through extensive mechanistic experiments, the authors propose a catalytic pathway that begins with the C–H activation of the carboxamide, forming metallacycle **XIX**. This is followed by a

reversible C–H deprotonation of the heteroarene by the iron intermediate, creating a transient species (**XX**) where the two reactants are linked via the coordination of the Q auxiliary with iron. Subsequently, the irreversible deprotonation of the *ortho* C−H bond of the carboxamide by -CH_2SiMe_3 leads to the formation of intermediate **XXI**. Reductive elimination of **XXI** produces the iron(II) intermediate **XXII**, which is then oxidized by 1,2-dichloropropane (1,2-DCP), completing the catalytic cycle (Scheme 1.22).

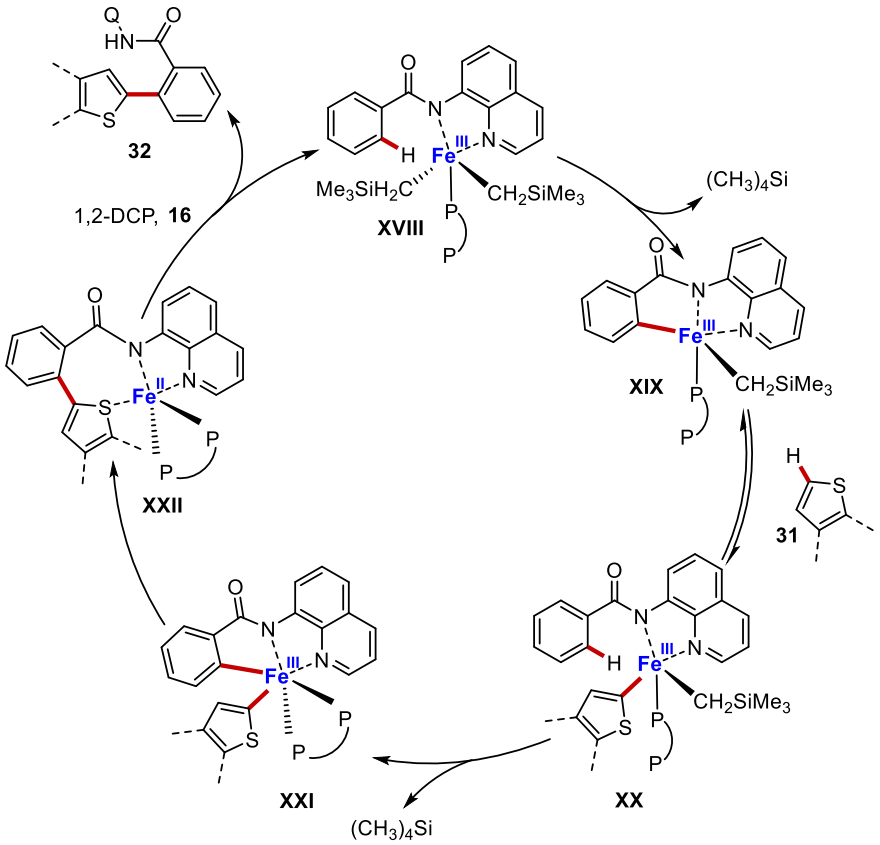

Scheme 1.22 Proposed mechanism for iron-catalyzed twofold C–H activation/cross coupling of carboxamides **16**.

1.3.3 Iron-Catalyzed C(sp^2)−H Functionalizations with Carbon Electrophiles

Despite significant advancements in iron-catalyzed C–H activations with nucleophilic coupling partners, most cases still require stoichiometric amounts of costly and toxic haloalkanes as oxidants to ensure catalyst turnover (Scheme 1.13, path a). In 2013, Nakamura and colleagues demonstrated for the first time that an electrophile (**33**) can serve as a coupling partner in iron-catalyzed C–H functionalization.[58] This reaction does not require an oxidant; instead, a non-nucleophilic base is necessary to deprotonate the C–H bond (Scheme 1.23). This protocol has promoted the development of methods for forming various bonds using different electrophiles that can react with the *in situ* generated iron species. These include alkyl electrophiles, allylic electrophiles, and amine electrophiles which were successfully employed in bidentate directing group-assisted low-valent iron catalysis.[59]

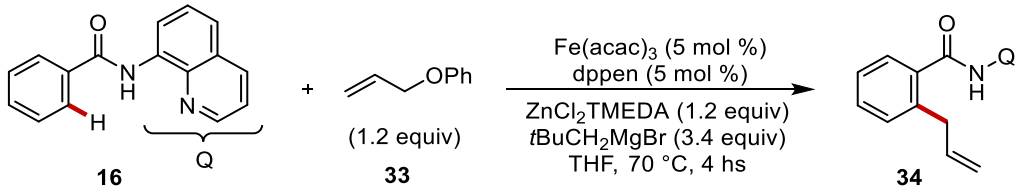

Scheme 1.23 Iron-catalyzed directed C(sp^2)–H allylation with allyl phenyl ethers.

In 2014 Nakamura established a novel protocol where alkenes, arenes, and heteroarenes with an 8-quinolylamide directing group are alkylated using primary and secondary alkyl tosylates, mesylates, and halides in the presence of $Fe(acac)_3$ as the catalyst and ArZnBr as a base (Scheme 1.24).[60] The ligand effect is crucial in this reaction, facilitating C−H alkylation while preventing unwanted cross-coupling or C−H arylation. The authors showed that bis(phosphine) ligands with a conjugated backbone were necessary for the reaction's success, whereas monodentate phosphine and bipyridine ligands proved completely ineffective, leading to the recovery of the starting quinolinamide.

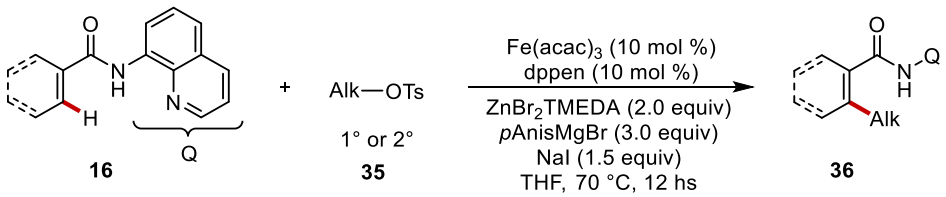

Scheme 1.24 Iron-catalyzed directed C(sp^2)–H alkylation with primary and secondary alkyl tosylates.

In the same year, Cook independently reported a unified strategy for iron catalyzed directed C−H alkylation of carboxamides (Scheme 1.25).[61] The iron-catalyzed conditions can be quickly

adjusted to suit a variety of significant electrophiles including benzyl halides (**37**) and unactivated secondary alkyl bromides (**39**). The key to enhance the catalytic efficiency was the slow addition of the Grignard reagent. Moreover, the reaction performed best when conducted over a short period of time, whereas the inclusion of zinc additives was surprisingly counterproductive. The authors suggested that the slow addition method and short reaction time lead to the formation of a highly reactive phenyliron species via transmetalation from PhMgBr. This species quickly coordinates with the quinolinamide substrate **16** in a turnover-limiting step, followed by rapid and irreversible C–H cleavage.

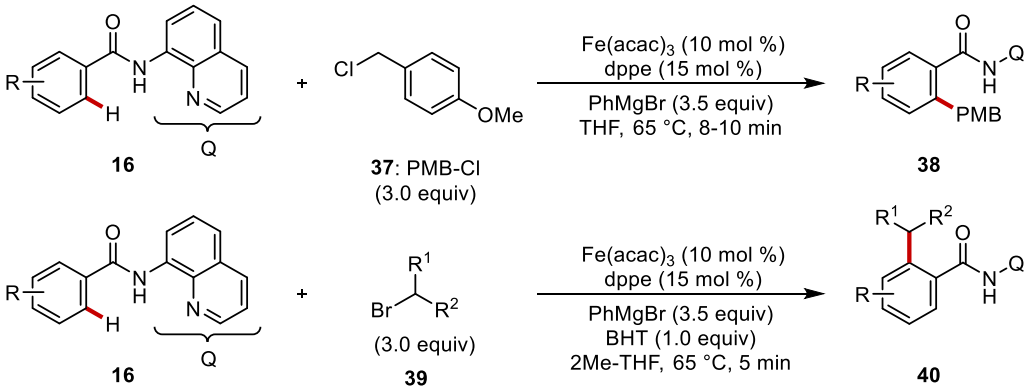

Scheme 1.25 Iron-catalyzed C(sp^2)–H benzylation and alkylation with secondary alkyl bromides.

In addition to their previous findings, Cook and coworkers also reported a robust iron-catalyzed *ortho* C(sp^2)–H alkylation of quinolinamides using primary electrophiles like unactivated alkyl bromides.[62] The reaction is conducted under mild conditions in bio-derived 2-methyltetrahydrofuran as solvent and completes in less than 10 minutes. Radical-clock experiments confirmed the radical nature of the alkyliron intermediate, as previously demonstrated by Nakamura.[58] The reaction of a cyclopropylmethyl bromide **41a** led to the production of the ring-opened product **42aa** (Scheme 1.26, a); while when 6-bromo-1-hexene **41b** was used as the reaction partner, the cyclized product **42ab** was formed along with the linear product **42ab'** in a 5:1 ratio suggesting a single-electron-transfer (SET)-type pathway in the C–Br cleavage (Scheme 1.26, b).

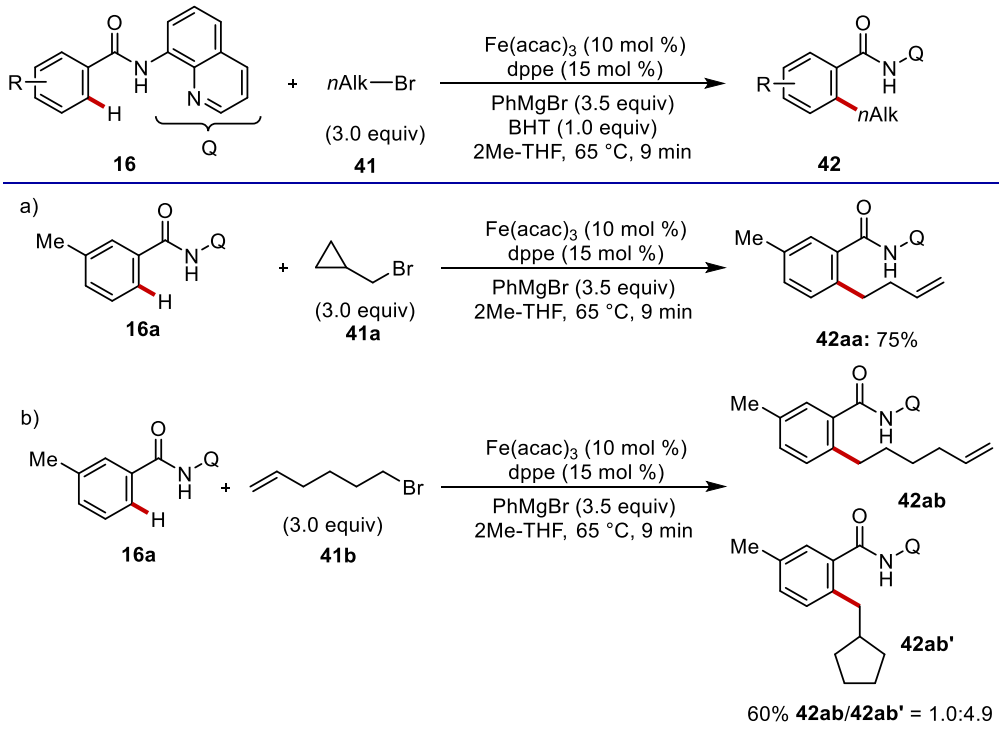

Scheme 1.26 Iron-catalyzed C(sp^2)–H alkylation with primary alkyl bromides.

In independent studies, Ackermann and coworkers developed an effective protocol for the iron-catalyzed C–H allylation of arenes, heteroarenes, and alkenes, assisted by triazole directing group with ample scope (Scheme 1.27).[63] The versatile catalyst was efficiently employed in the site-selective methylation, benzylation, and alkylation with challenging primary and secondary halides.

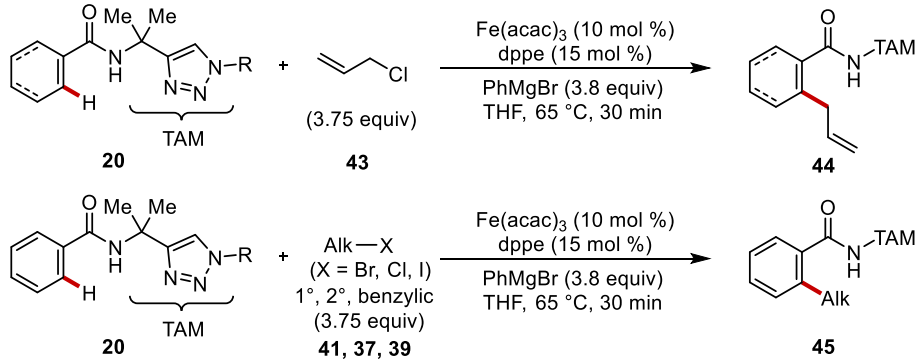

Scheme 1.27 Iron-catalyzed C(sp^2)–H allylation/alkylation by triazole assistance.

The mechanism of the versatile iron catalyst was thoroughly investigated by the authors, revealing consistency with a SET-type C–Hal cleavage. Notably, a new protocol was developed for the easy removal of the TAM auxiliary (Scheme 1.28). The use of nitrosonium tetrafluoroborate ($NOBF_4$)

facilitated the cleavage of the triazole directing group under extremely mild conditions, addressing a significant limitation of Q-directing group in C–H activation methodologies.

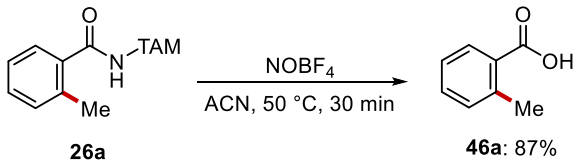

26a **46a**: 87%

Scheme 1.28 Mild removal of TAM directing group with $NOBF_4$.

In the scenario of iron promoted C–H bond functionalizations, Ackermann and coworkers made a significant breakthrough in 2017 by developing the first iron-catalyzed C–H alkynylation of arenes, heteroarenes, and alkenes (Scheme 1.29).[64] The reaction is conducted utilizing TIPS-bromoalkynes **47**, exploiting the assistance of the versatile TAM directing group which allowed the synthesis of a family of *ortho*-alkynylated carboxamides with high yields and site selectivity. This setup facilitated a sequential C–H alkynylation/annulation strategy with broad applicability, allowing for the iron-catalyzed synthesis of isoquinolones, pyridones, pyrrolones, and isoindolinones. A one-pot, two-step cascade involving C–H alkynylation and 6-*endo*-dig annulation was successfully carried out for the synthesis of isoquinolone **50** following the basic deprotection of the TMS group (Scheme 1.29, a). Additionally, when *ortho*-alkynylated benzamides, produced via C–H alkynylation of **47**, were subjected to standard desilylation conditions, a 5-*exo*-dig annulation provided isoindolinone derivatives **51** (Scheme 1.29, b).

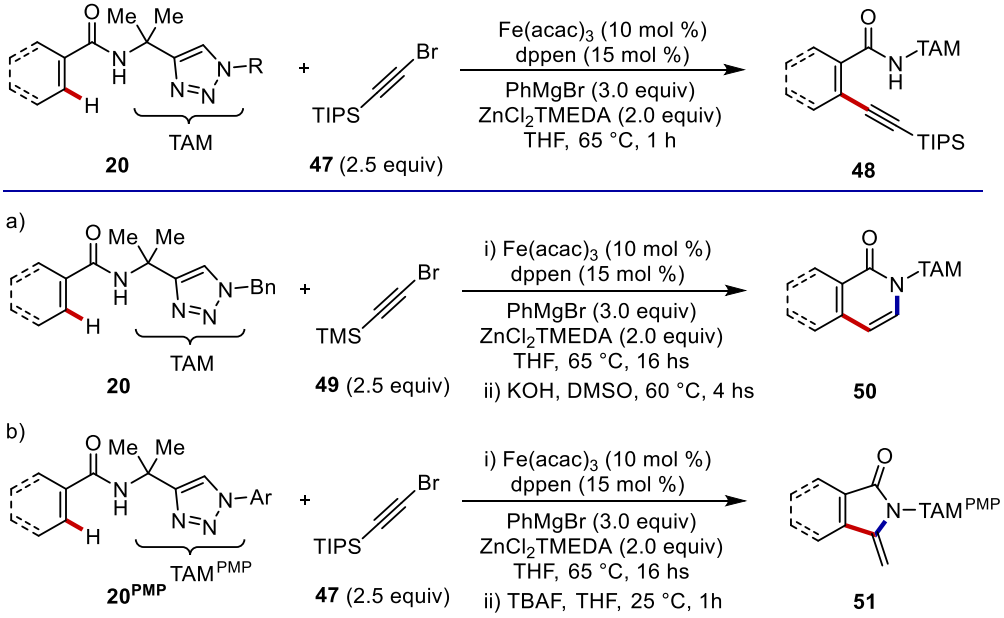

Scheme 1.29 Iron-catalyzed TAM-assisted alkynylation of C(sp^2)–H bonds with bromoalkynes. Sequential C–H alkynylation/annulation for a) isoquinolones synthesis; b) isoindolinones synthesis.

The proposed catalytic cycle begins with the coordination of the amide to the iron pre-catalyst in the presence of an organozinc reagent, forming intermediate **XXIII**. This intermediate is then converted into metallacycle **XXIV** through a reversible C–H bond activation. Subsequently, the regioselective insertion of the bromo-alkyne occurs, producing metallacycle **XXV**, which ultimately releases the desired product **48** and regenerates the active catalytic species via *β*–Br elimination.

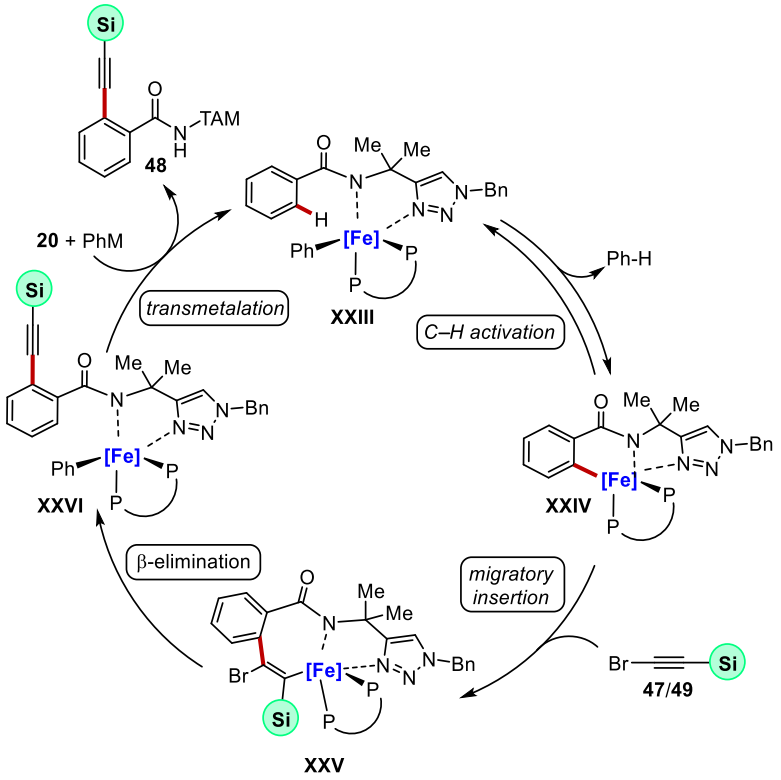

Scheme 1.30 Proposed mechanism for iron-catalyzed TAM-assisted C–H alkynylation.

In this introduction, the most representative examples of iron-catalyzed C–H functionalization have been highlighted, with a particular focus on oxidative C–H activations and C–H transformations with organic electrophiles. Significant advancements have been achieved through bidentate chelation assistance provided by 8-aminoquinoline or modular 1,2,3-triazoles, which enabled site-selective activation of C(sp^2)–H and more challenging C(sp^3)–H bonds. Further recent examples of transformations facilitated by the use of this versatile metal will be discussed in the introductions of the different chapters of this thesis, while more modern strategies such as bimetallic activations, ligand design for functionalizations of unsaturated molecules, isotopic labelling and photo-assisted C–H activation will not be covered.[65]

1.4 Triazoles as Efficient Directing Groups in Iron-Catalyzed C–H Activation

As discussed in Section 1.2, early reports in the field of C−H bond activation primarily concentrated on nondirected C−H bond activation, often utilizing heteroaromatic compounds as substrates.[66] However, this strategy has some drawbacks, including a limited range of substrates, unpredictable reactivity, poor site-selectivity, and the need for high catalyst loadings. Consequently, recent research has shifted towards directed C−H bond activation to address these issues. In this context, both monodentate and bidentate directing groups have been employed for assistance.[67] The preference for bidentate directing groups over monodentate ones is due to their easier metal coordination and adjustable coordinating properties, leading to their increased application in C−H bond activation. In 2005, Daugulis firstly introduced the quinolinamide and picolinamide bidentate directing groups for the palladium catalyzed *ortho* arylation of C(sp^2)−H and C(sp^3)−H bonds of amides.[44] These *N*-heterocycles used as directing groups, contain a coordinating N(sp^2) atom. The other coordinating site involves an NH group, which acts as an anionic coordinating site after deprotonation. The coordination of both an N(sp^2) atom and an anionic N(sp^3) atom to the metal center makes these *N*,*N*-bidentate directing group highly effective as chelating systems. Since this discovery of bidentate directing group-assisted C−H bond functionalizations, numerous studies have been published on this approach.[43a] Selecting the right bidentate directing group and appropriate metal catalysts is crucial to achieve specific functionalizations. Among the *N*,*N*-bidentate auxiliaries, the well-known ones include quinoline-based 8-aminoquinoline (Q), pyridine-based picolinamide (Pico), 2-pyridylisopropylamine (PIP)-derived amides, pyridine-2-sulfonamide (PyS), oxazoline-based amides; pyrazole-based amides; and triazole-based amides. Notably, all these directing groups function as monoanionic chelating systems.

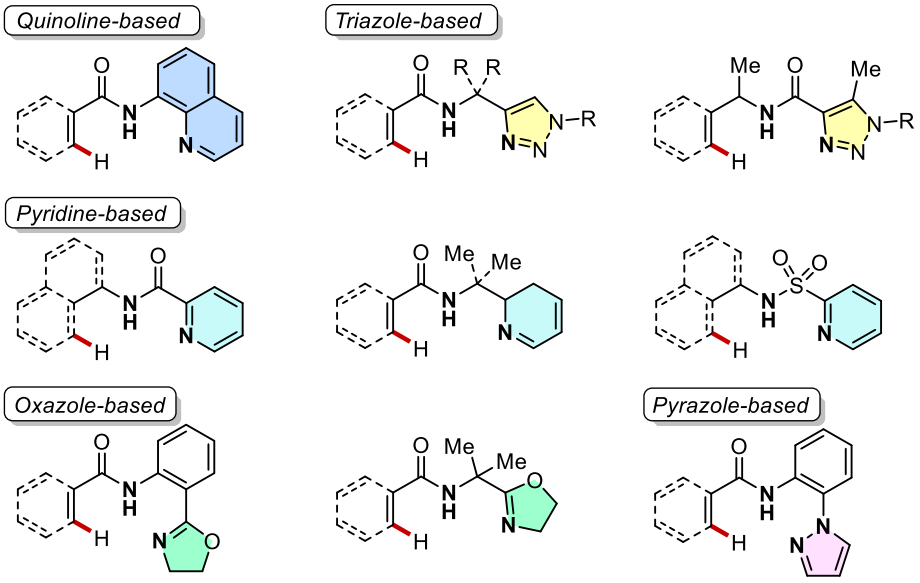

Scheme 1.31 *N,N*-bidentate directing groups.

As demonstrated by the numerous examples discussed previously (Section 1.3 Iron catalyzed C−H functionalizations), the 8-aminoquinoline directing group is predominant in the landscape of iron-catalyzed C−H activation reactions. However, despite its straightforward incorporation into target substrates, the Q auxiliary is limited by its restricted capacity for structural modifications and its often-difficult removal from the final products. Furthermore, its use in C−H activation reactions is often compromised by poor chemo-selectivity, which frequently leads to unwanted functionalizations of its aromatic ring.[68]

As a result of extensive research into the use of 1,2,3-triazole directing groups for C–H functionalizations,[69] in 2014 Ackermann firstly reported the use of a triazole-based directing group (TAM) in the Fe-catalyzed *ortho*-C−H arylation of aromatic and aliphatic amides with aryl Grignard reagents.[51] The straightforward and modular synthesis of triazoles is a significant advantage that has been exploited for the construction of a diverse family of 1,2,3-triazole-based directing groups including triazolyldimethylmethyl-amine (TAM), triazolyldihydrogenmethyl-amine (TAH) and trisubstituted triazole (TST). The modular forms of 1,2,3-triazoles can be synthetized *via* copper-catalyzed [3 + 2] cycloaddition between various substituted alkynes and organic azides that occurs under mild conditions, with excellent yields and complete regioselectivity.[70] Thus, the introduction of modular triazole-based bidentate directing groups paved the way for broader applications of iron catalyzed C−H functionalizations.[42 a, b]

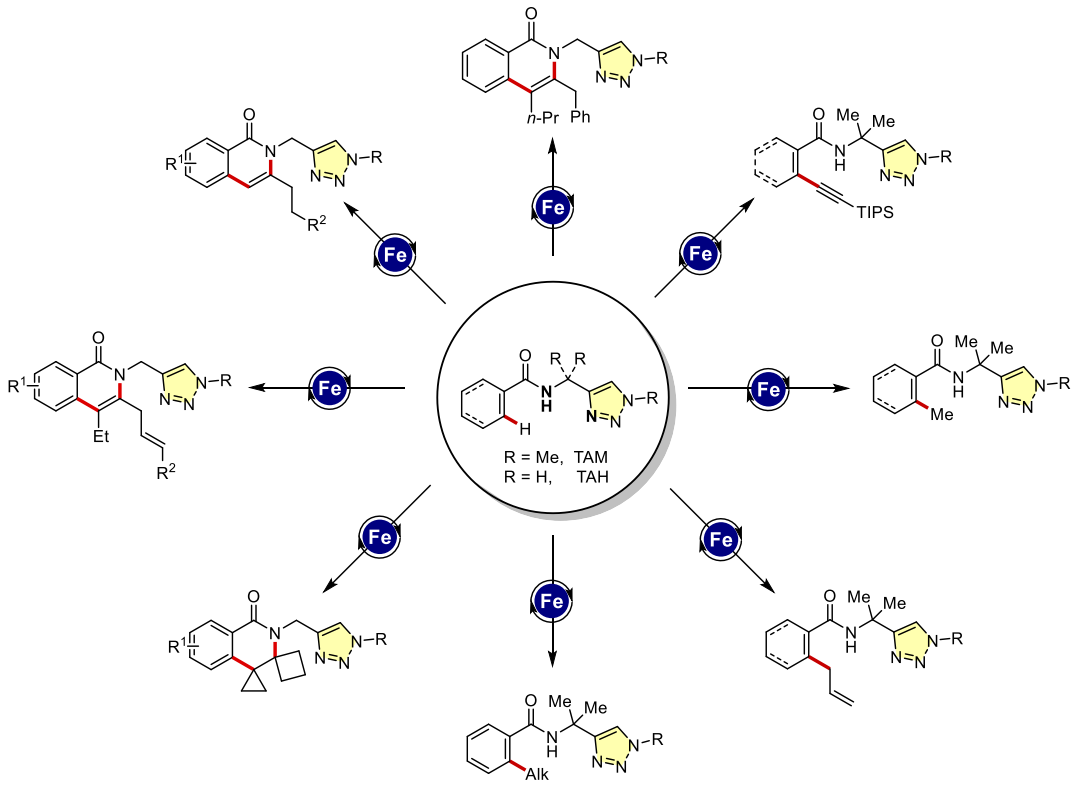

Scheme 1.32 Iron catalyzed C−H functionalizations enabled by 1,2,3-triazoles.

Although triazole is often regarded merely as a surrogate for 8-aminoquinoline or other *N*,*N*-bidentate groups, it has demonstrated the ability to promote various and different types of reactivity in iron-catalyzed C−H activation reactions. Furthermore, innovative mild methods have been developed for the efficient removal of this directing group. These methods circumvent the need for harsh acidic conditions and include techniques such as electrochemical deprotection. [63, 71] The availability of multiple synthetic methods for the removal of the triazole auxiliary increases the synthetic utility of this directing group, further promoting its application in the formation of new C−C and C−Heteroatom bonds. Therefore, research aimed at developing new iron-catalyzed C−H activation methodologies that leverage the assistance of this important directing group is crucial.

1.5 Objectives

Carbon–carbon bond (C–C) formation is a fundamental and essential process of modern organic synthesis. Alkylation reactions are particularly significant for C–C bond formation and are widely used in the synthesis of various compounds.[72] Over the past three decades, transition metal catalyzed C–H alkylation with traditional alkylation reagents, manly halides, has become a crucial method for the synthesis of complex molecules.[73] A significant advantage is represented by the direct addition of unactivated unsaturated compounds to C–H bond *via* an hydroarylation reaction to achieve alkylation reactions.[74] In fact, unsaturated compounds like alkenes and alkynes present several appealing advantages over traditional alkylation reagents. The alkylation reactions involving these compounds are typically free of by-products, with a perfect atom economy of the process since all the atoms from the substrates are ultimately incorporated in the products. Additionally, they are generally more cost-effective and readily available compared to their alkyl halide counterparts. Furthermore, using olefins can streamline syntheses, as many primary alkyl halides or sulfonates are ultimately synthesized from olefins.[2b, 75]

Even though there has been significant progress in iron catalyzed directed C–H alkylations alkylation, allylation and alkynylation using tosylate, mesylate and halides electrophiles coupling partner,[60, 61, 62, 63] the portfolio of direct C–H hydroarylation of unsaturated compounds is still quite restricted.[76] Therefore, there is a strong need to develop novel methods for site-selective iron catalyzed C–H functionalizations using readily available alkenes. In the first project we aimed to investigate the modular reactivity of the triazole directing group, in the iron-catalyzed C–H hydroarylation with olefins.

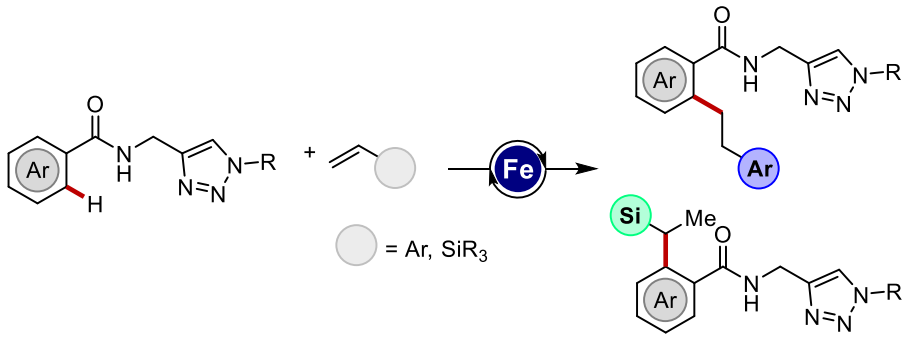

Scheme 1.33 Triazole-enabled, iron-catalyzed linear/branched selective C–H alkylations with alkenes.

Despite significant progress in organometallic iron-catalyzed C−H activations, the range of chemical transformations facilitated by this metal remains relatively limited, so the pursuit of new reactions is always encouraged. In the second project, we aimed to combine our aspiration to

explore the reactivity of unsaturated compounds with the goal of discovering new reactions in chelate-assisted iron catalyzed C–H functionalizations.

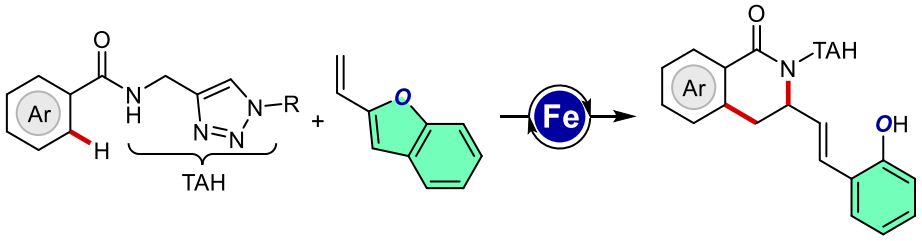

Scheme 1.34 Iron catalyzed C-H alkylation/ring opening with vinylbenzofurans enabled by triazoles.

Finally, within the purpose of utilizing unsaturated compounds, we envisioned to exploit the reactivity of allenes as versatile building blocks capable of enabling various types of C–H functionalizations. Specifically, the advantages of using these compounds were combined with the goal of achieving stereoselective synthesis of *Z*-olefins, which are directly produced by the insertion of allenes into C(sp^2)–H bonds promoted by iron catalysis.

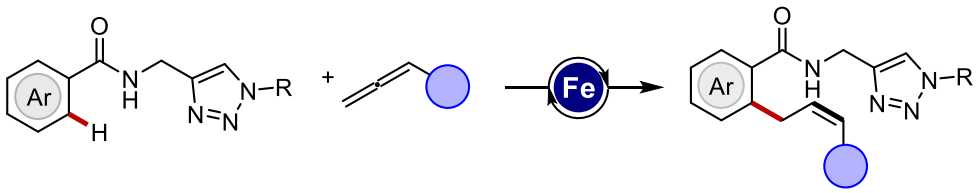

Scheme 1.35 *Z*-selective iron catalyzed C–H alkylation with allenes.

The experimental work for the projects discussed in Chapters 2, 3, and 4 of this thesis was conducted entirely at the University of Parma. The computational calculations presented in Chapter 3 were performed in collaboration with Professor Ackermann's research group. The research detailed in Chapter 5 and Chapter 6 was conducted during a six-month visiting stay in Professor Ackermann's group. The research work carried out during the six-month period at the Chiesi Farmaceutici laboratories is not included in this thesis due to intellectual property restrictions.

1.6 References

[1] C. R. H. Hale, C. Nilewskia, H. A. Ioannidou, K. C. Nicolaou, *Chem. Soc.Rev*. **2012**, *41*, 5185–5238.

[2] a) J. D. Hayler, D. K. Leahy, E. M. Simmons, *Organometallics* **2019**, *38*, 36−46; b) B. M. Trost, *Science* **1991**, *254*, 1471−1477; c) B. M. Trost, *Angew. Chem. Int. Ed.* **1995**, *34*, 259−281; d) B. M. Trost, *Science* **1983**, *219*, 245–250.

[3] R. A. Sheldon, *Green Chem.*, **2023**, *25*, 1704–1728.

[4] a) P. Anastas, N. Eghbali, *Chem. Soc. Rev*. **2010**, *39*, 301–312; b) P. T. Anastas, J. C. Warner, Green chemistry: theory and practice, Oxford University Press, Oxford [England], **1998**; c) P. T. Anastas, J. J. Breen, *Clean. Prod.* **1997**, *5*, 97–102.

[5] a) L. Ackermann, S.-L. You, M. Oestreich, S. Meng, D. MacFarlane, Y. Yin, *Trends Chem*. **2020**, *2*, 275–277; b) X. Zhang, M. Fevre, G. O. Jones, R. M. Waymouth, *Chem. Rev*. **2018**, *118*, 839–885; c) F. E. Celik, B. Peters, M.-O. Coppens, A. McCormick, R. F. Hicks, J. Ekerdt, *ACS Catal*. **2017**, *7*, 8628–8640.

[6] F. Mao, W. Ni, X. Xu, H. Wang, J. Wang, M. Ji, J. Li, *Molecules* **2016**, *21*, 75.

[7] a) A. Suzuki, *Angew. Chem. Int. Ed*. **2011**, *50*, 6722–6737; b) E. Negishi, *Angew. Chem. Int. Ed*. **2011**, *50*, 6738–6764; c) C. C. C. J. Seechurn, M. O. Kitching, T. J. Colacot, V. Snieckus, *Angew. Chem. Int. Ed*. **2012**, *51*, 5062–5085; d) P. Ruiz-Castillo, S. L. Buchwald, *Chem. Rev.* **2016**, *116*, 12564–12649; e) N. Miyaura, A. Suzuki, *Chem. Rev.* **1995**, *95*, 2457–2483.

[8] E. Negishi, Nobel Lecture, *Angew. Chem. Int. Ed*., **2011**, *50*, 6738–6764.

[9] a) R. G. Bergman, *Nature* **2007**, *446*, 391–393; b) T. Rogge, N. Kaplaneris, N. Chatani, J. Kim, S. Chang, B. Punji, L. L. Schafer, D. G. Musaev, J. Wencel-Delord, C. A. Roberts, R. Sarpong, Z. E. Wilson, M. A. Brimble, M. J. Johansson, L. Ackermann, *Nature Rev. Methods Primer* **2021**, *1*, 43; c) P. Gandeepan, T. Müller, D. Zell, G. Cera, S. Warratz, L. Ackermann, *Chem. Rev.* **2019**, *119*, 2192–2452; d) A. Dey, S. K. Sinha, T. K. Achar, D. Maiti, *Angew. Chem. Int. Ed*. **2019**, *58*, 10820–10843; e) Y. Park, Y. Kim, S. Chang, *Chem. Rev*. **2017**, *117*, 9247–9301; f) P. H. Dixneuf, H. Doucel, *C–H Bond Activation and Catalytic Functionalization II*, Springer International Publishing, Switzerland, **2016**; g) J. Yu, Z. Shi, *Acc. Chem. Res*. **2012**, *45*, 788–802; h) I. A. I. Mkhalid, J. H. Barnard, T. B. Marder, J. M. Murphy, J. F. Hartwig, *Chem. Rev*. **2010**, *110*, 890–931.

[10] a) J. Wencel-Delord, F. Glorius, *Nat. Chem*. **2013**, *5*, 369−375; b) T. Dalton, T. Faber, F. Glorius, *ACS Cent. Sci.* **2021**, *7*, 245–261.

[11] a) S. Rej, Y. Ano, N. Chatani, *Chem. Rev*. **2020**, *120*, 1788–1887; b) H. Yi, G. Zhang, H. Wang, Z. Huang, J. Wang, A. K. Singh, A. Lei, *Chem. Rev.* **2017**, *117*, 9016–9085. c) J. C. K. Chu, T. Rovis, *Angew. Chem. Int. Ed.* **2018**, *57*, 62–101.

[12] a) A. S. Goldman, K. I. Goldberg, *Activation and Functionalization of C–H Bonds*–ACS Symposium Series*,* 885, **2004**; b) K. M. Altus, J. A. Love, *Commun. Chem.* **2021**, *4*, 173.

[13] J. Kua, X. Xu, R. A. Periana, W. A. Goddard, *Organometallics* **2002**, *21*, 511– 525.

[14] a) M. E. Thompson, S. M. Baxter, A. R. Bulls, B. J. Burger, M. C. Nolan, B. D. Santarsiero, W. P. Schaefer, J. E. Bercaw, *J. Am. Chem. Soc.* **1987**, *109*, 1, 203–219; b) Z. Lin, *Coord. Chem. Rev.* **2007**, *251*, 2280–2291.

[15] D. Balcells, E. Clot, O. Eisenstein, *Chem. Rev.* **2010**, *110*, 749–823.

[16] a) T. R. Cundari, T. R. Klinckman, P. T. Wolczanski, *J. Am. Chem. Soc*. **2002**, *124*, 1481–1487; b) J. L. Bennett, P. T. Wolczanski, *J. Am. Chem. Soc.* **1997**, *119*, 10696–10719.

[17] a) L. Ackermann, *Chem. Rev*., **2011**, *111*, 1315–1345; b) L. Ackermann, *Acc. Chem. Res*. **2014**, *47*, 281–295.

[18] B. Biswas, M. Sugimoto, S. Sakaki, *Organometallics* **2000**, *19*, 3895–3908.

[19] a) S. I. Gorelsky, D. Lapointe, K. Fagnou, *J. Am. Chem. Soc.* **2008**, *130*, 10848– 10849; b) D. Lapointe, K. Fagnou, *Chem. Lett*., **2010**, *39*, 1118–1126.

[20] a) D. L. Davies, S. M. A. Donald, S. A. Macgregor, *J. Am. Chem. Soc*. **2005**, *127*, 13754–13755; b) Y. Boutadla, D. L. Davies, S. A. Macgregor, A. I. Poblador-Bahamonde, *Dalton Trans.* **2009**, 5887–5893.

[21] a) D. Zell, M. Bursch, V. Müller, S. Grimme, L. Ackermann, *Angew. Chem. Int. Ed*. **2017**, *56*, 10378–10382; b) W. Ma, R. Mei, G. Tenti, L. Ackermann, *Chem. Eur. J*. **2014**, *20*, 15248–15251.

[22] a) S. J. Blanksby, G. B. Ellison, *Acc. Chem. Res.*, **2003**, *36*, 255–263; b) X.-S. Xue, P. Ji, B. Zhou, J.-P. Cheng, *Chem. Rev.*, **2017**, *117*, 8622–8648.

[23] K. Shen, Y. Fu, J.-N. Li, L. Liu, Q.-X. Guo, *Tetrahedron* **2007**, *63*, 1568–1576.

[24] a) J. F. Hartwig*, Chem. Soc. Rev.,* **2011**, *40*, 1992–2002; b) C. Cheng, J. F. Hartwig, *Science*, **2014**, 343, 853–857.

[25] M. Zhang, Y. Zhang, X. Jie, H. Zhao, G. Li, W. Su, *Org. Chem. Front.*, **2014**, *1*, 843–895; b) C. Sambiagio, D. Schönbauer, R. Blieck, T. Dao-Huy, G. Pototschnig, P. Schaaf, T. Wiesinger, M. F. Zia, J. Wencel-Delord, T. Besset, B. U. W. Maes, M. Schnürch, *Chem. Soc. Rev.*, **2018**, *47*, 6603–6743.

[26] a) G. Rouquet, N. Chatani, *Angew. Chem. Int. Ed*. **2013**, *52*, 11726–11743; b) S. Rej, Y. Ano, N. Chatani, *Chem. Rev*. **2020**, *120*, 3, 1788–1887; c) O. Daugulis, J. Roane, L. D. Tran, *Acc. Chem. Res*. **2015**, *48*, 1053–1064.

[27] a) J. He, M. Wasa, K. S. L. Chan, Q. Shao, J.-Q. Yu, *Chem. Rev.* **2017**, *117*, 8754–8786; b) T. W. Lyons, M. S. Sanford, *Chem. Rev.* **2010**, *110*, 1147–1169.

[28] a) J. A. Leitch, C. G. Frost, *Chem. Soc. Rev.* **2017**, *46*, 7145–7153; b) P. B. Arockiam, C. Bruneau, P. H. Dixneuf, *Chem. Rev.* **2012**, *112*, 5879–5918.

[29] a) J. S. Wright, P. J. H. Scott, P. G. Steel, *Angew. Chem. Int. Ed*. **2021**, *60*, 2796–2821; b) Ł. Woźniak, J.-F. Tan, Q.-H. Nguyen, A. Madron du Vigné, V. Smal, Y.-X. Cao, N. Cramer, *Chem. Rev*. **2020**, *120*, 10516–10543.

[30] a) G. Song, F. Wang, X. Li, *Chem. Soc. Rev*. **2012**, *41*, 3651–3678; b) D. A. Colby, R. G. Bergman, J. A. Ellman, *Chem. Rev.* **2010**, *110*, 624–655.

[31] P. Gandeepan, T. Müller, D. Zell, G. Cera, S. Warratz, L. Ackermann, *Chem. Rev*. **2019**, *119*, 2192–2452.

[32] a) P. Enghag, *Encyclopedia of elements.* VCH, Weinheim, **2004**, p. 167; b) K. S. Egorova, V. P. Ananikov, *Angew. Chem. Int. Ed*. **2016**, *55*, 12150–12162.

[33] a) A. Fürstner, *ACS Cent. Sci*. **2016**, *2*, 778–789; b) A. Correa, O. Garcìa Mancheno, C. Bolm, *Chem. Soc. Rev.* **2008**, *37*, 1108; c) A. A. O. Sarhan, C. Bolm, *Chem. Soc. Rev*. **2009**, *38*, 2730; d) I. Bauer, H.-J. Knölker, *Chem. Rev*. **2015**, *115*, 3170–3387.

[34] a) M. Tamura, J. K. Kochi, *J. Am. Chem. Soc.* **1971**, *93*, 6, 1487–1489; b) S. M. Neumann, J. K. Kochi, *J. Org. Chem.* **1975**, *40*, 5, 599–606.

[35] G. Hata, H. Kondo, A. Miyake*, J. Am. Chem. Soc*. **1968**, *90*, 9, 2278–2281.

[36] a) D. H. R. Barton, D. Doller, *Acc. Chem. Res*. **1992**, *25*, 11, 504–512; b) J. W. Rahtke, E. L. Muetterties, *J. Am. Chem. Soc.* **1975**, *97*, 11, 3272–3273; c) M. V. Baker, L. D. Field, *J. Am. Chem. Soc*. **1987**, *109*, 9, 2825–2826.

[37] S. Camadanli, R. Beck, U. Flörke, H.-F Klein, *Organometallics* **2009**, *28*, 7, 2300–2310.

[38] W. D. Jones, G. P. Foster, J. M. Putinas, *J. Am. Chem. Soc*. **1987**, *109*, 5047−5048.

[39] N. Yoshikai, A. Matsumoto, J. Norinder, E. Nakamura, *Synlett* **2010**, *2*, 313−316.

[40] J. Norinder, A. Matsumoto, N. Yoshikai, E. Nakamura, *J. Am. Chem. Soc*. **2008**, *130*, 5858−5859.

[41] Y. Sun, H. Tang, K. Chen, L. Hu, J. Yao, S. Shaik, H. Chen, *J. Am. Chem. Soc.* **2016**, *138*, 11, 3715–3730.

[42] a) J. Mo, A. M. Messinis, J. Li, S. Warratz, L. Ackermann, *Acc. Chem. Res*. **2024**, *57*, 1, 10–22; b) M. Lanzi, G. Cera, *Molecules* **2020**, *25*, 1806; c) N. Yoshikai, *Isr. J. Chem*. **2017**, *57*, 1117–1130; d) R. Shang, L. Ilies, E. Nakamura, *Chem. Rev.* **2017**, *117*, 9086–9139; e) G. Pototschnig, N. Maulide, M. Schnürch, *Chem. Eur. J*. **2017**, *23*, 9206–9232; f) G. Cera, L. Ackermann, *Top. Curr. Chem*. **2016**, *374*, 57; g) C.-L. Sun, B.-J. Li, Z.-J. Shi, *Chem. Rev.* **2011**, *111*, 1293–1314; h) E. Nakamura, N. Yoshikai, *J. Org. Chem*. **2010**, *75*, 6061–6067.

[43] a) S. Rej, Y. Ano, N. Chatani, *Chem. Rev*. **2020**, *120*, 1788–1877; b) G. Rouquet, N. Chatani, *Angew. Chem. Int. Ed.* **2013**, *52*, 11726 – 11743.

[44] V. G. Zaitsev, D. Shabashov, O. Daugulis, *J. Am. Chem. Soc*. **2005**, *127*, 13154–13155.

[45] H. H. Al Mamari, E. Diers, L. Ackermann, *Chem. Eur. J*. **2014**, *20*, 9739–9743.

[46] N. Yoshikai, A. Matsumoto, J. Norinder, E. Nakamura, *Angew. Chem. Int. Ed*. **2009**, *48*, 2925 –2928.

[47] L. Ilies, E. Konno, Q. Chen, E. Nakamura, *Asian J. Org. Chem*. **2012**, *1*, 142 – 145.

[48] R. Shang, L. Ilies, A. Matsumoto, E. Nakamura, *J. Am. Chem. Soc.* **2013**, *135*, 16, 6030–6032.

[49] R. Shang, L. Ilies, S. Asako, E. Nakamura, *J. Am. Chem. Soc*. **2014**, *136*, 14349−1435.

[50] L. S. Fitzgerald, M. L. O'Duill, *Chem. Eur. J.* **2021**, *27*, 8411–8436.

[51] Q. Gu, H. H. Al Mamari, K. Graczyk, E. Diers, L. Ackermann, *Angew. Chem. Int. Ed*. **2014**, *53*, 3868–3871.

[52] L. Ilies, S. Ichikawa, S. Asako, T. Matsubara, E. Nakamura, *Adv. Synth. Catal.* **2015**, *357*, 2175–2179.

[53] R. Shang, L. Ilies, E. Nakamura, *J. Am. Chem. Soc.* **2015**, *137*, 24, 7660–7663.

[54] K. Graczyk, T. Haven, L. Ackermann, *Chem. Eur. J*. **2015**, *21*, 8812–8815.

[55] Z. Shen, G. Cera, T. Haven, L. Ackermann, *Org. Lett*. **2017**, *19*, 14, 3795–3798.

[56] T. E. Boddie, S. H. Carpenter, T. M. Baker, J. C. DeMuth, G. Cera, W. W. Brennessel, L. Ackermann, M. L. Neidig, *J. Am. Chem. Soc.* **2019**, *141*, 31, 12338–12345.

[57] T. Doba, T. Matsubara, L. Ilies, R. Shang, E. Nakamura, *Nat. Catal*. **2019**, *2*, 400–406.

[58] S. Asako, L. Ilies, E. Nakamura, *J. Am. Chem. Soc*. **2013**, *135*, 17755−17757.

[59] S. Rana, J. P. Biswas, S. Paul, An. Paika, D. Maiti, *Chem. Soc. Rev*. **2021**, *50*, 243−472.

[60] L. Ilies, T. Matsubara, S. Ichikawa, S. Asako, E. Nakamura, *J. Am. Chem. Soc*. **2014**, *136*, 38, 13126–13129.

[61] E. R. Fruchey, B. M. Monks, S. P. Cook, *J. Am. Chem. Soc*. **2014**, *136*, 38, 13130–13133.

[62] B. M. Monks, E. R. Fruchey, S. P. Cook, *Angew. Chem. Int. Ed*. **2014**, *53*, 11065–11069.

[63] G. Cera, T. Haven, L. Ackermann, *Angew. Chem. Int. Ed*. **2016**, *55*, 1484–1488.

[64] G. Cera, T. Haven, L. Ackermann, *Chem. Eur. J.* **2017**, *23*, 3577–3582.

[65] S. Cattani, G. Cera, *Chem Asian J*. **2024**, *19*, e202300897.

[66] a) K. R. Campos, *Chem. Soc. Rev*. **2007**, *36*, 1069−1084; b) J. F: Hartwig, M. A. Larsen, *ACS Cent. Sci*. **2016**, *2*, 281−292. c) S.-M. Wong, F.-Y. Kwong, *Strategies for Palladium-Catalyzed Non-Directed and Directed C−H Bond Functionalization*; A. R. Kapdi, D. Maiti, Elsevier: New York, 2017; pp 49−166.

[67] K. Murali, L. A. Machado, R. L. Carvalho, L. F. Pedrosa, R. Mukherjee, E. N. Da Silva Júnior, D. Maiti, *Chem. Eur. J*. **2021**, 27, 12453–12508.

[68] Z. Xu, X. Yang, S.-F. Yin, R. Qiu, *Top. Curr. Chem.* **2020**, *378*, 42.

[69] a) X. Ye, Z. He, T. Ahmed, K. Weise, N. G. Akhmedov, J. L. Petersen, X. Shi, *Chem. Sci.* **2013**, *4*, 3712–3716; b) H. H. Al Mamari, E. Diers, L. Ackermann, *Chem. Eur. J.* **2014**, *20*, 9739–9743.

[70] R. Huisgen, *Angew. Chem. Int. Ed*. **1963**, *2*, 565–598; b) R. Huisgen, *Angew. Chem. Int. Ed.* **1963**, *2*, 633–645.

[71] a) J. Mo, A. M. Messinis, J. C. A. Oliveira, S. Demeshko, F. Meyer, L. Ackermann, *ACS Catal.* **2021**, *11*, 3, 1053–1064; b) J. Mo, T. Müller, J. C. A. Oliveira, S. Demeshko, F. Meyer, L. Ackermann, *Angew. Chem. Int. Ed*. **2019**, *58*, 12874–12878.

[72] J. H. Docherty, T. M. Lister, G. Mcarthur, M. T. Findlay, P. Domingo-Legarda, J. Kenyon, S. Choudhary I. Larrosa, *Chem. Rev*. **2023**, *123*, 12, 7692–7760.

[73] a) S. B. Ankade, A. B. Shabade, V. Soni, B. Punji, *ACS Catal*. **2021**, *11*, 6, 3268–3292; b) L. Ackermann, *Chem. Commun.*, **2010**, *46*, 4866−4877.

[74] a) Z. Dong, Z. Ren, S. J. Thompson, Y. Xu, G. Dong, *Chem. Rev*. **2017**, *117*, 13, 9333–9403; b) F. Kakiuchi, S. Murai, *Acc. Chem. Res*. **2002**, *35*, 10, 826–834.

[75] a) T. Newhouse, P. S. Baran, R. W. Hoffmann, *Chem. Soc. Rev.* **2009**, *38*, 3010–3021; b) T. Ren, M. Patel, K. Blok, *Energy* **2006**, *31*, 425−451.

[76] a) N. Kimura, S. Katta, Y. Kitazawa, T. Kochi, F. Kakiuchi, *J. Am. Chem. Soc*. **2021**, *143*, 12, 4543–4549; b) A. M. Messinis, L. H. Finger, L. Hu, L. Ackermann, *J. Am. Chem. Soc*. **2020**, *142*, 30, 13102–13111; c) L. Ilies, Y. Zhou, H. Yang, T. Matsubara, R. Shang, E. Nakamura, *ACS Catal*. **2018**, *8*, 12, 11478–11482; d) M. Y. Wong, T. Yamakawa, N. Yoshikai, *Org. Lett*. **2015**, *17*, 3, 442–445; e) N. Kimura, T. Kochi, F. Kakiuchi, *J. Am. Chem. Soc*. **2017**, *139*, 42, 14849–14852.

2. Triazole-enabled, Iron-catalyzed Linear/Branched Selective C–H Alkylations with Alkenes

From this chapter:

S. Cattani, A. Secchi, L. Ackermann, G. Cera, *Org Biomol Chem*. **2023**, *21*, 1264–1269.

2.1 Introduction

2.1.1 Iron-Catalyzed C–H Alkylations with Alkenes

In recent years, 3d-transition metal catalysed C–H functionalizations has gained importance as a sustainable alternative to the traditionally used, but often toxic and costly, 4d and 5d transition metals.[1] Among these, iron catalysts stand out as a particularly advantageous alternative, being non-toxic, affordable, and naturally abundant.[2] Among the various strategies for C–H functionalization, direct C–H alkylations with readily available feedstocks like alkenes[3] stand out as a highly effective method for producing alkylarene derivatives. Originally developed by Lewis and Smith[4] and subsequently advanced by Murai with ruthenium catalysts[5] (Scheme 2.1, a), this approach has recently been extended to 3d metals such as nickel and cobalt.[6] Iron catalysts have also been effective in facilitating these transformations, particularly when used with ketones[7] or imines[8] as low-valent iron species (Scheme 2.1, b).

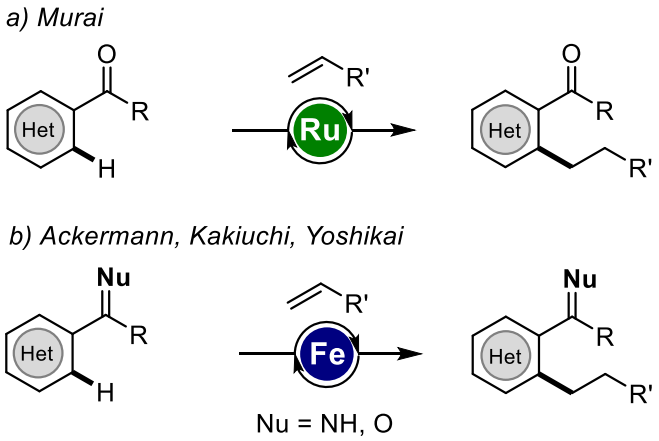

Scheme 2.1 Transition metals catalyzed C–H alkylations with alkenes.

The report made by Yoshikai and co-workers in 2015 represents the first example of iron-catalyzed hydroarylation involving directed C−H activation (Scheme 2.2).[8b] These reactions occur with vinylarenes and internal alkynes, respectively, through imine-directed C−H activation at the C2-position of indole substrates **I**. The catalytic system requires the use of an N-heterocyclic carbene as the ligand, an iron(III) salt and a Grignard reagent. The reaction facilitates alkylation and alkenylation reactions at the C2-position of indole. The reaction with olefins proceeds with complete Markovnikov selectivity delivering the branched alkylated products **IV**. When alkynes are employed as reaction partners, the *E*-hydroarilation products **V** are obtained with high levels of stereoselectivity.

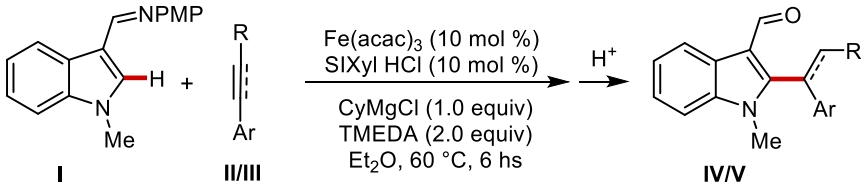

Scheme 2.2 Imine-directed iron catalyzed C–H alkylation of indoles with olefins and alkynes.

Following pioneering studies, where stoichiometric reactions involving the oxidative addition of C−H bonds to low-valent iron complexes have been described,[9] in 2017 Kakiuchi extended the iron catalyzed C−H alkylation with alkenes to aromatic ketones **VI** developing a simple reaction protocol that proceeds in the presence of only a $Fe(PMe_3)_4$ catalyst.[7d] The key features of this new C−H/olefin coupling are the complete anti-Markovnikov selectivity in the products **VIII** and the possibility to employ a wide array of differently functionalized olefins (Scheme 2.3).

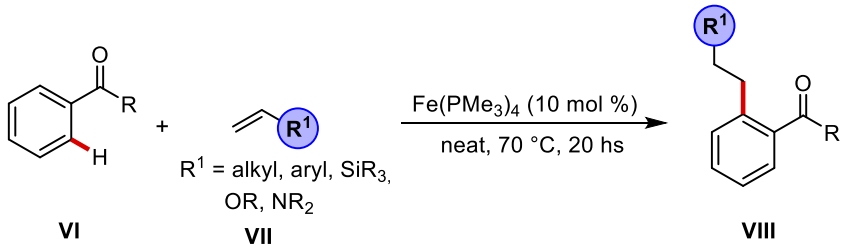

Scheme 2.3 Ketone-directed iron catalyzed C–H alkylation of aromatic ketones with olefins.

This method has the advantage of not requiring the introduction of a specially designed directing group, as the weakly coordinating oxygen in the carbonyl group is sufficient to promote the desired transformation. However, this protocol present significant limitations in terms of substrate scope of the aromatic ketones **VI**.

Additionally, iron-catalyzed C–H alkylations with alkyl halides have been found successful in functionalizing carboxylic acid derivatives like benzamides, utilizing bidentate directing groups.[10] More recently, to address the limitations related to the use of halides, iron-catalyzed C–H alkylations *via* carbometalation of alkenes have been developed by Nakamura's group (Scheme 2.4).[11] This method has enabled the hydroarylation of specific vinylarenes and vinylsilanes with complete anti-Markovnikov selectivity thanks to the aid of the bidentate 8-aminoquinoline (Q) directing group.

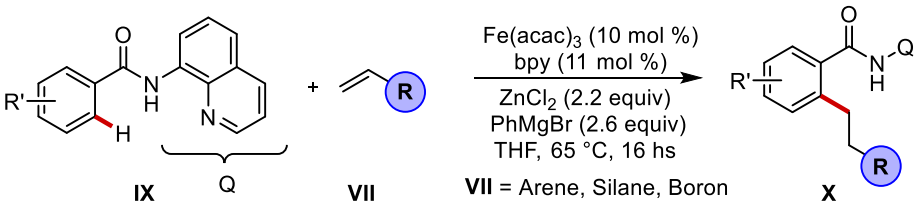

Scheme 2.4 Q-assisted iron-catalyzed C–H alkylation with olefins.

The authors propose a reaction mechanism that differs from the Murai-type reaction.[12] In the latter case, the ruthenium-catalyzed C–H/olefin coupling proceeds with the initial O-coordination of the ketone that promotes the C–H bond cleavage by the ruthenium complex $RuH_2(CO)(PPh_3)_3$, to give the ruthenium-hydride (Ru–H) species **Int1**. Afterwards, the complexation of the olefin and the addition of the Ru–H bond to the double bond *via* hydrometallation delivers the alkylated intermediate **Int3,** containing the hydrogen atom of the substrate. Finally, this intermediate undergoes reductive elimination to yield the corresponding coupling product **VIII** (Scheme 2.5).

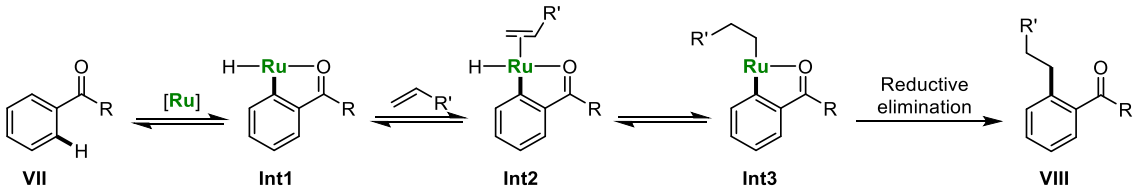

Scheme 2.5 Proposed mechanism for ruthenium-catalyzed C–H alkylation with olefins.

In contrast, in the iron-catalyzed C–H alkylation with alkenes, the cyclometalated intermediate **Int5** reacts with the olefin through a carbometalation process that leads to the installation of a 2-metalloalkyl chain at the *ortho* position of an aromatic or heteroaromatic carboxamide in **Int7**. The resulting alkyl zinc intermediate **Int8**, obtained after transmetalation, is stable and does not readily undergo demetalation; instead, it can be trapped by reaction with electrophiles such as HCl or allyl bromide (Scheme 2.6).

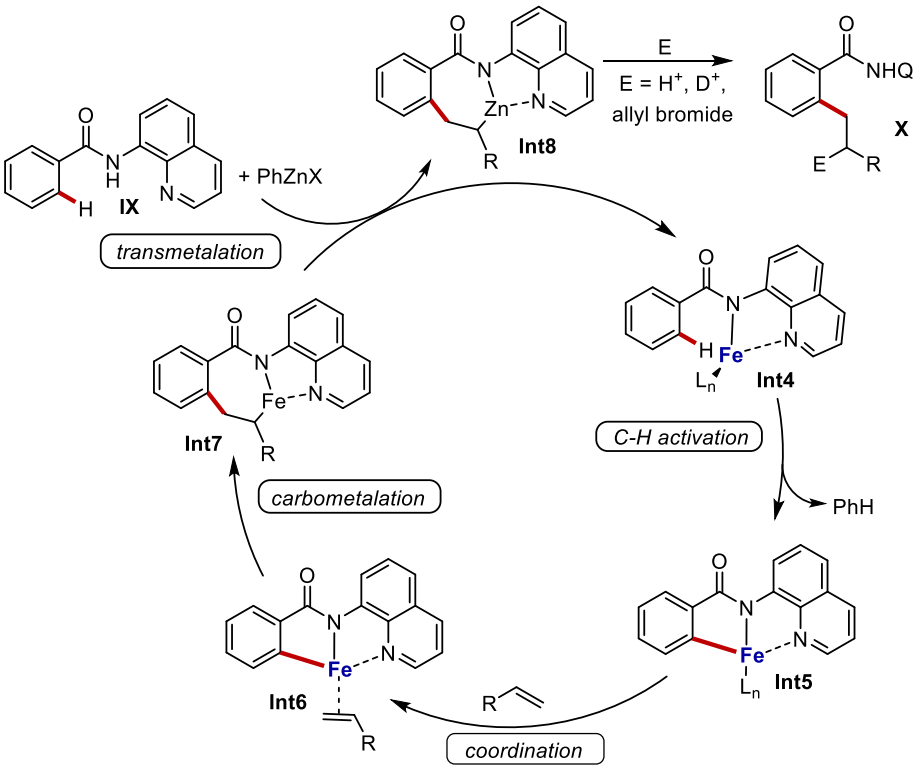

Scheme 2.6 Proposed mechanism for Q-assisted, iron-catalyzed C–H alkylation with olefins.

2.1.2 Triazole-based Directing Groups

Despite its widespread use in C–H functionalizations, the Q auxiliary has faced limitations due to its restricted potential for structural modifications and its often-difficult removal from the final products.[14] Triazoles, a versatile class of nitrogen heterocycles, are noteworthy for their modularity, accessibility, and bioactivity. The structural resemblance of triazoles to other functional groups allows for their incorporation into drug molecules, potentially enhancing bioactivity while replacing a peptide bond with a triazole can enhance peptide stability, making triazoles highly valuable in the development of peptidomimetics.[15]

Among these, the triazolyldimethylmethylamine (TAM) directing group has been particularly successful in C−H bond functionalizations with different metal catalysts. The development of this directing group for C−H bond functionalizations was primarily advanced by Shi and Ackermann.[16] Shi first reported the use of a triazole-based directing group in 2013 for Pd-catalyzed intramolecular cyclization and acetoxylation reactions, which involve C−Heteroatom bond formation.[16a] Following these groundbreaking works, the TAM directing group has been utilized in arylation, alkenylation, alkylation, allylation, alkynylation, and oxidative annulation reactions, as reported in the introduction of this thesis.

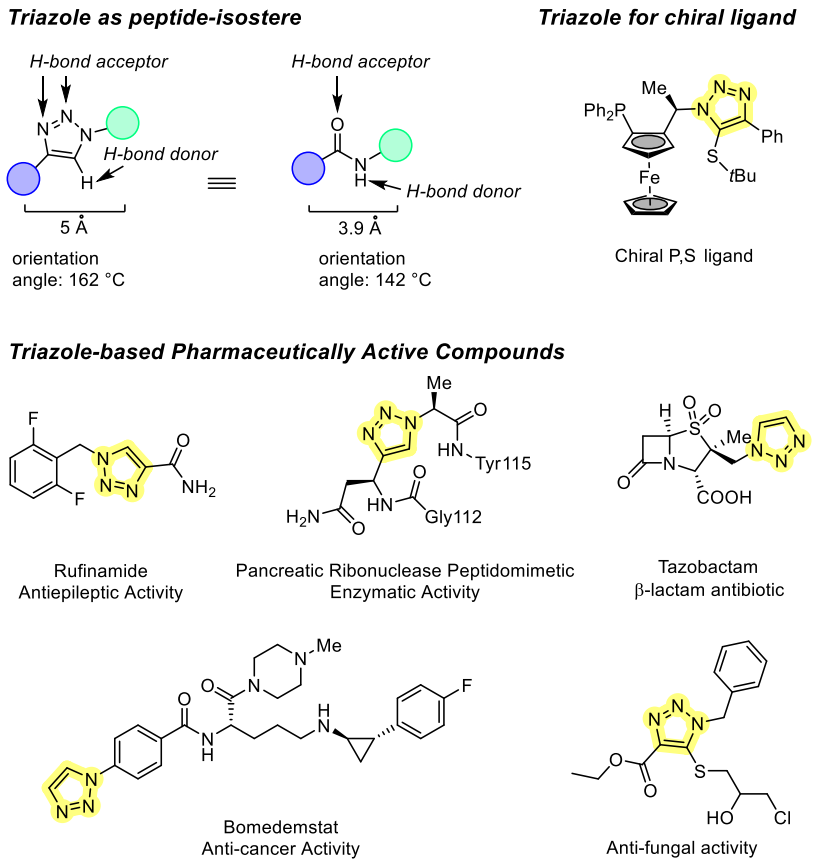

Scheme 2.7. Highly Modular 1,2,3-Triazoles.

2.2 Results and Discussion

Given the reported method that involves the use of 8-aminoquinoline as directing group, we envisioned to design a novel strategy for iron catalyzed alkene hydroarilation that exploits the modular and easily accessible triazole moiety. In this chapter we present a new strategy for iron-catalyzed C–H alkylations of benzamides with olefins enabled by *N*-triazole assistance. We disclosed a complementary reactivity with respect to the use of 8-aminoquinoline (Q), which enabled the synthesis of both linear and branched products, depending on the type of olefin used, with the same catalytic system.

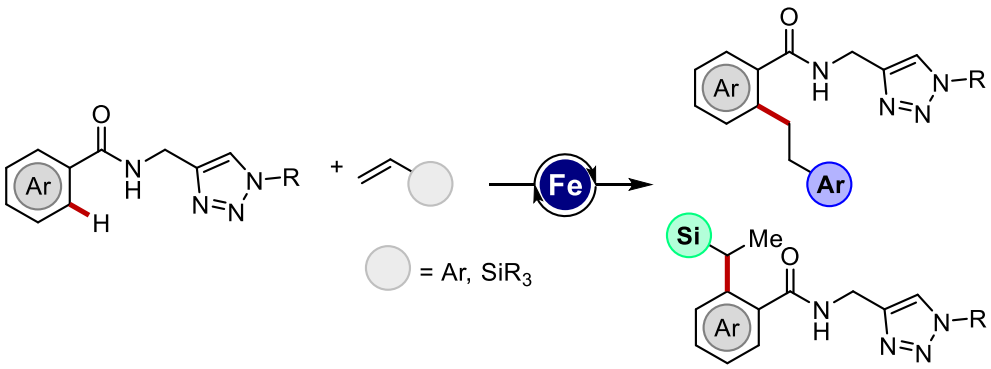

Scheme 2.8 Triazole-enabled, iron-catalyzed linear/branched selective C–H alkylations with alkenes.

2.2.1 Triazole-based Substrates

We started our investigation by probing different triazole-based directing groups for the iron-catalyzed C–H alkylations with alkenes. The desired substrates were prepared in a straightforward fashion starting from commercially available benzoic acids in two synthetic steps. One of them exploits the atom-economical "click" copper(I)-catalyzed 1,3-dipolar Huisgen cycloaddition between a propargylic amine derivative and an azide.[17]

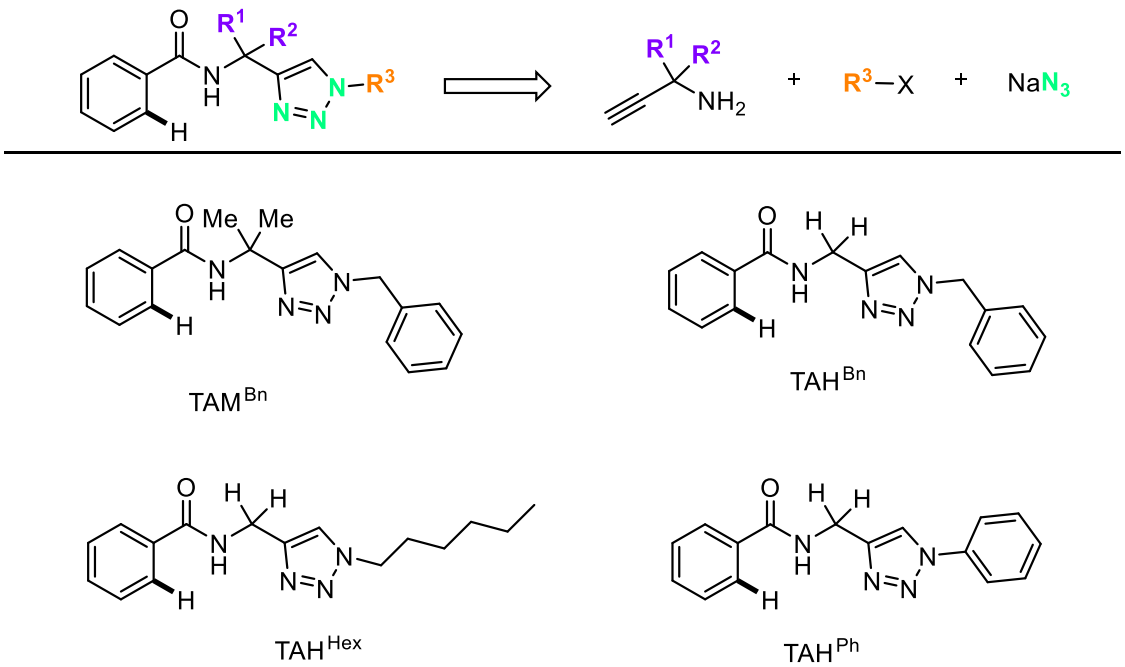

Scheme 2.9 Highly Modular 1,2,3-Triazole-based directing groups.

2.2.2 Optimization Studies

At first, we tested the triazolyldimethylmethyl (TAM) group (**1a**^{TAM}) which was previously found successful in alkylation and allylation reactions, among others.[18] The investigation began by probing the optimized conditions for the reaction reported by Nakamura[19] with the 8-aminoquinoline directing group that led to the isolation of our desired product **3aa**^{TAM} in 12% yield (Table 2.1, entry 1). Afterwards, we tested a series of bidentate ligands, both nitrogen and phosphine based, but none of them was found efficient in promoting the desired transformation (entries 3–6). Moreover, even the use of other zinc salts with or without the TMEDA as additive inhibited the reaction completely (entries 7–9). A small improvement in the isolated yield was registered only by increasing the catalyst and ligand loading up to 20% (entry 10).

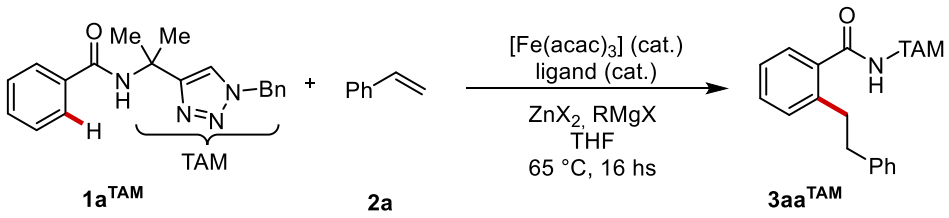

1a^{TAM} **2a** **3aa**^{TAM}

Entry[a]	Ligand	RMgX	ZnX_2	**3aa**^{TAM} (%)[b]
1	2,2'-bipy	PhMgBr	$ZnCl_2$TMEDA	18 (12)
2	2,2'-bipy	*i*-PrMgCl	$ZnBr_2$	n.d.
3	dppbz	PhMgBr	$ZnCl_2$TMEDA	n.d.
4	dppe	PhMgBr	$ZnCl_2$TMEDA	n.d.
5	1,10-phenantroline	PhMgBr	$ZnCl_2$TMEDA	n.d.
6	5,5'-dimetylbipy	PhMgBr	$ZnCl_2$TMEDA	n.d.
7	2,2'-bipy	PhMgBr	$ZnBr_2$TMEDA	n.d.
8	2,2'-bipy	PhMgBr	$ZnCl_2$	n.d.
9	2,2'-bipy	PhMgBr	$ZnBr_2$	n.d.
10	2,2'-bipy [c]	PhMgBr	$ZnBr_2$	25 (18)

[a]Reaction conditions: **1a** (0.2 mmol), **2a** (0.6 mmol), $Fe(acac)_3$ (0.03 mmol), ligand (0.03 mmol), RMgX (0.52 mmol), ZnX_2 (0.24 mmol), THF (0.5 mL). [b]Yields determined using 1,3,5-trimethoxybenzene as the internal standard. [c] $Fe(acac)_3$ (0.04 mmol), ligand (0.04 mmol). dppen = *cis*-1,2-bis(diphenylphosphino)ethylene, dppe = 1,2-bis(diphenylphosphino)ethane, dppbz = 1,2-bisdiphenylphosphinobenzene.

Table 2.1 Optimization of iron catalyzed C–H alkylation of benzamide **1a**^{TAM} with **2a**.

After this survey of reaction conditions, we thought that a modification of the geometry of the directing group could benefit the reaction outcome to afford satisfactory yields of the desired product. Given the limited results obtained with substrate **1a**$^{\mathbf{TAM}}$, we envisioned to employ the TAH directing group, without the *gem*-substitution on the methylene backbone, to evaluate the importance of the Thorpe-Ingold effect on the reaction.[20] We tested triazole amide **1a** in the proposed iron-catalyzed C–H hydroarylation, using styrene **2a** as the model reaction pattern. A 2,2'-bipyridine ligand, previously effective for the hydroarylation of Q-amide derivatives and to a lesser extent also of TAM derivative, did not cause any reactivity with complete recovery of the starting material. Employing a diphosphine ligand with a rigid backbone, such as dppbz, along with stoichiometric amounts of zinc salts and phenyl magnesium bromide, allowed the isolation of the desired product **3aa** in 38% yield, while also obtaining an *ortho*-arylated by-product **3aa′**. Notably, the inclusion of zinc salts was essential for promoting the desired reaction, with both $ZnBr_2$ and $ZnCl_2$ yielding comparable results (Table 2.2, entries 1–3). The use of TMEDA as an additive completely inhibited the catalytic activity (entries 4 and 5). Interestingly, both dppen and dppe proved to be optimal ligands for the transformation, producing **3aa** in good yields (entries 7 and 8). Specifically, the use of the less expensive dppe ligand became feasible by increasing the quantities of both PhMgBr and $ZnBr_2$, which enabled the isolation of **3aa** with greater efficiency (entry 9). The choice of the organometallic base in this catalytic system was crucial for achieving the desired reactivity. When *i*-PrMgBr was used as the additive, only small quantities of **3aa** were produced, and this occurred solely in the presence of dppen (entries 10 and 11).

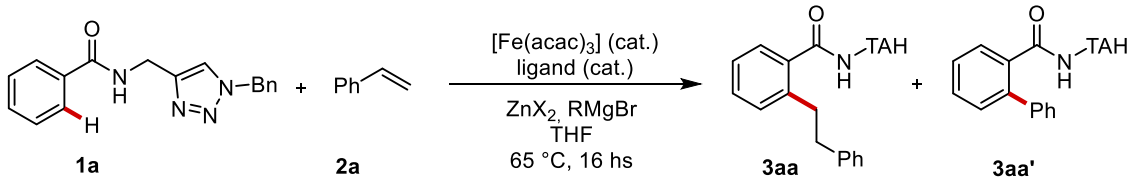

Entry[a]	Ligand	RMgBr	ZnX_2	**3aa** + **3aa'** (%)[b]
1	dppz	PhMgBr	$ZnBr_2$	44 (38) + 18
2	dppz	PhMgBr	$ZnCl_2$	37
3	dppz	PhMgBr	--	n.d.
4	dppz	PhMgBr	$ZnBr_2$TMEDA	n.d.
5	dppz	PhMgBr	$ZnCl_2$TMEDA	n.d.
6	2,2'-bipy	PhMgBr	$ZnBr_2$	n.d.
7	dppen	PhMgBr	$ZnBr_2$	77 (70) + 10
8	dppe	PhMgBr	$ZnBr_2$	68 (60) + 10
9[c]	dppe	PhMgBr	$ZnBr_2$	80 (71) + 7
10	dppen	*i*-PrMgBr	$ZnBr_2$	18
11	dppe	*i*-PrMgBr	$ZnBr_2$	n.d.

[a]Reaction conditions: **1a** (0.2 mmol), **2a** (0.6 mmol), $Fe(acac)_3$ (0.03 mmol), ligand (0.03 mmol), RMgBr (0.52 mmol), ZnX_2 (0.24 mmol), THF (0.5 mL). [b]Yields determined using 1,3,5-trimethoxybenzene as the internal standard. [c]PhMgBr (0.60 mmol), $ZnBr_2$ (0.40 mmol). In parenthesis, isolated yields.

Table 2.2 Optimization of iron catalyzed C–H alkylation of benzamide **1a** with styrene **2a**.

2.2.3 Substrate Scope

Under the optimized reaction conditions, we proceeded to investigate the scope of iron-catalyzed C–H alkylations (Scheme 2.10). A series of substituted vinylarenes **2** was subjected to iron catalysis. *para*-Substituted styrenes with both electron-donating groups (EDGs) and electron-withdrawing groups (EWGs) were well tolerated, yielding the corresponding products in moderate to good yields (**3ab**–**3ag**). Notably, a phosphine-substituted styrene **2h** also underwent the transformation, although with reduced yields of product **3ah**. Additionally, *meta*- and *ortho*-functionalized styrenes were examined, delivering alkylated benzamides **3ai**–**3ak** and **3bl**, which feature pharmacologically significant groups like the trifluoromethyl group and the naphthyl ring, among others. The method proved amenable for vinyl heteroarenes (**2m** and **2n**) and a vinyl ferrocenyl derivative as well, which delivered product **3ao**, albeit with a slightly lower yield.

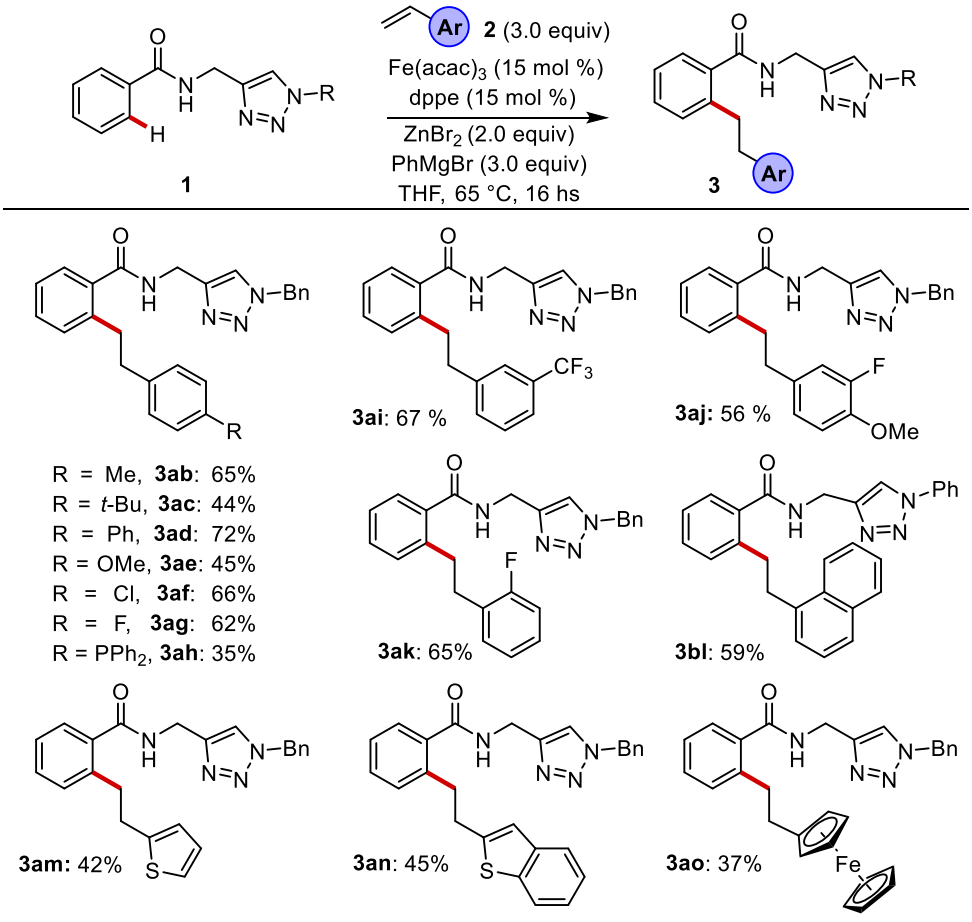

Scheme 2.10 Substrate scope of vinylarenes **2**.

We next explored the versatility of the method by submitting to the optimized catalytic conditions a family of differently decorated TAH benzamides. Different *N*-substitutions, as for amides **1b** and **1c**, were tolerated leading to the corresponding products in good yields. As for *para*- and *meta*- substituted TAH-benzamides **1d**–**1k**, the corresponding alkylated products **3da**–**3ka** were obtained in moderate to high yields both with electron donating and withdrawing groups. Notably, chloro and bromo substituent at the *para*-position **1g** and **1h** were efficiently converted in the desired products without any dehalogenation product being observed, proving the chemoselectivity of the reaction.

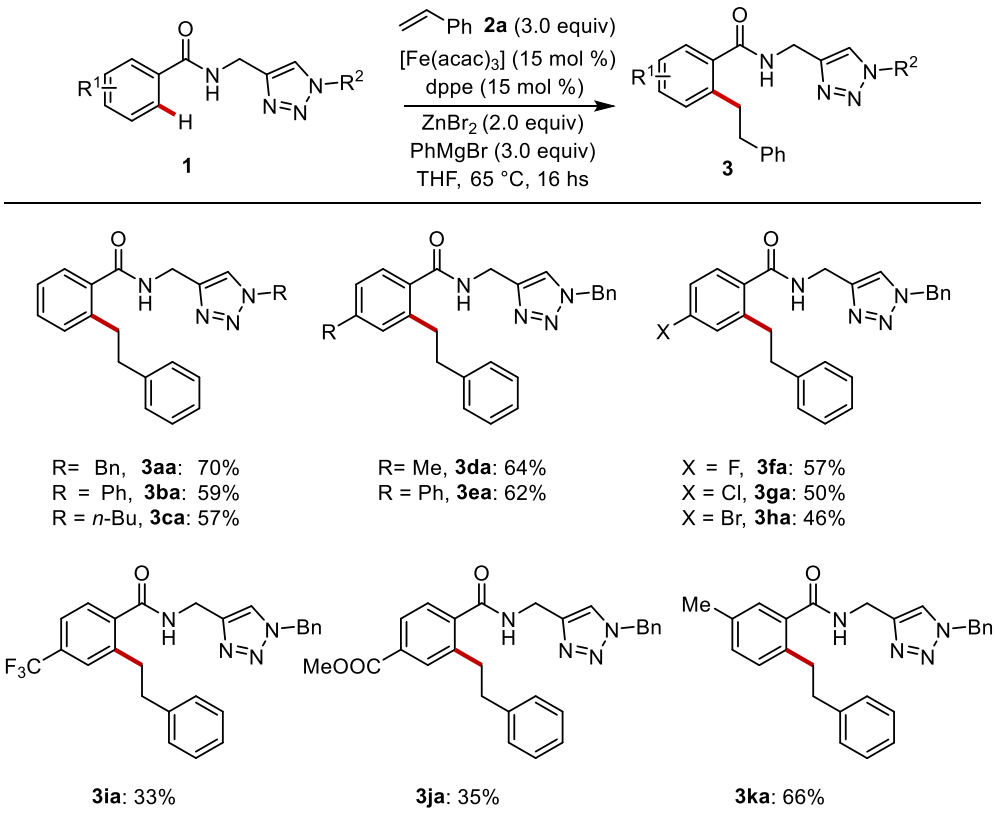

Scheme 2.11 Substrate scope of benzamides **2**.

Overall, our method displayed a good substrate scope and functional group tolerance, but we observed a poor reactivity of electronically deactivated and *ortho*-substituted benzamides above all. Furthermore, also more challenging substituted styrene derivatives were found unsuccessful in promoting the desired transformation. In particular, oxazolidinones, vinylpyridine and -OH protected derivatives failed to deliver the corresponding desired products (Scheme 2.12) under the optimized reaction conditions.

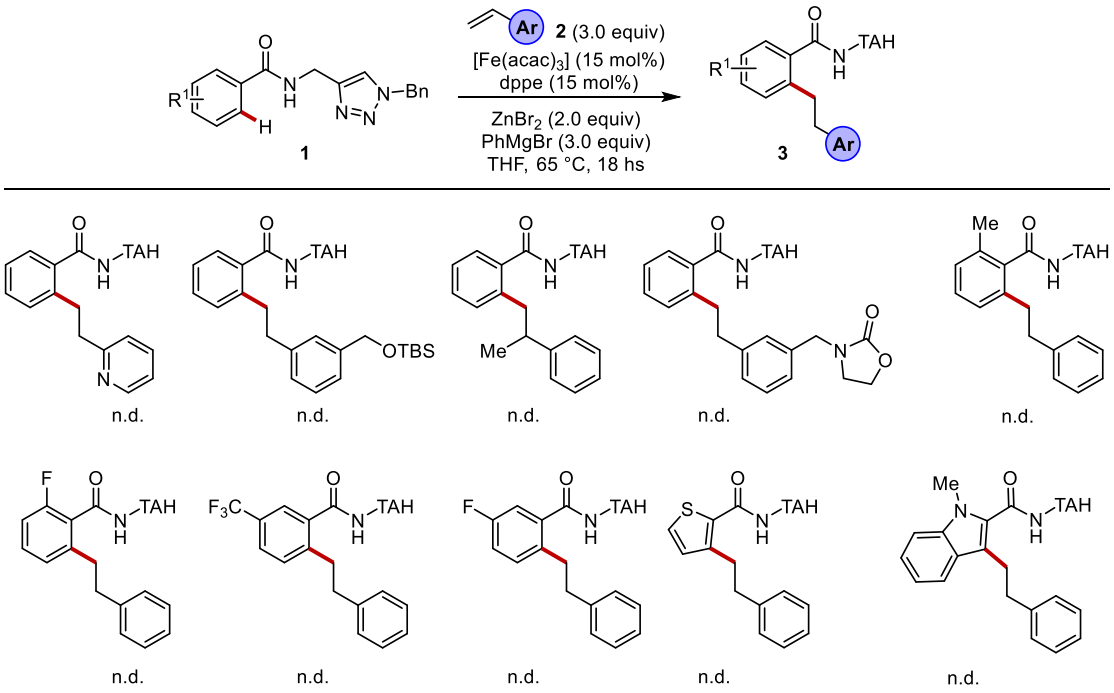

Scheme 2.12 Substrate scope limitations for C–H alkylation with vinylarenes.

Next, we investigated the reactivity of other types of alkenes among which vinylsilanes **4a** were found successful in promoting a unique reactivity in triazole-assisted iron catalyzed C–H alkylation. Here, only the branched alkylated product **5aa** was delivered when benzamide **1a** was submitted to the optimized catalytic conditions, albeit in low yield. For this reason, a brief optimization of the reaction parameters was conducted, and the use of the more electrophilic $ZnCl_2$ in place of $ZnBr_2$ was the key to achieve high yields (entry 4).

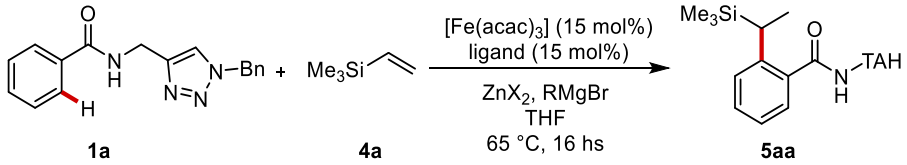

Entry[a]	Ligand	ZnX_2	**5aa** (%)[b]
1	dppen	$ZnBr_2$	25
2	dppe	$ZnBr_2$	53 (45)
3	dppe	$ZnCl_2$	73 (64)
4	dppe	--	n.d.

[a]Reaction conditions: **1a** (0.2 mmol), **4a** (0.6 mmol), $Fe(acac)_3$ (0.03 mmol), ligand (0.03 mmol), PhMgBr (0.6 mmol), ZnX_2 (0.4 mmol), THF (0.5 mL). [b]Yields determined using 1,3,5-trimethoxybenzene as the internal standard. In parenthesis, isolated yields.

Table 2.3 Variation of key parameters for iron-catalyzed C–H alkylation with vinylsilanes.

The substate scope was evaluated by submitting to the optimized reaction conditions a family of *meta*- and *para*-substituted benzamides to obtain the branched alkylated products **5** with moderate yields and functional group tolerance (Scheme 2.13). We observed that the nature of the substitution on the silyl group was crucial for achieving high regioselectivity and reactivity, as bulky substituents were generally not tolerated by the catalytic system. The best results in terms of regioselectivity were obtained with small R- groups on the silicon atom (**5aa**), while replacing a methyl substituent with a phenyl group resulted in a decreased selectivity (**5ac**).

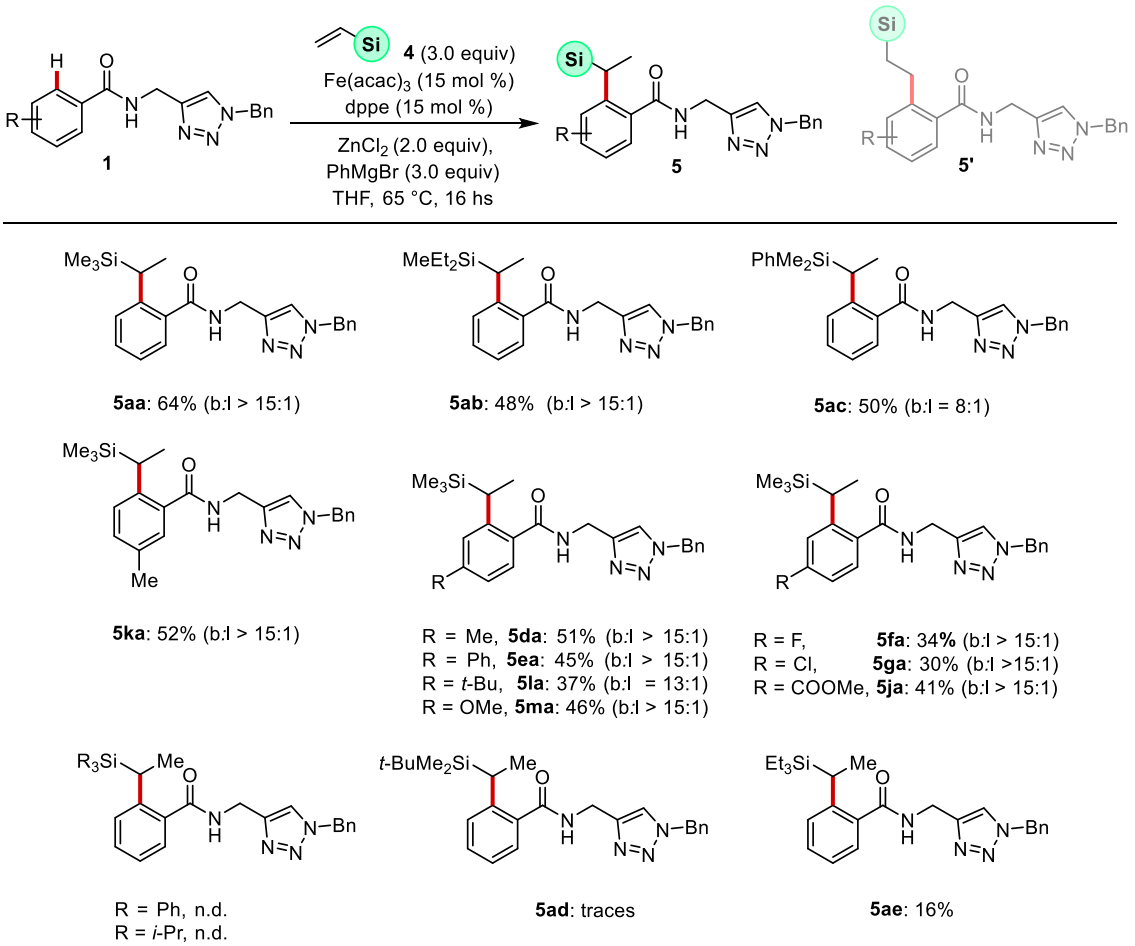

Scheme 2.13 Substrate scope and limitations of iron-catalyzed C–H alkylation with vinylsilanes **4**.

2.2.4 Mechanistic Investigation

Preliminary mechanistic experiments were conducted to gain insights into the reaction mechanism. Through inter- and intramolecular competition experiments with isotopically labelled compounds, we observed the absence of a primary isotopic effect, suggesting a facile C–H metalation step (Scheme 2.14 a, b). Additionally, model catalytic reactions using styrene **2a** and vinylsilane **4a** were quenched with DCl, leading to the selective labelling of the β-carbon of the alkyl chains in benzamides [D]-**3aa** and [D]-**5aa**, with 93% and 50% deuterium incorporation, respectively (Scheme 2.14 c, d). This supports the different structure of the proposed intermediates **Int3/Int3'** (Scheme 2.15) that derives from the nature of the alkenes employed in the transformation. These findings led us to hypothesize that a kinetically relevant carbometalation pathway is at play.[21]

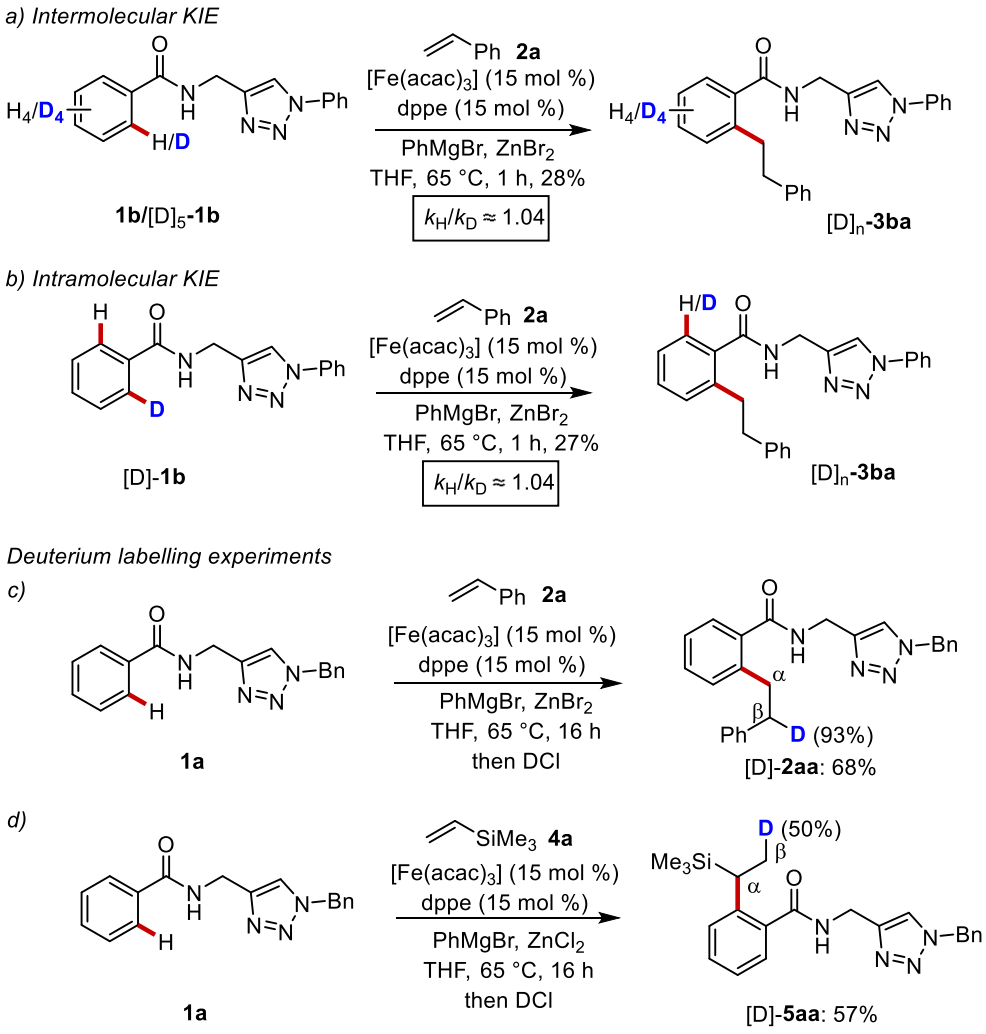

Scheme 2.14 Competition experiments and deuterium labelling.

2.2.5 Proposed Catalytic Cycle

Based on the mechanistic findings and prior research on the nature of iron-catalyzed C–H functionalization under bidentate assistance,[22] we propose a mechanism that begins with a facile C–H activation that from phenyliron(II) intermediate **Int1** delivers the cyclometalated species **Int2**. We propose that this step can occur *via* ligand-to-ligand hydrogen transfer (LLHT) or deprotonative σ-bond metathesis (DBM),[23] although a concerted oxidative addition cannot be excluded at this stage. Subsequently, coordination and product-determining carbometalation with alkenes **2** or **4** produce **Int3** or **Int3'**, where the site-selectivity of the carbon-iron bond is different depending on the nature of the alkene. After transmetalation with the arylzinc base, intermediate **Int3/Int3'** delivers the final product **3** or **5** and the active species of the catalyst, completing the catalytic cycle (Scheme 2.15).

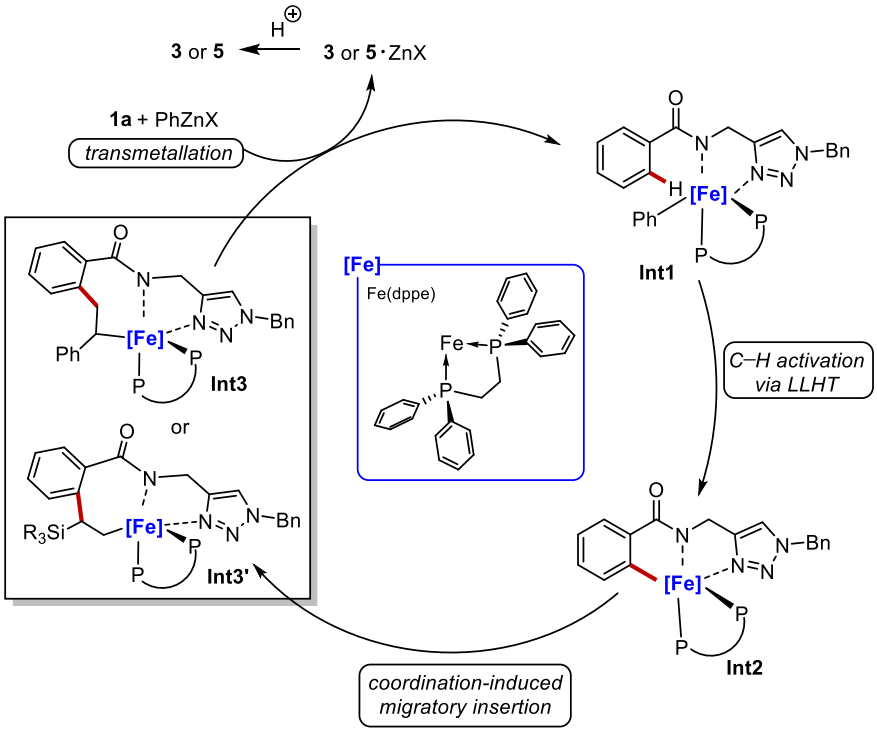

Scheme 2.15 Proposed catalytic cycle for iron-catalyzed C–H alkylation with alkenes.

2.2.6 Late-stage Diversifications

After a study on the key steps of the reaction mechanism, we further demonstrated the relevance of our new method by several late-stage synthetic manipulations of the *ortho*-alkylated products. We converted benzamide **3ah** into the corresponding phosphine gold(I) complex **6ah** in good yields (Scheme 2.16 a); while the C–Si bond in branched products, as for **5ea**, was transformed into a new C–C bond by a fluoride-mediated alkylation using benzaldehyde as the electrophile. Under these conditions, the protected alcohol **7ea** was synthesized in moderate yields as a mixture of diastereoisomers (Scheme 2.16 b). Lastly, we achieved the removal of the triazole directing group by means of acid hydrolysis to restore the carboxylic acid functional group on the aromatic ring (Scheme 2.16 c).

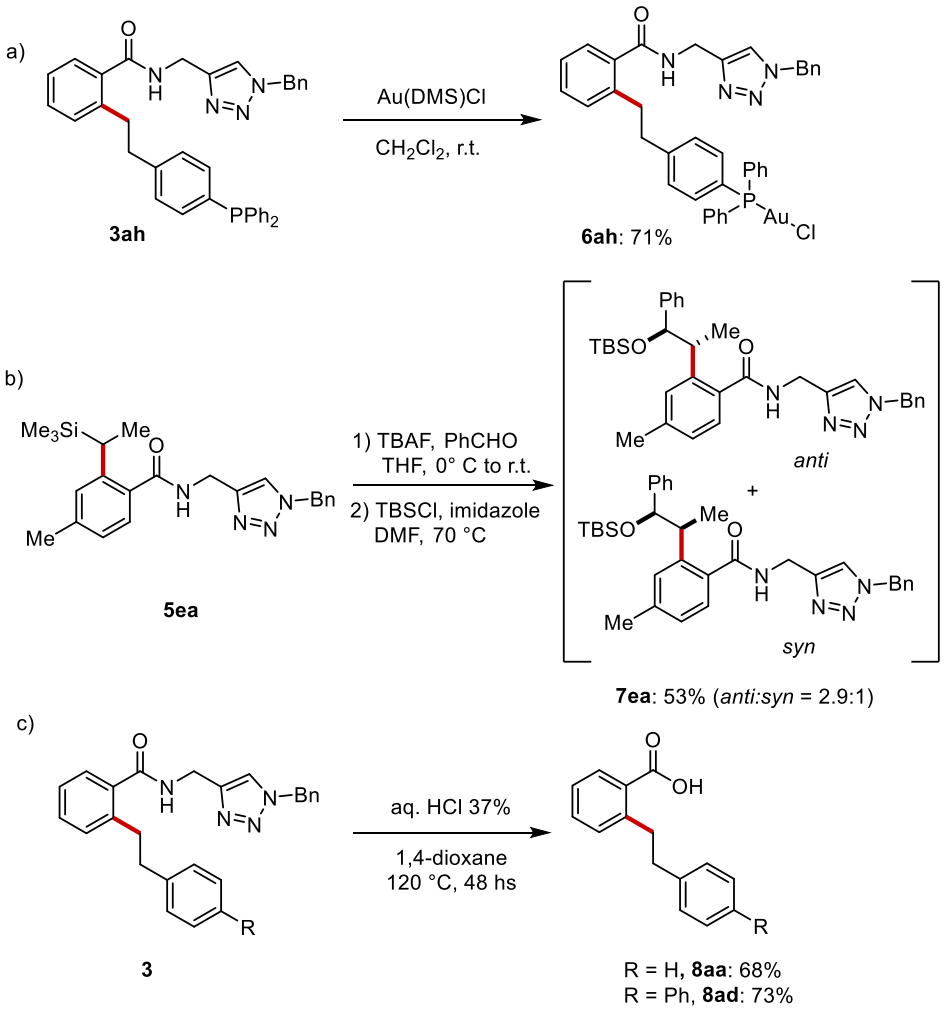

Scheme 2.16 Removal of directing group and late-stage manipulations of products.

2.3 Conclusions

In summary, in this section we presented a new method for iron-catalyzed C–H alkylation *via* carbometalation of alkenes that exploits triazole as the directing group. This strategy enabled the efficient synthesis of a variety of substituted alkyl benzamides, achieving high yields and demonstrating good tolerance to various functional groups, all while using Earth-abundant and non-toxic iron catalysts. Notably, the removable triazole directing group allowed the synthesis of both linear and branched benzamides based on the type of alkenes used, utilizing a single catalytic system. This method reveals for the first time that the geometry of triazole directing groups can control the regioselectivity in iron-catalyzed C–H alkylations, offering a complementary approach to the widely used 8-aminoquinoline moiety.

2.4 References

[1] P. Gandeepan, T. Müller, D. Zell, G. Cera, S. Warratz and L. Ackermann, *Chem. Rev.* **2019**, *119*, 2192.

[2] For recent general reviews on iron catalysis, see: a) S. Rana, J. P. Biswas, S. Paul, A. Paik, D. Maiti, *Chem. Rev.* **2021**, *50*, 243-472; b) A. Casnati, M. Lanzi, G. Cera, *Molecules*, **2020**, *25*, 3889; c) D. Wei, C. Darcel, *Chem. Rev*. **2019**, *4*, 2550–2610; d) I. T. Alt, C. Guttroff, B. Plietker, *Angew. Chem. Int. Ed.* **2017**, *56*, 10582 –10586; e) A. Fürstner, *ACS Cent. Sci*. **2016**, *2*, 778–789; f) K. S. Egorova,V. P. Ananikov, *Angew. Chem. Int. Ed.* **2016**, *55*, 12150 – 12162; g) I. Bauer, H.-J. Knölker, *Chem. Rev.* **2015**, *115*, 3170–3387. For recent reviews on iron-catalysed C–H functionalizations, see: h) S. Cattani, G. Cera, *Chem. Asian J.* **2024**, *19*, e202300897; i) R. Shang, L. Ilies, E. Nakamura, *Chem. Rev.* **2017**, *117*, 9086–9139; j) N. Yoshikai, *Isr. J. Chem*. **2017**, 57, 1117–1130; k) G. Cera, L. Ackermann, *Top. Curr. Chem*. **2017**, *374*, 191–224.

[3] For selected reviews, see: a) G. Evano, C. Theunissen, *Angew. Chem. Int. Ed*., **2019**, *58*, 7202-7236; b) Z. Dong, Z. Ren, S. J. Thompson, Y. Xu, G. Dong, *Chem. Rev.* **2017**, *117*, 9333–9403.

[4] L. N. Lewis, J. F. Smith, *J. Am. Chem. Soc*. **1986**, *108*, 2728–2735.

[5S. Murai, F. Kakiuchi, S. Sekine, Y. Tanaka, A. Kamatani, M. Sonoda, N. Chatani, *Nature* **1993**, *366*, 529–531.

[6] For selected examples with cobalt, see: a) D. Zell, M. Bursch, V. Müller, S. Grimme, L. Ackermann, *Angew. Chem. Int. Ed*. **2017**, *56*, 10378-10382; b) W. Xu, N. Yoshikai, *Angew. Chem. Int. Ed*. **2014**, *53*, 14166-14170; c) K. Gao, N. Yoshikai, *J. Am. Chem. Soc.* **2011**, *133*, 400–402; d) L. Ilies, L. Q. Chen, X. Zeng, E. Nakamura, *J. Am. Chem. Soc*. **2011**, *133*, 5221–5223. For nickel, see: e) N. I. Saper, A. Ohgi, D. W. Small, K. Semba, Y. Nakao, J. F. Hartwig, *Nat. Chem*., **2020**, *12*, 276–283; f) Y. Schramm, M. Takeuchi, K. Semba, Y. Nakao, J. F. Hartwig, *J. Am. Chem. Soc*. **2015**, *137*, 12215–12218; g) Y. Nakao, N. Kashihara, K. S. Kanyiva, T. Hiyama, *Angew. Chem. Int. Ed*. **2010**, *49*, 4451-4454; h) Y. Nakao, N. Kashihara, K. S. Kanyiva, T. Hiyama, *J. Am. Chem. Soc*. **2008**, *130*, 16170–16171.

[7]A. M. Messinis, J. C. A. Oliveira, A. C. Stückl, L. Ackermann, *ACS Catal*. **2022**, *12*, 4947–4960; b) N. Kimura, S. Katta, Y. Kitazawa, T. Kochi, F. Kakiuchi, *J. Am. Chem. Soc*. **2021**, *143*, 12, 4543–4549; c) A. M. Messinis, L. H. Finger, L. Hu and L. Ackermann, *J. Am. Chem. Soc*., **2020**, *142*, 13102–13111; d) N. Kimura, T. Kochi, F. Kakiuchi, *J. Am. Chem. Soc*. **2017**, *139*, 42, 14849–14852.

[8] J. Loup, D. Zell, J. C. A. Oliveira, H. Keil, D. Stalke, L. Ackermann, *Angew. Chem. Int. Ed.* **2017**, *56*, 14197-14201; b) M. Y. Wong, T. Yamakawa, N. Yoshikai, *Org. Lett.*, **2015**, *17, 3, 442–445*; c) Z.-J. Zhang, N. Jacob, S. Bhatia, P. Boos, X. Chen, J. C. DeMuth, A. M. Messinis, B. Bongsuiru Jei, J. C. A. Oliveira, A. Radović, M. L. Neidig, J. Wencel-Delord, L. Ackermann, *Nat Commun* **2024**, *15*, 3503.

[9] a) M. M. Bagga; P. L. Pauson, F. J. Preston, R. I. Reed, *Chem. Commun*. **1965**, 543-544; b) G. Hata, H. Kondo, A. Miyake, *J. Am. Chem .Soc*. **1968**, *90*, 9, 2278–2281; c) C. A. Tolman, S. D. Ittel, A. D. English, J. P. Jesson, *J. Am. Chem. Soc*. **1979**, *101, 7, 1742–1751*; d) M. V. Baker, L. D. Field, *J. Am. Chem. Soc*. **1986**, *108*, 7433; e) H.-F. Klein, S. Camadanli, R. Beck, D. Leukel, U. Flörke, *Angew. Chem., Int. Ed.* **2005**, *44*, 975-977; f) S. Camadanli, R. Beck, U. Flörke, H.-F. Klein, *Organometallics* **2009**, *28*, 2300–2310; g) L. Wang, H. Sun, X. Li, O. Fuhr, D. Fenske, *Dalton Trans*. **2016**, *45*, 18133–18141; h) R. Beck, S. Camadanli, U. Flörke, H.-F. Klein, *J. Organomet. Chem.* **2015**, *778*, 47–55.

[10] a) G. Cera, T. Haven, L. Ackermann, *Angew. Chem. Int. Ed.*, **2016**, *55*, 1484–1488; b) E. R. Fruchey, B. M. Monks, S. P. Cook, *J. Am. Chem. Soc.*, **2014**, *136*, 13130–13133; c) L. Ilies, T. Matsubara, S. Ichikawa, S. Asako, E. Nakamura, *J. Am. Chem. Soc*. **2014**, *136*, 38, 13126–13129; d) B. M. Monks, E. R. Fruchey, S. P. Cook, *Angew. Chem., Int. Ed*., **2014**, *53*, 41, 11065-11069; (e) S. Asako, L. Ilies, E. Nakamura, *J. Am. Chem. Soc*., **2013**, *135*, 47, 17755–17757.

[11] L. Ilies, Y. Zhou, H. Yang, T. Matsubara, R. Shang, E. Nakamura, *ACS Catal.* **2018**, *8*, 12, 11478–11482. [12] F. Kakiuchi, S. Murai, *Acc. Chem. Res*. **2002**, *35*, 826–834.

[13] X. Ye, Z. He, T. Ahmed, K. Weise, N. G. Akhmedov, J. L. Petersena, X. Shi, *Chem. Sci.* **2013**, *4*, 3712−3716.

[14] Z. Xu, X. Yang, S.-F. Yin, R. Qiu, *Top. Curr. Chem.* **2020**, *378*, 42.

[15] a) X. Jiang, X. Hao, L. Jing, G. Wu, D. Kang, X. Liu, P. Zhan, *Expert Opin. Drug Discovery* **2019**, *14*, 779−789; b) I. Avan, D. C. Hall, A. R. Katritzky, *Chem. Soc. Rev.* **2014**, *43*, 3575−3594; c) S. Kumar, S. L. Khokra, A. Yadav, *Futur. J. Pharm. Sci*. **2021**, *7*, 106.

[16] a) X. Ye, Z. He, T. Ahmed, K. Weise, N. G. Akhmedov, J. L. Petersen, X. Shi, *Chem. Sci.* **2013**, *4*, 3712–3716; b) H. H. Al Mamari, E. Diers, L. Ackermann, *Chem. Eur. J.* **2014**, *20*, 9739–9743.

[17] a) R. Huisgen, *Angew. Chem. Int. Ed*. **1963**, *2*, 565–598; b) R. Huisgen, *Angew. Chem. Int. Ed.* **1963**, *2*, 633–645.

[18] a) K. Graczyk, T. Haven, L. Ackermann, *Chem. Eur. J*. **2015**, *21*, 8812−8815; b) G. Cera, T. Haven, L. Ackermann, *Angew. Chem., Int. Ed.* **2016**, *55*, 1484−1488.

[19] L. Ilies, Y. Zhou, H. Yang, T. Matsubara, R. Shang, E. Nakamura, *ACS Catal*. **2018**, *8*, 12, 11478–11482.

[20] R. M. Beesley, C. K. Ingold, J. F. Thorpe, *J. Chem. Soc., Trans.*, **1915**, *107*, 1080−1106.

[21] a) L. Adak, M. Jin, S. Saito, T. Kawabata, T. Itoh, S. Ito, A. K. Sharma, N. J. Gower, P. Cogswell, J. Geldsetzer, H. Takaya, K. Isozaki, M. Nakamura, *Chem. Commun*. **2021**, *57*, 6975–6978; b) S. Ito, T. Itoh, M. Nakamura, *Angew. Chem. Int. Ed*. **2011**, *50*, 454 –457; c) Y. Wang, E. A. F. Fordyce, F. Y. Chen, H. W. Lam, *Angew. Chem. Int. Ed.* **2008**, *47*, 7350–7353; d) M. Nakamura, A. Hirai, E. Nakamura, *J. Am. Chem. Soc.* **2000**, *122*, 5, 978–979.

[22] a) J. C. DeMuth, Z. Song, S. H. Carpenter, T. E. Boddie, A. Radovic, T. M. Baker, O. Gutierrez, M. L. Neidig, *Chem. Sci*., **2021**, *12*, 9398–9407; b) T. E. Boddie, S. H. Carpenter, T. M. Baker, J. C. DeMuth, G. Cera, W. W. Brennessel, L. Ackermann, M. L. Neidig, *J. Am. Chem. Soc.* **2019**, *141*, 31, 12338–12345; c) Y. Sun, H. Tang, K. Chen, L. Hu, J. Yao, S. Shaik, H. Chen, *J. Am. Chem. Soc*. **2016**, *138*, 11, 3715–3730.

[23] a) R. N. Perutz, S. Sabo-Etienne, A. S. Weller, *Angew. Chem. Int. Ed*. **2022**, *61*, e202111462; b) R. N. Perutz, S. Sabo-Etienne, *Angew. Chem. Int. Ed.* **2007**, *46*, 2578–2592.

2.5 Experimental Section

2.5.1 Methods

All reactions were carried out in Schlenk tubes under a N_2 atmosphere using pre-dried glassware. THF was dried using a solvent purification system (SPS) from Inert. Yields refer to isolated compounds, estimated to be > 95% pure as determined by ^{1}H-NMR. Column chromatography was performed on silica gel 60 (40-63 mesh). Melting points were measured with an Electrothermal apparatus and are uncorrected. NMR spectra were recorded on a Bruker 400 MHz and JEOL 600 MHz using solvents as internal standards (7.26 ppm for ^{1}H NMR and 77.00 ppm for ^{13}C NMR for $CDCl_3$). The terms m, s, d, t, q, and quint represent multiplet, singlet, doublet, triplet, quadruplet, and quintuplet respectively, and the term bs means a broad signal. ^{13}C DEPTQ NMR spectra are reported for all compounds. Mass spectra were recorded in the ESI mode. Exact masses were recorded on a LTQ ORBITRAP XL Thermo Mass Spectrometer (ESI source).

2.5.2 Materials

PhMgBr (1.0 M in THF) was freshly prepared from Bromobenzene ≥99.5% (GC) and magnesium turnings in anhydrous THF and titrated prior to use with I_2 in THF. The solution of $ZnCl_2$ in THF (1.0 mol/L) was prepared in a Schlenk tube by melting anhydrous $ZnCl_2$ at 230 °C under vacuum for 3 hours. Then, dry THF was added and the solution was stirred until all the $ZnCl_2$ was dissolved. Anhydrous $ZnBr_2$ for catalytic reactions was weighted under air (90 mg, 0.06 mmol) and then transferred in a 1.0 mL Eppendorf vial. The Eppendorf vial was then placed in a BUCHI glass oven for drying under vacuum at 110 °C for 3 hours prior to use. Vinylferrocene (**2n**), 2-Vinylthiophene (**2m**), 2-Vinyl-1-benzothiophene (**2n**), 4-Fluorostyrene (**2g**), 3-(Trifluoromethyl) styrene (**2i**), 3-fluoro-4- methoxystyrene (**2j**), 2-Fluorostyrene (**2k**) and 4-vinyl-1,1'-biphenyl (**2d**) were synthesized according to known procedures.[1,2] 3-(Trifluoromethyl)benzoic acid and 4-(Trifluoromethyl)benzoic acid were obtained according to previously described methods.[3] Other chemicals were obtained from commercial sources and were used without further purification.

2.5.3 Synthesis of Benzamide Substrates

General procedure A: synthesis of benzamide substrates

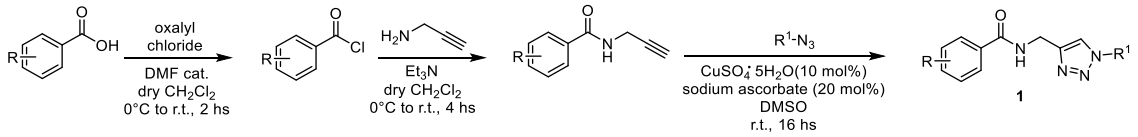

Oxalyl chloride (1.1 equiv.) was added dropwise to a mixture of the carboxylic acid (1.0 equiv.), DMF (cat.) in dry CH_2Cl_2 under a nitrogen atmosphere at 0 °C. The mixture was stirred at the same temperature for 2 hs upon which it was allowed to warm up to ambient temperature. The crude acyl chloride was cooled to 0 °C and it was added dropwise to a solution of propargylamine (1.5 equiv.), NEt_3 (3.0 equiv.) in dry CH_2Cl_2 (10 mL) at 0 °C under a nitrogen atmosphere. The mixture was initially stirred at the same temperature and then at ambient temperature for 4 hs. To the reaction was added sat. aqueous $NaHCO_3$ (20 mL). The aqueous layers were extracted with CH_2Cl_2 (3x20 mL). The combined organic extracts were washed with HCl (1.0 M, 20 mL), brine and dried over Na_2SO_4. The filtrate was concentrated under reduced pressure. The crude product was further submitted to the corresponding azide (1.5 equiv.), $CuSO_4 \cdot 5H_2O$ (10 mol %), sodium ascorbate (20 mol %) in DMSO (10 mL). After 16 hs, the reaction was quenched with sat. aqueous NH_4Cl (40 mL). The aqueous layers were extracted with EtOAc (3x40 mL). The combined organic extracts were dried over Na_2SO_4 and the filtrate was concentrated under reduced pressure. The crude product was purified by column chromatography on silica gel.

_N_-[(1-Benzyl-1_H_-1,2,3-triazol-4-yl)methyl]benzamide (1a)

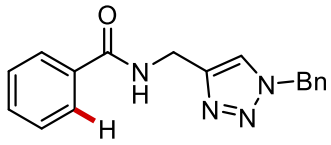

Representative procedure **A** was followed using benzoyl chloride (420 mg, 3.0 mmol) and benzyl azide (598 mg, 4.5 mmol). Purification by column chromatography on silica gel (*n*-Hexane/EtOAc 1:1→ 3:7) yielded **1a** (744 mg, 85%) as a white solid. M.p. = 122-123 °C. ^{1}H-NMR (400 MHz, $CDCl_3$): δ = 7.82 – 7.77 (m, 2H), 7.58 – 7.49 (m, 2H), 7.48 – 7.37 (m, 5H), 7.33 – 7.29 (m, 2H), 6.90 (bs, 1H), 5.53 (s, 2H), 4.72 (d, *J* = 5.6 Hz, 2H). ^{13}C-NMR (101 MHz, $CDCl_3$): δ = 167.5 (C_q), 134.5 (C_q), 134.0 (2 x C_q), 131.6 (CH), 129.1 (CH), 128.8 (CH), 128.5 (CH), 128.2 (2 x CH), 127.1 (CH), 54.3 (CH_2), 35.4 (CH_2). MS (ESI) *m/z* (relative intensity): 331 (15) $[M+K]^+$, 325 (20), 315 (100) $[M+Na]^+$, 293 (57) $[M+H]^+$. HR-MS (ESI) *m/z* calcd for $C_{17}H_{17}N_4O$ $[M+H]^+$ 293.1397, found 293.1392.

_N_-[2-(1-Benzyl-1_H_-1,2,3-triazol-4-yl)propan-2-yl]benzamide (1a^{TAM})

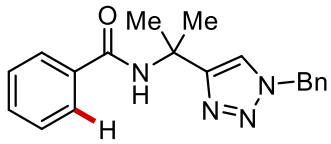

Representative procedure **A** was followed using benzoyl chloride (420 mg, 3.0 mmol), 1,1-dimethylpropargylamine (373 mg, 4.5 mmol) and benzyl azide (598 mg, 4.50 mmol). Purification by column chromatography on silica gel (*n*-Hexane/EtOAc 8:2→ 6:4) yielded **1a^{TAM}** (768 mg, 82%) as a white solid. M.p. = 152-153 °C. ^{1}H-NMR (400 MHz, $CDCl_3$): δ = 7.81 – 7.76 (m, 2H), 7.53 – 7.47 (m, 2H), 7.46 – 7.38 (m, 5H), 7.32-7.30 (m, 2H), 7.03 (bs, 1H), 5.54 (s, 2H), 1.88 (s, 6H). ^{13}C-NMR (101 MHz, $CDCl_3$): δ = 166.7 (C_q), 154.0 (C_q), 135.3 (C_q), 134.6 (C_q), 131.3 (CH), 129.1 (CH), 128.8 (CH), 128.5 (CH), 128.1 (CH), 126.9 (CH), 120.3 (CH), 54.2 (CH_2), 51.9 (C_q), 28.0 (CH_3). MS (ESI) *m/z* (relative intensity): 358 (12) $[M+K]^+$, 343 (100) $[M+Na]^+$, 321 (37) $[M+H]^+$, 200 (20), 172 (16). HR-MS (ESI) *m/z* calcd for $C_{19}H_{21}N_4O$ $[M+H]^+$ 321.1710, found 321.1716.

_N_-[(1-Phenyl-1_H_-1,2,3-triazol-4-yl)methyl]benzamide (1b)

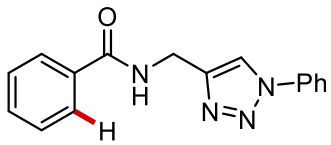

Representative procedure **A** was followed using benzoyl chloride (366 mg, 3.0 mmol) and azidobenzene (535 mg, 4.5 mmol). Purification by column chromatography on silica gel (*n*-Hexane/EtOAc 6:4→ 4:6) yielded **1b** (625 mg, 75%) as a white solid. M.p. = 167-168 °C. ^{1}H-NMR (400 MHz, $CDCl_3$): δ = 8.11 (s, 1H), 7.87 – 7.81 (m, 2H), 7.79 – 7.72 (m, 2H), 7.59 – 7.50 (m, 3H), 7.49-7.44 (m, 3H), 6.97 (s, 1H), 4.85 (d, *J* = 5.7 Hz, 2H). ^{13}C-NMR (101 MHz, $CDCl_3$): δ = 167.6 (C_q), 145.4 (C_q), 137.0 (C_q), 133.9 (C_q), 131.8 (CH), 129.8 (CH), 128.9 (CH), 128.6 (CH), 127.1 (CH), 120.9 (CH), 120.6 (CH), 35.4 (CH_2). MS (ESI) *m/z* (relative intensity): 301

(100) $[M+Na]^+$, 279 (60) $[M+H]^+$, 130 (12). HR-MS (ESI) *m/z* calcd for $C_{16}H_{15}N_4O$ $[M+H]^+$ 279.1240, found 279.1245.

_N_-[(1-Butyl-1_H_-1,2,3-triazol-4-yl)methyl]benzamide (1c)

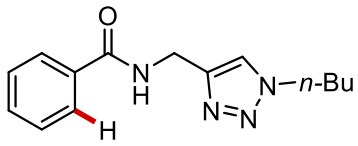

Representative procedure **A** was followed using benzoyl chloride (420 mg, 3.0 mmol) and 1-azidobutane (445 mg, 4.5 mmol). Purification by column chromatography on silica gel (*n*-Hexane/EtOAc 1:1→ 3:7) yielded **1c** (642 mg, 83%) as a white solid. M.p. = 84-85 °C. ^{1}H-NMR (400 MHz, CDCl3): δ = 7.83 – 7.81 (m, 2H), 7.64 (s, 1H), 7.53 – 7.49 (m, 1H), 7.46 – 7.41 (m, 2H), 7.07 (bs, 1H), 4.74 (d, *J* = 5.6 Hz, 2H), 4.36 (t, *J* = 7.3 Hz, 2H), 1.98 – 1.85 (quint, *J* = 7.6 Hz, 2H), 1.45 – 1.33 (sest, , *J* = 7.6 Hz, 2H), 0.97 (t, *J* = 7.4 Hz, 3H). ^{13}C-NMR (101 MHz, $CDCl_3$): δ = 167.4 (C_q), 144.5 (C_q), 134.0 (C_q), 131.7 (CH), 128.6 (CH), 127.0 (CH), 122.3 (CH), 50.2 (CH_2), 35.4 (CH_2), 32.2 (CH_2), 19.7 (CH_2), 13.4 (CH_3)**.** MS (ESI) *m/z* (relative intensity): 297 (15) $[M+K]^+$, 281 (100) $[M+Na]^+$, 259 (53) $[M+H]^+$. HR-MS (ESI) *m/z* calcd for $C_{14}H_{19}N_4O$ $[M+H]^+$ 259.1553, found 259.1561.

_N_-[(1-Benzyl-1_H_-1,2,3-triazol-4-yl)methyl]-4-methylbenzamide (1d)

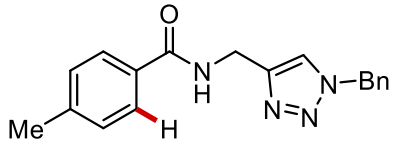

Representative procedure **A** was followed using 4-methylbenzoic acid (408 mg, 3.0 mmol) and benzyl azide (598 mg, 4.5 mmol). Purification by column chromatography on silica gel (*n*-Hexane/EtOAc 1:1→ 3:7) yielded **1d** (678 mg, 74%) as a white solid. M.p. = 164-165 °C. ^{1}H-NMR (400 MHz, $CDCl_3$): δ = 7.69 (d, *J* = 8.2 Hz, 2H), 7.56 (s, 1H), 7.39 – 7.36 (m, 3H), 7.30 – 7.29 (m, 2H), 7.23 (d, *J* = 7.9 Hz, 2H), 6.96 (bs, 1H), 5.52 (s, 2H), 4.70 (d, *J* = 5.6 Hz, 2H), 2.40 (s, 3H). ^{13}C-NMR (101 MHz, $CDCl_3$): δ = 167.3 (C_q), 145.2 (C_q), 142.1 (C_q), 134.5 (C_q), 131.1 (C_q), 129.2, (CH) 129.1 (CH), 128.8 (CH), 128.2 (CH), 127.0 (CH), 122.4 (CH), 54.3 (CH_2), 35.4 (CH_2), 21.5 (CH_3). ESI-MS calcd for $C_{18}H_{19}N_4O$ $[M+H]^+$ 307.15, found 307.18. MS (ESI) *m/z* (relative intensity): 329 (100) $[M+Na]^+$, 307 (69) $[M+H]^+$, 143 (229, 119 (39). HR-MS (ESI) *m/z* calcd for $C_{18}H_{19}N_4O$ $[M+H]^+$ 307.1553, found 307.1557.

_N_-[(1-Benzyl-1_H_-1,2,3-triazol-4-yl)methyl)-[1,1'-biphenyl]-4-carboxamide (1e)

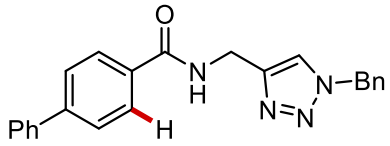

Representative procedure **A** was followed using [1,1'-biphenyl]-4-carboxylic acid (594 mg, 3.0 mmol) and benzyl azide (598 mg, 4.5 mmol). Purification by column chromatography on silica gel (*n*-Hexane/EtOAc 1:1→ 3:7) yielded **1e** (770 mg, 70%) as a white solid. M.p. = 212-213 °C. ^{1}H-NMR (400 MHz, $CDCl_3$): δ = 7.88 (d, *J* = 8.4 Hz, 2H), 7.67 (d, *J* =

8.4 Hz, 2H), 7.64 – 7.61 (m, 2H), 7.59 (s, 1H), 7.48 (t, *J* = 7.4 Hz, 2H), 7.43 – 7.37 (m, 4H), 7.31 (dd, *J* = 7.4, 2.2 Hz, 2H), 7.00 (bs, 1H), 5.54 (s, 2H), 4.75 (d, *J* = 5.1 Hz, 2H). ^{13}C-NMR (101 MHz, $CDCl_3$): δ = 167.1 (C_q), 144.5 (C_q), 140.0 (C_q), 134.4 (C_q), 132.6 (2 x C_q), 129.2 (CH), 128.9 (CH), 128.8 (CH), 128.2 (CH), 128.0 (CH), 127.5 (CH), 127.3 (CH), 127.2 (CH), 122.3 (CH), 54.3 (CH_2), 35.5 (CH_2). MS (ESI) *m/z* (relative intensity): 759 $[2M+Na]^+$ (100), 391 (48) $[M+Na]^+$, 269 (30) $[M+H]^+$. HR-MS (ESI) *m/z* calcd for $C_{23}H_{21}N_4O$ $[M+H]^+$ 369.1710, found 369.1706.

_N_-[(1-Benzyl-1_H_-1,2,3-triazol-4-yl)methyl]-4-fluorobenzamide (1f)

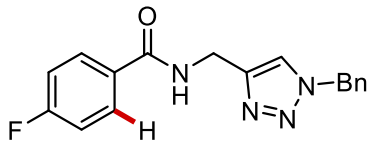

Representative procedure **A** was followed using 4-fluorobenzoic acid (420 mg, 3.0 mmol) and benzyl azide (598 mg, 4.5 mmol). Purification by column chromatography on silica gel (*n*-Hexane/EtOAc 1:1→ 3:7) yielded **1f** (650 mg, 70%) as a light-yellow solid. M.p. = 133-135 °C. ^{1}H-NMR (400 MHz, $CDCl_3$): δ = 7.88 – 7.81 (m, 2H), 7.60 (s, 1H), 7.45 (bs, 1H), 7.39 – 7.37 (m, 3H), 7.30 – 7.29 (m, 2H), 7.08 (t, *J* = 8.6 Hz, 2H), 5.51 (s, 2H), 4.68 (d, *J* = 5.6 Hz, 2H). ^{13}C-NMR (101 MHz, $CDCl_3$): δ = 166.4 (C_q), 164.8 (d, $^1J_{C\text{-}F}$ = 251 Hz, C_q), 145.01 (C_q), 134.35 (C_q), 130.1 (d, $^4J_{C\text{-}F}$ = 4 Hz, C_q), 129.5 (d, $^3J_{C\text{-}F}$ = 9 Hz, CH), 129.2 (CH), 128.9 (CH), 128.2 (CH), 122.53 (CH), 115.5 (d, $^2J_{C\text{-}F}$ = 22 Hz, CH), 54.33 (CH_2), 35.29 (CH_2). ^{19}F-NMR (565 MHz, $CDCl_3$): δ = -107.85 (ddd, *J* = 13.6, 8.5, 5.1 Hz). MS (ESI) *m/z* (relative intensity): 349 (34) $[M+K]^+$, 333 (100) $[M+Na]^+$, 311 (60) $[M+H]^+$. HR-MS (ESI) *m/z* calcd for $C_{17}H_{16}FN_4O$ $[M+H]^+$ 311.1303, found 311.1308.

_N_-[(1-Benzyl-1_H_-1,2,3-triazol-4-yl)methyl]-4-chlorobenzamide (1g)

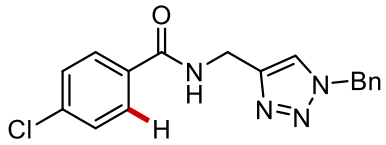

Representative procedure **A** was followed using 4-chlorobenzoic acid (468 mg, 3.0 mmol) and benzyl azide (598 mg, 4.5 mmol). Purification by column chromatography on silica gel (*n*-Hexane/EtOAc 1:1→ 3:7) yielded **1g** (782 mg, 80%) as a white solid. M.p. = 172-173 °C. ^{1}H-NMR (400 MHz, $CDCl_3$): δ = 7.75 (d, *J* = 8.5 Hz, 2H), 7.60 (bs, 1H), 7.41 – 7.38 (m, 5H), 7.34 – 7.29 (m, 2H), 7.16 (bs, 1H), 5.52 (s, 2H), 4.69 (d, *J* = 4.4 Hz, 2H). ^{13}C-NMR (101 MHz, $CDCl_3$): δ = 166.4 (C_q), 137.9 (C_q), 134.3 (C_q), 132.3 (2 x C_q), 129.2 (CH), 128.9 (CH), 128.8 (CH), 128.5 (2 x CH), 128.2 (CH), 54.4 (CH_2), 35.4 (CH_2). MS (ESI) *m/z* (relative intensity): 349 (100) $[M+Na]^+$, 327 (54) $[M+H]^+$. HR-MS (ESI) *m/z* calcd for $C_{17}H_{16}ClN_4O$ $[M+H]^+$ 327.1007, found 327.1012.

_N_-[(1-Benzyl-1_H_-1,2,3-triazol-4-yl)methyl]-4-bromobenzamide (1h)

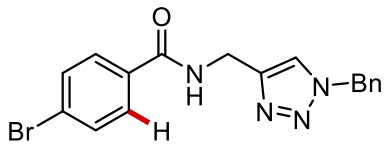

Representative procedure **A** was followed using 4-bromobenzoic acid (603 mg, 3.0 mmol) and benzyl azide (598 mg, 4.5 mmol). Purification by column chromatography on silica gel (*n*-Hexane/EtOAc 1:1→ 3:7) yielded **1h** (790 mg, 71%) as a white solid. M.p. = 176-178 °C. ^{1}H-NMR (400 MHz, $CDCl_3$): δ = 7.69 (d, *J* = 8.6 Hz, 2H), 7.57 (s, 1H), 7.55 (d, *J* = 8.6 Hz, 2H), 7.40 – 7.37 (m, 3H), 7.31 – 7.29 (m, 3H), 5.52 (s, 2H), 4.68 (d, *J* = 5.6 Hz, 2H). ^{13}C-NMR (101 MHz, $CDCl_3$): δ = 166.5 (C_q), 144.8 (C_q), 134.3 (C_q), 132.8 (C_q), 131.8 (CH), 129.2 (CH), 128.9 (CH), 128.7 (CH), 128.2 (CH), 126.4 (C_q), 122.4 (CH), 54.3 (CH_2), 35.4 (CH_2). MS (ESI) *m/z* (relative intensity): 409 (13) $[M+K]^+$, 393 (100) $[M+Na]^+$, 371 (29) $[M+H]^+$, 144 (49). HR-MS (ESI) *m/z* calcd for $C_{17}H_{16}BrN_4O$ $[M+H]^+$ 371.0502, found 371.0510.

_N_-[(1-Benzyl-1_H_-1,2,3-triazol-4-yl)methyl]-4-(trifluoromethyl)benzamide (1i)

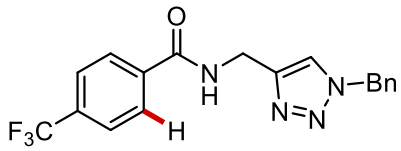

Representative procedure **A** was followed using 4-(trifluoromethyl) benzoic acid (570 mg, 3.0 mmol) and benzyl azide (598 mg, 4.5 mmol). Purification by column chromatography on silica gel (*n*-Hexane/EtOAc 1:1→ 3:7) yielded **1i** (702 mg, 65%) as a white solid. M.p. = 173-174 °C. ^{1}H-NMR (400 MHz, $CDCl_3$): δ = 7.93 (d, *J* = 8.2 Hz, 2H), 7.70 (d, *J* = 8.1 Hz, 2H), 7.57 (s, 1H), 7.41 – 7.38 (m, 3H), 7.32 – 7.29 (m, 2H), 7.24 (bs, 1H), 5.54 (s, 2H), 4.72 (d, *J* = 5.6 Hz, 2H). ^{13}C-NMR (101 MHz, $CDCl_3$): δ = 166.1 (C_q), 144.7 (C_q), 137.2 (C_q), 134.3 (C_q), 133.3 (q, $^{2}J_{C\text{-}F}$ = 32 Hz, C_q), 129.2 (CH), 129.0 (CH), 128.2 (CH), 127.6 (CH), 125.6 (q, $^{4}J_{C\text{-}F}$ = 4 Hz, CH), 123.7 (q, $^{1}J_{C\text{-}F}$ = 273 Hz, C_q), 122.5 (CH), 54.4 (CH_2), 35.4 (CH_2). ^{19}F-NMR (565 MHz, $CDCl_3$): δ = -62.9 (s). MS (ESI) *m/z* (relative

intensity): 383 (100) $[M+Na]^+$, 361 (55) $[M+H]^+$. HR-MS (ESI) *m/z* calcd for $C_{18}H_{16}F_3N_4O$ $[M+H]^+$ 361.1271, found 361.1268.

Methyl 4-{[(1-benzyl-1*H*-1,2,3-triazol-4-yl)methyl]carbamoyl}benzoate (1j)

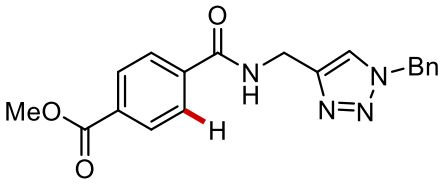

Representative procedure **B** was followed using 4-(methoxycarbonyl) benzoic acid (540 mg, 3.0 mmol) and benzyl azide (598 mg, 4.5 mmol). Purification by column chromatography on silica gel (*n*-Hexane/EtOAc 1:1→ 3:7) yielded **1j** (690 mg, 66%) as a white solid. M.p. = 174-176 °C. ^{1}H-NMR (400 MHz, $CDCl_3$): δ = 8.11 (d, *J* = 8.4 Hz, 2H), 7.86 (d, *J* = 8.6 Hz, 2H), 7.56 (s, 1H), 7.42 – 7.37 (m, 3H), 7.31 – 7.29 (m, 2H), 6.99 (s, 1H), 5.54 (s, 2H), 4.72 (d, *J* = 5.4 Hz, 2H), 3.96 (s, 3H). ^{13}C-NMR (101 MHz, $CDCl_3$): δ = 166.6 (C_q), 166.3 (C_q), 137.9 (C_q), 134.4 (C_q), 132.8 (2 x C_q), 129.8 (2 x CH), 129.2 (CH), 128.9 (CH), 128.2 (CH), 127.2 (CH), 54.4 (CH_2), 52.4 (CH_3), 35.4 (CH_2). MS (ESI) *m/z* (relative intensity): 723 (23) $[2M+Na]^+$, 545 (12), 351(100) $[M+H]^+$. HR-MS (ESI) *m/z* calcd for $C_{19}H_{19}N_4O_3$ $[M+H]^+$ 351.1452, found 351.1458.

***N*-[(1-Benzyl-1*H*-1,2,3-triazol-4-yl)methyl]-4-(tert-butyl)benzamide (1l)**

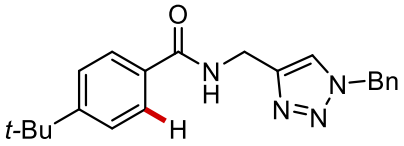

Representative procedure **A** was followed using 4-(*tert*-butyl)benzoic acid (534 mg, 3.0 mmol) and benzyl azide (598 mg, 4.5 mmol). Purification by column chromatography on silica gel (*n*-Hexane/EtOAc 1:1→ 3:7) yielded **1l** (616 mg, 59%) as a white solid. M.p. = 167–169 °C. ^{1}H-NMR (400 MHz, $CDCl_3$): δ = 7.73 (d, *J* = 7.7 Hz, 2H), 7.55 (s, 1H), 7.45 (d, *J* = 7.4 Hz, 2H), 7.40 – 7.37 (m, 3H), 7.30 – 7.27 (m, 2H), 6.94 (s, 1H), 5.52 (s, 2H), 4.70 (d, *J* = 5.6 Hz, 2H), 1.34 (s, 9H). ^{13}C-NMR (101 MHz, $CDCl_3$): δ = 167.3 (C_q), 155.2 (C_q), 145.2 (C_q), 134.5 (C_q), 131.1 (C_q), 129.2 (CH), 128.8 (CH), 128.2 (CH), 126.8 (CH), 125.5 (CH), 122.3 (CH), 54.3 (CH_2), 35.4 (CH_2), 34.9 (C_q), 31.2 (CH_3). MS (ESI) *m/z* (relative intensity): 719 $[2M+Na]^+$ (53), 542 (37), 387 (30) $[M+K]^+$, 371 (92) $[M+Na]^+$, 349 (100) $[M+H]^+$. HR-MS (ESI) *m/z* calcd for $C_{21}H_{25}N_4O$ $[M+H]^+$ 349.2023, found 349.2027.

***N*-[(1-Benzyl-1*H*-1,2,3-triazol-4-yl)methyl]-4-methoxybenzamide (1m)**

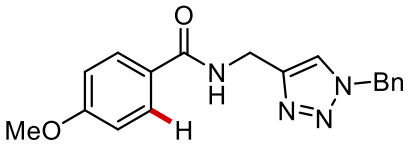

Representative procedure **A** was followed using 4-methoxybenzoic acid (456 mg, 3.0 mmol) and benzyl azide (598 mg, 4.5 mmol). Purification by column chromatography on silica gel (*n*-Hexane/EtOAc 1:1→ 3:7) yielded **1m** (589 mg, 61 %) as a white solid. M.p. = 134-136 °C. ^{1}H-NMR (400 MHz, $CDCl_3$): δ = 7.77 (d, *J* = 8.8 Hz, 2H), 7.56 (s, 1H),

7.39 – 7.35 (m, 3H), 7.30 – 7.27 (m, 2H), 6.95 (bs, 1H), 6.92 (d, J = 8.8 Hz, 2H), 5.51 (s, 2H), 4.68 (d, J = 5.6 Hz, 2H), 3.85 (s, 3H). ^{13}C-NMR (101 MHz, $CDCl_3$): δ = 166.9 (C_q), 162.3 (C_q), 145.3 (C_q), 134.5 (C_q), 129.2 (CH), 128.9 (CH), 128.8 (CH), 128.2 (CH), 126.3 (C_q), 122.3 (CH), 113.8 (CH), 55.4 (CH_3), 54.3 (CH_2), 35.4 (CH_2). MS (ESI) *m/z* (relative intensity): 667 $[2M+Na]^+$ (51), 503 (30), 361 (25) $[M+K]^+$, 345 (100) $[M+Na]^+$, 323 (68) $[M+H]^+$. HR-MS (ESI) *m/z* calcd for $C_{18}H_{19}N_4O_2$ $[M+H]^+$ 323.1502, found 323.1507.

_N_-[(1-Benzyl-1_H_-1,2,3-triazol-4-yl)methyl]-3-methylbenzamide (1k)

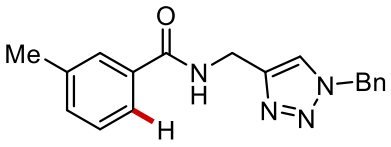

Representative procedure **A** was followed using *m*-toluoyl chloride (464 mg, 3.0 mmol) and benzyl azide (598 mg, 4.5 mmol). Purification by column chromatography on silica gel (*n*-Hexane/EtOAc 1:1→ 3:7) yielded **1k** (744 mg, 85%) as a white solid. M.p. = 143-144 °C. ^{1}H-NMR (400 MHz, $CDCl_3$): δ = 7.62 (s, 1H), 7.59 – 7.54 (m, 2H), 7.42 – 7.36 (m, 3H), 7.32 – 7.30 (m, 4H), 6.94 (bs, 1H), 5.53 (s, 2H), 4.71 (d, J = 4.9 Hz, 2H), 2.40 (s, 3H). ^{13}C-NMR (101 MHz, $CDCl_3$): δ = 167.7 (C_q), 138.4 (C_q), 134.5 (C_q), 133.9 (2 x C_q), 132.4 (CH), 129.2 (CH), 128.8 (CH), 128.4 (CH), 128.2 (2 x CH), 127.8 (CH), 124.1 (CH), 54.3 (CH_2), 35.3 (CH_2), 21.3 (CH_3). MS (ESI) *m/z* (relative intensity): 345 (16) $[M+K]^+$, 329 (100) $[M+Na]^+$, 307 (78) $[M+H]^+$. HR-MS (ESI) *m/z* calcd for $C_{18}H_{19}N_4O$ $[M+H]^+$ 307.1553, found 307.1550.

_N_-[(1-Benzyl-1_H_-1,2,3-triazol-4-yl)methyl]benzamide-d_5 ([D]$_5$-1a)

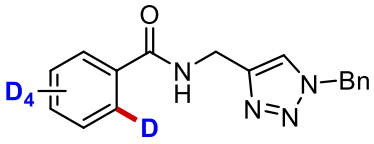

Representative procedure **A** was followed using d_5-benzoic acid (381 mg, 3.0 mmol) and benzyl azide (686 mg, 4.5 mmol). Purification by column chromatography on silica gel (*n*-Hexane/EtOAc 1:1→ 3:7) yielded [D]$_5$-**1a** (702 mg, 70%) as a white solid. M.p. = 128-129 °C. ^{1}H-NMR (400 MHz, $CDCl_3$): δ = 7.56 (s, 1H), 7.41 – 7.36 (m, 3H), 7.30 – 7.28 (m, 2H), 6.97 (bs, 1H), 5.52 (s, 2H), 4.71 (d, J = 5.6 Hz, 2H). ^{13}C-NMR (101 MHz, $CDCl_3$): δ = 167.4 (C_q), 145.0 (C_q), 134.4 (C_q), 133.8 (C_q), 131.2 (t, J = 24 Hz, CD), 129.2 (CH), 128.9 (CH), 128.1 (t, J = 24 Hz, CD), 128.2 (CH), 126.6 (t, J = 25 Hz, CD), 122.3 (CH), 54.3 (CH_2), 35.4 (CH_2). MS (ESI) *m/z* (relative intensity): 466 (35), 320 (53) $[M+Na]^+$, 298 (100) $[M+H]^+$. HR-MS (ESI) *m/z* calcd for $C_{17}H_{12}D_5N_4O$ $[M+H]^+$ 298.1711, found 298.1718.

_N_-[(1-Phenyl-1_H_-1,2,3-triazol-4-yl)methyl]benzamide-d_5 ([D]$_5$-1b)

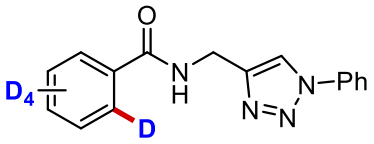

Representative procedure **A** was followed using d_5-benzoic acid (381 mg, 3.0 mmol) and azidobenzene (535 mg, 4.5 mmol). Purification by column chromatography on silica gel

(*n*-Hexane/EtOAc 1:1→ 3:7) yielded $[D]_5$-**1b** (577 mg, 68%) as a white solid. M.p. = 167-168 °C. ^{1}H-NMR (400 MHz, $CDCl_3$): δ = 8.11 (s, 1H), 7.76 – 7.73 (m, 2H), 7.57 – 7.51 (m, 2H), 7.49 – 7.44 (m, 1H), 7.09 (bs, 1H), 4.84 (d, *J* = 5.8 Hz, 2H). ^{13}C-NMR (101 MHz, $CDCl_3$): δ = 167.6 (C_q), 145.4 (C_q), 137.0 (C_q), 133.8 (C_q), 131.2 (t, *J* = 24 Hz, CD), 129.8 (CH), 128.9 (CH), 128.1 (t, *J* = 24 Hz, CD), 126.7 (t, *J* = 25 Hz, CD), 120.9 (CH), 120.6 (CH), 35.4 (CH_2). MS (ESI) *m/z* (relative intensity): 445 (16), 306 (30) $[M+Na]^+$, 284 (100) $[M+H]^+$. HR-MS (ESI) *m/z* calcd for $C_{16}H_{10}D_5N_4O$ $[M+H]^+$ 284.1481, found 284.1486.

_N_-[(1-Phenyl-1_H_-1,2,3-triazol-4-yl)methyl]benzamide-2-d ($[D]_1$-1b)

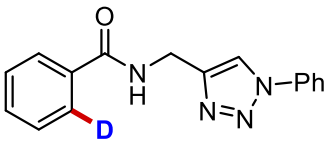

Representative procedure **A** was followed using benzoic-2-[d] acid (369 mg, 3.0 mmol) and azidobenzene (535 mg, 4.5 mmol). Purification by column chromatography on silica gel (*n*-Hexane/EtOAc 1:1→ 3:7) yielded $[D]_1$-**1b** (510 mg, 61%) as a white solid. M.p. = 169-170 °C. ^{1}H-NMR (400 MHz, $CDCl_3$): δ = 8.11 (s, 1H), 7.84 (dd, *J* = 8.1, 1.5 Hz, 1H), 7.76 – 7.73 (m, 2H), 7.54 (dtd, *J* = 7.6, 6.0, 1.2 Hz, 3H), 7.46 (ddt, *J* = 7.1, 6.0, 1.7 Hz, 3H), 7.08 (s, 1H), 4.83 (d, *J* = 5.7 Hz, 2H). ^{13}C-NMR (101 MHz, $CDCl_3$): δ = 167.5 (C_q), 145.4 (C_q), 134.0 (C_q), 133.9 (C_q), 131.8 (CH), 129.8 (CH), 128.9 (CH), 128.6 (CH), 128.5 (CH), 127.0 (d, *J* = 1 Hz, CH), 126.5 (t, *J* = 25 Hz, CD), 120.8 (CH), 120.6 (CH), 35.4 (CH_2). MS (ESI) *m/z* (relative intensity): 302 (26) $[M+Na]^+$, 280 (100) $[M+H]^+$, 130 (34). HR-MS (ESI) *m/z* calcd for $C_{16}H_{14}DN_4O$ $[M+H]^+$ 280.1230, found 284.1227.

2.5.4 Representative procedure for iron-catalyzed C–H alkylation with vinylarenes

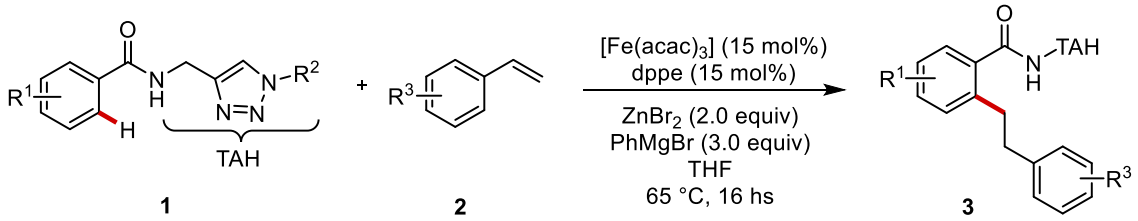

To a stirred solution of $Fe(acac)_3$ (10.6 mg, 0.03 mmol), dppe (11.9 mg, 0.03 mmol), zinc bromide (90.0 mg, 0.40 mmol, 2.0 equiv.) and **1** (0.20 mmol) in THF (0.4 mL) under N_2 atmosphere, PhMgBr (1.0 M in THF, 600 µL, 0.60 mmol, 3.0 equiv.) was added in a single portion. Then, **2** (0.60 mmol, 3.0 equiv.) was added and the mixture was placed in a pre-heated oil bath at 65 °C. After stirring for 16 hs, the reaction was cooled to room temperature and quenched by the addition of an aqueous solution of HCl (1.0 M, 5.0 mL). The reaction was extracted with CH_2Cl_2 (3x15 mL), and the combined organic extracts were dried over Na_2SO_4, filtered and concentrated. The crude product was purified by column chromatography on silica gel (*n*-Hexane/EtOAc).

2.5.5 Characterization Data of Products

***N*-[(1-Benzyl-1*H*-1,2,3-triazol-4-yl)methyl]-2-phenethylbenzamide (3aa)**

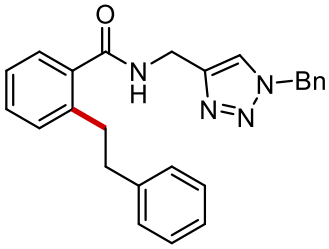

The representative procedure was followed using **1a** (58.5 mg, 0.20 mmol) and styrene **2a** (69 µL, 0.60 mmol). Purification by column chromatography on silica gel (*n*-Hexane/EtOAc 1:1) yielded **3aa** (56.3 mg, 71%) as a white solid. M.p. = 125-127 °C. ^{1}H-NMR (400 MHz, $CDCl_3$): δ = 7.53 (s, 1H), 7.37 – 7.30 (m, 5H), 7.26 – 7.17 (m, 7H), 7.08 – 7.06 (m, 2H), 6.15 (bs, 1H), 5.45 (s, 2H), 4.59 (d, *J* = 5.8 Hz, 2H), 3.04 (dd, *J* = 9.1, 6.5 Hz, 2H), 2.86 (dd, *J* = 9.2, 6.5 Hz, 2H). ^{13}C-NMR (101 MHz, $CDCl_3$): δ = 170.1 (C_q), 144.9 (C_q), 141.6 (C_q), 139.8 (C_q), 136.0 (C_q), 134.4 (C_q), 130.4 (CH), 130.1 (CH), 129.2 (CH), 128.8 (CH), 128.6 (CH), 128.3 (CH), 128.1 (CH), 126.9 (CH), 126.1 (CH), 125.9 (CH), 122.2 (CH), 54.2 (CH_2), 37.9 (CH_2), 35.4 (CH_2), 35.1 (CH_2). MS (ESI) *m/z* (relative intensity): 815 (24) $[2M+Na]^+$, 435 (32) $[M+K]^+$, 419 (49) $[M+Na]^+$, 397 (100) $[M+H]^+$. HR-MS (ESI) *m/z* calcd for $C_{25}H_{25}N_4O$ $[M+H]^+$ 397.2023, found 397.2018.

***N*-[2-(1-Benzyl-1*H*-1,2,3-triazol-4-yl)propan-2-yl]-2-phenethylbenzamide (3aa^{TAM})**

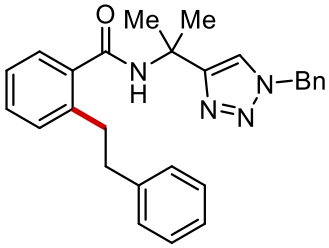

To a stirred solution of $Fe(acac)_3$ (7.0 mg, 0.02 mmol), bpy (3.4 mg, 0.022 mmol), $ZnBr_2$ (90 mg, 0.40 mmol, 2.00 equiv.) and **1a^{TAM}** (64.1 mg, 0.20 mmol) in THF (0.4 mL) under N_2 atmosphere, PhMgBr (1.0 M in THF, 600 µL, 0.6 mmol, 3.0 equiv.) was added in a single portion. Then, styrene **2a** (69 µL, 0.60 mmol, 3.0 equiv.) was added and the mixture was placed in a pre-heated oil bath at 65 °C. After stirring for 18 h, the reaction was cooled to room temperature and quenched by the addition of an aqueous solution of HCl (1.0 M, 5.0 mL). The reaction was extracted with CH_2Cl_2 (3x15 mL) and the combined organic extracts were dried over Na_2SO_4, filtered and concentrated. Purification by column chromatography on silica gel (*n*-Hexane/EtOAc 6:4) yielded **3aa^{TAM}** (16.1 mg, 19%) as a white solid. M.p. = 128-130 °C. ^{1}H-NMR (400 MHz, $CDCl_3$): δ = 7.51 (s, 1H), 7.41 – 7.36 (m, 4H), 7.34 – 7.29 (m, 3H), 7.28 – 7.17 (m, 6H), 7.17 – 7.12 (m, 2H), 5.48 (s, 2H), 3.05 (dd, *J* = 9.8, 6.3 Hz, 2H), 2.89 (dd, *J* = 9.8, 6.3 Hz, 2H), 1.87 (s, 6H). ^{13}C-NMR (101 MHz, $CDCl_3$): δ = 169.7 (C_q), 153.5 (C_q), 141.9 (C_q), 139.7 (C_q), 137.1 (C_q), 134.5 (C_q), 130.3 (CH), 129.7 (CH), 129.2 (CH), 128.8 (CH), 128.5 (CH), 128.3 (CH), 128.1 (CH), 126.9 (CH), 126.1 (CH), 125.9 (CH), 120.6 (CH), 54.3 (CH_2), 51.8 (C_q), 37.9 (CH_2), 35.3 (CH_2), 27.9 (CH_3). (ESI) *m/z* (relative intensity): 871 (10) $[2M+Na]^+$, 463 (16) $[M+K]^+$, 447 (29) $[M+Na]^+$, 425 (100) $[M+H]^+$. HR-MS (ESI) *m/z* calcd for $C_{27}H_{29}N_4O$ $[M+H]^+$ 425.2336, found 425.2340.

2-Phenethyl-*N*-[(1-phenyl-1*H*-1,2,3-triazol-4-yl)methyl]benzamide (3ba)

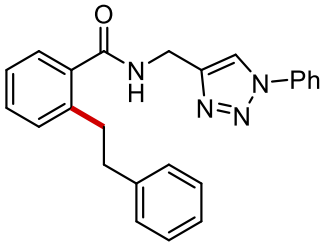

The representative procedure was followed using **1b** (55.7 mg, 0.20 mmol) and styrene **2a** (69 µL, 0.60 mmol). Purification by column chromatography on silica gel (*n*-Hexane/EtOAc 1:1) yielded **3ba** (45.1 mg, 59%) as a white solid. M.p. = 132-134 °C. ^{1}H-NMR (400 MHz, $CDCl_3$): δ = 8.08 (s, 1H), 7.70 – 7.68 (m, 2H), 7.55 – 7.50 (m, 2H), 7.48 – 7.44 (m, 1H), 7.39 – 7.35 (m, 2H), 7.26 – 7.13 (m, 5H), 7.10 – 7.07 (m, 2H), 6.23 (bs, 1H), 4.70 (d, *J* = 5.9 Hz, 2H), 3.10 (dd, *J* = 9.2, 6.5 Hz, 2H), 2.91 (dd, *J* = 9.2, 6.5 Hz, 2H). ^{13}C-NMR (101 MHz, $CDCl_3$): δ = 170.2 (C_q), 145.3 (C_q), 141.6 (C_q), 139.9 (C_q), 137.0 (C_q), 135.9 (C_q), 130.4 (CH), 130.2 (CH), 129.8 (CH), 128.8 (CH), 128.6 (CH), 128.3 (CH), 126.9 (CH), 126.1 (CH), 125.9 (CH), 120.6 (CH), 120.5 (CH), 38.1 (CH_2), 35.4 (CH_2), 35.2 (CH_2). MS (ESI) *m/z* (relative intensity): 787 (27) $[2M+Na]^+$, 593 (43), 405 (66) $[M+Na]^+$, 383 (100) $[M+H]^+$, 208 (12). HR-MS (ESI) *m/z* calcd for $C_{24}H_{23}N_4O$ $[M+H]^+$ 383.1866, found 383.1871.

***N*-[(1-Butyl-1*H*-1,2,3-triazol-4-yl)methyl]-2-phenethylbenzamide (3ca)**

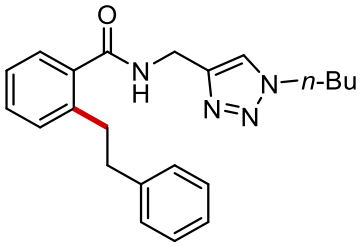

The representative procedure was followed using **1c** (51.7 mg, 0.20 mmol) and styrene **2a** (69 µL, 0.60 mmol). Purification by column chromatography on silica gel (*n*-Hexane/EtOAc 1:1) yielded **3ca** (41.3 mg, 57%) as a white solid. M.p. = 91-93 °C. ^{1}H-NMR (400 MHz, $CDCl_3$): δ = 7.59 (s, 1H), 7.37 – 7.32 (m, 2H), 7.27 – 7.16 (m, 5H), 7.12 – 7.09 (m, 2H), 6.24 (bs, 1H), 4.62 (d, *J* = 5.8 Hz, 2H), 4.28 (t, *J* = 7.2 Hz, 2H), 3.07 (dd, *J* = 9.3, 6.5 Hz, 2H), 2.89 (dd, *J* = 9.3, 6.5 Hz, 2H), 1.84 (quint, *J* = 7.2 Hz, 2H), 1.34 (sest, *J* = 7.4 Hz, 2H), 0.95 (t, *J* = 7.4 Hz, 3H). ^{13}C-NMR (101 MHz, $CDCl_3$): δ = 170.2 (C_q), 144.1 (C_q), 141.6 (C_q), 140.0 (C_q), 135.8 (C_q), 130.4 (CH), 130.2 (CH), 128.6 (CH), 128.3 (CH), 127.0 (CH), 126.2 (CH), 126.0 (CH), 122.7 (CH), 50.5 (CH_2), 38.0 (CH_2), 35.2 (CH_2), 34.9 (CH_2), 32.1 (CH_2), 19.7 (CH_2), 13.4 (CH_3). MS (ESI) *m/z* (relative intensity): 747 (18) $[2M+Na]^+$, 385 (44) $[M+Na]^+$, 363 (100) $[M+H]^+$. HR-MS (ESI) *m/z* calcd for $C_{22}H_{27}N_4O$ $[M+H]^+$ 363.2179, found 363.2183.

***N*-[(1-Benzyl-1*H*-1,2,3-triazol-4-yl)methyl]-2-(4-methylphenethyl)benzamide (3ab)**

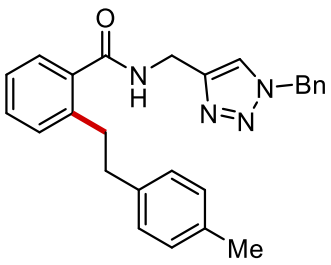

The representative procedure was followed using **1a** (58.5 mg, 0.20 mmol) and 4-methylstyrene **2b** (79 µL, 0.60 mmol). Purification by column chromatography on silica gel (*n*-Hexane/EtOAc 1:1) yielded **3ab** (53.4 mg, 65%) as a white solid. M.p. = 138-140 °C. ^{1}H-NMR (400 MHz, $CDCl_3$): δ = 7.53 (s, 1H),

7.39 – 7.29 (m, 5H), 7.27 – 7.18 (m, 4H), 7.06 (d, *J* = 7.7 Hz, 2H), 6.96 (d, *J* = 8.0 Hz, 2H), 6.18 (t, *J* = 5.9 Hz, 1H), 5.44 (s, 2H), 4.57 (d, *J* = 5.8 Hz, 2H), 3.01 (dd, *J* = 9.1, 6.5 Hz, 2H), 2.82 (dd, *J* = 9.1, 6.5 Hz, 2H), 2.31 (s, 3H). ^{13}C-NMR (101 MHz, $CDCl_3$): δ = 170.2 (C_q), 145.0 (C_q), 139.9 (C_q), 138.5 (C_q), 136.0 (C_q), 135.4 (C_q), 134.5 (C_q), 130.3 (CH), 130.1 (CH), 129.1 (CH), 129.0 (CH), 128.8 (CH), 128.5 (CH), 128.1 (CH), 126.9 (CH), 126.1 (CH), 122.2 (CH), 54.2 (CH_2), 37.5 (CH_2), 35.4 (CH_2), 35.2 (CH_2), 21.0 (CH_3). (ESI) *m/z* (relative intensity): 843 (30) $[2M+Na]^+$, 449 (13) $[M+K]^+$, 433 (52) $[M+Na]^+$, 411 (100) $[M+H]^+$. HR-MS (ESI) *m/z* calcd for $C_{26}H_{27}N_4O$ $[M+H]^+$ 411.2179, found 411.2181.

_N_-[(1-Benzyl-1_H_-1,2,3-triazol-4-yl)methyl]-2-[4-(tert-butyl)phenethyl]benzamide (3ac)

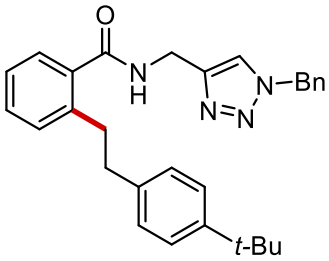

The representative procedure was followed using **1a** (58.5 mg, 0.20 mmol) and 4-*tert*-butylstyrene **2c** (110 µL, 0.60 mmol). Purification by column chromatography on silica gel (*n*-Hexane/EtOAc 1:1) yielded **3ac** (39.8 mg, 44%) as a white solid. M.p. = 129-131 °C. ^{1}H-NMR (400 MHz, $CDCl_3$): δ = 7.54 (s, 1H), 7.43 – 7.29 (m, 7H), 7.28 – 7.19 (m, 4H), 7.04 (d, *J* = 8.2 Hz, 2H), 6.20 (bs, 1H), 5.44 (s, 2H), 4.60 (d, *J* = 5.8 Hz, 2H), 3.02 (dd, *J* = 9.6, 6.4 Hz, 2H), 2.83 (dd, *J* = 9.6, 6.4 Hz, 2H), 1.32 (s, 9H). ^{13}C-NMR (101 MHz, $CDCl_3$): δ = 170.2 (C_q), 148.8 (C_q), 145.0 (C_q), 140.0 (C_q), 138.6 (C_q), 135.9 (C_q), 134.4 (C_q), 130.3 (CH), 130.1 (CH), 129.2 (CH), 128.8 (CH), 128.2 (CH), 128.0 (CH), 126.9 (CH), 126.1 (CH), 125.2 (CH), 122.3 (CH), 54.2 (CH_2), 37.4 (CH_2), 35.4 (CH_2), 35.0 (CH_2), 34.9 (C_q), 31.4 (CH_3). (ESI) *m/z* (relative intensity): 927 (37) $[2M+Na]^+$, 491 (20) $[M+K]^+$, 475 (39) $[M+Na]^+$, 453 (100) $[M+H]^+$. HR-MS (ESI) *m/z* calcd for $C_{29}H_{33}N_4O$ $[M+H]^+$ 453.2649, found 453.2647.

2-{2-[(1,1'-Biphenyl)-4-yl]ethyl}-_N_-((1-benzyl-1_H_-1,2,3-triazol-4-yl)methyl) benzamide (3ad)

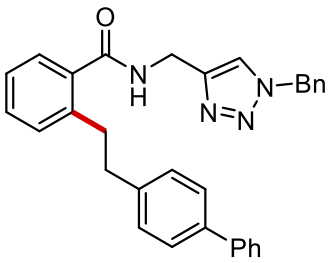

The representative procedure was followed using **1a** (58.5 mg, 0.20 mmol) and 4-vinyl-1,1'-biphenyl **2d** (108.2 mg, 0.60 mmol). Purification by column chromatography on silica gel (*n*-Hexane/EtOAc 1:1) yielded **3ad** (70.0 mg, 74%) as a white solid. M.p. = 155-156 °C. ^{1}H-NMR (400 MHz, $CDCl_3$): δ = 7.59 (dd, *J* = 8.3, 1.3 Hz, 2H), 7.51 – 7.49 (m, 3H), 7.45 (t, *J* = 7.6 Hz, 2H), 7.37 – 7.33 (m, 6H), 7.27 (bs, 1H), 7.26 – 7.20 (m, 4H), 7.16 (d, *J* = 8.2 Hz, 2H), 5.42 (s, 2H), 4.61 (d, *J* = 5.7 Hz, 2H), 3.09 (dd, *J* = 9.2, 6.4 Hz, 2H), 2.91 (dd, *J* = 9.3, 6.4 Hz, 2H). ^{13}C-NMR (101 MHz, $CDCl_3$): δ = 170.1 (C_q), 144.9 (C_q), 140.9 (C_q), 140.8 (C_q), 139.9 (C_q), 138.8 (C_q),

135.9 (C_q), 134.5 (C_q), 130.4 (CH), 130.2 (CH), 129.1 (2 x CH), 128.8 (2 x CH), 128.1 (CH), 127.1 (CH), 127.0 (2 x CH), 126.9 (CH), 126.2 (CH), 122.1 (CH), 54.2 (CH_2), 37.6 (CH_2), 35.5 (CH_2), 35.1 (CH_2). (ESI) *m/z* (relative intensity): 495 (28) $[M+Na]^+$, 473 (100) $[M+H]^+$. HR-MS (ESI) *m/z* calcd for $C_{31}H_{29}N_4O$ $[M+H]^+$ 473.2336, found 473.2333.

_N_-[(1-Benzyl-1_H_-1,2,3-triazol-4-yl)methyl]-2-(4-methoxyphenethyl)benzamide (3ae)

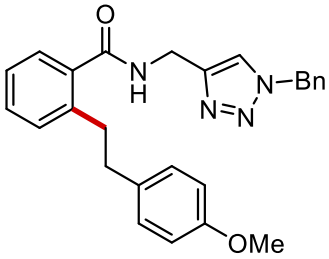

The representative procedure was followed using **1a** (58.5 mg, 0.20 mmol) and 4-methoxystyrene **2e** (80 µL, 0.60 mmol). Purification by column chromatography on silica gel (*n*-Hexane/EtOAc 1:1) yielded **3ae** (38.4 mg, 45%) as a white solid. M.p. = 114-116 °C. ^{1}H-NMR (400 MHz, $CDCl_3$): δ = 7.53 (s, 1H), 7.37 – 7.30 (m, 5H), 7.26 – 7.18 (m, 4H), 6.98 (d, *J* = 8.6 Hz, 2H), 6.79 (d, *J* = 8.6 Hz, 2H), 6.18 (t, *J* = 5.8 Hz, 1H), 5.46 (s, 2H), 4.59 (d, *J* = 5.7 Hz, 2H), 3.78 (s, 3H), 3.01 (dd, *J* = 8.9, 6.6 Hz, 2H), 2.80 (dd, *J* = 9.0, 6.6 Hz, 2H). ^{13}C-NMR (101 MHz, $CDCl_3$): δ = 170.1 (C_q), 157.9 (C_q), 145.0 (C_q), 139.9 (C_q), 136.0 (C_q), 134.5 (C_q), 133.6 (C_q), 130.4 (CH), 130.1 (CH), 129.5 (CH), 129.2 (CH), 128.8 (CH), 128.1 (CH), 126.9 (CH), 126.1 (CH), 122.2 (CH), 113.7 (CH), 55.3 (CH_3), 54.2 (CH_2), 37.0 (CH_2), 35.4 (CH_2), 35.3 (CH_2). (ESI) *m/z* (relative intensity): 875 (28) $[2M+Na]^+$, 465 (16) $[M+K]^+$, 449 (100) $[M+Na]^+$, 427 (88) $[M+H]^+$. HR-MS (ESI) *m/z* calcd for $C_{26}H_{27}N_4O_2$ $[M+H]^+$ 427.2129, found 427.2124.

_N_-[(1-Benzyl-1_H_-1,2,3-triazol-4-yl)methyl]-2-(4-chlorophenethyl)benzamide (3af)

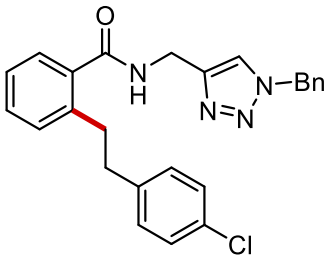

The representative procedure was followed using **1a** (58.5 mg, 0.20 mmol) and 4-chlorostyrene **2f** (76 µL, 0.60 mmol). Purification by column chromatography on silica gel (*n*-Hexane/EtOAc 1:1) yielded **3af** (56.9 mg, 66%) as a white solid. M.p. = 131-132 °C. ^{1}H-NMR (400 MHz, $CDCl_3$): δ = 7.53 (s, 1H), 7.38 – 7.32 (m, 5H), 7.28 – 7.23 (m, 3H), 7.21 (d, *J* = 8.3 Hz, 2H), 7.20 – 7.17 (m, 1H), 7.03 (d, *J* = 8.3 Hz, 2H), 6.32 (t, *J* = 5.5 Hz, 1H), 5.48 (s, 2H), 4.63 (d, *J* = 5.6 Hz, 2H), 3.03 (dd, *J* = 9.2, 6.5 Hz, 2H), 2.83 (dd, *J* = 9.2, 6.5 Hz, 2H). ^{13}C-NMR (101 MHz, $CDCl_3$): δ = 170.0 (C_q), 144.8 (C_q), 140.1 (C_q), 139.8 (C_q), 135.7 (C_q), 134.4 (C_q), 131.6 (C_q), 130.5 (CH), 130.2 (CH), 130.0 (CH), 129.2 (CH), 128.9 (CH), 128.3 (CH), 128.1 (CH), 127.0 (CH), 126.3 (CH), 122.1 (CH), 54.3 (CH_2), 37.2 (CH_2), 35.4 (CH_2), 35.1 (CH_2). (ESI) *m/z* (relative intensity): 883 (23) $[2M+Na]^+$, 453 (32) $[M+Na]^+$, 431 (100) $[M+H]^+$. HR-MS (ESI) *m/z* calcd for $C_{25}H_{24}ClN_4O$ $[M+H]^+$ 431.1633, found 431.1630.

_N_-[(1-Benzyl-1_H_-1,2,3-triazol-4-yl)methyl]-2-(4-fluorophenethyl)benzamide (3ag)

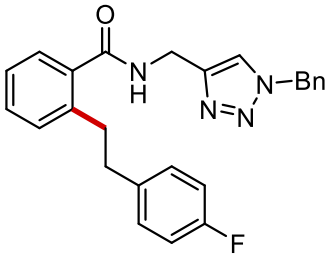

The representative procedure was followed using **1a** (58.5 mg, 0.20 mmol) and 4-fluorostyrene **2g** (72 µL, 0.60 mmol). Purification by column chromatography on silica gel (*n*-Hexane/EtOAc 1:1) yielded **3ag** (51.4 mg, 62%) as a white solid. M.p. = 121-122 °C. ^{1}H-NMR (400 MHz, $CDCl_3$): δ = 7.54 (s, 1H), 7.40 – 7.30 (m, 5H), 7.28 – 7.16 (m, 4H), 7.04 (dd, *J* = 8.5, 5.6 Hz, 2H), 6.92 (t, *J* = 8.7 Hz, 2H), 6.36 (t, *J* = 5.7 Hz, 1H), 5.48 (s, 2H), 4.63 (d, *J* = 5.7 Hz, 2H), 3.02 (dd, *J* = 9.2, 6.5 Hz, 2H), 2.83 (dd, *J* = 9.3, 6.5 Hz, 2H). ^{13}C-NMR (101 MHz, $CDCl_3$): δ = 170.0 (C_q), 161.3 (d, $^{1}J_{C\text{-}F}$ = 245 Hz, C_q), 139.8 (2 x C_q), 137.3 (d, $^{4}J_{C\text{-}F}$ = 3 Hz, C_q), 135.8 (C_q), 134.4 (C_q), 130.5 (CH), 130.2 (CH), 129.9 (d, $^{3}J_{C\text{-}F}$ = 7 Hz, CH), 129.2 (CH), 128.9 (CH), 128.6 (CH), 128.1 (CH), 127.0 (CH), 126.2 (CH), 122.1 (CH), 115.0 (d, $^{2}J_{C\text{-}F}$ = 21 Hz, CH), 54.3 (CH_2), 37.1 (CH_2), 35.4 (CH_2), 35.3 (CH_2). ^{19}F-NMR (565 MHz, $CDCl_3$): δ = -117.4 (ddd, *J* = 14.2, 8.9, 5.4 Hz). (ESI) *m/z* (relative intensity): 453 (77) $[M+K]^+$, 437 (81) $[M+Na]^+$, 415 (100) $[M+H]^+$**.** HR-MS (ESI) *m/z* calcd for $C_{25}H_{24}FN_4O$ $[M+H]^+$ 415.1929, found 415.1926.

_N_-[(1-Benzyl-1_H_-1,2,3-triazol-4-yl)methyl]-2-[4-(diphenylphosphanyl)phenethyl] benzamide (3ah)

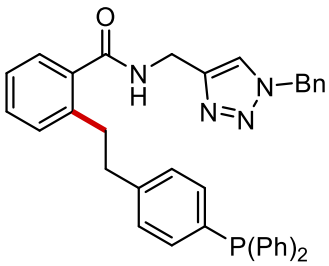

The representative procedure was followed using **1a** (58.5 mg, 0.20 mmol) and 4-(diphenylphosphino) styrene **2h** (80 µL, 0.60 mmol). Purification by column chromatography on silica gel (*n*-Hexane/EtOAc 1:1) yielded **3ah** (40.6 mg, 35%) as pale yellow waxy solid. ^{1}H-NMR (400 MHz, $CDCl_3$): δ = 7.53 (s, 1H), 7.38 – 7.29 (m, 15H), 7.26 – 7.18 (m, 6H), 7.11 (dd, *J* = 8.0, 1.5 Hz, 2H), 6.44 (bs, *J* = 5.2 Hz, 1H), 5.41 (s, 2H), 4.62 (d, *J* = 5.8 Hz, 2H), 3.03 (dd, *J* = 9.7, 6.4 Hz 2H), 2.85 (dd, *J* = 9.8, 6.3 Hz, 2H). ^{13}C-NMR (101 MHz, $CDCl_3$): δ = 170.0 (C_q), 144.8 (C_q), 142.6 (C_q), 140.0 (C_q), 137.4 (d, $J_{C\text{-}P}$ = 11 Hz, C_q), 135.7 (C_q), 134.4 (C_q), 134.2 (d, $J_{C\text{-}P}$ = 10 Hz, C_q), 133.9 (d, $J_{C\text{-}P}$ = 19 Hz, CH), 133.7 (d, $J_{C\text{-}P}$ = 19 Hz, CH), 130.4 (CH), 130.1 (CH), 129.2 (CH), 128.9 (CH), 128.8 (d, $J_{C\text{-}P}$ = 7 Hz, CH), 128.7 (CH), 128.5 (d, $J_{C\text{-}P}$ = 7 Hz, CH), 128.1 (CH), 127.0 (CH), 126.2 (CH), 122.2 (CH), 54.3 (CH_2), 37.7 (CH_2), 35.3 (CH_2), 35.1 (CH_2). ^{31}P-NMR (162 MHz, $CDCl_3$): δ = -6.29. (ESI) *m/z* (relative intensity): 603 (76) $[M+Na]^+$, 581 (100) $[M+H]^+$. HR-MS (ESI) *m/z* calcd for $C_{37}H_{34}N_4OP$ $[M+H]^+$ 581.2465, found 581.2461.

_N_-[(1-Benzyl-1_H_-1,2,3-triazol-4-yl)methyl]-2-[3-(trifluoromethyl)phenethyl] benzamide (3ai)

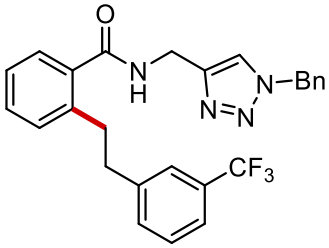

The representative procedure was followed using **1a** (58.5 mg, 0.20 mmol) and 3-(trifluoromethyl)styrene **2i** (89 µL, 0.60 mmol). Purification by column chromatography on silica gel (*n*-Hexane/EtOAc 1:1) yielded **3ai** (62.2 mg, 67%) as a white solid. M.p. = 149-150 °C. ^{1}H-NMR (400 MHz, $CDCl_3$): δ = 7.58 (bs, 1H), 7.44 (d, *J* = 7.7 Hz, 1H), 7.38 – 7.29 (m, 8H), 7.26 – 7.21 (m, 3H), 7.18 (d, *J* = 7.6, 1H), 6.42 (s, 1H), 5.49 (s, 2H), 4.65 (s, 2H), 3.08 – 3.04 (m, 2H), 2.95-2.91 (m, 2H). ^{13}C-NMR (101 MHz, $CDCl_3$): δ = 169.9 (C_q), 142.6 (C_q), 139.7 (C_q), 135.7 (C_q), 134.4 (C_q), 132.1 (2 x CH), 130.6 (C_q), 130.5 (CH), 130.5 (q, $^{2}J_{C\text{-}F}$ = 4 Hz, C_q), 130.3 (CH), 129.1 (CH), 128.9 (CH), 128.7 (CH), 128.1 (CH), 127.1 (CH), 126.4 (CH), 125.3 (q, $^{4}J_{C\text{-}F}$ = 4 Hz, CH), 124.3 (q, $^{1}J_{C\text{-}F}$ = 272 Hz, C_q), 122.8 (q, $^{3}J_{C\text{-}F}$ = 4 Hz, CH), 54.6 (CH_2), 37.7 (CH_2), 35.21 (CH_2), 29.7 (CH_2). ^{19}F-NMR (565 MHz, $CDCl_3$): δ = -62.3 (s). (ESI) *m/z* (relative intensity): 951 (14) $[2M+Na]^+$, 487 (100) $[M+Na]^+$, 465 (33) $[M+H]^+$. HR-MS (ESI) *m/z* calcd for $C_{26}H_{24}F_3N_4O$ $[M+H]^+$ 465.1897, found 465.1900.

_N_-[(1-Benzyl-1_H_-1,2,3-triazol-4-yl)methyl]-2-(3-fluoro-4-methoxyphenethyl) benzamide (3aj)

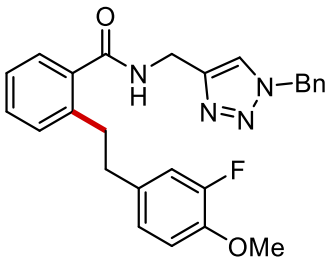

The representative procedure was followed using **1a** (58.5 mg, 0.20 mmol) and 3-fluoro-4-methoxystyrene **2j** (91.1 mg, 0.60 mmol). Purification by column chromatography on silica gel (*n*-Hexane/EtOAc 1:1) yielded **3aj** (49.8 mg, 56%) as a white solid. M.p. = 87-89 °C. ^{1}H-NMR (400 MHz, $CDCl_3$): δ = 7.55 (s, 1H), 7.38 – 7.32 (m, 6H), 7.27 – 7.26 (m, 1H), 7.24 – 7.18 (m, 2H), 6.86 – 6.81 (m, 2H), 6.76 (dd, *J* = 8.0 Hz, *J* = 4 Hz, 1H), 6.33 (bs, 1H), 5.50 (s, 2H), 4.64 (d, *J* = 5.7 Hz, 2H), 3.86 (s, 3H), 3.01 (dd, *J* = 9.2, 6.5 Hz, 2H), 2.79 (dd, *J* = 9.2, 6.5 Hz, 2H). ^{13}C-NMR (101 MHz, $CDCl_3$): δ = 170.0 (C_q), 153.4 (d, $^{1}J_{C\text{-}F}$ = 245 Hz C_q), 151.0 (C_q), 144.8 (C_q), 139.8 (C_q), 135.8 (C_q), 134.8 (d, $^{3}J_{C\text{-}F}$ = 7 Hz, C_q), 134.5 (C_q), 130.4 (CH), 130.2 (CH), 129.2 (CH), 128.8 (CH), 128.1 (CH), 126.9 (CH), 126.2 (CH), 124.1 (d, $^{4}J_{C\text{-}F}$ = 3 Hz, CH), 122.1 (CH), 116.2 (d, $^{2}J_{C\text{-}F}$ = 18 Hz, CH) 113.2 (d, $^{5}J_{C\text{-}F}$ = 2 Hz, CH), 56.3 (CH_3), 54.2 (CH_2), 37.0 (CH_2), 35.4 (CH_2), 35.2 (CH_2). ^{19}F-NMR (565 MHz, $CDCl_3$): δ= -135.53 (dd, *J* = 12.5, 8.7 Hz). (ESI) *m/z* (relative intensity): 445 (100) $[M+H]^+$. HR-MS (ESI) *m/z* calcd for $C_{26}H_{26}FN_4O_2$ $[M+H]^+$ 445.2034, found 445.2037.

_N_-[(1-Benzyl-1_H_-1,2,3-triazol-4-yl)methyl]-2-(2-fluorophenethyl)benzamide (3ak)

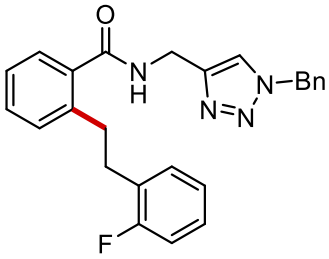

The representative procedure was followed using **1a** (58.5 mg, 0.20 mmol) and 2-fluorostyrene **2k** (73.3 mg, 0.60 mmol). Purification by column chromatography on silica gel (*n*-Hexane/EtOAc 1:1) yielded **3ak** (53.9 mg, 65%) as a white solid. M.p.= 128-130 °C. ^{1}H-NMR (400 MHz, $CDCl_3$): δ = 7.56 (s, 1H), 7.37 (dd, *J* = 5.0, 1.8 Hz, 3H), 7.32 (d, *J* = 7.4 Hz, 2H), 7.26 (dd, *J* = 4.5, 1.7 Hz, 2H), 7.24 – 7.18 (m, 2H), 7.17 – 7.13 (m, 1H), 7.06 (td, *J* = 7.5, 2.1 Hz, 1H), 7.01 (dd, *J* = 7.3, 1.2 Hz, 1H), 6.99 – 6.94 (m, 1H), 6.29 (bs, 1H), 5.50 (s, 2H), 4.64 (d, *J* = 5.7 Hz, 2H), 3.05 (dd, *J* = 9.2, 6.4 Hz, 2H), 2.90 (dd, *J* = 9.3, 6.4 Hz, 2H). ^{13}C-NMR (101 MHz, $CDCl_3$): δ = 170.0 (C_q), 161.1 (d, $^{1}J_{C\text{-}F}$ = 244 Hz C_q), 145.0 (C_q), 139.7 (C_q), 135.9 (C_q), 134.5 (C_q), 130.9 (d, $^{4}J_{C\text{-}F}$ = 5 Hz , CH), 130.5 (CH), 130.1 (CH), 129.1 (CH), 128.8 (CH), 128.3 (d, $^{3}J_{C\text{-}F}$ = 16 Hz C_q), 128.1 (CH), 127.7 (d, $^{6}J_{C\text{-}F}$ = 8 Hz , CH) , 126.9 (CH), 126.2 (CH), 123.9 (d, $^{5}J_{C\text{-}F}$ = 3 Hz , CH), 122.2 (CH), 115.1 (d, $^{2}J_{C\text{-}F}$ = 22 Hz , CH), 54.2 (CH_2), 35.4 (CH_2), 33.7 (CH_2), 31.0 (d, $^{7}J_{C\text{-}F}$ = 2 Hz, CH_2). ^{19}F-NMR (565 MHz, $CDCl_3$): δ = -118.75 (q, *J* = 8.8, 7.9 Hz). (ESI) *m/z* (relative intensity): 851 (16) $[2M+Na]^+$, 437 (27) $[M+Na]^+$, 415 (100) $[M+H]^+$. HR-MS (ESI) *m/z* calcd for $C_{25}H_{24}FN_4O$ $[M+H]^+$ 415.1929, found 415.1933.

2-[2-(Naphthalen-1-yl)ethyl]-_N_-[(1-phenyl-1_H_-1,2,3-triazol-4-yl)methyl]benzamide (3bl)

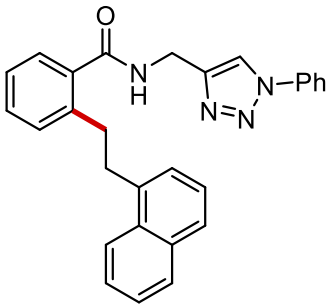

The representative procedure was followed using **1b** (55.6 mg, 0.20 mmol) and 1-vinylnaphthalene **2l** (89 µL, 0.60 mmol). Purification by column chromatography on silica gel (*n*-Hexane/EtOAc 1:1) yielded **3bl** (51.0 mg, 59%) as a white solid. M.p. = 143-145 °C. ^{1}H-NMR (400 MHz, $CDCl_3$): δ = 8.18 (d, *J* = 8.8 Hz, 1H), 8.00 (s, 1H), 7.85 (d, *J* = 8.4 Hz, 1H), 7.71 (d, *J* = 7.9 Hz, 1H), 7.60 – 7.57 (m, 2H), 7.56 – 7.51 (m, 1H), 7.50 – 7.37 (m, 5H), 7.35 – 7.30 (m, 3H), 7.24 (td, *J* = 7.4, 1.2 Hz, 1H), 7.17 (d, *J* = 6.8 Hz, 1H), 6.16 (t, *J* = 5.9 Hz, 1H), 4.52 (d, *J* = 5.8 Hz, 2H), 3.40 (dd, *J* = 9.3, 6.4 Hz, 2H), 3.24 (dd, *J* = 9.3, 6.4 Hz, 2H). ^{13}C-NMR (101 MHz, $CDCl_3$): δ = 170.2 (C_q), 145.3 (C_q), 140.3 (C_q), 137.7 (C_q), 136.9 (C_q), 136.0 (C_q), 133.8 (C_q), 131.9 (C_q), 130.5 (CH), 130.3 (CH), 129.7 (CH), 128.8 (CH), 128.7 (CH), 126.8 (CH), 126.8 (CH), 126.3 (CH), 126.2 (CH), 126.0 (CH), 125.6 (CH), 125.5 (CH), 124.0 (CH), 120.6 (CH), 120.4 (CH), 35.4 (CH_2), 35.1 (CH_2), 34.6 (CH_2). (ESI) *m/z* (relative intensity): 455 (100) $[M+Na]^+$, 433 (47) $[M+H]^+$. HR-MS (ESI) *m/z* calcd for $C_{28}H_{25}N_4O$ $[M+H]^+$ 433.2023, found 433.2025.

_N_-[(1-Benzyl-1_H_-1,2,3-triazol-4-yl)methyl]-2-[2-(thiophen-2-yl)ethyl]benzamide (3am)

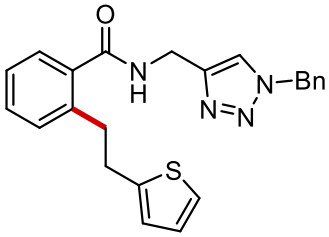

The representative procedure was followed using **1a** (58.5 mg, 0.20 mmol) and 2-vinylthiophene **2m** (66.1 mg, 0.60 mmol). Purification by column chromatography on silica gel (*n*-Hexane/EtOAc 1:1) yielded **3am** (33.8 mg, 42%) as a white solid. M.p. = 101-103 °C. ^{1}H-NMR (400 MHz, $CDCl_3$): δ = 7.56 (s, 1H), 7.39 – 7.32 (m, 5H), 7.27 – 7.20 (m, 4H), 7.09 (dd, *J* = 5.1, 1.2 Hz, 1H), 6.88 (dd, *J* = 5.1, 3.4 Hz, 1H), 6.66 (dd, *J* = 3.4, 1.1 Hz, 1H), 6.29 (s, 1H), 5.48 (s, 2H), 4.64 (d, *J* = 5.8 Hz, 2H), 3.09 (s, 4H). ^{13}C-NMR (101 MHz, $CDCl_3$): δ = 170.0 (C_q), 145.0 (C_q), 144.2 (C_q), 139.3 (C_q), 136.0 (C_q), 134.5 (C_q), 130.3 (CH), 130.2 (CH), 129.2 (CH), 128.8 (CH), 128.1 (CH), 126.9 (CH), 126.8 (CH), 126.3 (CH), 124.6 (CH), 123.2 (CH), 122.2 (CH), 54.2 (CH_2), 35.4 (CH_2), 35.4 (CH_2), 31.8 (CH_2). (ESI) *m/z* (relative intensity): 827 (20) $[2M+Na]^+$, 452 (17), 441 (30) $[M+K]^+$, 425 (100) $[M+Na]^+$, 403 (44) $[M+H]^+$. HR-MS (ESI) *m/z* calcd for $C_{23}H_{23}N_4OS$ $[M+H]^+$ 403.1587, found 403.1595.

2-[2-(Benzo[*b*]thiophen-2-yl)ethyl]-_N_-[(1-benzyl-1_H_-1,2,3-triazol-4-yl)methyl]benzamide (3an)

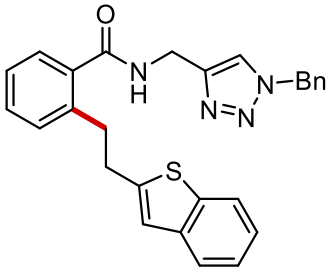

The representative procedure was followed using **1a** (58.5 mg, 0.20 mmol) and 2-vinylbenzo[*b*]thiophene **2n** (96.1 mg, 0.60 mmol). Purification by column chromatography on silica gel (*n*-Hexane/EtOAc 1:1) yielded **3an** (40.7 mg, 45%) as a white solid. M.p. = 94-96 °C. ^{1}H-NMR (400 MHz, $CDCl_3$): δ = 7.76 (d, *J* = 8.2 Hz, 1H), 7.66 (d, *J* = 8.0 Hz, 1H), 7.51 (s, 1H), 7.36 – 7.31 (m, 6H), 7.27 – 7.23 (m, 3H), 7.22 – 7.17 (m, 2H), 6.93 (s, 1H), 6.40 (bs, 1H), 5.39 (s, 2H), 4.60 (d, *J* = 5.8 Hz, 2H), 3.22 – 3.12 (m, 4H). ^{13}C-NMR (101 MHz, $CDCl_3$): δ = 170.0 (C_q), 145.3 (C_q), 144.9 (C_q), 140.1 (C_q), 139.4 (C_q), 139.3 (C_q), 135.8 (C_q), 134.4 (C_q), 130.4 (CH), 130.3 (CH), 129.1 (CH), 128.8 (CH), 128.1 (CH), 127.0 (CH), 126.4 (CH), 125.8 (CH), 124.1 (CH), 123.6 (CH), 122.8 (CH), 122.1 (CH), 121.0 (CH), 54.2 (CH_2), 35.3 (CH_2), 34.8 (CH_2), 32.6 (CH_2). (ESI) *m/z* (relative intensity): 927 (43) $[2M+Na]^+$, 475 (100) $[M+Na]^+$. HR-MS (ESI) *m/z* calcd for $C_{27}H_{24}N_4NaOS$ $[M+Na]^+$ 475.1743, found 475.1748.

_N_-[(1-Benzyl-1_H_-1,2,3-triazol-4-yl)methyl]-2-(2-(ferocenyl)ethyl)benzamide (3ao)

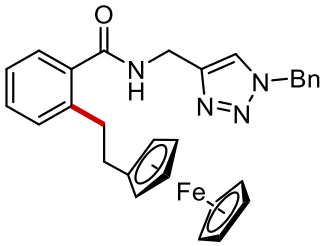

The representative procedure was followed using **1a** (58.5 mg, 0.20 mmol) and vinylferrocene **2o** (127.2 mg, 0.60 mmol). Purification by column chromatography on silica gel (*n*-Hexane/EtOAc 1:1) yielded **3ao** (37.3 mg, 37%) as an orange viscous oil. ^{1}H-NMR (400 MHz, $CDCl_3$): δ = 7.52 (s, 1H), 7.42 – 7.33 (m, 5H), 7.26 – 7.18 (m, 4H), 6.13 (bs, 1H), 5.48 (s, 2H), 4.58 (d, *J* = 5.7 Hz, 2H), 4.18 (s, 1H), 4.11 (s, 4H), 4.01 (s, 2H), 3.91 (s, 2H), 2.89 (t, *J* = 7.7 Hz, 2H), 2.61 (t, *J* = 7.6 Hz, 2H). ^{13}C-NMR (101 MHz, $CDCl_3$): δ = 170.2 (C_q), 145.0 (C_q), 139.9 (C_q), 136.2 (C_q), 134.6 (C_q), 130.1 (CH), 130.0 (CH), 129.2 (CH), 128.8 (CH), 128.2 (CH), 126.9 (CH), 126.0 (CH), 122.3 (CH), 88.3 (C_q), 68.8 (CH), 68.7 (CH), 68.4 (CH), 67.4 (CH), 54.2 (CH_2), 35.4 (CH_2), 34.5 (CH_2), 31.9 (CH_2). (ESI) *m/z* (relative intensity): 1031 (12) $[2M+Na]^+$, 543 (18) $[M+K]^+$, 527 (41) $[M+Na]^+$, 505 (100) $[M+H]^+$. HR-MS (ESI) *m/z* calcd for $C_{29}H_{29}FeN_4O$ $[M+H]^+$ 505.1686, found 505.1682.

_N_-[(1-Benzyl-1_H_-1,2,3-triazol-4-yl)methyl]-4-methyl-2-phenethylbenzamide (3da)

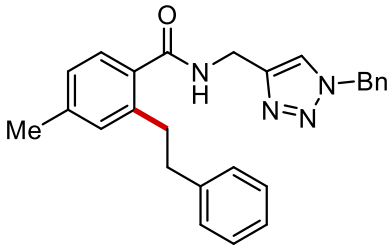

The representative procedure was followed using **1d** (61.3 mg, 0.20 mmol) and styrene **2a** (69 µL, 0.60 mmol). Purification by column chromatography on silica gel (*n*-Hexane/EtOAc 1:1) yielded **3da** (52.5 mg, 64%) as a white solid. M.p. = 125-127. ^{1}H-NMR (400 MHz, $CDCl_3$): δ = 7.52 (s, 1H), 7.37 – 7.35 (m, 3H), 7.26 – 7.23 (m, 4H), 7.21 – 7.15 (m, 2H), 7.10 (d, *J* = 6.5 Hz, 2H), 7.05 – 7.01 (m, 2H), 6.12 (s, 1H), 5.45 (s, 2H), 4.58 (d, *J* = 5.7 Hz, 2H), 3.02 (dd, *J* = 9.4, 6.4 Hz, 2H), 2.85 (dd, *J* = 9.5, 6.4 Hz, 2H), 2.35 (s, 3H). ^{13}C-NMR (101 MHz, $CDCl_3$): δ = 170.2 (C_q), 145.1 (C_q), 141.8 (C_q), 140.2 (C_q), 140.0 (C_q), 134.5 (C_q), 133.0 (C_q), 131.2 (CH), 129.1 (CH), 128.8 (CH), 128.6 (CH), 128.3 (CH), 128.1 (CH), 127.0 (CH), 126.7 (CH), 125.9 (CH), 122.2 (CH), 54.2 (CH_2), 38.1 (CH_2), 35.4 (CH_2), 35.2 (CH_2), 21.3 (CH_3). (ESI) *m/z* (relative intensity): 843 (27) $[2M+Na]^+$, 433 (40) $[M+Na]^+$, 411 (100) $[M+H]^+$. HR-MS (ESI) *m/z* calcd for $C_{26}H_{27}N_4O$ $[M+H]^+$ 411.2179 found 411.2181.

_N_-[(1-Benzyl-1_H_-1,2,3-triazol-4-yl)methyl]-3-phenethyl-[1,1'-biphenyl]-4-carboxamide (3ea)

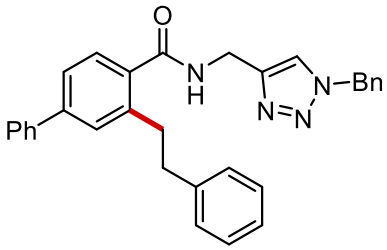

The representative procedure was followed using **1e** (73.7 mg, 0.20 mmol) and styrene **2a** (69 µL, 0.60 mmol). Purification by column chromatography on silica gel (*n*-Hexane/EtOAc 6:4) yielded **3ea** (58.6 mg, 62%) as a white solid. M.p. = 163-165 °C. ^{1}H-NMR (400 MHz, $CDCl_3$): δ = 7.57 – 7.52 (m, 3H), 7.49 – 7.40 (m, 6H), 7.40 – 7.35 (m, 4H), 7.27 – 7.25 (m, 3H), 7.22 – 7.17 (m, 1H), 7.13 – 7.08 (m, 2H), 6.27 (bs, 1H), 5.46 (s, 2H), 4.62 (d, *J* = 5.7 Hz, 2H), 3.12 (dd, *J* = 9.1, 6.5 Hz, 2H), 2.92 (dd, *J* = 9.0, 6.5 Hz, 2H). ^{13}C-NMR (101 MHz, $CDCl_3$): δ = 169.9 (C_q), 145.0 (C_q), 142.9 (C_q), 141.6 (C_q), 140.5 (C_q), 140.3 (C_q), 134.7 (C_q), 134.5 (C_q), 129.3 (CH), 129.2 (CH), 128.8 (2 x CH), 128.7 (CH), 128.4 (CH), 128.1 (CH), 127.8 (CH), 127.5 (CH), 127.2 (CH), 126.0 (CH), 124.8 (CH), 122.2 (CH), 54.2 (CH_2), 38.0 (CH_2), 35.5 (CH_2), 35.4 (CH_2). (ESI) *m/z* (relative intensity): 495 (47) $[M+Na]^+$, 473 (100) $[M+H]^+$. HR-MS (ESI) *m/z* calcd for $C_{31}H_{29}N_4O$ $[M+H]^+$ 473.2336 found 473.2339.

_N_-[(1-Benzyl-1_H_-1,2,3-triazol-4-yl)methyl]-4-fluoro-2-phenethylbenzamide (3fa)

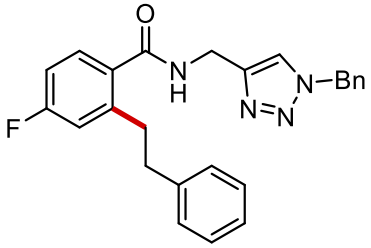

The representative procedure was followed using **1f** (62.1 mg, 0.20 mmol) and styrene **2a** (69 µL, 0.60 mmol). Purification by column chromatography on silica gel (*n*-Hexane/EtOAc 1:1) yielded **3fa** (47.3 mg, 57%) as a white solid. M.p. = 110-112 °C. ^{1}H-NMR (400 MHz, $CDCl_3$): δ = 7.52 (s, 1H), 7.38-7.36 (m, 4H), 7.27 – 7.23 (m, 4H), 7.19 – 7.16 (m, 1H), 7.07 (d, *J* = 6.9 Hz, 2H), 6.94 – 6.87 (m, 2H), 6.15 (t, *J* = 5.7 Hz, 1H), 5.46 (s, 2H), 4.57 (d, *J* = 5.7 Hz, 2H), 3.05 (dd, *J* = 8.9, 6.6 Hz, 2H), 2.86 (dd, *J* = 9.0, 6.5 Hz, 2H). ^{13}C-NMR (101 MHz, $CDCl_3$): δ = 169.2 (C_q), 163.4 (d, $^{1}J_{C\text{-}F}$ = 250 Hz C_q), 144.7 (C_q), 143.2 (d, $^{5}J_{C\text{-}F}$ = 9 Hz, C_q), 141.1 (C_q), 134.3 (C_q), 132.1 (d, $^{6}J_{C\text{-}F}$ = 3 Hz, C_q), 129.2 (CH), 129.0 (d, $^{4}J_{C\text{-}F}$ = 8 Hz, CH), 128.9 (CH), 128.6 (CH), 128.4 (CH), 128.2 (CH), 126.1 (CH), 122.2 (CH), 117.1 (d, $^{2}J_{C\text{-}F}$ = 21 Hz CH), 113.1 (d, $^{3}J_{C\text{-}F}$ = 21 Hz CH), 54.3 (CH_2), 37.6 (CH_2), 35.3 (CH_2), 35.0 (CH_2). ^{19}F-NMR (565 MHz, $CDCl_3$): δ= -110.28 – -110.36 (m). (ESI) *m/z* (relative intensity): 437 (39) $[M+Na]^+$, 415 (100) $[M+H]^+$. HR-MS (ESI) *m/z* calcd for $C_{25}H_{24}FN_4O$ $[M+H]^+$ 415.1929, found 415.1932.

_N_-[(1-Benzyl-1_H_-1,2,3-triazol-4-yl)methyl]-4-chloro-2-phenethylbenzamide (3ga)

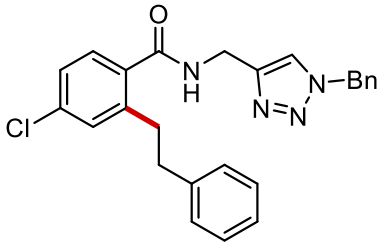

The representative procedure was followed using **1g** (65.4 mg, 0.20 mmol) and styrene **2a** (69 µL, 0.60 mmol). Purification by column chromatography on silica gel (*n*-Hexane/EtOAc 1:1) yielded **3ga** (43.1 mg, 50%) as a white solid. M.p. = 127-129 °C. ^{1}H-NMR (400 MHz, $CDCl_3$): δ = 7.51 (s, 1H), 7.38 – 7.36 (m, 3H), 7.27 – 7.23 (m, 6H), 7.19 (dd, *J* = 7.7, 1.5 Hz, 2H), 7.07 (d, *J* = 7.3 Hz, 2H), 6.14 (bs, 1H), 5.46 (s, 2H), 4.56 (d, *J* = 5.7 Hz, 2H), 3.02 (dd, *J* = 9.1, 6.5 Hz, 2H), 2.85 (dd, *J* = 9.1, 6.5 Hz, 2H). ^{13}C-NMR (101 MHz, $CDCl_3$): δ = 169.1 (C_q), 144.7 (C_q), 142.1 (C_q), 141.1 (C_q), 135.9 (C_q), 134.4 (C_q), 134.4 (C_q), 130.4 (CH), 129.2 (CH), 128.9 (CH), 128.6 (CH), 128.4 (CH), 128.3 (CH), 128.1 (CH), 126.3 (CH), 126.1 (CH), 122.1 (CH), 54.3 (CH_2), 37.7 (CH_2), 35.4 (CH_2), 34.9 (CH_2). (ESI) *m/z* (relative intensity): 453 (36) $[M+Na]^+$, 431 (100) $[M+H]^+$. HR-MS (ESI) *m/z* calcd for $C_{25}H_{24}ClN_4O$ $[M+H]^+$ 431.1633, found 431.1635.

_N_-[(1-Benzyl-1_H_-1,2,3-triazol-4-yl)methyl]-4-bromo-2-phenethylbenzamide (3ha)

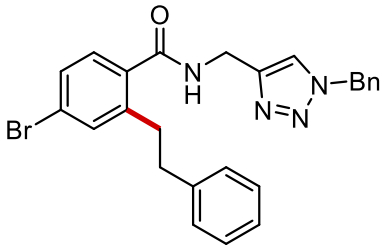

The representative procedure was followed using **1h** (74.2 mg, 0.20 mmol) and styrene **2a** (69 µL, 0.60 mmol). Purification by column chromatography on silica gel (*n*-Hexane/EtOAc 1:1) yielded **3ha** (43.7 mg, 46%) as a white solid. M.p. = 99-101 °C. ^{1}H-NMR (400 MHz, $CDCl_3$): δ = 7.51 (s, 1H), 7.39 – 7.33 (m, 5H), 7.26 – 7.23 (m, 4H), 7.19 – 7.17 (m, 2H), 7.06 (d, *J* = 6.8 Hz, 2H), 6.17 (s, 1H), 5.46 (s, 2H), 4.55 (d, *J* = 5.7 Hz, 2H), 3.00 (dd, *J* = 9.1, 6.4 Hz, 2H), 2.85 (dd, *J* = 9.2, 6.4 Hz, 2H). ^{13}C-NMR (101 MHz, $CDCl_3$): δ = 169.1 (C_q), 144.7 (C_q), 142.3 (C_q), 141.1 (C_q), 134.8 (C_q), 134.4 (C_q), 133.3 (CH), 129.2 (2 x CH), 128.9 (CH), 128.6 (CH), 128.5 (CH), 128.4 (CH), 128.1 (CH), 126.1 (CH), 124.3 (C_q), 122.1 (CH), 54.2 (CH_2), 37.7 (CH_2), 35.4 (CH_2), 34.9 (CH_2). (ESI) *m/z* (relative intensity): 497 (86) $[M+Na]^+$, 475 (100) $[M+H]^+$. HR-MS (ESI) *m/z* calcd for $C_{25}H_{24}BrN_4O$ $[M+H]^+$ 475.1128, found 475.1132.

_N_-[(1-Benzyl-1_H_-1,2,3-triazol-4-yl)methyl]-2-phenethyl-4-(trifluoromethyl) benzamide (3ia)

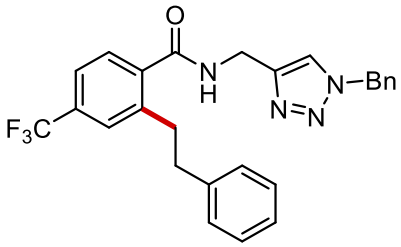

The representative procedure was followed using **1i** (61.3 mg, 0.20 mmol) and styrene **2a** (69 µL, 0.60 mmol). Purification by column chromatography on silica gel (*n*-Hexane/EtOAc 1:1) yielded **3ia** (30.7 mg, 33%) as a white solid. M.p. = 135-137 °C. ^{1}H-NMR (400 MHz, $CDCl_3$): δ =

7.53 (s, 1H), 7.48 – 7.45 (m, 2H), 7.42 (d, J = 7.8 Hz, 1H), 7.38 – 7.36 (m, 3H), 7.27 – 7.23 (m, 4H), 7.20 – 7.16 (m, 1H), 7.04 (d, J = 6.7 Hz, 2H), 6.21 (bs, 1H), 5.47 (s, 2H), 4.59 (d, J = 5.7 Hz, 2H), 3.07 (dd, J = 9.0, 6.6 Hz, 2H), 2.88 (dd, J = 8.9, 6.6 Hz, 2H). ^{13}C-NMR (101 MHz, $CDCl_3$): δ = 168.8 (C_q), 144.5 (C_q), 140.9 (C_q), 140.8 (C_q), 139.3 (C_q), 134.4 (C_q), 131.9 (q, $^2J_{C\text{-}F}$ = 33 Hz C_q), 129.2 (CH), 128.9 (CH), 128.6 (CH), 128.4 (CH), 128.1 (CH), 127.4 (CH), 127.1 (q, $^3J_{C\text{-}F}$ = 4 Hz, CH), 126.2 (CH), 123.6 (q, $^1J_{C\text{-}F}$ = 273 Hz, C_q), 123.0 (q, $^4J_{C\text{-}F}$ = 4 Hz, CH), 122.2 (CH), 54.3 (CH_2), 37.7 (CH_2), 35.4 (CH_2), 35.0 (CH_2). ^{19}F-NMR (565 MHz, $CDCl_3$): δ= -62.8 (s). (ESI) *m/z* (relative intensity): 487 (56) $[M+Na]^+$, 465 (100) $[M+H]^+$. HR-MS (ESI) *m/z* calcd for $C_{26}H_{24}F_3N_4O$ $[M+H]^+$ 465.1897 found 465.1901.

Methyl-4-{[(1-benzyl-1*H*-1,2,3-triazol-4-yl)methyl]carbamoyl}-3-phenethyl benzoate (3ja)

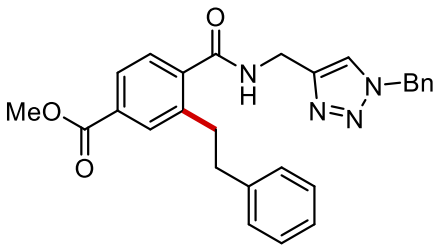

The representative procedure was followed using **1j** (70.1 mg, 0.20 mmol) and styrene **2a** (69 µL, 0.60 mmol). Purification by column chromatography on silica gel (*n*-Hexane/EtOAc 1:1) yielded **3ja** (31.8 mg, 35%) as a white solid. M.p. = 84-85 °C. ^{1}H-NMR (400 MHz, $CDCl_3$): δ = 7.95 (d, J = 1.7 Hz, 1H), 7.87 (dd, J = 7.9, 1.7 Hz, 1H), 7.52 (s, 1H), 7.39 – 7.33 (m, 5H), 7.28 – 7.21 (m, 3H), 7.20 – 7.15 (m, 1H), 7.05 (d, J = 6.8 Hz, 2H), 6.20 (bs, 1H), 5.45 (s, 2H), 4.56 (d, J = 5.7 Hz, 2H), 3.95 (s, 3H), 3.05 (dd, J = 9.2, 6.4 Hz, 2H), 2.88 (dd, J = 9.0, 6.5 Hz, 2H).^{13}C-NMR (101 MHz, $CDCl_3$): δ = 169.3 (C_q), 166.5 (C_q), 144.7 (C_q), 141.2 (C_q), 140.2 (C_q), 140.1 (C_q), 134.4 (C_q), 131.4 (C_q), 131.4 (CH), 129.2 (CH), 128.9 (CH), 128.6 (CH), 128.4 (CH), 128.1 (CH), 127.3 (CH), 127.0 (CH), 126.1 (CH), 122.2 (CH), 54.2 (CH_2), 52.3 (CH_3), 37.8 (CH_2), 35.4 (CH_2), 35.0 (CH_2). (ESI) *m/z* (relative intensity): 931 (68) $[2M+Na]^+$, 477 (100) $[M+Na]^+$, 455 (70) $[M+H]^+$. HR-MS (ESI) *m/z* calcd for $C_{27}H_{27}N_4O_3$ $[M+H]^+$ 455.2078 found 455.2081.

***N*-[(1-Benzyl-1*H*-1,2,3-triazol-4-yl)methyl]-5-methyl-2-phenethylbenzamide (3ka)**

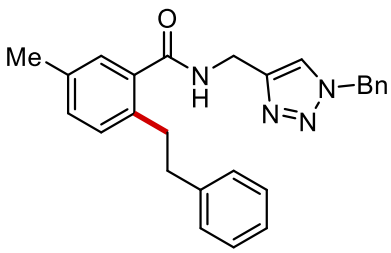

The representative procedure was followed using **1k** (61.3 mg, 0.20 mmol) and styrene **2a** (69 µL, 0.60 mmol). Purification by column chromatography on silica gel (*n*-Hexane/EtOAc 1:1) yielded **3ka** (54.2 mg, 66%) as a white solid. M.p. = 153-155 °C. ^{1}H-NMR (400 MHz, $CDCl_3$): δ = 7.53 (s, 1H), 7.37 – 7.35 (m, 3H), 7.26 – 7.22 (m, 4H), 7.18 – 7.14 (m, 2H), 7.12 – 7.10 (m, 2H), 7.09 – 7.05 (m, 2H), 6.09 (s, 1H), 5.46 (s, 2H), 4.58 (d, J = 5.7 Hz, 2H), 2.99 (dd, J = 9.1, 6.5 Hz, 2H), 2.84 (dd, J = 9.2, 6.4 Hz, 2H), 2.32 (s, 3H). ^{13}C-NMR

(101 MHz, $CDCl_3$): δ = 170.2 (C_q), 145.0 (C_q), 141.7 (C_q), 136.7 (C_q), 135.8 (C_q), 135.7 (C_q), 134.5 (C_q), 130.8 (CH), 130.3 (CH), 129.2 (CH), 128.8 (CH), 128.6 (CH), 128.3 (CH), 128.1 (CH), 127.4 (CH), 125.9 (CH), 122.2 (CH), 54.2 (CH_2), 38.0 (CH_2), 35.4 (CH_2), 34.7 (CH_2), 20.9 (CH_3). (ESI) *m/z* (relative intensity): 843 (60) $[2M+Na]^+$, 433 (62) $[M+Na]^+$, 411 (100) $[M+H]^+$. HR-MS (ESI) *m/z* calcd for $C_{26}H_{27}N_4O$ $[M+H]^+$ 411.2179 found 411.2184.

2.5.6 Representative procedure for Iron-Catalyzed C–H alkylation with vinylsilanes

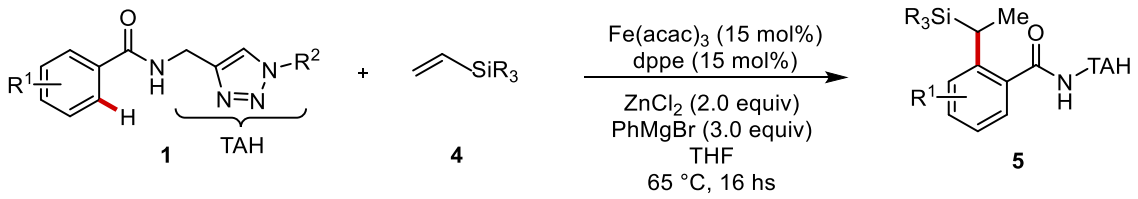

To a stirred solution of $Fe(acac)_3$ (10.6 mg, 0.03 mmol), dppe (11.9 mg, 0.03 mmol) zinc chloride (1.0 M in THF, 400 µL, 0.4 mmol, 2.0 equiv.) and **1** (0.20 mmol) under N_2 atmosphere, PhMgBr (1.0 M in THF, 600 µL, 0.6 mmol, 3.0 equiv.) was added in a single portion. Then, **4** (0.6 mmol, 3.0 equiv.) was added and the mixture was placed in a pre-heated oil bath at 65 °C. After stirring for 16 hs, the reaction was cooled to room temperature and quenched by the addition of an aqueous solution of HCl (1.0 M, 5.0 mL). The reaction was extracted with CH_2Cl_2 (3x15 mL) and the combined organic extracts were dried over Na_2SO_4, filtered and concentrated. The crude product was purified by column chromatography on silica gel (*n*-Hexane/EtOAc).

2.5.7 Characterization data for compounds 5

***N*-[(1-Benzyl-1*H*-1,2,3-triazol-4-yl)methyl]-2-[1-(trimethylsilyl)ethyl]benzamide (5aa)**

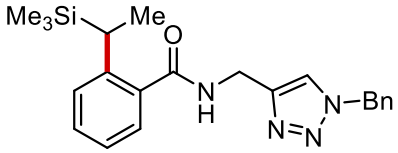

The representative procedure was followed using **1a** (58.5 mg, 0.20 mmol) and vinyltrimethylsilane **4a** (88 µL, 0.60 mmol). Purification by column chromatography on silica gel (*n*-Hexane/EtOAc 6:4) yielded **5aa** (50.1 mg, 64%, *b:l* = 20:1) as a white solid. M.p. = 84-85 °C. ^{1}H-NMR (400 MHz, $CDCl_3$): δ = 7.56 (s, 1H), 7.42 – 7.26 (m, 7H), 7.17 (dd, *J* = 7.9, 1.2 Hz, 1H), 7.08 (td, *J* = 7.4, 1.2 Hz, 1H), 6.49 (s, 1H), 5.52 (s, 2H), 4.66 (d, *J* = 5.7 Hz, 2H), 2.81 (q, *J* = 7.4 Hz, 1H), 1.34 (d, *J* = 7.4 Hz, 3H), -0.10 (s, 9H). ^{13}C-NMR (101 MHz, $CDCl_3$): δ = 170.5 (C_q), 145.3 (C_q), 144.9 (C_q), 134.8 (C_q), 134.4 (C_q), 129.9 (CH), 129.2 (CH), 128.9 (CH), 128.1 (CH), 127.5 (CH), 126.9 (CH), 124.1 (CH), 122.2 (CH), 54.3 (CH_2), 35.3 (CH_2), 24.6 (CH), 16.1 (CH_3), -2.9 (CH_3). (ESI) *m/z* (relative intensity): 807 (39) $[2M+Na]^+$, 415 (46) $[M+Na]^+$, 393(100) $[M+H]^+$, 144 (33). HR-MS (ESI) *m/z* calcd for $C_{22}H_{29}N_4OSi$ $[M+H]^+$ 393.2105, found 393.2109.

***N*-[(1-Benzyl-1*H*-1,2,3-triazol-4-yl)methyl]-2-{1-[diethyl(methyl)silyl]ethyl} benzamide (5ab)**

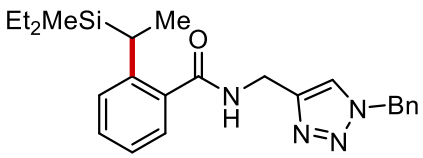

The representative procedure was followed using **1a** (58.5 mg, 0.2 mmol) and diethylmethylvinylsilane **4b** (77.0 mg, 0.60 mmol). Purification by column chromatography on silica gel (*n*-Hexane/EtOAc 1:1) yielded **5ab** (40.4 mg, 48%, *b:l* = 17:1) as a white solid. M.p. = 86-88 °C. ^{1}H-NMR (400 MHz, $CDCl_3$): δ = 7.56 (s, 1H), 7.44 – 7.37 (m, 3H), 7.36 – 7.29 (m, 3H), 7.28 – 7.25 (m, 1H), 7.21 (dd, *J* = 8.0, 1.2 Hz, 1H), 7.08 (td, *J* = 7.5, 1.3 Hz, 1H), 6.42 (s, 1H), 5.53 (s, 2H), 4.67 (dd, *J* = 5.7, 4.6 Hz, 2H), 2.87 (q, *J* = 7.5 Hz, 1H), 1.35 (d, *J* = 7.5 Hz, 3H), 0.84 (t, *J* = 7.9 Hz, 3H), 0.78 (t, *J* = 7.9 Hz, 3H), 0.53 – 0.35 (m, 4H), -0.12 (s, 3H). ^{13}C-NMR (101 MHz, $CDCl_3$): δ = 170.5 (C_q), 145.4 (C_q), 144.9 (C_q), 134.8 (C_q), 134.3 (C_q), 129.9 (CH), 129.2 (CH), 128.9 (CH), 128.2 (CH), 127.9 (CH), 127.0 (CH), 124.1 (CH), 122.2 (CH), 54.4 (CH_2), 35.2 (CH_2), 22.9 (CH), 16.6 (CH_3), 7.4 (CH_3), 7.4 (CH_3), 3.9 (CH_2), 3.8 (CH_2), -7.6 (CH_3). (ESI) *m/z* (relative intensity): 863 (25) $[2M+Na]^+$, 443 (100) $[M+Na]^+$, 421 (67) $[M+H]^+$, 377 (28). HR-MS (ESI) *m/z* calcd for $C_{24}H_{33}N_4OSi$ $[M+H]^+$ 421.2418, found 421.2427.

_N_-[(1-Benzyl-1_H_-1,2,3-triazol-4-yl)methyl]-2-{1-[dimethyl(phenyl)silyl]ethyl} benzamide (5ac)

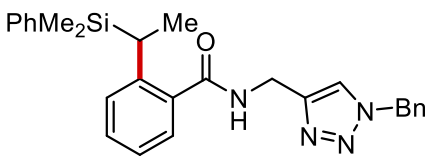

The representative procedure was followed using **1a** (58.5 mg, 0.20 mmol) and dimethylphenylvinylsilane **4c** (88 µL, 0.60 mmol). Purification by column chromatography on silica gel (*n*-Hexane/EtOAc 6:4) yielded **5ac** (45.5 mg, 50%, *b:l* = 8:1) as a colourless oil.^{1}H-NMR (400 MHz, $CDCl_3$): δ = 7.51 (s, 1H), 7.39 – 7.37 (m, 4H), 7.33 – 7.29 (m, 3H), 7.26 – 7.22 (m, 2H), 7.19 – 7.12 (m, 4H), 7.08 (td, *J* = 7.4, 1.2 Hz, 1H), 5.62 – 5.55 (m, 1H), 5.50 (d, *J* = 3.9 Hz, 2H), 4.49 (dd, *J* = 15.1, 5.9 Hz, 1H), 4.32 (dd, *J* = 15.1, 5.6 Hz, 1H), 2.96 (q, *J* = 7.4 Hz, 1H), 1.37 (d, *J* = 7.4 Hz, 3H), 0.28 (s, 3H), 0.19 (s, 3H). ^{13}C-NMR (101 MHz, $CDCl_3$): δ = 170.6 (C_q), 145.0 (C_q), 144.0 (C_q), 137.7 (C_q), 135.3 (C_q), 134.5 (C_q), 134.2 (CH), 129.7 (CH), 129.2 (CH), 129.1 (CH), 128.8 (CH), 128.2 (CH), 128.1 (CH), 127.6 (CH), 126.9 (CH), 124.3 (CH), 122.3 (CH), 54.3 (CH_2), 35.4 (CH_2), 24.7 (CH), 15.9 (CH_3), -4.9 (CH_3), -5.1 (CH_3). (ESI) *m/z* (relative intensity): 931 (89) $[2M+Na]^+$, 493 (20) $[M+K]^+$, 477 (100) $[M+Na]^+$, 455 (34) $[M+H]^+$, 377 (28). HR-MS (ESI) *m/z* calcd for $C_{27}H_{31}N_4OSi$ $[M+H]^+$ 455.2262, found 455.2266.

_N_-[(1-Benzyl-1_H_-1,2,3-triazol-4-yl)methyl]-5-methyl-2-[1-(trimethylsilyl)ethyl] benzamide (5ka)

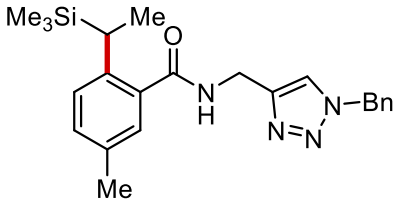

The representative procedure was followed using **1k** (61.3 mg, 0.20 mmol) and vinyltrimethylsilane **4a** (88 µL, 0.60 mmol). Purification by column chromatography on silica gel (*n*-Hexane/EtOAc 1:1) yielded **5ka** (42.5 mg, 52%, *b:l* = 15:1) as a white solid. M.p. = 157-159 °C. ^{1}H-NMR (400 MHz, $CDCl_3$): δ = 7.55 (s, 1H), 7.41 – 7.37 (m, 3H), 7.31 – 7.29 (m, 2H), 7.15 – 7.13 (m, 1H), 7.08 – 7.05 (m, 2H), 6.38 (bs, 1H), 5.53 (s, 2H), 4.66 (d, *J* = 5.7 Hz, 2H), 2.75 (q, *J* = 7.5 Hz, 1H), 2.29 (s, 3H), 1.32 (d, *J* = 7.5 Hz, 3H), -0.10 (s, 9H). ^{13}C-NMR (101 MHz, $CDCl_3$): δ = 170.6 (C_q), 145.0 (C_q), 142.0 (C_q), 134.7 (C_q), 134.5 (C_q), 133.6 (C_q), 130.7 (CH), 129.2 (CH), 128.9 (CH), 128.2 (CH), 127.5 (CH), 127.4 (CH), 122.1 (CH), 54.3 (CH_2), 35.3 (CH_2), 24.1 (CH), 20.7 (CH_3), 16.2 (CH_3), -3.0 (CH_3). (ESI) *m/z* (relative intensity): 835 (48) $[2M+Na]^+$, 445 (14) $[M+K]^+$, 429 (53) $[M+Na]^+$, 407 (100) $[M+H]^+$. HR-MS (ESI) *m/z* calcd for $C_{23}H_{31}N_4OSi$ $[M+H]^+$ 407.2262, found 407.2265.

_N_-[(1-Benzyl-1_H_-1,2,3-triazol-4-yl)methyl]-4-methyl-2-[1-(trimethylsilyl)ethyl] benzamide (5da)

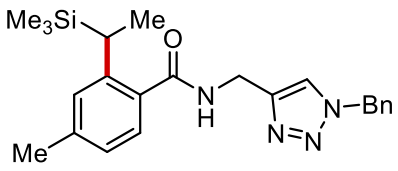

The representative procedure was followed using **1d** (61.3 mg, 0.20 mmol) and vinyltrimethylsilane **4a** (88 µL, 0.60 mmol). Purification by column chromatography on silica gel (*n*-Hexane/EtOAc 1:1) yielded **5da** (41.5 mg, 51%, *b:l* = 15:1) as a white solid. M.p.= 106-108 °C. ^{1}H-NMR (400 MHz, $CDCl_3$): δ = 7.55 (s, 1H), 7.40 – 7.37 (m, 3H), 7.30 (dd, *J* = 4.4, 2.4 Hz, 2H), 7.18 (d, *J* = 7.8 Hz, 1H), 6.97 (s, 1H), 6.88 (dd, *J* = 7.8, 1.0 Hz, 1H), 6.38 (bs, 1H), 5.53 (s, 2H), 4.65 (d, *J* = 5.7 Hz, 2H), 2.87 (q, *J* = 7.4 Hz, 1H), 2.34 (s, 3H), 1.34 (d, *J* = 7.5 Hz, 3H), -0.10 (s, 9H). ^{13}C-NMR (101 MHz, $CDCl_3$): δ = 170.6 (C_q), 145.4 (C_q), 145.1 (C_q), 139.8 (C_q), 134.4 (C_q), 131.9 (C_q), 129.2 (CH), 128.9 (CH), 128.2 (CH), 128.1 (CH), 127.0 (CH), 124.8 (CH), 122.1 (CH), 54.3 (CH_2), 35.3 (CH_2), 24.3 (CH), 21.6 (CH_3), 16.0 (CH_3), -3.0 (CH_3). (ESI) *m/z* (relative intensity): 835 (81) $[2M+Na]^+$, 429 (48) $[M+Na]^+$, 407 (100) $[M+H]^+$, 143 (14). HR-MS (ESI) *m/z* calcd for $C_{23}H_{31}N_4OSi$ $[M+H]^+$ 407.2262, found 407.2268.

_N_-[(1-Benzyl-1_H_-1,2,3-triazol-4-yl)methyl]-3-[1-(trimethylsilyl)ethyl]-[1,1'-biphenyl]-4-carboxamide (5ea)

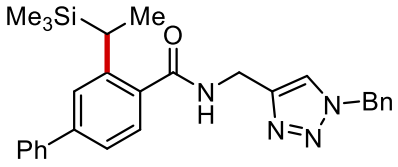

The representative procedure was followed using **1e** (73.7 mg, 0.20 mmol) and vinyltrimethylsilane **4a** (88 µL, 0.60 mmol). Purification by column chromatography on silica gel (*n*-Hexane/EtOAc 1:1) yielded **5ea** (42.2 mg, 45%, *b:l* = 16:1) as a white solid. M.p. = 171-172 °C.^{1}H-NMR (400 MHz, $CDCl_3$): δ = 7.58 – 7.56 (m, 3H), 7.47 (t, *J* = 7.4 Hz, 2H), 7.41 – 7.38 (m, 5H), 7.36 (s, 1H), 7.33 – 7.29 (m, 3H), 6.47 (t, *J* = 5.7 Hz, 1H), 5.54 (s, 2H), 4.69 (d, *J* = 5.7 Hz, 2H), 2.94 (q, *J* = 7.4 Hz, 1H), 1.41 (d, *J* = 7.5 Hz, 3H), -0.05 (s, 9H). ^{13}C-NMR (101 MHz, $CDCl_3$): δ = 170.3 (C_q), 146.0 (C_q), 144.9 (C_q), 142.7 (C_q), 140.7 (C_q), 134.4 (C_q), 133.6 (C_q), 129.2 (CH), 128.9 (CH), 128.8 (CH), 128.2 (CH), 127.7 (CH), 127.5 (CH), 127.2 (CH), 126.3 (CH), 123.0 (CH), 122.1 (CH), 54.3 (CH_2), 35.3 (CH_2), 24.6 (CH), 16.1 (CH_3), -2.9 (CH_3). (ESI) *m/z* (relative intensity): 469 (100) $[M+H]^+$. HR-MS (ESI) *m/z* calcd for $C_{28}H_{33}N_4OSi$ $[M+H]^+$ 469.2418, found 469.2423.

_N_-[(1-Benzyl-1_H_-1,2,3-triazol-4-yl)methyl]-4-chloro-2-(1-(trimethylsilyl)ethyl) benzamide (5fa)

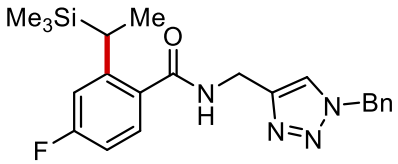

The representative procedure was followed using **1f** (62.1 mg, 0.20 mmol) and vinyltrimethylsilane **4a** (88 µL, 0.60 mmol). Purification by column chromatography on silica gel (*n*-Hexane/EtOAc 1:1) yielded **5fa** (27.9 mg, 34%, *b:l* =21:1) as a white solid. M.p. = 155-156 °C. ^{1}H-NMR (400 MHz, $CDCl_3$): δ = 7.56 (s, 1H), 7.40 (dd, *J* = 5.2, 1.9 Hz, 3H), 7.33 – 7.29 (m, 3H), 6.85 (dd, *J* = 10.9, 2.6 Hz, 1H), 6.77 (td, *J* = 8.2, 2.6 Hz, 1H), 6.55 (s, 1H), 5.53 (s, 2H), 4.65 (d, *J* = 5.5 Hz, 2H), 2.94 (qd, *J* = 7.4, 1.8 Hz, 1H), 1.33 (d, *J* = 7.4 Hz, 3H), -0.09 (s, 9H). ^{13}C-NMR (101 MHz, $CDCl_3$): δ = 169.7 (C_q), 163.7 (d, $^{1}J_{C\text{-}F}$ = 249 Hz, C_q), 149.2 (d, $^{5}J_{C\text{-}F}$ = 8.0 Hz, C_q), 149.14 (CH), 134.3 (2 x C_q) 130.7 (d, $^{6}J_{C\text{-}F}$ = 3 Hz, C_q), 129.2 (CH), 129.0 (d, $^{4}J_{C\text{-}F}$ = 9 Hz, CH), 129.0 (CH), 128.2 (CH), 122.2 (CH), 114.2 (d, $^{2}J_{C\text{-}F}$ = 22 Hz, CH), 111.0 (d, $^{3}J_{C\text{-}F}$ = 22 Hz, CH), 54.4 (CH_2), 35.2 (CH_2), 24.9 (d, $J_{C\text{-}F}$ = 2 Hz CH), 15.8 (CH_3), -3.1 (CH_3). ^{19}F-NMR (565 MHz, $CDCl_3$): δ= -110.2 – -110.3 (m). (ESI) *m/z* (relative intensity): 483 (10) $[2M+Na]^+$, 449 (27) $[M+K]^+$, 433 (100) $[M+Na]^+$, 411 (40) $[M+H]^+$. HR-MS (ESI) *m/z* calcd for $C_{22}H_{28}FN_4OSi$ $[M+H]^+$ 411.2011, found 411.2016.

_N_-[(1-Benzyl-1_H_-1,2,3-triazol-4-yl)methyl]-4-chloro-2-[1-(trimethylsilyl)ethyl] benzamide (5ga)

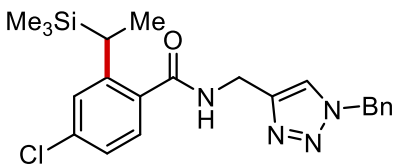

The representative procedure was followed using **1g** (65.4 mg, 0.20 mmol) and vinyltrimethylsilane **4a** (88 µL, 0.60 mmol). Purification by column chromatography on silica gel (*n*-Hexane/EtOAc 1:1) yielded **5ga** (25.6 mg, 30%, *b:l* = 22:1) as a white solid. M.p. = 121-122 °C. ^{1}H-NMR (400 MHz, $CDCl_3$): δ = 7.53 (s, 1H), 7.40 – 7.38 (m, 3H), 7.31 – 7.29 (m, 2H), 7.23 (d, *J* = 8.2 Hz, 1H), 7.14 (d, *J* = 2.1 Hz, 1H), 7.07 (dd, *J* = 8.2, 2.1 Hz, 1H), 6.44 (bs, 1H), 5.53 (s, 2H), 4.65 (d, *J* = 5.7 Hz, 2H), 2.86 (q, *J* = 7.4 Hz, 1H), 1.33 (d, *J* = 7.4 Hz, 3H), -0.08 (s, 9H). ^{13}C-NMR (101 MHz, $CDCl_3$): δ = 169.5 (C_q), 147.9 (C_q), 144.7 (C_q), 136.1 (C_q), 134.4 (C_q), 133.1 (C_q), 129.2 (CH), 128.9 (CH), 128.3 (CH), 128.2 (CH), 127.5 (CH), 124.3 (CH), 122.0 (CH), 54.3 (CH_2), 35.3 (CH_2), 24.8 (CH), 15.9 (CH_3), -3.1 (CH_3). (ESI) *m/z* (relative intensity): 875 (27) $[2M+Na]^+$, 449 (21) $[M+Na]^+$, 427 (100) $[M+H]^+$. HR-MS (ESI) *m/z* calcd for $C_{22}H_{28}ClN_4OSi$ $[M+H]^+$ 427.1715, found 427.1719.

Methyl-4-{[(1-benzyl-1*H*-1,2,3-triazol-4-yl)methyl]carbamoyl}-3-(1-(trimethylsilyl) ethyl)benzoate (5ja)

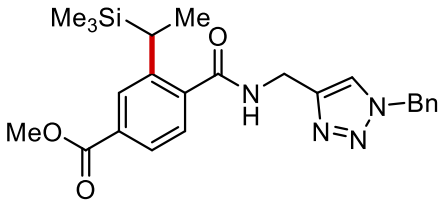

The representative procedure was followed using **1j** (70.1 mg, 0.20 mmol) and vinyltrimethylsilane **4a** (88 µL, 0.60 mmol). Purification by column chromatography on silica gel (*n*-Hexane/EtOAc 1:1) yielded **5ja** (37.0 mg, 41%, *b:l* =17:1) as a white solid. M.p. = 161-162 °C. ^{1}H-NMR (400 MHz, $CDCl_3$): δ = 7.85 (s, 1H), 7.73 (dd, *J* = 7.9, 1.7 Hz, 1H), 7.57 (s, 1H), 7.40 – 7.38 (m, 3H), 7.34 (d, *J* = 7.9 Hz, 1H), 7.30 – 7.29 (m, 2H), 6.66 (bs, 1H), 5.52 (s, 2H), 4.66 (d, *J* = 5.6 Hz, 2H), 3.92 (s, 3H), 2.78 (q, *J* = 7.4 Hz, 1H), 1.37 (d, *J* = 7.5 Hz, 3H), -0.09 (s, 9H). ^{13}C-NMR (101 MHz, $CDCl_3$): δ = 169.7 (C_q), 166.7 (C_q), 145.8 (C_q), 138.8 (C_q), 134.3 (2 x C_q), 131.2 (C_q). 129.2 (CH), 128.9 (CH), 128.6 (CH), 128.2 (CH), 127.1 (CH), 125.3 (CH), 122.2 (CH), 54.3 (CH_2), 52.3 (CH_3), 35.2 (CH_2), 24.9 (CH), 16.0 (CH_3), -3.0 (CH_3). (ESI) *m/z* (relative intensity): 489 (65) $[M+K]^+$, 473 (53) $[M+Na]^+$, 451 (100) $[M+H]^+$. HR-MS (ESI) *m/z* calcd for $C_{24}H_{31}N_4O_3Si$ $[M+H]^+$ 451.2160, found 451.2166.

***N*-[(1-Benzyl-1*H*-1,2,3-triazol-4-yl)methyl]-4-(*tert*-butyl)-2-[1-(trimethylsilyl) ethyl]benzamide (5la)**

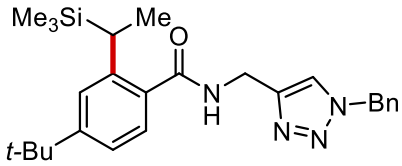

The representative procedure was followed using **1l** (69.7 mg, 0.20 mmol) and vinyltrimethylsilane **4a** (88 µL, 0.60 mmol). Purification by column chromatography on silica gel (*n*-Hexane/EtOAc 1:1) yielded **5la** (33.2 mg, 37%, *b:l* =13:1) as a white solid. M.p. = 142-143 °C. ^{1}H-NMR (400 MHz, $CDCl_3$): δ = 7.57 (s, 1H), 7.40 (dd, *J* = 5.0, 1.9 Hz, 3H), 7.31 (d, *J* = 2.8 Hz, 2H), 7.25 – 7.19 (m, 2H), 7.09 (dd, *J* = 8.0, 1.9 Hz, 1H), 6.47 (bs, 1H), 5.53 (s, 2H), 4.67 (d, *J* = 5.6 Hz, 2H), 2.88 (q, *J* = 7.4 Hz, 1H), 1.36 (d, *J* = 7.3 Hz, 3H), 1.31 (s, 9H), -0.10 (s, 9H).^{13}C-NMR (101 MHz, $CDCl_3$): δ = 170.6 (C_q), 152.9 (C_q), 144.9 (C_q), 134.2 (C_q), 131.8 (C_q), 129.2 (CH), 128.9 (CH), 128.6 (C_q), 128.2 (CH), 126.8 (CH), 124.8 (CH), 122.3 (CH), 121.0 (CH), 54.4 (CH_2), 35.1 (CH_2), 34.7 (C_q), 31.2 (CH_3), 24.5 (CH), 16.1 (CH_3), -3.0 (CH_3). (ESI) *m/z* (relative intensity): 487 (60) $[M+K]^+$, 471 (100) $[M+Na]^+$, 449 (20) $[M+H]^+$. HR-MS (ESI) *m/z* calcd for $C_{26}H_{37}N_4OSi$ $[M+H]^+$ 449.2731, found 449.2737.

_N_-[(1-Benzyl-1_H_-1,2,3-triazol-4-yl)methyl]-4-methoxy-2-[1-(trimethylsilyl) ethyl]benzamide (5ma)

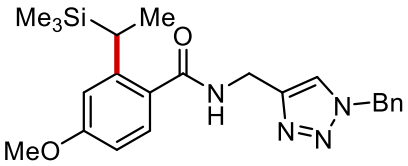

The representative procedure was followed using **1m** (64.5 mg, 0.20 mmol) and vinyltrimethylsilane **4a** (88 µL, 0.60 mmol). Purification by column chromatography on silica gel (*n*-Hexane/EtOAc 1:1) yielded **5ma** (38.9 mg, 46%, *b:l* = 22:1) as a colourless waxy solid. ^{1}H-NMR (400 MHz, $CDCl_3$): δ = 7.54 (s, 1H), 7.42 – 7.29 (m, 5H), 7.27 (d, *J* = 8.6 Hz, 1H), 6.69 (d, *J* = 2.5 Hz, 1H), 6.60 (dd, *J* = 8.5, 2.6 Hz, 1H), 6.40 (bs, 1H), 5.52 (s, 2H), 4.64 (d, *J* = 5.7 Hz, 2H), 3.81 (s, 3H), 3.01 (q, *J* = 7.4 Hz, 1H), 1.33 (d, *J* = 7.5 Hz, 3H), -0.09 (s, 9H).^{13}C-NMR (101 MHz, $CDCl_3$): δ = 170.2 (C_q), 160.8 (C_q), 148.1 (C_q), 145.1 (C_q), 134.5 (C_q), 129.2 (CH), 128.9 (CH), 128.7 (CH), 128.2 (CH), 127.3 (C_q), 122.1 (CH), 113.3 (CH), 108.9 (CH), 55.1 (CH_3), 54.3 (CH_2), 35.3 (CH_2), 24.4 (CH), 15.9 (CH_3), -3.0 (CH_3). (ESI) *m/z* (relative intensity): 445 (86) $[M+Na]^+$, 423 (100) $[M+H]^+$. HR-MS (ESI) *m/z* calcd for $C_{23}H_{31}N_4O_2Si$ $[M+H]^+$ 423.2211, found 423.2218.

2.5.8 Key Mechanistic Findings

Intermolecular KIE

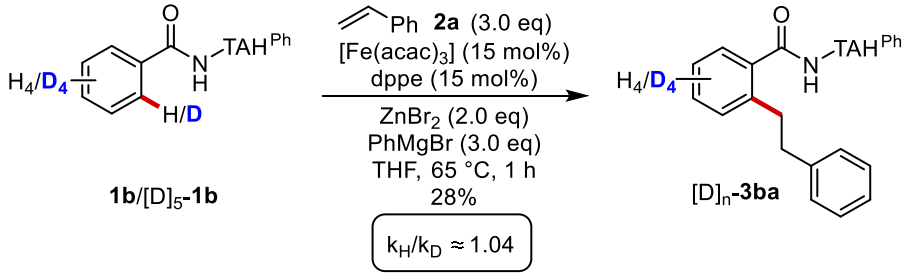

To a stirred solution of $Fe(acac)_3$ (10.6 mg, 0.03 mmol), dppe (11.9 mg, 0.03 mmol), zinc bromide (90.0 mg, 0.40 mmol), **1b** (27.8 mg, 0.10 mmol) and $[D]_5$-**1b** (28.3 mg, 0.10 mmol) in THF (0.4 mL) under N_2 atmosphere, PhMgBr (1.0 M in THF, 600 µl, 0.60 mmol) was added in a single portion. Then, styrene **2a** (69 µL, 0.60 mmol) was added and the mixture was placed in a pre-heated oil bath at 65 °C. After stirring for 1 h, the reaction was cooled to room temperature and quenched by the addition of an aqueous solution of HCl (1.0 M, 5.0 mL). The reaction was extracted with CH_2Cl_2 (3x15 mL) and the combined organic extracts were dried over Na_2SO_4, filtered and concentrated. The crude product was purified by column chromatography (*n*-Hexane/EtOAc). The mixture was analysed by 400 MHz ^{1}H-NMR spectroscopy to determine the ratio of **3ba**/$[D]_4$-**3ba** [(1.02/0.98 = 1.04)].

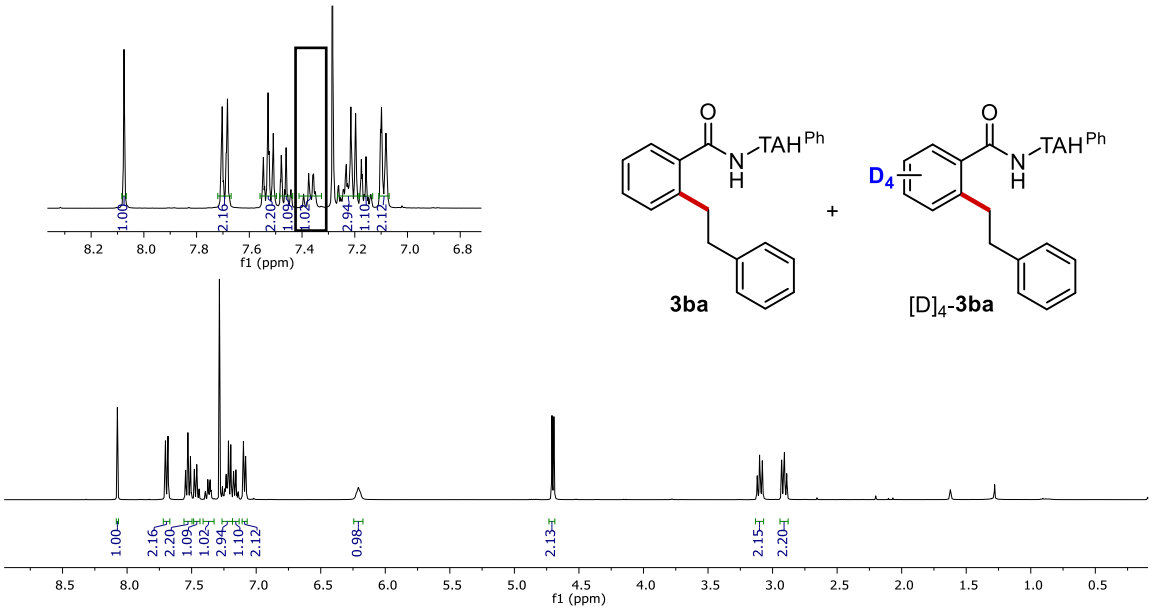

Intramolecular KIE

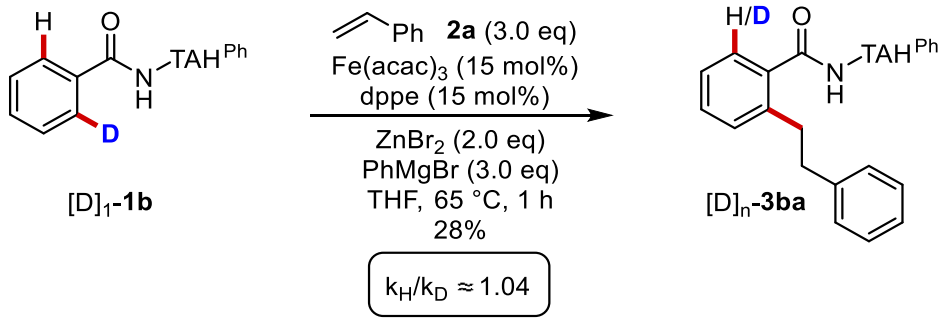

To a stirred solution of $Fe(acac)_3$ (10.6 mg, 0.03 mmol), dppe (11.9 mg, 0.03 mmol), zinc bromide (90.0 mg, 0.40 mmol) and [D]-**1b** (55.9 mg, 0.20 mmol) in THF (0.4 mL) under N_2 atmosphere, PhMgBr (1.0 M in THF, 600 µL, 0.60 mmol) was added in a single portion. Then, styrene **2a** (69 µL, 0.60 mmol) was added and the mixture was placed in a pre-heated oil bath at 65 °C. After stirring for 1 h, the reaction was cooled to room temperature and quenched by the addition of an aqueous solution of HCl (1.0 M, 5.0 mL). The reaction was extracted with CH_2Cl_2 (3x15 mL), and the combined organic extracts were dried over Na_2SO_4, filtered and concentrated. The crude product was purified by column chromatography (*n*-Hexane/EtOAc). The mixture was analysed by 400 MHz ^{1}H-NMR spectroscopy to determine the ratio of **3ba**/[D]-**3ba** [(1.0-0.49/0.49) = 1.04].

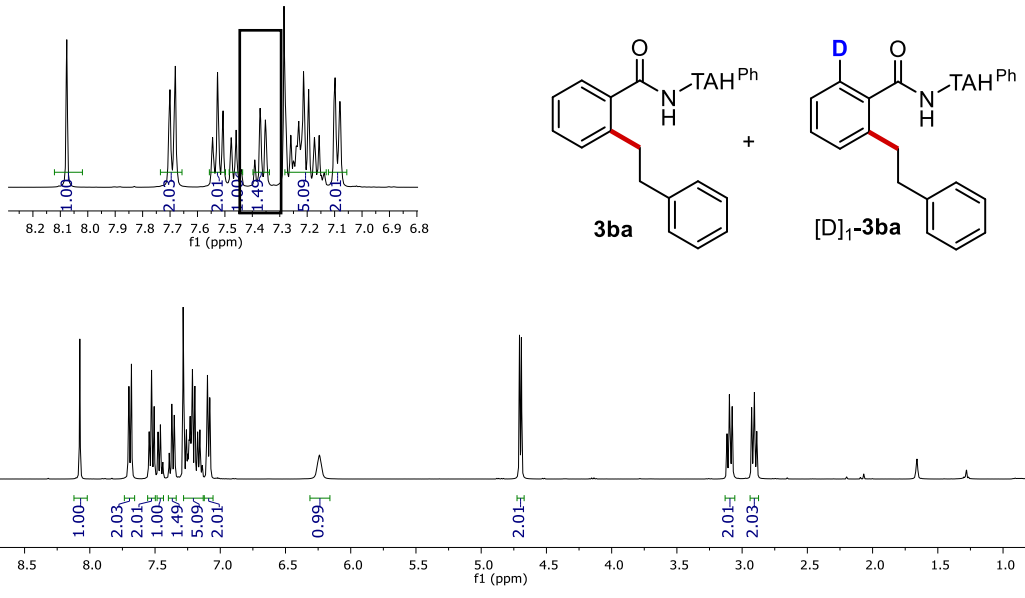

Reaction with DCl

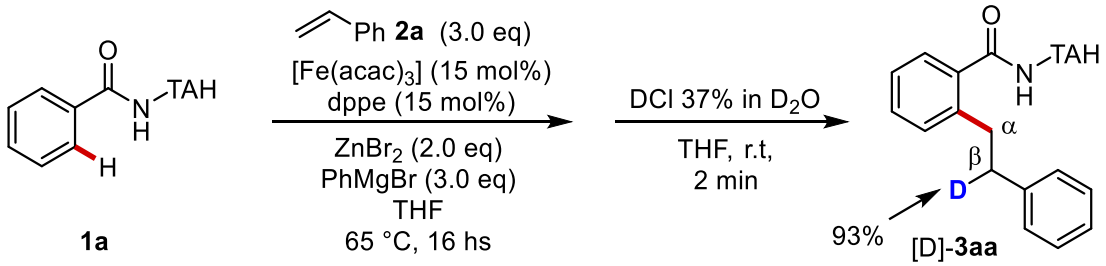

To a stirred solution of $Fe(acac)_3$ (10.6 mg, 0.03 mmol), dppe (11.9 mg, 0.03 mmol), zinc bromide (90.0 mg, 0.4 mmol) and **1a** (58.5 mg, 0.20 mmol) in THF (0.4 mL) under N_2 atmosphere, PhMgBr (1.0 M in THF, 600 µL, 0.60 mmol) was added in a single portion. Then, styrene **2a** (69 µL, 0.60 mmol) was added and the mixture was placed in a pre-heated oil bath at 65 °C. After stirring for 16 hs, the reaction was cooled to room temperature and quenched by the addition of 37% DCl in D_2O (1.5 mL). The reaction was extracted with CH_2Cl_2 (3x15 mL) and the combined organic extracts were dried over Na_2SO_4, filtered and concentrated. Purification by column chromatography on silica gel (*n*-Hexane/EtOAc 1:1) yielded [D]-**3aa** (53.8 mg, 68%) as a white solid. The amount of deuterium incorporation was determined by ^{1}H-NMR.

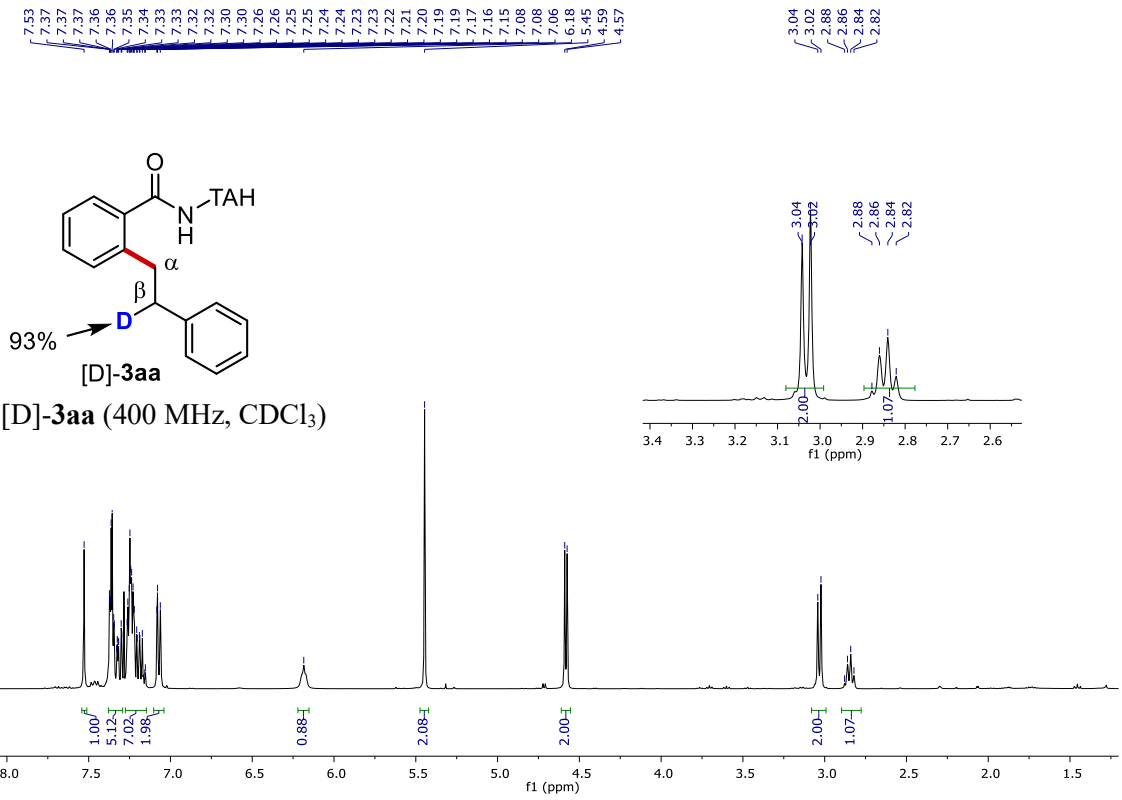

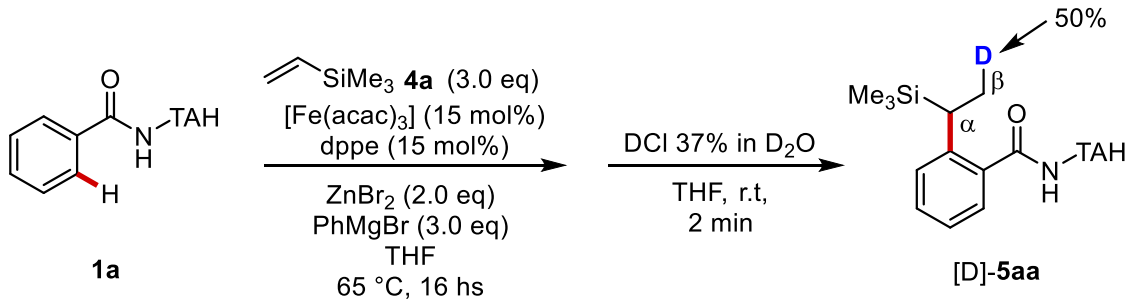

To a stirred solution of $Fe(acac)_3$ (10.6 mg, 0.03 mmol), dppe (11.9 mg, 0.03 mmol), zinc chloride (1.0 M in THF, 400 µL, 0.4 mmol, 2.0 equiv), and **1a** (58.5 mg, 0.20 mmol) under N_2 atmosphere, PhMgBr (1.0 M in THF, 600 µL, 0.60 mmol) was added in a single portion. Then, vinyltrimethylsilane **4a** (88 µL, 0.6 mmol) was added and the mixture was placed in a pre-heated oil bath at 65 °C. After stirring for 16 hs, the reaction was cooled to room temperature and quenched by the addition of 37% DCl in D_2O (1.5 mL). The reaction was extracted with CH_2Cl_2 (3x15 mL) and the combined organic extracts were dried over Na_2SO_4, filtered and concentrated. Purification by column chromatography on silica gel (*n*-Hexane/EtOAc 1:1) yielded [D]-**5aa** (44.9 mg, 57%) as a white solid. The amount of deuterium incorporation was determined by ^{1}H-NMR.

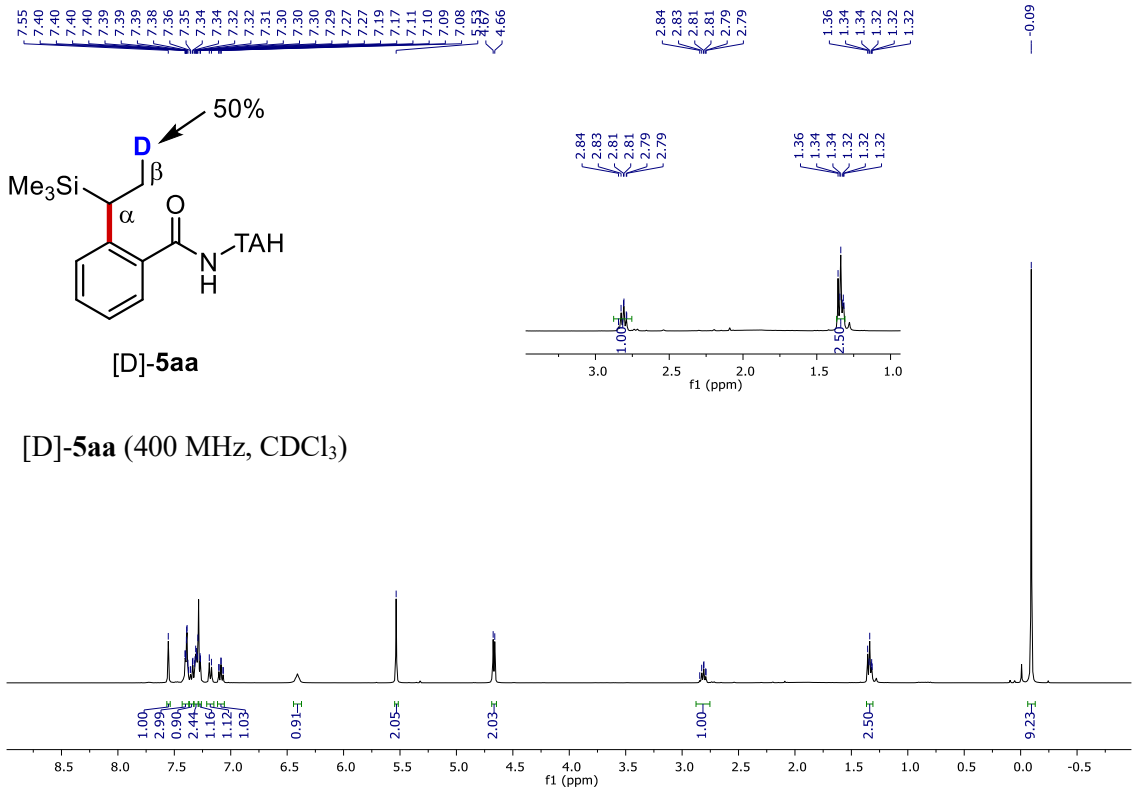

Reaction of [D]$_5$-1a

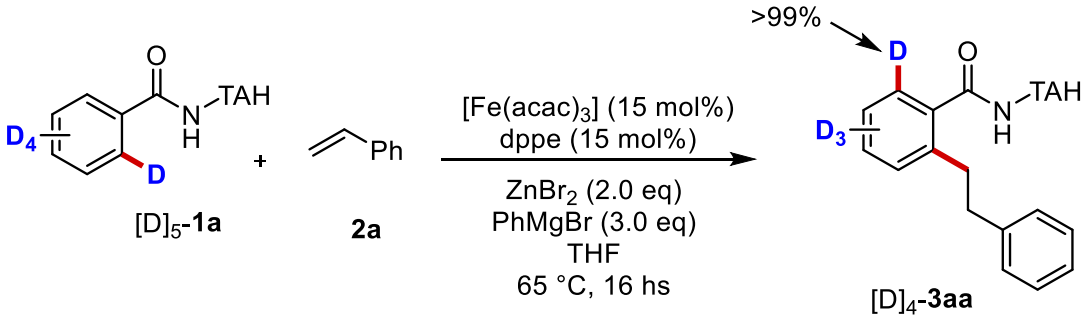

To a stirred solution of Fe(acac)$_3$ (10.6 mg, 0.03 mmol), dppe (11.9 mg, 0.03 mmol), zinc bromide (90.0 mg, 0.40 mmol) and [D]$_5$-**1a** (59.5 mg, 0.02 mmol) in THF (0.4 mL) under N_2 atmosphere, PhMgBr (1.0 M in THF, 600 µL, 0.60 mmol) was added in a single portion. Then, styrene **2a** (69 µL, 0.60 mmol) was added and the mixture was placed in a pre-heated oil bath at 65 °C. After stirring for 16 hs, the reaction was cooled to room temperature and quenched by the addition of an aqueous solution of HCl (1.0 M, 5.0 mL). The reaction was extracted with CH_2Cl_2 (3x15 mL), and the combined organic extracts were dried over Na_2SO_4, filtered and concentrated. Purification by column chromatography on silica gel (*n*-Hexane/EtOAc 1:1) yielded [D]$_4$-**3aa** (51.2 mg, 65 %) as a white solid. No hydrogen scrambling was observed by ^{1}H-NMR spectroscopy.

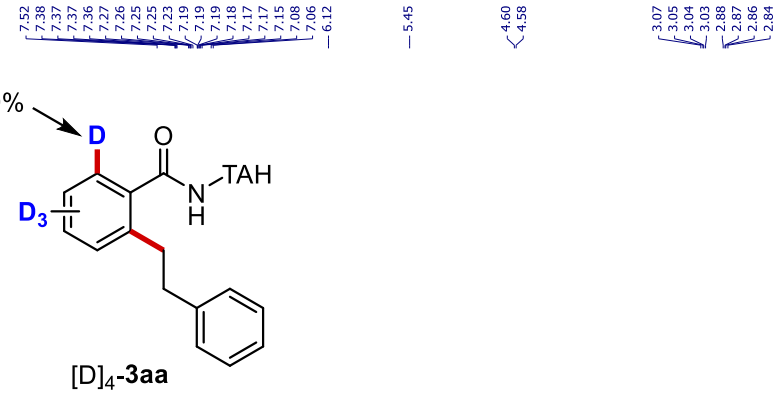

[D]$_4$-**3aa** (400 MHz, $CDCl_3$)

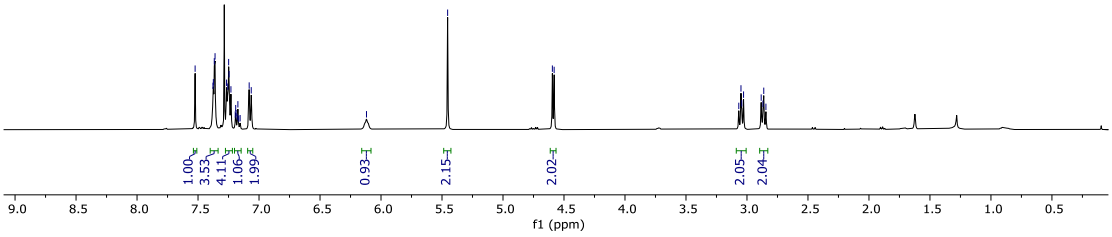

2.5.9 Late-stage synthetic manipulations

_N_-[(1-Benzyl-1_H_-1,2,3-triazol-4-yl)methyl]-2-[4-(diphenylphosphanyl)phenethyl] benzamide-AuCl (6ah)

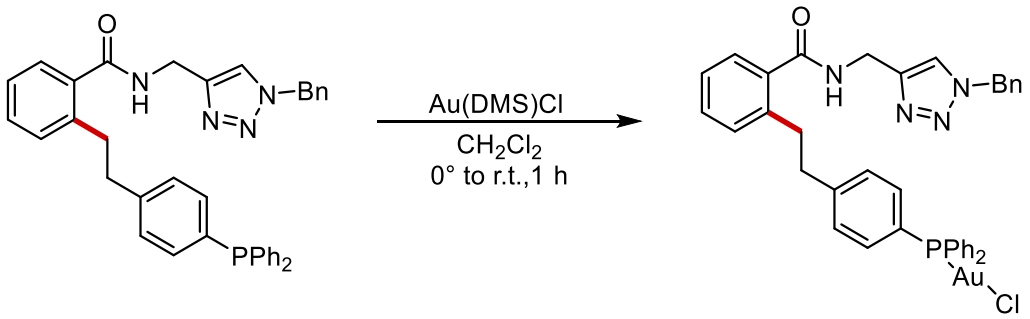

In a two-necked round bottom flask, under N_2 atmosphere, Au(DMS)Cl (10.7 mg, 0.036 mmol, 1.1 equiv.) was added to solution of **3ah** (19.1 mg, 0.032 mmol) in CH_2Cl_2 (3.0 mL) at 0 °C. The reaction was stirred at the same temperature for 30 min and then allowed to reach room temperature. After 1 h, the mixture was filtered through celite and washed with additional CH_2Cl_2 (20 mL). The volatiles were concentrated under reduced pressure and the crude product was purified by column chromatography on silica gel (*n*-Hexane/EtOAc 3:7) to yield **6ah** (18.5 mg, 71%) as a white waxy solid. ^{1}H-NMR (400 MHz, $CDCl_3$): δ = 7.55 – 7.46 (m, 12H), 7.41 – 7.33 (m, 6H), 7.27 – 7.24 (m, 5H), 7.18 (dd, *J* = 7.6, 1.3 Hz, 1H), 6.48 (bs, 1H), 5.48 (s, 2H), 4.66 (d, *J* = 5.6 Hz, 2H), 3.07 (dd, *J* = 9.8, 6.0 Hz, 2H), 2.95 (dd, *J* = 9.9, 6.1 Hz, 2H). ^{13}C-NMR (101 MHz, $CDCl_3$): δ = 169.8 (C_q), 146.5 (d, $J_{C\text{-}P}$ = 3 Hz, C_q), 144.6 (C_q), 139.7 (C_q), 135.5 (C_q), 134.3 (CH), 134.2 (CH), 134.0 (CH), 131.9 (d, $J_{C\text{-}P}$ = 3 Hz, CH), 130.4 (d, $J_{C\text{-}P}$ = 17 Hz, CH), 129.5 (d, $J_{C\text{-}P}$ = 17 Hz, CH), 129.2 (d, $J_{C\text{-}P}$ = 12 Hz, CH), 129.1 (CH), 128.9 (CH), 128.7 (C_q), 128.1 (CH), 127.1 (CH), 126.4 (CH), 125.9 (C_q), 125.3 (C_q), 122.0 (CH), 54.3 (CH_2), 37.7 (CH_2), 35.4 (CH_2), 35.1 (CH_2). ^{31}P-NMR (162 MHz, $CDCl_3$): δ = 32.5. (ESI) *m/z* (relative intensity): 813 (100) $[M+H]^+$, 777 (54) $[M\text{-}Cl]^+$. HR-MS (ESI) *m/z* calcd for $C_{37}H_{34}AuNOP$ $[M\text{-}Cl]^+$ 777.2058, found 777.2064.

_N_-[(1-Benzyl-1_H_-1,2,3-triazol-4-yl)methyl]-2-(1-[(*tert*-butyldimethylsilyl)oxy]-1-phenylpropan-2-yl)-4-methylbenzamide (7ea)

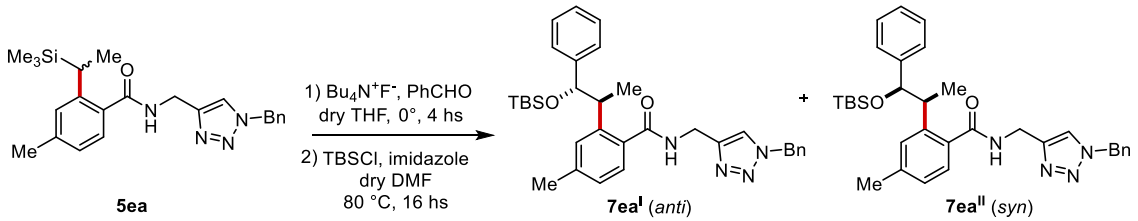

Tetra-*n*-butylammonium fluoride (75 µL, 1.0 M solution in THF, dried over molecular sieves, 0.422 mmol) was added to a solution of **5ea** (20.3 mg, 0.050 mmol) and freshly distilled benzaldehyde (27 µL, 0.165 mmol) in dry THF (2.0 mL), in an ice-bath and under N_2. The solution was stirred at 0 °C for 4 hs and saturated aqueous ammonium chloride solution (10 mL) was added. The aqueous phase was extracted with CH_2Cl_2 (3×10 mL). The combined organic extracts were washed with brine and dried over Na_2SO_4. The filtrate was concentrated under reduced pressure. The crude product was further submitted to *tert*-Butyldimethylsilyl chloride (11.3 mg, 0.075 mmol) in anhydrous DMF (2.0 mL) with imidazole (5.1 mg, 0.075 mmol). The solution was stirred at 70 °C. After 16 hs, the reaction was diluted with water and extracted with EtOAc (3x10 mL). The combined organic extracts were dried over Na_2SO_4 and the filtrate was concentrated under reduced pressure. Purification by column chromatography on silica gel (*n*-Hexane/EtOAc 2:8) yielded **7ea** as mixture of diastereoisomer (14.7 mg, 53% for two steps, *anti:syn* = 2.9:1) as a colourless oil.

7ea^{I}: ^{1}H-NMR (400 MHz, $CDCl_3$, *anti*): δ = 8.28 (bs, 1H), 7.60 (s, 1H), 7.42 (d, *J* = 7.8 Hz, 1H), 7.37 – 7.29 (m, 3H), 7.28 – 7.22 (m, 4H), 7.21 – 7.15 (m, 3H), 7.15 – 7.06 (m, 3H), 5.57 – 5.44 (m, 2H), 4.89 – 4.82 (m, 1H), 4.65 – 4.59 (m, 1H), 4.53 (d, *J* = 9.5 Hz, 1H), 3.31 (dq, *J* = 9.6, 6.9 Hz, 1H), 2.39 (s, 3H), 0.84 (d, *J* = 6.9 Hz, 3H), 0.52 (s, 9H), -0.31 (s, 6H). ^{13}C-NMR (101 MHz, $CDCl_3$): δ = 170.3 (C_q), 146.1 (C_q), 142.9 (C_q), 141.4 (C_q), 139.9 (C_q), 134.7 (C_q), 134.6 (C_q), 129.0 (CH), 128.6 (CH), 128.4 (2 x CH), 128.0 (CH), 127.8 (CH), 127.5 (CH), 127.2 (CH), 126.8 (CH), 122.7 (CH), 83.3 (CH), 54.2 (CH_2), 43.0 (CH), 35.5 (CH_2), 25.3 (CH_3), 21.5 (CH_3), 18.6 (CH_3), 17.9 (C_q), -5.6 (CH_3).

7ea^{II}:^{1}H-NMR (400 MHz, $CDCl_3$, *syn*): δ = 7.52 (s, 1H), 7.37 – 7.29 (m, 3H), 7.28 – 7.22 (m, 4H), 7.21 – 7.15 (m, 3H), 7.15 – 7.06 (m, 3H), 7.00 (d, *J* = 8.6 Hz, 1H), 5.77 (bs, 1H), 5.57 – 5.44 (m, 2H), 4.89 – 4.82 (m, 1H), 4.65 – 4.59 (m, 1H), 4.50 – 4.45 (m, 1H), 3.44 – 3.40 (m, 1H), 2.38 (s, 3H), 1.21 (d, *J* = 7.0 Hz, 3H), 0.90 (s, 9H), -0.42 (s, 6H). ^{13}C-NMR (101 MHz, $CDCl_3$): δ = 170.5 (C_q), 145.1 (C_q), 144.7 (C_q), 142.7 (C_q), 139.4 (C_q), 134.5 (C_q), 133.5 (C_q), 129.4 (CH), 129.2 (CH), 128.8 (CH), 128.1 (CH), 126.9 (CH), 126.7 (CH), 126.6 (2 X CH), 126.4 (CH), 122.2 (CH), 78.4 (CH), 54.2 (CH_2), 43.6 (CH), 35.4 (CH_2), 25.9 (CH_3), 21.5 (CH_3), 18.2 (C_q), 14.6 (CH_3), -5.0 (CH_3).

(ESI) *m/z* (relative intensity): 1154 (35) $[2M+Na]^+$, 577 (100) $[M+Na]^+$. HR-MS (ESI) *m/z* calcd for $C_{33}H_{43}N_4O_2Si$ $[M+H]^+$ 554.3077, found 554.3083.

2.5.10 Removal of the TAH directing group

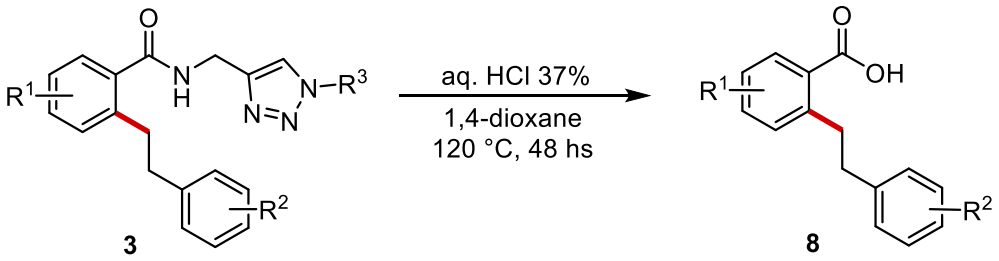

A solution of benzamide **3** (0.10 mmol) in aqueous HCl (3.0 mL, 37% w/w) and 1,4-dioxane (1.5 mL) was stirred at 120 °C for 48 hs. Then, the reaction mixture was diluted with water (15 mL) and extracted with CH_2Cl_2 (3x10 mL). The combined organic extracts were dried over Na_2SO_4, and the filtrate was concentrated under reduced pressure. The crude product was purified by column chromatography on silica gel (*n*-Hexane/EtOAc).

2-Phenethylbenzoic acid (8aa)

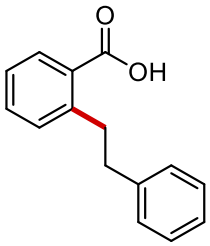

The representative procedure was followed using **3aa** (0.10 mmol, 39.6 mg). Purification by column chromatography on silica gel (*n*-Hexane/EtOAc 7:3) yielded **8aa** (15.4 mg, 68%) as a white solid. M.p. = 128-130 °C. ^{1}H-NMR (400 MHz, $CDCl_3$): δ = 10.72 (bs, 1H), 8.10 (dd, *J* = 7.9, 1.5 Hz, 1H), 7.50 (td, *J* = 7.5, 1.5 Hz, 1H), 7.37 – 7.29 (m, 3H), 7.28 – 7.19 (m, 4H), 3.41 – 3.30 (m, 2H), 3.02 – 2.92 (m, 2H). ^{13}C-NMR (101 MHz, $CDCl_3$): δ = 172.3 (C_q), 144.8 (C_q), 141.9 (C_q), 133.0 (CH), 131.8 (CH), 131.5 (CH), 128.6 (CH), 128.4 (CH), 128.0 (C_q), 126.3 (CH), 125.9 (CH), 38.1 (CH_2), 37.1 (CH_2). (ESI) *m/z* (relative intensity): 473 (100) $[2M+Na]^-$. HR-MS (ESI) *m/z* calcd for $C_{15}H_{15}O_2$ $[M+H]^+$ 227.1067, found 427.1072. The spectral data were in accordance with those reported in the literature.[4]

2-{2-[(1,1'-biphenyl)-4-yl]ethyl}benzoic acid (8ad)

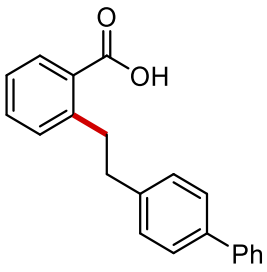

The representative procedure was followed using **3ad** (0.10 mmol, 47.2 mg). Purification by column chromatography on silica gel (*n*-Hexane/EtOAc 7:3) yielded **8ad** (22.1 mg, 73%) as a white solid. M.p. = 149-151 °C. ^{1}H-NMR (400 MHz, $CDCl_3$): δ = 8.13 (dd, *J* = 7.8, 1.5 Hz, 1H), 7.60 – 7.57 (m, 2H), 7.55 – 7.49 (m, 3H), 7.43 (t, *J* = 7.5 Hz, 2H), 7.37 – 7.29 (m, 5H), 3.42 – 3.37 (m, 2H), 3.03 – 2.99 (m, 2H). ^{13}C-NMR (101 MHz, $CDCl_3$): δ = 171.9 (C_q), 144.8 (C_q), 141.1 (C_q), 141.0 (C_q), 138.9 (C_q), 133.1 (CH), 131.9 (CH), 131.6 (CH), 129.0 (CH), 128.7 (CH), 127.9 (C_q), 127.1 (CH), 127.0 (CH), 126.9 (CH), 126.3 (CH), 37.8 (CH_2), 37.1 (CH_2). (ESI) *m/z* (relative intensity): 625 (93)

$[2M+Na]^+$, 325 (100) $[M+Na]^+$. HR-MS (ESI) *m/z* calcd for $C_{21}H_{19}O_2$ $[M+H]^+$ 303.1380, found 303.1384.

2.5.11 Additional References

[1] N. Camedda, A. Serafino, R. Maggi, F. Bigi, G. Cera and G. Maestri, *Synthesis*, **2020**, *52*, 1762–1772.

[2] X. Ma, Y. Liu, P. Liu, J. Xie, B. Dai and Z. Liu, *Appl. Organometal. Chem*. **2013**, *27*, 707–710.

[3] L. Sancineto, C. Tidei, L. Bagnoli, F. Marini, E. J. Lenardão and C. Santi, *Molecules*, **2015**, *20*, 10496–10510.

[4] R. Zhu, J. Jiang, X. Li, J. Deng and Y. Fu, *ACS Catal.*, **2017**, *7*, 11, 7520–7528.

3. Iron-Catalyzed C−H Alkylation/Ring Opening with Vinylbenzofurans Enabled by Triazoles

From this chapter:

S. Cattani, N. K. Pandit, M. Buccio, D. Balestri, L. Ackermann, G. Cera, *Angew. Chem. Int. Ed*. **2024**, *63*, e202404319.

3.1 Introduction

3.1.1 Iron-Catalyzed C–H Annulations

Transition metal-catalyzed C–H alkylations and annulations represent a well-established strategy for forming new C–C and C–Heteroatom bonds.[1] These reactions typically employ unsaturated compounds, such as olefins and alkynes, as reaction partners. The reaction mechanism generally involves a migratory insertion of the unsaturated moiety into a cyclometalated species[2] that gives rise to different products with a selectivity that is primarily influenced by the choice of reaction parameters as depicted in Scheme 3.1.

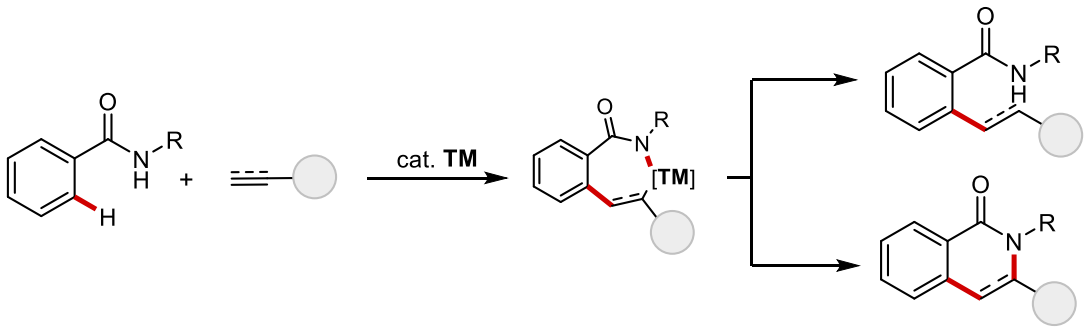

Scheme 3.1 General scheme for TM-catalyzed C–H alkylation and annulations reactions.

Alkynes, which can coordinate with low-valent iron species through their π-systems, have been used to promote C–H annulation reactions. In 2011 Nakamura firstly reported the iron-catalyzed oxidative [4 + 2] benzannulation of 2-biaryl and 2-alkenylphenyl Grignard reagents **I** with internal or terminal alkynes **II** to synthesize phenanthrene derivatives **III** (Scheme 3.2).[3] Due to the high activity of the iron-based catalytic system, the oxidative coupling occurs under mild conditions and enables the formation of sterically congested systems with remarkable chemoselectivity.

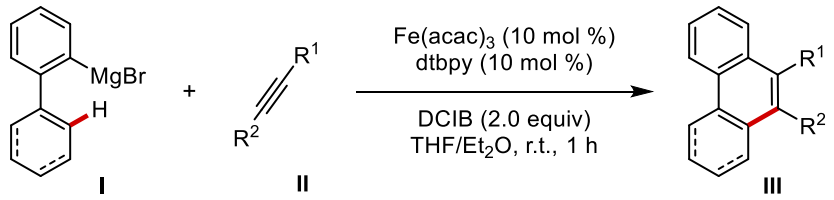

Scheme 3.2 Iron-catalyzed [4 + 2] benzannulation of alkynes with aryl Grignard reagents.

Additionally, the authors developed a similar method for iron-catalyzed oxidative [2 + 2 + 2] annulations of aryl Grignard reagents **IV** with two molecules of an internal alkyne.[4] Mechanistically, the reaction is proposed to proceed *via* iron-catalyzed carbometalation of alkyne

II with aryl Grignard reagent **IV**, followed by intramolecular C–H activation to form the five-membered ferracycle **Int2**. The insertion of a second molecule of alkyne then forms **Int3**, which undergoes reductive elimination and oxidation to yield the final product **V** and regenerate the active iron species (Scheme 3.3).

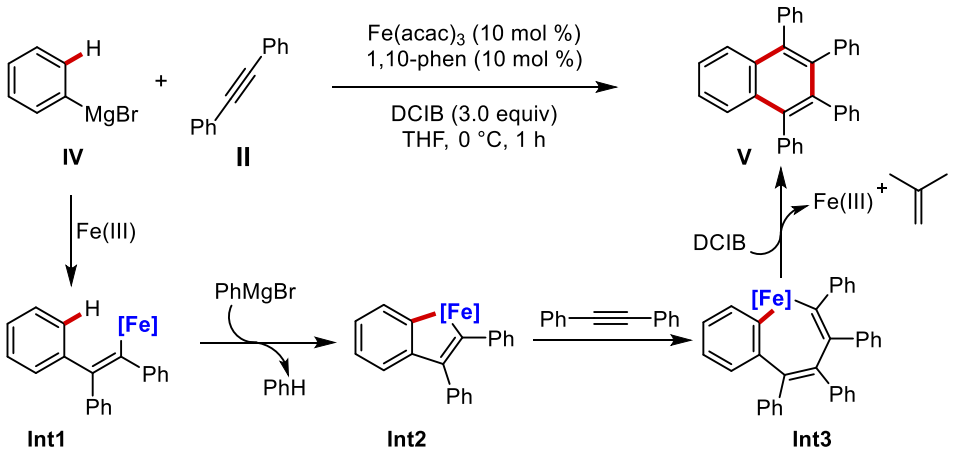

Scheme 3.3 Iron-catalyzed [2 + 2 + 2] benzannulation of alkynes with aryl Grignard reagents.

As for chelation-assisted annulation reactions, two characteristic examples are represented by the works of Nakamura[5] and Ackermann.[6] In the work reported by Nakamura's group the reaction of 8-aminoquinoline decorated benzamide **VI** with an internal alkyne (e.g., 4-octyne) yielded either the alkenylated product **VII** or the annulated product **VII'**, depending on the choice of organometallic base (Scheme 3.4).[5] When a mono-organozinc halide was employed as the base (1.5 eq. $ZnBr_2$TMEDA, 3.0 eq. Me_3SiCH_2Cl) the major product obtained was the alkenylated compound, regardless of the presence or absence of the oxidant (1,2-DCP). However, the use of a di-organozinc base (1.5 eq. $ZnBr_2$TMEDA, 5.0 eq. Me_3SiCH_2Cl) in the presence of 1,2-DCP exclusively produced the cyclized product **VII'**. This represents a successful example where the selectivity of the reaction depends on the choice of reaction parameters.

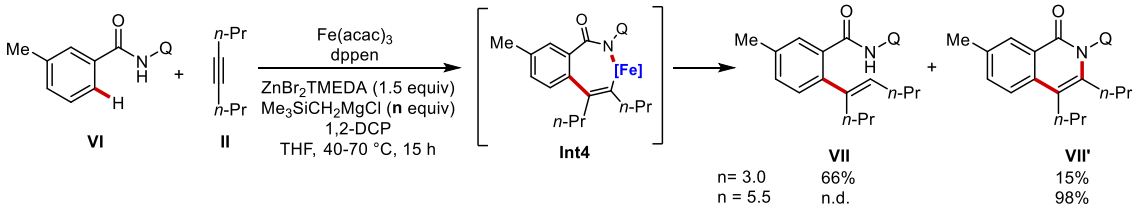

Scheme 3.4 Diversification of reaction routes of Q-assisted iron catalyzed C–H functionalization with **II**.

In the work reported by the Ackermann group the TAH auxiliary was exploited for the synthesis of isoquinolones *via* alkyne annulation (Scheme 3.5).[6] The optimized reaction conditions involve

the use of $ZnBr_2$•TMEDA and 1,2-dichloroisobutane (DCIB) as the oxidant. The authors propose a reaction mechanism initiated by a facile C–H activation to form a five-membered metallacycle **Int6** that subsequently undergoes migratory insertion of the alkyne forming a 7-membered metallacycle **Int7** that represents the key intermediate for the C–N bond formation. Subsequently, oxidation by DCIB followed by reductive elimination leads to the formation of the annulation product.

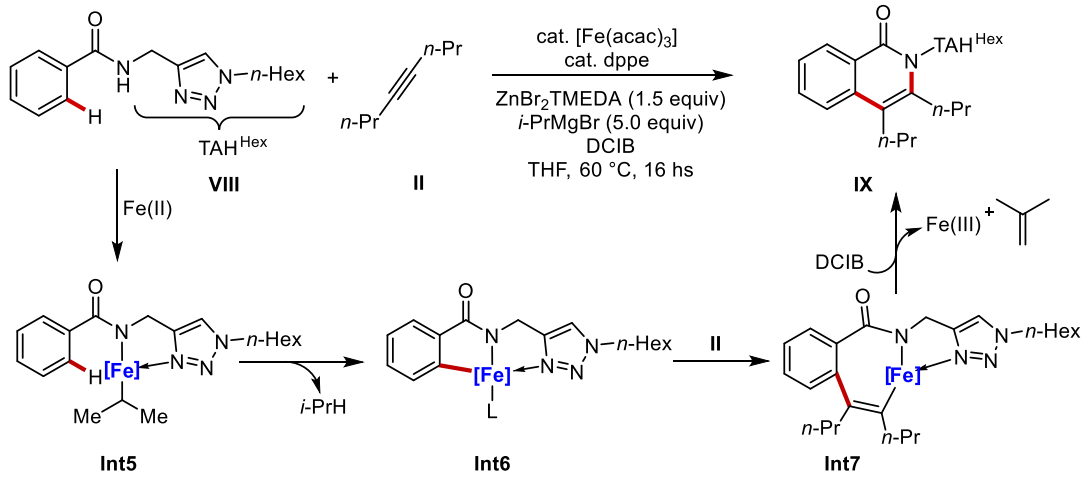

Scheme 3.5 TAH-assisted iron catalyzed C–H/N–H functionalization for alkynes annulation.

A further breakthrough for iron-catalyzed annulation reactions was achieved with the use of unsaturated substrates having an oxygen-based leaving group in the vicinal position, such as propargyl acetates (**X**), as reported by Ackermann.[7] When conducting the reaction with propargyl acetates, the external oxidant is no longer necessary to achieve the desired cyclization, as the reaction mechanism is different (Scheme 3.6).

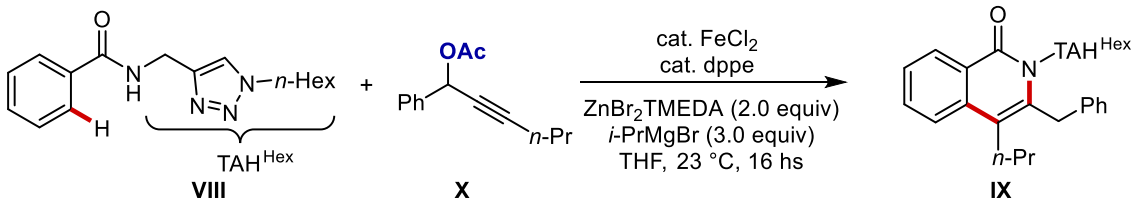

Scheme 3.6 TAH-assisted iron catalyzed C–H/N–H functionalization with propargyl acetates.

Mechanistically, it has been proposed that the reaction begins with the deprotonation of benzamide **VIII** by a Grignard reagent or an isopropylzinc species as depicted in Scheme 3.7. The substrate then coordinates with the Fe(dppe) complex generated in situ *via* chelation of the triazolylamide. The proximity of the iron to the *ortho* C–H bond, facilitated by the coordination of the directing group, allows for its activation *via* ligand-to-ligand hydrogen transfer (LLHT),

leading to the formation of the cyclometalated iron species (**Int6**). Subsequently, the propargyl acetate **X** coordinates to the iron center and undergoes a migratory insertion into the Fe–C bond. The resulting vinyliron species (**Int9**) then undergoes a C–O bond cleavage, yielding the allenyl intermediate **Int10** and releasing an acetate ion that remains coordinated to the iron. The insertion of the allene moiety into the N–Fe bond then forms the annulated iron intermediate **Int11**, which releases the isoquinolone product **IX** through proto-demetalation, regenerating the catalytically active species.

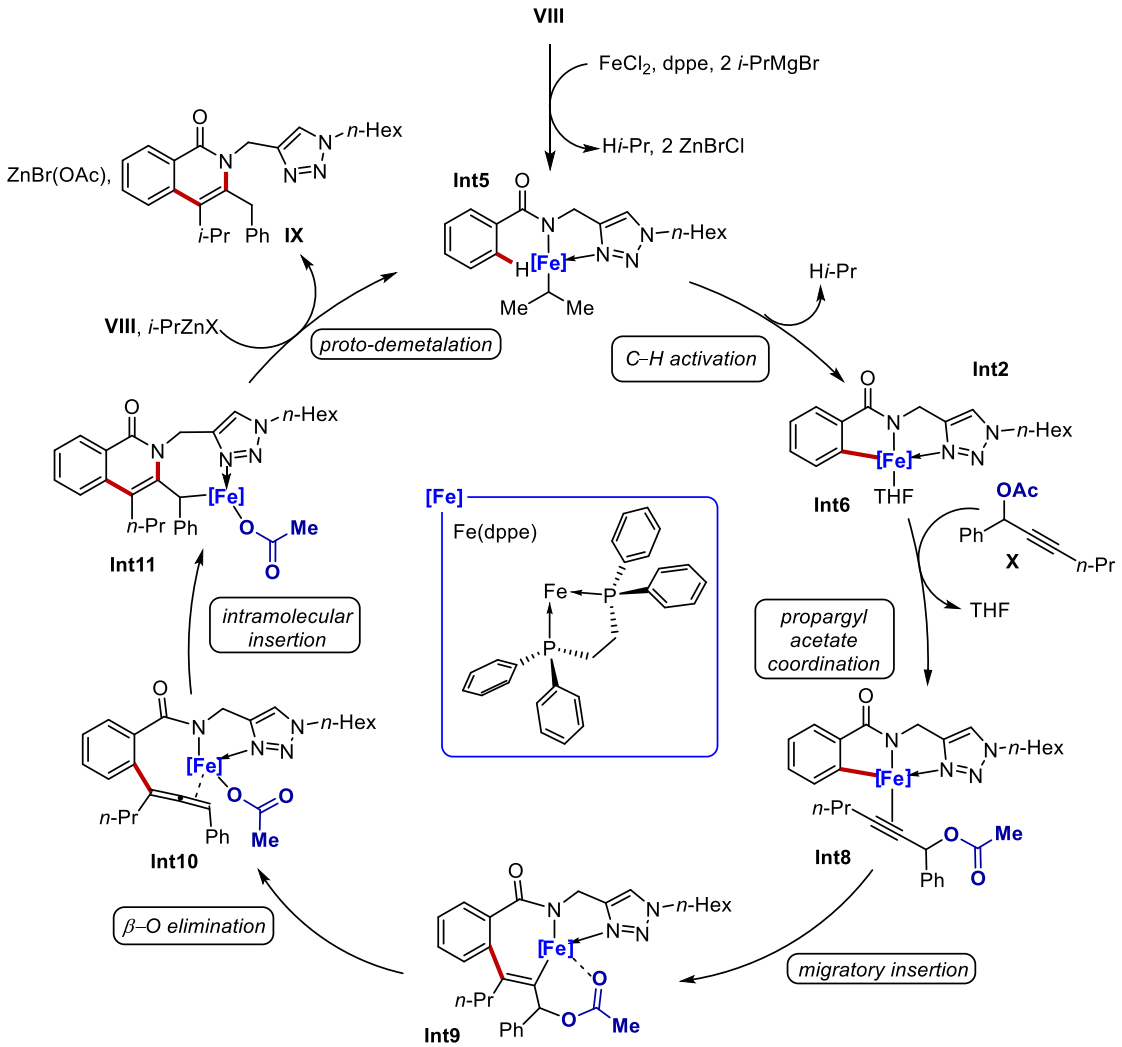

Scheme 3.7 Proposed mechanism for iron catalyzed C–H/N–H annulation with propargyl acetates.

Representative reports addressing chelation-assisted iron-catalyzed C–H functionalization reactions with olefins were discussed in the previous section. In these cases, the reaction with alkenes leads to the formation of either linear or branched alkylation products, depending on their nature.[8]

After investigating simple alkynes and alkenes, researchers turned their attention to more structurally complex substrates like bicyclopropylidenes (BCPs). BCPs are particularly unique because their ring strain imparts reactivity beyond that of typical C−C double bonds. Thus in 2021, the Ackermann group introduced the first iron-catalyzed C−H/C−C annulation using bicyclopropylidenes (BCPs) facilitated by triazole directing groups.[9] A notable aspect of this new protocol is its chemo-selectivity, which is influenced by the choice of the leaving group on BCPs (Scheme 3.8). Thus, isoquinolone derivatives **XII** were synthesized using the acyloxy (OAc) leaving group on the BCP moiety **XI** (Scheme 3.8, a). In contrast, bispiro-fused isoquinolone derivatives **XIV** were produced by switching to alkyl ether (OMe) BCPs **XIII** (Scheme 3.8, b).

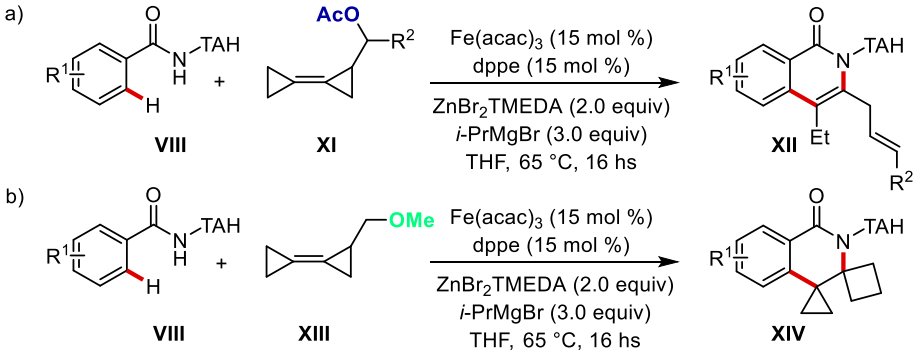

Scheme 3.8 Iron-catalyzed C−H/C−C annulation with bicyclopropylidenes by TAH assistance.

The proposed catalytic cycle, based on detailed experimental and ^{57}Fe Mössbauer spectroscopic studies (Scheme 3.9), suggests that the cycle begins with a facile C−H activation, potentially occurring via LLHT, to generate the cyclometalated intermediate **Int6**. Following the coordination and migratory insertion of BCP, **Int13** is formed. Subsequent reductive elimination and *β*−C elimination of **Int13** delivers intermediate **Int14**, which can proceed through two different pathways (A and B) depending on the leaving group on the BCP moiety. In pathway A, intermediate **Int14** undergoes *β*−C elimination to form **Int15**, followed by LLHT to produce isoquinolone **XII**. Conversely, when OMe is the leaving group (pathway B), migratory insertion of the alkene into the Fe−C bond forms intermediate **Int16**, which then undergoes LLHT to deliver the bispiro-fused isoquinolone **XIV**.

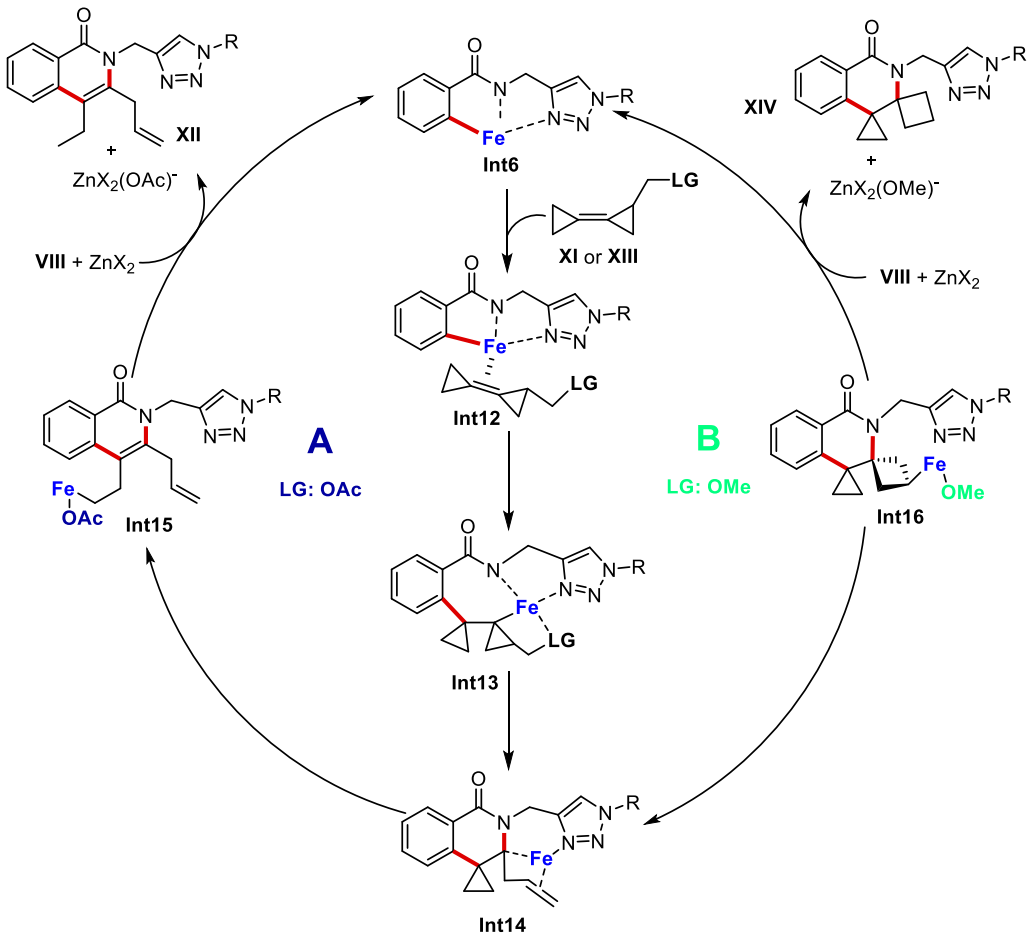

Scheme 3.9 Proposed mechanism for iron-catalyzed C−H/C−C annulation with BCPs.

3.1.2 Benzofurans

Benzofurans are an important class of heterocyclic compounds frequently found in natural products and bioactive molecules.[10] Their ease of synthesis and the ability to selectively modify their structure have made these heterocycles essential components in medicinal chemistry and drug discovery.[11] Benzofurans are electron-rich aromatic systems that can participate in a variety of reactions typical of heterocyclic aromatic compounds, including Friedel-Crafts acylations, formylations, nitrations, and functionalizations via metalation of the acidic proton at the 2-position as depicted in Scheme 3.10.

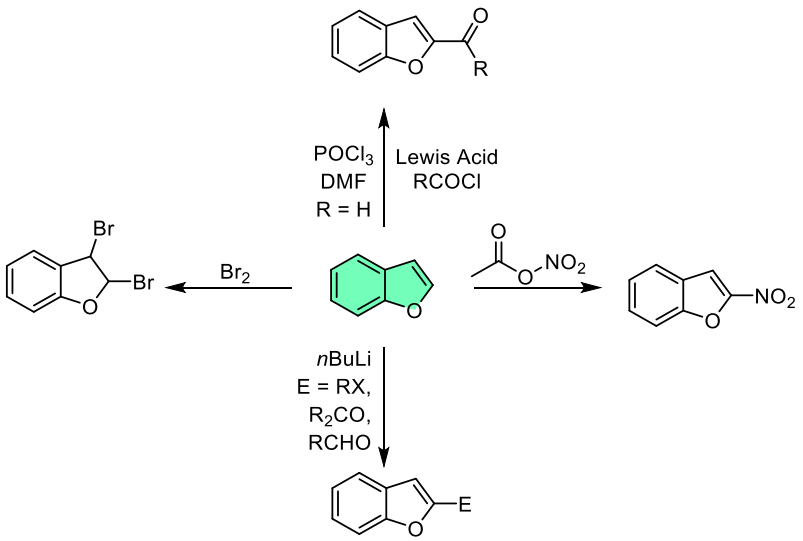

Scheme 3.10 Examples of classical reactivity of benzofurans.

Exploring the catalytic ring-opening of benzofurans can potentially unlock new and unique chemical reactivity. In this context, the few examples involving C−O bond cleavage of these compounds and their subsequent transformations are particularly valuable. These methods, which often utilize organometallic reagents alongside transition-metal complexes, offer promising strategies for producing functionalized phenols (Scheme 3.11).[12] Based on the seminal report made by Wenkert that exploit a nickel-based catalyst in the presence of a Grignard reagent,[13] chemists have recently harnessed the potential of catalytic arylation and alkylation reactions of benzofuran using stoichiometric organometallic reagents through C(sp^2)–O bond cleavage. For example, Wang successfully reported a nickel-catalyzed reductive cross-electrophile coupling between 2,3-nonsubstituted benzofuran and alkyl halides.[14] Additionally, Yorimitsu has reported the ring-opening coupling of benzofurans using either B_2pin_2 or disilane.[15]

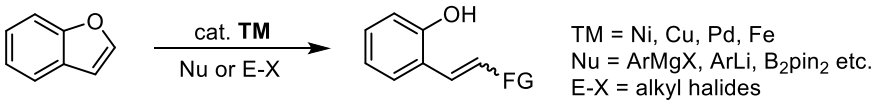

Scheme 3.11 General scheme for transition metal catalyzed ring-opening of benzofurans.

As for iron promoted ring-opening of benzofurans, in 2016 Kambe reported an example where the reaction occurs in the presence of a Grignard reagent.[16] The reaction mechanism proposed by the authors (Scheme 3.12) suggests that the catalytically active species is either Fe(I) or Fe(0), generated *in situ* by reduction with the Grignard reagent. Following the reduction, a phenyl group coordinates to the metal center, forming the anionic complex **Int18**. This complex undergoes a carbometalation reaction on the carbon-carbon double bond of the benzofuran **XV**, yielding the cyclometallated intermediate **Int19**. This latter then evolves through a *β*-oxygen elimination reaction, leading to the formation of the desired phenolic product **XVI** after the reaction is quenched. However, the ring-opening product was obtained without control on the stereochemistry of the double bond, resulting in a mixture of *E* and *Z* isomers.

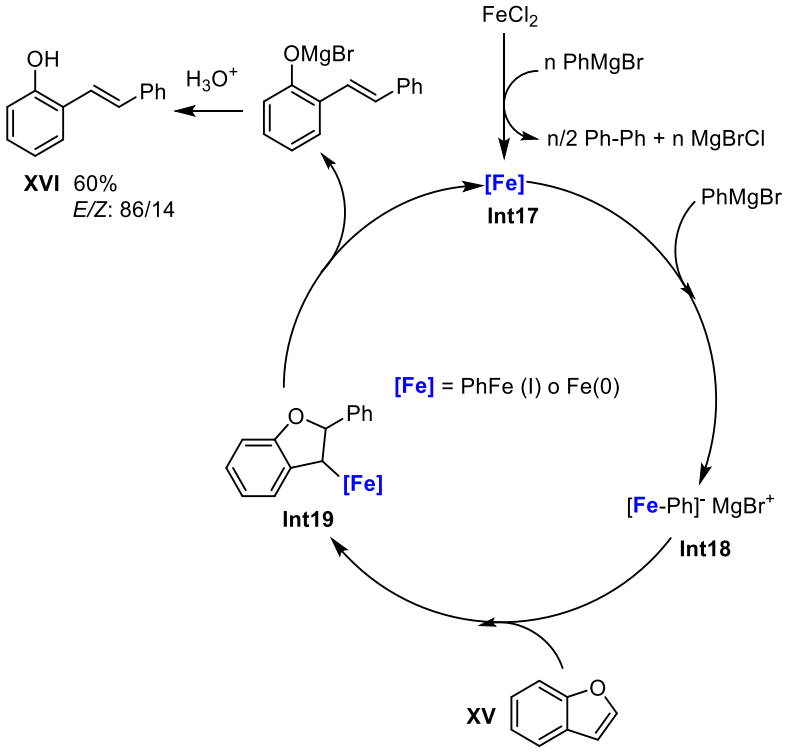

Scheme 3.12 Proposed mechanism for iron catalyzed cross-coupling reaction of benzofuran.

3.2 Results and Discussion

Although significant progress has been made in organometallic iron-catalyzed C–H activations, the range of chemical transformations facilitated by this metal remains limited.[17] Consequently, there is a strong need for discovering new reaction pathways. In this project, we hypothesized that 2-vinyl benzofurans could serve as effective substrates for iron-catalyzed C–H functionalizations. Inspired by our previous findings on triazole-assisted iron-catalyzed C–H alkylations with olefins,[8b] we started our investigation by testing a triazole-functionalized benzamide in the presence of 2-vinylbenzofuran. Notably, the iron catalysis facilitated a cascade reaction that resulted in the formation of a complex isoquinolone derivative, where a 2-(prop-1-en-1-yl)phenol pendant, produced through a challenging *β*–O elimination for the ring-opening of the benzofuran ring, is generated with complete *E*-selectivity (Scheme 3.13).

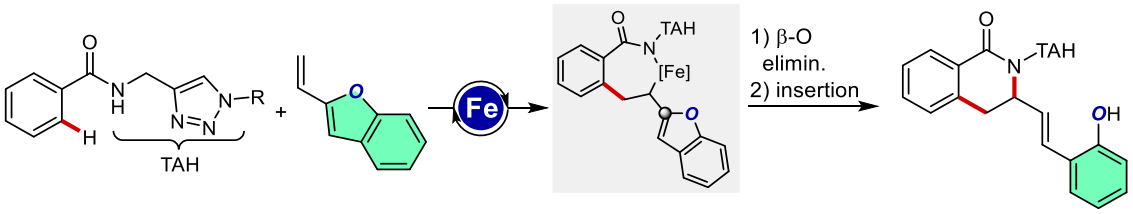

Scheme 3.13 Iron catalyzed C–H alkylation/ring opening with vinylbenzofurans enabled by triazoles.

3.2.1 Optimization Studies

Our study commenced by submitting benzamide **1a** in the presence of 2-vinylbenzofuran **2a** under various reaction conditions. As we previously observed with alkenes as reaction partner, the transformation is promoted by bidentate phosphorous ligands, as shown in Table 3.1, while 2,2'-bipyridine failed to induce any reaction (entry 5). The best results were obtained with a diphosphine ligand with a rigid, aromatic backbone, such as dppbz, with PhMgBr (3.0 equiv), and $ZnCl_2$ (2.0 equiv) as zinc salt (entries 7, 8). Substituting $Fe(acac)_3$ with other iron(II) and iron(III) salts not only reduced yields but also led to the formation of by-product **3'aa** (entries 11, 12). Other organomagnesium reagents, previously shown to be effective in promoting iron-catalyzed C–H functionalizations, were not suitable in this case (entries 8, 9).[17] In stark contrast, other transition metals, such as cobalt, nickel, or palladium, did not facilitate any transformation under otherwise identical conditions (entries 14-16). Finally, the role of zinc was examined; the presence of zinc proved crucial for the reactivity of the iron catalysts, whereas using it as a TMEDA adduct was detrimental (entries 10, 11).[18]

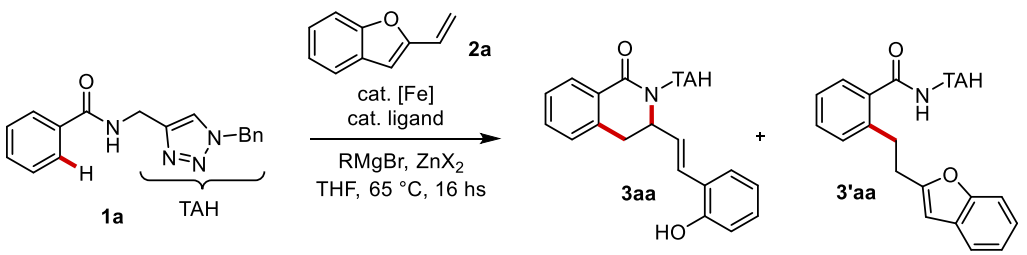

Entry[a]	Catalyst	Ligand	RMgBr	ZnX_2	**3aa** + **3'aa**(%)[b]
1	$Fe(acac)_3$	dppe	PhMgBr	$ZnBr_2$	50 (45) + trace
2	$Fe(acac)_3$	dppe	PhMgBr	$ZnCl_2$	47 (42) + trace
3	$Fe(acac)_3$	dppen	PhMgBr	$ZnBr_2$	53 (49) + trace
4	$Fe(acac)_3$	dppen	PhMgBr	$ZnCl_2$	38 (35) + trace
5	$Fe(acac)_3$	2,2'-bipy	PhMgBr	$ZnCl_2$	n.d.
6	$Fe(acac)_3$	dppbz	PhMgBr	$ZnBr_2$	(25)
7	$Fe(acac)_3$	dppbz	PhMgBr	$ZnCl_2$	72 (67) + trace
8[c]	$Fe(acac)_3$	dppbz	PhMgBr	$ZnCl_2$	76 (72) + trace
9[d]	$Fe(acac)_3$	dppbz	PhMgBr	$ZnCl_2$	62 + trace
10[e]	$Fe(acac)_3$	dppbz	PhMgBr	$ZnCl_2$	50 + trace
11	$FeCl_3$	dppbz	PhMgBr	$ZnCl_2$	37 + 14

12	$FeCl_2$	dppbz	PhMgBr	$ZnCl_2$	30 + trace
13	$Fe(acac)_3$	dppbz	EtMgBr	$ZnCl_2$	n.d.
14	$Fe(acac)_3$	dppbz	$TMSCH_2MgBr$	$ZnCl_2$	n.d.
15	$Fe(acac)_3$	dppbz	PhMgBr	--	n.d.
16	$Fe(acac)_3$	dppbz	PhMgBr	$ZnCl_2TMEDA$	n.d.
17	$Pd(OAc)_2$	dppbz	PhMgBr	$ZnCl_2$	n.d.
18	$Ni(acac)_2$	dppbz	PhMgBr	$ZnCl_2$	n.d.
19	$Co(acac)_2$	dppbz	PhMgBr	$ZnCl_2$	n.d.

[a]Reaction conditions: **1a** (0.2 mmol), **2a** (0.6 mmol), [Fe] (0.03 mmol), ligand (0.03 mmol), RMgBr (0.6 mmol), ZnX_2 (0.4 mmol), THF (0.3 mL). [b]Yields determined using 1,3,5-trimethoxybenzene as the internal standard. In parenthesis, isolated yields. [c]THF (0.5 mL). [d]RMgBr (0.52 mmol), ZnX_2 (0.24 mmol). [e] [Fe] (0.02 mmol), ligand (0.02 mmol).

Table 3.1 Optimization of iron catalyzed C–H alkylation/ring opening with **2a**.

To unequivocally establish the atom connectivity present in **3aa**, its structure was confirmed by single-crystal X-ray analysis. Suitable crystals for X-ray diffraction were obtained by slow diffusion of hexane in an ethyl acetate solution of compound **3aa.**

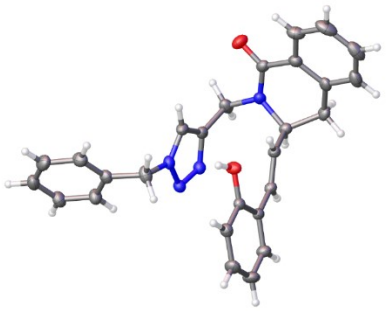

Figure 3.1 X-ray structure of product **3aa** (CCDC 2314708).

Given the reported reactivity of benzofuran in iron-catalyzed ring opening reaction in the presence of a Grignard reagent,[16] we decided to perform a stability test of compound **2a** under the optimized catalytic reaction conditions. After the quenching, we submitted the crude of the reaction to ^{1}H NMR analysis and we observed that without the presence of **1a**, the 2-vinylbenzofuran substrate **2a** remains unchanged after the reaction. In fact, from the stack plot of the crude and the ^{1}H NMR of the pure starting material we can only observe the diagnostic peaks of **2a**, along with the biphenyl that is formed during the reaction.

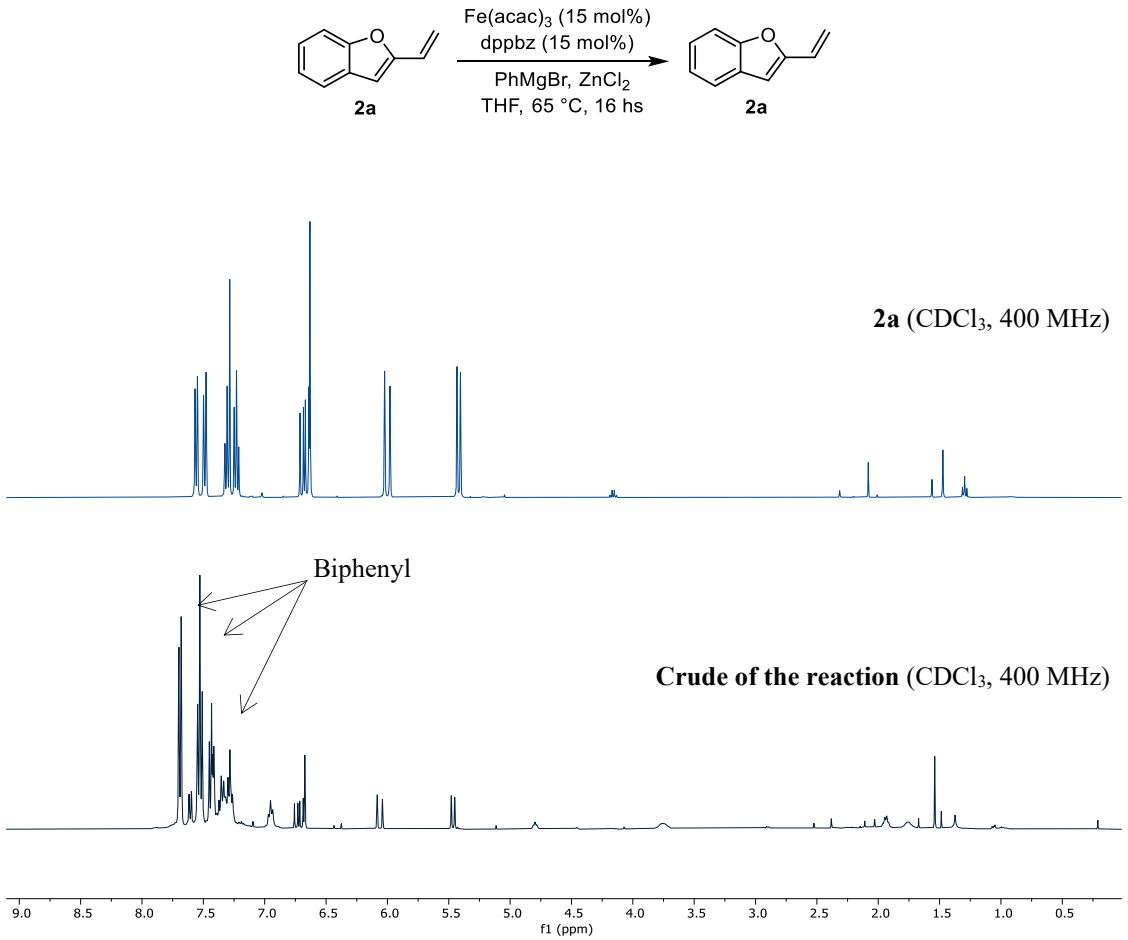

Scheme 3.14 Stability test of 2-vinylbenzofuran **2a** under the catalytic reaction conditions.

To demonstrate the unique reactivity of **2a** under the optimized reaction conditions we also tested other vinylarene compounds under the iron catalytic regime. Hence, both 2-vinylbenzothiophene **2o** and 2-vinylindole derivative **2p** reacted with model substate **1a** with the sole formation of linear hydroarilation products in low yields. Additionally, we also synthetized derivatives **2q** and **2r** with the vinylic moiety at the 3 and 7 positions of the benzofuran ring, respectively. The reaction with substrate **2q** failed to deliver any product, while **2r** reacted only following the hydroarylation pathway without the formation of the corresponding annulation product. This latter experiment highlights the importance of the cyclometalated species that is formed during the catalysis that needs to have the correct geometry in order to promote the *β*-oxygen elimination over the simple hydroarilation of the olefin.

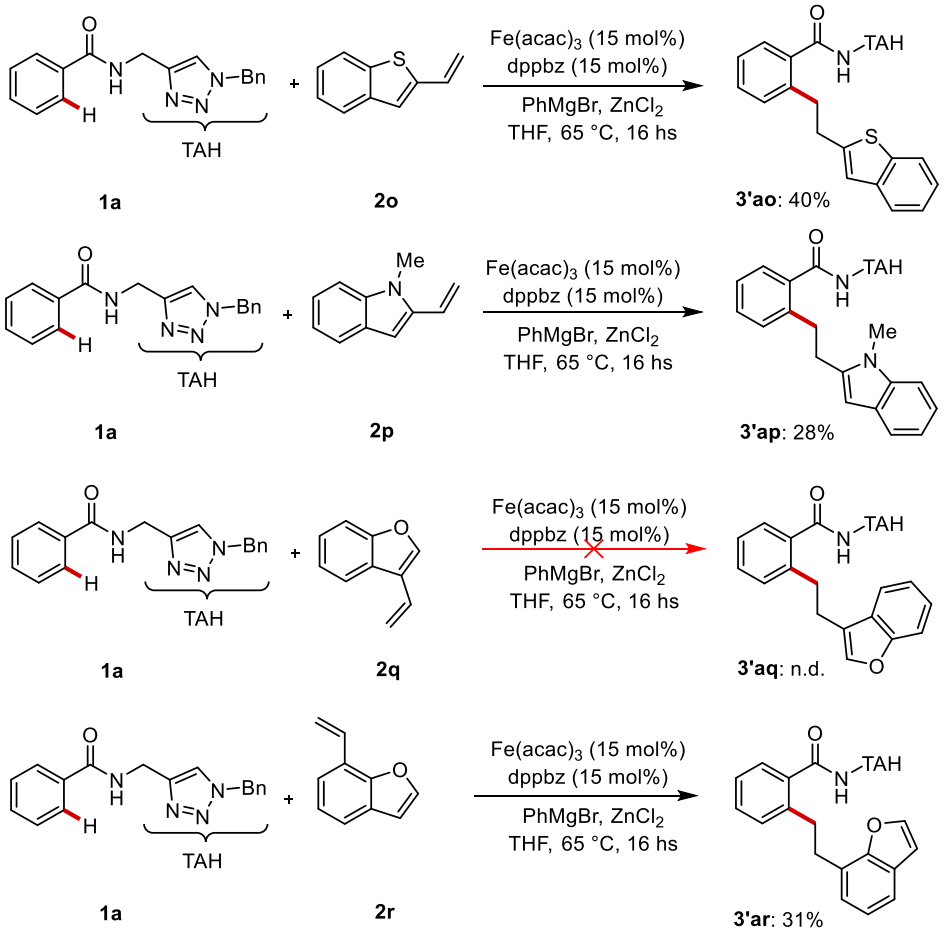

Scheme 3.15 Limitations for other vinylarene compounds.

We also evaluated the reactivity of 2-vinylbenzofuran **2a** in the presence of other directing groups, in particular 8-aminoquinoline (Q) which is one of the most widely used in iron-catalyzed C–H functionalizations.[8a] We conducted a brief screening of reaction conditions using model substrate **4a**, but the only product delivered under iron catalysis was the 1*H*-inden-3-amine derivative **5aa**. In particular, only a moderate yield of this product was obtained employing the 2,2'-bipy ligand in place of a phosphine-based one. This finding highlights the role of triazole directing group that provides the suitable geometry to promote the ring-opening of the benzofuran moiety.[19]

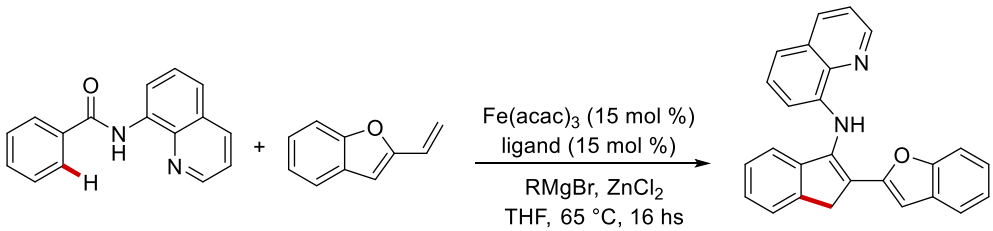

4a **2a** **5aa**

Entry[a]	Catalyst	Ligand	RMgBr	**5aa**[b]
1	$Fe(acac)_3$	2,2'-bipy	PhMgBr	36
2	$Fe(acac)_3$	dppe	PhMgBr	27
3	$Fe(acac)_3$	dppen	PhMgBr	25
4	$Fe(acac)_3$	dppbz	PhMgBr	26

[a]Reaction conditions: **4a** (0.2 mmol), **2a** (0.6 mmol), [Fe] (0.03 mmol), ligand (0.03 mmol), PhMgBr (0.6 mmol), $ZnCl_2$ (0.4 mmol), THF (0.3 mL). [b]Isolated yields.

Table 3.2 Screening of reaction conditions for benzamide **4a**.

The structure of compound **5aa** was determined by 1D and 2D NMR spectroscopy and confirmed by single-crystal X-ray analysis. Suitable crystals for X-ray diffraction were obtained by slow diffusion of hexane in an ethyl acetate solution of compound **5aa.**

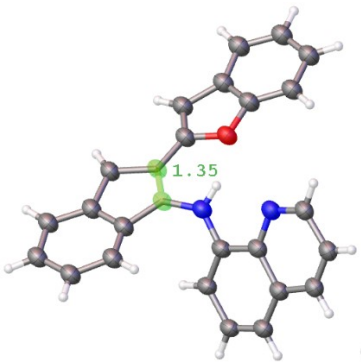

Figure 3.2 X-ray structure of product **3aa** (CCDC 2314709).

3.2.2 Substrate Scope

We synthetized various methylene-tethered triazoles (**1b-e**) that were successfully submitted to the devised protocol, delivering the corresponding isoquinolones (**3ba-de**) in good yields. Product **3ea** represent an excellent example of chemoselectivity of the iron-catalyzed transformation. In fact, here we don't observe the insertion of the terminal double bond of the triazole alkyl pendant, but only the reaction of the substrate with the 2-vinylbenzofuran. Benzamides substituted with electron-rich groups at the *para* and *meta* positions generally outperformed their electron-poor counterparts. In these cases, by-products **3'** were detected only in trace amounts via ^{1}H-NMR analysis of the crude reaction mixtures. Interestingly, this minimal by-product formation was also observed for fluoro- and bromo-substituted benzamides (**1m-n**). Conversely, substrates with electron-withdrawing groups produced variable amounts of by-products (**3'na-pa**, **3'sa**), which could be isolated after chromatographic purification. Substitution at the *ortho*-position hindered the cascade sequence, resulting in low yields of C−H alkylated benzamide **3'ta**.[20] A naphthalene ring was also converted into the corresponding product **3ua** in good yields, while electron-rich heterocycles showed diverse outcomes. For example, the indole derivative **1v** produced both compounds **3va** and **3'va**, whereas thiophene **1w** yielded only thieno [2,3-*c*] pyridone **3wa** in moderate yields.

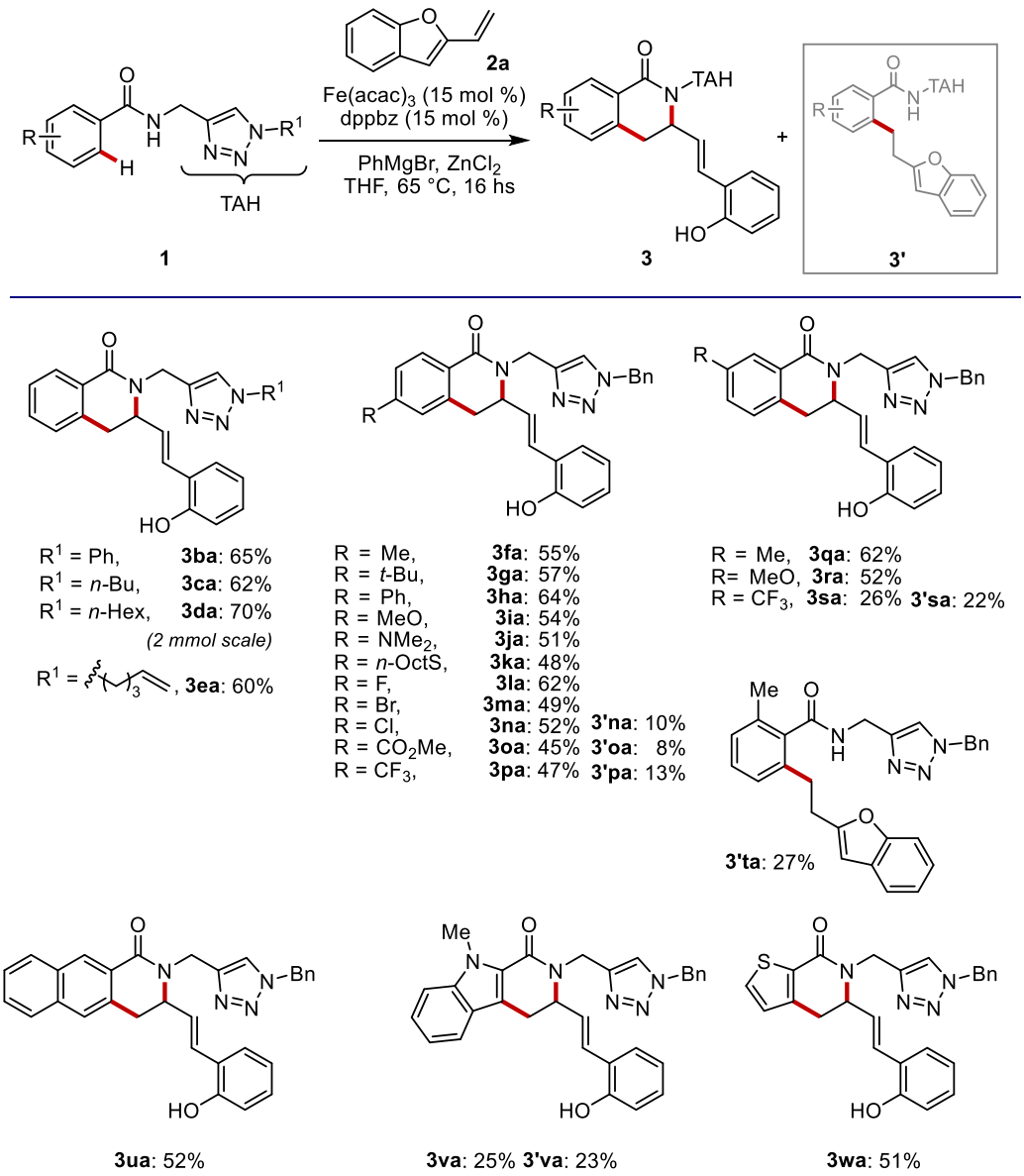

Scheme 3.16 Substrate scope of benzamides **1**.

Afterwards, we synthetized a series of diversely substituted 2-vinylbenzofuran derivatives that were submitted to the iron-catalyzed cascade C–H annulation. These compounds were obtained starting from the corresponding commercially available salicylaldehydes, following a three-step procedure (Scheme 3.17). After a first step of alkylation of the phenolic moiety with bromoacetaldehyde diethyl acetal (**XVIII**), the benzofuran ring is formed by the acid-catalyzed one-pot acetal hydrolysis and condensation (**XIX**). Finally, the aldehyde at the 2-position is converted in the desired double bond by a Wittig olefination reaction. The 2-vinylbenzofurans **2** obtained from this synthesis are decorated with both electron-donating and electron-withdrawing groups, mainly at the 5 position to evaluate the different impact on the stability of the transient phenolate intermediate that derives from the ring-opening reaction.

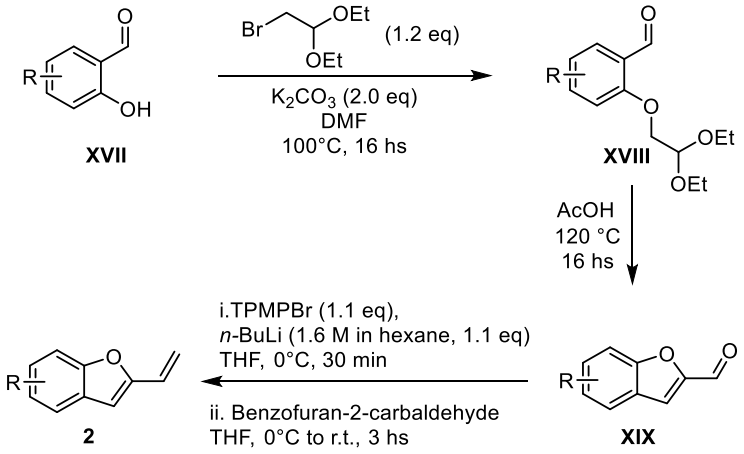

Scheme 3.17 General procedure for the synthesis of 2-vinyl benzofuran substrates **2**.

When we submitted the 5-substituted 2-vinylbenzofurans to the catalytic conditions we observed an opposite trend with respect to the one revealed for benzamide derivatives (Scheme 3.18). Electron-donating groups **2b–d**, led to the formation of both isoquinolones **3ab–ad** and alkylated by-products **3'ab–ad** in variable yields. In contrast, when catalytic reactions were performed using 2-vinylbenzofurans decorated with electron-withdrawing groups **2f–h**, isoquinolones **3af–ah** were the only products that could be isolated from the reaction mixture. In the same way as before, also here the fluoro-containing vinylbenzofuran **2e** represents a deviation from this trend since both compounds **3ae** and **3'ae** were isolated after the catalytic reaction in overall moderate yields. Substrates with functional groups at other positions of the benzofuran ring were also tested under identical reaction conditions. 2-vinylbenzofuran **2i** substituted at the 6-position with a methoxy group reacted smoothly leading to the formation of **3ai** in good yields. Contrarily, a 7-methoxy-2-vinylbenzofuran analogue **2j** turned out to be more challenging. A similar outcome was observed when 5,7-dichloro-2-vinylbenzofuran **2k** was used as the reaction pattern. In all these cases, no formation of by-products **3'** was detected in the reaction mixtures. 2-Vinylnaphtho[2,1-*b*]furan **2l** turned out to be reactive under the iron catalytic regime. However, **3'al** was the only product delivered, although in fair yield.

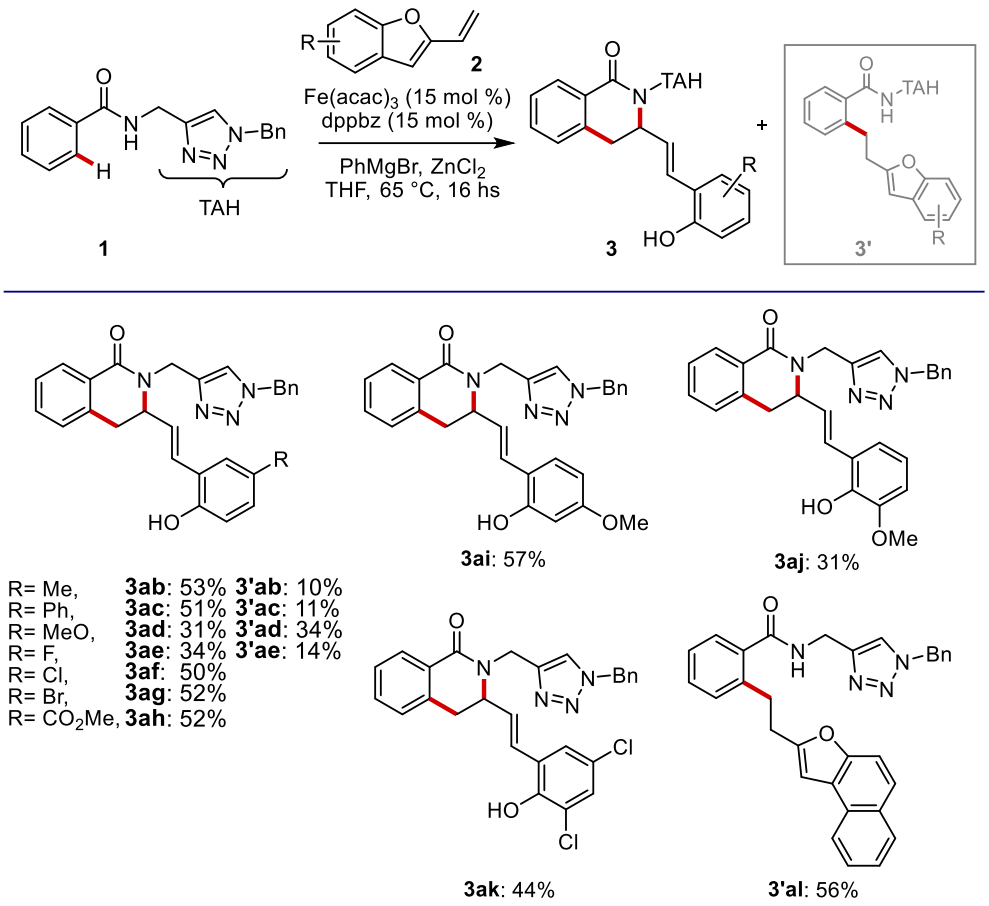

Scheme 3.18 Substrate scope of 2-vinylbenzofurans **2**.

After succeeding in the development of the catalytic conditions that promote the ring-opening of 2-vinylbenzofuran we also tested our method with biomass-derived 2-vinylfuran derivatives. When the reaction was performed with simple 2-vinylfuran **6a** we did not observe the formation of any product. We suppose that this is probably due to its very low boiling point that prevents to have the right concentration in the reaction media or its low stability under the reaction conditions. Given this result, we synthetized and tested under otherwise identical reaction conditions compound **6b**. Hence, the presence of the methyl group at the 5 position was found to be mandatory to promote a challenging cascade C–H annulation leading to compound **7ab**, functionalized with a β,γ-unsaturated ketone pendant.

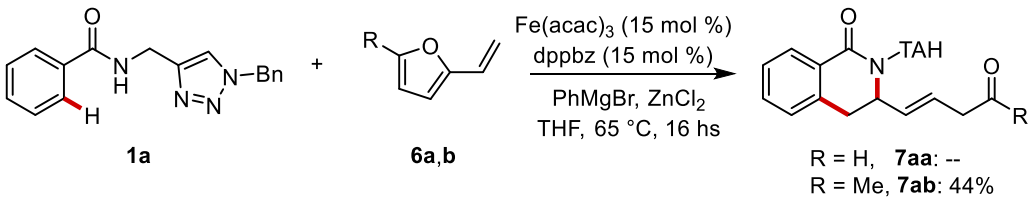

Scheme 3.19 Reaction with 2-vinylfurans **6**.

The desired product **7ab** was isolated in 44% yield without observing the formation of the linear hydroarilation product. The formation of the β,γ-unsaturated ketone supports our hypothesis that the reaction proceeds via an enolate intermediate that is formed after the ring-opening of the furan (Scheme 3.20) which secure the carbonyl functional group towards the reaction with the Grignard and arylzinc species during the reaction.

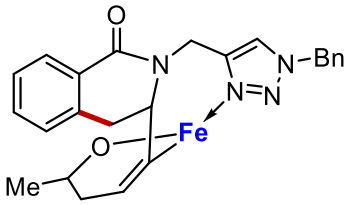

Scheme 3.20 Hypothesized intermediate from 2-vinylfuran **6b**.

3.2.3 Mechanistic Investigation

Given the unique features of the developed iron-catalyzed C–H cascade annulation, we conducted mechanistic experiment to get more insights on the reaction mechanism. Inter- and intramolecular competition experiments using deuterium-labelled compound [D]$_5$–**1b** revealed a lack of primary kinetic isotope effect. These results support a facile C–H cleavage which is not the rate-determining step of the overall reaction.

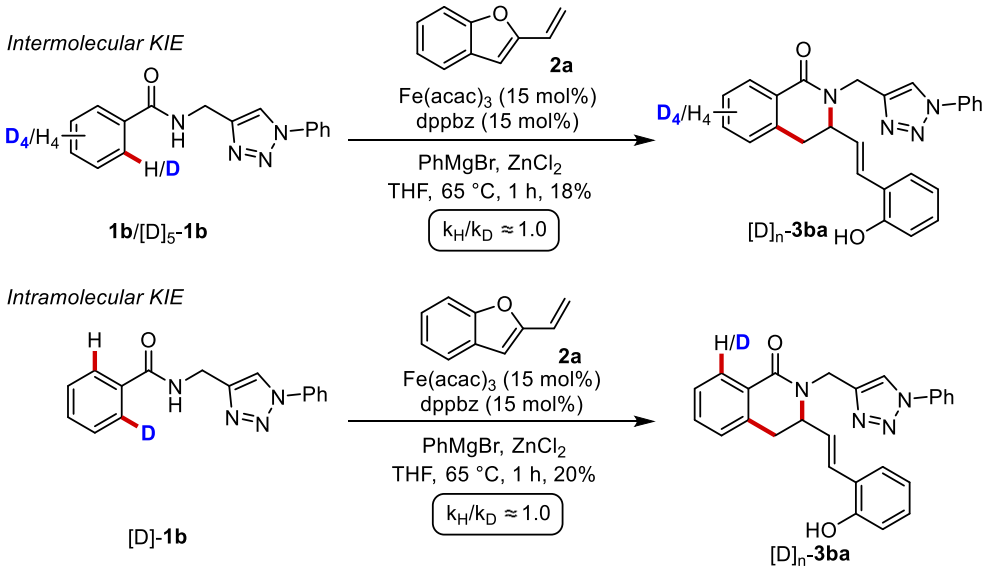

Scheme 3.21 KIE studies of iron-catalyzed C–H annulation with vinylbenzofuran **2a**.

Compound [D]$_5$–**1a** was then subjected to the optimal catalytic conditions, resulting in the formation of the corresponding product without observation of significant deuterium scrambling at the *ortho*-position (Scheme 3.22, a). This result indicates that the C–H activation step is likely to be irreversible. A deuterated 2-vinylbenzofuran, [D]$_n$–**2a**, was synthesized and reacted with benzamide **1a**. This reaction yielded isoquinolone [D]$_n$–**3aa** in good yields, with retention of deuterium content (Scheme 3.22, b). Additionally, when the model reaction was quenched by the addition of DCl, selective labelling occurred at only one vinylic position (Scheme 3.22, c). These observations do not support a reaction mechanism initiated by oxidative addition of the iron followed by olefin hydrometallation.

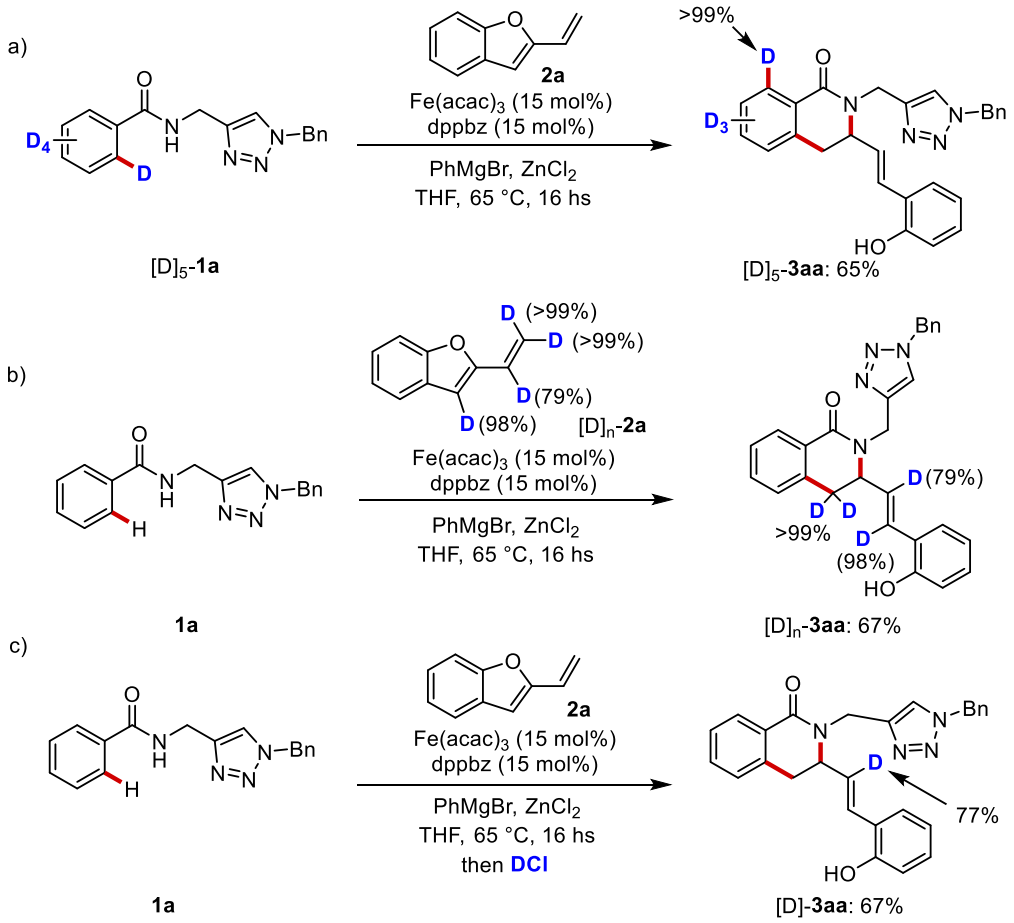

Scheme 3.22 Experiments with isotopically labelled substrates.

To further elucidate the mechanism of the iron-catalyzed transformation facilitated by the triazole directing group, DFT calculations were performed at the PW6B95-D4/def2-TZVPP + SMD(THF)//TPSS-D3(BJ)/def2-SVP level of theory (Figure 3.3). These studies were conducted in collaboration with the research group of Prof. Dr. Lutz Ackermann. Substrate **1a** and 2-vinylbenzofuran **2a** were selected as models for the iron-catalyzed C–H activation process. Given the characteristics of the iron(II) complexes, the reaction pathway was computed for all three possible spin states: singlet (low-spin), triplet (intermediate-spin), and quintet (high-spin) (1,3 and 5 respectively, Figure 3.3).[21] We identified and analyzed four elementary steps involved in the cascade C–H annulation process. These steps can be rationalized as: a) C–H activation, b) alkene migratory insertion, c) *β*-oxygen elimination and d) allene migratory insertion. The computational analysis of the C–H activation step is in line with a ligand-to-ligand hydrogen transfer mechanism (LLHT)[22] via **TS(1-2)**^{1}, with an activation energy of 18.3 kcal mol^{-1}. The low energy barrier is attributed to an into-play spin-crossover that determines a drastic reduction of the energy barrier when compared to the quintet **TS(1–2)** surface. After a facile olefin coordination to form **Int3** we have the migratory insertion step through **TS(3–4)** with an energy

barrier of 24.0 kcal mol^{-1}. Here as well, spin cross-over was observed from a quintet **Int3** to a singlet **TS(3–4)** surface, delivering **Int4** in a quintet state. After the olefin rotation, the **Int4'** undergoes *β*–O-elimination via **TS(4'–5),**[23] which revealed to be endergonic with an energy barrier of 28.1 kcal mol^{-1}, delivering **Int5** with an η^2-allene coordination. This will undergo intramolecular migratory insertion into the N–Fe bond to form **Int6** with an energy barrier of 38.3 kcal mol^{-1}. This result indicates that the intramolecular migratory insertion event is the rate determining step of the reaction.

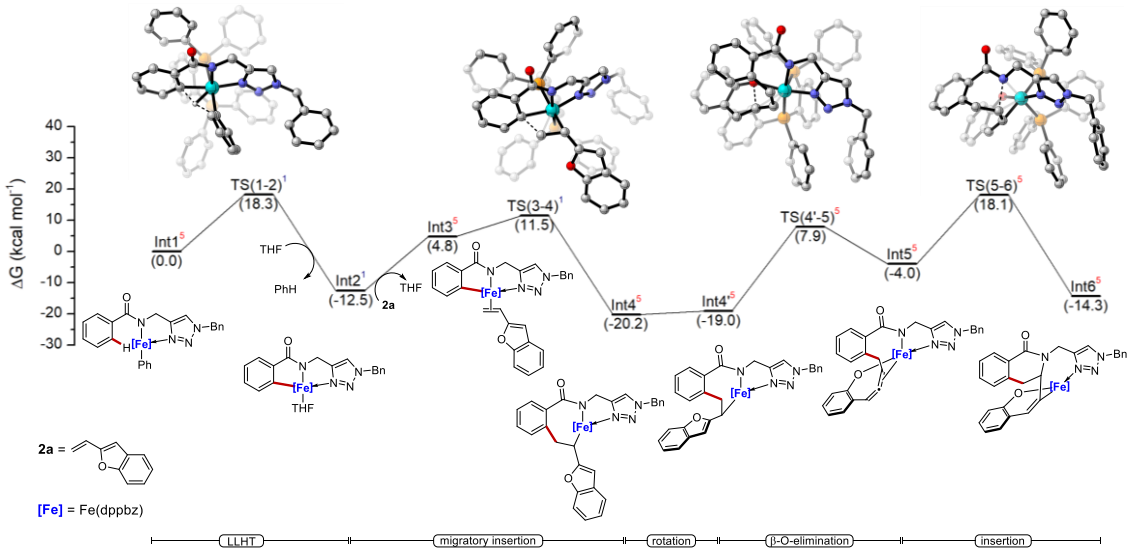

Figure 3.3 Computed Gibbs free energy profile ($\Delta G_{338.15}$) in kcal mol^{-1} for the iron-catalyzed cascade C−H annulation with 2-vinylbenzofuran at the PW6B95-D4/def2-TZVPP+SMD(THF)//TPSS-D3(BJ)/def2-SVP level of theory. Non-relevant hydrogens in the transition state structures were omitted for clarity. Superscripted 1, 3, and 5 represents singlet, triplet and quintet spin states, respectively.

We also performed a computational Hammett plot analysis at the same level of theory. We identified the *β*–O-elimination step as the point of deviation from the investigated pathway which leads to the formation of linear by-products **3'**. The analysis showed that more electron-withdrawing substituents at the *meta* and *para* positions of the benzamide substrate may facilitate the formation of linear by-products **3'**. The low-chemoselectivity could be also a result of the proto-demetalation step of **Int4** that releases by-product **3'** that becomes competitive in the presence of electron-withdrawing, more acidic substrates.[24] In contrast, electron-rich substituents were shown to largely favour the formation of isoquinolones **3** (See Experimental section for more details).

3.2.4 Proposed Catalytic Cycle

Based on our mechanistic findings, we propose a catalytic cycle that begins with a facile C–H activation via LLHT (Scheme 3.23). This is followed by the coordination of vinylbenzofuran **2a**, leading to a rapid migratory insertion that forms the key iron species **Int4**. This intermediate then undergoes a rotation of the side-chain arm, allowing for an endergonic *cis*-*β*–O elimination, resulting in **Int5**. The next step involves a rate-determining intramolecular insertion into the N–Fe bond, forming **Int6**. Finally, the product **3aa** is released through proto-demetalation, regenerating the active iron species.

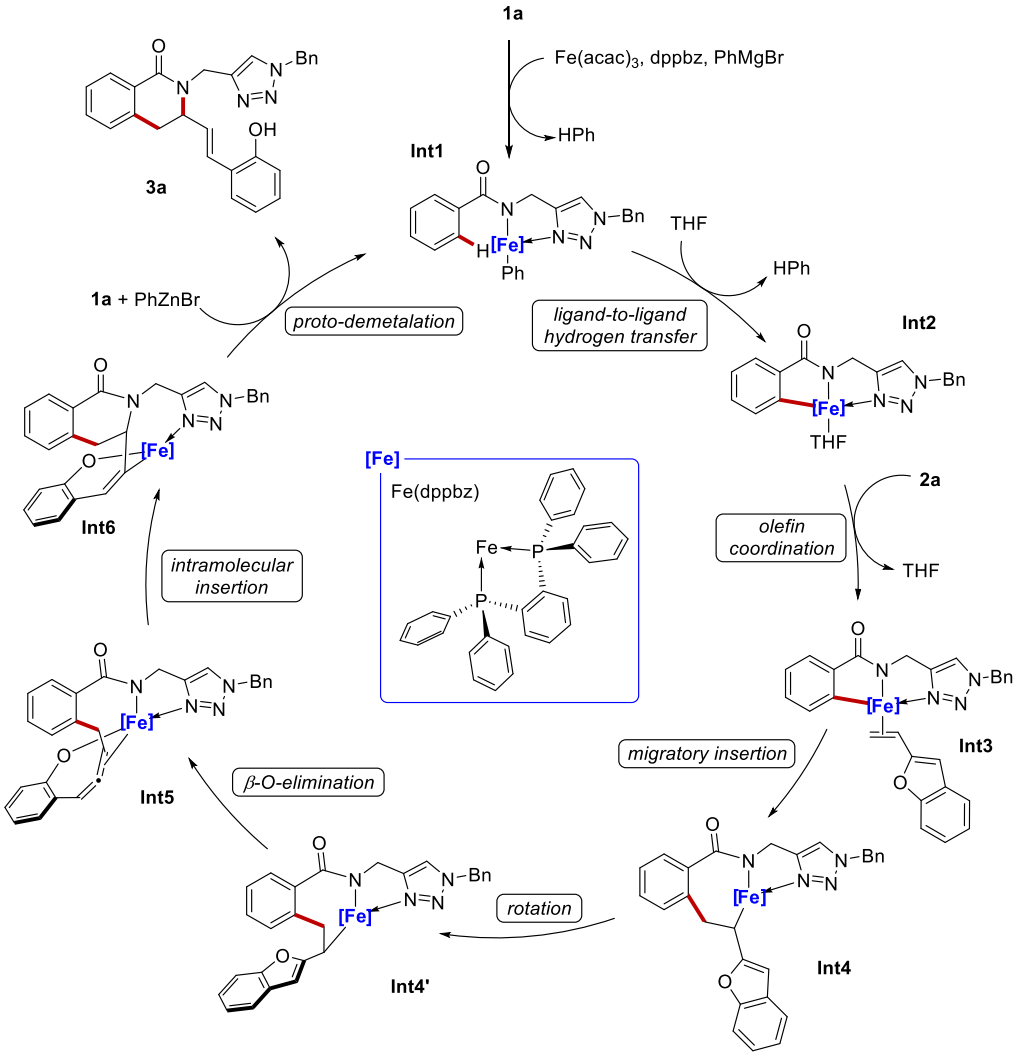

Scheme 3.23 Proposed reaction mechanism.

3.2.5 Late-stage Diversifications

We demonstrated the versatility of the iron catalysis by several late-stage diversifications. In particular, the isoquinolone product is synthetically valuable due to the presence of a phenolic pendant on the C3 position. This feature allows for further functionalizations, leading to the synthesis of more complex derivatives. It is well-known that aryl triflates can undergo oxidative addition reactions with palladium-based catalysts. Therefore, the phenol was converted into a triflate using trifluoromethanesulfonic anhydride (Scheme 3.24, a) to explore the feasibility of further functionalizations through palladium catalyzed cross-coupling reactions. Specifically, compound **8aa** was subjected to a Suzuki cross-coupling reaction to afford derivative **9aa**, a Sonogashira cross-coupling with trimethylsilylacetilene to produce **11a** and a Buchwald-Hartwig reaction with benzylamine to synthetize derivative **12aa**. Additionally, the treatment of **8aa** with formic acid in the presence of a palladium catalyst led to the reduction of the phenolic moiety in compound **10aa**. The post-synthetic modifications were not limited to the phenol functional group but also extended to the triazole motif. First, the treatment with $LiAlH_4$ enabled the reduction of the triazolyl amide to an amine (**13aa**, Scheme 3.24, f). Lastly, we employed a new triazole directing group, functionalized with a terminal alkene moiety (**3ea**), which was further derivatized through a representative olefin cross-metathesis with methylacrylate, yielding product **14ea** (Scheme 3.24, g).

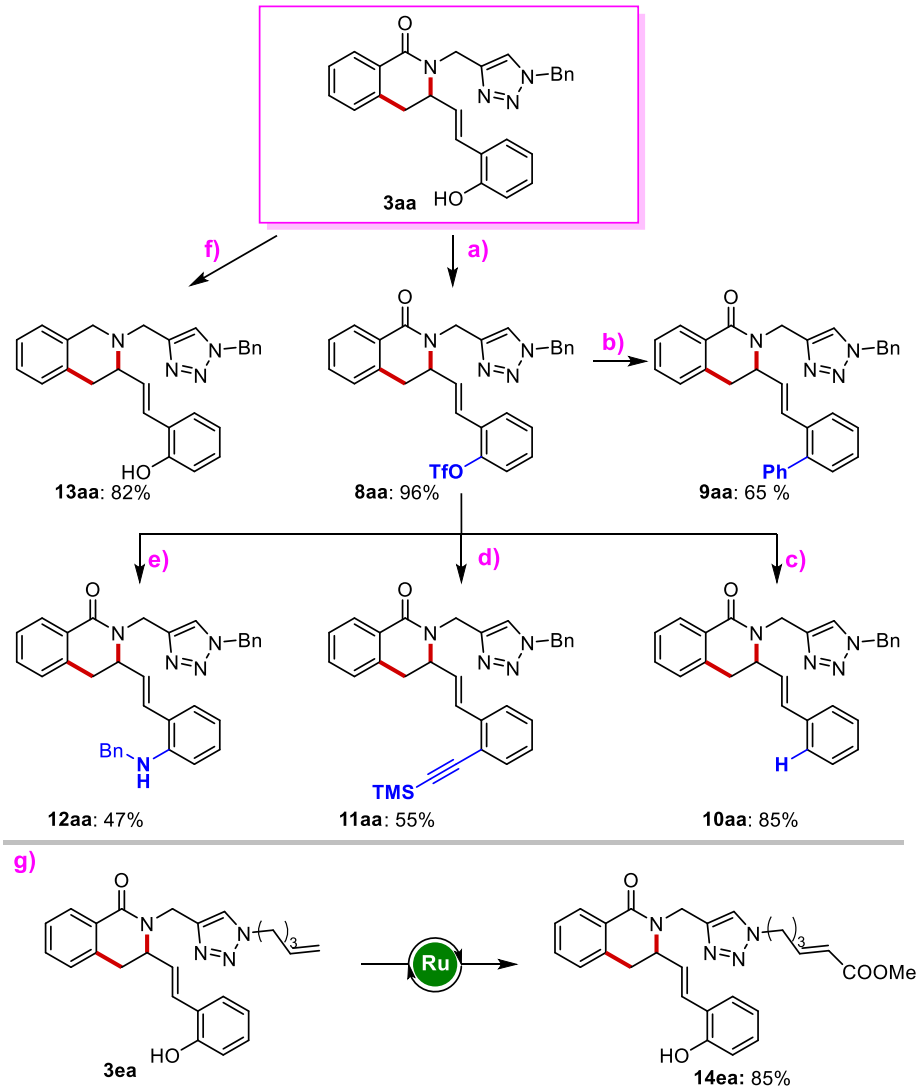

Scheme 3.24 Late-stage synthetic diversification of **3aa** and **3ea**.

Unfortunately, we failed in the removal of the triazole directing group. We tried common chemical methods including hydrolysis under acidic or basic conditions and oxidative methods, but all these trials were unsuccessful (Table 3.3, entries 1-9). Further, we also attempted to perform an electrochemical deprotection that was previously found successful for related substrates.[7] However, the high reactivity of the heterocyclic moiety, that presents a very acidic C–H bond, an alkene and a phenol, hampered the selectivity of the electro-removal. In all the cases (Table 3.3, entries 10-13), starting material **1a** was the major product that could be observed along with its broad decomposition.

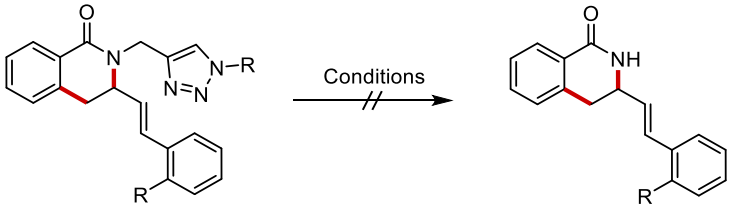

Entry	R	Conditions
1	OH (**3aa**)	Conc. aq. HCl (1 ml), dioxane, 120 °C, 16 hs
2	OH (**3aa**)	NaOH (5.0 equiv.), THF, 65 °C, 16 h
3	OH (**3aa**)	HOTf (2.0 equiv), DCM, 0 °C, 2 hs
4	OH (**3aa**)	BF_3 Et_2O (1.5 equiv), dry MeOH, 130 °C, 16 hs
5	OH (**3aa**)	$NOBF_4$ (2.0 equiv), MeCN, 50 °C, 16 hs
6	H (**10aa**)	HOTf (2.0 equiv), DCM, 0 °C, 16 hs
7	H (**10aa**)	Conc. aq. HCl (1mL), dioxane, 120 °C, 16 hs
8	H (**10aa**)	CAN (3.0 equiv), CH_3CN (1 mL), 80 °C, 16 hs
9	H (**10aa**)	Pd/C (cat.) ammonium formate, MeOH (80° C), 16 hs
10	OH (**3aa**)	RVC anode, stainless steel cathode, $ZnBr_2$TMEDA (2.0 equiv), *i*PrMgBr (3.0 equiv), 60 °C, CCE at 10 mA, 16 hs
11	H (**10aa**)	RVC anode, stainless steel cathode, $ZnBr_2$TMEDA (2.0 equiv), *i*PrMgBr (3.0 equiv), 60 °C, CCE at 10 mA, 16 hs
12	H (**10aa**)	RVC anode, stainless steel cathode, $ZnBr_2$TMEDA (2.0 equiv), *i*PrMgBr (3.0 equiv), 60 °C, CCE at 2 mA, 16 hs
13	H (**10aa**)	RVC anode, stainless steel cathode, $ZnBr_2$TMEDA (2.0 equiv), Bu_4NBF_4 (2.0 equiv), *i*PrMgBr (3.0 equiv), 60 °C, CCE at 2 mA, 16 hs

Table 3.3 Attempts for removal of TAH directing group.

3.3 Conclusions

In summary, in this section we presented the synthesis of highly functionalized isoquinolones through a cascade C–H annulation with 2-vinylbenzofurans, facilitated by Earth-abundant and non-toxic iron catalysts. The versatility of iron catalysis was evidenced by several late-stage modifications of the phenol and triazole directing group. Notably, the triazole directing group was crucial in promoting a novel reaction mechanism in iron catalysis, involving an unprecedented *β*–O elimination that drives C(sp^2)–O activation of benzofuran heterocyclic scaffolds. Both computational and experimental studies identified spin-crossover phenomena and fast C–H activation as key factors in the efficiency of the iron catalysis.

3.4 References

[1] For selected recent reviews, see: a) D. Mandal, S. Roychowdhury, J. P. Biswas, S. Maiti, D. Maiti, *Chem. Soc. Rev*. **2022**, *51*, 7358–7426; b) G. Ewano, C. Theunissen, *Angew. Chem. Int. Ed*. **2019**, *58*, 7202–7236; c) Z. Dong, Z. Ren, S. J. Thompson, Y. Xu, G. Dong, *Chem. Rev*. **2017**, *117*, 9333–9403; d) M. Gulías, J. L. Mascareñas, *Angew. Chem. Int. Ed*. **2016**, *55*,11000–11019.

[2] a) S. Murai, F. Kakiuchi, S. Sekine, Y. Tanaka, A. Kamatani, M. Sonoda, N. Chatani, *Nature* **1993**, *366*, 529–531; b) L. N. Lewis, J. F. Smith, *J. Am. Chem. Soc*. **1986**, *108*, 2728–2735.

[3] A. Matsumoto, L. Ilies, E. Nakamura, *J. Am. Chem. Soc*. **2011**, *133*, 6557– 6559.

[4] L. Ilies, A. Matsumoto, M. Kobayashi, N. Yoshikai, E. Nakamura, *Synlett* **2012**, *23*, 2381–2384.

[5] T. Matsubara, L. Ilies, E. Nakamura, *Chem. Asian J*. **2016**, *11*, 380–384.

[6] G. Cera, T. Haven, L. Ackermann, *Chem. Commun*. **2017**, *53*, 6460–6463.

[7] J. Mo, T. Müller, J. C. A. Oliveira, S. Demeshko, F. Meyer, L. Ackermann, *Angew. Chem. Int. Ed*. **2019**, *58*, 12874–12878.

[8] a) L. Ilies, Y. Zhou, H. Yang, T. Matsubara, R. Shang, E. Nakamura, *ACS Catal.* **2018**, *8*, 12, 11478–11482; b) S. Cattani, A. Secchi, L. Ackermann, G. Cera, *Org. Biomol. Chem*. **2023**, 21, 1264–126.

[9] J. Mo, A. M. Messinis, J. C. A. Oliveira, S. Demeshko, F. Meyer, L. Ackermann, *ACS Catal*. **2021**, 11, 1053−1064.

[10] Y.-H. Miao, Y.-H. Hu, J. Yang, T. Liu, J. Sun, X.-J. Wang, *RSC Adv*. **2019**, *9*, 27510–27540.

[11] J. Yu, L. Huang, *ChemCatChem* **2023**, *15*, e202300986.

[12] For selected examples, see: a) C. Lu, Y. Lin, M. Wang, J. Zhou, S. Wang, H. Jiang, K. Kang, L. Huang, *ACS Catal*. **2023**, *13*, 2432–2442; b) L. A. Perego, S. Wagschal, R. Grüber, P. Fleurat-Lessard, L. El Kaïm, L. Grimaud, *Adv. Synth. Catal*. **2019**, *361*, 151–159; c) Q.-F. Xu-Xu, Q.-Q.Liu, X. Zhang, S.-L. You, *Angew. Chem. Int*. *Ed*. **2018**, *57*, 15204–15208; d) S. Tsuchiya, H. Saito, K. Nogi, H. Yorimitsu, *Org. Lett.* **2017**, *19*, 5557–5560; e) L. Guo, M. Leiendecker, C. C. Hsiao, C. Baumann, M. Rueping, *Chem. Commun*. **2015**, *51*, 1937–1940; f) K. Itami, S. Tanaka, K. Sunahara, G. Tatsuta, A. Mori, *Asian J. Org. Chem*. **2015**, *4*, 477–481; g) S. Yow, A. E. Nako, L. Neveu, A. J. P. White, M. R. Crimmin, *Organometallics* **2013**, 32, 5260–5262; h) J. Cornella, R. Martin, *Org. Lett.* **2013**, *15*, 6298–6301.

[13] E. Wenkert, E. L. Michelotti, C. S. Swindell, *J. Am. Chem. Soc.* **1979**, *101*, 2246–2247.

[14] D. Ding, H. Dong, C. Wang, *CCS Chemistry* **2022**, *4*, 548–556.

[15] a) H. Saito, S. Otsuka, K. Nogi, H. Yorimitsu, *J. Am. Chem. Soc.* **2016**, *138*, 47, 15315–15318; b) H. Saito, K. Nogi, H. Yorimitsu, *Angew. Chem. Int. Ed.* **2018**, *57*, 11030–11034.

[16] T. Iwasaki, R. Akimoto, H. Kuniyasu, N. Kambe, *Chem. Asian J.* **2016**, *11*, 2834–2837.

[17] a) J. Mo, T. Müller, J. C. A. Oliveira, L. Ackermann, *Angew. Chem. Int. Ed.* **2018**, 57, 77197–723; b) G. Cera, T. Haven, L. Ackermann, *Chem. Commun*. **2017**, *53*, 6460–6463; c) T. Matsubara, L. Ilies, E. Nakamura, *Chem. Asian J*. **2016**, *11*, 380–384; d) Q. Gu, H. H. Al Mamari, K. Graczyk, E. Diers, L. Ackermann, *Angew. Chem. Int. Ed*. **2014**, *53*, 3868–3871.

[18] N. J. Bakkas, M. L. Neidig, *ACS Catal*. **2021**, *11*, 8493–8503.

[19] For metal-catalyzed C–H hydroarylations of 2-vinylbenzofurans that occur without ring-openings, see: a) Y. Zhang, J. Struwe, L. Ackermann, *Angew. Chem. Int. Ed*. **2020**, *59*, 15076–15080; b) R.-P. Li, Z.-W. Shen, Q.-J. Wu, J. Zhang, H.-M. Sun, *Org. Lett.* **2019**, *21*, 5055–5058; c) Z.-J. Jia, C. Merten, R. Gontla, C. G. Daniliuc, A. P. Antonchick, H. Waldmann, *Angew. Chem. Int. Ed*. **2017**, *56*, 2429–2434; d) W. Xu, N. Yoshikai, *Angew. Chem. Int. Ed*. **2014**, *53*, 14166–14170; e) P.-S. Lee, N. Yoshikai, *Angew. Chem. Int. Ed*. **2013**, *52*, 1240–1244.

[20] Y.-M. Wei, M.-F. Wang, X.-F. Duan**,** *Org. Lett.* **2019**, *21*, 16, 6471–6475.

[21] Y. Sun, H. Tang, K. Chen, L. Hu, J. Yao, S. Shaik, H. Chen, *J. Am. Chem. Soc.* **2016**, *138*, 3715–3730.

[22] a) T. Rogge, J. C. A. Oliveira, R. Kuniyil, L. Hu, L. Ackermann, *ACS Catal*. **2020**, *10*, 10551–10558; b) J. Loup, D. Zell, J. C. A. Oliveira, H. Keil, D. Stalke, L. Ackermann, *Angew. Chem. Int. Ed*. **2017**, *56*, 14197–124201; c) S. Tang, O. Eisenstein, Y. Nakao, S. Sakaki, *Organometallics* **2017**, *36*, 2761–2771; d) J. Guihaumé, S. Halbert, O. Eisenstein, R. N. Perutz, *Organometallics* **2012**, *31*, 1300–1314; e) L. Ackermann, *Chem. Rev*. **2011**, *111*, 1315–1345.

[23] For related contributions with [Pd], see: a) H.-Q. Ni, J.-C. Dai, S. Yang, R. P. Loach, M. D. Chuba, I. J. McAlpine, P. K. M. Engle, *Angew. Chem. Int. Ed*. **2023**, *62*, e2023065; b) J. Yang, Y. Zhang, R. Zhu, Y. Xue, *J. Phys. Chem. A* **2021**, *125*, 9267–9278; c) V. T. Tran, J. A. Gurak Jr, K. S. Yang, K. M. Engle, *Nat. Chem*. **2018**, *10*, 1126–1133; For early reports: d) M. Lautens, S. Hiebert, *J. Am. Chem. Soc*. **2004**, *126*, 1437–1447; e) M. Lautens, S. Hiebert, J.-L. Renaud, *J. Am. Chem. Soc.* **2001**, *123*, 6834–6839; For a review: f) J. Le Bras, J. Muzart, *Tetrahedron* **2012**, *68*, 10065–10113.

[24] P. E. Piszel, B. J. Orzolek, A. K. Olszewski, M. E. Rotella, A. M. Spiewak, M. C. Kozlowski, D. J. Weix, *J. Am. Chem. Soc*. **2023**, *145*, 8517–8528.

3.5 Experimental Section

3.5.1 General remarks

Methods

All reactions were carried out in Schlenk tubes under a N_2 atmosphere using pre-dried glassware. THF was dried using a solvent purification system (SPS) from Inert. Yields refer to isolated compounds, estimated to be > 95% pure as determined by ^{1}H-NMR. Column chromatography was performed on silica gel 60 (40-63 mesh). Melting points were measured with an Electrothermal apparatus and are uncorrected. NMR spectra were recorded on a Bruker 400 MHz and JEOL 600 MHz using solvents as internal standards (7.26 ppm for ^{1}H-NMR and 77.00 ppm for ^{13}C-NMR for $CDCl_3$). The terms m, s, d, t, q, and quint represent multiplet, singlet, doublet, triplet, quadruplet, and quintuplet respectively, and the term bs means a broad signal. ^{13}C-DEPTQ NMR spectra are reported for all compounds. Mass spectra were recorded in the ESI mode. Exact masses were recorded on a LTQ ORBITRAP XL Thermo Mass Spectrometer (ESI source).

Materials

PhMgBr (1.0 M in THF) was freshly prepared from Bromobenzene ≥99.5% (GC) and magnesium turnings in anhydrous THF and titrated prior to use using I_2 in THF. The solution of $ZnCl_2$ in THF (1.0 mol/L) was prepared in a Schlenk tube by melting anhydrous $ZnCl_2$ at 230 °C under vacuum for 3 hours. Then, dry THF was added and the solution was stirred until all the $ZnCl_2$ was dissolved. Benzamides **1a-h**, **1k-o**[1], 2-vinylbenzo[*b*]thiophene (**2o**)[2], 1-methyl-2-vinyl-1*H*-indole (**2p**)[3] and 3-vinylbenzofuran (**2q**)[4] were synthesized according to known procedures. Other chemicals were obtained from commercial sources and were used without further purification.

3.5.2 Synthesis of Vinylbenzofuran Substrates

General procedure A: synthesis and characterization of 2-vinylbenzofuran substrates[5]

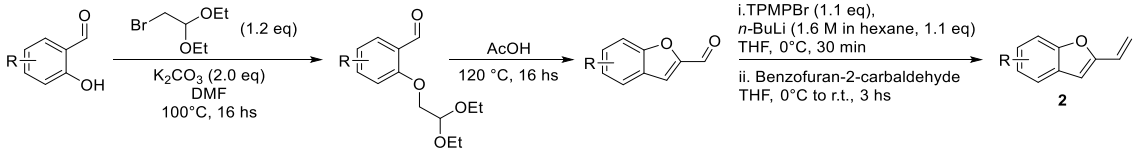

***Step 1*:** A 100 mL round-bottomed flask was charged with salicylaldehyde (20.0 mmol, 1.0 equiv.), bromoacetaldehyde diethyl acetal (30.0 mmol, 1.2 equiv.), anhydrous K_2CO_3 (40.0 mmol, 2.0 equiv.) and dry DMF (20 mL). The resulting suspension was stirred overnight at 100 °C. After cooling, the reaction mixture was diluted with EtOAc (200 mL) and filtered through a pad of celite. The clear filtrate was concentrated under reduced pressure. Purification by flash chromatography (*n*-Hexane/EtOAc) of the oily residue provided the desired product.

Step 2: The resulting 2-(2,2-Diethoxyethoxy)benzaldehyde was dissolved in acetic acid (0.5 M) and refluxed for 16 hs. Most of the acetic acid was evaporated under reduced pressure and the residue was dissolved in Et_2O (100 mL) and extracted with sat. aqueous $NaHCO_3$ solution (3x20 mL). The organic phase was dried over Na_2SO_4 and concentrated under reduced pressure. Purification by flash chromatography (*n*-Hexane/EtOAc) provided the desired product.

Step 3: To a suspension of methyltriphenylphosphonium bromide (TPMPBr, 1.1 equiv.) in dry THF (0.1 M) was added *n*-BuLi (1.6 M in *n*-Hexane, 1.1 equiv.) dropwise at 0 °C under nitrogen. After stirring for 30 min, a solution of benzofuran-2-carbaldehyde (1.0 equiv.) in dry THF (0.2 M) was added dropwise. The reaction mixture was warmed to room temperature and the progress of the reaction was monitored by TLC. After the reaction was completed, the reaction mixture was quenched with sat. aqueous NH_4Cl (50 mL) and extracted with EtOAc (2x100 mL). The combined organic layers were dried over Na_2SO_4 and concentrated under reduced pressure. Purification by flash chromatography (*n*-Hexane/EtOAc) provided desired product.

General procedure B: synthesis and characterization of 2-vinylbenzofuran substrates[6]

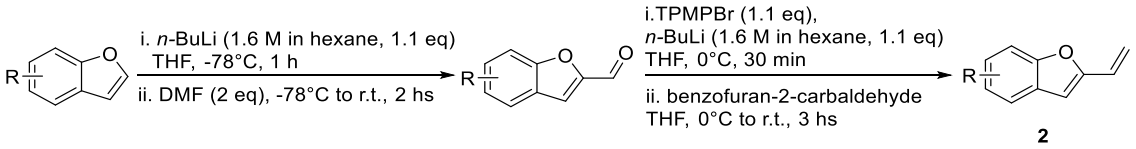

Step 1: To a solution of benzofuran (20.0 mmol, 1.0 equiv.) in dry THF (0.2 M) cooled at -78 °C under nitrogen was added *n*-BuLi (22.0 mmol, 1.6 M in n-Hexane, 1.1 equiv.), dropwise. After stirring the mixture for 1 h at -78 °C, DMF (40.0 mmol, 2.0 equiv.) was added dropwise and stirred for another hour at -78 °C and then allowed to reach room temperature. After the complete consumption of benzofuran, judged by TLC (*n*-Hexane/EtOAc), the reaction was quenched with sat. aqueous NH_4Cl (10 mL). The aqueous layer was extracted with EtOAc (2x100 mL) and the combined organic layers were dried over Na_2SO_4 and concentrated under reduced pressure. Purification by flash chromatography (*n*-Hexane/EtOAc) provided the desired product.

Step 2: To a suspension of methyltriphenylphosphonium bromide (TPMPBr,1.1 equiv.) in dry THF (0.1 M) was added *n*-BuLi (1.6 M in *n*-Hexane, 1.1 equiv.) dropwise at 0 °C under nitrogen. After stirring for 30 min, a solution of benzofuran-2-carbaldehyde (1.0 equiv.) in dry THF (0.2 M) was added dropwise. The reaction mixture was warmed to room temperature and the progress of the reaction was monitored by TLC. After the reaction was completed, the reaction mixture was quenched with sat. aqueous NH_4Cl (50 mL) and extracted with EtOAc (2x100 mL). Purification by flash chromatography (*n*-Hexane/EtOAc) provided desired product.

2-Vinylbenzofuran (2a)

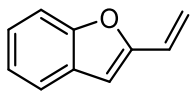

Following general procedure **B**, the title compound was isolated as a colourless liquid (2.45 g, 85%, over two steps). ^{1}H-NMR (400 MHz, $CDCl_3$): δ = 7.55 (dd, *J* = 7.7, 0.8 Hz, 1H), 7.48 (dd, *J* = 8.2, 1.0 Hz, 1H), 7.30 (td, *J* = 7.4, 1.5 Hz 1H), 7.22 (td, *J* = 7.5, 1.0 Hz, 1H), 6.67 (dd, *J* = 17.5, 11.2 Hz, 1H), 6.63 (s, 1H), 5.99 (dd, *J* = 17.5, 1.2 Hz, 1H), 5.41 (dd, *J* = 11.1, 1.2 Hz, 1H). ^{13}C-NMR (101 MHz, $CDCl_3$): δ = 154.9 (C_q), 154.8 (C_q), 128.8 (C_q), 125.3 (CH), 124.7 (CH), 122.8 (CH), 121.0 (CH), 115.8 (CH_2), 111.0 (CH), 104.8 (CH). MS (EI) *m/z*: 144 [$M^{+\bullet}$]. The spectral and MS data were in accordance with those reported in literature.[7]

5-Methyl-2-vinylbenzofuran (2b)

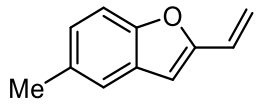

Following general procedure **A**, the title compound was isolated as a yellow liquid (0.79 g, 25%, over three steps). ^{1}H-NMR (400 MHz, $CDCl_3$): δ = 7.36 (d, *J* = 8.3 Hz, 1H), 7.35 – 7.33 (m, 1H), 7.11 (dd, *J* = 8.4, 1.8 Hz, 1H), 6.66 (dd, *J* = 17.4, 11.2 Hz, 1H), 6.56 (s, 1H), 5.97 (dd, *J* = 17.6, 1.5 Hz, 1H), 5.39 (dd, *J* = 11.2, 1.3 Hz, 1H), 2.46 (s, 3H). ^{13}C-NMR (101 MHz, $CDCl_3$): δ = 155.0 (C_q), 153.2 (C_q), 132.2 (C_q), 128.9 (C_q), 125.9 (CH), 125.4 (CH), 120.8 (CH), 115.4 (CH_2), 110.5 (CH), 104.6 (CH), 21.3 (CH_3). MS (EI) *m/z*: 158 [$M^{+\bullet}$].

5-Phenyl-2-vinylbenzofuran (2c)

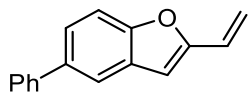

Following general procedure **A**, the title compound was isolated as a white solid (0.59 g, 37%, over three steps). M.p.= 100-101 °C. ^{1}H-NMR (400 MHz, $CDCl_3$): δ = 7.74 (t, *J* = 1.3 Hz, 1H), 7.67 – 7.62 (m, 2H), 7.53 (d, *J* = 1.3 Hz, 2H), 7.47 (dd, *J* = 8.4, 6.9 Hz, 2H), 7.40 – 7.34 (m, 1H), 6.73 – 6.64 (m, 2H), 6.05 – 5.98 (m, 1H), 5.44 (dd, *J* = 11.2, 1.3 Hz, 1H). ^{13}C-NMR (101 MHz, $CDCl_3$): δ = 155.5 (C_q), 154.4 (C_q), 141.6 (C_q), 136.5 (C_q), 129.4 (C_q), 128.8 (CH), 127.4 (CH), 126.9 (CH), 125.3 (CH), 124.4 (CH), 119.5 (CH), 116.0 (CH_2), 111.1 (CH), 104.9 (CH). MS (EI) *m/z*: 220 [$M^{+\bullet}$].

5-Methoxy-2-vinylbenzofuran (2d)

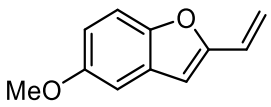

Following general procedure **A**, the title compound was isolated as a pale yellow solid (0.37 g, 31%, over three steps). M.p. = 41-42 °C. ^{1}H-NMR (400 MHz, $CDCl_3$): δ = 7.36 (d, *J* = 8.9 Hz, 1H), 7.01 (d, *J* = 2.6 Hz, 1H), 6.90 (dd, *J* = 8.9, 2.6 Hz, 1H), 6.64 (dd, *J* = 17.5, 11.2 Hz, 1H), 6.57 (s, 1H), 5.96 (dd, *J* = 17.5, 1.2 Hz, 1H), 5.39 (dd, *J* = 11.3, 1.3 Hz, 1H), 3.86 (s, 3H). ^{13}C-NMR (101 MHz, $CDCl_3$): δ = 155.9 (C_q), 155.7 (C_q), 149.8 (C_q), 129.4 (C_q), 125.4 (CH), 115.6 (CH_2), 113.4 (CH), 111.5 (CH), 104.9 (CH), 103.4 (CH), 55.9 (CH_3). MS (EI) *m/z*: 174 [$M^{+\bullet}$].

5-Fluoro-2-vinylbenzofuran (2e)

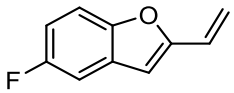

Following general procedure **A**, the title compound was isolated as a yellow liquid (0.74 g, 23%, over three steps). ^{1}H-NMR (400 MHz, $CDCl_3$): δ = 7.39 (ddd, *J* = 8.9, 4.1, 0.9 Hz, 1H), 7.20 (dd, *J* = 8.5, 2.6 Hz, 1H), 7.01 (td, *J* = 9.1, 2.7 Hz, 1H), 6.65 (dd, *J* = 17.5, 11.2 Hz, 1H), 6.59 (s, 1H), 6.00 (dd, *J* = 17.5, 1.1 Hz, 1H), 5.44 (dd, *J* = 11.2, 1.2 Hz, 1H). ^{13}C-NMR (101 MHz, $CDCl_3$): δ = 159.2 (d, $^{1}J_{C\text{-}F}$ = 239 Hz, C_q), 156.6 (C_q), 151.0 (C_q), 129.6 (d, $^{3}J_{C\text{-}F}$ = 11 Hz, C_q), 125.1 (CH), 116.5 (CH_2), 112.2 (d, $^{2}J_{C\text{-}F}$ = 26 Hz, CH), 111.6 (d, $^{3}J_{C\text{-}F}$ = 10 Hz, CH), 106.4 (d, $^{2}J_{C\text{-}F}$ = 25 Hz, CH), 104.8 (d, $^{5}J_{C\text{-}F}$ = 4 Hz, CH). ^{19}F-NMR (565 MHz, $CDCl_3$): δ = -121.0 – -121.1 (m). MS (EI) *m/z*: 162 [$M^{+\bullet}$].

5-Chloro-2-vinylbenzofuran (2f)

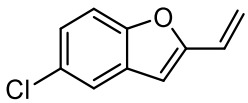

Following general procedure **A**, the title compound was isolated as a white solid (0.36 g, 41%, over three steps). M.p. = 66-67 °C. ^{1}H-NMR (400 MHz, $CDCl_3$): δ = 7.51 (d, *J* = 2.1 Hz, 1H), 7.39 (d, *J* = 8.8 Hz, 1H), 7.25 (dd, *J* = 8.7, 2.1 Hz, 1H), 6.64 (dd, *J* = 17.5, 11.2 Hz, 1H), 6.56 (s, 1H), 6.01 (dd, *J* = 17.5, 1.1 Hz, 1H), 5.45 (dd, *J* = 11.2, 1.1 Hz, 1H). ^{13}C-NMR (101 MHz, $CDCl_3$): δ = 156.2 (C_q), 153.1 (C_q), 130.2 (C_q), 128.3 (C_q), 125.0 (CH), 124.8 (CH), 120.5 (CH), 116.8 (CH_2), 112.0 (CH), 104.2 (CH). MS (EI) *m/z*: 178 [$M^{+\bullet}$].

5-Bromo-2-vinylbenzofuran (2g)

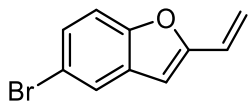

Following general procedure **A**, the title compound was isolated as a white solid (0.14 g, 22%, over three steps). M.p. = 67-69 °C. ^{1}H-NMR (400 MHz, $CDCl_3$): δ = 7.67 (d, *J* = 1.9 Hz, 1H), 7.40 – 7.32 (m, 2H), 6.64 (dd, *J* = 17.5, 11.2 Hz, 1H), 6.56 (s, 1H), 6.00 (dd, *J* = 17.4, 1.2 Hz, 1H), 5.45 (dd, *J* = 11.2, 1.2 Hz, 1H). ^{13}C-NMR (101 MHz, $CDCl_3$): δ = 156.1 (C_q), 153.5 (C_q), 130.8 (C_q), 127.5 (CH), 124.9 (CH), 123.6 (CH), 116.9 (CH_2), 115.8 (C_q), 112.5 (CH), 104.0 (CH). MS (EI) *m/z*: 222 [$M^{+\bullet}$].

Methyl 2-vinylbenzofuran-5-carboxylate (2h)

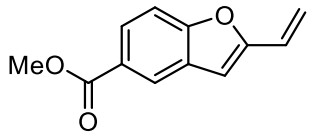

Following general procedure **A**, the title compound was isolated as a white solid (0.32 g, 28%, over three steps). M.p.= 91-93 °C. ^{1}H-NMR (400 MHz, $CDCl_3$): δ = 8.28 (dd, *J* = 1.8, 0.7 Hz, 1H), 8.02 (dd, *J* = 8.7, 1.7 Hz, 1H), 7.49 (dt, *J* = 8.6, 0.8 Hz, 1H), 6.73 – 6.62 (m, 2H), 6.08 – 5.98 (m, 1H), 5.47 (dd, *J* = 11.3, 1.2 Hz, 1H), 3.96 (s, 3H). ^{13}C-NMR (101 MHz, $CDCl_3$): δ = 167.3 (C_q), 157.3 (C_q), 156.2 (C_q), 128.9 (C_q), 126.5 (CH), 125.2 (C_q), 124.9 (CH), 123.4 (CH), 116.8 (CH_2), 110.9 (CH), 104.9 (CH), 52.1 (CH_3). MS (EI) *m/z*: 202 [$M^{+\bullet}$].

6-Methoxy-2-vinylbenzofuran (2i)

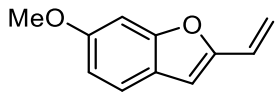

Following general procedure **A**, the title compound was isolated as a pale yellow viscous oil (1.03 g, 48%, over three steps). ^{1}H-NMR (400 MHz, $CDCl_3$): δ = 7.40 (d, *J* = 8.5 Hz, 1H), 7.03 (d, *J* = 2.4 Hz, 1H), 6.86 (dd, *J* = 8.5, 2.2 Hz, 1H), 6.62 (dd, *J* = 17.4, 11.2 Hz, 1H), 6.54 (s, 1H), 5.89 (dd, *J* = 17.5, 1.3 Hz, 1H), 5.33 (dd, *J* = 11.3, 1.3 Hz, 1H), 3.88 (s, 3H). ^{13}C-NMR (101 MHz, $CDCl_3$): δ = 158.4 (C_q), 155.8 (C_q), 154.2 (C_q), 125.3 (CH), 122.2 (C_q), 121.1 (CH), 114.2 (CH_2), 111.8 (CH), 104.7 (CH), 95.7 (CH), 55.7 (CH_3). MS (EI) *m/z*: 174 [$M^{+\bullet}$].

7-Methoxy-2-vinylbenzofuran (2j)

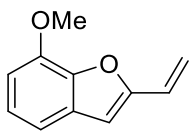

Following general procedure **A**, the title compound was isolated as a pale-yellow liquid (1.67 g, 49%, over three steps). ^{1}H-NMR (400 MHz, $CDCl_3$): δ = 7.17 – 7.13 (m, 2H), 6.86 – 6.79 (m, 1H), 6.72 – 6.64 (m, 1H), 6.63 (s, 1H), 6.04 (dd, *J* = 17.6, 1.2 Hz, 1H), 5.41 (dd, *J* = 11.3, 1.2 Hz, 1H), 4.05 (s, 3H). ^{13}C-NMR (101 MHz,

$CDCl_3$): δ = 155.1 (C_q), 145.2 (C_q), 143.9 (C_q), 130.5 (C_q), 125.1 (CH), 123.5 (CH), 116.1 (CH_2), 113.4 (CH), 107.0 (CH), 104.8 (CH), 56.1 (CH_3). MS (EI) *m/z*: 174 [$M^{+\bullet}$].

5,7-Dichloro-2-vinylbenzofuran (2k)

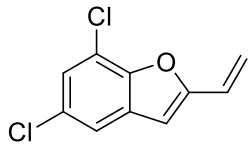

Following general procedure **A**, the title compound was isolated as a pale-yellow solid (0.51 g, 22%, over three steps). M.p. = 49-51 °C. ^{1}H-NMR (400 MHz, $CDCl_3$): δ = 7.41 (d, *J* = 1.9 Hz, 1H), 7.29 (d, *J* = 2.0 Hz, 1H), 6.65 (dd, *J* = 17.5, 11.3 Hz, 1H), 6.60 (s, 1H), 6.15 – 6.07 (m, 1H), 5.52 (dd, *J* = 11.2, 1.1 Hz, 1H). ^{13}C-NMR (101 MHz, $CDCl_3$): δ = 156.9 (C_q), 149.2 (C_q), 131.1 (C_q), 128.6 (C_q), 124.7 (CH), 124.5 (CH), 119.2 (CH_2), 118.1 (C_q), 104.4 (CH). MS (EI) *m/z*: 212 [$M^{+\bullet}$].

2-Vinylnaphtho[2,1-b]furan (2l)

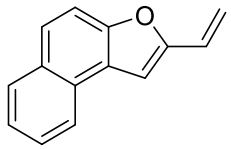

Following general procedure **A**, the title compound was isolated as a white solid (0.13 g, 10%, over three steps). M.p. = 65-66 °C. ^{1}H-NMR (400 MHz, $CDCl_3$): δ = 8.12 (dt, *J* = 8.3, 1.1 Hz, 1H), 7.98 – 7.93 (m, 1H), 7.74 (d, *J* = 8.9 Hz, 1H), 7.65 (dd, *J* = 8.9, 0.9 Hz, 1H), 7.60 (ddd, *J* = 8.2, 6.9, 1.3 Hz, 1H), 7.50 (ddd, *J* = 8.2, 6.9, 1.3 Hz, 1H), 7.13 (s, 1H), 6.76 (dd, *J* = 17.5, 11.2 Hz, 1H), 6.02 (dd, *J* = 17.4, 1.1 Hz, 1H), 5.42 (dd, *J* = 11.2, 1.2 Hz, 1H). ^{13}C-NMR (101 MHz, $CDCl_3$): δ = 154.4 (C_q), 152.3 (C_q), 130.4 (C_q), 128.8 (CH), 127.6 (C_q), 126.3 (CH), 125.6 (CH), 125.3 (CH), 124.6 (CH), 124.1 (C_q), 123.4 (CH), 114.9 (CH_2), 112.2 (CH), 103.8 (CH). MS (EI) *m/z*: 194 [$M^{+\bullet}$].

5-(*tert*-Butyl)-2-vinylbenzofuran (2m)

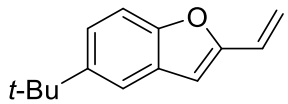

Following general procedure **A**, the title compound was isolated as a pale-yellow solid (0.72 g, 18%, over three steps). M.p.= 69-71 °C. ^{1}H-NMR (400 MHz, $CDCl_3$): δ = 7.55 (d, *J* = 1.7 Hz, 1H), 7.43 – 7.34 (m, 2H), 6.66 (dd, *J* = 17.4, 11.2 Hz, 1H), 6.59 (s, 1H), 5.96 (dd, *J* = 17.5, 1.4 Hz, 1H), 5.38 (dd, *J* = 11.2, 1.3 Hz, 1H), 1.41 (s, 9H). ^{13}C-NMR (101 MHz, $CDCl_3$): δ = 155.0 (C_q), 153.0 (C_q), 145.8 (C_q), 128.5 (C_q), 125.4 (CH), 122.7 (CH), 117.2 (CH), 115.3 (CH_2), 110.3 (CH), 105.0 (CH), 34.7 (Cq), 31.9 (CH_3). MS (EI) *m/z*: 200 [$M^{+\bullet}$].

3-Methyl-2-vinylbenzofuran (2n)

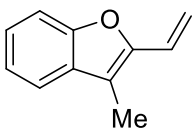

Following general procedure **B**, the title compound was isolated as a colourless liquid (2.21 g, 70%, over two steps). ^{1}H-NMR (400 MHz, $CDCl_3$): δ = 7.50 (dd, *J* = 7.7, 1.5 Hz, 1H), 7.47 – 7.42 (m, 1H), 7.34 – 7.28 (m, 1H), 7.27 – 7.20 (m, 1H), 6.75 (ddd, *J* = 17.5, 11.3, 1.3 Hz, 1H), 5.93 (dd, *J* = 17.3, 1.9 Hz, 1H), 5.38 (d, *J* = 11.1 Hz, 1H), 2.29 (s, 3H). ^{13}C-NMR (101 MHz, $CDCl_3$): δ = 154.0 (C_q), 150.3 (C_q), 130.4 (C_q), 124.8 (CH), 123.3 (CH), 122.3 (CH), 119.4 (CH), 114.2 (CH_2), 113.2 (C_q), 110.8 (CH), 8.0 (CH_3). MS (EI) *m/z*: 158 [$M^{+\bullet}$].

7-vinylbenzofuran (2r)

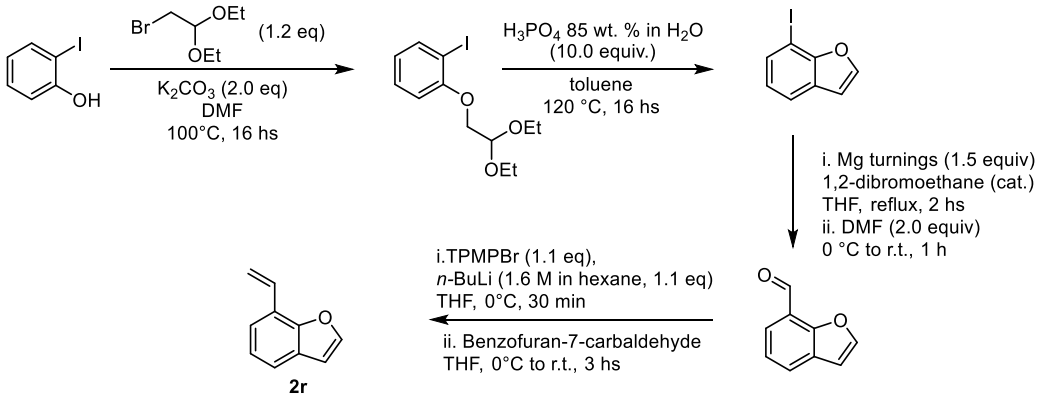

Step 1: A 100 mL round-bottomed flask was charged with 2-Iodophenol (10.0 mmol, 1.0 equiv.), bromoacetaldehyde diethyl acetal (12.0 mmol, 1.2 equiv.), anhydrous K_2CO_3 (20.0 mmol, 2.0 equiv.) and dry DMF (10 mL). The resulting suspension was stirred overnight at 100 °C. After cooling, the reaction mixture was diluted with EtOAc (100 mL) and filtered through a pad of celite. The clear filtrate was concentrated under reduced pressure. Purification by flash chromatography (*n*-Hexane/EtOAc) of the oily residue provided the desired product.

Step 2: The resulting 1-(2,2-diethoxyethoxy)-2-iodobenzene was dissolved in toluene (0.5 M) and H_3PO_4 85 wt. % in H_2O (10.0 equiv.) was added. The solution was stirred under reflux for 16 hs. The residue was dissolved in Et_2O (100 mL) and extracted with saturated aqueous $NaHCO_3$ solution (2x50 mL). The organic phase was dried over Na_2SO_4 and concentrated under reduced pressure. Purification by flash chromatography (*n*-Hexane/EtOAc) provided the desired product.

***Step 3*[8]:** A drop of 1,2-dibromoethane was added to a suspension of Mg turnings (1.5 equiv) in dry THF (1.0 M). The reaction mixture was stirred and then a solution of 7-iodobenzofuran (1.0 quiv) in dry THF (1.0 M) was added. The reaction mixture was heated to reflux for 2 hs. Then the

solution was cooled to 0 °C and DMF (2.0 equiv) was added dropwise. The reaction mixture was warmed to room temperature and stirred for 1 h. After, the reaction mixture was quenched with sat. aqueous NH_4Cl (50 mL) and extracted with EtOAc (2x100 mL). The combined organic layers were dried over Na_2SO_4 and concentrated under reduced pressure. Purification by flash chromatography (*n*-Hexane/EtOAc) provided desired product.

Step 4: To a suspension of methyltriphenylphosphonium bromide (TPMPBr, 1.1 equiv.) in dry THF (0.1 M) was added *n*-BuLi (1.6 M in *n*-Hexane, 1.1 equiv.) dropwise at 0 °C under nitrogen. After stirring for 30 min, a solution of benzofuran-7-carbaldehyde (1.0 equiv.) in dry THF (0.2 M) was added dropwise. The reaction mixture was warmed to room temperature and the progress of the reaction was monitored by TLC. After the reaction was completed, the reaction mixture was quenched with sat. aqueous NH_4Cl (50 mL) and extracted with EtOAc (2x50 mL). The combined organic layers were dried over Na_2SO_4 and concentrated under reduced pressure. The crude was purified by chromatography on silica gel (*n*-Hexane) yielding **2r** (518 mg, 36% over four steps) as a colourless liquid. ^{1}H-NMR (400 MHz, $CDCl_3$): δ = 7.71 (d, *J* = 2.2 Hz, 1H), 7.54 (dd, *J* = 7.7, 1.3 Hz, 1H), 7.35 (dd, *J* = 7.5, 1.2 Hz, 1H), 7.25 (t, *J* = 7.6 Hz, 1H), 7.03 (dd, *J* = 17.7, 11.3 Hz, 1H), 6.82 (d, *J* = 2.2 Hz, 1H), 6.26 (dd, *J* = 17.7, 1.3 Hz, 1H), 5.55 (dd, *J* = 11.4, 1.4 Hz, 1H). ^{13}C-NMR (101 MHz, $CDCl_3$): δ = 152.5 (C_q), 144.9 (CH), 131.7 (CH), 127.9 (C_q), 123.1 (CH), 122.9 (CH), 122.4 (C_q), 120.5 (CH), 117.4 (CH_2), 106.6 (CH). MS (EI) *m/z*: 144 [$M^{+\bullet}$].

2-vinylbenzofuran ([D]$_n$-2a)[9]

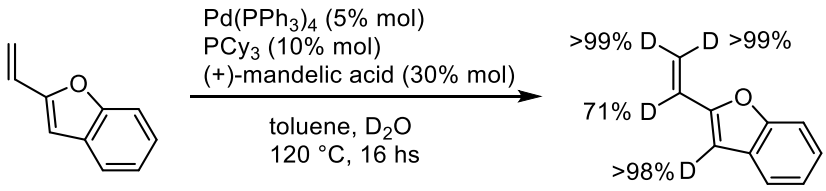

In an oven dried tube, **2a** (432.0 mg, 3.0 mmol), $Pd(PPh_3)_4$ (173.2 mg, 0.05 mmol), PCy_3 (84.1 mg, 0.1 mmol) and (+)-mandelic acid (136.9 mg, 0.3 mmol) were added sequentially and purged with nitrogen three times. Subsequently, toluene (500 µL, 0.1 M) and D_2O (50 mmol, 50 equiv.) were added under N_2 atmosphere, and the tube placed in a pre-heated oil bath at 120 °C overnight. The reaction mixture was then cooled down at room temperature and CH_2Cl_2 (10 mL) was added. The mixture was concentrated under reduced pressure and the crude purified by chromatography on silica gel (*n*-Hexane) yielding **[D]$_n$-2a** (279 mg, 63%) as a colourless liquid. The amount of deuterium incorporation was determined by ^{1}H-NMR.

3.4.3 Synthesis of Benzamide Substrates

General procedure C: synthesis of benzamide substrates

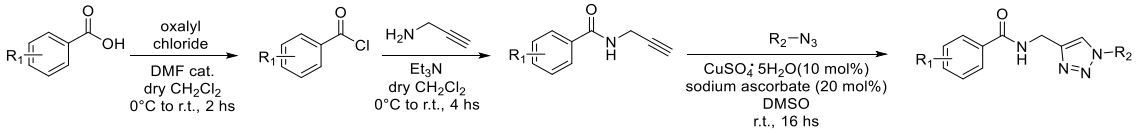

Oxalyl chloride (1.1 equiv) was added dropwise to a mixture of the carboxylic acid (1.0 equiv), DMF (cat.) in dry CH_2Cl_2 (10 mL) under a nitrogen atmosphere at 0 °C. The mixture was stirred at the same temperature for 2 hs upon which it was allowed to warm up to ambient temperature. The crude acyl chloride was cooled to 0 °C and it was added dropwise to a solution of propargylamine (1.5 equiv), NEt_3 (3.0 equiv) in dry CH_2Cl_2 (10 mL) at 0 °C under a nitrogen atmosphere. The mixture was initially stirred at the same temperature and then at ambient temperature for 4 hs. To the reaction was added sat. aqueous $NaHCO_3$ (20 mL). The aqueous layers were extracted with CH_2Cl_2 (3x20 mL). The combined organic extracts were washed with HCl (1.0 M, 20 mL), brine and dried over Na_2SO_4. The filtrate was concentrated under reduced pressure. The crude product was further submitted to the corresponding azide (1.5 equiv), $CuSO_4 \cdot 5H_2O$ (10 mol %), sodium ascorbate (20 mol %) in DMSO (10 mL). After 16 hs, the reaction was quenched with sat. aqueous NH_4Cl (40 mL). The aqueous layers were extracted with EtOAc (3x40 mL). The combined organic extracts were dried over Na_2SO_4 and the filtrate was concentrated under reduced pressure. The crude product was purified by column chromatography on silica gel.

_N_-[(1-(Pent-4-en-1-yl)-1_H_-1,2,3-triazol-4-yl]methyl)benzamide (1e)

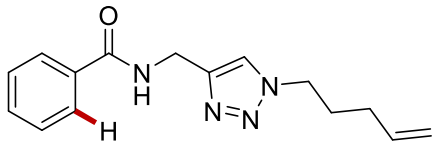

The general procedure **C** was followed using benzoyl chloride (422 mg, 3.0 mmol) and 5-azidopent-1-ene (500 mg, 4.5 mmol). Purification by column chromatography (*n*-Hexane/EtOAc 1:1→ 3:7) yielded **1x** (324 mg, 40%) as a white solid. M.p.= 77-79 °C. ^{1}H-NMR (400 MHz, $CDCl_3$): δ = 7.85 – 7.79 (m, 2H), 7.63 (s, 1H), 7.55 – 7.49 (m, 1H), 7.47 – 7.42 (m, 2H), 7.05 (s, 1H), 5.79 (ddt, *J* = 16.9, 10.3, 6.4 Hz, 1H), 5.12 – 5.03 (m, 2H), 4.74 (d, *J* = 5.6 Hz, 2H), 4.36 (t, *J* = 7.0 Hz, 2H), 2.16 – 2.08 (m, 2H), 2.07 – 1.99 (m, 2H). ^{13}C-NMR (101 MHz, $CDCl_3$): δ = 167.4 (C_q), 144.6 (C_q), 136.4 (CH), 134.0 (C_q), 131.7 (CH), 128.6 (CH), 127.0 (CH), 122.4 (CH), 116.3 (CH_2), 49.6 (CH_2), 35.4 (CH_2), 30.4 (CH_2), 29.2 (CH_2). MS (ESI) *m/z* (relative intensity): 293 (44) $[M+Na]^+$, 271 (100) $[M+H]^+$. HR-MS (ESI) *m/z* calcd for $C_{15}H_{19}N_4O$ $[M+H]^+$ 271.1553, found 271.1557.

_N_-[(1-Benzyl-1_H_-1,2,3-triazol-4-yl)methyl]-4-(dimethylamino)benzamide (1j)

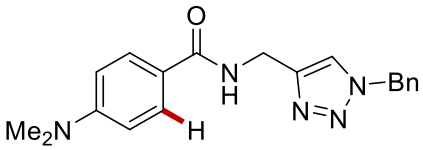

The general procedure **C** was followed using 4-(dimethylamino)benzoic acid (495 mg, 3.0 mmol) and benzyl azide (598 mg, 4.5 mmol). Purification by precipitation (*n*-Hexane/EtOAc) yielded **1j** (452 mg, 45%) as a white solid. M.p.= 201-202 °C. ^{1}H-NMR (400 MHz, $CDCl_3$): δ = 7.70 (d, *J* = 8.6 Hz, 2H), 7.57 (bs, 1H), 7.37 (d, *J* = 6.2 Hz, 3H), 7.31 – 7.25 (m, 2H), 6.80 (bs, 1H), 6.66 (d, *J* = 8.5 Hz, 2H), 5.50 (s, 2H), 4.69 (s, 2H), 3.02 (s, 6H). ^{13}C-NMR (101 MHz, $CDCl_3$): δ = 167.3 (C_q), 152.6 (2 x C_q), 134.5 (C_q), 129.1 (CH), 128.8 (CH), 128.5 (2 x CH), 128.1 (CH), 120.7 (C_q), 111.0 (CH), 54.3 (CH_2), 40.1 (CH_3), 35.3 (CH_2). MS (ESI) *m/z* (relative intensity): 358 (100) $[M+Na]^+$, 336 (52) $[M+H]^+$. HR-MS (ESI) *m/z* calcd for $C_{19}H_{22}N_5O$ $[M+H]^+$ 336.1819, found 336.1815.

_N_-[(1-Benzyl-1_H_-1,2,3-triazol-4-yl)methyl]-4-(octylthio)benzamide (1k)

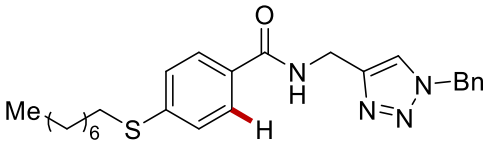

The general procedure **C** was followed using 4-(octylthio)benzoic acid (799 mg, 3.0 mmol) and benzyl azide (598 mg, 4.5 mmol). Purification by column chromatography (*n*-Hexane/EtOAc 1:1→ 3:7) yielded **1k** (680 mg, 52%) as a white solid. M.p.= 150-152 °C. ^{1}H-NMR (400 MHz, $CDCl_3$): δ = 7.72 (d, *J* = 7.8 Hz, 2H), 7.39 (d, *J* = 6.1 Hz, 3H), 7.15 (bs, 1H), 7.28 (d, *J* = 6.9 Hz, 5H), 5.51 (s, 2H), 4.73 (bs, 2H), 2.97 (t, *J* = 7.4 Hz, 2H), 1.68 (p, *J* = 7.3 Hz, 2H), 1.45 (p, *J* = 7.0 Hz, 2H), 1.37 – 1.23 (m, 8H), 0.95 – 0.85 (m, 3H). ^{13}C-NMR (101 MHz, $CDCl_3$): δ = 166.9 (C_q), 142.7 (C_q), 134.3 (2 x C_q), 130.4 (C_q), 129.2 (2 x CH), 128.9 (CH), 128.2 (CH), 127.5 (CH), 127.0 (CH), 54.7 (CH_2), 35.3 (CH_2), 32.4 (CH_2), 31.8 (CH_2), 29.2 (CH_2), 29.1 (CH_2), 28.9 (CH_2), 28.8 (CH_2), 22.6 (CH_2), 14.1 (CH_3). MS (ESI) *m/z* (relative intensity): 475 (15) $[M+K]^+$, 459 (100) $[M+Na]^+$, 437 (52) $[M+H]^+$.HR-MS (ESI) *m/z* calcd for $C_{25}H_{33}N_4OS$ $[M+H]^+$ 437.2370, found 437.2373.

_N_-[(1-Benzyl-1_H_-1,2,3-triazol-4-yl)methyl]-3-methoxybenzamide (1r)

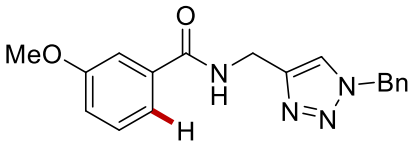

The general procedure **C** was followed using 3-methoxybenzoic acid (456 mg, 3.0 mmol) and benzyl azide (598 mg, 4.5 mmol). Purification by column chromatography (*n*-Hexane/EtOAc 1:1→ 3:7) yielded **1r** (560 mg, 58%) as a white solid. M.p.= 99-100 °C. ^{1}H-NMR (400 MHz, $CDCl_3$): δ = 7.59 (s, 1H), 7.39 – 7.35 (m, 4H), 7.34 – 7.26 (m, 5H), 7.03 (ddd, *J* = 7.8, 2.6, 1.3 Hz, 1H), 5.50 (s, 2H), 4.68 (d, *J* = 5.6 Hz, 2H), 3.82 (s, 3H). ^{13}C-NMR (101 MHz, $CDCl_3$): δ = 167.3 (C_q), 159.8 (C_q), 153.5 (C_q), 135.4 (C_q), 134.3 (C_q), 129.6 (CH), 129.2 (2 x CH), 128.9 (CH), 128.2 (2 x CH), 118.8 (CH), 118.1 (CH), 112.2 (CH), 55.5 (CH_3), 54.4 (CH_2), 35.4 (CH_2). MS (ESI) *m/z* (relative intensity): 667 (51) $[2M+Na]^+$, 361 (25) $[M+K]^+$, 345 (100) $[M+Na]^+$, 323 (68) $[M+H]^+$. HR-MS (ESI) *m/z* calcd for $C_{18}H_{19}N_4O_2$ $[M+H]^+$ 323.1502, found 323.1505.

_N_-[(1-Benzyl-1_H_-1,2,3-triazol-4-yl)methyl]-3-(trifluoromethyl)benzamide (1s)

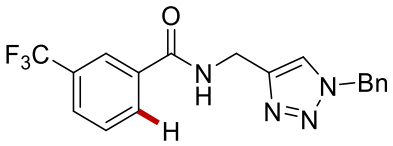

The general procedure **C** was followed using 3-(Trifluoromethyl)benzoic acid (570 mg, 3.0 mmol) and benzyl azide (598 mg, 4.5 mmol). Purification by column chromatography (*n*-Hexane/EtOAc 1:1→ 3:7) yielded **1s** (710 mg, 66%) as a white solid. M.p.= 127-128 °C. ^{1}H-NMR (400 MHz, $CDCl_3$): δ = 8.15 (s, 1H), 8.05 (d, *J* = 8.2 Hz, 1H), 7.94 (bs, 1H), 7.74 (d, *J* = 7.9 Hz, 1H), 7.65 (s, 1H), 7.53 (t, *J* = 8.0 Hz, 1H), 7.39 – 7.37 (m, 3H), 7.30 – 7.28 (m, 2H), 5.52 (s, 2H), 4.70 (d, *J* = 5.5 Hz, 2H). ^{13}C-NMR (101 MHz, $CDCl_3$): δ = 166.1 (C_q), 134.8 (2 x C_q), 134.3 (C_q), 131.0 (q, $^{2}J_{C-F}$ = 33 Hz, C_q), 130.5 (CH), 129.2 (CH), 129.1 (CH), 128.9 (CH), 128.2 (2 x CH), 128.1 (q, $^{3}J_{C-F}$ = 4 Hz, CH), 124.4 (q, $^{4}J_{C-F}$= 4 Hz, CH), 123.7 (q, $^{1}J_{C-F}$ = 274 Hz, C_q), 54.4 (CH_2), 35.3 (CH_2). ^{19}F-NMR (565 MHz, $CDCl_3$): δ = -62.6 (s). MS (ESI) *m/z* (relative intensity): 383 (100) $[M+Na]^+$, 361 (51) $[M+H]^+$. HR-MS (ESI) *m/z* calcd for $C_{18}H_{16}F_3N_4O$ $[M+H]^+$ 361.1271, found 361.1276.

_N_-[(1-Benzyl-1_H_-1,2,3-triazol-4-yl)methyl]-2-methylbenzamide (1t)

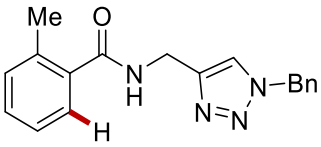

The general procedure **C** was followed using 2-methylbenzoic acid (408 mg, 3.0 mmol) and benzyl azide (598 mg, 4.5 mmol). Purification by column chromatography (*n*-Hexane/EtOAc 1:1→ 3:7) yielded **1t** (624 mg, 68%) as a white solid. M.p.= 112-114 °C. ^{1}H-NMR (400 MHz, $CDCl_3$):

δ = 7.56 (s, 1H), 7.42 – 7.37 (m, 3H), 7.36 (dd, *J* = 7.5, 1.5 Hz, 1H), 7.34 – 7.29 (m, 3H), 7.23 – 7.16 (m, 2H), 6.50 (bs, 1H), 5.53 (s, 2H), 4.68 (d, *J* = 5.7 Hz, 2H), 2.40 (s, 3H). ^{13}C-NMR (101 MHz, $CDCl_3$): δ = 170.1 (C_q), 145.1 (C_q), 136.2 (C_q), 135.8 (C_q), 134.5 (C_q), 131.1 (CH), 130.1 (CH), 129.2 (CH), 128.8 (CH), 128.1 (CH), 126.8 (CH), 125.7 (CH), 122.2 (CH), 54.3 (CH_2), 35.3 (CH_2), 19.8 (CH_3). MS (ESI) *m/z* (relative intensity): 329 (100) $[M+Na]^+$, 307 (69) $[M+H]^+$, 143 (229, 119 (39). HR-MS (ESI) *m/z* calcd for $C_{18}H_{19}N_4O$ $[M+H]^+$ 307.1553, found 307.1557.

_N_-[(1-Benzyl-1_H_-1,2,3-triazol-4-yl)methyl]-2-naphthamide (1u)

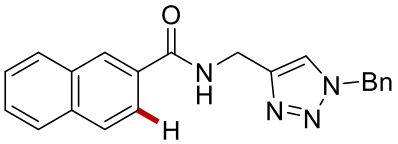

The general procedure **C** was followed using 2-naphthoic acid (516 mg, 3.0 mmol) and benzyl azide (598 mg, 4.5 mmol). Purification by column chromatography (*n*-Hexane/EtOAc 1:1→ 3:7) yielded **1u** (718 mg, 70%) as a white solid. M.p.= 183-184 °C. ^{1}H-NMR (400 MHz, $CDCl_3$): δ = 8.33 (3, 1H), 7.95 – 7.84 (m, 4H), 7.60 (d, *J* = 1.5 Hz, 1H), 7.59 – 7.52 (m, 2H), 7.40 – 7-37 (m, 3H), 7.33 – 7.29 (m, 2H), 7.17 (bs, 1H), 5.54 (s, 2H), 4.78 (d, *J* = 5.3 Hz, 2H). ^{13}C-NMR (101 MHz, $CDCl_3$): δ = 167.5 (C_q), 145.0 (C_q), 134.8 (C_q), 134.4 (C_q), 132.6 (C_q), 131.2 (C_q), 129.2 (CH), 129.0 (CH), 128.9 (CH), 128.5 (CH), 128.2 (CH), 127.8 (2 x CH), 127.6 (CH), 126.8 (CH), 123.6 (CH), 122.3 (CH), 54.3 (CH_2), 35.5 (CH_2). MS (ESI) *m/z* (relative intensity): 707 (46) $[2M+Na]^+$, 365 (48) $[M+Na]^+$, 343 (100) $[M+H]^+$. HR-MS (ESI) *m/z* calcd for $C_{21}H_{19}N_4O$ $[M+H]^+$ 343.1553, found 343.1556.

_N_-[(1-Benzyl-1_H_-1,2,3-triazol-4-yl)methyl]-1-methyl-1_H_-indole-2-carboxamide (1v)

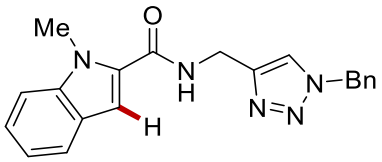

The general procedure **C** was followed using 1-methyl-1*H*-indole-2-carboxylic acid (525 mg, 3.0 mmol) and benzyl azide (598 mg, 4.5 mmol). Purification by column chromatography (*n*-Hexane/EtOAc 1:1→ 3:7) yielded **1v** (642 mg, 62%) as a white solid. M.p.= 172-174 °C. ^{1}H-NMR (400 MHz, $CDCl_3$): δ = 7.61 (dd, *J* = 8.0, 1.0 Hz, 1H), 7.56 (s, 1H), 7.42 – 7.35 (m, 4H), 7.34 (dd, *J* = 6.7, 1.2 Hz, 1H), 7.31 – 7.27 (m, 2H), 7.19 (bs, 1H), 7.15 (ddd, *J* = 8.0, 6.6, 1.3 Hz, 1H), 6.90 (d, *J* = 0.8 Hz, 1H), 5.52 (s, 2H), 4.70 (d, *J* = 5.7 Hz, 2H), 4.02 (s, 3H). ^{13}C-NMR (101 MHz, $CDCl_3$): δ = 162.6 (C_q), 145.1 (C_q), 139.1 (C_q), 134.5 (C_q), 131.5 (C_q), 129.2 (CH), 128.9 (CH), 128.2 (CH), 126.0 (C_q), 124.1 (CH), 122.3 (CH), 121.9 (CH), 120.5 (CH), 110.1 (CH), 104.4 (CH), 54.3 (CH_2), 35.0 (CH_2), 31.5 (CH_3). MS (ESI) *m/z* (relative intensity): 368 (100) $[M+Na]^+$, 346 (47) $[M+H]^+$. HR-MS (ESI) *m/z* calcd for $C_{20}H_{20}N_5O$ $[M+H]^+$ 346.1662, found 346.1664.

_N_-[(1-Benzyl-1_H_-1,2,3-triazol-4-yl)methyl]thiophene-2-carboxamide (1w)

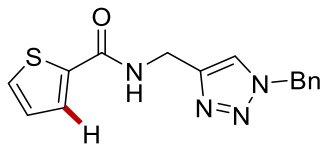

The general procedure **C** was followed using 2-Thiophenecarboxylic acid (384 mg, 3.0 mmol) and benzyl azide (598 mg, 4.5 mmol). Purification by column chromatography (*n*-Hexane/EtOAc 1:1→ 3:7) yielded **1w** (570 mg, 64%) as a white solid. M.p.= 130-132 °C. ^{1}H-NMR (400 MHz, $CDCl_3$): δ = 7.64 - 7.54 (m, 3H), 7.45 (d, *J* = 4.7 Hz, 1H), 7.37 – 7.35 (m, 3H), 7.29 – 7.27 (m, 2H), 7.03 – 7.01 (m, 1H), 5.50 (s, 2H), 4.65 (d, *J* = 5.2 Hz, 2H). ^{13}C-NMR (101 MHz, $CDCl_3$): δ = 162.1 (C_q), 138.8 (C_q), 138.7 (C_q), 134.4 (C_q), 130.2 (CH), 129.1 (CH), 128.8 (CH), 128.4 (CH), 128.2 (2 x CH), 127.7 (CH), 54.3 (CH_2), 35.2 (CH_2). MS (ESI) *m/z* (relative intensity): 321 (62) $[M+Na]^+$, 299 (100) $[M+H]^+$, 143 (11). HR-MS (ESI) *m/z* calcd for $C_{15}H_{15}N_4OS$ $[M+H]^+$ 299.0961, found 299.0957.

3.4.4 Representative Procedure for Iron-Catalyzed C–H Alkylation/Ring Opening with Vinylbenzofurans

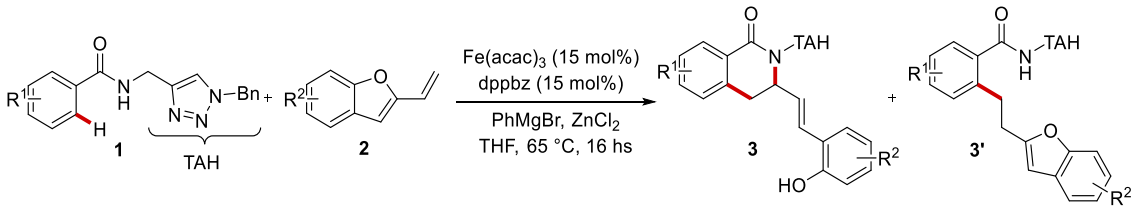

To a stirred solution of $Fe(acac)_3$ (10.6 mg, 0.03 mmol), dppbz (13.4 mg, 0.03 mmol), $ZnCl_2$ (1.0 M in THF, 400 µL, 0.4 mmol, 2.0 equiv) and **1** (0.20 mmol) under N_2 atmosphere, PhMgBr (1.0 M in THF, 600 µL, 0.6 mmol, 3.0 equiv) was added in a single portion. Then, **2** (0.6 mmol, 3.0 equiv) was added and the mixture was placed in a pre-heated oil bath at 65 °C. After stirring for 16 hs, the reaction was cooled to room temperature and quenched by the addition of an aqueous solution of HCl (1.0 M, 5 mL). The reaction was extracted with CH_2Cl_2 (3x10 mL) and the combined organic extracts were dried over Na_2SO_4, filtered and concentrated. The crude product was purified by column chromatography on silica gel (*n*-Hexane/EtOAc).

3.4.5 Stability test of vinylbenzofuran 2a under the catalytic reaction conditions

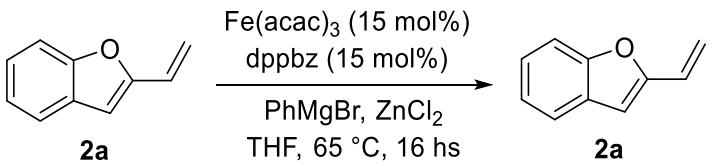

To a stirred solution of $Fe(acac)_3$ (26.5 mg, 0.075 mmol), dppbz (33.5 mg, 0.075 mmol), $ZnCl_2$ (1.0 M in THF, 1.0 mL, 1.0 mmol, 2.0 equiv) and **2a** (72.1 mg, 0.5 mmol) under N_2 atmosphere, PhMgBr (1.0 M in THF, 1.5 mL, 1.5 mmol, 3.0 equiv) was added in a single portion. Then, the mixture was placed in a pre-heated oil bath at 65 °C. After stirring for 16 hs, the reaction was cooled to room temperature and quenched by the addition of an aqueous solution of HCl (1.0 M, 5 mL). The reaction was extracted with CH_2Cl_2 (3x10 mL) and the combined organic extracts were dried over Na_2SO_4, filtered and concentrated. Purification by column chromatography on silica gel (*n*-Hexane) yielded **2a** (63.1 mg, 90%) as a colourless oil.

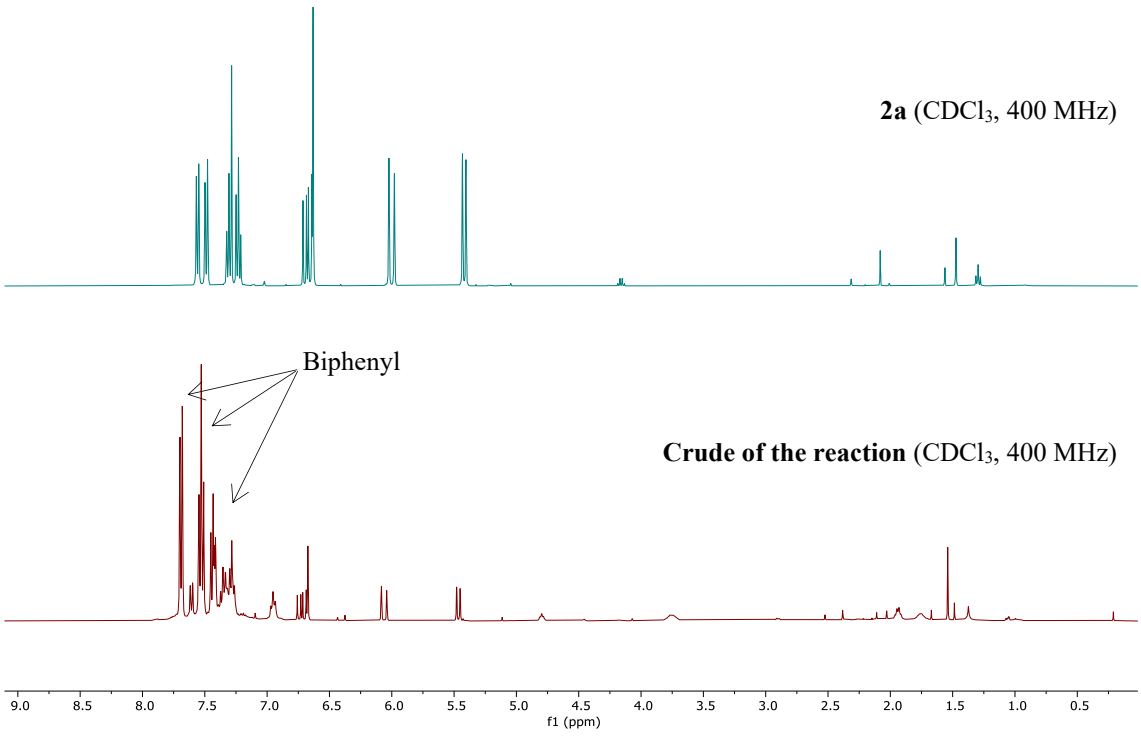

3.4.6 Characterization Data of Products

(*E*)-2-[(1-Benzyl-1*H*-1,2,3-triazol-4-yl)methyl]-3-(2-hydroxystyryl)-3,4-dihydroisoquinolin-1(2*H*)-one (3aa)

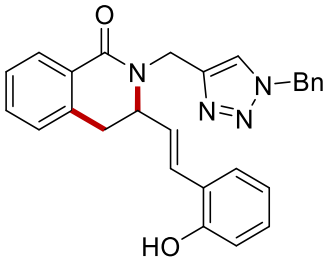

The representative procedure was followed using **1a** (58.5 mg, 0.2 mmol) and **2a** (81 µL, 0.6 mmol). Purification by column chromatography on silica gel (*n*-hexane/EtOAc 1:1) yielded **3aa** (63.1 mg, 72%) as a white solid. M.p.= 157-159 °C. ^{1}H-NMR (400 MHz, $CDCl_3$): δ= 8.80 (bs, 1H), 8.06 (dd, *J* = 7.7, 1.4 Hz, 1H), 7.72 (s, 1H), 7.44 (td, *J* = 7.5, 1.5 Hz, 1H), 7.37 – 7.36 (m, 4H), 7.28 – 7.26 (m, 2H), 7.21 (dd, *J* = 7.7, 1.7 Hz, 1H), 7.16 – 7.12 (m, 2H), 7.07 (d, *J* = 15.8 Hz, 1H), 7.02 (dd, *J* = 8.1, 1.2 Hz, 1H), 6.82 (td, *J* = 7.5, 1.2 Hz, 1H), 6.06 (dd, *J* = 15.8, 8.9 Hz, 1H), 5.57 – 5.43 (m, 2H), 5.14 (d, *J* = 14.8 Hz, 1H), 4.64 – 4.58 (m, 1H), 4.52 (d, *J* = 14.8 Hz, 1H), 3.31 (dd, *J* = 15.9, 5.9 Hz, 1H), 2.95 (dd, *J* = 16.0, 4.4 Hz, 1H). ^{13}C-NMR (101 MHz, $CDCl_3$): δ= 164.3 (C_q), 154.6 (C_q), 144.8 (C_q), 136.4 (C_q), 134.2 (C_q), 132.2 (CH), 129.7 (CH), 129.2 (CH), 129.1 (CH), 128.9 (CH), 128.7 (C_q), 128.3 (CH), 127.9 (CH), 127.7 (CH), 127.5 (CH), 127.2 (CH), 127.1 (CH), 124.1 (CH), 123.8 (C_q), 120.0 (CH), 116.7 (CH), 59.9 (CH), 54.5 (CH_2), 40.4 (CH_2), 34.2 (CH_2). MS (ESI) *m/z* (relative intensity): 459 (100) $[M+Na]^+$, 437 (78) $[M+H]^+$. HR-MS (ESI) *m/z* calcd for $C_{27}H_{25}N_4O_2$ $[M+H]^+$ 437.1972, found 437.1975.

The rest of the mass balance was accounted for substrate **1a** (12.8 mg 22%).

***N*-[2-(Benzofuran-2-yl)-1*H*-inden-3-yl]quinolin-8-amine (5aa)**

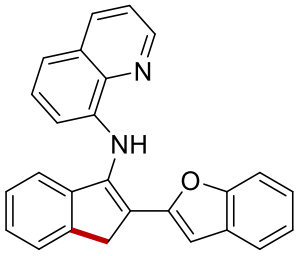

To a stirred solution of $Fe(acac)_3$ (10.6 mg, 0.03 mmol), 2,2'-bipy (4.7 mg, 0.03 mmol) $ZnCl_2$ (1.0 M in THF, 400 µL, 0.4 mmol, 2.0 equiv) and **4a** (49.7 mg, 0.20 mmol) under N_2 atmosphere, PhMgBr (1.0 M in THF, 600 µL, 0.6 mmol, 3.0 equiv) was added in a single portion. Then, **2a** (81 µL, 0.6 mmol, 3.0 equiv) was added and the mixture was placed in a pre-heated oil bath at 65 °C. After stirring for 16 hs, the reaction was cooled to room temperature and quenched by the addition of an aqueous solution of HCl (1.0 M, 5 mL). The reaction was extracted with CH_2Cl_2 (3x10 mL) and the combined organic extracts were dried over Na_2SO_4, filtered and concentrated. Purification by column chromatography on silica gel (*n*-Hexane/EtOAc 95:5) yielded **5aa** (26.9 mg, 36%) as an orange solid. M.p.= 148-150 °C. ^{1}H-NMR (400 MHz, $CDCl_3$): δ = 8.97 (dd, *J* = 4.2, 1.7 Hz, 1H), 8.77 (s, 1H), 8.21 (dd, *J* = 8.3, 1.7 Hz, 1H), 7.59 – 7.55 (m, 1H), 7.53 (dd, *J* = 8.3, 4.2 Hz, 1H), 7.51 –

7.47 (m, 1H), 7.47 – 7.40 (m, 2H), 7.37 – 7.29 (m, 4H), 7.26 (dd, *J* = 6.2, 1.4 Hz, 2H), 7.25 – 7.16 (m, 2H), 6.87 (dd, *J* = 7.5, 1.3 Hz, 1H), 6.74 (d, *J* = 0.9 Hz, 1H), 4.04 (s, 2H).^{13}C-NMR (101 MHz, $CDCl_3$): δ = 154.2 (C_q), 153.5 (C_q), 147.8 (CH), 142.1 (C_q), 142.0 (C_q), 139.6 (C_q), 138.8 (C_q), 138.6 (C_q), 136.2 (CH), 129.2 (C_q), 128.8 (C_q), 127.2 (CH), 126.3 (CH), 126.0 (CH), 124.0 (CH), 123.9 (CH), 122.9 (CH), 121.6 (CH), 121.2 (CH), 120.6 (CH), 119.8 (C_q), 116.9 (CH), 111.0 (CH), 110.9 (CH), 103.6 (CH), 36.8 (CH_2). MS (ESI) *m/z* (relative intensity): 375 (100) $[M+H]^+$. HR-MS (ESI) *m/z* calcd for $C_{26}H_{19}N_2O$ $[M+H]^+$ 375.1492, found 375.1493.

(*E*)-3-(2-Hydroxystyryl)-2-[(1-phenyl-1*H*-1,2,3-triazol-4-yl)methyl]-3,4-dihydroisoquinolin-1(2*H*)-one (3ba)

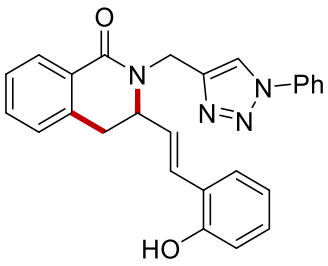

The representative procedure was followed using **1b** (55.6 mg, 0.2 mmol) and **2a** (81 µL, 0.6 mmol). Purification by column chromatography on silica gel (*n*-Hexane/EtOAc 1:1) yielded **3ba** (54.8 mg, 65%) as a white waxy solid. ^{1}H-NMR (400 MHz, $CDCl_3$): δ= 8.52 (bs, 1H), 8.23 (s, 1H), 8.11 (dd, *J* = 7.7, 1.5 Hz, 1H), 7.75 – 7.72 (m, 2H), 7.55 – 7.48 (m, 2H), 7.48 – 7.42 (m, 2H), 7.41 – 7.33 (m, 2H), 7.27 – 7.22 (m, 1H), 7.19 – 7.13 (m, 1H), 7.10 (d, *J* = 15.3 Hz, 1H), 7.02 (dd, *J* = 8.2, 1.2 Hz, 1H), 6.82 (td, *J* = 7.4, 1.2 Hz, 1H), 6.13 (dd, *J* = 15.8, 8.7 Hz, 1H), 5.29 (d, *J* = 14.9 Hz, 1H), 4.70 – 4.63 (m, 1H), 4.59 (d, *J* = 14.8 Hz, 1H), 3.36 (dd, *J* = 15.9, 5.9 Hz, 1H), 2.99 (dd, *J* = 16.0, 4.5 Hz, 1H). ^{13}C-NMR (101 MHz, $CDCl_3$): δ= 164.5 (C_q), 154.5 (C_q), 145.2 (2 x C_q), 136.9 (C_q), 136.4 (C_q), 132.2 (CH), 130.3 (CH), 129.7 (CH), 129.3 (CH), 128.9 (CH), 127.9 (CH), 127.7 (CH), 127.5 (CH), 127.3 (CH), 127.2 (CH), 123.7 (C_q), 122.4 (CH), 120.6 (CH), 120.1 (CH), 116.6 (CH), 60.0 (CH), 40.5 (CH_2), 34.3 (CH_2). MS (ESI) *m/z* (relative intensity): 867 (33) $[2M+Na]^+$, 799 (52), 501 (61), 445 (100) $[M+Na]^+$, 437 (78) $[M+H]^+$, 377 (80). HR-MS (ESI) *m/z* calcd for $C_{26}H_{23}N_4O_2$ $[M+H]^+$ 423.1815, found 423.1818.

(*E*)-2-[(1-Butyl-1*H*-1,2,3-triazol-4-yl)methyl]-3-(2-hydroxystyryl)-3,4-dihydroisoquinolin-1(2*H*)-one (3ca)

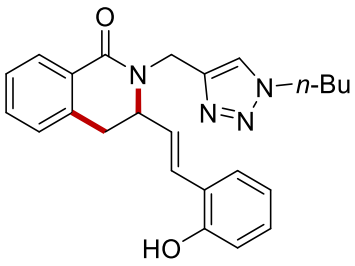

The representative procedure was followed using **1c** (51.6 mg, 0.2 mmol) and **2a** (81 µL, 0.6 mmol). Purification by column chromatography on silica gel (*n*-Hexane/EtOAc 1:1) yielded **3ca** (50.1 mg, 62%) as a white waxy solid. ^{1}H-NMR (400 MHz, $CDCl_3$): δ= 9.34 (bs, 1H), 8.10 (dd, *J* = 7.7, 1.5 Hz, 1H), 7.78 (s, 1H), 7.44 (td, *J* = 7.5, 1.5 Hz, 1H), 7.37 (td, *J* = 7.5, 1.2 Hz, 1H), 7.23 (dd, *J* = 7.7, 1.7 Hz, 1H), 7.18 – 7.10 (m, 3H), 7.05 (dd, *J* = 8.1, 1.3 Hz, 1H), 6.80 (td, *J* = 7.4, 1.2 Hz, 1H), 6.08 (dd, *J* = 15.8, 8.9 Hz, 1H), 5.20 (d, *J* = 14.8 Hz, 1H), 4.68 – 4.60 (m, 1H), 4.49 (d, *J* = 14.8 Hz, 1H), 4.34 (q, *J* = 7.2 Hz, 2H), 3.31 (dd, *J* = 15.9, 6.0 Hz, 1H), 2.94 (dd, *J* = 16.0, 4.0 Hz, 1H), 1.93 – 1.84 (m, 2H), 1.36 (q, *J* = 7.5 Hz, 2H), 0.96 (t, *J* = 7.4 Hz, 3H). ^{13}C-NMR (101 MHz, $CDCl_3$): δ= 164.3 (C_q), 154.7 (C_q), 144.3 (C_q), 136.4 (C_q), 132.1 (CH), 129.7 (CH), 129.2 (CH), 128.8 (C_q), 127.9 (CH), 127.7 (CH), 127.3 (CH), 127.2 (CH), 127.1 (CH), 124.1 (CH), 123.8 (C_q), 119.9 (CH), 116.7 (CH), 59.9 (CH), 50.4 (CH_2), 40.5 (CH_2), 34.2 (CH_2), 32.1 (CH_2), 19.7 (CH_2), 13.4 (CH_3). MS (ESI) *m/z* (relative intensity): 425 (100) $[M+Na]^+$, 403 (34) $[M+H]^+$.HR-MS (ESI) *m/z* calcd for $C_{24}H_{27}N_4O_2$ $[M+H]^+$ 403.2129, found 403.2132.

(*E*)-2-[(1-Hexyl-1*H*-1,2,3-triazol-4-yl)methyl]-3-(2-hydroxystyryl)-3,4-dihydroisoquinolin-1(2*H*)-one (3da)

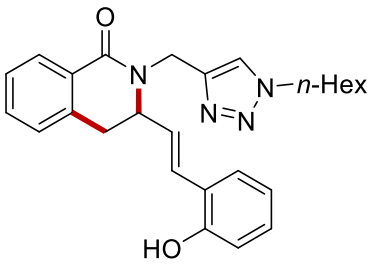

The representative procedure was followed using **1d** (57.3 mg, 0.2 mmol) and **2a** (81 µL, 0.6 mmol). Purification by column chromatography on silica gel (*n*-Hexane/EtOAc 1:1) yielded **3da** (48.4 mg, 70%) as a white solid. M.p.= 128-130 °C. ^{1}H-NMR (400 MHz, $CDCl_3$): δ = 9.62 (bs, 1H), 8.09 (dd, *J* = 7.7, 1.5 Hz, 1H), 7.79 (s, 1H), 7.47 – 7.40 (m, 1H), 7.36 (td, *J* = 7.6, 1.3 Hz, 1H), 7.27 – 7.20 (m, 1H), 7.17 (d, *J* = 10.8 Hz, 1H), 7.14 (d, *J* = 2.6 Hz, 1H), 7.10 (dd, *J* = 7.0, 1.6 Hz, 1H), 7.06 (dd, *J* = 8.1, 1.4 Hz, 1H), 6.78 (td, *J* = 7.4, 1.4 Hz, 1H), 6.09 (dd, *J* = 15.8, 8.8 Hz, 1H), 5.23 (d, *J* = 14.8 Hz, 1H), 4.66 (ddd, *J* = 9.2, 6.2, 3.5 Hz, 1H), 4.44 (d, *J* = 14.8 Hz, 1H), 4.40 – 4.25 (m, 2H), 3.31 (dd, *J* = 15.9, 6.1 Hz, 1H), 2.91 (dd, *J* = 16.1, 3.5 Hz, 1H), 1.89 (q, *J* = 7.3 Hz, 2H), 1.38 – 1.23 (m, 6H), 0.94 – 0.81 (m, 3H). ^{13}C-NMR (101 MHz, $CDCl_3$): δ = 164.2 (C_q), 154.9 (C_q), 144.4 (C_q), 136.4 (C_q), 132.2 (CH), 129.2 (2 x CH), 128.7 (C_q), 127.8 (2 x CH), 127.2 (CH), 126.9 (CH), 126.7 (CH), 124.0 (CH), 123.7 (C_q), 119.7 (CH), 116.5 (CH), 59.8 (CH), 50.7 (CH_2), 40.6 (CH_2), 34.2 (CH_2), 31.1 (CH_2), 30.1 (CH_2), 26.1 (CH_2), 22.4 (CH_2),

13.9 (CH_3). MS (ESI) *m/z* (relative intensity): 883 (10) $[2M+Na]^+$, 431 (100) $[M+H]^+$. HR-MS (ESI) *m/z* calcd for $C_{26}H_{31}N_4O_2$ $[M+H]^+$ 431.2441, found 431.2446.

The reaction was repeated using 2.0 mmol of **1d**. The representative procedure was followed using **2a** (0.81 mL, 0.6 mmol). Purification by column chromatography on silica gel (*n*-hexane/EtOAc 1:1) yielded **3da** (480 mg, 70%) as a white solid.

(*E*)-3-(2-Hydroxystyryl)-2-{[1-(pent-4-en-1-yl)-1*H*-1,2,3-triazol-4-yl]methyl}-3,4-dihydroisoquinolin-1(2*H*)-one (3ea)

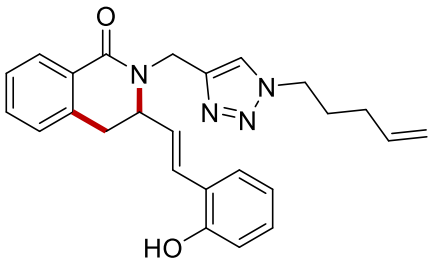

The representative procedure was followed using **1e** (54.1 mg, 0.2 mmol) and **2a** (81 µL, 0.6 mmol). Purification by column chromatography on silica gel (*n*-Hexane/EtOAc 1:1) yielded **3ea** (49.7 mg, 60%) as a colourless oil. ^{1}H-NMR (400 MHz, $CDCl_3$): δ = 9.13 (bs, 1H), 8.09 (dd, *J* = 7.7, 1.4 Hz, 1H), 7.78 (s, 1H), 7.44 (td, *J* = 7.4, 1.5 Hz, 1H), 7.39 – 7.34 (m, 1H), 7.22 (dd, *J* = 7.7, 1.7 Hz, 1H), 7.18 – 7.08 (m, 3H), 7.03 (dd, *J* = 8.2, 1.3 Hz, 1H), 6.80 (t, *J* = 7.7 Hz, 1H), 6.08 (dd, *J* = 15.8, 8.8 Hz, 1H), 5.77 (ddt, *J* = 16.8, 10.2, 6.3 Hz, 1H), 5.18 (dd, *J* = 14.8, 1.6 Hz, 1H), 5.10 – 5.01 (m, 2H), 4.66 – 4.58 (m, 1H), 4.51 (dd, *J* = 14.8, 2.2 Hz, 1H), 4.41 – 4.27 (m, 2H), 3.32 (dd, *J* = 15.9, 6.0 Hz, 1H), 2.95 (dd, *J* = 16.0, 4.2 Hz, 1H), 2.12 – 1.98 (m, 4H). ^{13}C-NMR (101 MHz, $CDCl_3$): δ = 164.3 (C_q), 154.7 (C_q), 144.3 (C_q), 136.4 (C_q), 136.4 (CH), 132.2 (CH), 129.7 (CH), 129.2 (CH), 128.7 (C_q), 128.5 (CH), 127.9 (CH), 127.7 (CH), 127.2 (CH), 127.1 (CH), 124.2 (CH), 123.8 (C_q), 119.9 (CH), 116.7 (CH), 116.4 (CH_2), 60.0 (CH), 49.8 (CH_2), 40.5 (CH_2), 34.2 (CH_2), 30.4 (CH_2), 29.1 (CH_2). MS (ESI) *m/z* (relative intensity): 437 (33) $[M+Na]^+$, 415 (100) $[M+H]^+$. HR-MS (ESI) *m/z* calcd for $C_{25}H_{27}N_4O_2$ $[M+H]^+$ 415.2129, found 415.2127.

(*E*)-2-[(1-Benzyl-1*H*-1,2,3-triazol-4-yl)methyl]-3-(2-hydroxystyryl)-6-methyl-3,4-dihydroisoquinolin-1(2*H*)-one (3fa)

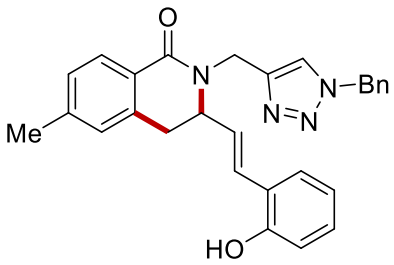

The representative procedure was followed using **1f** (61.2 mg, 0.2 mmol) and **2a** (81 µL, 0.6 mmol). Purification by column chromatography on silica gel (*n*-Hexane/EtOAc 1:1) yielded **3fa** (49.5 mg, 55%) as a white solid. M.p.= 101-102 °C. ^{1}H-NMR (400 MHz, $CDCl_3$): δ = 8.76 (s, 1H), 7.94 (d, *J*

= 7.9 Hz, 1H), 7.71 (s, 1H), 7.39 – 7.34 (m, 3H), 7.26 (m, 2H), 7.22 (dd, *J* = 7.7, 1.7 Hz, 1H), 7.16 – 7.11 (m, 2H), 7.08 – 7.00 (m, 2H), 6.96 (d, *J* = 1.6 Hz, 1H), 6.82 (td, *J* = 7.5, 1.2 Hz, 1H), 6.06 (dd, *J* = 15.8, 8.8 Hz, 1H), 5.56 – 5.43 (m, 2H), 5.12 (d, *J* = 14.8 Hz, 1H), 4.57 (dd, *J* = 9.2, 4.9 Hz, 1H), 4.54 – 4.47 (m, 1H), 3.26 (dd, *J* = 15.9, 5.8 Hz, 1H), 2.90 (dd, *J* = 16.0, 4.5 Hz, 1H), 2.37 (s, 3H). ^{13}C-NMR (101 MHz, $CDCl_3$): δ = 164.4 (C_q), 154.6 (C_q), 144.9 (C_q), 142.7 (C_q), 136.3 (C_q), 134.2 (C_q), 129.6 (CH), 129.2 (2 x CH), 128.9 (CH), 128.3 (CH), 128.2 (CH), 128.0 (CH), 127.9 (CH), 127.7 (CH), 127.2 (CH), 126.1 (C_q), 124.1 (CH), 123.9 (C_q), 120.0 (CH), 116.7 (CH), 60.0 (CH), 54.4 (CH_2), 40.4 (CH_2), 34.2 (CH_2), 21.6 (CH_3). MS (ESI) *m/z* (relative intensity): 923 (31) $[2M+Na]^+$, 473 (100) $[M+Na]^+$, 451 (76) $[M+H]^+$. HR-MS (ESI) *m/z* calcd for $C_{28}H_{27}N_4O_2$ $[M+H]^+$ 451.2129, found 451.2134.

(*E*)-2-[(1-Benzyl-1*H*-1,2,3-triazol-4-yl)methyl]-6-(*tert*-butyl)-3-(2-hydroxystyryl)-3,4-dihydroisoquinolin-1(2*H*)-one (3ga)

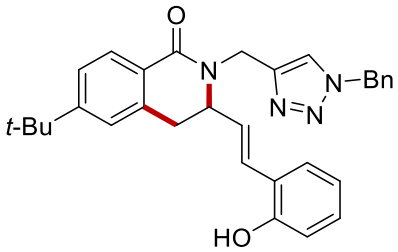

The representative procedure was followed using **1g** (69.6 mg, 0.2 mmol) and **2a** (81 µL, 0.6 mmol). Purification by column chromatography on silica gel (*n*-Hexane/EtOAc 1:1) yielded **3ga** (56.1 mg, 57%) as a white solid. M.p.= 99-101 °C. ^{1}H-NMR (400 MHz, $CDCl_3$): δ = 8.84 (bs, 1H), 7.99 (d, *J* = 8.2 Hz, 1H), 7.70 (s, 1H), 7.40 – 7.33 (m, 5H), 7.28 – 7.20 (m, 3H), 7.15 – 7.13 (m, 1H), 7.08 – 7.00 (m, 2H), 6.83 (td, *J* = 7.5, 1.2 Hz, 1H), 6.08 (dd, *J* = 15.8, 8.9 Hz, 1H), 5.49 (q, *J* = 14.8 Hz, 2H), 5.13 (d, *J* = 14.9 Hz, 1H), 4.56 (dt, *J* = 8.7, 5.2 Hz, 1H), 4.51 (d, *J* = 14.8 Hz, 1H), 3.29 (dd, *J* = 15.9, 5.8 Hz, 1H), 2.95 (dd, *J* = 15.9, 4.9 Hz, 1H), 1.33 (s, 9H). ^{13}C-NMR (101 MHz, $CDCl_3$): δ = 164.4 (C_q), 155.8 (C_q), 154.7 (C_q), 144.9 (C_q), 136.1 (C_q), 134.2 (C_q), 129.9 (CH), 129.2 (2 x CH), 128.9 (CH), 128.2 (CH), 128.1 (CH), 127.8 (CH), 127.2 (CH), 126.0 (C_q), 124.5 (CH), 124.3 (CH), 124.1 (CH), 123.9 (C_q), 119.9 (CH), 116.8 (CH), 60.1 (CH), 54.4 (CH_2), 40.3 (CH_2), 35.0 (C_q), 34.6 (CH_2), 31.2 (CH_3). MS (ESI) *m/z* (relative intensity): 493 (100) $[M+H]^+$, 478 (60). HR-MS (ESI) *m/z* calcd for $C_{31}H_{33}N_4O_2$ $[M+H]^+$ 493.2598, found 493.2599.

(*E*)-2-[(1-Benzyl-1*H*-1,2,3-triazol-4-yl)methyl]-3-(2-hydroxystyryl)-6-phenyl-3,4-dihydroisoquinolin-1(2*H*)-one (3ha)

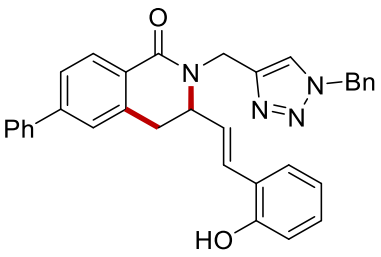

The representative procedure was followed using **1h** (73.6 mg, 0.2 mmol) and **2a** (81 µL, 0.6 mmol). Purification by column chromatography on silica gel (*n*-Hexane/EtOAc 1:1) yielded **3ha** (65.5 mg, 64%) as a white solid. M.p.= 109-111 °C. ^{1}H-NMR (400 MHz, $CDCl_3$): δ = 8.91 – 8.82 (m, 1H), 8.13 (d, *J* = 8.1 Hz, 1H), 7.73 (s, 1H), 7.62 – 7.57 (m, 3H), 7.49 – 7.44 (m, 2H), 7.42 – 7.35 (m, 5H), 7.29 (s, 1H), 7.28 – 7.22 (m, 2H), 7.17 – 7.08 (m, 2H), 7.04 (dd, *J* = 8.2, 1.2 Hz, 1H), 6.82 (td, *J* = 7.4, 1.2 Hz, 1H), 6.11 (dd, *J* = 15.8, 8.8 Hz, 1H), 5.59 – 5.44 (m, 2H), 5.16 (d, *J* = 14.8 Hz, 1H), 4.65 (dt, *J* = 9.7, 5.2 Hz, 1H), 4.54 (d, *J* = 14.8 Hz, 1H), 3.37 (dd, *J* = 15.9, 5.8 Hz, 1H), 3.01 (dd, *J* = 16.0, 4.4 Hz, 1H). ^{13}C-NMR (101 MHz, $CDCl_3$): δ = 164.1 (C_q), 154.7 (C_q), 144.9 (C_q), 144.9 (C_q), 140.0 (C_q), 136.9 (C_q), 134.2 (C_q), 129.4 (CH), 129.2 (CH), 129.2 (CH), 128.9 (2 x CH), 128.5 (CH), 128.3 (CH), 128.1 (CH), 127.5 (C_q), 127.2 (CH), 127.1 (2 x CH), 126.4 (CH), 125.9 (CH), 124.1 (CH), 123.7 (C_q), 119.9 (CH), 116.6 (CH), 59.9 (CH), 54.5 (CH_2), 40.5 (CH_2), 34.4 (CH_2). MS (ESI) *m/z* (relative intensity): 1125 (23), 1047 (100) $[2M+Na]^+$, 535 (31) $[M+Na]^+$, 513 (11) $[M+H]^+$. HR-MS (ESI) *m/z* calcd for $C_{33}H_{29}N_4O_2$ $[M+H]^+$ 513.2285, found 513.2287.

(*E*)-2-[(1-Benzyl-1*H*-1,2,3-triazol-4-yl)methyl]-3-(2-hydroxystyryl)-6-methoxy-3,4-dihydroisoquinolin-1(2*H*)-one (3ia)

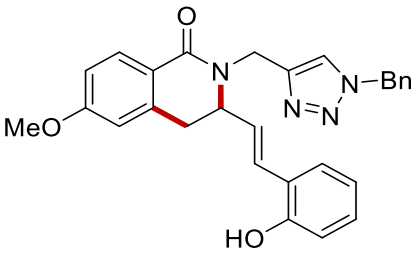

The representative procedure was followed using **1i** (64.5 mg, 0.2 mmol) and **2a** (81 µL, 0.6 mmol). Purification by column chromatography on silica gel (*n*-Hexane/EtOAc 1:1) yielded **3ia** (50.3 mg, 54%) as a white solid. M.p.= 98-100 °C. ^{1}H-NMR (400 MHz, $CDCl_3$): δ = 8.78 (s, 1H), 8.00 (d, *J* = 8.6 Hz, 1H), 7.70 (s, 1H), 7.38 – 7.34 (m, 3H), 7.28 – 7.25 (m, 2H), 7.22 (dd, *J* = 7.7, 1.7 Hz, 1H), 7.16 – 7.12 (m, 1H), 7.09 – 7.00 (m, 2H), 6.88 – 6.80 (m, 2H), 6.64 (d, *J* = 2.5 Hz, 1H), 6.07 (dd, *J* = 15.8, 8.8 Hz, 1H), 5.56 – 5.42 (m, 2H), 5.11 (d, *J* = 14.8 Hz, 1H), 4.57 (dt, *J* = 9.6, 5.2 Hz, 1H), 4.50 (d, *J* = 14.8 Hz, 1H), 3.84 (s, 3H), 3.28 (dd, *J* = 15.9, 5.8 Hz, 1H), 2.92 (d, *J* = 4.7 Hz, 1H). ^{13}C-NMR (101 MHz, $CDCl_3$): δ = 164.3 (C_q), 162.6 (C_q), 154.6 (C_q), 144.9 (C_q), 138.5 (C_q), 134.2 (C_q), 130.1 (CH), 129.9 (CH), 129.2 (2 x CH), 128.9 (CH), 128.2 (CH), 128.0 (CH), 127.3 (CH), 124.1 (CH), 123.9 (C_q), 121.6 (C_q),

120.0 (CH), 116.8 (CH), 112.7 (CH), 112.5 (CH), 60.0 (CH), 55.4 (CH_3), 54.4 (CH_2), 40.3 (CH_2), 34.6 (CH_2). MS (ESI) *m/z* (relative intensity): 1085 (44), 955 (87) $[2M+Na]^+$, 719 (100), 489 (23) $[M+Na]^+$, 467 (64) $[M+H]^+$, 415 (31). HR-MS (ESI) *m/z* calcd for $C_{28}H_{27}N_4O_3$ $[M+H]^+$ 467.2078, found 467.2081.

(*E*)-2-[(1-Benzyl-1*H*-1,2,3-triazol-4-yl)methyl]-6-(dimethylamino)-3-(2-hydroxystyryl)-3,4-dihydroisoquinolin-1(2*H*)-one (3ja)

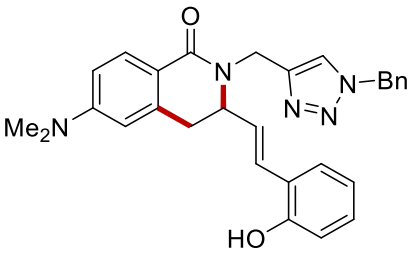

The representative procedure was followed using **1j** (67.1 mg, 0.2 mmol) and **2a** (81 µL, 0.6 mmol). Purification by column chromatography on silica gel (CH_2Cl_2/EtOAc 1:1) yielded **3ja** (37.4 mg, 39%) as a pale-yellow solid. M.p.= 96-98 °C. ^{1}H-NMR (400 MHz, $CDCl_3$): δ = 7.92 (d, *J* = 8.8 Hz, 1H), 7.70 (s, 1H), 7.37 – 7.33 (m, 4H), 7.28 – 7.21 (m, 3H), 7.16 – 7.12 (m, 1H), 7.05 – 7.00 (m, 2H), 6.82 (t, *J* = 7.4 Hz, 1H), 6.62 (dd, *J* = 8.8, 2.5 Hz, 1H), 6.35 (d, *J* = 2.6 Hz, 1H), 6.08 (dd, *J* = 15.8, 8.9 Hz, 1H), 5.48 (q, *J* = 14.8 Hz, 2H), 5.11 (d, *J* = 14.7 Hz, 1H), 4.55 – 4.44 (m, 2H), 3.24 (dd, *J* = 15.8, 5.6 Hz, 1H), 3.03 (s, 6H), 2.93 – 2.84 (m, 1H). ^{13}C-NMR (101 MHz, $CDCl_3$): δ = 165.0 (C_q), 154.6 (2 x C_q), 152.7 (C_q), 145.3 (C_q), 138.0 (C_q), 134.3 (C_q), 129.6 (CH), 129.1 (2 x CH), 129.0 (CH), 128.8 (CH), 128.2 (2 x CH), 127.3 (CH), 124.1 (CH), 119.9 (CH), 116.7 (CH), 116.6 (C_q), 110.2 (CH), 109.5 (CH), 60.1 (CH), 54.4 (CH_2), 40.1 (CH_3), 40.1 (CH_2), 35.0 (CH_2). MS (ESI) *m/z* (relative intensity): 502 (53) $[M+Na]^+$, 480 (27) $[M+H]^+$, 292 (100). HR-MS (ESI) *m/z* calcd for $C_{29}H_{30}N_5O_2$ $[M+H]^+$ 480.2394, found 480.2398.

(*E*)-2-[(1-Benzyl-1*H*-1,2,3-triazol-4-yl)methyl]-3-(2-hydroxystyryl)-6-(octylthio)-3,4-dihydroisoquinolin-1(2*H*)-one (3ka)

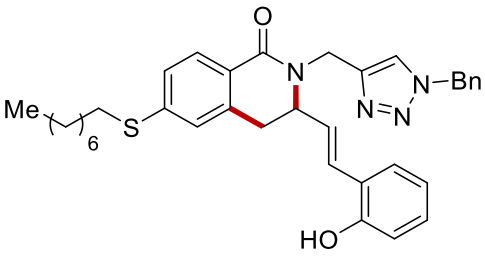

The representative procedure was followed using **1k** (87.3 mg, 0.2 mmol) and **2a** (81 µL, 0.6 mmol). Purification by column chromatography on silica gel (*n*-Hexane/EtOAc 1:1) yielded **3ka** (46.5 mg, 40%) as a white solid. M.p. = 115-117 °C. ^{1}H-NMR (400 MHz, $CDCl_3$): δ = 9.11 (bs, 1H), 7.94 (d, *J* = 8.2 Hz, 1H), 7.70 (s, 1H), 7.41 – 7.33 (m, 3H), 7.28 – 7.18 (m, 4H), 7.16 – 7.07 (m, 2H), 7.04 (dd, *J* = 8.1, 1.2 Hz, 1H), 7.00 (d, *J* = 1.8 Hz, 1H), 6.81 (td, *J* = 7.5, 1.2 Hz, 1H), 6.07 (dd, *J* = 15.8, 8.8

Hz, 1H), 5.58 – 5.42 (m, 2H), 5.15 (d, *J* = 14.9 Hz, 1H), 4.61 (ddd, *J* = 9.4, 5.9, 3.9 Hz, 1H), 4.45 (d, *J* = 14.9 Hz, 1H), 3.26 (dd, *J* = 15.9, 6.0 Hz, 1H), 2.97 (t, *J* = 7.4 Hz, 2H), 2.87 (dd, *J* = 16.1, 3.9 Hz, 1H), 1.69 (p, *J* = 7.4 Hz, 2H), 1.50 – 1.39 (m, 2H), 1.39 – 1.22 (m, 8H), 0.95 – 0.83 (m, 3H). ^{13}C-NMR (101 MHz, $CDCl_3$): δ = 164.0 (C_q), 154.7 (C_q), 144.8 (C_q), 143.5 (C_q), 136.8 (C_q), 134.2 (C_q), 129.5 (CH), 129.2 (2 x CH), 128.9 (CH), 128.3 (2 x CH), 127.1 (2 x CH), 125.4 (CH), 125.4 (C_q), 125.2 (CH), 124.1 (CH), 123.7 (C_q), 119.9 (CH), 116.6 (CH), 59.8 (CH), 54.5 (CH_2), 40.4 (CH_2), 34.3 (CH_2), 32.1 (CH_2), 31.8 (CH_2), 29.2 (CH_2), 29.1 (CH_2), 28.9 (CH_2), 28.8 (CH_2), 22.7 (CH_2), 14.1 (CH_3). MS (ESI) *m/z* (relative intensity): 603 (100) $[M+Na]^+$, 581 (85) $[M+H]^+$. HR-MS (ESI) *m/z* calcd for $C_{35}H_{41}N_4O_2S$ $[M+H]^+$ 581.2945, found 581.2947.

(*E*)-2-[(1-Benzyl-1*H*-1,2,3-triazol-4-yl)methyl]-6-fluoro-3-(2-hydroxystyryl)-3,4-dihydroisoquinolin-1(2*H*)-one (3la)

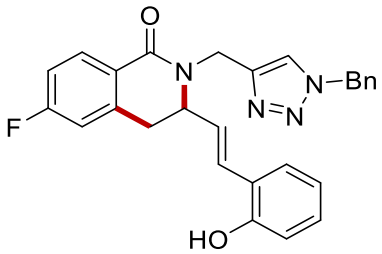

The representative procedure was followed using **1l** (62.0 mg, 0.2 mmol) and **2a** (81 µL, 0.6 mmol). Purification by column chromatography on silica gel (*n*-Hexane/EtOAc 1:1) yielded **3la** (56.3 mg, 62%) as a white solid. M.p.= 84-85 °C. ^{1}H-NMR (400 MHz, $CDCl_3$): δ = 8.99 (bs, 1H), 8.07 (dd, *J* = 8.7, 5.7 Hz, 1H), 7.70 (s, 1H), 7.40 – 7.34 (m, 3H), 7.27 (d, *J* = 2.3 Hz, 1H), 7.22 (dd, *J* = 7.7, 1.7 Hz, 1H), 7.16 – 7.12 (m, 2H), 7.08 (d, *J* = 15.8 Hz, 1H), 7.05 – 6.99 (m, 2H), 6.87 – 6.81 (m, 2H), 6.06 (dd, *J* = 15.8, 8.7 Hz, 1H), 5.57 – 5.43 (m, 2H), 5.13 (d, *J* = 14.9 Hz, 1H), 4.65 – 4.59 (m, 1H), 4.48 (d, *J* = 14.8 Hz, 1H), 3.30 (dd, *J* = 16.1, 5.9 Hz, 1H), 2.92 (dd, *J* = 16.1, 4.3 Hz, 1H). ^{13}C-NMR (101 MHz, $CDCl_3$): δ = 165.0 (d, $^1J_{C\text{-}F}$ = 253 Hz, C_q), 163.4 (C_q), 154.6 (C_q), 144.7 (C_q), 139.2 (d, $^5J_{C\text{-}F}$ = 9 Hz, C_q), 134.1 (C_q), 130.7 (d, $^4J_{C\text{-}F}$ = 8 Hz, CH), 129.9 (CH), 129.3 (CH), 129.2 (CH), 128.9 (CH), 128.3 (CH), 127.2 (CH), 127.1 (CH), 125.1 (d, $^6J_{C\text{-}F}$ = 3 Hz, C_q), 124.1 (CH), 123.7 (C_q), 120.0 (CH), 116.7 (CH), 114.5 (d, $^2J_{C\text{-}F}$ = 22 Hz, CH), 114.4 (d, $^3J_{C\text{-}F}$ = 22 Hz, CH), 59.8 (CH), 54.5 (CH_2), 40.4 (CH_2), 34.2 (CH_2). ^{19}F-NMR (565 MHz, $CDCl_3$): δ = -107.03 (td, *J* = 8.5, 5.5 Hz). MS (ESI) *m/z* (relative intensity): 931 (37) $[2M+Na]^+$, 477 (100) $[M+Na]^+$, 455 (19) $[M+H]^+$. HR-MS (ESI) *m/z* calcd for $C_{27}H_{24}FN_4O_2$ $[M+H]^+$ 455.1878, found 455.1880.

(*E*)-2-[(1-Benzyl-1*H*-1,2,3-triazol-4-yl)methyl]-6-bromo-3-(2-hydroxystyryl)-3,4-dihydroisoquinolin-1(2*H*)-one (3ma)

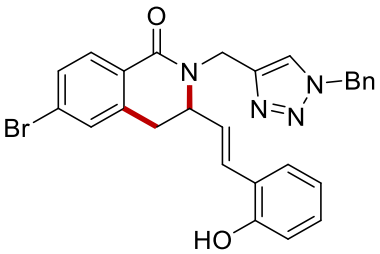

The representative procedure was followed using **1m** (74.2 mg, 0.2 mmol) and **2a** (81 µL, 0.6 mmol). Purification by column chromatography on silica gel (*n*-Hexane/EtOAc 1:1) yielded **3ma** (30.9 mg, 30%) as a white solid. M.p.= 85-87 °C. ^{1}H-NMR (400 MHz, $CDCl_3$): δ = 8.87 (bs, 1H), 7.91 (d, *J* = 8.3 Hz, 1H), 7.69 (s, 1H), 7.48 (dd, *J* = 8.3, 2.0 Hz, 1H), 7.38 – 7.36 (m, 3H), 7.32 (d, *J* = 1.9 Hz, 1H), 7.28 – 7.26 (m, 2H), 7.22 (dd, *J* = 7.8, 1.8 Hz, 1H), 7.13 (td, *J* = 7.7, 1.7 Hz, 1H), 7.06 (d, *J* = 16.1 Hz, 1H), 7.01 (dd, *J* = 8.1, 1.2 Hz, 1H), 6.82 (td, *J* = 7.6, 1.1 Hz, 1H), 6.05 (dd, *J* = 15.8, 8.7 Hz, 1H), 5.57 – 5.44 (m, 2H), 5.13 (d, *J* = 14.8 Hz, 1H), 4.67 – 4.59 (m, 1H), 4.51 – 4.44 (m, 1H), 3.29 (dd, *J* = 16.0, 6.0 Hz, 1H), 2.89 (dd, *J* = 16.1, 4.0 Hz, 1H). ^{13}C-NMR (101 MHz, $CDCl_3$): δ = 163.5 (C_q), 154.6 (C_q), 144.6 (C_q), 138.3 (C_q), 134.1 (C_q), 130.6 (CH), 130.5 (CH), 129.9 (CH), 129.6 (CH), 129.3 (CH), 129.2 (CH), 128.9 (CH), 128.3 (CH), 127.7 (C_q), 127.2 (CH), 126.8 (CH), 126.8 (C_q), 124.0 (CH), 123.6 (C_q), 120.0 (CH), 116.7 (CH), 59.8 (CH), 54.5 (CH_2), 40.5 (CH_2), 33.9 (CH_2). MS (ESI) *m/z* (relative intensity): 515 (100) $[M+H]^+$, 478 (26), 384 (21). HR-MS (ESI) *m/z* calcd for $C_{27}H_{24}BrN_4O_2$ $[M+H]^+$ 515.1077, found 515.1081.

(*E*)-2-[(1-benzyl-1*H*-1,2,3-triazol-4-yl)methyl]-6-chloro-3-(2-hydroxystyryl)-3,4-dihydroisoquinolin-1(2*H*)-one (3na) / 2-[2-(Benzofuran-2-yl)ethyl]-*N*-[(1-benzyl-1*H*-1,2,3-triazol-4-yl)methyl]-4-chlorobenzamide (3'na)

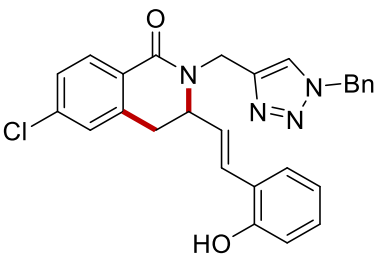

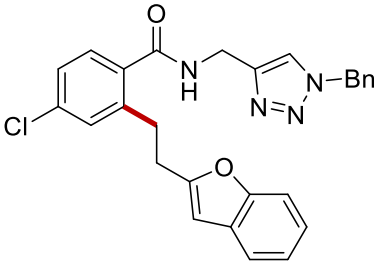

The representative procedure was followed using **1n** (65.2 mg, 0.2 mmol) and **2a** (81 µL, 0.6 mmol). Purification by a first column chromatography on silica gel (*n*-Hexane/EtOAc 1:1) afforded a mixture of the two products which were further purified by preparative thin layer chromatography (SiO_2, *n*-Hexane/acetone 7:3) to yield **3na** (46.6 mg, 52%) as a white solid and **3'na** (11.4 mg, 10%) as a colourless oil.

3na: M.p. = 95-97 °C. ^{1}H-NMR (400 MHz, $CDCl_3$): δ = 9.16 (s, 1H), 7.99 (d, *J* = 8.3 Hz, 1H), 7.70 (s, 1H), 7.40 – 7.35 (m, 3H), 7.32 (dd, *J* = 8.4, 2.1 Hz, 1H), 7.29 – 7.26 (m, 2H), 7.23 (dd, *J* = 7.7, 1.6 Hz, 1H), 7.17 – 7.12 (m, 2H), 7.12 – 7.08 (m, 1H), 7.05 (dd, *J* = 8.2, 1.2 Hz, 1H), 6.82 (td, *J* = 7.4, 1.2 Hz, 1H), 6.06 (dd, *J* = 15.8, 8.7 Hz, 1H), 5.59 – 5.42 (m, 2H), 5.16 (d, *J* = 14.9 Hz, 1H), 4.66 (ddd, *J* = 9.2, 6.1, 3.5 Hz, 1H), 4.43 (d, *J* = 14.9 Hz, 1H), 3.28 (dd, *J* = 16.0, 6.0 Hz, 1H), 2.88 (dd, *J* = 16.2, 3.6 Hz, 1H). ^{13}C-NMR (101 MHz, $CDCl_3$): δ = 163.4 (C_q), 154.7 (C_q), 144.6 (C_q), 138.3 (C_q), 138.1 (C_q), 134.1 (C_q), 129.5 (CH), 129.5 (CH), 129.3 (CH), 129.2 (CH), 128.9 (CH), 128.3 (CH), 127.7 (CH), 127.5 (CH), 127.2 (C_q), 127.1 (CH), 126.4 (CH), 124.1 (CH), 123.5 (C_q), 119.9 (CH), 116.5 (CH), 59.7 (CH), 54.5 (CH_2), 40.5 (CH_2), 34.0 (CH_2). MS (ESI) *m/z* (relative intensity): 493 (100) $[M+Na]^+$, 471 (28) $[M+H]^+$. HR-MS (ESI) *m/z* calcd for $C_{27}H_{24}ClN_4O_2$ $[M+H]^+$ 471.1582, found 471.1585.

3'na: ^{1}H-NMR (400 MHz, $CDCl_3$): δ = 7.51 (s, 1H), 7.48 (dt, *J* = 7.2, 1.0 Hz, 1H), 7.44 – 7.40 (m, 1H), 7.36 – 7.33 (m, 3H), 7.31 (d, *J* = 8.2 Hz, 1H), 7.26 – 7.18 (m, 6H), 6.50 (bs, 1H), 6.33 (d, *J* = 1.0 Hz, 1H), 5.43 (s, 2H), 4.58 (d, *J* = 5.7 Hz, 2H), 3.18 (dd, *J* = 8.9, 6.9 Hz, 2H), 3.04 (dd, *J* = 8.8, 6.6 Hz, 2H). ^{13}C-NMR (101 MHz, $CDCl_3$): δ = 168.9 (C_q), 157.8 (C_q), 154.7 (C_q), 144.7 (C_q), 141.6 (C_q), 136.1 (C_q), 134.4 (C_q), 134.1 (C_q), 130.4 (CH), 129.1 (CH), 128.8 (C_q), 128.8 (CH), 128.4 (CH), 128.1 (CH), 126.5 (CH), 123.4 (CH), 122.6 (CH), 122.1 (CH), 120.4 (CH), 110.8 (CH), 102.6 (CH), 54.2 (CH_2), 35.3 (CH_2), 31.3 (CH_2), 30.1 (CH_2). MS (ESI) *m/z* (relative intensity): 493 (100) $[M+Na]^+$. HR-MS (ESI) *m/z* calcd for $C_{27}H_{24}ClN_4O_2$ $[M+H]^+$ 471.1582, found 471.1586.

The rest of the mass balance was accounted for substrate **1n** (20.2 mg 31%).

Methyl-(*E*)-2-[(1-benzyl-1*H*-1,2,3-triazol-4-yl)methyl]-3-(2-hydroxystyryl)-1-oxo-1,2,3,4-tetrahydroisoquinoline-6-carboxylate (3oa) / Methyl 3-[2-(benzofuran-2-yl)ethyl]-4-{[(1-benzyl-1*H*-1,2,3-triazol-4-yl)methyl]carbamoyl}benzoate (3'oa)

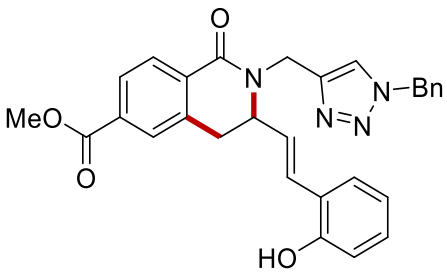

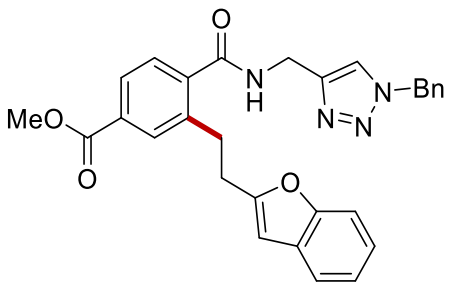

The representative procedure was followed using **1o** (70.0 mg, 0.2 mmol) and **2a** (81 µL, 0.6 mmol). Purification by a first column chromatography on silica gel (*n*-Hexane/EtOAc 1:1)

afforded a mixture of the two products which were further purified by preparative thin layer chromatography (SiO_2, *n*-Hexane/acetone 7:3) to yield **3oa** (44.5 mg, 45%) as a white waxy solid and **3'oa** (8.4 mg, 8%) as a colourless oil.

3oa: ^{1}H-NMR (400 MHz, $CDCl_3$): δ = 9.00 (s, 1H), 8.13 (d, *J* = 8.1 Hz, 1H), 8.01 (dd, *J* = 8.1, 1.7 Hz, 1H), 7.86 – 7.84 (m, 1H), 7.72 (s, 1H), 7.40 – 7.34 (m, 3H), 7.29 – 7.26 (m, 2H), 7.23 – 7.19 (m, 1H), 7.16 – 7.08 (m, 2H), 7.03 (dd, *J* = 8.1, 1.2 Hz, 1H), 6.80 (td, *J* = 7.5, 1.2 Hz, 1H), 6.04 (dd, *J* = 15.8, 8.7 Hz, 1H), 5.59 – 5.42 (m, 2H), 5.16 (d, *J* = 14.8 Hz, 1H), 4.69 (ddd, *J* = 9.2, 6.0, 3.7 Hz, 1H), 4.48 (d, *J* = 14.7 Hz, 1H), 3.94 (s, 3H), 3.34 (dd, *J* = 16.0, 6.0 Hz, 1H), 2.98 (dd, *J* = 16.1, 3.7 Hz, 1H). ^{13}C-NMR (101 MHz, $CDCl_3$): δ = 166.4 (C_q), 163.3 (C_q), 154.7 (C_q), 144.5 (C_q), 136.5 (C_q), 134.1 (C_q), 133.2 (C_q), 132.4 (C_q), 129.5 (CH), 129.3 (CH), 129.2 (CH), 129.0 (CH), 128.9 (CH), 128.3 (CH), 128.2 (CH), 128.0 (CH), 127.1 (CH), 126.4 (CH), 124.1 (CH), 123.5 (C_q), 119.9 (CH), 116.5 (CH), 59.7 (CH), 54.5 (CH_2), 52.4 (CH_3), 40.6 (CH_2), 34.0 (CH_2). MS (ESI) *m/z* (relative intensity): 517 (76) $[M+Na]^+$, 495 (100) $[M+H]^+$. HR-MS (ESI) *m/z* calcd for $C_{29}H_{27}N_4O_4$ $[M+H]^+$ 495.2027, found 495.2028.

3'oa: ^{1}H-NMR (400 MHz, $CDCl_3$): δ = 7.52 (s, 1H), 7.47 (dd, *J* = 7.7, 1.4 Hz, 1H), 7.44 – 7.39 (m, 2H), 7.34 (m, 4H), 7.25 – 7.15 (m, 5H), 6.53 (bs, 1H), 6.32 (d, *J* = 1.1 Hz, 1H), 5.42 (s, 2H), 4.59 (d, *J* = 5.7 Hz, 2H), 3.91 (s, 3H), 3.22 (dd, *J* = 8.8, 6.7 Hz, 2H), 3.06 (t, *J* = 7.7 Hz, 2H). ^{13}C-NMR (101 MHz, $CDCl_3$): δ = 169.0 (C_q), 166.3 (C_q), 157.9 (C_q), 154.7 (C_q), 144.6 (C_q), 139.9 (C_q), 139.7 (C_q), 134.4 (C_q), 131.6 (C_q), 131.4 (CH), 129.1 (CH), 128.8 (CH), 128.8 (C_q), 128.1 (CH), 127.6 (CH), 127.1 (CH), 123.4 (CH), 122.5 (CH), 122.1 (CH), 120.4 (CH), 110.8 (CH), 102.6 (CH), 54.2 (CH_2), 52.3 (CH_3), 35.3 (CH_2), 31.3 (CH_2), 30.2 (CH_2). MS (ESI) *m/z* (relative intensity): 1011 (32) $[2M+Na]^+$, 517 (100) $[M+Na]^+$, 495 (44) $[M+H]^+$. HR-MS (ESI) *m/z* calcd for $C_{29}H_{27}N_4O_4$ $[M+H]^+$ 495.2027, found 495.2025.

The rest of the mass balance was accounted for substrate **1o** (25.9 mg 37%).

(*E*)-2-[(1-Benzyl-1*H*-1,2,3-triazol-4-yl)methyl]-3-(2-hydroxystyryl)-6-(trifluoromethyl)-3,4-dihydroisoquinolin-1(2*H*)-one (3pa) / 2-[2-(benzofuran-2-yl)ethyl]-*N*-[(1-benzyl-1*H*-1,2,3-triazol-4-yl)methyl]-4-(trifluoromethyl)benzamide (3'pa)

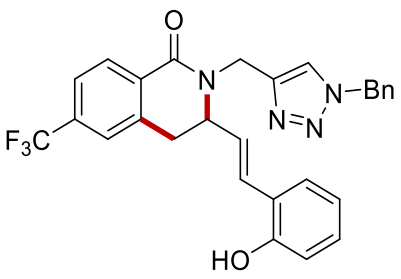

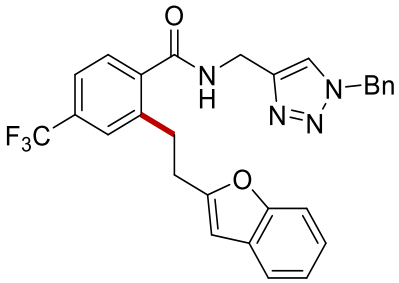

The representative procedure was followed using **1p** (73.2 mg, 0.2 mmol) and **2a** (81 µL, 0.6 mmol). Purification by a first column chromatography on silica gel (*n*-Hexane/EtOAc 1:1) afforded a mixture of the two products which were further purified by preparative thin layer chromatography (SiO_2, *n*-Hexane/acetone 7:3) to yield **3pa** (47.3 mg, 47%) as a white solid and **3'pa** (13.3 mg, 13%) as a colourless oil.

3pa: M.p. = 167-169 °C. ^{1}H-NMR (400 MHz, $CDCl_3$): δ = 9.08 (bs, 1H), 8.18 (d, *J* = 8.1 Hz, 1H), 7.71 (s, 1H), 7.61 (dd, *J* = 8.2, 1.7 Hz, 1H), 7.43 (d, *J* = 1.7 Hz, 1H), 7.38 (m, 3H), 7.30 (s, 2H), 7.23 (dd, *J* = 7.7, 1.6 Hz, 1H), 7.16 (s, 1H), 7.14 – 7.11 (m, 1H), 7.04 (dd, *J* = 8.1, 1.2 Hz, 1H), 6.82 (td, *J* = 7.5, 1.2 Hz, 1H), 6.05 (dd, *J* = 15.8, 8.7 Hz, 1H), 5.59 – 5.44 (m, 2H), 5.18 (d, *J* = 14.8 Hz, 1H), 4.71 (ddd, *J* = 9.2, 6.0, 3.6 Hz, 1H), 4.47 (d, *J* = 14.8 Hz, 1H), 3.35 (dd, *J* = 16.1, 6.1 Hz, 1H), 2.98 (dd, *J* = 16.2, 3.7 Hz, 1H). ^{13}C-NMR (101 MHz, $CDCl_3$): δ = 162.9 (C_q), 154.6 (C_q), 144.4 (C_q), 137.1 (C_q), 134.1 (C_q), 133.7 (q, $^2J_{C-F}$ = 33 Hz C_q), 131.8 (C_q), 129.8 (CH), 129.4 (CH), 129.2 (CH), 129.0 (CH), 128.5 (CH), 128.3 (CH), 127.1 (CH), 126.3 (CH), 124.7 (q, $^3J_{C-F}$ = 4 Hz, CH), 124.1 (m, CH), 124.1 (CH), 123.6 (q, $^1J_{C-F}$ = 273 Hz, C_q), 123.4 (C_q), 120.0 (CH), 116.6 (CH), 59.6 (CH), 54.5 (CH_2), 40.6 (CH_2), 34.1 (CH_2). ^{19}F-NMR (565 MHz, $CDCl_3$): δ= -62.9 (s). MS (ESI) *m/z* (relative intensity): 527 (71) $[M+Na]^+$. HR-MS (ESI) *m/z* calcd for $C_{28}H_{24}F_3N_4O_2$ $[M+H]^+$ 505.1846, found 505.1848.

3'pa: ^{1}H-NMR (400 MHz, $CDCl_3$): δ = 7.52 (s, 1H), 7.52 – 7.45 (m, 4H), 7.42 (d, *J* = 8.1 Hz, 1H), 7.37 – 7.33 (m, 3H), 7.24 – 7.19 (m, 4H), 6.60 (bs, 1H), 6.32 (d, *J* = 1.0 Hz, 1H), 5.43 (s, 2H), 4.60 (d, *J* = 5.7 Hz, 2H), 3.27 – 3.18 (m, 2H), 3.06 (dd, *J* = 8.9, 6.6 Hz, 2H). ^{13}C-NMR (101 MHz, $CDCl_3$): δ = 168.6 (C_q), 157.6 (C_q), 154.7 (C_q), 144.5 (C_q), 140.4 (C_q), 139.1 (C_q), 134.4 (C_q), 132.1 (q, $^2J_{C-F}$ = 33 Hz, C_q), 129.2 (CH), 128.9 (CH), 128.7 (C_q), 128.07 (CH), 127.4 (CH), 127.14 (q, $^4J_{C-F}$ = 4 Hz, CH), 123.6 (q, $^1J_{C-F}$ = 273 Hz, C_q), 123.5 (CH), 123.4 (q, $^3J_{C-F}$ = 4 Hz, CH), 122.6 (CH), 122.1 (CH), 120.4 (CH), 110.8 (CH), 102.8 (CH), 54.3 (CH_2), 35.4 (CH_2), 31.5 (CH_2), 30.1 (CH_2). ^{19}F-NMR (565 MHz, $CDCl_3$): δ= -62.9 (s). MS (ESI) *m/z* (relative intensity):

527 (100) $[M+Na]^+$, 505 (84) $[M+H]^+$. HR-MS (ESI) *m/z* calcd for $C_{28}H_{24}F_3N_4O_2$ $[M+H]^+$ 505.1846, found 505.1850.

The rest of the mass balance was accounted for substrate **1p** (23.1 mg, 32%).

(*E*)-2-[(1-Benzyl-1*H*-1,2,3-triazol-4-yl)methyl]-3-(2-hydroxystyryl)-7-methyl-3,4-dihydroisoquinolin-1(2*H*)-one (3qa)

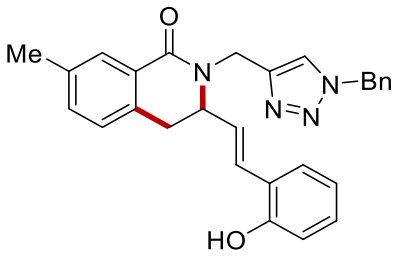

The representative procedure was followed using **1q** (61.2 mg, 0.2 mmol) and **2a** (81 µL, 0.6 mmol). Purification by column chromatography on silica gel (*n*-Hexane/EtOAc 1:1) yielded **3qa** (55.8 mg, 62%) as a white solid. M.p.= 86-88 °C. ^{1}H-NMR (400 MHz, $CDCl_3$): δ = 8.72 (d, *J* = 4.5 Hz, 1H), 7.90 – 7.86 (m, 1H), 7.71 (s, 1H), 7.39 – 7.35 (m, 3H), 7.28 – 7.20 (m, 4H), 7.18 – 7.12 (m, 1H), 7.08 – 7.01 (m, 3H), 6.82 (d, *J* = 1.2 Hz, 1H), 6.06 (dd, *J* = 15.8, 8.8 Hz, 1H), 5.50 (q, *J* = 14.7 Hz, 2H), 5.11 (d, *J* = 14.8 Hz, 1H), 4.60 – 4.50 (m, 2H), 3.26 (dd, *J* = 15.8, 5.8 Hz, 1H), 2.91 (dd, *J* = 15.9, 4.7 Hz, 1H), 2.39 (s, 3H). ^{13}C-NMR (101 MHz, $CDCl_3$): δ = 164.5 (C_q), 154.5 (C_q), 144.8 (C_q), 136.9 (C_q), 134.2 (C_q), 133.3 (C_q), 132.9 (CH), 130.0 (CH), 129.2 (2 x CH), 128.9 (CH), 128.5 (C_q), 128.3 (CH), 128.2 (2 x CH), 127.5 (CH), 127.3 (CH), 124.2 (CH), 124.0 (C_q), 120.1 (CH), 116.8 (CH), 60.2 (CH), 54.4 (CH_2), 40.5 (CH_2), 33.9 (CH_2), 21.1 (CH_3). MS (ESI) *m/z* (relative intensity): 1002 (31), 923 (100) $[2M+Na]^+$, 473 (71) $[M+Na]^+$, 451 (17) $[M+H]^+$. HR-MS (ESI) *m/z* calcd for $C_{28}H_{27}N_4O_2$ $[M+H]^+$ 451.2129, found 451.2132.

(*E*)-2-[(1-Benzyl-1*H*-1,2,3-triazol-4-yl)methyl]-3-(2-hydroxystyryl)-7-methoxy-3,4-dihydroisoquinolin-1(2*H*)-one (3ra)

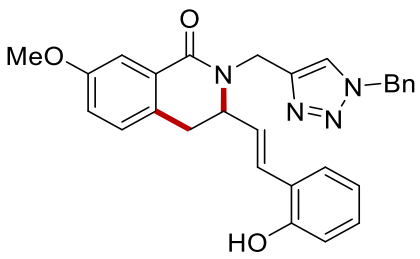

The representative procedure was followed using **1r** (64.5 mg, 0.2 mmol) and **2a** (81 µL, 0.6 mmol). Purification by column chromatography on silica gel (*n*-Hexane/EtOAc 1:1) yielded **3ra** (48.5 mg, 52%) as a white waxy solid. ^{1}H-NMR (400 MHz, $CDCl_3$): δ = 8.57 (s, 1H), 7.70 (s, 1H), 7.59 (d, *J* = 2.7 Hz, 1H), 7.40 – 7.34 (m, 3H), 7.28 – 7.25 (m, 2H), 7.21 (dd, *J* = 7.7, 1.7 Hz, 1H), 7.15 (td, *J* = 7.7, 1.7 Hz, 1H), 7.10 – 6.98 (m, 4H), 6.83 (td, *J* = 7.5, 1.2 Hz, 1H), 6.07 (dd, *J* = 15.8, 8.8 Hz, 1H), 5.50 (q, *J* = 14.8 Hz, 2H), 5.10 (d, *J* =

14.8 Hz, 1H), 4.60 – 4.52 (m, 2H), 3.85 (s, 3H), 3.24 (dd, *J* = 15.7, 5.8 Hz, 1H), 2.90 (dd, *J* = 15.8, 4.8 Hz, 1H). ^{13}C-NMR (101 MHz, $CDCl_3$): δ = 164.3 (C_q), 158.8 (C_q), 154.5 (C_q), 144.7 (C_q), 134.2 (C_q), 129.9 (CH), 129.6 (C_q), 129.2 (2 x CH), 128.9 (CH), 128.8 (CH), 128.5 (C_q), 128.2 (CH), 128.0 (CH), 127.3 (CH), 124.1 (CH), 123.9 (C_q), 120.1 (CH), 119.5 (CH), 116.8 (CH), 111.3 (CH), 60.3 (CH), 55.5 (CH_3), 54.5 (CH_2), 40.5 (CH_2), 33.4 (CH_2). MS (ESI) *m/z* (relative intensity): 479 (35), 467 (100) $[M+H]^+$. HR-MS (ESI) *m/z* calcd for $C_{28}H_{27}N_4O_3$ $[M+H]^+$ 467.2078, found 467.2082.

(*E*)-2-[(1-Benzyl-1*H*-1,2,3-triazol-4-yl)methyl]-3-(2-hydroxystyryl)-7-(trifluoromethyl)-3,4-dihydroisoquinolin-1(2*H*)-one (3sa) / 2-[2-(Benzofuran-2-yl)ethyl]-*N*-[(1-benzyl-1*H*-1,2,3-triazol-4-yl)methyl]-5-(trifluoromethyl)benzamide (3'sa)

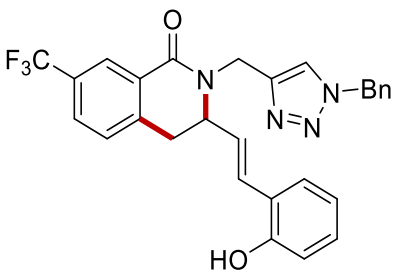

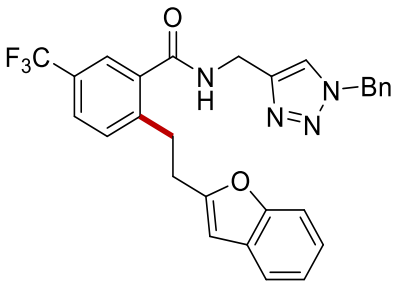

The representative procedure was followed using **1s** (73.2 mg, 0.2 mmol) and **2a** (81 µL, 0.6 mmol). Purification by a first column chromatography on silica gel (*n*-Hexane/EtOAc 1:1) afforded a mixture of the two products which were further purified by preparative thin layer chromatography (SiO_2, *n*-Hexane/acetone 7:3) to yield **3sa** (26.2 mg, 26%) as a white waxy solid and **3'sa** (22.1 mg, 22%) as a colourless oil.

3sa: ^{1}H-NMR (400 MHz, $CDCl_3$): δ = 8.81 (s, 1H), 8.36 (d, *J* = 2.0 Hz, 1H), 7.72 (s, 1H), 7.68 (dd, *J* = 8.0, 2.0 Hz, 1H), 7.41 – 7.36 (m, 3H), 7.32 – 7.29 (m, 3H), 7.22 (dd, *J* = 7.8, 1.7 Hz, 1H), 7.17 – 7.13 (m, 1H), 7.11 (d, *J* = 15.8 Hz, 1H), 7.03 (dd, *J* = 8.1, 1.2 Hz, 1H), 6.83 (td, *J* = 7.5, 1.2 Hz, 1H), 6.04 (dd, *J* = 15.8, 8.8 Hz, 1H), 5.60 – 5.44 (m, 2H), 5.14 (d, *J* = 14.8 Hz, 1H), 4.70 – 4.65 (m, 1H), 4.52 (d, *J* = 14.8 Hz, 1H), 3.36 (dd, *J* = 16.3, 5.9 Hz, 1H), 3.02 (dd, *J* = 16.3, 4.3 Hz, 1H). ^{13}C-NMR (101 MHz, $CDCl_3$): δ = 162.9 (C_q), 154.6 (C_q), 144.4 (C_q), 140.1 (C_q), 134.1 (C_q), 130.3 (CH), 129.7 (q, $^2J_{C\text{-}F}$ = 33 Hz, C_q), 129.4 (CH), 129.4 (C_q), 129.2 (CH), 129.0 (CH), 128.6 (q, $^4J_{C\text{-}F}$ = 4 Hz, CH), 128.3 (2 x CH), 127.2 (CH), 126.8 (CH), 125.1 (q, $^3J_{C\text{-}F}$ = 4 Hz, CH), 124.2 (CH), 123.8 (q, $^1J_{C\text{-}F}$ = 273 Hz, C_q), 123.5 (C_q), 120.1 (CH), 116.7 (CH), 59.7 (CH), 54.5 (CH_2), 40.5 (CH_2), 34.2 (CH_2). ^{19}F-NMR (565 MHz, $CDCl_3$): δ= -62.6 (s). MS (ESI) *m/z* (relative

intensity): 527 (100) $[M+Na]^+$, 505 (76) $[M+H]^+$. HR-MS (ESI) *m/z* calcd for $C_{28}H_{24}F_3N_4O_2$ $[M+H]^+$ 505.1846, found 505.1847.

3'sa: ^{1}H-NMR (400 MHz, $CDCl_3$): δ = 7.61 (s, 1H), 7.57 (dd, *J* = 8.2, 1.9 Hz, 1H), 7.53 (s, 1H), 7.49 – 7.46 (m, 1H), 7.45 – 7.41 (m, 1H), 7.36 – 7.34 (m, 3H), 7.32 (d, *J* = 8.1 Hz, 1H), 7.25 – 7.19 (m, 4H), 6.70 (bs, 1H), 6.31 (d, *J* = 1.0 Hz, 1H), 5.44 (s, 2H), 4.62 (d, *J* = 5.7 Hz, 2H), 3.24 (t, *J* = 7.6 Hz, 2H), 3.06 (t, *J* = 7.6 Hz, 2H). ^{13}C-NMR (101 MHz, $CDCl_3$): δ = 168.5 (C_q), 157.6 (C_q), 154.7 (C_q), 144.5 (C_q), 143.5 (C_q), 136.4 (C_q), 134.4 (C_q), 130.9 (CH), 129.3 (q, $^2J_{C\text{-}F}$ = 33 Hz C_q), 129.2 (CH), 128.9 (CH), 128.7 (C_q), 128.1 (CH), 126.8 (q, $^4J_{C\text{-}F}$ = 4 Hz, CH), 124.0 (q, $^3J_{C\text{-}F}$ = 4 Hz, CH) , 123.7 (q, $^1J_{C\text{-}F}$ = 273 Hz, C_q), 123.5 (CH), 122.6 (CH), 122.2 (CH), 120.4 (CH), 110.8 (CH), 102.8 (CH), 54.2 (CH_2), 35.4 (CH_2), 31.4 (CH_2), 30.0 (CH_2). ^{19}F-NMR (565 MHz, $CDCl_3$): δ= -62.4 (s). MS (ESI) *m/z* (relative intensity): 1031 (24) $[2M+Na]^+$, 527 (70) $[M+Na]^+$, 505 (100) $[M+H]^+$. HR-MS (ESI) *m/z* calcd for $C_{28}H_{24}F_3N_4O_2$ $[M+H]^+$ 505.1846, found 505.1845.

The rest of the mass balance was accounted for substrate **1s** (21.5 mg, 30%).

2-[2-(Benzofuran-2-yl)ethyl]-*N*-[(1-benzyl-1*H*-1,2,3-triazol-4-yl)methyl]-6-methylbenzamide (3'ta)

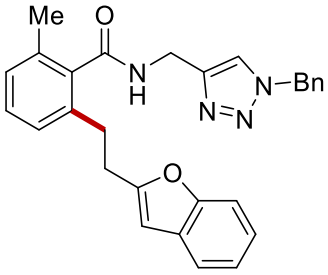

The representative procedure was followed using **1t** (61.2 mg, 0.2 mmol) and **2a** (81 µL, 0.6 mmol). Purification by column chromatography on silica gel (*n*-Hexane/EtOAc 1:1) yielded **3'ta** (24.3 mg, 27%) as a pale-yellow solid. M.p.= 102-104 °C. ^{1}H-NMR (400 MHz, $CDCl_3$): δ = 7.73 – 7.66 (m, 1H), 7.54 (s, 1H), 7.50 – 7.47 (m, 1H), 7.45 – 7.42 (m, 1H), 7.36 – 7.31 (m, 3H), 7.26 – 7.14 (m, 4H), 7.05 – 7.02 (m, 2H), 6.38 (t, *J* = 5.9 Hz, 1H), 6.31 (d, *J* = 1.0 Hz, 1H), 5.34 (s, 2H), 4.65 (d, *J* = 5.8 Hz, 2H), 3.05 – 2.90 (m, 4H), 2.21 (s, 3H). ^{13}C-NMR (101 MHz, $CDCl_3$): δ = 170.2 (C_q), 158.3 (C_q), 154.6 (C_q), 144.8 (C_q), 137.3 (C_q), 136.9 (C_q), 134.5 (C_q), 134.4 (C_q), 133.5 (CH), 129.1 (CH), 128.8 (CH), 128.8 (C_q), 128.2 (CH), 127.9 (CH), 126.5 (CH), 123.4 (CH), 122.6 (CH), 122.3 (CH), 120.4 (CH), 110.8 (CH), 102.3 (CH), 54.1 (CH_2), 35.1 (CH_2), 31.3 (CH_2), 30.4 (CH_2), 19.1 (CH_3). MS (ESI) *m/z* (relative intensity): 479 (100), 473 (36) $[M+Na]^+$, 463 (45). HR-MS (ESI) *m/z* calcd for $C_{28}H_{27}N_4O_2$ $[M+H]^+$ 451.2129, found 451.2132.

(*E*)-2-[(1-Benzyl-1*H*-1,2,3-triazol-4-yl)methyl]-3-(2-hydroxystyryl)-3,4-dihydrobenzo [g]isoquinolin-1(2*H*)-one (3ua)

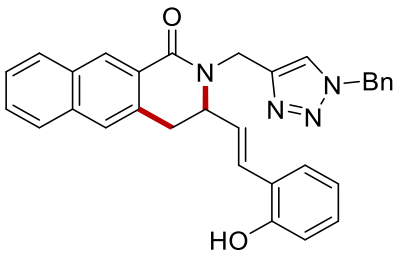

The representative procedure was followed using **1u** (68.4 mg, 0.2 mmol) and **2a** (81 µL, 0.6 mmol). Purification by column chromatography on silica gel (*n*-Hexane/EtOAc 1:1) yielded **3ua** (50.5 mg, 52%) as a white solid. M.p.= 96-98 °C. ^{1}H-NMR (400 MHz, $CDCl_3$): δ = 8.62 (s, 1H), 8.46 (bs, 1H), 7.95 (dd, *J* = 8.1, 1.3 Hz, 1H), 7.80 (dd, *J* = 8.2, 1.2 Hz, 1H), 7.74 (s, 1H), 7.60 (s, 1H), 7.58 – 7.54 (m, 1H), 7.52 – 7.48 (m, 1H), 7.39 – 7.34 (m, 3H), 7.26 (m, 2H), 7.19 – 7.04 (m, 3H), 7.00 (dd, *J* = 8.1, 1.2 Hz, 1H), 6.79 (td, *J* = 7.5, 1.2 Hz, 1H), 6.04 (dd, *J* = 15.8, 8.8 Hz, 1H), 5.57 – 5.44 (m, 2H), 5.16 (d, *J* = 14.8 Hz, 1H), 4.70 – 4.64 (m, 1H), 4.61 (d, *J* = 14.8 Hz, 1H), 3.47 (dd, *J* = 15.5, 5.6 Hz, 1H), 3.13 (dd, *J* = 15.7, 4.3 Hz, 1H). ^{13}C-NMR (101 MHz, $CDCl_3$): δ = 164.3 (C_q), 154.4, (C_q) 144.7 (C_q), 135.1 (C_q), 134.2 (C_q), 132.5 (C_q), 132.2 (C_q), 129.7 (CH), 129.4 (CH), 129.2 (2 x CH), 129.1 (CH), 128.9 (CH), 128.2 (CH), 128.0 (CH), 127.8 (CH), 127.3 (CH), 127.1 (CH), 126.8 (C_q), 126.1 (2 x CH), 124.2 (CH), 123.8 (C_q), 120.1 (CH), 116.7 (CH), 60.3 (CH), 54.5 (CH_2), 40.9 (CH_2), 34.8 (CH_2). MS (ESI) *m/z* (relative intensity): 995 (54) $[2M+Na]^+$, 927 (64), 509 (61) $[M+Na]^+$, 487 (100) $[M+H]^+$, 463 (56). HR-MS (ESI) *m/z* calcd for $C_{31}H_{27}N_4O_2$ $[M+H]^+$ 487.2129, found 487.2130.

(*E*)-2-[(1-Benzyl-1*H*-1,2,3-triazol-4-yl)methyl]-3-(2-hydroxystyryl)-9-methyl-2,3,4,9-tetrahydro-1*H*-pyrido[3,4-b]indol-1-one (3va) / 3-[2-(Benzofuran-2-yl)ethyl]-*N*-[(1-benzyl-1*H*-1,2,3-triazol-4-yl)methyl]-1-methyl-1*H*-indole-2-carboxamide (3'va)

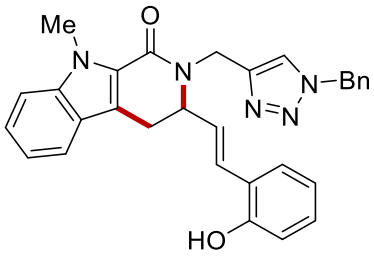

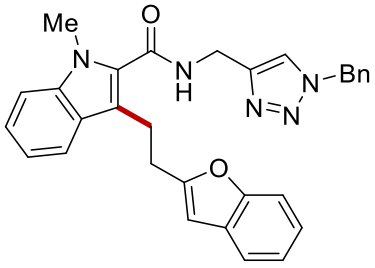

The representative procedure was followed using **1v** (69.1 mg, 0.2 mmol) and **2a** (81 µL, 0.6 mmol). Purification by a first column chromatography on silica gel (*n*-Hexane/EtOAc 1:1) afforded a mixture of the two products which were further purified by preparative thin layer chromatography (SiO_2, *n*-Hexane/acetone 7:3) to yield **3va** (24.5 mg, 25%) as a pale-yellow waxy solid and **3'va** (22.5 mg, 23%) as a pale-yellow oil.

3va: ^{1}H NMR (400 MHz, $CDCl_3$) δ 7.68 (s, 1H), 7.56 (d, *J* = 8.1 Hz, 1H), 7.48 (dd, *J* = 12.2, 7.6 Hz, 1H), 7.41 – 7.34 (m, 5H), 7.28 – 7.22 (m, 2H), 7.19 – 7.12 (m, 2H), 7.11 – 7.06 (m, 2H), 7.00 (dd, *J* = 8.2, 1.2 Hz, 1H), 6.81 (td, *J* = 7.5, 1.2 Hz, 1H), 6.25 (dd, *J* = 15.8, 9.0 Hz, 1H), 5.50 (q, *J* = 14.8 Hz, 2H), 5.17 (d, *J* = 15.1 Hz, 1H), 4.65 (m, 1H), 4.52 (d, *J* = 15.0 Hz, 1H), 4.13 (s, 3H), 3.33 (dd, *J* = 16.2, 6.4 Hz, 1H), 3.14 – 3.02 (m, 1H). ^{13}C-NMR (101 MHz, $CDCl_3$): δ = 161.2 (C_q), 154.6 (C_q), 145.1 (C_q), 139.4 (C_q), 134.2 (C_q), 129.6 (CH), 129.2 (2 x CH), 128.9 (CH), 128.2 (2 x CH), 127.2 (CH), 125.6 (C_q), 124.8 (CH), 124.3 (2 x C_q), 123.9 (CH), 120.4 (CH), 120.1 (CH), 120.0 (CH), 117.0 (C_q), 116.7 (CH), 110.2 (CH), 61.8 (CH), 54.5 (CH_2), 39.2 (CH_2), 31.3 (CH_3), 27.0 (CH_2). MS (ESI) *m/z* (relative intensity): 512 (66) $[M+Na]^+$, 490 (100) $[M+H]^+$. HR-MS (ESI) *m/z* calcd for $C_{30}H_{28}N_5O_2$ $[M+H]^+$ 490.2238, found 490.2236.

3'va: ^{1}H-NMR (400 MHz, $CDCl_3$): δ = 7.67 (d, *J* = 8.0 Hz, 1H), 7.46 – 7.38 (m, 3H), 7.38 – 7.32 (m, 5H), 7.26 – 7.14 (m, 5H), 6.62 (bs, 1H), 6.31 (s, 1H), 5.45 (s, 2H), 4.59 (d, *J* = 5.8 Hz, 2H), 3.79 (s, 3H), 3.33 (t, *J* = 7.4 Hz, 2H), 3.14 (t, *J* = 7.4 Hz, 2H). ^{13}C-NMR (101 MHz, $CDCl_3$): δ = 162.8 (C_q), 157.9 (C_q), 144.9 (C_q), 138.0 (2 x C_q), 134.5 (C_q), 133.6 (C_q), 130.2 (CH), 129.1 (2 x CH), 128.8 (CH), 128.1 (2 x CH), 126.4 (2 x C_q), 124.1 (CH), 123.6 (CH), 122.7 (CH), 120.5 (CH), 120.0 (CH), 119.9 (CH), 115.4 (C_q), 110.9 (CH), 110.0 (CH), 103.2 (CH), 54.2 (CH_2), 35.3 (CH_2), 31.3 (CH_3), 29.7 (CH_2), 23.6 (CH_2). MS (ESI) *m/z* (relative intensity): 512 (100) $[M+Na]^+$. HR-MS (ESI) *m/z* calcd for $C_{30}H_{28}N_5O_2$ $[M+H]^+$ 48490.2238, found 490.2239.

(*E*)-6-[(1-Benzyl-1*H*-1,2,3-triazol-4-yl)methyl]-5-(2-hydroxystyryl)-5,6-dihydrothieno[2,3-c]pyridin-7(4*H*)-one (3wa)

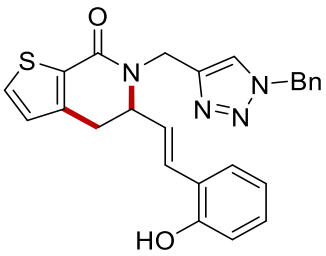

The representative procedure was followed using **1w** (59.6 mg, 0.2 mmol) and **2a** (81 µL, 0.6 mmol). Purification by column chromatography on silica gel (*n*-Hexane/EtOAc 1:1) yielded **3wa** (45.1 mg, 51%) as a white waxy solid. ^{1}H-NMR (400 MHz, $CDCl_3$): δ = 9.08 (bs, 1H), 7.70 (s, 1H), 7.48 (d, *J* = 4.9 Hz, 1H), 7.37 (m, 3H), 7.31 – 7.24 (m, 3H), 7.16 (td, *J* = 7.6, 1.6 Hz, 1H), 7.10 (d, *J* = 15.7 Hz, 1H), 7.05 (dd, *J* = 8.1, 1.2 Hz, 1H), 6.88 (d, *J* = 4.9 Hz, 1H), 6.87 – 6.82 (m, 1H), 6.15 (dd, *J* = 15.8, 9.0 Hz, 1H), 5.60 – 5.41 (m, 2H), 5.13 (d, *J* = 15.0 Hz, 1H), 4.62 (dt, *J* = 9.2, 5.7 Hz, 1H), 4.46 (d, *J* = 15.0 Hz, 1H), 3.19 (dd, *J* = 16.4, 6.3 Hz, 1H), 2.96 (dd, *J* = 16.4, 5.1 Hz, 1H). ^{13}C-NMR (101 MHz, $CDCl_3$): δ = 161.3 (C_q), 154.7 (C_q), 144.7 (C_q), 142.2 (C_q), 134.2 (C_q), 131.4 (CH), 131.1 (C_q), 130.4 (CH), 129.3 (CH), 129.2 (CH), 128.9 (CH), 128.3 (CH), 127.7 (CH), 127.2 (CH), 127.1 (CH), 124.3 (CH), 123.9 (C_q), 120.0 (CH), 116.8 (CH), 61.5 (CH),

54.5 (CH_2), 39.3 (CH_2), 31.0 (CH_2). MS (ESI) *m/z* (relative intensity): 465 (54) $[M+Na]^+$, 443 (100) $[M+H]^+$. HR-MS (ESI) *m/z* calcd for $C_{25}H_{23}N_4O_2S$ $[M+H]^+$ 443.1536, found 443.1539.

(*E*)-2-[(1-Benzyl-1*H*-1,2,3-triazol-4-yl)methyl]-3-(2-hydroxy-5-methylstyryl)-3,4-dihydroisoquinolin-1(2*H*)-one (3ab) / *N*-[(1-Benzyl-1*H*-1,2,3-triazol-4-yl)methyl]-2-[2-(5-methylbenzofuran-2-yl)ethyl]benzamide (3'ab)

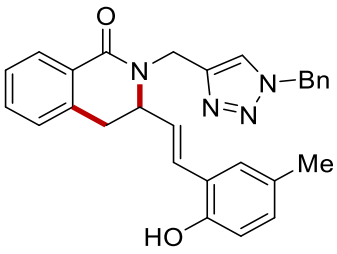

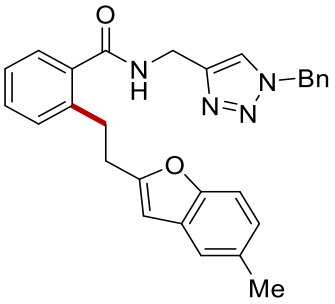

The representative procedure was followed using **1a** (58.5 mg, 0.2 mmol) and **2b** (94.8 mg, 0.6 mmol). Purification by a first column chromatography on silica gel (*n*-Hexane/EtOAc 1:1) afforded a mixture of the two products which were further purified by preparative thin layer chromatography (SiO_2, *n*-Hexane/acetone 7:3) to yield **3ab** (47.8 mg, 53%) as a white solid and **3'ab** (9.0 mg, 10%) as a colourless oil.

3ab: M.p.= 79-80 °C. ^{1}H-NMR (400 MHz, $CDCl_3$): δ = 8.54 (bs, 1H), 8.07 (dd, *J* = 7.7, 1.5 Hz, 1H), 7.71 (s, 1H), 7.44 (td, *J* = 7.4, 1.5 Hz, 1H), 7.39 – 7.34 (m, 4H), 7.27 (m, 2H), 7.16 (d, *J* = 7.4 Hz, 1H), 7.08 – 7.01 (m, 2H), 6.95 – 6.91 (m, 2H), 6.05 (dd, *J* = 15.7, 8.8 Hz, 1H), 5.58 – 5.42 (m, 2H), 5.14 (d, *J* = 14.9 Hz, 1H), 4.61 (ddd, *J* = 9.5, 6.0, 4.4 Hz, 1H), 4.49 (d, *J* = 14.8 Hz, 1H), 3.31 (dd, *J* = 15.9, 5.9 Hz, 1H), 2.94 (dd, *J* = 16.0, 4.2 Hz, 1H), 2.23 (s, 3H). ^{13}C-NMR (101 MHz, $CDCl_3$): δ = 164.2 (C_q), 152.3 (C_q), 144.8 (C_q), 136.4 (C_q), 134.2 (C_q), 132.1 (CH), 129.8 (CH), 129.7 (CH), 129.2 (CH), 129.0 (C_q), 128.9 (CH), 128.7 (C_q), 128.2 (CH), 127.9 (CH), 127.7 (CH), 127.5 (CH), 127.1 (2 x CH), 124.1 (CH), 123.4 (C_q), 116.5 (CH), 59.9 (CH), 54.4 (CH_2), 40.5 (CH_2), 34.2 (CH_2), 20.5 (CH_3). MS (ESI) *m/z* (relative intensity): 489 (20) $[M+K]^+$, 451 (100) $[M+H]^+$, 317 (28). HR-MS (ESI) *m/z* calcd for: $C_{28}H_{27}N_4O_2$ $[M+H]^+$ 451.2129, found 451.2131.

3'ab: M.p.= 124-126 °C. ^{1}H-NMR (400 MHz, $CDCl_3$): δ = 7.54 (s, 1H), 7.37 – 7.32 (m, 5H), 7.31 (d, *J* = 1.5 Hz, 1H), 7.26 – 7.19 (m, 5H), 7.03 (dd, *J* = 8.4, 1.8 Hz, 1H), 6.44 (bs, 1H), 6.24 (d, *J* = 1.0 Hz, 1H), 5.43 (s, 2H), 4.62 (d, *J* = 5.7 Hz, 2H), 3.18 (dd, *J* = 8.6, 6.8 Hz, 2H), 3.02 (dd, *J* = 8.7, 6.6 Hz, 2H), 2.43 (s, 3H). ^{13}C -NMR (101 MHz, $CDCl_3$): δ = 169.9 (C_q), 158.4 (C_q), 153.0

(C_q), 144.9 (C_q), 139.4 (C_q), 135.7 (C_q), 134.5 (C_q), 131.8 (C_q), 130.4 (CH), 130.3 (CH), 129.1 (CH), 129.0 (C_q), 128.8 (CH), 128.1 (CH), 126.9 (CH), 126.4 (CH), 124.4 (CH), 122.2 (CH), 120.2 (CH), 110.2 (CH), 102.3 (CH), 54.2 (CH_2), 35.3 (CH_2), 31.5 (CH_2), 30.4 (CH_2), 21.3 (CH_3). MS (ESI) *m/z* (relative intensity): 479 (64), 473 (87) $[M+Na]^+$, 451 (100) $[M+H]^+$, 317 (28). HR-MS (ESI) *m/z* calcd for: $C_{28}H_{27}N_4O_2$ $[M+H]^+$ 451.2129, found 451.2126.

(*E*)-2-[(1-Benzyl-1*H*-1,2,3-triazol-4-yl)methyl]-3-{2-[4-hydroxy-(1,1'-biphenyl)-3-yl]vinyl}-3,4-dihydroisoquinolin-1(2*H*)-one (3ac) / *N*-[(1-Benzyl-1*H*-1,2,3-triazol-4-yl)methyl]-2-[2-(5-phenylbenzofuran-2-yl)ethyl]benzamide (3'ac)

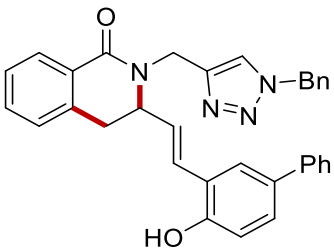

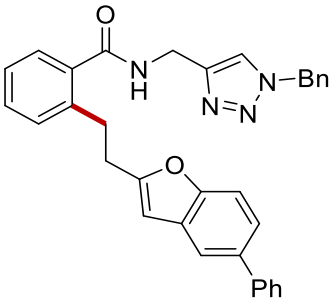

The representative procedure was followed using **1a** (58.5 mg, 0.2 mmol) and **2c** (132.2 mg, 0.6 mmol). Purification by a first column chromatography on silica gel (*n*-Hexane/EtOAc 1:1) afforded a mixture of the two products which were further purified by preparative thin layer chromatography (SiO_2, *n*-Hexane/acetone 7:3) to yield **3ac** (52.3 mg, 51%) as a white solid and **3'ac** (11.2 mg, 11%) as a colourless oil.

3ac: M.p.= 88-90 °C. ^{1}H-NMR (400 MHz, $CDCl_3$): δ = 9.51 (bs, 1H), 8.08 (dd, *J* = 7.7, 1.4 Hz, 1H), 7.75 (s, 1H), 7.55 – 7.51 (m, 2H), 7.46 – 7.40 (m, 4H), 7.40 – 7.34 (m, 6H), 7.32 – 7.29 (m, 1H), 7.27 (m, 2H), 7.19 (d, *J* = 16.2 Hz, 1H), 7.16 – 7.13 (m, 1H), 6.15 (dd, *J* = 15.8, 8.8 Hz, 1H), 5.59 – 5.44 (m, 2H), 5.20 (d, *J* = 14.9 Hz, 1H), 4.68 (ddd, *J* = 9.4, 6.0, 3.8 Hz, 1H), 4.50 (d, *J* = 14.9 Hz, 1H), 3.34 (dd, *J* = 15.9, 6.0 Hz, 1H), 2.96 (dd, *J* = 16.1, 3.9 Hz, 1H). ^{13}C-NMR (101 MHz, $CDCl_3$): δ = 164.3 (C_q), 154.4 (C_q), 144.8 (C_q), 141.0 (C_q), 136.3 (C_q), 134.1 (C_q), 133.1 (C_q), 132.2 (CH), 129.6 (CH), 129.2 (CH), 128.9 (CH), 128.7 (CH), 128.6 (C_q), 128.3 (CH), 128.0 (CH), 127.9 (CH), 127.7 (CH), 127.5 (CH), 127.2 (CH), 126.8 (CH), 126.6 (CH), 125.8 (CH), 124.2 (CH), 124.0 (C_q), 117.0 (CH), 60.0 (CH), 54.5 (CH_2), 40.5 (CH_2), 34.2 (CH_2). MS (ESI) *m/z* (relative intensity): 513 (100) $[M+H]^+$, 347 (24). HR-MS (ESI) *m/z* calcd for: $C_{33}H_{29}N_4O_2$ $[M+H]^+$ 513.2285, found 513.2289.

3'ac: ^{1}H-NMR (400 MHz, $CDCl_3$): δ = 7.68 – 7.60 (m, 3H), 7.53 (s, 1H), 7.49 – 7.44 (m, 5H), 7.40 – 7.31 (m, 5H), 7.24 (m, 2H), 7.21 (m, 2H), 6.49 (bs, 1H), 6.37 (s, 1H), 5.43 (s, 2H), 4.64 (d, *J* = 5.7 Hz, 2H), 3.23 (t, *J* = 7.7 Hz, 2H), 3.07 (t, *J* = 7.7 Hz, 2H). ^{13}C-NMR (101 MHz, $CDCl_3$): δ = 169.9 (C_q), 159.1 (C_q), 154.3 (C_q), 144.9 (C_q), 141.8 (C_q), 139.4 (C_q), 136.2 (C_q), 135.7 (C_q), 134.4 (C_q), 130.4 (CH), 130.3 (CH), 129.4 (C_q), 129.1 (CH), 128.8 (CH), 128.7 (CH), 128.0 (CH), 127.4 (CH), 127.0 (CH), 126.8 (CH), 126.4 (CH), 122.9 (CH), 122.1 (CH), 118.9 (CH), 110.9 (CH), 102.7 (CH), 54.2 (CH_2), 35.4 (CH_2), 31.5 (CH_2), 30.4 (CH_2). MS (ESI) *m/z* (relative intensity): 513 (33) $[M+H]^+$, 479 (100), 463 (43). HR-MS (ESI) *m/z* calcd for: $C_{33}H_{29}N_4O_2$ $[M+H]^+$ 513.2285, found 513.2288.

(*E*)-2-[(1-Benzyl-1*H*-1,2,3-triazol-4-yl)methyl]-3-(2-hydroxy-5-methoxystyryl)-3,4-dihydroisoquinolin-1(2*H*)-one (3ad) / *N*-[(1-Benzyl-1*H*-1,2,3-triazol-4-yl)methyl]-2-[2-(5-methoxybenzofuran-2-yl)ethyl]benzamide (3'ad)

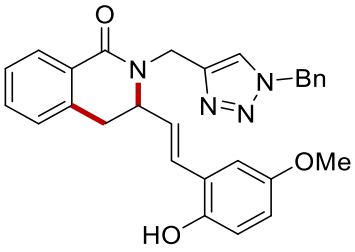

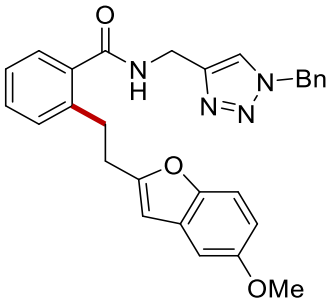

The representative procedure was followed using **1a** (58.5 mg, 0.2 mmol) and **2d** (104 mg, 0.6 mmol). Purification by a first column chromatography on silica gel (*n*-Hexane/EtOAc 1:1) afforded a mixture of the two products which were further purified by preparative thin layer chromatography (SiO_2, *n*-Hexane/acetone 6:4) to yield **3ad** (28.9 mg, 31%) as a white solid and **3'ad** (31.7 mg, 34%) as a colourless oil.

3ad: M.p.= 173-175 °C. ^{1}H-NMR (400 MHz, $CDCl_3$): δ = 8.06 (dd, *J* = 7.8, 1.4 Hz, 1H), 8.03 (bs, 1H), 7.70 (s, 1H), 7.44 (td, *J* = 7.4, 1.5 Hz, 1H), 7.37 (m, 4H), 7.26 (m, 2H), 7.17 (d, *J* = 7.4 Hz, 1H), 7.00 (d, *J* = 15.7 Hz, 1H), 6.96 – 6.92 (m, 1H), 6.73 (d, *J* = 7.0 Hz, 2H), 6.04 (dd, *J* = 15.8, 8.8 Hz, 1H), 5.54 – 5.44 (m, 2H), 5.08 (d, *J* = 14.8 Hz, 1H), 4.63 – 4.54 (m, 2H), 3.75 (s, 3H), 3.32 (dd, *J* = 15.9, 5.8 Hz, 1H), 2.96 (dd, *J* = 16.0, 4.8 Hz, 1H). ^{13}C-NMR (101 MHz, $CDCl_3$): δ = 164.2 (C_q), 153.2 (C_q), 148.6 (C_q), 144.8 (C_q), 136.3 (C_q), 134.2 (C_q), 132.2 (CH), 129.7 (CH), 129.2 (CH), 128.9 (CH), 128.7 (C_q), 128.2 (CH), 127.9 (CH), 127.7 (CH), 127.2 (CH), 124.4 (C_q), 124.1 (CH), 117.5 (CH), 115.7 (CH), 114.9 (CH), 112.0 (CH), 60.0 (CH), 55.9 (CH_3), 54.4 (CH_2),

40.5 (CH_2), 34.2 (CH_2). MS (ESI) *m/z* (relative intensity): 955 (47) $[2M+Na]^+$, 859 (22), 467 (100) $[M+H]^+$. HR-MS (ESI) *m/z* calcd for $C_{28}H_{27}N_4O_3$ $[M+H]^+$ 467.2078, found 467.2080.

3'ad: ^{1}H-NMR (400 MHz, $CDCl_3$): δ = 7.53 (s, 1H), 7.38 – 7.33 (m, 4H), 7.33 – 7.29 (m, 2H), 7.25 – 7.19 (m, 4H), 6.94 (d, *J* = 2.6 Hz, 1H), 6.82 (dd, *J* = 8.9, 2.6 Hz, 1H), 6.44 (bs, 1H), 6.25 (d, *J* = 1.0 Hz, 1H), 5.44 (s, 2H), 4.62 (d, *J* = 5.7 Hz, 2H), 3.84 (s, 3H), 3.18 (dd, *J* = 8.5, 6.8 Hz, 2H), 3.02 (dd, *J* = 8.5, 6.8 Hz, 2H). ^{13}C-NMR (101 MHz, $CDCl_3$): δ = 169.9 (C_q), 159.2 (C_q), 155.8 (C_q), 149.6 (C_q), 144.9 (C_q), 139.4 (C_q), 135.7 (C_q), 134.5 (C_q), 130.4 (CH), 130.3 (CH), 129.5 (C_q), 129.1 (CH), 128.8 (CH), 128.1 (CH), 126.9 (CH), 126.4 (CH), 122.1 (CH), 111.6 (CH), 111.1 (CH), 103.2 (CH), 102.7 (CH), 55.9 (CH_3), 54.2 (CH_2), 35.4 (CH_2), 31.5 (CH_2), 30.5 (CH_2). MS (ESI) *m/z* (relative intensity): 955 (14) $[2M+Na]^+$, 489 (100) $[M+Na]^+$, 467 (21) $[M+H]^+$. HR-MS (ESI) *m/z* calcd for $C_{28}H_{27}N_4O_3$ $[M+H]^+$ 467.2078, found 467.2075.

(*E*)-2-[(1-Benzyl-1*H*-1,2,3-triazol-4-yl)methyl]-3-(5-fluoro-2-hydroxystyryl)-3,4-dihydroisoquinolin-1(2*H*)-one (3ae) / *N*-[(1-Benzyl-1*H*-1,2,3-triazol-4-yl)methyl]-2-[2-(5-fluorobenzofuran-2-yl)ethyl]benzamide (3'ae)

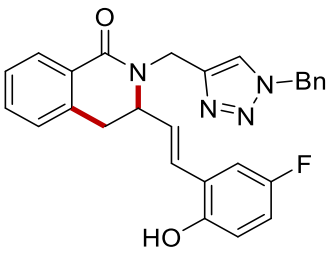

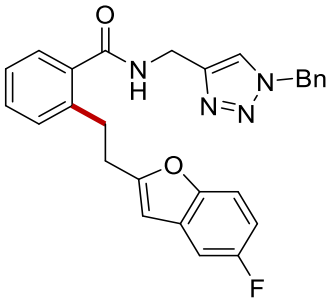

The representative procedure was followed using **1a** (58.4 mg, 0.2 mmol) and **2e** (97.2 mg, 0.6 mmol). Purification by a first column chromatography on silica gel (*n*-Hexane/EtOAc 1:1) afforded a mixture of the two products which were further purified by preparative thin layer chromatography (SiO_2, *n*-Hexane/acetone 7:3) to yield **3ae** (30.9 mg, 34%) as a white waxy solid and **3'ae** (12.7 mg, 14%) as a colourless oil.

3ae: ^{1}H-NMR (400 MHz, $CDCl_3$): δ = 9.27 (bs, 1H), 8.06 (dd, *J* = 7.8, 1.5 Hz, 1H), 7.73 (s, 1H), 7.45 (td, *J* = 7.5, 1.5 Hz, 1H), 7.41 – 7.34 (m, 4H), 7.28 – 7.24 (m, 2H), 7.16 (d, *J* = 7.4 Hz, 1H), 7.11 – 7.05 (m, 1H), 6.99 (dd, *J* = 8.9, 4.8 Hz, 1H), 6.90 (dd, *J* = 9.4, 3.1 Hz, 1H), 6.82 (ddd, *J* = 8.8, 7.9, 3.1 Hz, 1H), 6.03 (dd, *J* = 15.8, 8.9 Hz, 1H), 5.59 – 5.42 (m, 2H), 5.13 (d, *J* = 14.8 Hz, 1H), 4.61 (ddd, *J* = 9.3, 6.0, 3.7 Hz, 1H), 4.47 (d, *J* = 14.9 Hz, 1H), 3.32 (dd, *J* = 15.9, 6.0 Hz, 1H), 2.92 (dd, *J* = 16.0, 3.7 Hz, 1H). ^{13}C-NMR (101 MHz, $CDCl_3$): δ = 164.1 (C_q), 156.6 (d, $^1J_{C-}$

$_F$ = 237 Hz, C_q), 150.8 (d, $^4J_{C-F}$ = 2 Hz, C_q), 144.7 (C_q), 136.1 (C_q), 134.1 (C_q), 132.3 (CH), 129.2 (CH), 129.0 (CH), 128.7 (CH), 128.6 (C_q), 128.3 (CH), 128.1 (CH), 127.9 (CH), 127.7 (CH), 127.3 (CH), 124.7 (d, $^3J_{C-F}$ = 7 Hz, C_q), 124.3 (CH), 117.4 (d, $^3J_{C-F}$ = 8 Hz, CH) , 115.5 (d, $^2J_{C-F}$ = 23 Hz, CH) , 112.7 (d, $^2J_{C-F}$ = 23 Hz, CH), 59.8 (CH), 54.5 (CH_2), 40.6 (CH_2), 34.1 (CH_2). ^{19}F-NMR (565 MHz, $CDCl_3$): δ= -124.95 (td, *J* = 8.5, 4.4 Hz). MS (ESI) *m/z* (relative intensity): 931 (100) $[2M+Na]^+$, 477 (55) $[M+Na]^+$. HR-MS (ESI) *m/z* calcd for $C_{27}H_{24}FN_4O_2$ $[M+H]^+$ 455.1883, found 455.1886.

3'ae: ^{1}H-NMR (400 MHz, $CDCl_3$): δ = 7.54 (s, 1H), 7.40 – 7.30 (m, 6H), 7.26 – 7.19 (m, 4H), 7.12 (dd, *J* = 8.7, 2.7 Hz, 1H), 6.96 – 6.89 (m, 1H), 6.52 (bs, 1H), 6.29 (d, *J* = 1.0 Hz, 1H), 5.46 (s, 2H), 4.63 (d, *J* = 5.7 Hz, 2H), 3.19 (dd, *J* = 8.6, 6.8 Hz, 2H), 3.04 (dd, *J* = 8.7, 6.7 Hz, 2H). ^{13}C-NMR (101 MHz, $CDCl_3$): δ = 169.8 (C_q), 160.4 (C_q), 159.1 (d, $^1J_{C-F}$ = 237 Hz, C_q), 150.9 (C_q), 144.8 (C_q), 139.3 (C_q), 135.6 (C_q), 134.4 (C_q), 130.4 (CH), 130.3 (CH), 129.7 (d, $^3J_{C-F}$ = 11 Hz, C_q), 129.1 (CH), 128.8 (CH), 128.1 (CH), 127.0 (CH), 126.5 (CH), 122.1 (CH), 111.2 (d, $^3J_{C-F}$ = 10 Hz, CH), 110.7 (d, $^2J_{C-F}$ = 26 Hz, CH), 105.9 (d, $^2J_{C-F}$ = 25 Hz, CH), 102.8 (d, $^4J_{C-F}$ = 4 Hz, CH), 54.2 (CH_2), 35.4 (CH_2), 31.4 (CH_2), 30.4 (CH_2). ^{19}F-NMR (565 MHz, $CDCl_3$): δ= -121.57 – -121.62 (m). MS (ESI) *m/z* (relative intensity): 931 (75) $[2M+Na]^+$, 477 (100) $[M+Na]^+$. HR-MS (ESI) *m/z* calcd for $C_{27}H_{24}FN_4O_2$ $[M+H]^+$ 455.1883, found 455.1886.

(*E*)-2-[(1-Benzyl-1*H*-1,2,3-triazol-4-yl)methyl]-3-(5-chloro-2-hydroxystyryl)-3,4-dihydroisoquinolin-1(2*H*)-one (3af)

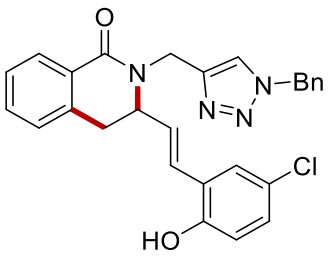

The representative procedure was followed using **1a** (58.5 mg, 0.2 mmol) and **2f** (106.8 mg, 0.6 mmol). Purification by column chromatography on silica gel (*n*-Hexane/EtOAc 1:1) yielded **3af** (47.1 mg, 50%) as a white waxy solid. ^{1}H-NMR (400 MHz, $CDCl_3$): δ = 8.80 (s, 1H), 8.06 (dd, *J* = 7.8, 1.4 Hz, 1H), 7.73 (s, 1H), 7.47 (td, *J* = 7.4, 1.5 Hz, 1H), 7.40 – 7.35 (m, 4H), 7.27 (m, 2H), 7.19 (d, *J* = 7.4 Hz, 1H), 7.14 (d, *J* = 2.6 Hz, 1H), 7.11 (dd, *J* = 8.5, 2.6 Hz, 1H), 6.97 (d, *J* = 2.8 Hz, 1H), 6.94 (d, *J* = 4.4 Hz, 1H), 6.01 (dd, *J* = 15.8, 8.9 Hz, 1H), 5.50 (d, *J* = 3.3 Hz, 2H), 5.00 (d, *J* = 14.8 Hz, 1H), 4.66 (d, *J* = 14.8 Hz, 1H), 4.53 (dt, *J* = 9.0, 5.6 Hz, 1H), 3.32 (dd, *J* = 15.9, 5.6 Hz, 1H), 3.00 (dd, *J* = 16.0, 5.6 Hz, 1H). ^{13}C-NMR (101 MHz, $CDCl_3$): δ = 164.3 (C_q), 153.3 (C_q), 144.5 (C_q), 136.2 (C_q), 134.1 (C_q), 132.3 (CH), 129.5 (CH), 129.4 (CH), 129.2 (2 x CH), 128.9 (CH), 128.6 (C_q), 128.3 (CH), 128.0 (CH), 127.6 (CH), 127.3 (CH), 126.8 (CH), 125.6 (C_q), 124.8 (C_q), 124.4 (CH), 118.3 (CH), 60.1 (CH), 54.5 (CH_2), 40.5 (CH_2), 34.1 (CH_2). MS

(ESI) *m/z* (relative intensity): 963 (100) $[2M+Na]^+$, 571 (26), 493 (92) $[M+Na]^+$, 471 (15) $[M+H]^+$. HR-MS (ESI) *m/z* calcd for $C_{27}H_{24}ClN_4O_2$ $[M+H]^+$ 471.1582, found 471.1585.

(*E*)-2-[(1-Benzyl-1*H*-1,2,3-triazol-4-yl)methyl]-3-(5-bromo-2-hydroxystyryl)-3,4-dihydroisoquinolin-1(2*H*)-one (3ag)

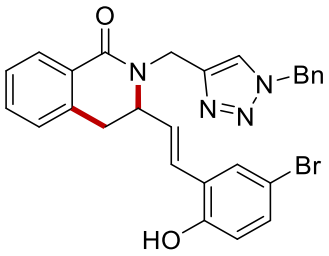

The representative procedure was followed using **1a** (58.5 mg, 0.2 mmol) and **2g** (133.7 mg, 0.6 mmol). Purification by column chromatography on silica gel (*n*-Hexane/EtOAc 1:1) yielded **3ag** (53.5 mg, 52%) as a white solid. M.p.= 96-98 °C. ^{1}H-NMR (400 MHz, $CDCl_3$): δ = 9.59 (bs, 1H), 8.07 (dd, *J* = 7.7, 1.5 Hz, 1H), 7.74 (s, 1H), 7.45 (dd, *J* = 7.5, 1.4 Hz, 1H), 7.42 – 7.34 (m, 4H), 7.29 (d, *J* = 3.4 Hz, 3H), 7.22 (dd, *J* = 8.6, 2.4 Hz, 1H), 7.17 (d, *J* = 7.4 Hz, 1H), 7.08 – 7.00 (m, 1H), 6.96 (d, *J* = 8.6 Hz, 1H), 6.02 (dd, *J* = 15.8, 8.9 Hz, 1H), 5.51 (q, *J* = 14.8 Hz, 2H), 5.09 (d, *J* = 15.1 Hz, 1H), 4.58 (dt, *J* = 9.8, 5.0 Hz, 1H), 4.55 – 4.46 (m, 1H), 3.32 (dd, J = 15.9, 6.0 Hz, 1H), 2.94 (dd, J = 15.9, 4.0 Hz, 1H). ^{13}C-NMR (101 MHz, $CDCl_3$): δ = 164.2 (C_q), 153.9 (C_q), 144.6 (C_q), 136.1 (C_q), 134.0 (C_q), 132.3 (CH), 131.8 (CH), 129.5 (CH), 129.2 (2 x CH), 129.0 (CH), 128.6 (C_q), 128.3 (2 x CH), 127.9 (CH), 127.7 (CH), 127.3 (CH), 126.0 (C_q), 124.4 (CH), 118.5 (CH), 111.8 (C_q), 60.0 (CH), 54.6 (CH_2), 40.5 (CH_2), 34.1 (CH_2). MS (ESI) *m/z* (relative intensity): 1053 (65) $[2M+Na]^+$, 537 (57) $[M+Na]^+$, 515 (100) $[M+H]^+$. HR-MS (ESI) *m/z* calcd for $C_{27}H_{24}BrN_4O_2$ $[M+H]^+$ 515.1077, found 515.1079.

Methyl-(*E*)-3-{2-{2-[(1-benzyl-1*H*-1,2,3-triazol-4-yl)methyl]-1-oxo-1,2,3,4-tetrahydroisoquinolin-3-yl}vinyl}-4-hydroxybenzoate (3ah)

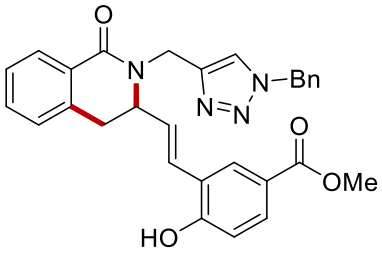

The representative procedure was followed using **1a** (58.5 mg, 0.2 mmol) and **2h** (121.3 mg, 0.6 mmol). Purification by column chromatography on silica gel (*n*-Hexane/EtOAc 1:1) yielded **3ah** (51.4 mg, 52%) as a pale-yellow solid. M.p.= 101-102 °C. ^{1}H-NMR (400 MHz, $CDCl_3$): δ = 10.2 (bs, 1H), 8.07 (dd, *J* = 7.7, 1.5 Hz, 1H), 7.91 (d, *J* = 2.2 Hz, 1H), 7.88 – 7.82 (m, 1H), 7.76 (d, *J* = 2.5 Hz, 1H), 7.49 – 7.43 (m, 1H), 7.41 – 7.35 (m, 4H), 7.31 – 7.29 (m, 2H), 7.18 (d, *J* = 7.4 Hz, 1H), 7.12 – 7.04 (m, 2H), 6.12 (dd, *J* = 15.6, 9.0 Hz, 1H), 5.52 (q, *J* = 14.8 Hz, 2H), 5.15 – 5.06 (m, 1H), 4.64 – 4.48 (m, 2H), 3.88 (d, *J* = 1.5 Hz, 3H), 3.32 (dd, *J* = 16.0, 5.8 Hz, 1H), 2.99 (d, *J* = 16.1 Hz, 1H). ^{13}C-NMR (101 MHz, $CDCl_3$): δ = 167.0 (C_q), 164.3 (C_q),

159.1 (C_q), 144.6 (C_q), 136.2 (C_q), 134.0 (C_q), 132.3 (CH), 131.0 (CH), 129.4 (CH), 129.3 (CH), 129.2 (CH), 129.0 (CH), 128.8 (CH), 128.6 (C_q), 128.3 (CH), 128.0 (CH), 127.7 (CH), 127.3 (CH), 124.5 (CH), 123.9 (C_q), 121.7 (C_q), 116.5 (CH), 60.1 (CH), 54.6 (CH_2), 51.9 (CH_3), 40.4 (CH_2), 34.1 (CH_2). MS (ESI) *m/z* (relative intensity): 1011 (11) $[2M+Na]^+$, 762 (21), 517 (21) $[M+Na]^+$, 495 (100) $[M+H]^+$. HR-MS (ESI) *m/z* calcd for $C_{29}H_{27}N_4O_4$ $[M+H]^+$ 495.2027, found 495.2023.

(*E*)-2-[(1-Benzyl-1*H*-1,2,3-triazol-4-yl)methyl]-3-(2-hydroxy-4-methoxystyryl)-3,4-dihydroisoquinolin-1(2*H*)-one (3ai)

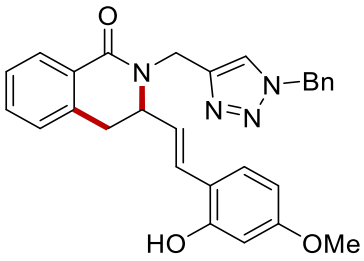

The representative procedure was followed using **1a** (58.5 mg, 0.2 mmol) and **2i** (104 mg, 0.6 mmol). Purification by column chromatography on silica gel (*n*-Hexane/EtOAc 1:1) yielded **3ai** (53.2 mg, 57%) as a white solid. M.p. = 188-190 °C. ^{1}H-NMR (400 MHz, $CDCl_3$): δ = 9.35 (bs, 1H), 8.06 (dd, *J* = 7.7, 1.4 Hz, 1H), 7.74 (s, 1H), 7.45 – 7.40 (m, 1H), 7.39 – 7.32 (m, 4H), 7.27 (dd, *J* = 7.1, 3.2 Hz, 2H), 7.15 (dd, *J* = 8.0, 4.6 Hz, 2H), 7.06 (d, *J* = 15.7 Hz, 1H), 6.69 (d, *J* = 2.5 Hz, 1H), 6.39 (dd, *J* = 8.6, 2.5 Hz, 1H), 5.96 (dd, *J* = 15.8, 9.0 Hz, 1H), 5.57 – 5.42 (m, 2H), 5.14 (d, *J* = 14.8 Hz, 1H), 4.60 (ddd, *J* = 9.5, 5.9, 4.1 Hz, 1H), 4.47 (d, *J* = 14.8 Hz, 1H), 3.74 (s, 3H), 3.30 (dd, *J* = 15.9, 5.9 Hz, 1H), 2.93 (dd, *J* = 16.0, 4.1 Hz, 1H). ^{13}C-NMR (101 MHz, $CDCl_3$): δ = 164.2 (C_q), 160.7 (C_q), 155.9 (C_q), 144.9 (C_q), 136.5 (C_q), 134.2 (C_q), 132.1 (CH), 129.2 (2 x CH), 128.9 (CH), 128.7 (C_q), 128.2 (CH), 127.8 (2 x CH), 127.7 (CH), 127.1 (CH), 124.9 (CH), 124.2 (CH), 116.6 (C_q), 106.3 (CH), 101.9 (CH), 60.2 (CH), 55.3 (CH_3), 54.5 (CH_2), 40.4 (CH_2), 34.4 (CH_2). MS (ESI) *m/z* (relative intensity): 489 (61) $[M+Na]^+$, 467 (100) $[M+H]^+$, 316 (62). HR-MS (ESI) *m/z* calcd for $C_{28}H_{27}N_4O_3$ $[M+H]^+$ 467.2078, found 467.2082.

(*E*)-2-[(1-Benzyl-1*H*-1,2,3-triazol-4-yl)methyl]-3-(2-hydroxy-3-methoxystyryl)-3,4-dihydroisoquinolin-1(2*H*)-one (3aj)

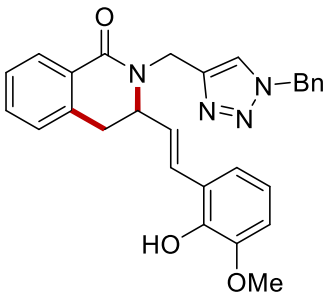

The representative procedure was followed using **1a** (58.4 mg, 0.2 mmol) and **2j** (104.4 mg, 0.6 mmol). Purification by column chromatography on silica gel (*n*-Hexane/EtOAc 1:1) yielded **3aj** (20.5 mg, 22%) as a yellow waxy solid ^{1}H-NMR (400 MHz, $CDCl_3$): δ = 8.07 (d, *J* = 1.4 Hz, 1H), 7.61 (s, 1H), 7.42 (td, *J* = 7.4, 1.5 Hz, 1H), 7.37 – 7.33 (m, 3H), 7.27 – 7.24 (m, 2H), 7.15 (d, *J* = 7.4 Hz, 1H), 6.89 – 6.82 (m, 2H), 6.77 – 6.73 (m, 2H), 6.19 (dd, *J* = 15.9, 8.1 Hz, 1H), 5.97 (bs, 1H), 5.56 – 5.42 (m, 3H), 5.32 (d, *J* = 14.9 Hz, 1H), 4.66 – 4.58 (m, 1H), 4.32 (d, *J* = 14.9 Hz, 1H), 3.88 (s, 3H), 3.38 (dd, *J* = 15.9, 6.3 Hz, 1H), 2.93 (dd, *J* = 15.9, 2.7 Hz, 1H). ^{13}C-NMR (101 MHz, $CDCl_3$): δ = 164.0 (C_q), 146.7 (C_q), 145.3 (C_q), 143.5 (C_q), 136.2 (C_q), 134.5 (C_q), 132.0 (CH), 129.1 (CH), 128.9 (C_q), 128.7 (CH), 128.2 (CH), 127.9 (CH), 127.7 (CH), 127.5 (CH), 127.2 (CH), 127.1 (CH), 123.1 (CH), 122.4 (C_q), 119.4 (CH), 119.3 (CH), 109.8 (CH), 59.0 (CH), 56.1 (CH_3), 54.2 (CH_2), 40.7 (CH_2), 34.1 (CH_2). MS (ESI) *m/z* (relative intensity): 955 (100) $[2M+Na]^+$, 489 (38) $[M+Na]^+$. HR-MS (ESI) *m/z* calcd for $C_{28}H_{27}N_4O_3$ $[M+H]^+$ 467.2083, found 467.2080.

(*E*)-2-[(1-Benzyl-1*H*-1,2,3-triazol-4-yl)methyl]-3-(3,5-dichloro-2-hydroxystyryl)-3,4-dihydroisoquinolin-1(2*H*)-one (3ak)

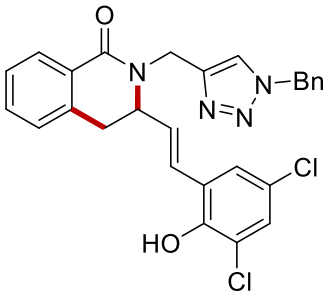

The representative procedure was followed using **1a** (58.5 mg, 0.2 mmol) and **2k** (127.8 mg, 0.6 mmol). Purification by column chromatography on silica gel (*n*-Hexane/EtOAc 1:1) yielded **3ak** (44.3 mg, 44%) as a white waxy solid. ^{1}H-NMR (400 MHz, $CDCl_3$): δ = 8.08 (dd, *J* = 7.7, 1.5 Hz, 1H), 7.64 (s, 1H), 7.45 (td, *J* = 7.4, 1.5 Hz, 1H), 7.37 (m, 4H), 7.27 (m, 2H), 7.23 (d, *J* = 2.4 Hz, 1H), 7.17 (d, *J* = 7.4 Hz, 1H), 7.11 (d, *J* = 2.5 Hz, 1H), 6.89 (bs, 1H), 6.81 (d, *J* = 15.8 Hz, 1H), 6.12 (dd, *J* = 15.9, 8.2 Hz, 1H), 5.49 (q, *J* = 14.8 Hz, 2H), 5.22 (d, *J* = 14.9 Hz, 1H), 4.63 – 4.56 (m, 1H), 4.42 (d, *J* = 14.9 Hz, 1H), 3.36 (dd, *J* = 15.9, 6.0 Hz, 1H), 2.95 (dd, *J* = 16.0, 4.1 Hz, 1H). ^{13}C-NMR (101 MHz, $CDCl_3$): δ = 164.1 (C_q), 148.1 (C_q), 144.8 (C_q), 135.9 (C_q), 134.3 (C_q), 132.2 (CH), 130.4 (CH), 129.2 (CH), 128.8 (CH), 128.7 (C_q), 128.2 (2 x CH), 128.0 (CH), 127.9 (CH), 127.6 (CH), 127.3 (CH), 126.0 (C_q), 125.8 (CH), 125.1 (C_q), 123.5 (CH), 121.5 (C_q), 59.0 (CH), 54.3 (CH_2), 40.5 (CH_2), 33.9 (CH_2). MS (ESI) *m/z* (relative intensity): 528 (30) $[M+Na]^+$,

505 (100) $[M+H]^+$. HR-MS (ESI) *m/z* calcd for $C_{27}H_{23}Cl_2N_4O_2$ $[M+H]^+$ 505.1193, found 505.1196.

_N_-[(1-Benzyl-1_H_-1,2,3-triazol-4-yl)methyl]-2-{2-[naphtho(2,1-b)furan-2-yl]ethyl}benzamide (3'al)

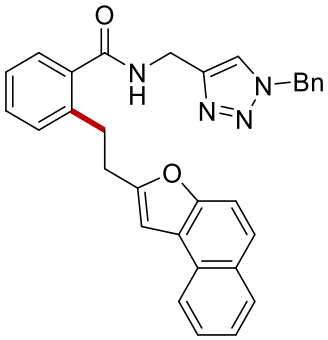

The representative procedure was followed using **1a** (58.5 mg, 0.2 mmol) and **2l** (116.4 mg, 0.6 mmol). Purification by column chromatography on silica gel (*n*-Hexane/EtOAc 1:1) yielded **3'al** (54.3 mg, 56%) as a yellow waxy solid. ^{1}H-NMR (400 MHz, $CDCl_3$): δ = 8.07 (d, *J* = 8.2 Hz, 1H), 7.94 (d, *J* = 8.2 Hz, 1H), 7.67 (d, *J* = 8.9 Hz, 1H), 7.61 (d, *J* = 9.0 Hz, 1H), 7.59 – 7.55 (m, 1H), 7.50 – 7.45 (m, 2H), 7.39 – 7.33 (m, 2H), 7.33 – 7.29 (m, 3H), 7.27 – 7.22 (m, 2H), 7.16 (m, 2H), 6.84 (s, 1H), 6.42 (bs, 1H), 5.38 (s, 2H), 4.62 (d, *J* = 5.7 Hz, 2H), 3.31 – 3.23 (m, 2H), 3.15 (t, *J* = 7.7 Hz, 2H). ^{13}C-NMR (101 MHz, $CDCl_3$): δ = 169.9 (C_q), 157.7 (C_q), 151.9 (C_q), 144.9 (C_q), 139.4 (C_q), 135.7 (C_q), 134.4 (C_q), 130.4 (CH), 130.3 (CH), 130.2 (C_q), 129.1 (CH), 128.8 (CH), 128.7 (CH), 128.0 (CH), 127.5 (C_q), 127.0 (CH), 126.4 (CH), 126.0 (CH), 124.2 (CH), 124.0 (CH), 123.9 (C_q), 123.5 (CH), 122.1 (CH), 112.2 (CH), 101.7 (CH), 54.1 (CH_2), 35.4 (CH_2), 31.8 (CH_2), 30.6 (CH_2). MS (ESI) *m/z* (relative intensity): 509 (30) $[M+Na]^+$, 487(100) $[M+H]^+$. HR-MS (ESI) *m/z* calcd for $C_{31}H_{27}N_4O_2$ $[M+H]^+$ 487.2129, found 487.2133.

(_E_)-2-[(1-Benzyl-1_H_-1,2,3-triazol-4-yl)methyl]-3-[5-(*tert*-butyl)-2-hydroxystyryl]-3,4-dihydroisoquinolin-1(2_H_)-one (3am)

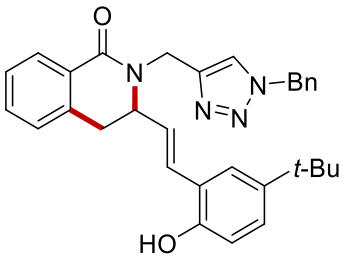

The representative procedure was followed using **1a** (58.5 mg, 0.2 mmol) and **2m** (120.0 mg, 0.6 mmol). Purification by column chromatography on silica gel (*n*-Hexane/EtOAc 1:1) yielded **3am** as a white waxy solid (26.6 mg, 27%). ^{1}H-NMR (400 MHz, $CDCl_3$): δ = 8.32 (bs, 1H), 8.07 (dd, *J* = 7.8, 1.4 Hz, 1H), 7.71 (s, 1H), 7.44 (td, *J* = 7.5, 1.5 Hz, 1H), 7.40 – 7.33 (m, 4H), 7.29 – 7.27 (m, 2H), 7.22 – 7.14 (m, 3H), 7.00 (d, *J* = 15.9 Hz, 1H), 6.96 – 6.91 (m, 1H), 6.10 (dd, *J* = 15.8, 8.6 Hz, 1H), 5.57 – 5.43 (m, 2H), 5.14 (d, *J* = 14.8 Hz, 1H), 4.59 (dt, *J* = 8.6, 5.4 Hz, 1H), 4.54 (d, *J* = 14.8 Hz, 1H), 3.30 (dd, *J* = 15.9, 5.8 Hz, 1H), 2.99 (dd, *J* = 16.0, 5.3 Hz, 1H), 1.29 (s, 9H). ^{13}C-NMR (101 MHz, $CDCl_3$): δ = 164.4 (C_q), 152.3 (C_q), 144.8 (C_q), 142.7 (C_q), 136.4 (C_q), 134.2 (C_q), 132.1 (CH), 130.8 (CH), 129.2 (CH), 128.9 (CH), 128.7 (C_q), 128.3 (CH), 127.9

(2 x CH), 127.6 (CH), 127.1 (CH), 126.4 (CH), 124.2 (CH), 124.1 (CH), 123.0 (C_q), 116.4 (CH), 60.0 (CH), 54.4 (CH_2), 40.3 (CH_2), 34.2 (CH_2), 34.1 (C_q), 31.6 (CH_3). MS (ESI) *m/z* (relative intensity): 515 (45) $[M+Na]^+$, 493 (100) $[M+H]^+$. HR-MS (ESI) *m/z* calcd for $C_{31}H_{33}N_4O_2$ $[M+H]^+$ 493.2598, found 493.2595.

_N_-[(1-Benzyl-1_H_-1,2,3-triazol-4-yl)methyl]-2-[2-(3-methylbenzofuran-2-yl)ethyl]benzamide (3'an)

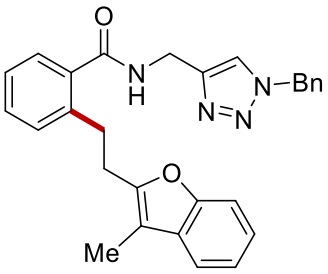

The representative procedure was followed using **1a** (58.5 mg, 0.2 mmol) and **2n** (94.9 mg, 0.6 mmol). Purification by column chromatography on silica gel (*n*-Hexane/EtOAc 1:1) yielded **3'an** (24.6 mg, 27%) as a viscous oil. ^{1}H-NMR (400 MHz, $CDCl_3$): δ = 7.53 (s, 1H), 7.41 – 7.30 (m, 6H), 7.30 – 7.26 (m, 1H), 7.25 – 7.21 (m, 3H), 7.19 (m, 2H), 7.13 (d, *J* = 7.6 Hz, 1H), 6.37 (bs, 1H), 5.45 (s, 2H), 4.54 (d, *J* = 5.7 Hz, 2H), 3.15 (t, *J* = 7.3 Hz, 2H), 3.01 (t, *J* = 7.4 Hz, 2H), 1.89 (s, 3H). ^{13}C-NMR (101 MHz, $CDCl_3$): δ = 169.9 (C_q), 153.9 (C_q), 153.1 (C_q), 145.0 (C_q), 139.6 (C_q), 135.8 (C_q), 134.5 (C_q), 130.6 (CH), 130.3 (C_q), 130.2 (CH), 129.1 (CH), 128.8 (CH), 128.1 (CH), 126.9 (CH), 126.3 (CH), 123.2 (CH), 122.2 (CH), 122.0 (CH), 118.8 (CH), 110.6 (CH), 110.6 (C_q), 54.2 (CH_2), 35.3 (CH_2), 32.0 (CH_2), 28.5 (CH_2), 7.5 (CH_3). MS (ESI) *m/z* (relative intensity): 473 (100) $[M+Na]^+$, 451 (47) $[M+H]^+$. HR-MS (ESI) *m/z* calcd for $C_{28}H_{27}N_4O_2$ $[M+H]^+$ 451.2129, found 451.2127.

2-[2-(Benzo[*b*]thiophen-2-yl)ethyl]-_N_-[(1-benzyl-1_H_-1,2,3-triazol-4-yl)methyl]benzamide (3'ao)

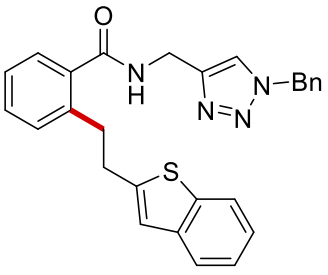

The representative procedure was followed using **1a** (58.5 mg, 0.20 mmol) and **2o** (96.1 mg, 0.60 mmol). Purification by column chromatography on silica gel (*n*-Hexane/EtOAc 1:1) yielded **3'ao** (36.2 mg, 40%) as a white solid. M.p. = 94-96 °C. ^{1}H-NMR (400 MHz, $CDCl_3$): δ = 7.76 (d, *J* = 8.2 Hz, 1H), 7.66 (d, *J* = 8.0 Hz, 1H), 7.51 (s, 1H), 7.36 – 7.31 (m, 6H), 7.27 – 7.23 (m, 3H), 7.22 – 7.17 (m, 2H), 6.93 (s, 1H), 6.40 (bs, 1H), 5.39 (s, 2H), 4.60 (d, *J* = 5.8 Hz, 2H), 3.22 – 3.12 (m, 4H). ^{13}C-NMR (101 MHz, $CDCl_3$): δ = 170.0 (C_q), 145.3 (C_q), 144.9 (C_q), 140.1 (C_q), 139.4 (C_q), 139.3 (C_q), 135.8 (C_q), 134.4 (C_q), 130.4 (CH), 130.3 (CH), 129.1 (CH), 128.8 (CH), 128.1 (CH), 127.0 (CH), 126.4 (CH), 125.8 (CH), 124.1 (CH), 123.6 (CH), 122.8 (CH), 122.1 (CH), 121.0

(CH), 54.2 (CH_2), 35.3 (CH_2), 34.8 (CH_2), 32.6 (CH_2). (ESI) *m/z* (relative intensity): 927 (43) $[2M+Na]^+$, 475 (100) $[M+H]^+$. HR-MS (ESI) *m/z* calcd for $C_{27}H_{24}N_4NaOS$ $[M+Na]^+$ 475.1743, found 475.1748.

_N_-[(1-Benzyl-1_H_-1,2,3-triazol-4-yl)methyl]-2-(2-(1-methyl-1_H_-indol-2-yl)ethyl)benzamide (3'ap)

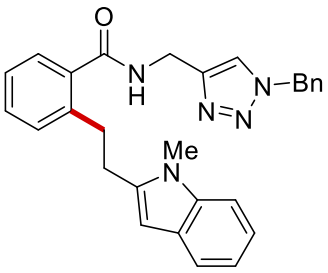

The representative procedure was followed using **1a** (58.5 mg, 0.2 mmol) and **2p** (94.3 mg, 0.6 mmol). Purification by column chromatography on silica gel (*n*-Hexane/EtOAc 1:1) yielded **3'ap** (25.2 mg, 28%) as a colourless oil. ^{1}H-NMR (400 MHz, $CDCl_3$): δ = 7.53 (d, *J* = 7.8 Hz, 1H), 7.41 (s, 1H), 7.40 – 7.32 (m, 5H), 7.28 – 7.22 (m, 3H), 7.19 – 7.14 (m, 3H), 7.10 – 7.05 (m, 1H), 6.28 (bs, 1H), 6.18 (s, 1H), 5.30 (s, 2H), 4.46 (d, *J* = 5.7 Hz, 2H), 3.57 (s, 3H), 3.15 (dd, *J* = 8.8, 6.7 Hz, 2H), 3.01 (dd, *J* = 8.8, 6.7 Hz, 2H). ^{13}C-NMR (101 MHz, $CDCl_3$): δ = 170.0 (C_q), 144.9 (C_q), 140.4 (C_q), 139.6 (C_q), 137.3 (C_q), 136.1 (C_q), 134.5 (C_q), 130.5 (CH), 130.3 (CH), 129.1 (CH), 128.8 (CH), 128.0 (CH), 127.8 (C_q), 126.9 (CH), 126.4 (CH), 122.2 (CH), 120.7 (CH), 119.8 (CH), 119.3 (CH), 108.9 (CH), 99.0 (CH), 54.0 (CH_2), 35.3 (CH_2), 32.7 (CH_2), 29.3 (CH_3), 29.2 (CH_2). (ESI) *m/z* (relative intensity): 472 (56) $[M+Na]^+$, 450 (100) $[M+H]^+$. HR-MS (ESI) *m/z* calcd for $C_{28}H_{28}N_5O$ $[M+H]^+$ 450.2288, found 450.2285.

2-(2-(Benzofuran-7-yl)ethyl)-_N_-[(1-benzyl-1_H_-1,2,3-triazol-4-yl)methyl]benzamide (3'ar)

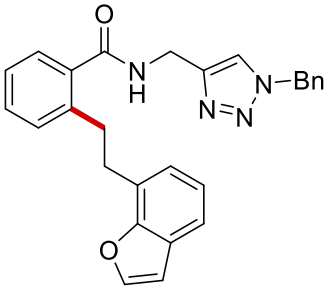

The representative procedure was followed using **1a** (58.5 mg, 0.2 mmol) and **2r** (86.5 mg, 0.6 mmol). Purification by column chromatography on silica gel (*n*-Hexane/EtOAc 1:1) yielded **3'ar** (26.4 mg, 31%) as a colourless oil. ^{1}H-NMR (400 MHz, $CDCl_3$): δ = 7.59 (d, *J* = 2.2 Hz, 1H), 7.52 (s, 1H), 7.43 (dd, *J* = 7.7, 1.2 Hz, 1H), 7.37 – 7.29 (m, 5H), 7.24 (dd, *J* = 7.7, 1.5 Hz, 1H), 7.22 – 7.16 (m, 3H), 7.11 (t, *J* = 7.5 Hz, 1H), 6.96 (dd, *J* = 6.9, 1.4 Hz, 1H), 6.75 (d, *J* = 2.2 Hz, 1H), 6.31 (t, *J* = 5.8 Hz, 1H), 5.40 (s, 2H), 4.55 (d, *J* = 5.8 Hz, 2H), 3.20 – 3.14 (m, 4H). ^{13}C-NMR (101 MHz, $CDCl_3$): δ = 170.1 (C_q), 145.1 (C_q), 144.7 (CH), 139.9 (C_q), 136.0 (C_q), 134.5 (C_q), 130.4 (CH), 130.0 (CH), 129.1 (CH), 128.8 (CH), 128.1 (CH), 127.1 (C_q), 126.8 (CH), 126.1 (CH), 125.3 (C_q), 124.4 (CH), 122.8 (CH), 122.2 (CH), 119.1 (CH), 117.8 (C_q), 106.7 (CH), 54.2

(CH_2), 35.4 (CH_2), 33.4 (CH_2), 31.9 (CH_2). (ESI) *m/z* (relative intensity): 459 (100) $[M+Na]^+$, 434 (71) $[M+H]^+$. HR-MS (ESI) *m/z* calcd for $C_{27}H_{25}N_4O_2$ $[M+H]^+$ 437.1972, found 437.1976.

(*E*)-2-[(1-Benzyl-1*H*-1,2,3-triazol-4-yl)methyl]-3-(4-oxopent-1-en-1-yl)-3,4-dihydroisoquinolin-1(2*H*)-one (7b)

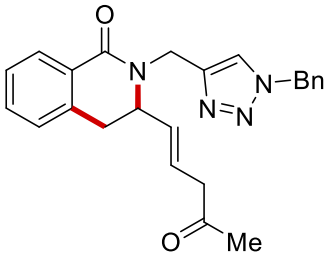

The representative procedure was followed using **1a** (58.5 mg, 0.2 mmol) and **6** (94.9 mg, 0.6 mmol). Purification by column chromatography on silica gel (*n*-Hexane/EtOAc 1:1) yielded **7b** (35.2 mg, 44%) as a viscous oil. ^{1}H-NMR (400 MHz, $CDCl_3$): δ = 8.04 (dd, *J* = 7.7, 1.5 Hz, 1H), 7.60 (s, 1H), 7.45 – 7.32 (m, 5H), 7.29 – 7.26 (m, 2H), 7.13 (d, *J* = 7.4 Hz, 1H), 5.75 (m, 1H), 5.59 – 5.42 (m, 3H), 5.26 (d, *J* = 14.9 Hz, 1H), 4.47 (td, *J* = 6.9, 2.5 Hz, 1H), 4.25 (d, *J* = 14.9 Hz, 1H), 3.30 (dd, *J* = 15.8, 6.3 Hz, 1H), 3.05 (ddd, *J* = 7.5, 4.1, 1.3 Hz, 2H), 2.81 (dd, *J* = 15.9, 2.6 Hz, 1H), 2.02 (s, 3H). ^{13}C-NMR (101 MHz, $CDCl_3$): δ = 206.0 (C_q), 163.9 (C_q), 145.1 (C_q), 135.9 (C_q), 134.5 (C_q), 132.1 (CH), 131.5 (CH), 129.1 (CH), 128.9 (C_q), 128.8 (CH), 128.2 (CH), 127.8 (CH), 127.7 (CH), 127.1 (CH), 125.6 (CH), 123.0 (CH), 57.8 (CH), 54.2 (CH_2), 46.7 (CH_2), 40.6 (CH_2), 33.7 (CH_2), 29.4 (CH_3). MS (ESI) *m/z* (relative intensity): 439 (11) $[M+K]^+$, 423 (36) $[M+Na]^+$, 401 (100) $[M+H]^+$. HR-MS (ESI) *m/z* calcd for C24H25N4O2 $[M+H]^+$ 401.1972, found 401.1975.

3.4.7 Key mechanistic findings

Intermolecular KIE

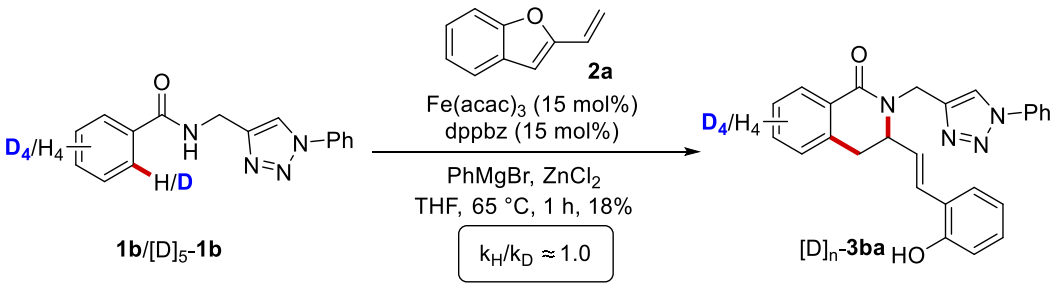

To a stirred solution of $Fe(acac)_3$ (10.6 mg, 0.03 mmol), dppbz (11.9 mg, 0.03 mmol), zinc chloride (1.0 M in THF, 400 µL, 0.4 mmol), **1b** (27.8 mg, 0.10 mmol) and $[D]_5$-**1b** (28.3 mg, 0.10 mmol) under N_2 atmosphere, PhMgBr (1.0 M in THF, 600 µL, 0.60 mmol) was added in a single portion. Then, 2-vinylbenzofuran **2a** (81 µL, 0.60 mmol) was added and the mixture was placed in a pre-heated oil bath at 65 °C. After stirring for 1 h, the reaction was cooled to room temperature and quenched by the addition of an aqueous solution of HCl (1.0 M, 5 mL). The reaction was extracted with CH_2Cl_2 (3x10 mL), and the combined organic extracts were dried over Na_2SO_4, filtered and concentrated. The crude product was purified by column chromatography (*n*-Hexane/EtOAc). The mixture was analysed by 400 MHz ^{1}H-NMR spectroscopy to determine the ratio of **3ba**/$[D]_4$-**3ba** [(0.51/0.49) = 1.04].

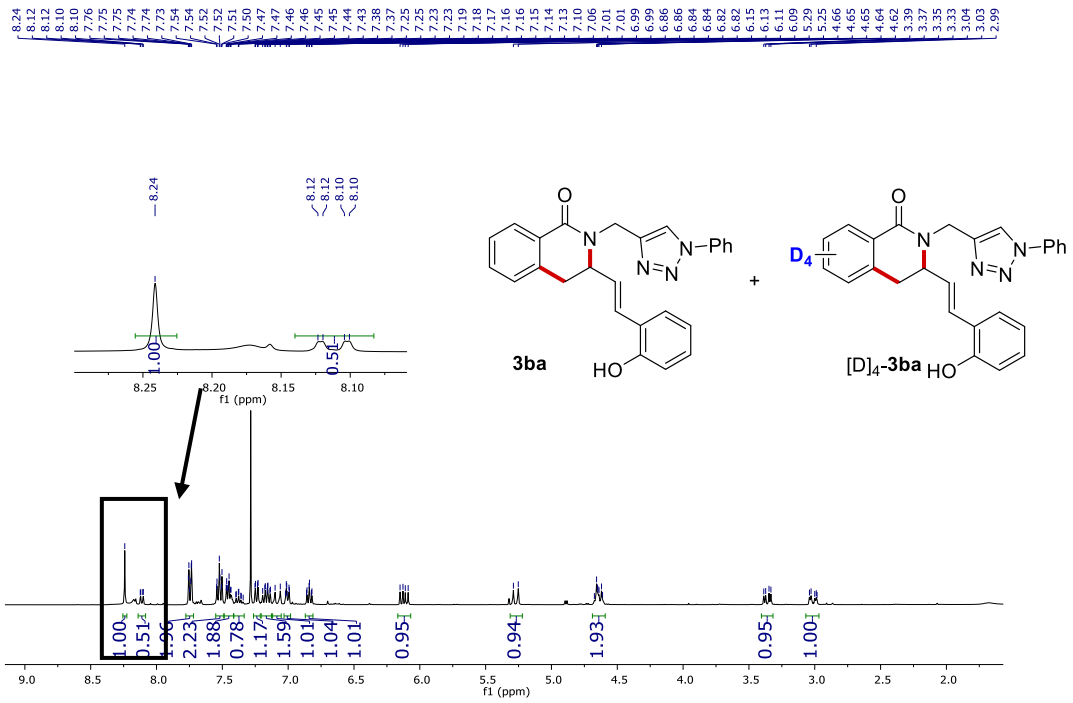

Intramolecular KIE

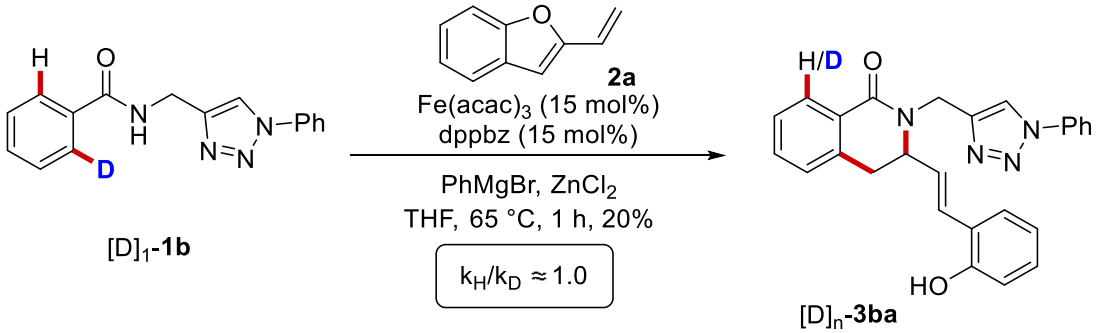

To a stirred solution of $Fe(acac)_3$ (10.6 mg, 0.03 mmol), dppz (11.9 mg, 0.03 mmol), zinc chloride (1.0 M in THF, 400 µL, 0.4 mmol) and $[D]_1$-**1b** (55.9 mg, 0.20 mmol) under N_2 atmosphere, PhMgBr (1.0 M in THF, 600 µL, 0.60 mmol) was added in a single portion. Then, 2-vinylbenzofuran **2a** (81 µL, 0.60 mmol) was added and the mixture was placed in a pre-heated oil bath at 65 °C. After stirring for 1 h, the reaction was cooled to room temperature and quenched by the addition of an aqueous solution of HCl (1.0 M, 5 mL). The reaction was extracted with CH_2Cl_2 (3x10 mL), and the combined organic extracts were dried over Na_2SO_4, filtered and concentrated. The crude product was purified by column chromatography (*n*-Hexane/EtOAc). The mixture was analysed by 400 MHz ^{1}H-NMR spectroscopy to determine the ratio of **3ba**/$[D]_1$-**3ba** [(1.0-0.49/0.49) = 1.04].

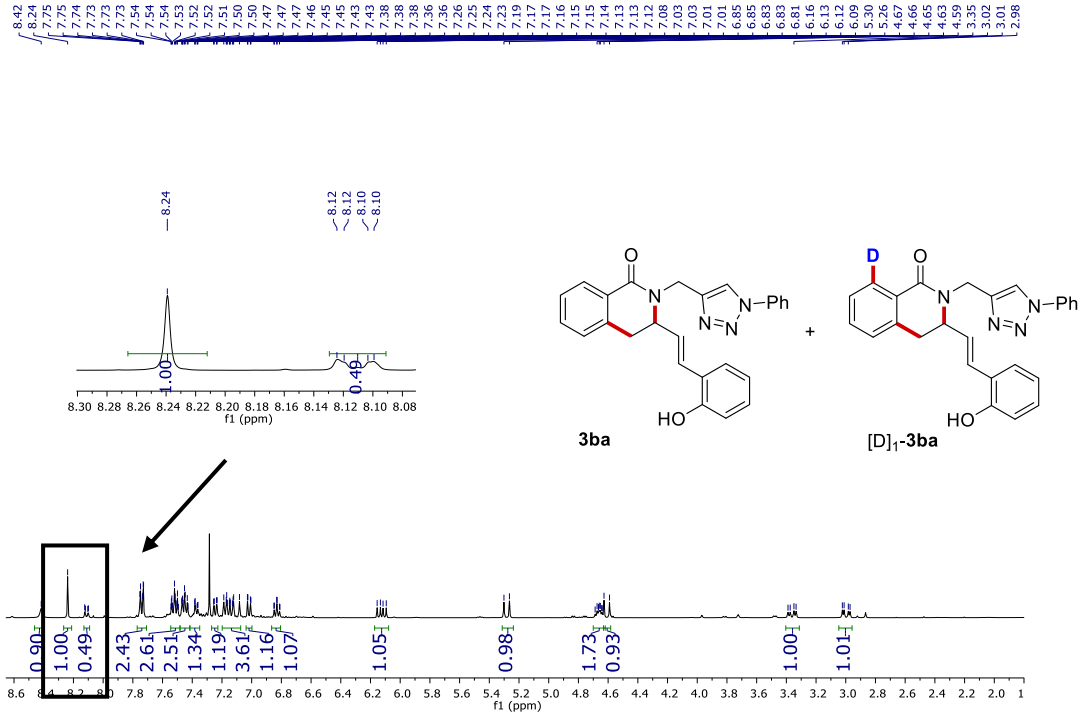

Reaction with Isotopically-labelled Substrates

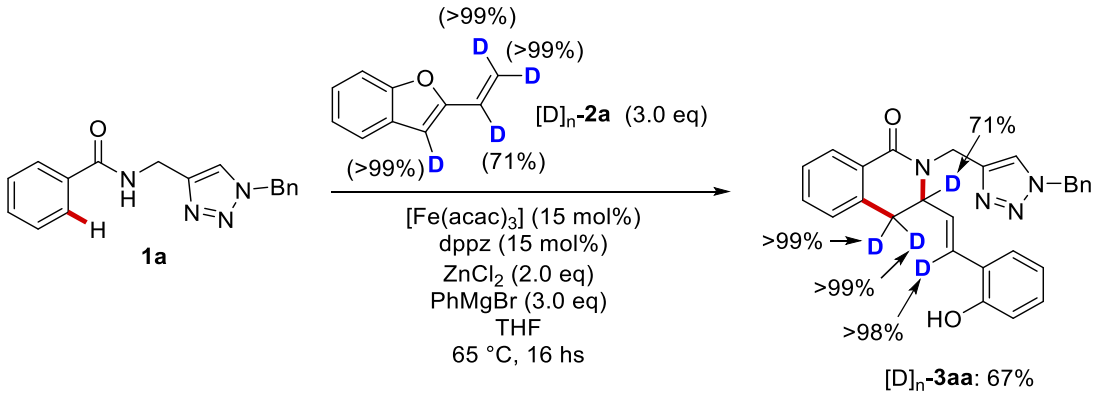

To a stirred solution of $Fe(acac)_3$ (10.6 mg, 0.03 mmol), dppz (13.4 mg, 0.03 mmol), zinc chloride (1.0 M in THF, 400 µL, 0.4 mmol) and **1a** (58.5 mg, 0.20 mmol) under N_2 atmosphere, PhMgBr (1.0 M in THF, 600 µL, 0.60 mmol) was added in a single portion. Then, 2-vinylbenzofuran $[D]_n$-**2a** (81 µL, 0.60 mmol) was added and the mixture was placed in a pre-heated oil bath at 65 °C. After stirring for 16 hs, the reaction was cooled to room temperature and quenched by the addition of an aqueous solution of HCl (1.0 M, 5 mL). The reaction was extracted with CH_2Cl_2 (3x10 mL) and the combined organic extracts were dried over Na_2SO_4, filtered and concentrated. Purification by column chromatography on silica gel (*n*-Hexane/EtOAc 1:1) yielded $[D]_n$-**3aa** (58.5 mg, 67%) as a white solid.

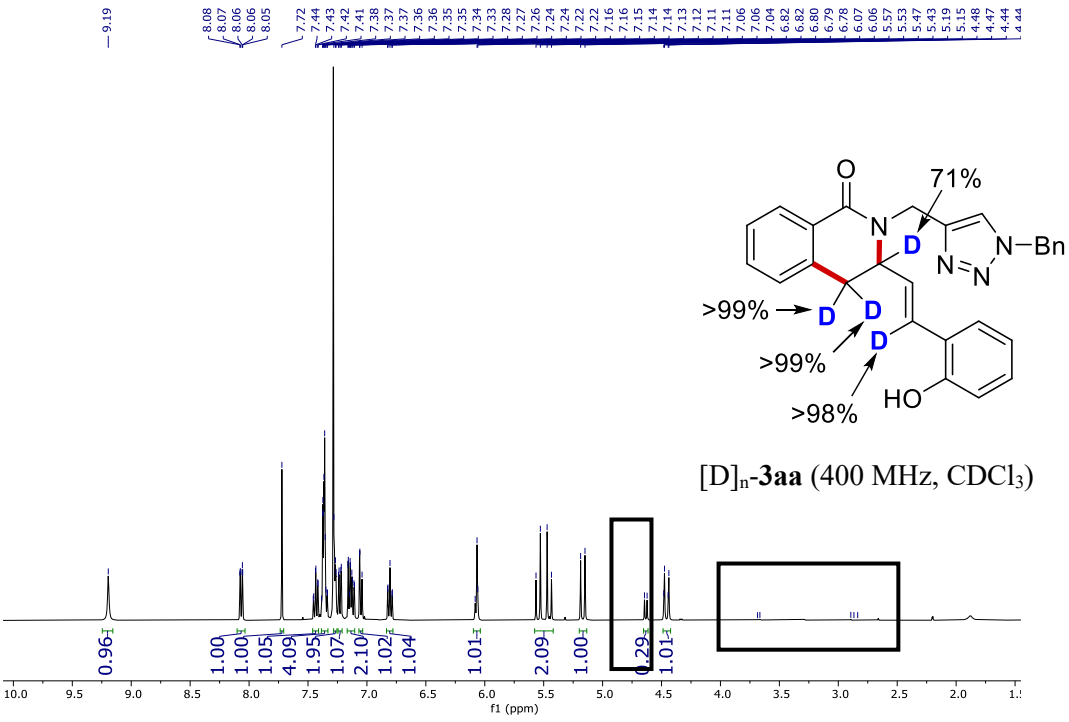

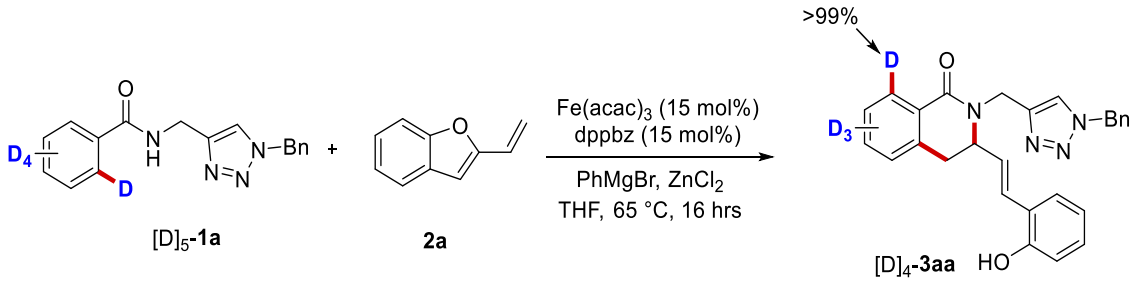

To a stirred solution of $Fe(acac)_3$ (10.6 mg, 0.03 mmol), dppz (13.4 mg, 0.03 mmol), zinc chloride (1.0 M in THF, 400 µL, 0.4 mmol) and $[D]_5$-**1a** (59.4 mg, 0.20 mmol) under N_2 atmosphere, PhMgBr (1.0 M in THF, 600 µL, 0.60 mmol) was added in a single portion. Then, 2-vinylbenzofuran **2a** (81 µL, 0.60 mmol) was added and the mixture was placed in a pre-heated oil bath at 65 °C. After stirring for 16 hs, the reaction was cooled to room temperature and quenched by the addition of an aqueous solution of HCl (1.0 M, 5 mL). The reaction was extracted with CH_2Cl_2 (3x10 mL) and the combined organic extracts were dried over Na_2SO_4, filtered and concentrated. Purification by column chromatography on silica gel (*n*-Hexane/EtOAc 1:1) yielded $[D]_4$-**3aa** (58.5 mg, 65%) as a white solid.

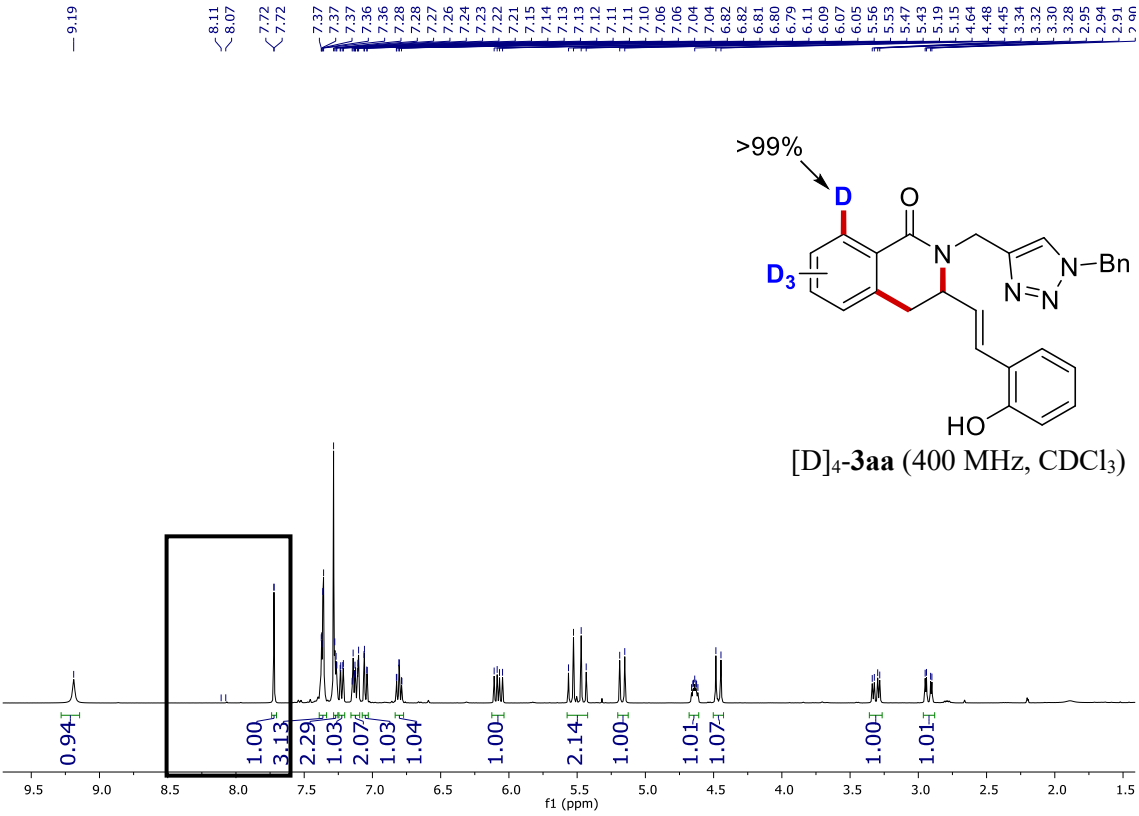

Reaction with DCl

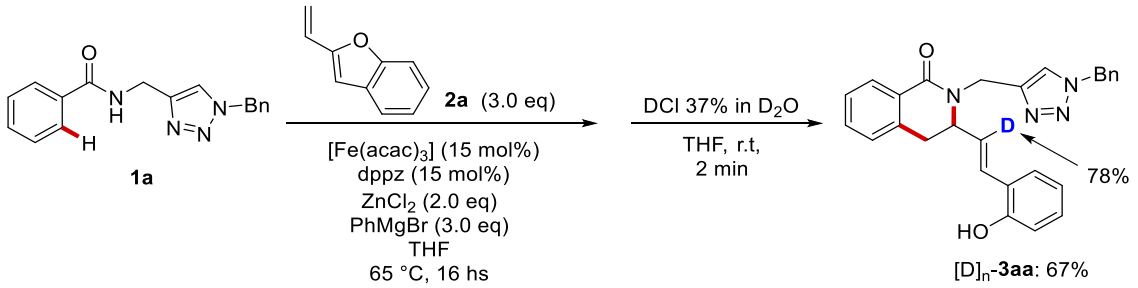

To a stirred solution of $Fe(acac)_3$ (10.6 mg, 0.03 mmol), dppz (13.4 mg, 0.03 mmol), zinc chloride (1.0 M in THF, 400 µL, 0.4 mmol) and **1a** (58.5 mg, 0.20 mmol) under N_2 atmosphere, PhMgBr (1.0 M in THF, 600 µL, 0.60 mmol) was added in a single portion. Then, 2-vinylbenzofuran **2a** (81 µL, 0.60 mmol) was added and the mixture was placed in a pre-heated oil bath at 65 °C. After stirring for 16 hs, the reaction was cooled to room temperature and quenched by the addition of 37% DCl in D_2O (1.5 mL). The reaction was extracted with CH_2Cl_2 (3x10 mL) and the combined organic extracts were dried over Na_2SO_4, filtered and concentrated. Purification by column chromatography on silica gel (*n*-hexane/EtOAc 1:1) yielded $[D]_n$-**3aa** (58.5 mg, 67%) as a white solid. The amount of deuterium incorporation was determined by ^{1}H-NMR.

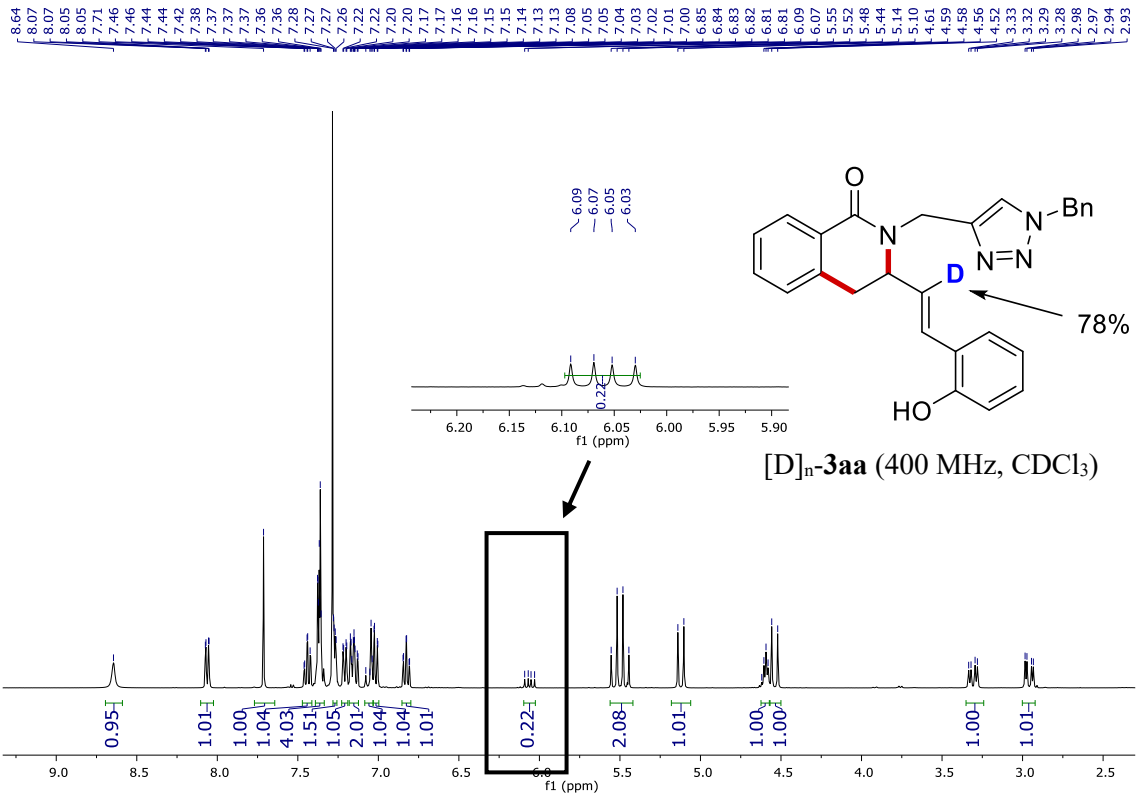

3.4.8 Late-stage synthetic manipulations

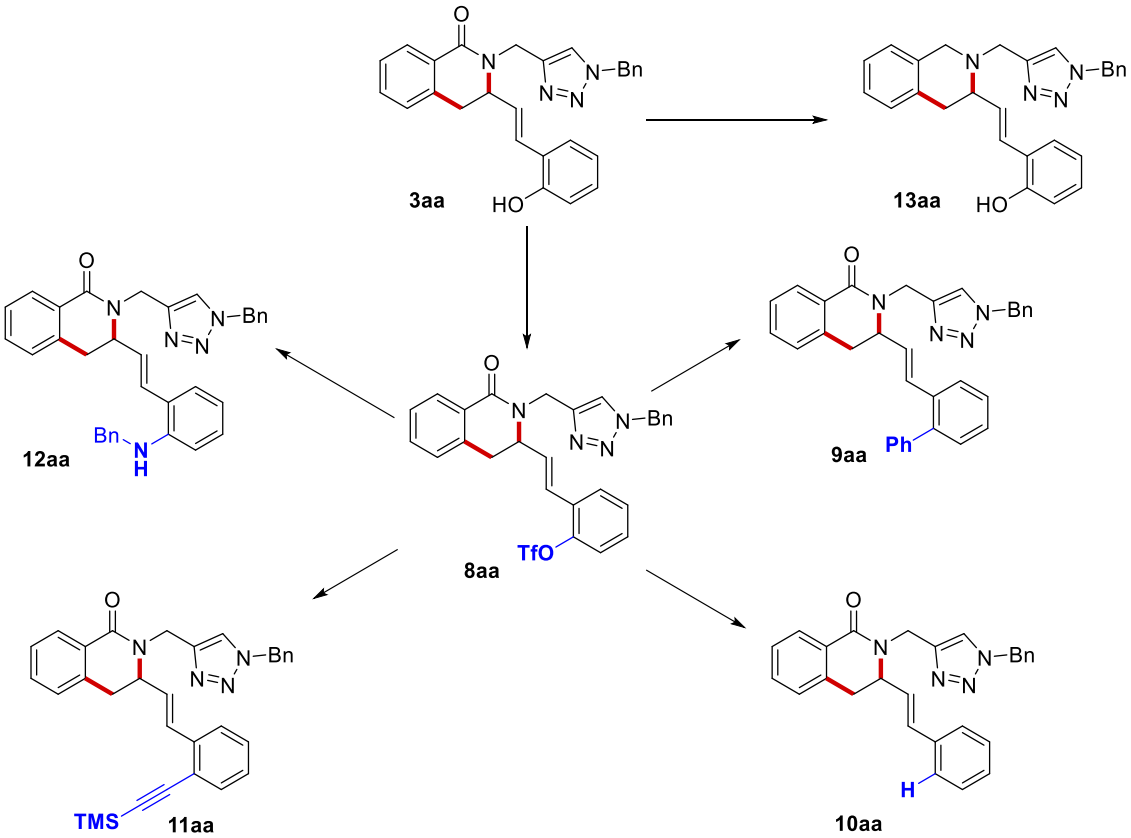

Figure S1: Late-stage synthetic diversification **of 3aa**.

(*E*)-2-(2-(2-((1-benzyl-1*H*-1,2,3-triazol-4-yl)methyl)-1-oxo-1,2,3,4-tetrahydroisoquinolin-3-yl)vinyl)phenyl trifluoromethanesulfonate (8aa)

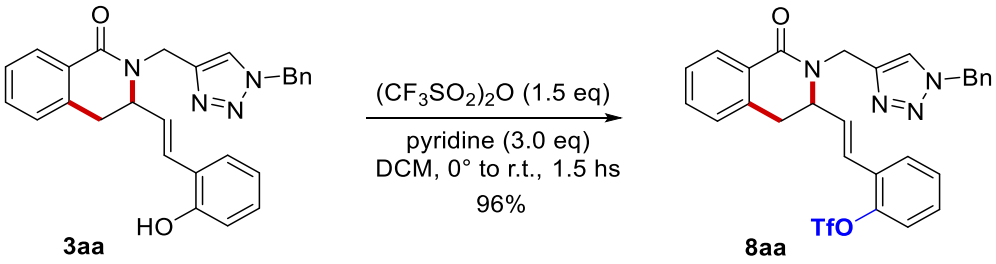

To a solution of **3aa** (100 mg, 0.23 mmol, 1.0 equiv.) in dry CH_2Cl_2 (1.0 mL), pyridine (56 µL, 1.0 mmol, 3.0 equiv.) was added. Then trifluoromethanesulfonic anhydride (58 µL, 0.35 mmol, 1.5 equiv.) was added dropwise at 0 °C. The solution was allowed to warm to room temperature and stirring was continued for 1.5 hours. The reaction was quenched with H_2O (1.0 mL) and the mixture was extracted with CH_2Cl_2 (2x5 mL). The combined organic extracts were dried over Na_2SO_4, filtered and concentrated. Purification by column chromatography on silica gel (*n*-Hexane/EtOAc 1:1) yielded **8aa** (125 mg, 96%) as a brown waxy solid. ^{1}H-NMR (400 MHz, $CDCl_3$): δ = 8.08 (dd, *J* = 7.7, 1.5 Hz, 1H), 7.63 (s, 1H), 7.47 – 7.44 (m, 1H), 7.42 (dd, *J* = 7.4, 1.6 Hz, 1H), 7.39 – 7.33 (m, 4H), 7.33 – 7.29 (m, 3H), 7.27 (d, *J* = 1.9 Hz, 1H), 7.25 – 7.21 (m, 1H), 7.16 (d, *J* = 7.4 Hz, 1H), 6.73 (dd, *J* = 15.8, 1.1 Hz, 1H), 6.23 (dd, *J* = 15.8, 7.4 Hz, 1H), 5.50 (q, *J* = 14.8 Hz, 2H), 5.34 (d, *J* = 14.9 Hz, 1H), 4.77 – 4.71 (m, 1H), 4.29 (d, *J* = 14.9 Hz, 1H), 3.42 (dd, *J* = 15.9, 6.4 Hz, 1H), 2.94 (dd, *J* = 16.0, 2.6 Hz, 1H). ^{13}C-NMR (101 MHz, $CDCl_3$): δ = 163.8 (C_q), 146.7 (C_q), 145.0 (C_q), 135.7 (2 x C_q), 134.5 (C_q), 132.2 (2 x CH), 129.9 (C_q), 129.4 (CH), 129.1 (CH), 128.8 (2 x CH), 128.4 (CH), 128.2 (CH), 128.0 (CH), 127.7 (CH), 127.3 (CH), 124.5 (CH), 123.1 (CH), 121.7 (CH), 118.5 (q, $^1J_{C\text{-}F}$ = 318 Hz, C_q), 58.3 (CH), 54.2 (CH_2), 40.8 (CH_2), 33.6 (CH_2). ^{19}F-NMR (565 MHz, $CDCl_3$): δ = -73.4 (s). MS (ESI) *m/z* (relative intensity): 591 (100) $[M+Na]^+$. HR-MS (ESI) *m/z* calcd for $C_{28}H_{23}F_3N_4O_4S$ $[M+H]^+$ 569.1470, found 569.1473.

(*E*)-3-(2-([1,1'-biphenyl]-2-yl)vinyl)-2-((1-benzyl-1H-1,2,3-triazol-4-yl)methyl)-3,4-dihydroisoquinolin-1(2*H*)-one (9aa)

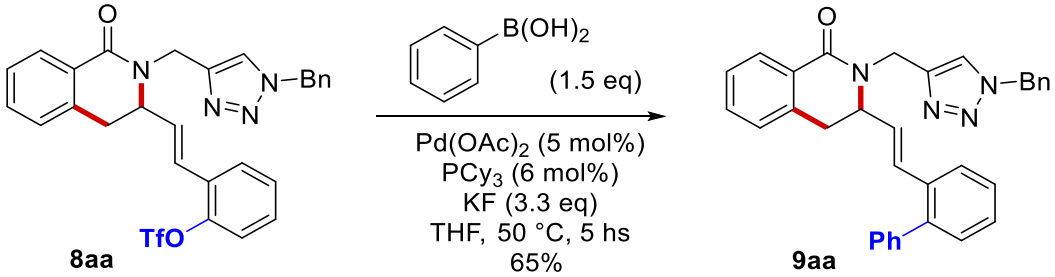

A 10 mL reaction tube was charged with $Pd(OAc)_2$ (1.1 mg, 0.005 mmol, 5 mol%), Cy_3P (1.7 mg, 0.006 mmol, 6 mol%), phenylboronic acid (18.3 mg, 0.15 mmol, 1.5 equiv), KF (19.1 mg, 0.33 mmol, 3.3 equiv) and **8aa** (56.8 mg, 0.1 mmol, 1.0 equiv.). The tube was evacuated and backfilled with nitrogen three times and then THF (0.3 mL) was added by syringe. The resulting mixture was stirred at 50 °C for 5 hs. The crude was filtered through a pad of celite and washed with EtOAc (3x2 mL), then concentrated under reduced pressure. Purification by column chromatography on silica gel (*n*-Hexane/EtOAc 6:4) yielded **9aa** (32.2 mg, 65%) as a pale-yellow waxy solid. ^{1}H-NMR (400 MHz, $CDCl_3$): δ = 8.04 (dd, *J* = 7.6, 1.5 Hz, 1H), 7.54 (s, 1H), 7.46 – 7.34 (m, 8H), 7.32 – 7.23 (m, 6H), 7.21 – 7.17 (m, 2H), 7.13 (d, *J* = 7.4 Hz, 1H), 6.51 (dd, *J* = 15.8, 1.2 Hz, 1H), 6.02 (dd, *J* = 15.8, 7.1 Hz, 1H), 5.55 – 5.39 (m, 2H), 5.22 (d, *J* = 14.9 Hz, 1H), 4.62 – 4.50 (m, 1H), 4.17 (d, *J* = 14.9 Hz, 1H), 3.33 (dd, *J* = 15.8, 6.4 Hz, 1H), 2.86 (dd, *J* = 15.9, 2.5 Hz, 1H). ^{13}C-NMR (101 MHz, $CDCl_3$): δ = 163.8 (C_q), 145.2 (C_q), 140.9 (C_q), 140.4 (C_q), 136.0 (C_q), 134.5 (C_q), 134.3 (C_q), 132.0 (CH), 131.3 (CH), 130.2 (CH), 129.6 (CH), 129.1 (CH), 128.9 (C_q), 128.8 (CH), 128.2 (2 x CH), 128.1 (CH), 127.9 (CH), 127.8 (CH), 127.7 (CH), 127.4 (CH), 127.2 (CH), 127.1 (CH), 126.4 (CH), 123.0 (CH), 58.3 (CH), 54.2 (CH_2), 41.0 (CH_2), 33.8 (CH_2). MS (ESI) *m/z* (relative intensity): 519 (100) $[M+Na]^+$, 497 (18) $[M+H]^+$. HR-MS (ESI) *m/z* calcd for $C_{33}H_{29}N_4O$ $[M+H]^+$ 497.2336, found 497.2335.

(*E*)-2-((1-Benzyl-1*H*-1,2,3-triazol-4-yl)methyl)-3-styryl-3,4-dihydroisoquinolin-1(2*H*)-one (10aa)

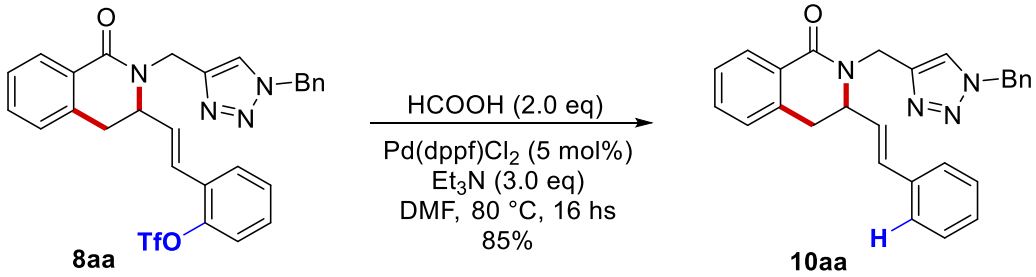

A 10 mL reaction tube was charged with $Pd(dppf)Cl_2$ (2.5 mg, 0.005 mmol, 5 mol%), and **8aa** (56.8 mg, 0.1 mmol, 1 equiv.). The tube was evacuated and backfilled with nitrogen three times and then DMF (0.3 mL) was added by syringe. Then triethylamine (42 µL, 0.3 mmol, 3.0 equiv.) was added followed by formic acid (8 µL, 0.2 mmol, 2.0 equiv.). The resulting mixture was stirred at 80 °C for 16 hs. The crude was filtered through a pad of celite and washed with EtOAc (3x2 mL), then concentrated under reduced pressure. Purification by column chromatography on silica gel (*n*-Hexane/EtOAc 6:4) yielded **10aa** (32.2 mg, 85%) as a white solid. M.p.= 40-42 °C. ^{1}H-NMR (400 MHz, $CDCl_3$): δ = 8.09 (dd, *J* = 7.7, 1.5 Hz, 1H), 7.60 (s, 1H), 7.43 (td, *J* = 7.5, 1.5 Hz, 1H), 7.40 – 7.34 (m, 4H), 7.29 (m, 3H), 7.28 – 7.21 (m, 4H), 7.15 (d, *J* = 7.4 Hz, 1H), 6.56 (dd, *J* = 15.8, 1.0 Hz, 1H), 6.10 (dd, *J* = 15.8, 7.8 Hz, 1H), 5.55 – 5.41 (m, 2H), 5.34 (d, *J* = 14.9 Hz, 1H), 4.67 – 4.63 (m, 1H), 4.29 (d, *J* = 14.9 Hz, 1H), 3.39 (dd, *J* = 15.9, 6.4 Hz, 1H), 2.90 (dd, *J* = 16.0, 2.4 Hz, 1H). ^{13}C-NMR (101 MHz, $CDCl_3$): δ = 163.9 (C_q), 145.2 (C_q), 136.0 (C_q), 135.9 (C_q), 134.4 (C_q), 132.6 (CH), 132.1 (CH), 129.1 (CH), 128.8 (CH), 128.8 (C_q), 128.6 (CH), 128.2 (CH), 128.0 (CH), 127.9 (CH), 127.7 (CH), 127.2 (CH), 126.6 (CH), 126.5 (CH), 123.0 (CH), 58.3 (CH), 54.2 (CH_2), 40.6 (CH_2), 33.9 (CH_2). MS (ESI) *m/z* (relative intensity): 863 (54) $[2M+Na]^+$, 443 (16) $[M+Na]^+$, 421 (100) $[M+H]^+$. HR-MS (ESI) *m/z* calcd for $C_{27}H_{25}N_4O$ $[M+H]^+$ 421.2023, found 421.2027.

(*E*)-2-((1-Benzyl-1*H*-1,2,3-triazol-4-yl)methyl)-3-(2-((trimethylsilyl)ethynyl)styryl)-3,4-dihydroisoquinolin-1(2*H*)-one (11aa)

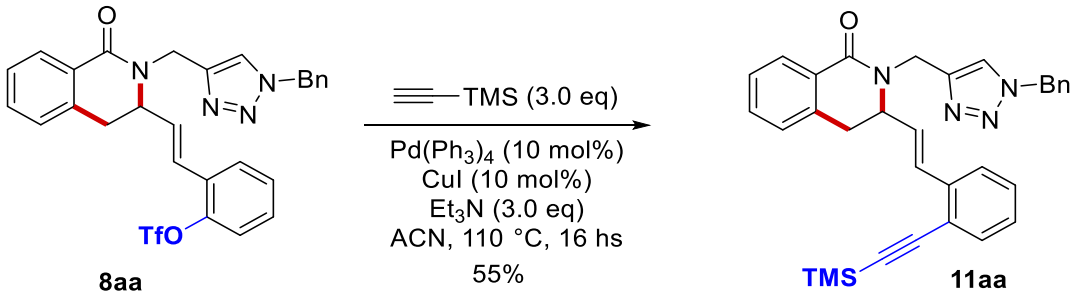

A 10 mL reaction tube was charged with $Pd(Ph_3)_4$ (12.0 mg, 0.01 mmol, 10 mol%), CuI (1.9 mg, 0.01 mmol, 10 mol%) and **8aa** (56.8 mg, 0.1 mmol, 1.0 equiv.). The tube was evacuated and backfilled with nitrogen three times and then ACN (0.5 mL) was added by syringe. Then triethylamine (42 µL, 0.3 mmol, 3.0 equiv.) was added followed by Trimethylsilylacetylene (37 µL, 0.3 mmol, 3.0 equiv.). The resulting mixture was stirred at 110 °C for 16 hs. The crude was filtered through a pad of celite and washed with EtOAc (3x2 mL), then concentrated under reduced pressure. Purification by column chromatography on silica gel (*n*-Hexane/EtOAc 6:4) yielded **11aa** (28.5 mg, 55%) as a sticky dark-yellow solid. ^{1}H-NMR (400 MHz, $CDCl_3$): δ = 8.08 (dd, *J* = 7.6, 1.5 Hz, 1H), 7.62 (s, 1H), 7.43 (m, 2H), 7.39 – 7.32 (m, 5H), 7.29 – 7.25 (m, 2H), 7.23 – 7.18 (m, 1H), 7.15 (m, 2H), 7.04 (dd, *J* = 16.0, 1.0 Hz, 1H), 6.21 (dd, *J* = 15.9, 7.5 Hz, 1H), 5.57 – 5.40 (m, 2H), 5.36 (d, *J* = 14.9 Hz, 1H), 4.74 – 7.69 (m, 1H), 4.31 (d, *J* = 14.9 Hz, 1H), 3.41 (dd, *J* = 15.9, 6.4 Hz, 1H), 2.94 (dd, *J* = 16.0, 2.5 Hz, 1H), 0.31 (s, 9H). ^{13}C-NMR (101 MHz, $CDCl_3$): δ = 163.8 (C_q), 145.2 (C_q), 137.7 (C_q), 135.9 (C_q), 134.5 (C_q), 133.0 (CH), 132.1 (CH), 130.4 (CH), 129.1 (CH), 128.9 (C_q), 128.8 (CH), 128.7 (CH), 128.6 (CH), 128.2 (CH), 127.9 (CH), 127.7 (CH), 127.5 (CH), 127.2 (CH), 125.2 (CH), 123.1 (CH), 121.9 (C_q), 103.1 (C_q), 99.7 (C_q), 58.4 (CH), 54.2 (CH_2), 40.8 (CH_2), 33.8 (CH_2), 0.1 (CH_3). MS (ESI) *m/z* (relative intensity): 1055 (10) $[2M+Na]^+$, 517 (100) $[M+H]^+$. HR-MS (ESI) *m/z* calcd for $C_{32}H_{33}N_4OSi$ $[M+H]^+$ 517.2418, found 517.2423.

2-((1-Benzyl-1*H*-1,2,3-triazol-4-yl)methyl)-3-(2-(benzylamino)styryl)-3,4-dihydroisoquinolin-1(2*H*)-one (12aa)

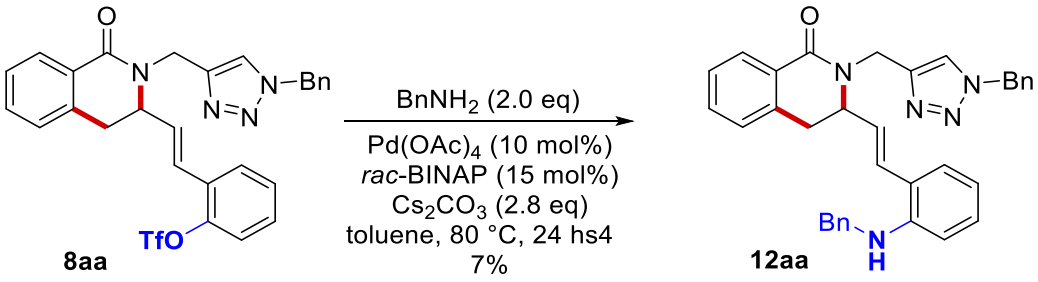

A 10 mL reaction tube was charged with $Pd(OAc)_2$ (2.2 mg, 0.01 mmol, 10 mol%), *rac*-BINAP (9.3 mg, 0.015 mmol, 15 mol%), Cs_2CO_3 (91.2 mg, 0.28 mmol, 2.8 equiv.) and **8aa** (56.8 mg, 0.1 mmol, 1.0 equiv.). The tube was evacuated and backfilled with nitrogen three times and then toluene (0.2 mL) was added by syringe followed by benzylamine (22 µL, 0.2 mmol, 2.0 equiv.). The resulting mixture was stirred at 80 °C for 24 hs. The crude was filtered through a pad of celite and washed with EtOAc (3x2 mL), then concentrated under reduced pressure. Purification by column chromatography on silica gel (*n*-Hexane/EtOAc 6:4) yielded **12aa** (24.7 mg, 47%) as a brown solid. M.p. = 93-95 °C. ^{1}H-NMR (400 MHz, $CDCl_3$): δ = 8.02 (dd, *J* = 7.7, 1.4 Hz, 1H), 7.62 (s, 1H), 7.41 – 7.27 (m, 11H), 7.25 – 7.19 (m, 2H), 7.15 – 7.11 (m, 1H), 7.09 (d, *J* = 7.4 Hz, 2H), 6.69 – 6.53 (m, 3H), 5.92 (dd, *J* = 15.5, 7.5 Hz, 1H), 5.45 (q, *J* = 14.8 Hz, 2H), 5.20 (d, *J* = 14.8 Hz, 1H), 4.65 – 4.57 (m, 1H), 4.53 (d, *J* = 14.8 Hz, 1H), 4.37 (d, *J* = 2.4 Hz, 2H), 3.36 (dd, *J* = 15.8, 6.0 Hz, 1H), 2.94 (dd, *J* = 15.9, 3.8 Hz, 1H). ^{13}C-NMR (101 MHz, $CDCl_3$): δ = 164.2 (C_q), 145.3 (C_q), 145.0 (C_q), 139.5 (C_q), 136.2 (C_q), 134.5 (C_q), 132.1 (CH), 129.4 (CH), 129.1 (2 x CH), 128.9 (C_q), 128.8 (CH), 128.7 (CH), 128.6 (CH), 128.1 (CH), 127.8 (CH), 127.7 (CH), 127.5 (CH), 127.4 (CH), 127.2 (CH), 127.1 (CH), 123.4 (CH), 122.7 (C_q), 117.2 (CH), 111.1 (CH), 58.9 (CH), 54.2 (CH_2), 48.0 (CH_2), 40.7 (CH_2), 34.1 (CH_2). MS (ESI) *m/z* (relative intensity): 548 (21) $[M+Na]^+$, 526 (100) $[M+H]^+$. HR-MS (ESI) *m/z* calcd for $C_{34}H_{32}N_5O$ $[M+H]^+$ 526.2601, found 526.2605.

(*E*)-2-(2-(2-((1-Benzyl-1*H*-1,2,3-triazol-4-yl)methyl)-1,2,3,4-tetrahydroisoquinolin-3 yl)vinyl)phenol (13aa)

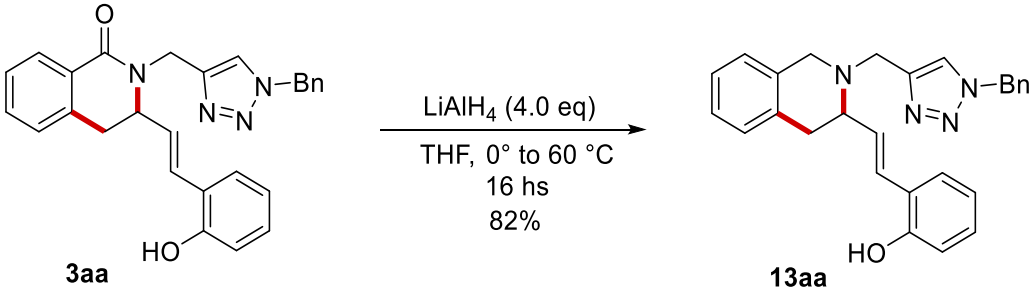

To a solution of **3aa** (43.6 mg, 0.1 mmol, 1.0 equiv.) in dry THF (1.0 mL), $LiAlH_4$ (15.2 mg, 0.4 mmol, 4.0 equiv.) was added at 0 °C. The solution was allowed to warm to room temperature and then placed in a pre-heated oil bath at 70 °C. After stirring for 16 hs, the reaction was cooled to room temperature and quenched with ice. The mixture was extracted with CH_2Cl_2 (2x5 mL) and the combined organic extracts were dried over Na_2SO_4, filtered and concentrated. Purification by column chromatography on silica gel (*n*-Hexane/EtOAc 1:1) yielded **13aa** (34.5 mg, 82%) as a colourless oil. ^{1}H-NMR (400 MHz, $CDCl_3$): δ = 8.81 (bs, 1H), 7.37 (s, 1H), 7.34 (m, 3H), 7.25 – 7.14 (m, 5H), 7.08 (td, *J* = 4.9, 3.3 Hz, 2H), 7.05 – 6.98 (m, 1H), 6.86 – 6.78 (m, 2H), 6.57 – 6.47 (m, 2H), 5.50 (d, *J* = 14.7 Hz, 1H), 5.36 – 5.27 (m, 1H), 4.08 (d, *J* = 14.2 Hz, 1H), 4.02 (d, *J* = 15.5 Hz, 1H), 3.92 (d, *J* = 14.1 Hz, 1H), 3.84 (d, *J* = 15.5 Hz, 1H), 3.44 (m, 1H), 3.08 – 2.93 (m, 2H). ^{13}C-NMR (101 MHz, $CDCl_3$): δ = 154.8 (C_q), 143.9 (C_q), 134.3 (C_q), 133.5 (C_q), 133.22 (C_q), 131.8 (CH), 130.3 (CH), 129.1 (CH), 128.8 (CH), 128.6 (3 x CH), 128.2 (CH), 126.5 (CH), 126.4 (CH), 125.9 (CH), 124.1 (C_q), 123.4 (CH), 119.8 (CH), 116.4 (CH), 61.8 (CH), 54.2 (CH_2), 53.5 (CH_2), 48.6 (CH_2), 35.1 (CH_2). MS (ESI) *m/z* (relative intensity): 423 (100) $[M+H]^+$. HR-MS (ESI) *m/z* calcd for $C_{27}H_{27}N_4O$ $[M+H]^+$ 423.2179, found 423.2176.

Methyl (*E*)-6-{4-[(3-((*E*)-2-hydroxystyryl)-1-oxo-3,4-dihydroisoquinolin-2(1*H*)-yl)methyl]-1*H*-1,2,3-triazol-1-yl}hex-2-enoate (14ea)

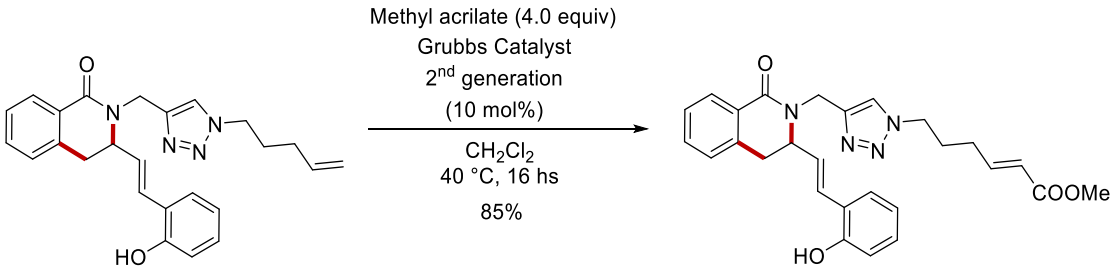

A 10 mL reaction tube was charged with **3ea** (41.5 mg, 0.1 mmol, 1.0 equiv.) and was evacuated and backfilled with nitrogen three times and then dry and degassed CH_2Cl_2 (1.0 mL) was added by syringe. Then methyl acrylate (36 µL, 0.4 mmol, 4.0 mmol), and Grubbs Catalyst 2nd generation (8.4 mg, 10 mol %, 0.01 equiv.) were added. The resulting mixture was stirred at 40 °C for 16 hs. The crude was filtered through a pad of celite and washed with EtOAc (3x2 mL), then concentrated under reduced pressure. Purification by column chromatography on silica gel (*n*-Hexane/EtOAc 1:1) yielded **14ea** (40.1 mg, 85%) as a pale-yellow oil. ^{1}H-NMR (400 MHz, $CDCl_3$): δ = 8.88 (bs, 1H), 8.09 (dd, *J* = 7.8, 1.5 Hz, 1H), 7.78 (s, 1H), 7.45 (dd, *J* = 7.4, 1.5 Hz, 1H), 7.37 (dd, *J* = 7.6, 1.3 Hz, 1H), 7.22 (dd, *J* = 7.7, 1.7 Hz, 1H), 7.17 (d, *J* = 7.4 Hz, 1H), 7.12 (dd, *J* = 7.4, 1.6 Hz, 1H), 7.07 (d, *J* = 15.8 Hz, 1H), 7.01 (dd, *J* = 8.1, 1.2 Hz, 1H), 6.90 (dt, *J* = 15.7, 6.9 Hz, 1H), 6.81 (dd, *J* = 7.4, 1.1 Hz, 1H), 6.07 (dd, *J* = 15.8, 8.8 Hz, 1H), 5.86 (dt, *J* = 15.8, 1.6 Hz, 1H), 5.15 (d, *J* = 14.8 Hz, 1H), 4.65 – 4.58 (m, 1H), 4.55 (d, *J* = 14.9 Hz, 1H), 4.40 – 4.29 (m, 2H), 3.75 (s, 3H), 3.34 (dd, *J* = 15.9, 5.9 Hz, 1H), 2.96 (dd, *J* = 16.0, 4.2 Hz, 1H), 2.27 – 2.18 (m, 2H), 2.12 – 2.03 (m, 2H). ^{13}C-NMR (101 MHz, $CDCl_3$): δ = 166.7 (C_q), 164.3 (C_q), 154.6 (C_q), 146.5 (CH), 144.5 (C_q), 136.4 (C_q), 132.2 (CH), 129.6 (CH), 129.2 (CH), 128.7 (C_q), 127.9 (CH), 127.7 (CH), 127.4 (CH), 127.2 (CH), 127.1 (CH), 124.2 (CH), 123.7 (C_q), 122.4 (CH), 120.0 (CH), 116.6 (CH), 60.0 (CH), 51.6 (CH_3), 49.6 (CH_2), 40.6 (CH_2), 34.2 (CH_2), 28.8 (CH_2), 28.4 (CH_2). MS (ESI) *m/z* (relative intensity): 473 (100) $[M+H]^+$. HR-MS (ESI) *m/z* calcd for $C_{27}H_{29}N_4O_4$ $[M+H]^+$ 473.2183, found 473.2187.

3.4.9 Computational Studies

For the DFT calculations details please refer to the Supporting Information file of the following publication:

S. Cattani, N. K. Pandit, M. Buccio, D. Balestri, L. Ackermann, G. Cera, *Angew. Chem. Int. Ed*. **2024**, *63*, e202404319.

https://doi.org/10.1002/anie.202404319

3.4.10 Additional References

[1] S. Cattani, A. Secchi, L. Ackermann, G. Cera, *Org. Biomol. Chem*. **2023**, *21*, 1264–1269.

[2] S. Movahhed, J. Westphal, M. Dindaroğlu, A. Falk, H.-G. Schmalz, *Chem. Eur. J*. **2016**, *22*, 7381–7384.

[3] J. Rojas-Martín, M. Veguillas, M. Ribagorda, M. C. Carreño, *Org. Lett.* **2013**, *15*, 5686–5689.

[4] M.W. Gribble, Jr., M. T. Pirnot, J. S. Bandar, R. Y. Liu, S. L. Buchwald, *J. Am. Chem. Soc*. **2017**, *139*, 2192–2195.

[5] L. A. Perego, S. Wagschal, R. Gruber, P. Fleurat-Lessard, L. El Kaim, L. Grimaud, *Adv. Synth. Catal.* **2019**, *361*, 151–159.

[6] S. Senaweera, J. D. Weaver, *Chem. Commun*. **2017**, *53*, 7545–7548.

[7] H. Seo, A. Liu, T. F. Jamison, *J. Am. Chem. Soc*. **2017**, *139*, 13969–13972.

[8] M. Hansen, S. E. Jacobsen, S. Plunkett, G. E. Liebscher, J. D. McCorvy, H. Bräuner-Osborne, J. L. Kristensen, *Bioorg. Med. Chem*. **2015**, *23*, 3933–3937.

[9] G. Cera, N. Della Ca', G. Maestri, *Chem. Sci.* **2019**, *10*, 10297–10304.

[10] M. J. Frisch, G. W. Trucks, H. B. Schlegel, G. E. Scuseria, M. A. Robb, J. R. Cheeseman, G. Scalmani, V. Barone, G. A. Petersson, H. Nakatsuji, X. Li, M. Caricato, A. V. Marenich, J. Bloino, B. G. Janesko, R. Gomperts, B. Mennucci, H. P. Hratchian, J. V. Ortiz, A. F. Izmaylov, J. L. Sonnenberg, D. Williams-Young, F. Ding, F. Lipparini, F. Egidi, J. Goings, B. Peng, A. Petrone, T. Henderson, D. Ranasinghe, V. G. Zakrzewski, J. Gao, N. Rega, G. Zheng, W. Liang, M. Hada, M. Ehara, K. Toyota, R. Fukuda, J. Hasegawa, M. Ishida, T. Nakajima, Y. Honda, O. Kitao, H. Nakai, T. Vreven, K. Throssell, J. A. Montgomery, Jr., J. E. Peralta, F. Ogliaro, M. J.

Bearpark, J. J. Heyd, E. N. Brothers, K. N. Kudin, V. N. Staroverov, T. A. Keith, R. Kobayashi, J. Normand, K. Raghavachari, A. P. Rendell, J. C. Burant, S. S. Iyengar, J. Tomasi, M. Cossi, J. M. Millam, M. Klene, C. Adamo, R. Cammi, J. W. Ochterski, R. L. Martin, K. Morokuma, O. Farkas, J. B. Foresman, D. J. Fox, *Gaussian 16, Revision A.03, Gaussian*, Inc., Wallingford CT, **2016**.

[11] J. M. Tao, J. P. Perdew, V. N. Staroverov, G. E. Scuseria, *Phys. Rev. Lett.* **2003**, *91*, 146401.

[12] a) S. Grimme, S. Ehrlich, L. Goerigk, *J. Comput. Chem*. **2011**, *32*, 1456–1465; b) S. Grimme, J. Antony, S. Ehrlich, H. Krieg, *J. Chem. Phys*. **2010**, 132, 154104.

[13] a) F. Weigend, Phys. *Chem. Chem. Phys*. **2006**, *8*, 1057–1065; b) F. Weigend, R. Ahlrichs, *Phys. Chem. Chem. Phys*. **2005**, *7*, 3297–3305; c) A. Schaefer, C. Huber, R. Ahlrichs, *J. Chem. Phys.* **1994**, *100*, 5829–583; d) A. Schaefer, H. Horn, R. Ahlrichs, *J. Chem. Phys*. **1992**, *97*, 2571–2577.

[14] K. Fukui, *Acc. Chem. Res*. **1981**, *14*, 363–368.

[15] Zhao, D. G. Truhlar, *J. Phys. Chem. A* **2005**, *109*, 5656–5667.

[16] A. V. Marenich, C. J. Cramer, D. G. Truhlar, *J. Phys. Chem. B* **2009**, *113*, 6378–6396.

4. Stereoselective Iron-catalyzed C–H Alkylations with Allenes: Expedient Access to Internal *Z*-Olefins

4.1 Introduction

4.1.1 Allenes in Transition Metal-Catalyzed C–H Functionalizations

Allenes, found in various natural products, pharmaceuticals, and functional materials, exhibit unique reactivity in organic synthesis.[1] Their recognition and use as versatile building blocks have significantly increased in recent decades.[2] Due to their flexibility, allenes can participate in diverse nucleophilic and electrophilic addition reactions, as well as cycloadditions and cyclizations. Allenes were found to be an interesting coupling partner in transition-metal-catalyzed C–H functionalization reactions.[3] The reactivity of allenes in carbometalation processes is mainly influenced by the formation of metal-allyl or metal-alkenyl intermediates (Scheme 4.1) This is achieved by the selective insertion of an organometallic species into the allene framework, enabling a variety of reactions. The steric and electronic properties of substituents significantly affect the insertion pattern, resulting in a wide range of regio-, chemo-, and stereoselectivities, which presents considerable challenges to control in C–H functionalization reactions involving allenes.

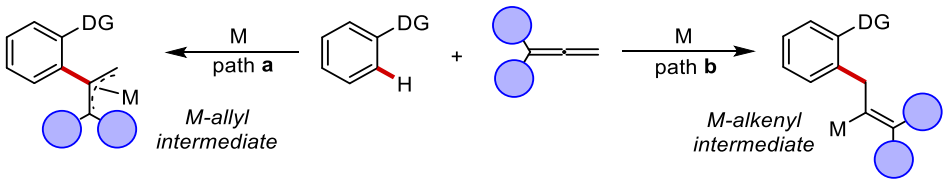

Scheme 4.1 Different reaction pathways of allenes in carbometalation.

The first report of a catalytic C–H activation process involving allenes was presented by Krische in 2009.[4] This pioneer study highlighted the reaction between various (hetero)aromatic and α,β-unsaturated carboxamides with 1,1-dimethylallene, using cationic iridium complexes as catalysts (Scheme 4.2). This transformation produced prenylated products with excellent regioselectivity and high yields. Inspired by Krische's seminal work, numerous C–H functionalization reactions involving allenes and other transition metals have since been developed.[5]

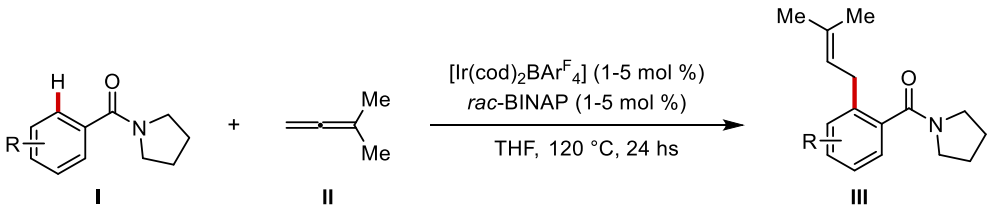

Scheme 4.2 Iridium catalyzed C−H prenylation of carboxamides with 1,1-dimethylallene.

In 2016 Cheng and coworkers reported the first use of allenes as coupling partners in C–H activation reactions *via* cobalt catalysis.[6] This research introduces a novel cobalt-catalyzed [5 + 1] annulation reaction between 2-vinylphenols and allenes, which delivers a wide family of cyclization products containing a chromene core, achieved in high yields. The proposed mechanism involves the C−H activation of the vinyl group of **IV**, insertion of the allene, and an unusual intramolecular regioselective phenoxide addition, where the oxygen−cobalt bond nucleophilically attacks the central carbon of the π-allylic group, forming six-membered chromene heterocycles **VI** under mild reaction conditions.

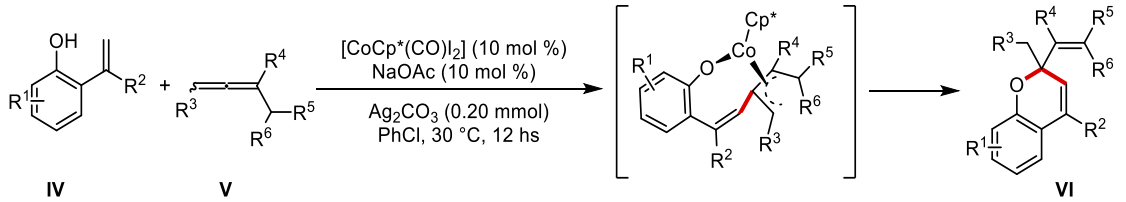

Scheme 4.3 Iridium catalyzed C−H prenylation of carboxamides with 1,1-dimethylallene.

Since this first report, significant progress has been made in the C–H functionalization of allenes using first-row transition metals. Despite significant advancements and developments with affordable 3d-TM catalysts, the use of iron for C–H functionalization with allenes has only recently overcome its challenges.

4.1.2 Iron-Catalyzed C–H Functionalizations with Allenes

A breakthrough in C–H activation using allenes with an inexpensive, non-toxic iron catalyst was reported by Ackermann in 2018.[7] In this report, iron catalysts enable a versatile allene annulations through a distinctive C−H/N−H/C−O/C−H functionalization sequence with triazolyl benzamides (**VII** and **VIII**). Control experiments performed with other leaving groups on the allene moiety revealed that allenyl acetates **IX** were the most suitable choice for the transformation. This robust catalytic system operates without external oxidants, at mild reaction conditions, leading to the efficient synthesis of differently substituted isoquinolone derivatives.

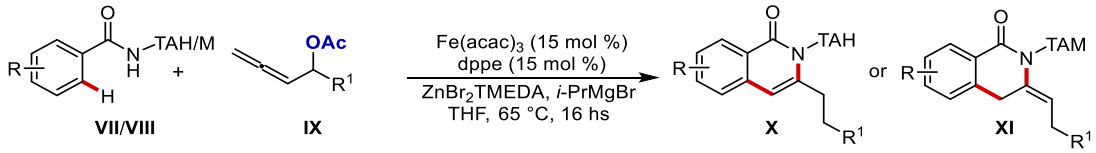

Scheme 4.4 Iron-catalyzed C−H/N−H/C−O/C−H functionalization with allenes **2**.

The authors propose a catalytic cycle initiated by a facile C−H activation step (**Int1**), followed by allene migratory insertion to deliver **Int2**. This undergoes oxidation-induced reductive elimination, leading to the formation of the iron allyl complex **Int3**. Detailed mechanistic studies have uncovered an unprecedented intramolecular C−H activation *via* 1,4-iron migration pathway resulting in the stabilized allylic-benzylic iron **Int4**. A proto-demetalation step produces *exo*-methylene-3,4-dihydroisoquinoline **XI**, which subsequently isomerizes to yield the corresponding isoquinolone **X**. According to the proposed reaction mechanism, the leaving group actively participates in the catalytic cycle by initiating a reductive elimination step, followed by the 1,4-iron migration (Scheme 4.5).

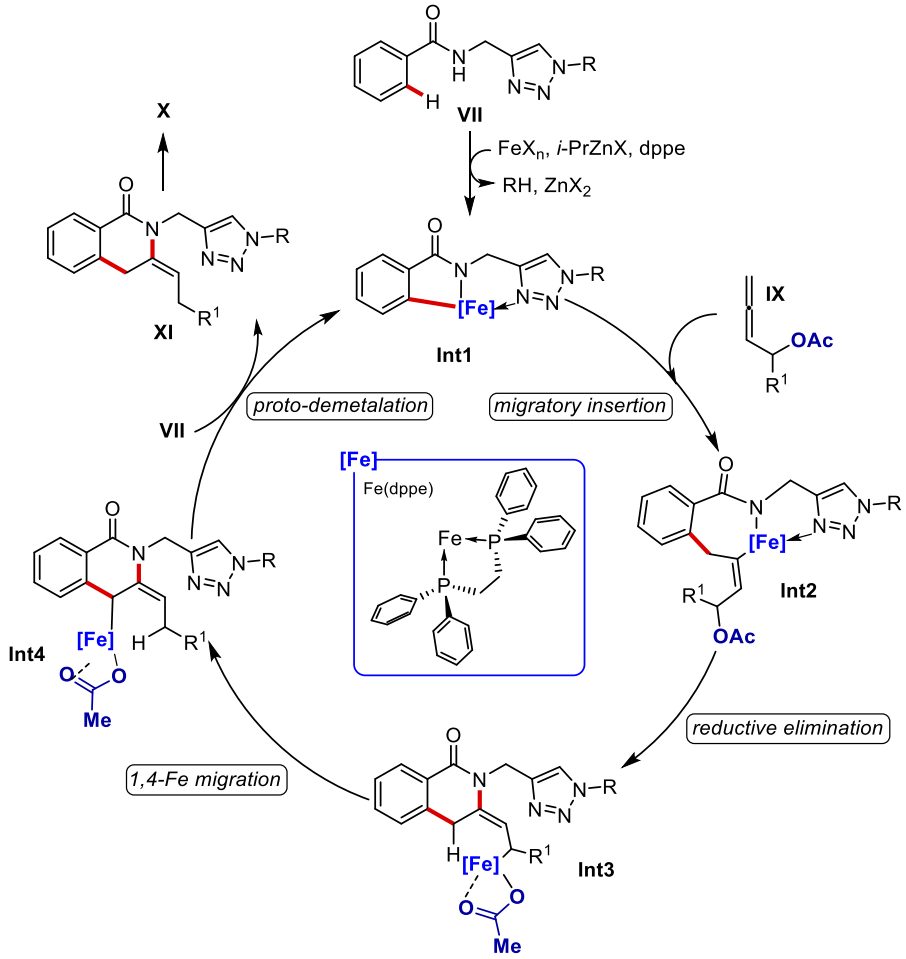

Scheme 4.5 Proposed catalytic cycle for the C−H/N−H/C−O/C−H activation.

The absence of the acetate group on the allene structure (**XII**) prevents the reductive elimination step, rendering the catalytic reaction inefficient and resulting only in the formation of the alkylation product **XIII**, as depicted in Scheme 4.6.

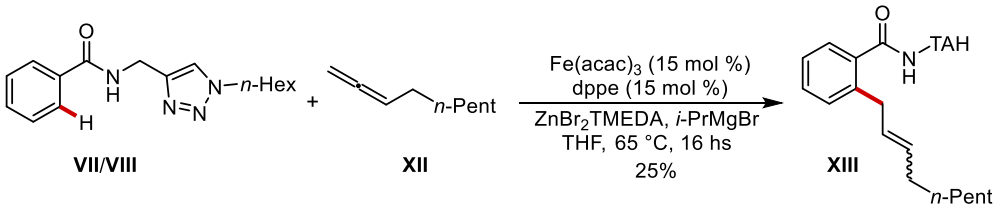

Scheme 4.6 Reaction without acetate leaving group on allene.

Inspired from the work of Kakiuchi,[8] in 2020 the same research group reported the iron-catalyzed C−H hydroarylation of ketones with allenes achieved by weak oxygen coordination (Scheme 4.7).[5b] This represent the first method which utilizes a weakly-coordinating directing group

(**XIV**) for the functionalization with allenes, as previous transformations were limited to strong-coordinating bidentate directing groups.

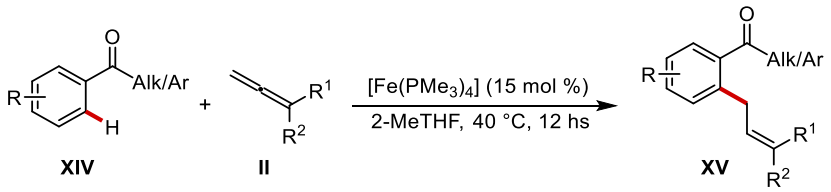

Scheme 4.7 Iron-catalyzed C−H alkylation of phenones with allenes **II**.

The mechanism of the iron catalyst was investigated in great detail through the structural characterization of key cyclometalated intermediates, kinetic analysis and comprehensive computational studies. As shown in Scheme 4.8, the catalytic cycle begins with the decoordination of one PMe_3 ligand from the $Fe(PMe_3)_4$ catalyst, followed by the coordination of phenone **XIV** to form the agostic complex **Int5**. Next, oxidative addition of **Int1** produces the iron(II) hydride intermediate **Int6** which rapidly isomerizes to **Int7**. The dissociation of one PMe_3 ligand from **Int7** creates a coordinatively unsaturated complex that, upon coordination with allene **II**, forms **Int8**. The authors proposed that the decoordination of PMe_3 is the rate-determining step of the catalytic reaction. Following the migratory insertion of the allene, intermediate **Int9** is generated. Finally, PMe_3 coordination, followed by reductive elimination and ligand exchange, regenerates $[Fe(PMe_3)_3]$ as the active catalyst and produces the desired product **XV**. Although this method presents a broad substrate scope with good to excellent yields, there are several limitations. Notably, it requires the use of 1,1-disubstituted allenes with bulky substituents, as the reactivity is completely shut down with less hindered ones or monosubstituted allenes. Moreover, the authors observed significant limitations in terms of functional group tolerance, as halogens, esters, nitriles, hydroxyl, and nitro groups, among others, were not suitable for the reaction.

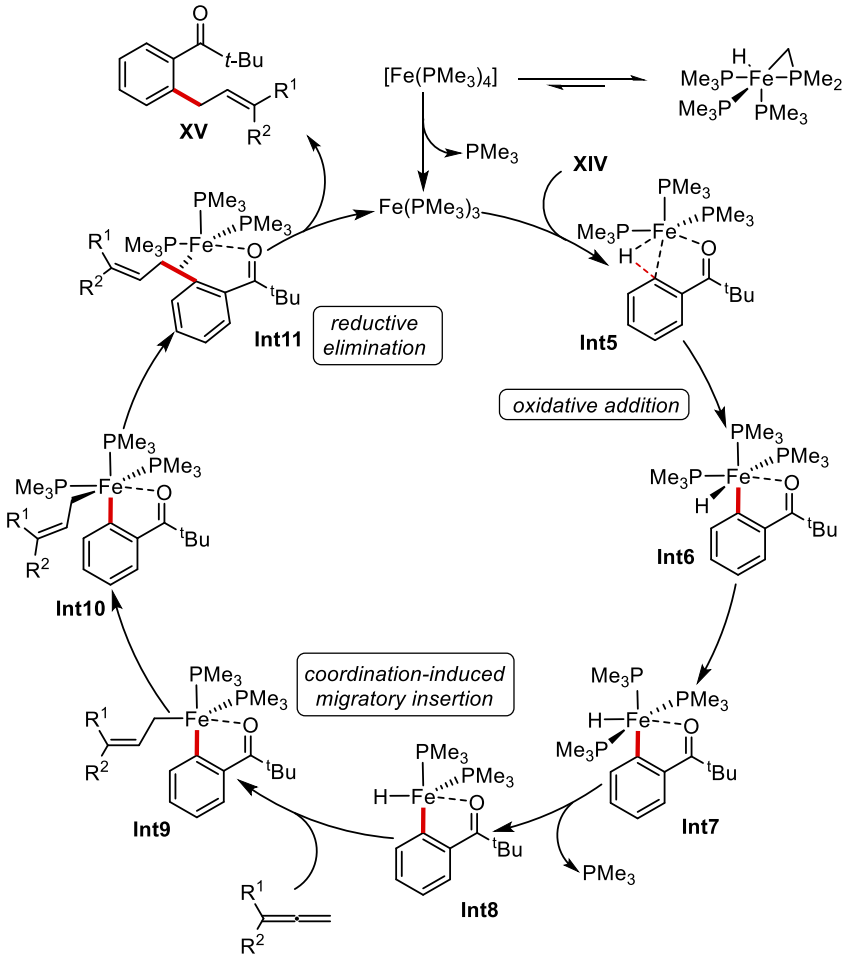

Scheme 4.8 Proposed catalytic cycle for iron-catalyzed C−H alkylation of phenones with allenes.

Significant progress in iron-catalyzed C–H functionalization reactions has been achieved by developing protocols for the site-selective activation of C(sp^2)–H bonds through chelation assistance with bidentate directing groups. Novel synthetic strategies leverage the coordination of an electron-deficient metal to a π-bond, thereby increasing the acidity of adjacent C–H bonds.[9] Consequently, after the deprotonative cleavage of the C–H bond, the resulting organometallic complex can undergo subsequent reactions with electrophiles, leading to entirely new functionalizations. In 2021, the Wang group reported an unprecedented iron-catalyzed method for functionalizing simple terminal allenes **XVI** at the internal, sterically less-accessible C(sp^2)−H bond.[10] This approach is suitable for synthesizing α-aminoalkyl 1,1-disubstituted allenes **XVIII** with high chemo- and regioselectivity. The transformation employs a cationic cyclopentadienyliron dicarbonyl complex, $[Cp^*Fe(CO)_2(thf)]^+BF_4^-$, as the catalyst. This complex enhances the acidity of the allenylic α-C−H bonds adjacent to the iron-complexed π-bond, thereby facilitating the contrasteric C−H functionalization upon reaction with an *in situ* generated iminium electrophile (Scheme 4.9).

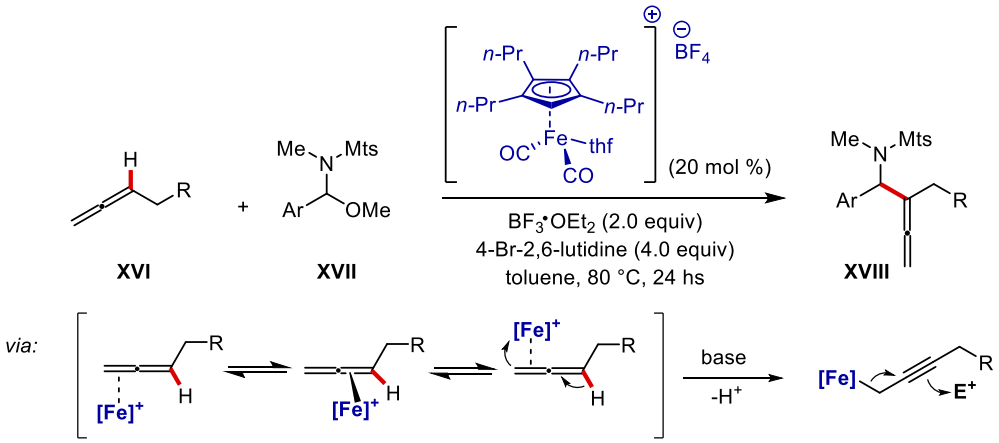

Scheme 4.9 Iron-catalyzed contrasteric functionalization of allenic C(sp^2)–H bonds.

4.1.3 Stereoselective Synthesis of *Z*-Olefins *via* C−H activation

Olefins are important intermediates in organic synthesis, commonly found in pharmaceuticals and other biologically active compounds.[11] Their defining feature is the presence of a π bond, which restricts rotation around the carbon−carbon σ-bond, imparting structural rigidity. This restricted rotation results in two distinct stereoisomeric forms of disubstituted alkenes, known as *E* and *Z* isomers.[12] One major challenge in olefins synthesis is controlling the stereochemical configuration (*E* or *Z*), which significantly affects their chemical and physical properties. While synthetic methods for *E*-olefins are well-established, synthesizing thermodynamically less stable *Z*-olefins remains a complex problem.

In recent years, transition-metal-catalyzed C−H activations have emerged as a powerful tool for the synthesis of value-added olefins using unsaturated hydrocarbons as reaction partners. Despite these advancements, C−H activation methods for synthesizing *Z*-olefins are still rare and mainly limited to the functionalization of heterocyclic indole substrates. Cobalt catalysts have been used for C−H/C−C activations of vinylcyclopropanes **XX** to synthesize *Z*-olefins (Scheme 4.10).[13] In this seminal report by Ackermann group, a cationic cobalt(III) catalyst enables the reaction under mild conditions with high levels of chemo- and diastereoselectivity.

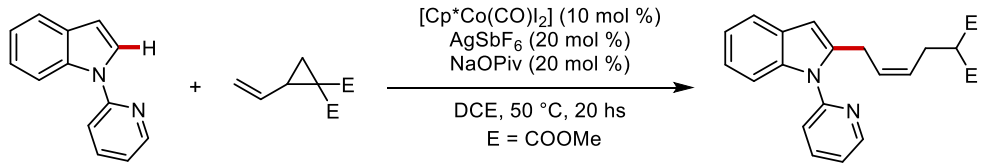

Scheme 4.10 Cobalt catalyzed C−H/C−C activation of indoles with vinylcyclopropanes.

Additionally, manganese-catalyzed C−H allylations with specifically designed allenyl ethylene carbonates **XXIII** have recently been reported as an effective method for producing alkenes with high *Z*-selectivity, attributed to the substantial steric hindrance imposed by the substituent on the allene moiety (Scheme 4.11).[14]

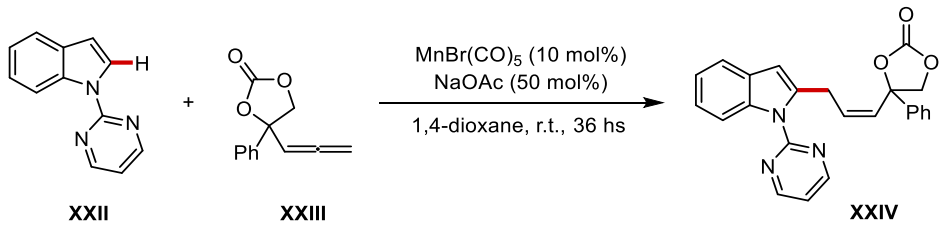

Scheme 4.11 Manganese catalyzed C−H/allylation of indoles with allenyl ethylene carbonates.

From a mechanistic perspective, the coordination of the allene to the cyclometalated species occurs in a stereoselective manner, as the allene approaches the metal with the enantioface that results in the least steric repulsion between its bulky substituent and the manganese ligands (Mode B, Scheme 4.12). Preliminary studies by the authors indicated that enhancing the Thorpe-Ingold effect from α-monosubstitution to α-trisubstitution on the allene moiety significantly amplifies steric congestion. This increase in steric hindrance consequently elevates the *Z*/*E* ratio, ultimately achieving exclusive *Z*-selectivity in the products.

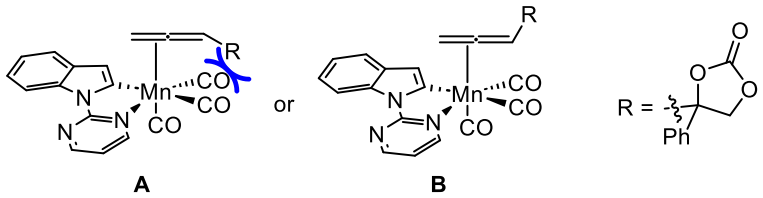

Scheme 4.12 Plausible coordination mode of allenyl ethylene carbonates for *Z*-selectivity.

The main limitation of this method lies in the need to synthesize allenes substituted at the α-position with bulky and difficult-to-install functional groups (**XXIII**). Additionally, the method's applicability is restricted to α-trisubstituted allenes, as α-monosubstitution and disubstitution led to poor levels of *Z*-selectivity.

4.2 Results and Discussion

4.2.1 Stereoselective Iron-catalyzed C−H Alkylations with Allenes: Expedient Access to Internal *Z*-Olefins

The synthesis of *Z*-olefins through *ortho* C−H activation of common benzamides remains largely unexplored. Among transition metal catalysts, iron stands out due to its abundance in the Earth's crust, cost-effectiveness, and low toxicity. Based on our recent discoveries regarding iron-catalyzed C−H activations using triazoles, we considered the potential of utilizing readily available allenes to investigate *Z*-selective, iron-catalyzed C−H alkylations. Our goal was to control the stereochemistry of the iron catalysis by leveraging the geometric constraints provided by the triazole directing group and the orthogonal cumulative π bonds of allenes, aiming for the synthesis of internal, disubstituted olefins.

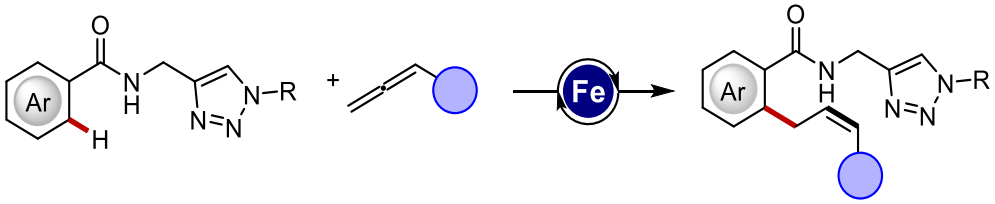

Scheme 4.13 *Z*-selective iron catalyzed C−H alkylation with allenes.

4.2.2 Optimization Studies

We started our investigation by probing triazolyl benzamide **1a** to various reaction conditions using mono-substituted allene **2a** which was readily obtained from the commercially available 1-octyne *via* the Crabbè-Ma reaction.[15] The optimized conditions for achieving *Z*-selective C−H alkylation involved using a bidentate diphosphine ligand like dppe, along with $ZnCl_2$ (2.0 equivalents) and PhMgBr (3.0 equivalents) as the base (entry 2). Among the ligands tested, 2,2'-bipyridine (entry 3) did not promote the desired transformation, while the structure of the diphosphine ligands had a significant impact on the outcome. More rigid ligands like dppen and dppbz resulted in lower yields of product **3aa** (entries 4-7). Using alkyl magnesium reagents hindered the catalysis, in contrast with previous reports on iron-catalyzed C−H annulations (entry 9). Zinc salts were also crucial; $ZnCl_2$ performed generally better than $ZnBr_2$, but when $ZnCl_2$ was used as a TMEDA adduct, no transformation occurred (entry 10). Similarly, the absence of $ZnCl_2$ negatively affected the iron-catalyzed C−H alkylation with allenes (entry 11). Other iron pre-catalysts such as $FeCl_2$ were effective for this reaction (entry 12), whereas commonly used transition metals like cobalt, nickel, or palladium did not facilitate any transformation under the same conditions (entries 13-15). This result highlighted the unique nature of the iron catalytic system. Moreover, the catalytic transformation was effective even at 25 °C, yielding **3aa** in good amounts (entry 16).

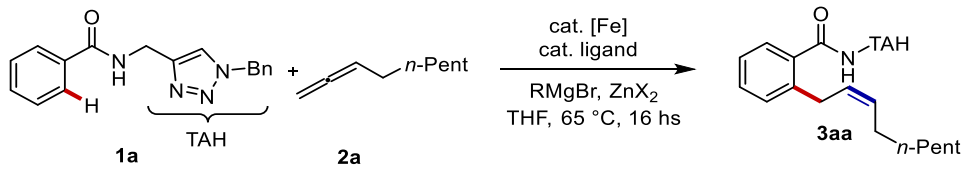

Entry[a]	Catalyst	Ligand	RMgBr	ZnX_2	**3aa** (%)[b]
1	$Fe(acac)_3$	dppe	PhMgBr	$ZnBr_2$	53
2	$Fe(acac)_3$	dppe	PhMgBr	$ZnCl_2$	80 (77)
3	$Fe(acac)_3$	2,2'-bipy	PhMgBr	$ZnCl_2$	n.d.
4	$Fe(acac)_3$	dppen	PhMgBr	$ZnBr_2$	45
5	$Fe(acac)_3$	dppen	PhMgBr	$ZnCl_2$	82 (78)
6	$Fe(acac)_3$	dppbz	PhMgBr	$ZnCl_2$	11
7	$Fe(acac)_3$	dppbz	PhMgBr	$ZnBr_2$	10
8[c]	$Fe(acac)_3$	dppe	PhMgBr	$ZnCl_2$	54 (50)
9	$Fe(acac)_3$	dppe	*i*-PrMgBr	$ZnCl_2$	20

10	$Fe(acac)_3$	dppe	PhMgBr	$ZnCl_2$TMEDA	n.d.
11	$Fe(acac)_3$	dppe	PhMgBr	--	n.d.
12	$FeCl_2$	dppe	PhMgBr	$ZnCl_2$	72
13	$Pd(OAc)_2$	dppe	PhMgBr	$ZnCl_2$	n.d.
14	$Ni(acac)_2$	dppe	PhMgBr	$ZnCl_2$	n.d.
15	$Co(acac)_2$	dppe	PhMgBr	$ZnCl_2$	n.d.
16[d]	$Fe(acac)_3$	dppe	PhMgBr	$ZnCl_2$	(70)

[a]Reaction conditions: **1a** (0.2 mmol), **2a** (0.4 mmol), [Fe] (0.03 mmol), ligand (0.03 mmol), RMgBr (0.6 mmol), ZnX_2 (0.4 mmol), THF (0.2 mL). [b]Yields determined using 1,3,5-trimethoxybenzene as the internal standard. In parenthesis, isolated yields. [c]THF (0.5 mL). [d] at 25 °C. dppe = 1,2-bis (diphenylphosphino)ethane; dppbz = 1,2-bis(diphenylphosphino) benzene; dppen = *cis*-1,2-bis(diphenylphosphino)ethene.

Table 4.1 Optimization of iron catalyzed C–H alkylation of benzamide **1a** with allene **2a**.

It is noteworthy that the widely used 8-aminoquinoline (Q) directing group was unsuitable for this type of transformation. Despite the screening of reaction parameters, we were unable to isolate any C−H alkylation product (Table 4.2). All the reaction led to a broad decomposition of the starting material. Upon analysis of the crude reaction mixtures *via* proton nuclear magnetic resonance and mass spectrometry, no experimental evidence was found to indicate the formation of the anticipated product.

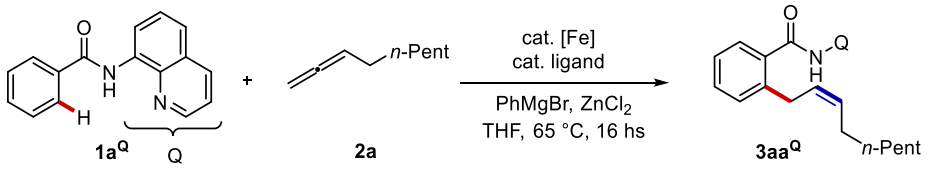

Entry[a]	Catalyst	Ligand	RMgBr	**3aa^{Q}**[b]
1	$Fe(acac)_3$	2,2'-bipy	PhMgBr	n.d.
2	$Fe(acac)_3$	dppe	PhMgBr	n.d.
3	$Fe(acac)_3$	dppen	PhMgBr	n.d.
4	$Fe(acac)_3$	dppbz	PhMgBr	n.d.

[a]Reaction conditions: **1a^{Q}** (0.2 mmol), **2a** (0.4 mmol), [Fe] (0.03 mmol), ligand (0.03 mmol), PhMgBr (0.6 mmol), $ZnCl_2$ (0.4 mmol), THF (0.3 mL). [b]Isolated yields.

Table 4.2: Screening of reaction conditions for Q-benzamide **1a^{Q}**.

4.2.3 Substrate Scope

Under the optimized catalytic conditions, we explored the substrate scope of the *Z*-selective, iron-catalyzed C−H alkylation protocol with benzamide derivatives (Scheme 4.14). Various methylene-tethered triazoles (**1b-d**) were compatible, although they produced the corresponding products (**3ba-da**) in moderate yields. A wide range of benzamides, functionalized with either electron-rich or electron-withdrawing groups at the *para* and *meta* positions, were generally well-suited for the reaction. Notably, the challenging nitrile derivative was also retained under the catalytic conditions (**3oa**). Importantly, the iron-catalyzed C−H alkylation protocol was effective in the presence of the synthetically versatile boronate group, yielding compound **3pa.** Finally, several heterocyclic compounds such as thiophene, benzo[*b*]thiophene and indole derivatives (**1u-w**) were smoothly converted into the corresponding products with good yields and chemoselectivity. In general, our protocol exhibits good yields and broad functional group tolerance. However, substitution at the *ortho*-position hinders the reaction, resulting in low yields of C−H alkylated benzamide **3xa**.

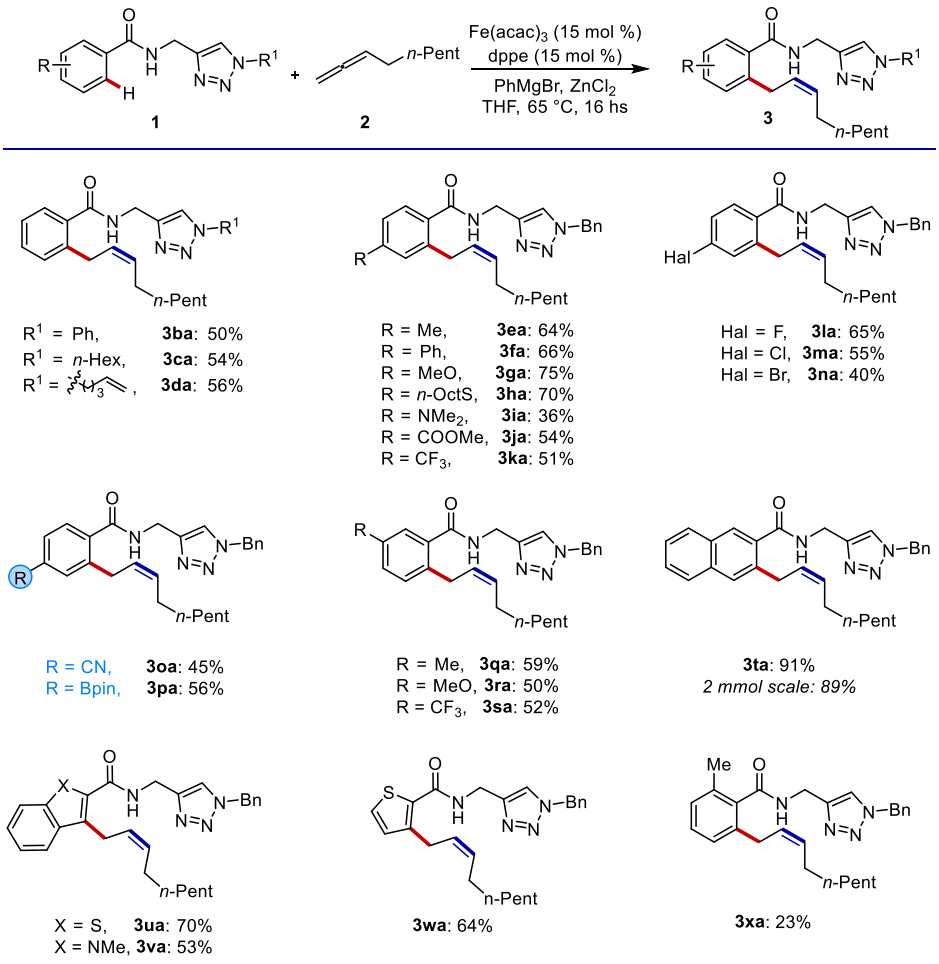

Scheme 4.14 Substrate scope of benzamides **1**.

Our method led to the synthesis of a broad family of alkylated products **3** with exclusive *Z*-selectivity, as confirmed by NMR analysis and single-crystal X-ray diffraction of compound **3ia** and **3la** as in example. The X-ray structure unequivocally confirms the *Z*-stereoisomerism of the double bond formed in the product formed after the alkylation reaction with the allene. Suitable crystals for X-ray diffraction were obtained by slow diffusion of hexane in an ethyl acetate solution of compound **5aa** and **3al.**

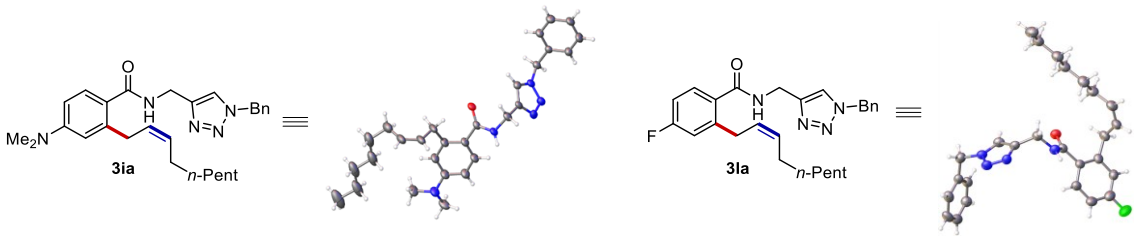

Figure 4.1: X-ray structures of products **3ia** and **3la**.

Next, we synthesized a variety of monosubstituted allenes with diverse decorations and used them as substrates for the iron-catalyzed C−H alkylation protocol (Scheme 4.15). All these compounds were obtained from commercially available terminal alkynes through common synthetic procedures. Both alkyl- and aryl-substituted allenes were efficiently converted into the corresponding products (**3ab-ad**) with good yields. Allenes attached to (thio)ethers and carbazole moieties were also well-tolerated (**3ae-ag**). A silyl-protected allenyl ether yielded the corresponding unprotected alcohol (**3ah**) directly after acidic work-up of the catalytic reaction. The iron catalysis demonstrated remarkable functional group tolerance, as compounds **3ai-ak**, functionalized with alkyl chlorides and esters, were all produced in good yields. Encouraged by these results, we extended the scope of the iron catalysis by synthesizing monosubstituted allenes decorated with complex synthetic scaffolds. For example, L-menthol and cholesterol-functionalized benzamides (**3al-am**) were obtained in synthetically useful yields, as well as a D-mannose diacetonide derivative (**3an**). Additionally, the effectiveness of the C−H alkylation method was confirmed when applied to pyrene and calix[4]arene macrocycle.

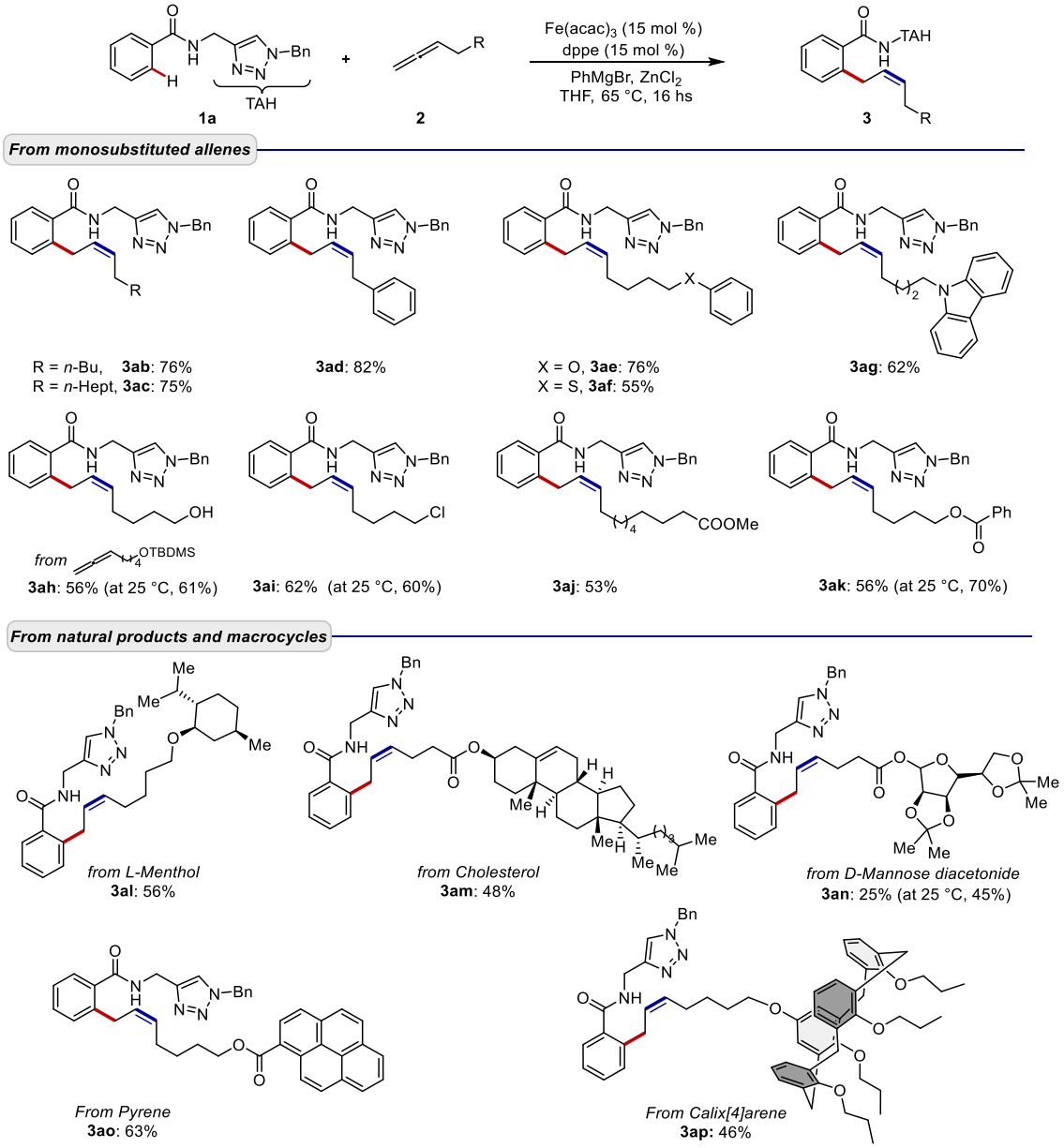

Scheme 4.15 Substrate scope for monosubstituted allenes **2**.

The reactivity of 1,1-disubstituted allenes was further investigated. Therefore, we synthetized a small family of 1,1-disubstituted allenylic compounds, which were submitted to the iron-catalyzed C–H alkylation protocol. The 1,1-alkyl allenes **2q** and **2s** were obtained starting from the corresponding commercially available alkyne, following a three-step procedure (Scheme 4.16). The first step involves a hydroxy methylation reaction of the alkyne using *n*-BuLi and paraformaldehyde. The product is then converted into the corresponding tosylate through a reaction with tosyl chloride in Et_2O in the presence of KOH. After protection, a final step of allylic substitution of the tosylate group with *n*-PentMgBr in the presence of a copper(I) salt was performed to deliver the desired products.

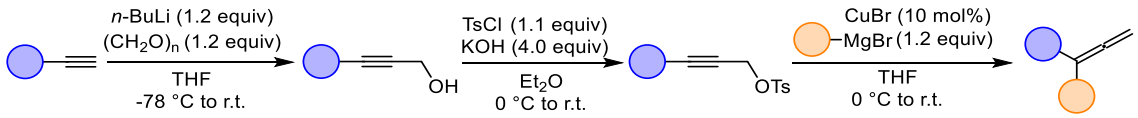

Scheme 4.16 General procedure for the synthesis of 1,1-alkyl allenes **2**.

In addition to the previously mentioned 1,1-alkyl allenes, two other asymmetric 1,1-disubstituted allenes (**2r**, **2t**), each containing a phenyl and an alkyl group, were synthesized. These allenes were obtained following a three-step procedure starting from the corresponding commercially available ketones (Scheme 4.17). The first step involves the addition of TMS-acetylene to the ketone using a strong base such as *n*-BuLi. The TMS group is then removed using TBAF in THF, which quantitatively delivers the corresponding terminal alkynyl intermediate. Finally, the desired allenes are obtained through the propargylic reduction using $AlCl_3$ and $LiAlH_4$.

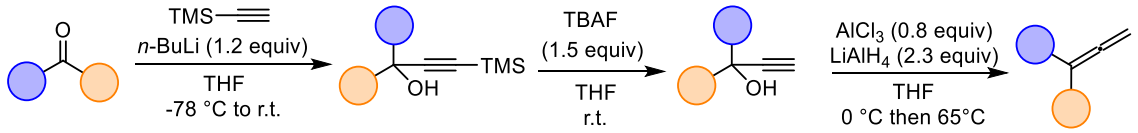

Scheme 4.17 General procedure for the synthesis of 1,1-alkyl, aryl allenes **2**.

After synthetizing the desired 1,1 disubstituted allenes, they were submitted to the optimized catalytic system (Scheme 4.18). A dialkyl derivative, such as **2q**, was reacted under standard conditions, resulting in product **3qa** with high yields. The remarkable *Z*-selectivity was also maintained for asymmetrical disubstituted allenes. Specifically, when allenes **2r-t** were subjected to iron catalysis, the corresponding products **3ar-at** were obtained with complete to high stereoselectivity and very good yields.

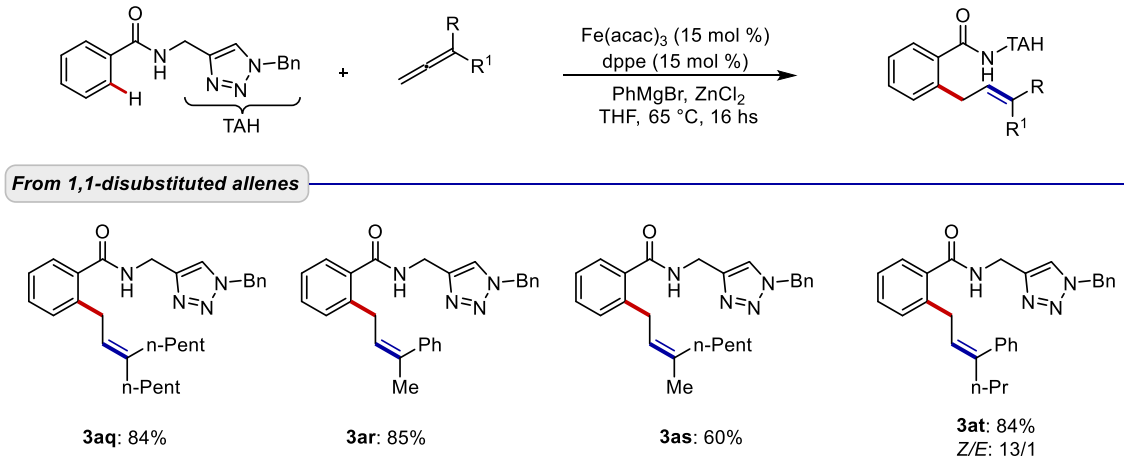

Scheme 4.18 Substrate scope for 1,1-disubstituted allenes **2**.

Among the catalytic products with 1,1-disubstituted allenes, the only one that showed the formation of the *E* isomer along with the *Z* main product was derivative **3at** with a 13:1 *Z*/*E* ratio. In contrast, product **3ar**, with a methyl and phenyl substituents, and product **3as**, with two different sterically hindered alkyl substituents, were obtained exclusively in the *Z*-configuration. In compound **3at**, the presence of the bulkier *n*-propyl group along with the phenyl one resulted in the possibility for the intermediate generated during the reaction to evolve into products with either the *Z* or *E* double bond configuration. The absolute configurations of the compounds were determined using 2D NMR spectroscopy, specifically through selective NOESY experiments, which unequivocally assigned the *Z*-isomerism to the double bonds of the alkylation products (See Experimental Part for more details).

Given the successful outcomes obtained from iron catalyzed C–H alkylation with both monosubstituted and disubstituted allenes, we decided to synthesize a racemic 1,1,3-trisubstituted allene **2u** which was obtained following a two-steps procedure (Scheme 4.19). The first and second steps, performed in a one-pot fashion, consist in the hydroxy methylation of phenylacetylene with acetaldehyde using *n*-BuLi as the base, followed by the *in situ* protection of the resulting propargylic alcohol with acetic anhydride. After purification, the intermediate was

submitted to an allylic substitution reaction using *n*-PentMgBr in the presence of a copper(I) salt and a lithium salt, yielding the desired product **2u**.

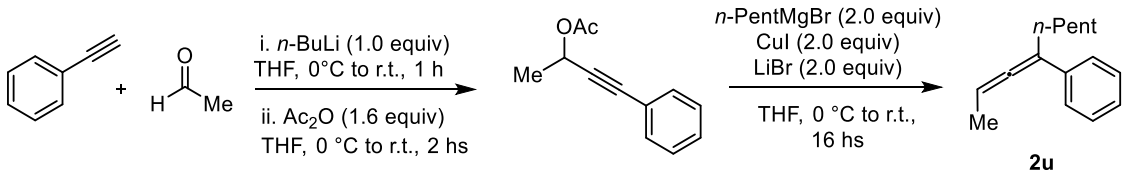

Scheme 4.19 Synthetic route for 1,1,3-trisubstituted allene **2u**.

The 1,1,3-trisubstituted allene was then tested under the optimized reaction conditions. However, despite achieving good stereocontrol, product **3au** was obtained only in low yields.

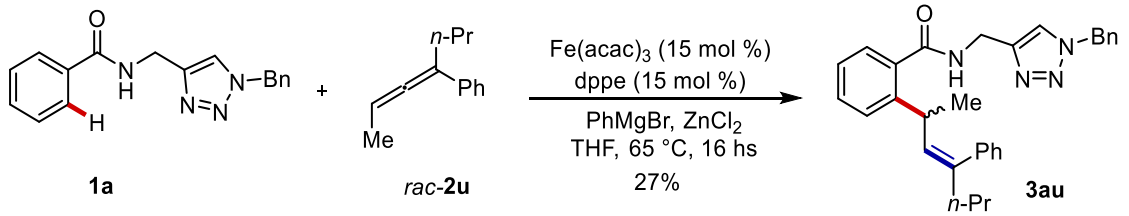

Scheme 4.20 Catalytic reaction with 1,1,3-trisubstituted allene **2u**.

4.2.4 Mechanistic Investigation

A series of mechanistic experiments were carried out to understand the catalyst working mode. Competition experiments using isotopically labelled benzamides [D]$_5$-**1b** and [D]-**1b** indicated no significant primary kinetic isotope effect (Scheme 4.21, a and b). Additionally, electron-deficient arenes **1k**/**1s** exhibited higher reactivity than their electron-rich counterparts **1e**/**1q** (Scheme 4.21, c and d). These observations suggest that the C−H metalation occurs through a ligand-to-ligand hydrogen transfer (LLHT) mechanism and is not rate-determining.

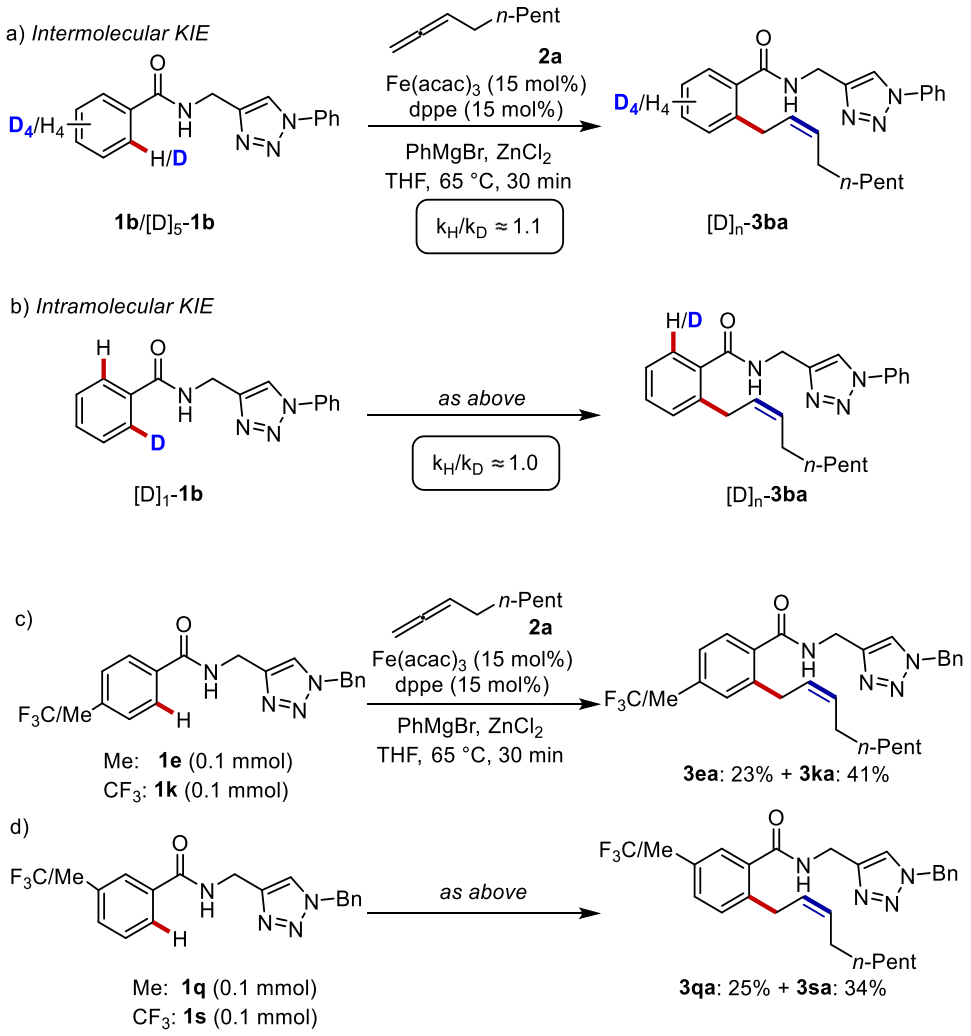

Scheme 4.21 KIE studies and competition experiments of iron-catalyzed C–H alkylation with allene **2a**.

The mechanistic investigation was extended by probing the reactivity of different isotopically labelled compounds. Under optimal catalytic conditions, compound [D]$_5$–**1a** was converted into the corresponding product without significant deuterium scrambling at the *ortho*-position (Scheme 4.22, a). This strongly suggests that the C−H activation process is irreversible. Additionally, when deuterated allene [D]$_2$-**2a** was used, the resulting product [D]$_2$-**3aa** retained its deuterium content completely (Scheme 4.22, b), supporting an irreversible migratory insertion step.

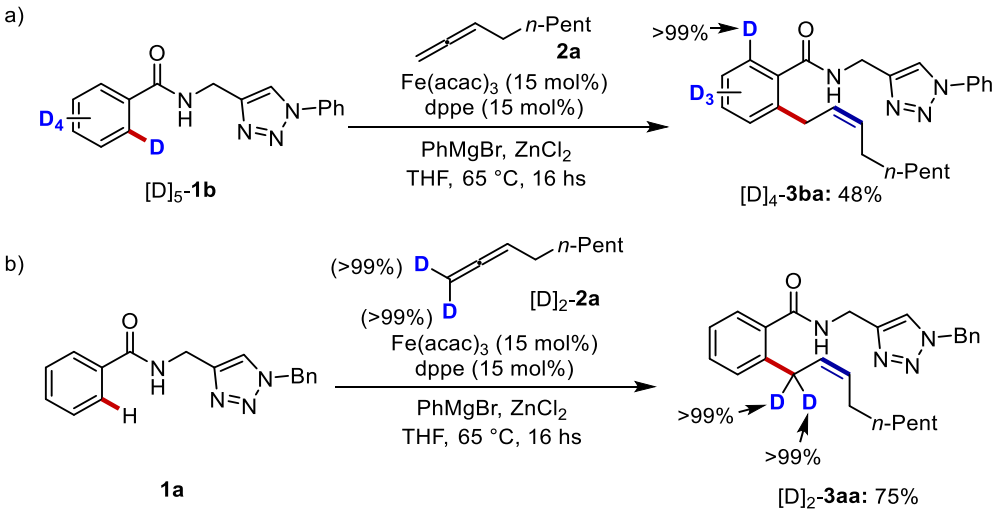

Scheme 4.22 Experiments with isotopically labelled substrates.

Finally, a competition experiment was conducted by submitting to the iron catalyst benzamide **1a** with an equimolar mixture of allene **2a** and styrene **4a** (Scheme 4.23). After 1 hour, only compound **3aa** was observed in the reaction mixture. This indicates that the migratory insertion of allenes into the key cyclometalated iron species is more favourable than that of styrenes.

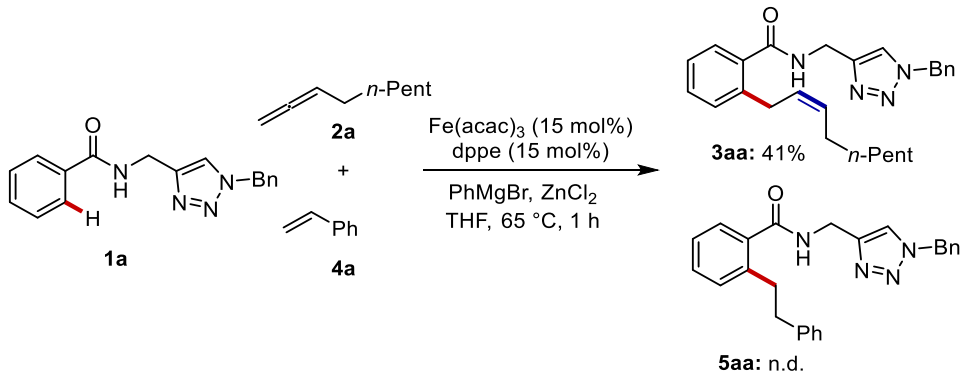

Scheme 4.23 Competition experiment with styrene.

Based on the results obtained, all catalytic alkylation products are linear, with no detectable formation of branched isomers. This suggests that the carbometalation step leads exclusively to the formation of the M-alkenyl intermediate rather than the M-allyl intermediate, which could otherwise evolve into a branched product.

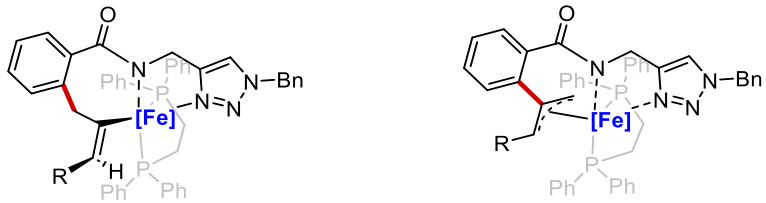

Scheme 4.24 Comparison between M-alkenyl and M-allyl intermediates.

4.2.5 Proposed Catalytic Cycle

From experimental data and prior mechanistic insights, we propose a catalytic cycle that begins with an easy C−H activation *via* a ligand-to-ligand hydrogen transfer (LLHT), resulting in the formation of intermediate **Int2**. This is followed by a stereo-determining, coordination-driven migratory insertion of the allene, producing the crucial cyclometalated species **Int3**. The high stereoselectivity that promotes the formation of *Z*-type alkenes is likely due to a preferred insertion from the less-shielded π face of allenes **2**. Finally, a proto-demetalation step yields product **3** and regenerates the active iron species **Int1**.

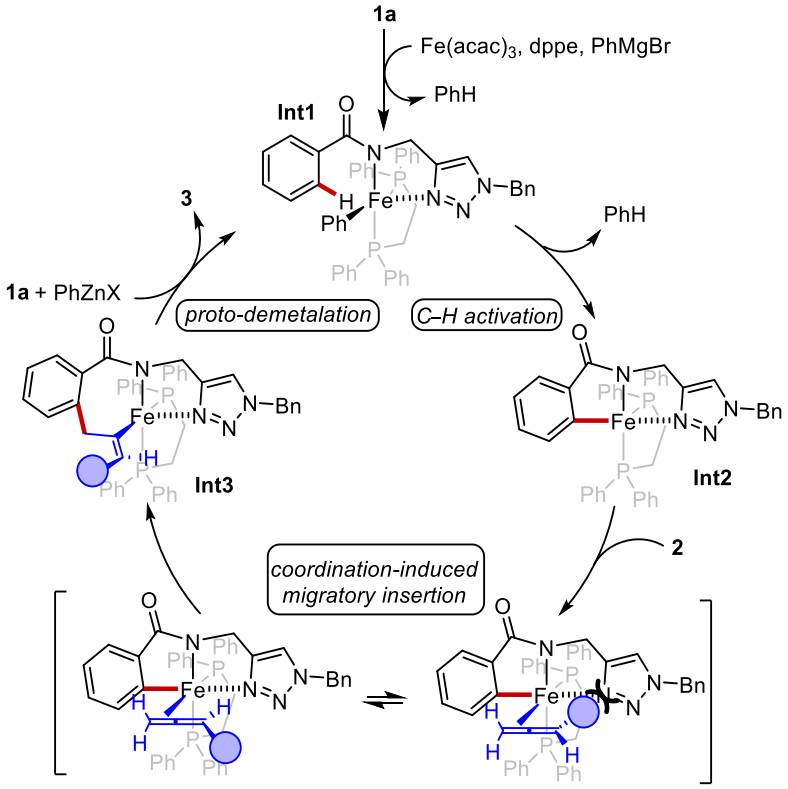

Scheme 4.25 Proposed reaction mechanism.

4.2.6 Removal of TAH Group and Late-stage Diversifications

The practical application of the iron-catalyzed C−H alkylation method was ultimately showcased through various orthogonal modifications of the triazole directing group (Scheme 4.26). For instance, compound **3ra** was converted into carboxylic acid **6ra** by initially protecting the secondary amide as a *tert*-butyloxycarbamate, followed by basic hydrolysis (Scheme 4.26, a). Through this two-step protocol, a mild deprotection of the directing group was achieved to restore the carboxylic acid functional group. Notably, **6ra** maintained the *Z*-configuration of the olefinic segment. The functionalization of **3aa** as a carbamate was further exploited to directly transform the amide into ketone **7aa** via a simple reaction with PhMgBr (Scheme 4.26, b). The use of m-CPBA facilitated a novel oxidative deprotection strategy for **3ab**, resulting in a synthetically versatile 3,4-dihydrocoumarin derivative **8ab** (Scheme 4.26, c). Finally, the TAH directing group could also be removed under acidic reaction conditions to afford the isochromanone derivative **9aa** (Scheme 4.26, d).

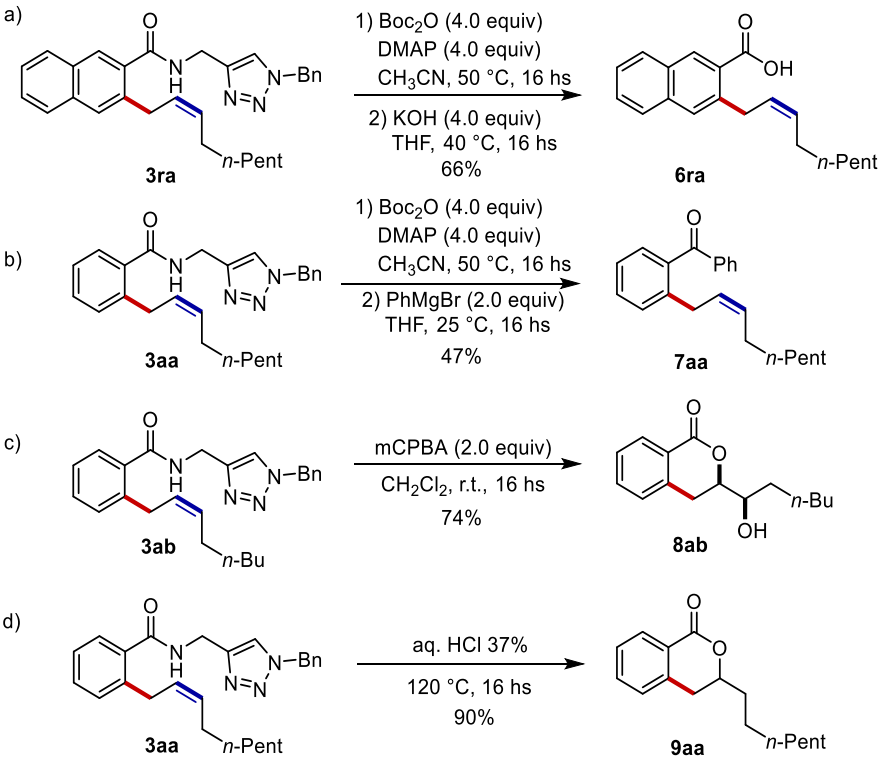

Scheme 4.26 TAH removal and late-stage synthetic diversification.

4.3 Conclusions

In conclusion, in this section we presented a novel method for the stereoselective synthesis of internal *Z*-olefins through iron-catalyzed C−H alkylations with allenes. This iron-catalyzed process exploits the unique properties of bioisosteric triazole directing groups to produce a wide range of alkylated benzamides, demonstrating broad scope and functional group tolerance, even with challenging boronate esters or nitriles. The newly developed protocol was found effective in the C−H alkylations with both monosubtituted and 1,1-disubstituted allenes, providing the desired product with excellent levels of *Z*-selectivity. Ultimately, the triazole could be removed, allowing straightforward access to a variety of synthetically valuable carbonyl-based compounds.

4.4 References

[1] a) A. Hoffmann-Roder, N. Krause, *Angew. Chem. Int. Ed.* **2004***, 43, 1196–1216*; b) P. Rivera-Fuentes, F. Diederich, *Angew. Chem. Int. Ed.* **2012**, *51*, 2818–2828; c) S. Yu, S. Ma, *Angew. Chem. Int. Ed.* **2012**, *51*, 3074–3112.

[2] a) S. Ma, *Chem. Rev*. **2005**, *105*, 7, 2829–2872; b) J. Ye, S. Ma, *Acc. Chem. Res*. **2014**, *47*, 989−1000; c) B. Yang, Y. Qiu, J. E. Backvall, *Acc. Chem. Res*. **2018**, *51*, 1520−1531.

[3] For recent reviews see: a) S.-M. Deng, Y.-X. Zhao, C. Wang, *Tetrahedron Chem*, 8, **2023**, 100049; b) X.-Lei Han, P.-Peng Lin, Q. Li, *Chinese Chemical Letters* **2019**, 30, 8, 1495–1502.

[4] Y.J. Zhang, E. Skucas, M.J. Krische *Org. Lett.* **2009**, *11*, 18, 4248–4250.

[5] For selected examples of C–H activation with allenes, see: [Fe] a) A. M. Messinis, J. C. A. Oliveira, C. Stückl, L. Ackermann, *ACS Catal.* **2022**, *12*, 9, 4947–4960; b) A. M. Messinis, L. H. Finger, L. Hu, L. Ackermann, *J. Am. Chem. Soc.* **2020**, *142*, 13102–13111; [Co] c) Y. Lin, T. von Münchow, L. Ackermann, *ACS Catal.* **2023**, *13*, 9713–9723; d) X.-J. Si, X. Zhao, J. Wang, X. Wang, Y. Zhang, D. Yang, M. P. Song, J.-L. Niu, *Chem. Sci.* **2023**, *14*, 7291–7303; e) T. H. Meyer, J. C. A. Oliveira, S. C. Sau, N. W. J. Ang, L. Ackermann, *ACS Catal.* **2018**, *8*, 9140−9147; f) S. Zhai, S. Qiu, X. Chen, C. Tao, Y. Li, B. Cheng, H. Wang, H. Zhai, *ACS Catal.* **2018**, *8*, 6645−6649; g) S. Nakanowatari, R. Mei, M. Feldt, L. Ackermann, *ACS Catal.* **2017**, *7*, 2511−2515; h) N. Thrimurtulu, A. Dey, D. Maiti, C. M. R. Volla, *Angew. Chem., Int. Ed.* **2016**, *55*, 12361−12365; [Ni] i) S. Nakanowatari, T. Müller, J. C. A. Oliveira, L. Ackermann, *Angew. Chem., Int. Ed.* **2017**, *56*, 15891−15895; [Ru] j) S. Nakanowatari, L. Ackermann, *Chem. -Eur. J.* **2015**, *21*, 16246−16251; [Rh] k) D.-S. Kong, Y.-F. Wang, Y.-S. Zhao, Q.-H. Li, Y.-X. Chen, P. Tian, G.-Q. Lin, *Org. Lett.* **2018**, *20*,1154−1157; l) Z.-J. Jia, C. Merten, R. Gontla, C. G. Daniliuc, A. P. Antonchick, H. Waldmann, *Angew. Chem., Int. Ed.* **2017**, *56*, 2429−2434; m) R. Zeng, S. Wu, C. Fu, S. Ma, *J. Am. Chem. Soc.* **2013**, *135*, 18284−18287; n) B. Ye, N. Cramer, *J. Am. Chem. Soc.* **2013**, *135*, 636−639; o) H. Wang, B. Beiring, D.-G. Yu, K. D. Collins, F. Glorius, *Angew. Chem., Int. Ed.* **2013**, *52*, 12430−12434; p) H. Wang, F. Glorius, *Angew. Chem. Int. Ed.* **2012**, *51*, 7318−7322; q) D. N. Tran, N. Cramer, *Angew. Chem., Int. Ed.* **2010**, *49*, 8181−8184.

[6] R. Kuppusamy, K. Muralirajan, C.H. Cheng, *ACS Catal.* **2016**, *6*, 6, 3909–3913.

[7] J. Mo, T. Müller, J. C. A. Oliveira, L. Ackermann, *Angew. Chem. Int. Ed*., **2018**, *57*, 7719 – 7723.

[8] N. Kimura, T. Kochi, F. Kakiuchi, *J. Am. Chem. Soc.* **2017**, *139*, 14849−14852.

[9] For a similar strategy applied to alkenyl C–H functionalization with different metals see: a) J. M. Schomaker, W. C. Boyd, I. C. Stewart, F. D. Toste, R. G. Bergman, *J. Am. Chem. Soc*. **2008**, *130*, 3777–3779; b) W. C. Boyd, M. R. Crimmin, L. E. Rosebrugh, J. M. Schomaker, R. G. Bergman, F. D. Toste, *J. Am. Chem. Soc*. **2010**, *132*, 16365–16367; c) C. Zhao, F. D. Toste, R. G. Bergman, *J. Am. Chem. Soc*. **2011**, *133*, 10787–10789; d) C. Zhao, M. R. Crimmin, F.D. Toste, R.G. Bergman, *Acc. Chem. Res.* **2014**, *47*, 517–529.

[10] Y. Wang, S. G. Scrivener, X.-D. Zuo, R. Wang, P. N. Palermo, E. Murphy, A. C. Durham, Y.-M. Wang, *J. Am. Chem. Soc.* **2021**, *143*, 14998–15004.

[11] J. M. J. Williams, Preparation of Alkenes: A Practical Approach; Oxford University Press: Oxford, U.K., **1996**.

[12] J. E. Blackwood, C. L. Gladys, K. L. Loening, A. E, Petrarca, J. E. Rush, *J. Am. Chem. Soc.* **1968**, *90*, 509.

[13] D. Zell, Q. Bu, M. Feldt, L. Ackermann, *Angew. Chem. Int. Ed.* **2016**, 55, 7408–7412.

[14] D. V. Kumar, B. Sundararaju, *J. Org. Chem.* **2024**, *89*, 10087–10092.

[15] J. Kuang, S. Ma, *J. Org. Chem.*, **2009**, *74*, 1763–1765.

4.5 Experimental Section

4.4.1 General remarks

Methods

All reactions were carried out in Schlenk tubes under a N_2 atmosphere using pre-dried glassware. THF was dried using a solvent purification system (SPS) from Inert. Yields refer to isolated compounds, estimated to be > 95% pure as determined by ^{1}H-NMR. Column chromatography was performed on silica gel 60 (40-63 mesh). Melting points were measured with an Electrothermal apparatus and are uncorrected. NMR spectra were recorded on a Bruker 400 MHz and JEOL 600 MHz using solvents as internal standards (7.26 ppm for ^{1}H-NMR and 77.00 ppm for ^{13}C-NMR for $CDCl_3$). The terms m, s, d, t, q, and quint represent multiplet, singlet, doublet, triplet, quadruplet, and quintuplet respectively, and the term bs means a broad signal. ^{13}C-DEPTQ NMR spectra are reported for all compounds. Mass spectra were recorded in the ESI mode. Exact masses were recorded on a LTQ ORBITRAP XL Thermo Mass Spectrometer (ESI source).

Materials

PhMgBr (1.0 M in THF) was freshly prepared from Bromobenzene ≥99.5% (GC) and magnesium turnings in anhydrous THF and titrated prior to use using I_2 in THF. The solution of $ZnCl_2$ in THF (1.0 mol/L) was prepared in a Schlenk tube by melting anhydrous $ZnCl_2$ at 230 °C under vacuum for 3 hours. Then, dry THF was added and the solution was stirred until all the $ZnCl_2$ was dissolved.

4.4.2 Synthesis of Benzamide Substrates

General procedure A: synthesis of benzamide substrates

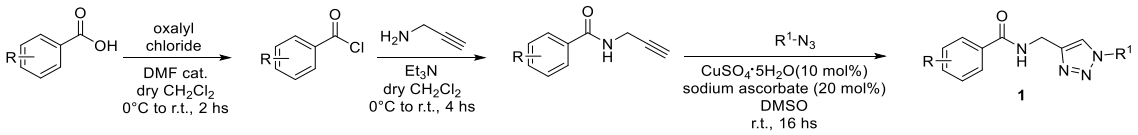

Oxalyl chloride (1.1 equiv.) was added dropwise to a mixture of the carboxylic acid (1.0 equiv.), DMF (cat.) in dry CH_2Cl_2 under a nitrogen atmosphere at 0 °C. The mixture was stirred at the same temperature for 2 hs upon which it was allowed to warm up to ambient temperature. The crude acyl chloride was cooled to 0 °C and it was added dropwise to a solution of propargylamine (1.5 equiv.), NEt_3 (3.0 equiv.) in dry CH_2Cl_2 (10 mL) at 0 °C under a nitrogen atmosphere. The mixture was initially stirred at the same temperature and then at ambient temperature for 4 hs. To the reaction was added sat. aqueous $NaHCO_3$ (20 mL). The aqueous layers were extracted with CH_2Cl_2 (3x20 mL). The combined organic extracts were washed with HCl (1.0 M, 20 mL), brine and dried over Na_2SO_4. The filtrate was concentrated under reduced pressure. The crude product was further submitted to the corresponding azide (1.5 equiv.), $CuSO_4 \cdot 5H_2O$ (10 mol %), sodium ascorbate (20 mol %) in DMSO (10 mL). After 16 hs, the reaction was quenched with sat. aqueous NH_4Cl (40 mL). The aqueous layers were extracted with EtOAc (3x40 mL). The combined organic extracts were dried over Na_2SO_4 and the filtrate was concentrated under reduced pressure. The crude product was purified by column chromatography on silica gel.

General procedure B: synthesis of benzamide substrates

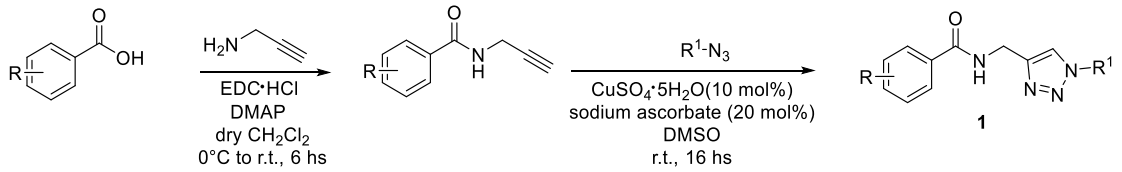

Propargylamine (1.2 equiv.) was added dropwise to a mixture of the carboxylic acid (1.0 equiv.), EDC•HCl (1.2 equiv.) and DMAP (cat.) in dry CH_2Cl_2 under a nitrogen atmosphere at 0 °C. The mixture was initially stirred at the same temperature and then at ambient temperature for 6 hs. To the reaction was added sat. aqueous $NaHCO_3$ (20 mL). The aqueous layers were extracted with CH_2Cl_2 (3x20 mL). The combined organic extracts were washed with HCl (1.0 M, 20 mL), brine and dried over Na_2SO_4. The filtrate was concentrated under reduced pressure. The crude product was further submitted to the corresponding azide (1.5 equiv.), $CuSO_4 \cdot 5H_2O$ (10 mol %), sodium

ascorbate (20 mol %) in DMSO (10 mL). After 16 hs, the reaction was quenched with sat. aqueous NH_4Cl (40 mL). The aqueous layers were extracted with EtOAc (3x40 mL). The combined organic extracts were dried over Na_2SO_4 and the filtrate was concentrated under reduced pressure. The crude product was purified by column chromatography on silica gel.

Amides **1a-1n, 1q-t, 1v-x** were synthetized according to the general procedure **A** starting from the carboxylic acid derivative or directly from the corresponding acyl chloride. The characterization data were consistent with those reported in the literature.[1, 2]

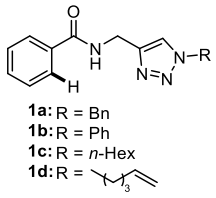

1a: R = Bn
1b: R = Ph
1c: R = *n*-Hex
1d: R =

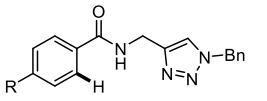

1e: R = Me
1f: R = Ph
1g: R = OMe
1h: R = *n*-OctS
1i: R = NMe_2
1j: R = COOMe
1k: R = CF_3
1l: R = F
1m: R = Cl
1n: R= Br
1o: R = CN
1p: R = Bpin

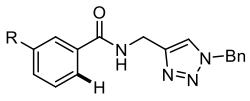

1q: R = Me
1r: R = OMe
1s: R = CF_3

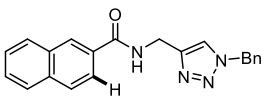

1t

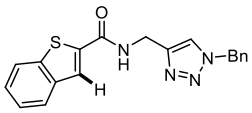

1u

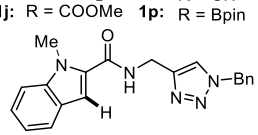

1v

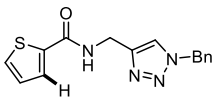

1w

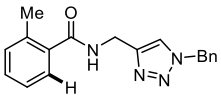

1x

_N_-[(1-Benzyl-1_H_-1,2,3-triazol-4-yl)methyl]-4-cyanobenzamide (1o)

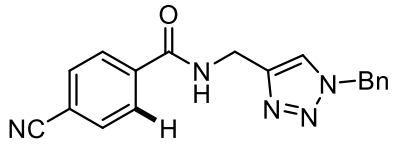

The general procedure *B* was followed using 4-cyanobenzoic acid (441 mg, 3.0 mmol) and benzyl azide (598 mg, 4.5 mmol). Purification by column chromatography (**n**-Hexane/EtOAc 1:1→ 3:7) yielded *1o* (561 mg, 59%) as a white solid. M.p.= 176-177 °C. ^{1}H-NMR (400 MHz, $CDCl_3$): δ = 7.95 (d, *J* = 8.4 Hz, 2H), 7.81 (t, *J* = 5.4 Hz, 1H), 7.70 (d, *J* = 8.3 Hz, 2H), 7.63 (s, 1H), 7.40 (dd, *J* = 5.1, 1.9 Hz, 3H), 7.33 – 7.29 (m, 2H), 5.53 (s, 2H), 4.69 (d, *J* = 5.3 Hz, 2H). ^{13}C-NMR (101 MHz, $CDCl_3$): δ = 165.7 (C_q), 137.9 (2 x C_q), 134.2 (C_q), 132.4 (CH), 129.2 (CH), 129.0 (CH), 128.2 (CH), 127.9 (2 x CH), 118.1 (C_q), 115.1 (C_q), 54.4 (CH_2), 35.4 (CH_2). MS (ESI) *m/z* (relative intensity): 340 (100) $[M+Na]^+$, 318 (52) $[M+H]^+$. HR-MS (ESI) *m/z* calcd for $C_{18}H_{16}N_5O$ $[M+H]^+$ 318.1349, found 318.1347.

_N_-[(1-Benzyl-1_H_-1,2,3-triazol-4-yl)methyl]-4-(4,4,5,5-tetramethyl-1,3,2-dioxaborolan-2-yl)benzamide (1p)

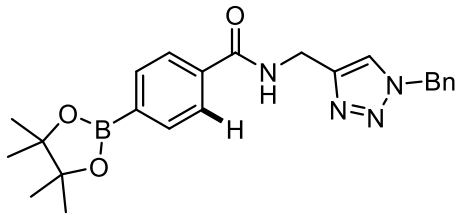

The general procedure *B* was followed using 14-(4,4,5,5-tetramethyl-1,3,2-dioxaborolan-2-yl) benzoic acid (744 mg, 3.0 mmol) and benzyl azide (598 mg, 4.5 mmol). Purification by column chromatography (**n**-Hexane/EtOAc 1:1→ 3:7) yielded *1p* (527 mg, 42%) as a white solid. M.p.= 149-150 °C. ^{1}H-NMR (400 MHz, $CDCl_3$): δ = 7.87 (d, *J* = 7.8 Hz, 2H), 7.78 (d, *J* = 8.1 Hz, 2H), 7.56 (s, 1H), 7.39 – 7.37 (m, 3H), 7.32 – 7.29 (m, 2H), 7.03 (t, *J* = 5.6 Hz, 1H), 5.52 (s, 2H), 4.71 (d, *J* = 5.4 Hz, 2H), 1.37 (s, 12H). ^{13}C-NMR (101 MHz, $CDCl_3$): δ = 167.3 (C_q), 145.0 (C_q), 136.1 (C_q), 135.1 (CH), 134.4 (C_q), 129.2 (CH), 128.9 (CH), 128.2 (CH), 126.1 (CH), 122.4 (CH), 84.2 (C_q), 54.3 (CH_2), 35.4 (CH_2), 24.9 (CH_3). The carbon directly attached to the boron atom was not detected due to quadrupolar broadening.[3] MS (ESI) *m/z* (relative intensity): 441 (100) $[M+Na]^+$. HR-MS (ESI) *m/z* calcd for $C_{23}H_{28}BN_4O_3$ $[M+H]^+$ 419.2249, found 419.2253.

_N_-[(1-Benzyl-1_H_-1,2,3-triazol-4-yl)methyl]benzo[_b_]thiophene-2-carboxamide (1u)

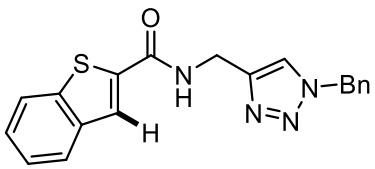

The general procedure *A* was followed using benzo[*b*]thiophene-2-carboxylic acid (534 mg, 3.0 mmol) and benzyl azide (598 mg, 4.5 mmol). Purification by column chromatography (**n**-Hexane/EtOAc 1:1→ 3:7) yielded *1u* (679 mg, 65%) as a white solid. M.p.= 204-205 °C. ^{1}H-NMR (400 MHz, $CDCl_3$): δ = 7.89 – 7.81 (m, 2H), 7.80 (d, *J* = 0.8 Hz, 1H), 7.59 (s, 1H), 7.47 – 7.37 (m, 5H), 7.32 – 7.29 (m, 2H), 7.03 (t, *J* = 5.7 Hz, 1H), 5.54 (s, 2H), 4.73 (d, *J* = 5.7 Hz, 2H). ^{13}C-NMR (101 MHz, $CDCl_3$): δ = 162.4 (C_q), 141.0 (C_q), 139.1 (C_q), 138.1 (C_q), 134.4 (2 x C_q), 129.2 (CH), 128.9 (CH), 128.2 (2 x CH), 126.4 (CH), 125.5 (CH), 125.1 (CH), 124.9 (CH), 122.7 (CH), 54.4 (CH_2), 35.4 (CH_2). MS (ESI) *m/z* (relative intensity): 371 (76) $[M+Na]^+$, 349 (100) $[M+H]^+$. HR-MS (ESI) *m/z* calcd for $C_{19}H_{17}N_4OS$ $[M+H]^+$ 349.1118, found 349.1116.

4.4.3 Synthesis of Allenes Substrates

General procedure C for monosubstituted allene synthesis[4]

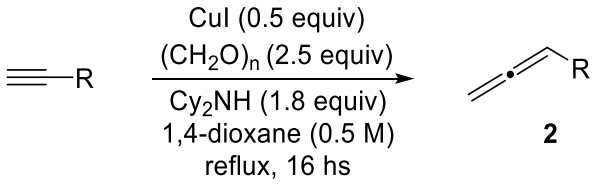

Copper iodide (0.5 equiv.), $(CH_2O)_n$ (2.5 equiv.), 1,4-dioxane (0.5 M), the corresponding alkyne (1.0 equiv.) and dicyclohexylamine (1.8 equiv.) were added sequentially into a two-neck flask equipped with a magnetic stir bar and a reflux condenser, under nitrogen atmosphere. The resulting mixture was then stirred under reflux for 16 hs. Subsequently, water and Et_2O were added and then the aqueous solution was separated and extracted with Et_2O. The organic layers were then dried over anhydrous Na_2SO_4 and filtered through celite to remove insoluble solids. The filtrate was concentrated, and the residue was purified by column chromatography on silica gel to afford the desired allene **2**.

General procedure D for 1,1-disubstituted allene synthesis *via* Allylic Substitution[5]

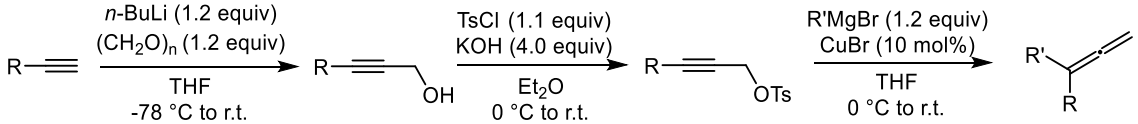

Step 1. To a solution of the corresponding alkyne in THF (1.25 M) cooled to –78 °C, *n*-BuLi (2.5 M in *n*-Hexane, 1.2 equiv.) was added dropwise. The reaction mixture was allowed to warm to 0 °C and stirred for 1 h. Then the solution was cooled to –78 °C again and paraformaldehyde (1.2 equiv.) was added. The reaction mixture was allowed to warm to r.t. and stirred for 16 hs. To the reaction was added sat. aqueous NH_4Cl (20 mL) and the aqueous layer was extracted with Et_2O (3x20 mL). The combined organic extracts were dried over Na_2SO_4 and the filtrate was concentrated under reduced pressure. The crude product was directly used in the next step without further purification.

Step 2. To a solution of the corresponding propargylic alcohol in Et_2O (0.5 M) was added tosyl chloride (1.2 equiv.). The reaction mixture was cooled to 0 °C, then KOH (freshly pestled, 3 g / 10 mmol substrate) was added in small portions. The reaction mixture was warmed to room temperature and the progress of the reaction was monitored by TLC. After the reaction was

completed, to the reaction mixture was added iced water and the aqueous phase was extracted with Et_2O (3×50 mL). The combined organic phases were washed with brine and dried over Na_2SO_4 and the filtrate was concentrated under reduced pressure. The crude product was directly use in the next step without further purification.

Step 3. To a solution of the corresponding tosylate (1.0 equiv.) in THF (0.5 M) was added CuBr (10 mol %). The reaction mixture was cooled to 0 °C, then the corresponding Grignard reagent (1.25 equiv., 1.0 M in THF) was added dropwise. The reaction mixture was allowed to warm to room temperature and stirred until the complete consumption of the starting material, judged by TLC (*n*-Hexane/EtOAc). Afterwards, it was quenched by the addition of a saturated aqueous solution of NH_4Cl (10 mL) followed by extraction with Et_2O (3×20 mL). The combined organic extracts were dried over Na_2SO_4 and the filtrate was concentrated under reduced pressure. The crude product was purified by column chromatography on silica gel.

General procedure E for 1,1-disubstituted allene synthesis from Ketones

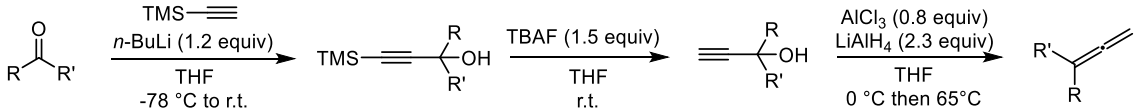

Step 1. To a solution of trimethylsilylacetylene (1.2 equiv.) in THF (1.25 M) cooled to –78 °C, *n*-BuLi (2.5 M in *n*-Hexane, 1.2 equiv.) was added dropwise. After being stirred at the same temperature for 30 min, a solution of the desired ketone (1.0 equiv.) in THF was added over a period of 10 min. The reaction mixture was allowed to warm to r.t. and stirred until the complete consumption of the starting material, judged by TLC (*n*-Hexane/EtOAc). Afterwards, it was quenched by the addition of a saturated aqueous solution of NH_4Cl (10 mL) followed by extraction with Et_2O (3×20 mL). The combined organic extracts were dried over Na_2SO_4 and the filtrate was concentrated under reduced pressure. The crude product was directly use in the next step without further purification or purified by a short pad on silica gel (if necessary).

Step 2. To a solution of the corresponding TMS-propargylic alcohol in THF (0.5 M) was added tetrabutylammonium fluoride (1.5 equiv.). The reaction mixture was stirred at room temperature until the complete consumption of the starting material, judged by TLC (*n*-Hexane/EtOAc). Afterwards, water was added and the aqueous layer was extracted with EtOAc (3x40 mL). The combined organic extracts were dried over Na_2SO_4 and the filtrate was concentrated under reduced pressure. The crude product was directly use in the next step without further purification.

Step 3.[5] A suspension of $AlCl_3$ (0.8 equiv.) in THF (1 mL / 100 mg $AlCl_3$) was cooled to 0 °C followed by a slow addition of a suspension of $LiAlH_4$ (2.3 equiv.) in THF (1 mL / mmol $LiAlH_4$). After stirring for 15 minutes a solution of the corresponding propargylic alcohol in THF (2.0 M) was added. The reaction mixture was heated under reflux for 16 hs. Afterwards, it was cooled to 0 °C and quenched by a slow addition of an aqueous solution of NaOH (15% w/w) and additional water. The aqueous layer was extracted with Et_2O (3×20 mL) and the combined organic extracts were dried over Na_2SO_4. The filtrate was concentrated under reduced pressure and purified by column chromatography on silica gel.

Nona-1,2-diene (2a)

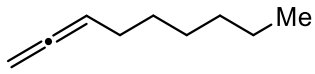

The compound was synthesized from 1-Octyne (4.4 mL, 30.0 mmol, 1.0 equiv.) according to general procedure **C**. The crude product was purified by column chromatography on silica gel (pure *n*-Pentane), affording **2a** (1.5 g, 42%) as a colourless liquid. ^{1}H-NMR (400 MHz, $CDCl_3$): δ = 5.12 (p, *J* = 6.8 Hz, 1H), 4.67 (dt, *J* = 6.5, 3.2 Hz, 2H), 2.07 – 1.97 (m, 2H), 1.49 – 1.24 (m, 8H), 0.91 (t, *J* = 7.0 Hz, 3H). The NMR data are consistent with the reported literatures.[6]

Octa-1,2-diene (2b)

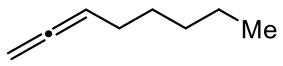

The compound was synthesized from 1-Heptyne (3.9 mL, 30.0 mmol, 1.0 equiv.) according to general procedure **C**. The crude product was purified by column chromatography on silica gel (pure *n*-Pentane), affording **2b** (1.1 g, 35%) as a colourless liquid. ^{1}H-NMR (400 MHz, $CDCl_3$): δ = 5.12 (p, *J* = 6.8 Hz, 1H), 4.67 (dt, *J* = 6.5, 3.2 Hz, 2H), 2.08 – 1.96 (m, 2H), 1.51 – 1.39 (m, 2H), 1.39 – 1.24 (m, 4H), 0.91 (t, *J* = 6.9 Hz, 3H). The NMR data are consistent with the reported literatures.[7]

Undeca-1,2-diene (2c)

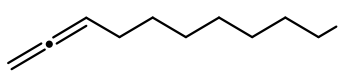

The compound was synthesized from 1-Decyne (1.8 mL, 10.0 mmol, 1.0 equiv.) according to general procedure **C**. The crude product was purified by column chromatography on silica gel (pure *n*-Pentane), affording **2c** (0.81 g, 53%) as a colourless liquid. ^{1}H-NMR (400 MHz, $CDCl_3$): δ = 5.12 (p, *J* = 6.8 Hz, 1H), 4.67

(dt, *J* = 6.5, 3.2 Hz, 2H), 2.07 – 1.97 (m, 2H), 1.49 – 1.39 (m, 2H), 1.39 – 1.25 (m, 10H), 0.91 (t, *J* = 6.9 Hz, 3H). The NMR data are consistent with the reported literatures.[4]

Buta-2,3-dien-1-ylbenzene (2d)

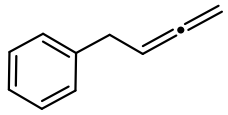

The compound was synthesized from 3-Phenyl-1-propyne (2.4 mL, 20.0 mmol, 1.0 equiv.) according to general procedure **C**. The crude product was purified by column chromatography on silica gel (pure *n*-Hexane), affording **2d** (1.82 g, 70%) as a colourless liquid. ^{1}H-NMR (400 MHz, $CDCl_3$): δ = 7.34 (dd, *J* = 8.1, 6.7 Hz, 2H), 7.29 – 7.22 (m, 3H), 5.31 (p, *J* = 7.0 Hz, 1H), 4.75 (dt, *J* = 6.5, 2.9 Hz, 2H), 3.40 (dt, *J* = 7.3, 2.9 Hz, 2H). The NMR data are consistent with the reported literatures.[8]

(Hepta-5,6-dien-1-yloxy)benzene (2e)

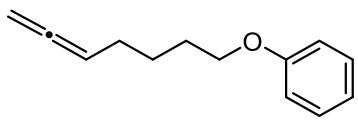

The compound **2e** was synthesized according to the following two step procedure.

Step 1. To a two-neck round-bottom flask was added phenol (471 mg, 5.0 mmol, 1.0 equiv.), 5-Hexyn-1-ol (589 mg, 6.0 mmol, 1.2 equiv.), triphenylphosphine (1.57 g, 6.0 mmol, 1.0 equiv.), and THF (5.0 mL). The reaction mixture was cooled to 0 °C and then diisopropylazodicarboxylate (1.18 mL, 6.0 mmol, 1.2 equiv.) was added dropwise. The mixture was initially stirred at the same temperature and then at ambient temperature for 16 hs. To the reaction was added sat. aqueous $NaHCO_3$ (20 mL). The aqueous layers were extracted with CH_2Cl_2 (3x20 mL). The combined organic extracts were dried over Na_2SO_4 and the filtrate was concentrated under reduced pressure. The crude product was purified by column chromatography on silica gel (*n*-Hexane/EtOAc).

Step 2. Compound **2e** was synthesized from the corresponding alkyne according to general procedure **C**. The crude product was purified by flash chromatography on silica gel (*n*-Hexane/EtOAc 95:5), affording **2e** (424 mg, 45%, over two steps) as a colourless oil. ^{1}H-NMR (400 MHz, $CDCl_3$): δ = 7.33 – 7.29 (m, 2H), 7.00 – 6.87 (m, 3H), 5.14 (p, *J* = 6.7 Hz, 1H), 4.70 (dt, *J* = 6.6, 3.2 Hz, 2H), 3.99 (t, *J* = 6.5 Hz, 2H), 2.14 – 2.07 (m, 2H), 1.89 – 1.82 (m, 2H), 1.68 – 1.59 (m, 2H). The NMR data are consistent with the reported literatures.[9]

Hepta-5,6-dien-1-yl(phenyl)sulfane (2f)

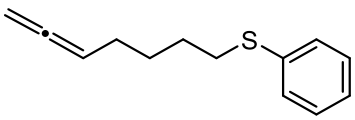

The compound **2f** was synthesized according to the following two step procedure.

Step 1. To a solution of thiophenol (550 mg, 5.0 mmol, 1.0 equiv.) in acetone (12.0 mL) was added K_2CO_3 (1.04 g, 7.5 mmol, 1.5 equiv.). The reaction mixture was stirred at room temperature for 30 min and then 6-chloro-1-hexyne (874 mg, 7.5 mmol, 1.5 equiv.) was added. The mixture was heated under reflux for 16 hs. To the reaction was added sat. aqueous $NaHCO_3$ (20 mL). The aqueous layers were extracted with CH_2Cl_2 (3x20 mL). The combined organic extracts were dried over Na_2SO_4 and the filtrate was concentrated under reduced pressure. The crude product was purified by column chromatography on silica gel (*n*-Hexane/EtOAc).

Step 2. Compound **2f** was synthesized from the corresponding alkyne according to general procedure **C**. The crude product was purified by flash chromatography on silica gel (*n*-Hexane/EtOAc 95:5), affording **2f** (378 mg, 37%, over two steps) as a colourless oil. ^{1}H-NMR (400 MHz, $CDCl_3$): δ = 7.37 – 7.33 (m, 2H), 7.33 – 7.27 (m, 2H), 7.23 – 7.15 (m, 1H), 5.10 (p, *J* = 6.7 Hz, 1H), 4.68 (dt, *J* = 6.6, 3.2 Hz, 2H), 2.95 (t, *J* = 7.3 Hz, 2H), 2.08 – 2.01 (m, 2H), 1.77 – 1.68 (m, 2H), 1.63 – 1.54 (m, 2H). ^{13}C-NMR (101 MHz, $CDCl_3$): δ = 208.5 (C_q), 136.9 (C_q), 128.9 (2 x CH), 125.7 (CH), 89.6 (CH), 74.9 (CH_2), 33.4 (CH_2), 28.6 (CH_2), 28.2 (CH_2), 27.7 (CH_2). MS (ESI) *m/z* (relative intensity): 227 (31) $[M+Na]^+$, 205 (100) $[M+H]^+$. HR-MS (ESI) *m/z* calcd for $C_{13}H_{17}S$ $[M+H]^+$ 205.1045, found 205.1047.

9-(Hepta-5,6-dien-1-yl)-9*H*-carbazole (2g)

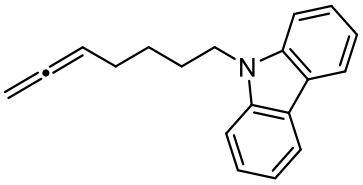

The compound **2g** was synthesized according to the following two step procedure.

Step 1. To a solution of carbazole (502 mg, 3.0 mmol, 1.0 equiv.) in toluene (4.0 mL) were added 6-chloro-1-hexyne (525 mg, 4.5 mmol, 1.5 equiv.) and tetrabutylammonium bromide (48.0 mg, 5 mol %). Afterwards, a solution of NaOH in water (156 mg in 180 µL, 1.3 equiv.) was added and the reaction mixture was placed in a pre-heated oil bath and stirred at 80 °C for 24 hs. Afterwards, the reaction was cooled to room temperature and then water was added. The aqueous layer was extracted with EtOAc (3x40 mL). The combined organic extracts were dried over Na_2SO_4 and the filtrate was concentrated under reduced pressure. The crude product was purified by column chromatography on silica gel (*n*-Hexane/EtOAc).

Step 2. Compound **2g** was synthesized from the corresponding alkyne according to general procedure **C**. The crude product was purified by flash chromatography on silica gel (*n*-Hexane/EtOAc 95:5), affording **2g** (329 mg, 42%, over two steps) as a colourless oil. ^{1}H-NMR (400 MHz, $CDCl_3$): δ = 8.14 (d, *J* = 7.8 Hz, 2H), 7.50 (t, *J* = 7.8 Hz, 2H), 7.44 (d, *J* = 8.1 Hz, 2H), 7.28 – 7.23 (m, 2H), 5.08 (p, *J* = 6.7 Hz, 1H), 4.66 (dt, *J* = 6.5, 3.2 Hz, 2H), 4.35 (t, *J* = 7.2 Hz, 2H), 2.11 – 2.04 (m, 2H), 1.96 (p, *J* = 7.4 Hz, 2H), 1.56 (p, *J* = 7.4 Hz, 2H). ^{13}C-NMR (101 MHz, $CDCl_3$): δ = 208.5 (C_q), 140.4 (C_q), 125.6 (CH), 122.8 (C_q), 120.4 (CH), 118.8 (CH), 108.6 (CH), 89.5 (CH), 75.0 (CH_2), 42.9 (CH_2), 28.3 (CH_2), 27.9 (CH_2), 26.7 (CH_2). MS (ESI) *m/z* (relative intensity): 284 (100) $[M+Na]^+$. HR-MS (ESI) *m/z* calcd for $C_{19}H_{20}N$ $[M+H]^+$ 262.1590, found 262.1593.

Tert-butyl(hepta-5,6-dien-1-yloxy)dimethylsilane (2h)

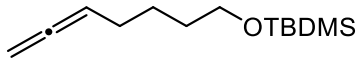

The compound **2h** was synthesized according to the following two step procedure.

Step 1. To a solution of 5-Hexyn-1-ol (490 mg, 5.0 mmol, 1.0 equiv.) in anhydrous THF (10 mL) were added imidazole (0.51 g, 7.5 mmol, 1.5 equiv.) and TBSCl (0.9 g, 6.0 mmol, 1.2 equiv.). The reaction mixture was stirred at ambient temperature for 16 hs. To the reaction was added sat. aqueous $NaHCO_3$ (20 mL). The aqueous layers were extracted with CH_2Cl_2 (3x20 mL). The combined organic extracts were dried over Na_2SO_4 and the filtrate was concentrated under reduced pressure. The crude product was directly use in the next step without further purification.

Step 2. Compound **2h** was synthesized from the corresponding alkyne according to general procedure **C**. The crude product was purified by flash chromatography on silica gel (*n*-Hexane/EtOAc 95:5), affording **2h** (396 mg, 35%, over two steps) as a colourless oil. ^{1}H-NMR (400 MHz, $CDCl_3$): δ = 5.12 (p, *J* = 6.7 Hz, 1H), 4.68 (dt, *J* = 6.6, 3.2 Hz, 2H), 3.64 (t, *J* = 6.4 Hz, 2H), 2.08 – 2.01 (m, 2H), 1.62 – 1.53 (m, 2H), 1.53 – 1.43 (m, 2H), 0.92 (s, 9H), 0.07 (s, 6H). The NMR data are consistent with the reported literatures.[10]

7-Chlorohepta-1,2-diene (2i)

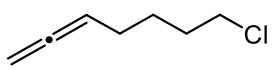

The compound was synthesized from 6-Chloro-1-hexyne (2.4 mL, 20.0 mmol, 1.0 equiv.) according to general procedure **C**. The crude product was purified by column chromatography on silica gel (pure *n*-Hexane), affording **2i** (1.2 g, 46%) as a colourless liquid. ^{1}H-NMR (400 MHz, $CDCl_3$): δ = 5.12 (p, *J* = 6.7 Hz, 1H), 4.70 (dt, *J* = 6.6,

3.2 Hz, 2H), 3.57 (t, *J* = 6.7 Hz, 2H), 2.09 – 2.02 (m, 2H), 1.90 – 1.79 (m, 2H), 1.65 – 1.55 (m, 2H). The NMR data are consistent with the reported literatures.[6]

Methyl dodeca-10,11-dienoate (2j)

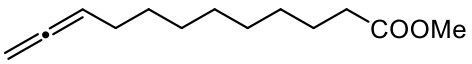

The compound was synthesized from Methyl undec-10-ynoate (2.4 mL, 20.0 mmol, 1.0 equiv.) according to general procedure **C**. The crude product was purified by column chromatography on silica gel (pure *n*-Hexane), affording **2j** (1.2 g, 46%) as a colourless liquid. ^{1}H-NMR (400 MHz, $CDCl_3$): δ = 5.11 (p, *J* = 6.8 Hz, 1H), 4.67 (dt, *J* = 6.6, 3.2 Hz, 2H), 3.69 (s, 3H), 2.32 (t, *J* = 7.5 Hz, 2H), 2.04 – 1.97 (m, 2H), 1.69 – 1.59 (m, 2H), 1.44 – 1.27 (m, 10H). The NMR data are consistent with the reported literatures.[11]

Hepta-5,6-dien-1-yl benzoate (2k)

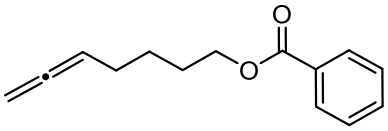

The compound **2k** was synthesized according to the following two step procedure.

Step 1. To a solution of 5-Hexyn-1-ol (490 mg, 5.0 mmol, 1.0 equiv.) in anhydrous CH_2Cl_2 (10 mL) were added DMAP (cat.), pyridine (1.20 mL, 7.5 mmol, 3.0 equiv.) and benzoyl chloride (0.88 mL, 7.5 mmol, 1.5 equiv.) at 0 °C. The mixture was initially stirred at the same temperature and then at room temperature for 16 hs. To the reaction was added sat. aqueous $NaHCO_3$ (20 mL). The aqueous layers were extracted with CH_2Cl_2 (3x20 mL). The combined organic extracts were washed with HCl (1.0 M, 20 mL), brine and dried over Na_2SO_4 and the filtrate was concentrated under reduced pressure. The crude product was purified by column chromatography on silica gel (*n*-Hexane/EtOAc).

Step 2. Compound **2k** was synthesized from the corresponding alkyne according to general procedure **C**. The crude product was purified by flash chromatography on silica gel (*n*-Hexane/EtOAc 95:5), affording **2k** (389 mg, 36%, over two steps) as a colourless oil. ^{1}H-NMR (400 MHz, $CDCl_3$): δ = 8.07 (dd, *J* = 8.3, 1.4 Hz, 2H), 7.62 – 7.54 (m, 1H), 7.47 (dd, *J* = 8.4, 7.0 Hz, 2H), 5.14 (p, *J* = 6.7 Hz, 1H), 4.70 (dt, *J* = 6.6, 3.2 Hz, 2H), 4.36 (t, *J* = 6.6 Hz, 2H), 2.15 – 2.08 (m, 2H), 1.89 – 1.79 (m, 2H), 1.67 – 1.54 (m, 2H). The NMR data are consistent with the reported literatures.[12]

(1*S*,2*R*,5*R*)-2-(Hepta-5,6-dien-1-yloxy)-1-isopropyl-4-methylcyclohexane (2l)

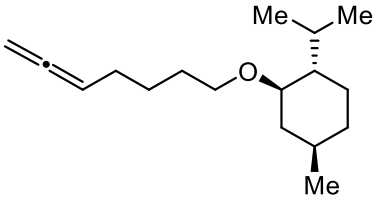

The compound **2l** was synthesized according to the following two step procedure.

Step 1. To a solution of L-Menthol (516 mg, 3.3 mmol, 1.0 equiv.) in anhydrous DMF (5.0 mL) was added NaH (50% dispersion in mineral oil, 240 mg, 5.0 mmol, 1.5 equiv.). The reaction mixture was stirred at room temperature for 30 min and then Hex-5-yn-1-yl 4-methylbenzenesulfonate (1.26 g, 5.0 mmol, 1.5 equiv.) was added. The mixture was heated at 40 °C for 16 hs. To the reaction was added sat. aqueous $NaHCO_3$ (20 mL). The aqueous layers were extracted with CH_2Cl_2 (3x20 mL). The combined organic extracts were dried over Na_2SO_4 and the filtrate was concentrated under reduced pressure. The crude product was purified by column chromatography on silica gel (*n*-Hexane/EtOAc).

Step 2. Compound **2l** was synthesized from the corresponding alkyne according to general procedure **C**. The crude product was purified by flash chromatography on silica gel (*n*-Hexane/EtOAc 95:5), affording **2l** (140 mg, 17%, over two steps) as a colourless oil. ^{1}H-NMR (400 MHz, $CDCl_3$): δ = 5.11 (p, *J* = 6.8 Hz, 1H), 4.67 (dt, *J* = 6.5, 3.2 Hz, 2H), 3.65 (dt, *J* = 9.2, 6.1 Hz, 1H), 3.28 (dt, *J* = 9.2, 6.6 Hz, 1H), 3.01 (td, *J* = 10.6, 4.1 Hz, 1H), 2.24 (pd, *J* = 7.0, 2.7 Hz, 1H), 2.14 – 2.09 (m, 1H), 2.08 – 2.01 (m, 2H), 1.70 – 1.56 (m, 4H), 1.56 – 1.44 (m, 2H), 1.41 – 1.31 (m, 1H), 1.28 – 1.18 (m, 1H), 1.04 – 0.96 (m, 1H), 0.95 – 0.90 (m, 6H), 0.89 – 0.83 (m, 2H), , 0.79 (d, *J* = 7.0 Hz, 3H). ^{13}C-NMR (101 MHz, $CDCl_3$): δ = 208.6 (C_q), 89.9 (CH), 79.2 (CH), 74.6 (CH_2), 68.3 (CH_2), 48.3 (CH), 40.5 (CH_2), 34.7 (CH_2), 31.6 (CH), 29.7 (CH_2), 28.1 (CH_2), 25.8 (CH_2), 25.6 (CH), 23.4 (CH_2), 22.4 (CH_3), 21.0 (CH_3), 16.2 (CH_3). MS (ESI) *m/z* (relative intensity): 251 (100) $[M+H]^+$. HR-MS (ESI) *m/z* calcd for $C_{17}H_{31}O$ $[M+H]^+$ 251.2369, found 251.2367.

(3*S*,8*S*,9*S*,10*R*,13*R*,14*S*,17*R*)-10,13-Dimethyl-17-[(*R*)-6-methylheptan-2-yl]-2,3,4,7,8,9,10,11,12,13,14,15,16,17-tetradecahydro-1*H*-cyclopenta[*a*]phenanthren-3-yl hexa-4,5-dienoate (2m)

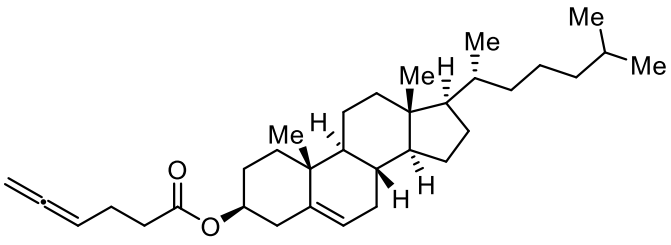

The compound **2m** was synthesized according to the following two step procedure.

Step 1. To a solution of 5-Pentynoic acid (177 mg, 1.8 mmol, 1.2 equiv.), *N*-(3-Dimethylaminopropyl)-*N*'-ethylcarbodiimide hydrochloride (345 mg, 1.8 mmol, 1.2 equiv.) and DMAP (18.0 mg, 0.15 mmol, 0.1 equiv.) in CH_2Cl_2 (10 mL) was added cholesterol (580 mg, 1.5 mmol, 1.0 equiv.). The reaction mixture was allowed to stir at room temperature for 16 hs. After completion, the reaction mixture was extracted with water and CH_2Cl_2 (2x20 mL). The organic layer was washed with brine, dried with Na_2SO_4, and concentrated under reduced pressure. Purification by flash chromatography on silica gel (*n*-Hexane/EtOAc) provided the desired product.

Step 2. Compound **2m** was synthesized from the corresponding alkyne according to general procedure **C**. The crude product was purified by flash chromatography on silica gel (*n*-Hexane/EtOAc 95:5), affording **2m** (284 mg, 40%, over two steps) as a pale-yellow oil. ^{1}H-NMR (400 MHz, $CDCl_3$): δ = 5.40 (dd, *J* = 4.8, 1.9 Hz, 1H), 5.19 (p, *J* = 6.4 Hz, 1H), 4.73 (dt, *J* = 6.7, 3.4 Hz, 2H), 4.70 – 4.59 (m, 1H), 2.46 – 2.42 (m, 2H), 2.37 – 2.30 (m, 4H), 2.06 – 1.96 (m, 2H), 1.91 – 1.83 (m, 3H), 1.65 – 1.44 (m, 7H), 1.44 – 1.09 (m, 12H), 1.05 – 0.96 (m, 5H), 0.94 (d, *J* = 6.5 Hz, 3H), 0.90 – 0.88 (m, 6H), 0.70 (s, 3H). ^{13}C-NMR (101 MHz, $CDCl_3$): δ = 208.4 (C_q), 172.4 (C_q), 139.7 (C_q), 122.7 (CH), 88.8 (CH), 76.0 (CH_2), 73.9 (CH), 56.7 (CH), 56.1 (CH), 50.0 (CH), 42.3 (C_q), 39.7 (CH_2), 39.5 (CH_2), 38.1 (CH_2), 37.0 (CH_2), 36.6 (C_q), 36.2 (CH_2), 35.8 (CH), 33.7 (CH_2), 31.9 (CH_2), 31.9 (CH), 28.2 (CH_2), 28.0 (CH), 27.8 (CH_2), 24.3 (CH_2), 23.8 (CH_2), 23.3 (CH_2), 22.8 (CH_3), 22.6 (CH_3), 21.0 (CH_2), 19.3 (CH_3), 18.7 (CH_3), 11.9 (CH_3). MS (ESI) *m/z* (relative intensity):503 (100) $[M+Na]^+$, 481 (58) $[M+H]^+$. HR-MS (ESI) *m/z* calcd for $C_{33}H_{53}O_2$ $[M+H]^+$ 481.4040, found 481.4044.

(3a*S*,6*R*,6a*S*)-6-(2,2-Dimethyl-1,3-dioxolan-4-yl)-2,2-dimethyltetrahydrofuro[3,4-*d*][1,3]dioxol-4-yl hexa-4,5-dienoate (2n)

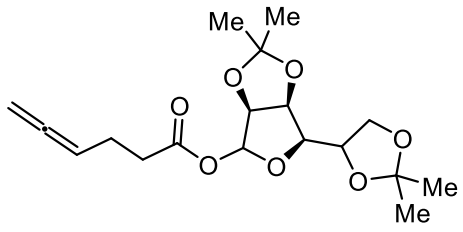

The compound **2n** was synthesized according to the following two step procedure.

Step 1. To a solution of 5-pentynoic acid (343 mg, 3.5 mmol, 1.2 equiv.), *N*-(3-Dimethylaminopropyl)-*N*'-ethylcarbodiimide hydrochloride (670 mg, 3.5 mmol, 1.2 equiv.) and DMAP (18 mg, 0.15 mmol, 0.1 equiv) in CH_2Cl_2 (10 mL) was added D-Mannose diacetonide (758 mg, 2.9 mmol, 1.0 equiv.). The reaction mixture was allowed to stir at room temperature for 16 h. After completion, the reaction mixture was quenched with water and extracted with ethyl acetate. The organic layer was washed with brine, dried with Na_2SO_4, and

concentrated under reduced pressure. Purification by flash chromatography on silica gel (*n*-Hexane/EtOAc) provided the desired product.

Step 2. Compound **2n** was synthesized from the corresponding alkyne according to general procedure **B**. The crude product was purified by flash chromatography on silica gel (*n*-Hexane/EtOAc 95:5), affording **2n** (497 mg, 50%, over two steps) as a colourless oil. ^{1}H-NMR (400 MHz, $CDCl_3$): δ = 6.16 (s, 1H), 5.19 (p, *J* = 6.4 Hz, 1H), 4.87 (dd, *J* = 5.9, 3.6 Hz, 1H), 4.76 (dt, *J* = 6.9, 3.5 Hz, 2H), 4.71 (d, *J* = 5.9 Hz, 1H), 4.44 – 4.40 (m, 1H), 4.12 (dd, *J* = 8.9, 6.1 Hz, 1H), 4.06 – 4.02 (m, 2H), 2.51 – 2.44 (m, 2H), 2.38 – 2.29 (m, 2H), 1.51 (s, 3H), 1.48 (s, 3H), 1.40 (s, 3H), 1.36 (s, 3H). ^{13}C-NMR (101 MHz, $CDCl_3$): δ = 208.3 (C_q), 171.4 (C_q), 113.3 (C_q), 109.4 (C_q), 100.7 (CH), 88.5 (CH), 85.1 (CH), 82.3 (CH), 79.3 (CH), 76.3 (CH_2)72.9 (CH), 66.8 (CH_2), 33.2 (CH_2), 27.0 (CH_3), 26.0 (CH_3), 25.2 (CH_3), 24.7 (CH_3), 22.8 (CH_2). MS (ESI) *m/z* (relative intensity):377 (63) $[M+Na]^+$, 355 (100) $[M+H]^+$. HR-MS (ESI) *m/z* calcd for $C_{33}H_{53}O_2$ $[M+H]^+$ 481.4040, found 481.4044.

Hepta-5,6-dien-1-yl pyrene-1-carboxylate (2o)

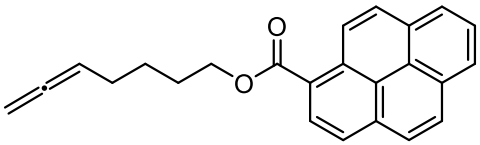

The compound **2o** was synthesized according to the following two step procedure.

Step 1. To a solution of 1-Pyrenecarboxylic acid (887 mg, 3.6 mmol, 1.2 equiv.), *N*-(3-Dimethylaminopropyl)-*N*'-ethylcarbodiimide hydrochloride (690 mg, 3.6 mmol, 1.2 equiv.) and DMAP (18 mg, 0.15 mmol, 0.1 equiv.) in CH_2Cl_2 (15 mL) was added 5-Hexyn-1-ol (294 mg, 3.0 mmol, 1.0 equiv). The reaction mixture was allowed to stir at room temperature for 16 hs. After completion, the reaction mixture was quenched with water and extracted with ethyl acetate. The organic layer was washed with brine, dried with Na_2SO_4, and concentrated under reduced pressure. Purification by flash chromatography on silica gel (*n*-Hexane/EtOAc) provided the desired product.

Step 2. Compound **2o** was synthesized from the corresponding alkyne according to general procedure **C**. The crude product was purified by flash chromatography on silica gel (*n*-Hexane/EtOAc 95:5), affording **2o** (643 mg, 63%, over two steps) as a pale-yellow oil. ^{1}H-NMR (400 MHz, $CDCl_3$): δ = 9.29 (d, *J* = 9.5 Hz, 1H), 8.65 (d, *J* = 8.1 Hz, 1H), 8.30 – 8.23 (m, 3H), 8.21 – 8.17 (m, 2H), 8.12 – 8.05 (m, 2H), 5.19 (p, *J* = 6.7 Hz, 1H), 4.74 (dt, *J* = 6.6, 3.2 Hz, 2H), 4.55 (t, *J* = 6.6 Hz, 2H), 2.21 – 2.14 (m, 2H), 2.02 – 1.94 (m, 2H), 1.77 – 1.68 (m, 2H). ^{13}C-NMR (101 MHz, $CDCl_3$): δ = 208.6 (C_q), 168.1 (C_q), 134.3 (C_q), 131.1 (2 x C_q), 130.4 (C_q), 129.6 (CH),

129.4 (CH), 128.4 (CH), 127.2 (CH), 126.3 (CH), 126.3 (CH), 126.2 (CH), 125.0 (CH), 124.9 (C_q), 124.3 (C_q), 124.1 (CH), 123.9 (C_q), 89.6 (CH), 75.1 (CH_2), 65.2 (CH_2), 28.3 (CH_2), 27.9 (CH_2), 25.7 (CH_2). MS (ESI) *m/z* (relative intensity): 341 (100) $[M+H]^+$. MS (ESI) *m/z* (relative intensity):377 (63) $[M+Na]^+$, 355 (100) $[M+H]^+$. HR-MS (ESI) *m/z* calcd for $C_{24}H_{21}O_2$ $[M+H]^+$ 341.1536, found 341.1535.

1^5-(Hepta-5,6-dien-1-yloxy)-1^2,3^2,5^2,7^2-tetrapropoxy-calix[4]arene (2p)

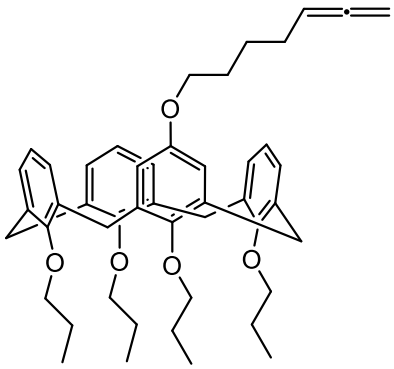

The compound **2p** was synthesized according to the following two step procedure.

Step 1. To a two-neck round-bottom flask was added hydroxy-calix[4]arene[13] (304.0 mg, 0.5 mmol), 5-Hexyn-1-ol (58.9 mg, 0.6 mmol, 1.2 equiv.), triphenylphosphine (157.4 mg, 0.6 mmol, 1.2 equiv), and THF (2.0 mL). The reaction mixture was cooled to 0 °C and then diisopropylazodicarboxylate (118 µL, 0.6 mmol, 1.2 equiv.) was added dropwise. The mixture was initially stirred at the same temperature and then at ambient temperature for 16 hs. To the reaction was added sat. aqueous $NaHCO_3$ (20 ml). The aqueous layers were extracted with CH_2Cl_2 (3x20 mL). The combined organic extracts were dried over Na_2SO_4 and the filtrate was concentrated under reduced pressure. The crude product was purified by column chromatography on silica gel.

Step 2. Compound **2p** was synthesized from the corresponding alkyne according to general procedure **B**. The crude product was purified by flash chromatography on silica gel (*n*-Hexane/EtOAc 95:5), affording **2p** (77.3 mg, 23%, over two steps) as a colourless oil. ^{1}H-NMR (400 MHz, $CDCl_3$): δ = 6.77 – 6.71 (m, 4H), 6.65 (t, *J* = 7.4 Hz, 2H), 6.51 (s, 3H), 6.04 (s, 2H), 5.13 (p, *J* = 6.7 Hz, 1H), 4.69 (dt, *J* = 6.6, 3.2 Hz, 2H), 4.46 (t, *J* = 13.3 Hz, 4H), 3.91 – 3.82 (m, 6H), 3.78 (t, *J* = 7.3 Hz, 2H), 3.64 (t, *J* = 6.5 Hz, 2H), 3.14 (dd, *J* = 24.5, 13.4 Hz, 4H), 2.10 – 2.03 (m, 2H), 1.97 – 1.89 (m, 8H), 1.73 – 1.65 (m, 2H), 1.56 – 1.49 (m, 2H), 1.07 – 0.94 (m, 12H). ^{13}C-NMR (101 MHz, $CDCl_3$): δ = 208.6 (C_q), 156.9 (C_q), 156.4 (C_q), 153.5 (C_q), 150.3 (C_q), 135.5 (2 x C_q), 135.4 (C_q), 134.9 (C_q), 128.3 (2 x CH), 128.0 (CH), 121.9 (CH), 121.8 (CH), 113.6 (CH), 89.8 (CH), 76.8 (CH_2), 76.7 (CH_2), 76.6 (CH_2), 74.9 (CH_2), 67.4 (CH_2), 31.2 (CH_2), 31.0 (CH_2), 28.8 (CH_2), 28.0 (CH_2), 25.6 (CH_2), 23.3 (2 x CH_2), 23.2 (CH_2), 10.5 (2 x CH_3), 10.3 (CH_3). MS (ESI) *m/z* (relative intensity): 726 (100) $[M+Na]^+$. HR-MS (ESI) *m/z* calcd for $C_{47}H_{59}O_5$ $[M+H]^+$ 703.4357, found 703.4359.

6-Vinylideneundecane (2q)

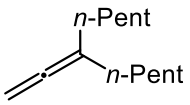

The compound was synthesized from 1-heptyne (962 mg, 10.0 mmol, 1.0 equiv.) according to general procedure **D**. The crude product was purified by column chromatography on silica gel (pure *n*-Hexane), affording **2q** (649 mg, 36%, over three steps) as a colourless liquid. ^{1}H-NMR (400 MHz, $CDCl_3$): δ = 4.65 (p, *J* = 3.2 Hz, 2H), 1.97 – 1.90 (m, 4H), 1.44 (p, *J* = 7.3 Hz, 4H), 1.34 – 1.28 (m, 8H), 0.91 (t, *J* = 6.8 Hz, 6H). The NMR data are consistent with the reported literatures.[14]

Buta-2,3-dien-2-ylbenzene (2r)

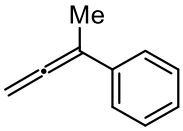

The compound was synthesized from Acetophenone (2.4 g, 20.0 mmol, 1.0 equiv.) according to general procedure **E**. The crude product was purified by column chromatography on silica gel (pure *n*-Hexane), affording **2r** (416 mg, 16%, over three steps) as a colourless liquid. ^{1}H-NMR (400 MHz, $CDCl_3$): δ = 7.47 – 7.43 (m, 2H), 7.36 (dd, *J* = 8.6, 7.0 Hz, 2H), 7.26 – 7.20 (m, 1H), 5.06 (q, *J* = 3.2 Hz, 2H), 2.14 (t, *J* = 3.2 Hz, 3H). The NMR data are consistent with the reported literatures.[15]

3-Methylocta-1,2-diene (2s)

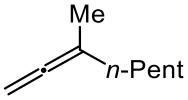

The compound was synthesized from but-2-yn-1-ol (701 mg, 10.0 mmol, 1.0 equiv.) according to general procedure **D**. The crude product was purified by column chromatography on silica gel (pure *n*-Pentane), affording **2s** (298 mg, 24%, over two steps) as a colourless liquid. ^{1}H-NMR (400 MHz, $CDCl_3$): δ = 4.60 (h, *J* = 3.2 Hz, 2H), 1.97 – 1.92 (m, 2H), 1.70 (t, *J* = 3.1 Hz, 3H), 1.50 – 1.41 (m, 2H), 1.36 – 1.27 (m, 4H), 0.91 (t, *J* = 6.8 Hz, 3H). The NMR data are consistent with the reported literatures.[16]

Hexa-1,2-dien-3-ylbenzene (2t)

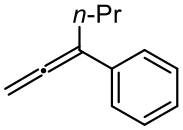

The compound was synthesized from Butyrophenone (3.0 g, 20.0 mmol, 1.0 equiv.) according to general procedure **E**. The crude product was purified by column chromatography on silica gel (pure *n*-Hexane), affording **2t** (538 mg, 17%, over three steps) as a colourless liquid. ^{1}H-NMR (400 MHz, $CDCl_3$): δ = 7.44 (d, *J* = 7.4 Hz, 2H), 7.34 (dd, *J* = 8.5, 6.9 Hz, 2H), 7.22 (t, *J* = 7.3 Hz, 1H), 5.09 (t, *J* = 3.3 Hz, 2H), 2.48 – 2.39 (m, 2H), 1.67 – 1.56 (m, 2H), 1.02 (t, *J* = 7.4 Hz, 3H). ^{13}C-NMR (101 MHz, $CDCl_3$): δ = 208.7 (C_q), 136.5 (C_q), 128.3 (CH), 126.5 (CH), 126.0 (CH), 104.8 (C_q), 78.0 (CH_2), 31.6 (CH_2), 21.1 (CH_2), 14.0 (CH_3). MS (ESI) *m/z* (relative intensity): 181 (100) $[M+Na]^+$. HR-MS (ESI) *m/z* calcd for $C_{12}H_{15}$ $[M+H]^+$ 159.1168, found 159.1165.

Hepta-2,3-dien-4-ylbenzene (2u)

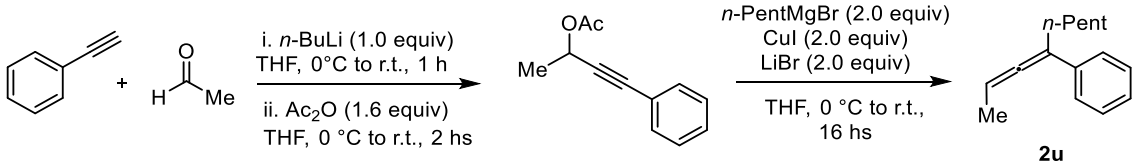

The compound **2u** was synthesized according to the following two step procedure.[17]

Step 1: To a solution of phenyl acetylene (0.88 mL, 8.0 mmol, 1.0 equiv.) in THF (1.0 M) was added *n*-BuLi (2.5 M in *n*-Hexane, 3.2 mL, 8.0 mmol, 1.0 equiv.) at 0 °C under N_2 atmosphere. The mixture was stirred at 0 °C for 30 min and then acetaldehyde (450 mL, 8.0 mmol, 1.0 equiv.) was added. The mixture was stirred for 30 min at room temperature and then acetic anhydride (1.2 m L, 12.8 mmol, 1.6 equiv.) was added at 0 °C. The mixture was stirred for additional 2 hs at room temperature before adding water. The aqueous solution was extracted with EtOAc (3x15 mL). The combined organic layers were dried over Na_2SO_4, filtered, and concentrated under reduced pressure. The residue was purified by flash chromatography on silica gel to afford the propargyl acetate which was directly use in the next step.

Step 2: To a 50 mL Schlenk flask were added CuI (866 mg, 4.56 mmol, 2.0 equiv.), LiBr (392 mg, 4.56 mmol, 2.0 equiv.), THF (0.25 M), and then *n*-PentMgBr (1.0 M in THF, 4.56 mmol, 2.0 equiv.) under N_2 atmosphere at 0 °C. The mixture was stirred for 30 min at room temperature and then the propargyl acetate was added at 0 °C. The resulting mixture was stirred overnight at room temperature. Afterwards, the reaction mixture was poured into a beaker with a mixture of saturated aqueous Na_2CO_3 solution and *n*-Hexane (1:1, v/v). The mixture was filtered to remove the solid. The filtrate was extracted with EtOAc (3x15 mL) and the combined organic layers were

dried over Na_2SO_4, filtered, and concentrated under reduced pressure. The crude product was purified by flash chromatography on silica gel (pure *n*-Hexane), affording **2u** (316 mg, 20%, over two steps) as a colourless oil. ^{1}H-NMR (400 MHz, $CDCl_3$): δ = 7.40 – 7.37 (m, 2H), 7.30 (t, *J* = 7.7 Hz, 2H), 7.18 – 7.15 (m, 1H), 5.45 (qt, *J* = 6.8, 3.0 Hz, 1H), 2.44 – 2.33 (m, 2H), 1.75 (dd, *J* = 7.0, 0.8 Hz, 3H), 1.56 – 1.50 (m, 3H), 1.40 – 1.30 (m, 3H), 0.89 (t, *J* = 7.1, 3H). ^{13}C-NMR (101 MHz, $CDCl_3$): δ = 204.7 (C_q), 137.7 (C_q), 128.3 (CH), 126.3 (CH), 126.0 (CH), 98.5 (C_q), 88.8 (CH), 31.6 (CH_2), 29.9 (CH_2), 27.6 (CH_2), 22.6 (CH_2), 14.4 (CH_3), 14.1 (CH_3). MS (ESI) *m/z* (relative intensity): 223 (100) $[M+Na]^+$. HR-MS (ESI) *m/z* calcd for $C_{15}H_{21}$ $[M+H]^+$ 201.1638, found 201.1635.

Nona-1,2-diene ([D]$_2$-2a)

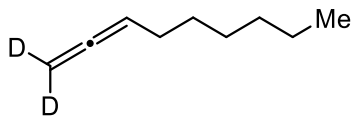

The compound was synthesized from 1-Octyne (0.88 mL, 6.0 mmol, 1.0 equiv.) and Paraformaldehyde-d_2 (0.48 g, 15.0 mmol, 2.5 equiv.) according to general procedure **C**. The crude product was purified by column chromatography on silica gel (pure *n*-Pentane), affording **[D]$_2$-2a** (0.34 g, 45%) as a colourless liquid. The amount of deuterium content was determined to be >99% by ^{1}H-NMR.

4.4.4 Optimization of reaction conditions

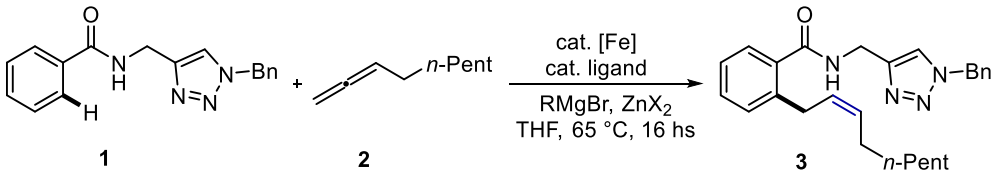

Entry[a]	Catalyst	Ligand	RMgBr	ZnX_2	**3aa** (%)[b]
1	$Fe(acac)_3$	dppe	PhMgBr	$ZnBr_2$	53
2	$Fe(acac)_3$	dppe	PhMgBr	$ZnCl_2$	80 (77)
3	$Fe(acac)_3$	dppen	PhMgBr	$ZnBr_2$	45
4	$Fe(acac)_3$	dppen	PhMgBr	$ZnCl_2$	82 (78)
5	$Fe(acac)_3$	2,2'-bipy	PhMgBr	$ZnCl_2$	n.d.
6	$Fe(acac)_3$	dppbz	PhMgBr	$ZnCl_2$	11
7	$Fe(acac)_3$	dppbz	PhMgBr	$ZnBr_2$	10
8[c]	$Fe(acac)_3$	dppe	PhMgBr	$ZnCl_2$	54 (50)
12	$Fe(acac)_3$	dppe	*i*-PrMgBr	$ZnCl_2$	20
13	$FeCl_2$	dppe	PhMgBr	$ZnCl_2$	72
14	$Pd(OAc)_2$	dppe	PhMgBr	$ZnCl_2$	n.d.
15	$Ni(acac)_2$	dppe	PhMgBr	$ZnCl_2$	n.d.
16	$Co(acac)_2$	dppe	PhMgBr	$ZnCl_2$	n.d.

[a]Reaction conditions: **1a** (0.2 mmol), **2a** (0.4 mmol), [Fe] (0.03 mmol), ligand (0.03 mmol), RMgBr (0.6 mmol), ZnX_2 (0.4 mmol), THF (0.2 mL). [b]Yields determined using 1,3,5-trimethoxybenzene as the internal standard. In parenthesis, isolated yields. [c]THF (0.5 mL). dppe = 1,2-bis (diphenylphosphino)ethane; dppbz = 1,2-bis(diphenylphosphino) benzene; dppen = *cis*-1,2-bis(diphenylphosphino)ethene.

4.4.5 Evaluation of 8-aminoquinoline directing group

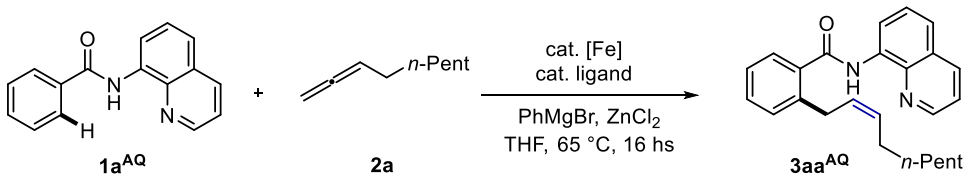

Entry[a]	Catalyst	Ligand	RMgBr	**3aa**^{AQ}[b]
1	$Fe(acac)_3$	2,2'-bipy	PhMgBr	n.d.
2	$Fe(acac)_3$	dppe	PhMgBr	n.d.
3	$Fe(acac)_3$	dppen	PhMgBr	n.d.
4	$Fe(acac)_3$	dppbz	PhMgBr	n.d.

[a]Reaction conditions: **1a**^{AQ} (0.2 mmol), **2a** (0.4 mmol), [Fe] (0.03 mmol), ligand (0.03 mmol), PhMgBr (0.6 mmol), $ZnCl_2$ (0.4 mmol), THF (0.3 mL). [b]Isolated yields.

All the reaction led to a broad decomposition of the starting material. Upon analysis of the crude reaction mixtures via proton nuclear magnetic resonance and mass spectrometry, no experimental evidence was found to indicate the formation of the anticipated product. A representative ^{1}H-NMR spectrum is provided, which notably lacks the characteristic doublet typically attributed to allylic protons in the expected product.

Crude ^{1}H-NMR of **Entry 1** (400 MHz, $CDCl_3$)

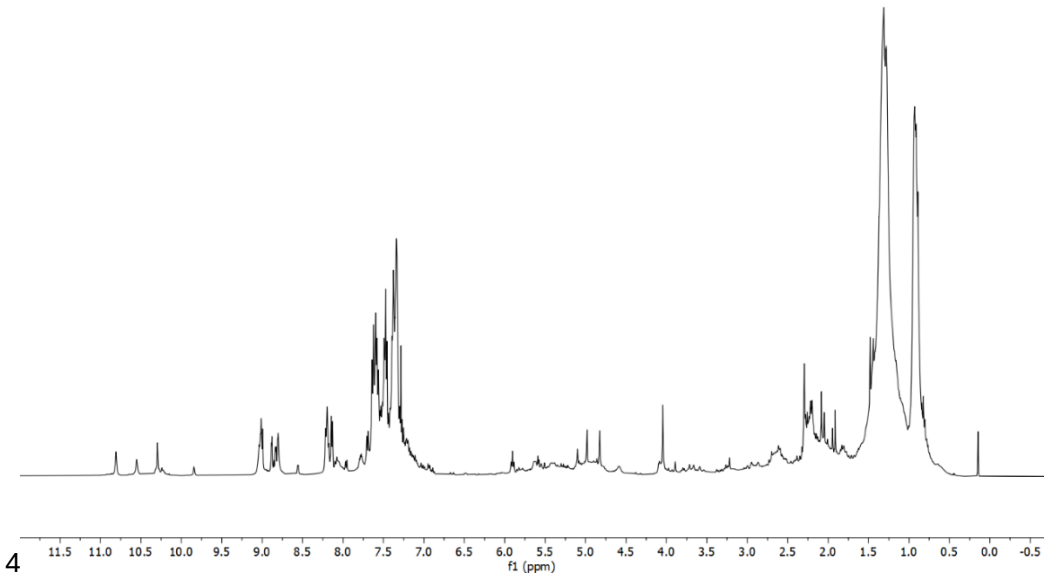

4

4.4.6 Representative Procedure for Iron-Catalyzed C–H Allylation with Allenes

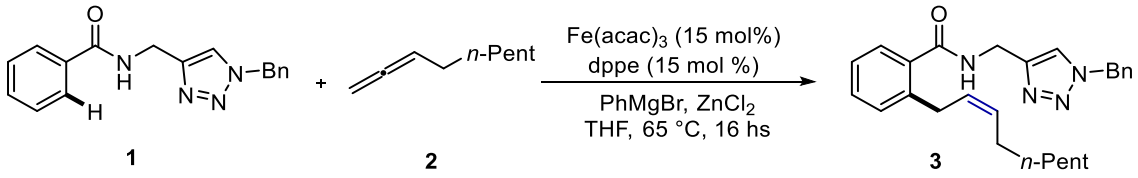

To a stirred solution of $Fe(acac)_3$ (10.6 mg, 0.03 mmol), dppe (12.0 mg, 0.03 mmol), $ZnCl_2$ (1.0 M in THF, 400 µL, 0.4 mmol, 2.0 equiv.) and **1** (0.20 mmol) in THF (200 µL) under N_2 atmosphere, PhMgBr (1.0 M in THF, 600 µL, 0.6 mmol, 3.0 equiv.) was added in a single portion. Then, **2** (0.4 mmol, 2.0 equiv.) was added and the mixture was placed in a pre-heated oil bath at 65 °C. After stirring for 16 hs, the reaction was cooled to room temperature and quenched by the addition of an aqueous solution of HCl (1.0 M, 5 mL). The reaction was extracted with CH_2Cl_2 (3x10 mL) and the combined organic extracts were dried over Na_2SO_4, filtered and concentrated. The crude product was purified by column chromatography on silica gel (*n*-Hexane/EtOAc).

4.4.7 Characterization Data of Products

(*Z*)-*N*-[(1-Benzyl-1*H*-1,2,3-triazol-4-yl)methyl]-2-(non-2-en-1-yl)benzamide (3aa)

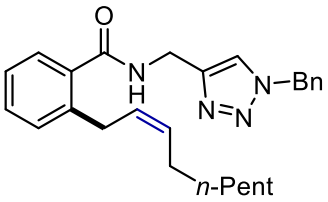

The representative procedure was followed using **1a** (58.5 mg, 0.2 mmol) and **2a** (49.6 mg, 0.4 mmol). Purification by column chromatography on silica gel (*n*-Hexane/EtOAc 1:1) yielded **3aa** (64.1 mg, 77%) as a white waxy solid. ^{1}H-NMR (400 MHz, $CDCl_3$): δ = 7.56 (s, 1H), 7.44 – 7.29 (m, 7H), 7.26 (d, *J* = 7.9 Hz, 1H), 7.21 (t, *J* = 7.4 Hz, 1H), 6.54 (s, 1H), 5.53 (s, 2H), 5.45 (m, 2H), 4.67 (d, *J* = 5.7 Hz, 2H), 3.54 (d, *J* = 5.3 Hz, 2H), 2.11 (q, *J* = 8.2, 7.4 Hz, 2H), 1.43 – 1.25 (m, 8H), 0.90 (t, *J* = 6.5 Hz, 3H). ^{13}C-NMR (101 MHz, $CDCl_3$): δ = 170.0 (C_q), 144.9 (C_q), 139.5 (C_q), 135.6 (C_q), 134.4 (C_q), 131.5 (CH), 130.3 (CH), 130.0 (CH), 129.2 (CH), 128.9 (CH), 128.1 (CH), 127.6 (CH), 127.0 (CH), 126.0 (CH), 122.2 (CH), 54.3 (CH_2), 35.4 (CH_2), 31.8 (CH_2), 30.9 (CH_2), 29.6 (CH_2), 29.1 (CH_2), 27.3 (CH_2), 22.7 (CH_2), 14.1 (CH_3). MS (ESI) *m/z* (relative intensity): 855 (28) $[2M+Na]^+$, 439 (100) $[M+Na]^+$. HR-MS (ESI) *m/z* calcd for $C_{26}H_{33}N_4O$ $[M+H]^+$ 417.2649, found 417.2646.

(*Z*)-2-(non-2-en-1-yl)-*N*-[(1-phenyl-1*H*-1,2,3-triazol-4-yl)methyl]benzamide (3ba)

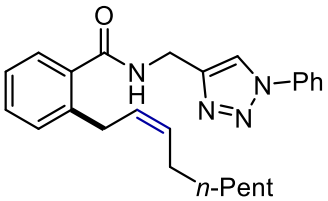

The representative procedure was followed using **1b** (55.6 mg, 0.2 mmol) and **2a** (49.6 mg, 0.4 mmol). Purification by column chromatography on silica gel (*n*-Hexane/EtOAc 1:1) yielded **3ba** (40.2 mg, 50%) as a pale-yellow solid. M.p.= 97-98 °C. ^{1}H-NMR (400 MHz, $CDCl_3$): δ = 8.11 (s, 1H), 7.78 – 7.73 (m, 2H), 7.55 (t, *J* = 7.6 Hz, 2H), 7.50 – 7.44 (m, 1H), 7.40 (dd, *J* = 7.5, 1.5 Hz, 1H), 7.36 (dd, *J* = 7.5, 1.5 Hz, 1H), 7.25 (dd, *J* = 9.2, 1.3 Hz, 1H), 7.21 (dd, *J* = 7.5, 1.3 Hz, 1H), 6.64 (bs, 1H), 5.54 – 5.43 (m, 2H), 4.79 (d, *J* = 5.8 Hz, 2H), 3.59 (d, *J* = 4.7 Hz, 2H), 2.14 – 2.07 (m, 2H), 1.36 – 1.25 (m, 8H), 0.92 – 0.86 (m, 3H). ^{13}C-NMR (101 MHz, $CDCl_3$): δ = 170.2 (C_q), 145.3 (C_q), 139.5 (C_q), 137.0 (C_q), 135.6 (C_q), 131.5 (CH), 130.3 (CH), 130.0 (CH), 129.8 (CH), 128.9 (CH), 127.7 (CH), 127.1 (CH), 126.1 (CH), 120.7 (CH), 120.5 (CH), 35.4 (CH_2), 31.8 (CH_2), 31.0 (CH_2), 29.6 (CH_2), 29.0 (CH_2), 27.4 (CH_2), 22.7 (CH_2), 14.1 (CH_3). MS (ESI) *m/z* (relative intensity): 425 (100) $[M+Na]^+$, 403 (61) $[M+H]^+$. HR-MS (ESI) *m/z* calcd for $C_{25}H_{31}N_4O$ $[M+H]^+$ 403.2492, found 403.2495.

(*Z*)-*N*-[(1-Hexyl-1*H*-1,2,3-triazol-4-yl)methyl]-2-(non-2-en-1-yl)benzamide (3ca)

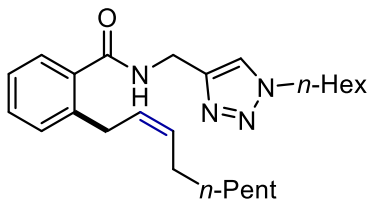

The representative procedure was followed using **1c** (57.3 mg, 0.2 mmol) and **2a** (49.6 mg, 0.4 mmol). Purification by column chromatography on silica gel (*n*-Hexane/EtOAc 1:1) yielded **3ca** (44.3 mg, 54%) as a pale-yellow oil. ^{1}H-NMR (400 MHz, $CDCl_3$): δ = 7.62 (s, 1H), 7.38 – 7.32 (m, 2H), 7.26 (d, *J* = 7.4 Hz, 1H), 7.20 (td, *J* = 7.4, 1.3 Hz, 1H), 6.58 (t, *J* = 5.8 Hz, 1H), 5.54 – 5.41 (m, 2H), 4.69 (d, *J* = 5.7 Hz, 2H), 4.35 (t, *J* = 7.3 Hz, 2H), 3.57 (d, *J* = 5.5 Hz, 2H), 2.16 – 2.07 (m, 2H), 1.91 (dd, *J* = 9.1, 5.3 Hz, 2H), 1.40 – 1.25 (m, 14H), 0.93 – 0.86 (m, 6H). ^{13}C-NMR (101 MHz, $CDCl_3$): δ = 170.1 (C_q), 144.5 (C_q), 139.5 (C_q), 135.7 (C_q), 131.4 (CH), 130.2 (CH), 130.0 (CH), 127.7 (CH), 127.0 (CH), 126.0 (CH), 122.1 (CH), 50.4 (CH_2), 35.4 (CH_2), 31.8 (CH_2), 31.1 (CH_2), 30.9 (CH_2), 30.2 (CH_2), 29.6 (CH_2), 29.1 (CH_2), 27.3 (CH_2), 26.2 (CH_2), 22.7 (CH_2), 22.4 (CH_2), 14.1 (CH_3), 14.0 (CH_3). MS (ESI) *m/z* (relative intensity): 433 (32) $[M+Na]^+$, 411 (100) $[M+H]^+$. HR-MS (ESI) *m/z* calcd for $C_{25}H_{39}N_4O$ $[M+H]^+$ 411.3118, found 411.3116.

(*Z*)-2-(Non-2-en-1-yl)-*N*-{[1-(pent-4-en-1-yl)-1*H*-1,2,3-triazol-4-yl]methyl}benzamide (3da)

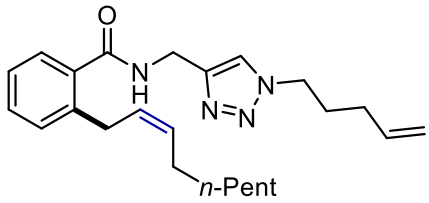

The representative procedure was followed using **1d** (54.1 mg, 0.2 mmol) and **2a** (49.6 mg, 0.4 mmol). Purification by column chromatography on silica gel (*n*-Hexane/EtOAc 1:1) yielded **3da** (44.2 mg, 56%) as a pale-yellow oil. ^{1}H-NMR (400 MHz, $CDCl_3$): δ = 7.63 (s, 1H), 7.36 – 7.31 (m, 2H), 7.24 (t, *J* = 7.4 Hz, 1H), 7.18 (td, *J* = 7.4, 1.3 Hz, 1H), 6.72 (t, *J* = 5.8 Hz, 1H), 5.83 – 5.73 (m, 1H), 5.52 – 5.41 (m, 2H), 5.10 – 5.03 (m, 2H), 4.66 (d, *J* = 5.8 Hz, 2H), 4.34 (t, *J* = 7.0 Hz, 2H), 3.55 (d, *J* = 5.7 Hz, 2H), 2.14 – 2.07 (m, 4H), 2.06 – 1.98 (m, 2H), 1.37 – 1.27 (m, 8H), 0.91 – 0.87 (m, 3H). ^{13}C-NMR (101 MHz, $CDCl_3$): δ = 170.1 (C_q), 144.6 (C_q), 139.4 (C_q), 136.4 (CH), 131.4 (C_q), 130.2 (CH), 129.9 (CH), 127.7 (CH), 127.0 (CH), 126.0 (2 x CH), 122.3 (CH), 116.3 (CH_2), 49.6 (CH_2), 35.4 (CH_2), 31.8 (CH_2), 30.9 (CH_2), 30.4 (CH_2), 29.6 (CH_2), 29.2 (CH_2), 29.0 (CH_2), 27.3 (CH_2), 22.7 (CH_2), 14.1 (CH_3). MS (ESI) *m/z* (relative intensity): 417 (100) $[M+Na]^+$. HR-MS (ESI) *m/z* calcd for $C_{24}H_{35}N_4O$ $[M+H]^+$ 395.2805, found 395.2810.

(*Z*)-*N*-[(1-Benzyl-1*H*-1,2,3-triazol-4-yl)methyl]-4-methyl-2-(non-2-en-1-yl)benzamide (3ea)

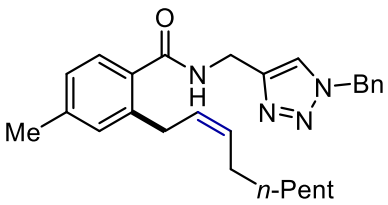

The representative procedure was followed using **1e** (61.2 mg, 0.2 mmol) and **2a** (49.6 mg, 0.4 mmol). Purification by column chromatography on silica gel (*n*-Hexane/EtOAc 1:1) yielded **3ea** (55.0 mg, 64%) as a white waxy solid. ^{1}H-NMR (400 MHz, $CDCl_3$): δ = 7.55 (s, 1H), 7.39 (dd, *J* = 5.7, 1.8 Hz, 3H), 7.29 (m, 2H), 7.26 (d, *J* = 7.8 Hz, 1H), 7.06 (d, *J* = 1.7 Hz, 1H), 7.00 (dd, *J* = 7.8, 1.7 Hz, 1H), 6.50 (t, *J* = 5.8 Hz, 1H), 5.52 (s, 2H), 5.47 – 5.43 (m, 2H), 4.66 (d, *J* = 5.7 Hz, 2H), 3.53 (d, *J* = 5.4 Hz, 2H), 2.34 (s, 3H), 2.14 – 2.08 (m, 2H), 1.36 – 1.27 (m, 8H), 0.90 (d, *J* = 6.9 Hz, 3H). ^{13}C-NMR (101 MHz, $CDCl_3$): δ = 170.1 (C_q), 145.1 (C_q), 140.4 (C_q), 139.6 (C_q), 134.5 (C_q), 132.7 (C_q), 131.3 (CH), 130.8 (CH), 129.2 (CH), 128.8 (CH), 128.1 (CH), 127.9 (CH), 127.1 (CH), 126.6 (CH), 122.2 (CH), 54.3 (CH_2), 35.4 (CH_2), 31.8 (CH_2), 30.9 (CH_2), 29.6 (CH_2), 29.1 (CH_2), 27.3 (CH_2), 22.7 (CH_2), 21.3 (CH_3), 14.1 (CH_3). MS (ESI) *m/z* (relative intensity): 453 (100) $[M+Na]^+$. HR-MS (ESI) *m/z* calcd for $C_{27}H_{35}N_4O$ $[M+H]^+$ 431.2805, found 431.2808.

(*Z*)-*N*-((1-Benzyl-1*H*-1,2,3-triazol-4-yl)methyl)-3-(non-2-en-1-yl)-[1,1'-biphenyl]-4-carboxamide (3fa)

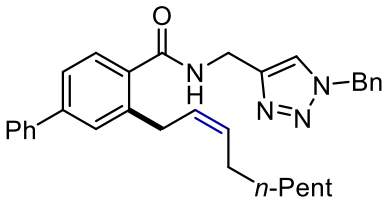

The representative procedure was followed using **1f** (73.6 mg, 0.2 mmol) and **2a** (49.6 mg, 0.4 mmol). Purification by column chromatography on silica gel (*n*-Hexane/EtOAc 1:1) yielded **3fa** (64.9 mg, 66%) as a white waxy solid. ^{1}H-NMR (400 MHz, $CDCl_3$): δ = 7.60 – 7.56 (m, 3H), 7.49 – 7.42 (m, 5H), 7.40 – 7.37 (m, 4H), 7.32 – 7.29 (m, 2H), 6.58 (t, *J* = 5.7 Hz, 1H), 5.54 (s, 2H), 5.53 – 5.48 (m, 2H), 4.70 (d, *J* = 5.7 Hz, 2H), 3.67 – 3.58 (m, 2H), 2.18 – 2.12 (m, 2H), 1.42 – 1.23 (m, 8H), 0.92 – 0.87 (m, 3H). ^{13}C-NMR (101 MHz, $CDCl_3$): δ = 169.8 (C_q), 145.0 (C_q), 143.1 (C_q), 140.3 (C_q), 140.1 (C_q), 134.5 (C_q), 134.4 (C_q), 131.7 (CH), 129.2 (CH), 128.9 (CH), 128.8 (2 x CH), 128.1 (CH), 127.8 (CH), 127.6 (2 x CH), 127.2 (CH), 124.7 (CH), 122.2 (CH), 54.3 (CH_2), 35.5 (CH_2), 31.8 (CH_2), 31.1 (CH_2), 29.6 (CH_2), 29.1 (CH_2), 27.4 (CH_2), 22.7 (CH_2), 14.1 (CH_3). MS (ESI) *m/z* (relative intensity): 515 (28) $[M+Na]^+$, 493 (100) $[M+H]^+$. HR-MS (ESI) *m/z* calcd for $C_{32}H_{37}N_4O$ $[M+H]^+$ 493.2962, found 493.2965.

(*Z*)-*N*-[(1-Benzyl-1*H*-1,2,3-triazol-4-yl)methyl]-4-methoxy-2-(non-2-en-1-yl)benzamide (3ga)

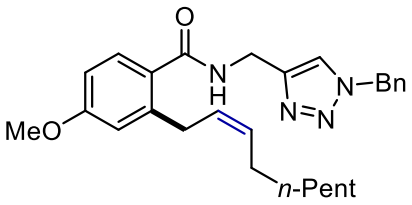

The representative procedure was followed using **1g** (64.5 mg, 0.2 mmol) and **2a** (49.6 mg, 0.4 mmol). Purification by column chromatography on silica gel (*n*-Hexane/EtOAc 1:1) yielded **3ga** (66.9 mg, 75%) as a pale-yellow solid. M.p.= 63-64 °C. ^{1}H-NMR (400 MHz, $CDCl_3$): δ = 7.55 (s, 1H), 7.42 – 7.36 (m, 3H), 7.34 (d, *J* = 8.5 Hz, 1H), 7.29 (d, *J* = 6.3 Hz, 2H), 6.79 (d, *J* = 2.6 Hz, 1H), 6.71 (dd, *J* = 8.5, 2.6 Hz, 1H), 6.46 (t, *J* = 5.7 Hz, 1H), 5.53 (s, 2H), 5.47 (q, *J* = 6.1 Hz, 2H), 4.65 (d, *J* = 5.7 Hz, 2H), 3.81 (s, 3H), 3.56 (d, *J* = 5.6 Hz, 2H), 2.11 (q, *J* = 6.6 Hz, 2H), 1.40 – 1.26 (m, 8H), 0.93 – 0.86 (m, 3H). ^{13}C-NMR (101 MHz, $CDCl_3$): δ = 169.7 (C_q), 161.0 (C_q), 145.1 (C_q), 142.0 (C_q), 134.5 (C_q), 131.7 (CH), 129.2 (CH), 128.9 (CH), 128.8 (CH), 128.1 (CH), 128.0 (C_q), 127.5 (CH), 122.2 (CH), 115.6 (CH), 110.9 (CH), 55.3 (CH_3), 54.3 (CH_2), 35.4 (CH_2), 31.8 (CH_2), 31.1 (CH_2), 29.6 (CH_2), 29.1 (CH_2), 27.4 (CH_2), 22.7 (CH_2), 14.1 (CH_3). MS (ESI) *m/z* (relative intensity): 469 (100) $[M+Na]^+$, 447 (82) $[M+H]^+$. HR-MS (ESI) *m/z* calcd for $C_{27}H_{35}N_4O_2$ $[M+H]^+$ 447.2755, found 447.2763.

(*Z*)-*N*-[(1-Benzyl-1*H*-1,2,3-triazol-4-yl)methyl]-2-(non-2-en-1-yl)-4-(octylthio)benzamide (3ha)

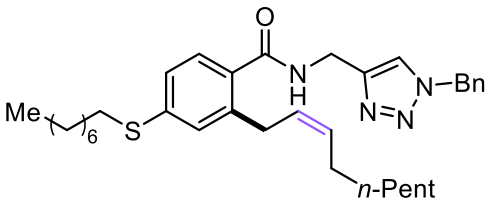

The representative procedure was followed using **1h** (87.3 mg, 0.2 mmol) and **2a** (49.6 mg, 0.4 mmol). Purification by column chromatography on silica gel (*n*-Hexane/EtOAc 1:1) yielded **3ha** (78.4 mg, 70%) as a pale-yellow solid. M.p.= 75-76 °C. ^{1}H-NMR (400 MHz, $CDCl_3$): δ = 7.54 (s, 1H), 7.41 – 7.37 (m, 3H), 7.31 – 7.26 (m, 3H), 7.16 (d, *J* = 1.9 Hz, 1H), 7.10 (dd, *J* = 8.0, 1.9 Hz, 1H), 6.46 (bs, 1H), 5.53 (s, 2H), 5.52 – 5.40 (m, 2H), 4.66 (d, *J* = 5.7 Hz, 2H), 3.53 (d, *J* = 6.4 Hz, 2H), 2.92 (t, *J* = 7.4 Hz, 2H), 2.10 (q, *J* = 6.9 Hz, 2H), 1.66 (p, *J* = 7.3 Hz, 2H), 1.46 – 1.25 (m, 18H), 0.93 – 0.87 (m, 6H). ^{13}C-NMR (101 MHz, $CDCl_3$): δ = 169.6 (C_q), 144.9 (C_q), 140.3 (2 x C_q), 134.4 (C_q), 132.3 (C_q), 131.8 (CH), 129.2 (CH), 129.0 (CH), 128.9 (CH), 128.1 (CH), 127.6 (CH), 127.3 (CH), 125.0 (CH), 122.1 (CH), 54.3 (CH_2), 35.4 (CH_2), 32.7 (CH_2), 31.8 (2 x CH_2), 30.9 (CH_2), 29.6 (CH_2), 29.2 (2 x CH_2), 29.1 (CH_2), 29.0 (CH_2), 28.9 (CH_2), 27.4 (CH_2), 22.7 (2 x CH_2), 14.1 (2 x CH_3). MS (ESI) *m/z* (relative intensity): 583 (100) $[M+Na]^+$, 561 (18) $[M+H]^+$. HR-MS (ESI) *m/z* calcd for $C_{34}H_{49}N_4OS$ $[M+H]^+$ 561.3622, found 561.3629.

(*Z*)-*N*-[(1-Benzyl-1*H*-1,2,3-triazol-4-yl)methyl]-4-(dimethylamino)-2-(non-2-en-1-yl)benzamide (3ia)

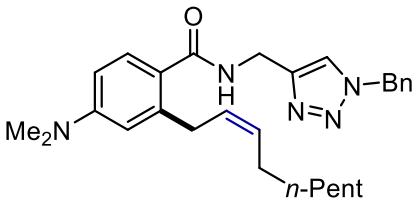

The representative procedure was followed using **1i** (67.1 mg, 0.2 mmol) and **2a** (49.6 mg, 0.4 mmol). Purification by column chromatography on silica gel (*n*-Hexane/EtOAc 1:1) yielded **3ia** (33.0 mg, 36%) as a yellow solid. M.p.= 96-98 °C. ^{1}H-NMR (400 MHz, $CDCl_3$): δ = 7.55 (s, 1H), 7.39 – 7.35 (m, 3H), 7.31 (d, *J* = 8.6 Hz, 1H), 7.29 – 7.25 (m, 2H), 6.55 – 6.43 (m, 3H), 5.51 (s, 2H), 5.49 – 5.42 (m, 2H), 4.64 (d, *J* = 5.8 Hz, 2H), 3.60 (d, *J* = 5.7 Hz, 2H), 2.97 (s, 6H), 2.13 (q, *J* = 6.6 Hz, 2H), 1.36 – 1.26 (m, 8H), 0.90 (t, *J* = 6.7 Hz, 3H). ^{13}C-NMR (101 MHz, $CDCl_3$): δ = 170.0 (C_q), 151.7 (C_q), 145.6 (C_q), 141.6 (C_q), 134.6 (C_q), 131.1 (CH), 129.1 (CH), 129.0 (CH), 128.8 (CH), 128.4 (CH), 128.1 (CH), 122.6 (C_q), 122.3 (CH), 113.2 (CH), 109.1 (CH), 54.2 (CH_2), 40.2 (CH_3), 35.4 (CH_2), 31.9 (CH_2), 31.7 (CH_2), 29.7 (CH_2), 29.1 (CH_2), 27.4 (CH_2), 22.7 (CH_2), 14.1 (CH_3). MS (ESI) *m/z* (relative intensity): 482 (56) $[M+Na]^+$, 460 (100) $[M+H]^+$. HR-MS (ESI) *m/z* calcd for $C_{28}H_{38}N_5O$ $[M+H]^+$ 460.3071, found 460.3076.

Methyl (*Z*)-4-{[(1-benzyl-1*H*-1,2,3-triazol-4-yl)methyl]carbamoyl}-3-(non-2-en-1-yl)benzoate (3ja)

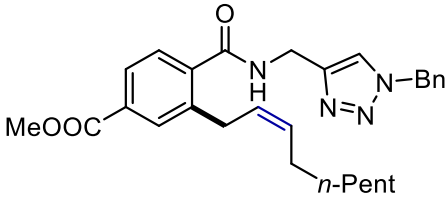

The representative procedure was followed using **1j** (70.0 mg, 0.2 mmol) and **2a** (49.6 mg, 0.4 mmol). Purification by column chromatography on silica gel (*n*-Hexane/EtOAc 1:1) yielded **3ja** (51.2 mg, 54%) as a white waxy solid. ^{1}H-NMR (400 MHz, $CDCl_3$): δ = 7.92 (d, *J* = 1.6 Hz, 1H), 7.86 (dd, *J* = 7.9, 1.7 Hz, 1H), 7.56 (s, 1H), 7.42 – 7.36 (m, 4H), 7.31 – 7.26 (m, 2H), 6.66 (t, *J* = 5.6 Hz, 1H), 5.53 (s, 2H), 5.52 – 5.40 (m, 2H), 4.67 (d, *J* = 5.7 Hz, 2H), 3.93 (s, 3H), 3.56 (d, *J* = 6.6 Hz, 2H), 2.11 (q, *J* = 6.9 Hz, 2H), 1.38 – 1.26 (m, 8H), 0.92 – 0.87 (m, 3H). ^{13}C-NMR (101 MHz, $CDCl_3$): δ = 169.2 (C_q), 166.5 (C_q), 144.6 (C_q), 139.8 (C_q), 139.7 (C_q), 134.4 (C_q), 132.1 (CH), 131.6 (C_q), 131.1 (CH), 129.2 (CH), 128.9 (CH), 128.1 (CH), 127.3 (CH), 127.1 (CH), 126.9 (CH), 122.1 (CH), 54.3 (CH_2), 52.3 (CH_3), 35.4 (CH_2), 31.8 (CH_2), 30.8 (CH_2), 29.5 (CH_2), 29.0 (CH_2), 27.4 (CH_2), 22.7 (CH_2), 14.1 (CH_3). MS (ESI) *m/z* (relative intensity): 497 (100) $[M+Na]^+$, 475 (12) $[M+H]^+$. HR-MS (ESI) *m/z* calcd for $C_{28}H_{35}N_4O_3$ $[M+H]^+$ 475.2704, found 475.2706.

(*Z*)-*N*-[(1-Benzyl-1*H*-1,2,3-triazol-4-yl)methyl]-2-(non-2-en-1-yl)-4-(trifluoromethyl) benzamide (3ka)

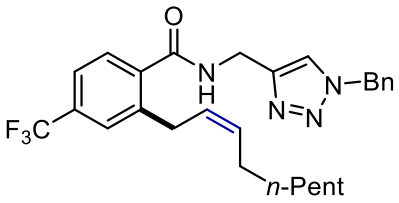

The representative procedure was followed using **1k** (73.2 mg, 0.2 mmol) and **2a** (49.6 mg, 0.4 mmol). Purification by column chromatography on silica gel (*n*-Hexane/EtOAc 1:1) yielded **3ka** (54.9 mg, 56%) as a white solid. M.p.= 93-95 °C. ^{1}H-NMR (400 MHz, $CDCl_3$): δ = 7.55 (s, 1H), 7.51 (s, 1H), 7.47 (d, *J* = 1.8 Hz, 2H), 7.40 – 7.38 (m, 3H), 7.32 – 7.29 (m, 2H), 6.64 (s, 1H), 5.55 – 5.50 (m, 3H), 5.48 – 5.40 (m, 1H), 4.68 (d, *J* = 5.6 Hz, 2H), 3.60 – 3.53 (m, 2H), 2.10 (qd, *J* = 7.3, 1.4 Hz, 2H), 1.38 – 1.27 (m, 8H), 0.90 (t, *J* = 6.8 Hz, 3H). ^{13}C-NMR (101 MHz, $CDCl_3$): δ = 168.8 (C_q), 144.5 (C_q), 140.5 (C_q), 139.0 (C_q), 134.4 (C_q), 132.7 (CH), 132.1 (q, $^{2}J_{C\text{-}F}$ = 32 Hz C_q), 129.2 (CH), 128.9 (CH), 128.1 (CH), 127.4 (CH), 126.7 (q, $^{4}J_{C\text{-}F}$ = 4 Hz, CH), 126.3 (CH), 123.7 (q, $^{1}J_{C\text{-}F}$ = 272 Hz, C_q), 122.9 (q, $^{3}J_{C\text{-}F}$ = 4 Hz, CH), 122.1 (CH), 54.3 (CH_2), 35.4 (CH_2), 31.8 (CH_2), 30.7 (CH_2), 29.5 (CH_2), 29.0 (CH_2), 27.4 (CH_2), 22.6 (CH_2), 14.1 (CH_3). ^{19}F-NMR (565 MHz, $CDCl_3$): δ = -62.8 (s). MS (ESI) *m/z* (relative intensity): 507 (100) $[M+Na]^+$, 485 (18) $[M+H]^+$. HR-MS (ESI) *m/z* calcd for $C_{27}H_{32}F_3N_4O$ $[M+H]^+$ 485.2523, found 485.2527.

(*Z*)-*N*-[(1-Benzyl-1*H*-1,2,3-triazol-4-yl)methyl]-4-fluoro-2-(non-2-en-1-yl)benzamide (3la)

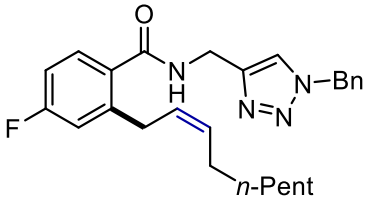

The representative procedure was followed using **1l** (62.0 mg, 0.2 mmol) and **2a** (49.6 mg, 0.4 mmol). Purification by column chromatography on silica gel (*n*-Hexane/EtOAc 1:1) yielded **3la** (56.4 mg, 65%) as a pale-yellow solid. M.p.= 81-82 °C. ^{1}H-NMR (400 MHz, $CDCl_3$): δ = 7.55 (s, 1H), 7.43 – 7.33 (m, 4H), 7.32 – 7.29 (m, 2H), 6.96 (dt, *J* = 10.0, 2.4 Hz, 1H), 6.91 – 6.85 (m, 1H), 6.52 (bs, 1H), 5.57 – 5.48 (m, 3H), 5.47 – 5.39 (m, 1H), 4.66 (d, *J* = 5.9 Hz, 2H), 3.54 (d, *J* = 7.0 Hz, 2H), 2.09 (q, *J* = 7.0 Hz, 2H), 1.38 – 1.26 (m, 8H), 0.94 – 0.86 (m, 3H). ^{13}C-NMR (101 MHz, $CDCl_3$): δ = 169.1 (C_q), 163.7 (d, $^{1}J_{C\text{-}F}$ = 249 Hz, C_q), 144.8 (C_q), 142.9 (d, $^{5}J_{C\text{-}F}$ = 8 Hz, C_q), 134.4 (C_q), 132.3 (CH), 131.7 (d, $^{6}J_{C\text{-}F}$ = 3 Hz, C_q), 129.2 (CH), 129.1 (d, $^{4}J_{C\text{-}F}$ = 9 Hz, CH), 128.9 (CH), 128.11 (CH), 126.6 (CH), 122.1 (CH), 116.7 (d, $^{2}J_{C\text{-}F}$ = 22 Hz, CH), 112.8 (d, $^{3}J_{C\text{-}F}$ = 22 Hz, CH), 54.3 (CH_2), 35.4 (CH_2), 31.8 (CH_2), 30.8 (CH_2), 29.6 (CH_2), 29.0 (CH_2), 27.3 (CH_2), 22.7 (CH_2), 14.1 (CH_3). ^{19}F-NMR (565 MHz, $CDCl_3$): δ = -110.01 – -110.07 (m). MS (ESI) *m/z* (relative intensity): 457 (70) $[M+Na]^+$, 435 (100) $[M+H]^+$. HR-MS (ESI) *m/z* calcd for $C_{26}H_{32}FN_4O$ $[M+H]^+$ 435.2555, found 435.2559.

(*Z*)-*N*-[(1-Benzyl-1*H*-1,2,3-triazol-4-yl)methyl]-4-chloro-2-(non-2-en-1-yl)benzamide (3ma)

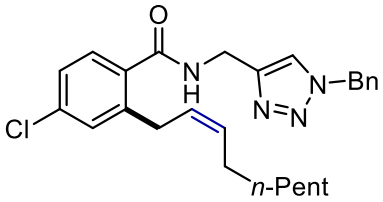

The representative procedure was followed using **1m** (65.2 mg, 0.2 mmol) and **2a** (49.6 mg, 0.4 mmol). Purification by column chromatography on silica gel (*n*-Hexane/EtOAc 1:1) yielded **3ma** (49.5 mg, 55%) as a white solid. M.p.= 92-93 °C. ^{1}H-NMR (400 MHz, $CDCl_3$): δ = 7.54 (s, 1H), 7.39 (dd, *J* = 5.2, 2.1 Hz, 3H), 7.31 – 7.28 (m, 3H), 7.25 (d, *J* = 2.1 Hz, 1H), 7.18 (dd, *J* = 8.1, 1.9 Hz, 1H), 6.55 (s, 1H), 5.56 – 5.47 (m, 3H), 5.46 – 5.39 (m, 1H), 4.66 (d, *J* = 5.6 Hz, 2H), 3.52 (d, *J* = 7.0 Hz, 2H), 2.09 (q, *J* = 7.2, 6.6 Hz, 2H), 1.38 – 1.27 (m, 8H), 0.93 – 0.88 (m, 3H). ^{13}C-NMR (101 MHz, $CDCl_3$): δ = 169.0 (C_q), 144.7 (C_q), 141.7 (C_q), 136.2 (C_q), 134.4 (C_q), 134.0 (C_q), 132.3 (CH), 130.0 (CH), 129.2 (CH), 128.9 (CH), 128.4 (CH), 128.1 (CH), 126.6 (CH), 126.1 (CH), 122.1 (CH), 54.3 (CH_2), 35.4 (CH_2), 31.8 (CH_2), 30.7 (CH_2), 29.5 (CH_2), 29.0 (CH_2), 27.3 (CH_2), 22.7 (CH_2), 14.1 (CH_3). MS (ESI) *m/z* (relative intensity): 473 (100) $[M+Na]^+$, 451 (14) $[M+H]^+$. MS (ESI) *m/z* (relative intensity): 473 (70) $[M+Na]^+$, 451 (100) $[M+H]^+$. HR-MS (ESI) *m/z* calcd for $C_{26}H_{32}ClN_4O$ $[M+H]^+$ 451.2259, found 451.2267.

(*Z*)-*N*-[(1-Benzyl-1*H*-1,2,3-triazol-4-yl)methyl]-4-bromo-2-(non-2-en-1-yl)benzamide (3na)

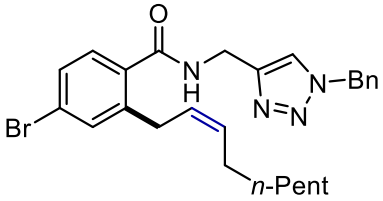

The representative procedure was followed using **1n** (74.2 mg, 0.2 mmol) and **2a** (49.6 mg, 0.4 mmol). Purification by column chromatography on silica gel (*n*-Hexane/EtOAc 1:1) yielded **3na** (39.6 mg, 40%) as a pale-yellow waxy solid. ^{1}H-NMR (400 MHz, $CDCl_3$): δ = 7.55 (s, 1H), 7.40 – 7.36 (m, 4H), 7.33 (dd, *J* = 8.1, 2.1 Hz, 1H), 7.29 – 7.26 (m, 2H), 7.22 (d, *J* = 8.1 Hz, 1H), 6.69 (t, *J* = 5.7 Hz, 1H), 5.55 – 5.47 (m, 3H), 5.46 – 5.37 (m, 1H), 4.64 (d, *J* = 5.6 Hz, 2H), 3.51 (d, *J* = 7.1 Hz, 2H), 2.09 (q, *J* = 7.1 Hz, 2H), 1.35 – 1.27 (m, 8H), 0.94 – 0.85 (m, 3H). ^{13}C-NMR (101 MHz, $CDCl_3$): δ = 169.1 (C_q), 144.7 (C_q), 141.9 (C_q), 134.5 (C_q), 134.4 (C_q), 132.9 (CH), 132.3 (CH), 129.2 (CH), 129.1 (CH), 128.9 (CH), 128.6 (CH), 128.1 (CH), 126.6 (CH), 124.5 (C_q), 122.2 (CH), 54.3 (CH_2), 35.4 (CH_2), 31.8 (CH_2), 30.6 (CH_2), 29.5 (CH_2), 29.0 (CH_2), 27.3 (CH_2), 22.7 (CH_2), 14.1 (CH_3). MS (ESI) *m/z* (relative intensity): 517 (34) $[M+Na]^+$, 495 (100) $[M+H]^+$. HR-MS (ESI) *m/z* calcd for $C_{26}H_{32}BrN_4O$ $[M+H]^+$ 495.1754, found 495.1759.

(*Z*)-*N*-[(1-Benzyl-1*H*-1,2,3-triazol-4-yl)methyl]-4-cyano-2-(non-1-en-1-yl)benzamide (3oa)

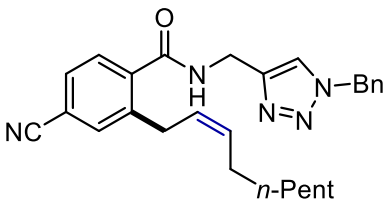

The representative procedure was followed using **1o** (63.5 mg, 0.2 mmol) and **2a** (49.6 mg, 0.4 mmol). Purification by column chromatography on silica gel (*n*-Hexane/EtOAc 1:1) yielded **3oa** (39.7 mg, 45%) as a colourless oil. ^{1}H-NMR (400 MHz, $CDCl_3$): δ = 7.57 – 7.54 (m, 2H), 7.52 (dd, *J* = 7.8, 1.5 Hz, 1H), 7.45 (d, *J* = 7.9 Hz, 1H), 7.42 – 7.36 (m, 3H), 7.30 (d, *J* = 3.5 Hz, 2H), 6.67 (bs, 1H), 5.61 – 5.55 (m, 1H), 5.54 (s, 2H), 5.45 – 5.37 (m, 1H), 4.67 (d, *J* = 5.5 Hz, 2H), 3.54 (d, *J* = 7.2 Hz, 2H), 2.13 – 1.96 (m, 2H), 1.40 – 1.28 (m, 8H), 0.94 – 0.85 (m, 3H). ^{13}C-NMR (101 MHz, $CDCl_3$): δ = 168.2 (C_q), 140.9 (C_q), 139.8 (2 x C_q), 134.3 (C_q), 133.4 (CH), 133.1 (CH), 129.8 (CH), 129.2 (2 x CH), 129.0 (CH), 128.1 (CH), 127.7 (CH), 125.7 (CH), 118.2 (C_q), 114.0 (C_q), 54.4 (CH_2), 35.4 (CH_2), 31.8 (CH_2), 30.5 (CH_2), 29.5 (CH_2), 29.0 (CH_2), 27.4 (CH_2), 22.7 (CH_2), 14.1 (CH_3). MS (ESI) *m/z* (relative intensity): 905 (21) $[2M+Na]^+$, 464 (100) $[M+Na]^+$, 442 (42) $[M+H]^+$. HR-MS (ESI) *m/z* calcd for $C_{27}H_{32}N_5O$ $[M+H]^+$ 442.2601, found 442.2606.

(*Z*)-*N*-[(1-Benzyl-1*H*-1,2,3-triazol-4-yl)methyl]-2-(non-2-en-1-yl)-4-(4,4,5,5-tetramethyl-1,3,2-dioxaborolan-2-yl)benzamide (3pa)

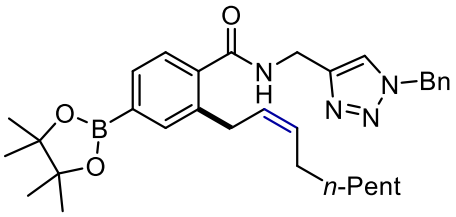

The representative procedure was followed using **1p** (83.7 mg, 0.2 mmol) and **2a** (49.6 mg, 0.4 mmol). Purification by column chromatography on silica gel (*n*-Hexane/EtOAc 1:1) yielded **3pa** (60.8 mg, 56%) as a colourless oil. ^{1}H-NMR (400 MHz, $CDCl_3$): δ = 7.68 (s, 1H), 7.64 (dd, *J* = 7.5, 1.2 Hz, 1H), 7.56 (s, 1H), 7.39 – 7.36 (m, 3H), 7.33 (d, *J* = 7.6 Hz, 1H), 7.30 – 7.26 (m, 2H), 6.55 (t, *J* = 5.7 Hz, 1H), 5.52 (s, 2H), 5.50 – 5.38 (m, 2H), 4.65 (d, *J* = 5.7 Hz, 2H), 3.59 – 3.49 (m, 2H), 2.11 (q, *J* = 6.5 Hz, 2H), 1.35 (s, 12H), 1.34 – 1.26 (m, 8H), 0.93 – 0.87 (m, 3H). ^{13}C-NMR (101 MHz, $CDCl_3$): δ = 169.9 (C_q), 145.0 (C_q), 139.5 (C_q), 138.6 (C_q), 138.1 (C_q), 136.5 (CH), 134.5 (C_q), 132.4 (CH), 131.2 (CH), 129.2 (CH), 128.8 (CH), 128.1 (CH), 128.0 (CH), 126.3 (CH), 122.2 (CH), 84.0 (C_q), 54.3 (CH_2), 35.4 (CH_2), 31.8 (CH_2), 31.1 (CH_2), 29.6 (CH_2), 29.0 (CH_2), 27.4 (CH_2), 24.9 (CH_3), 22.7 (CH_2), 14.2 (CH_3). MS (ESI) *m/z* (relative intensity): 565 (100) $[M+Na]^+$, 543 (43) $[M+H]^+$. HR-MS (ESI) *m/z* calcd for $C_{32}H_{43}BN_4O_3Na$ $[M+Na]^+$ 565.3326, found 565.3330.

(*Z*)-*N*-[(1-Benzyl-1*H*-1,2,3-triazol-4-yl)methyl]-5-methyl-2-(non-2-en-1-yl)benzamide (3qa)

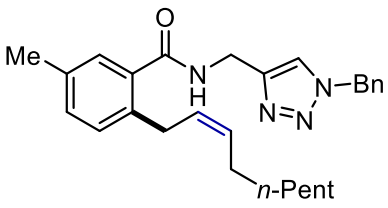

The representative procedure was followed using **1q** (61.2 mg, 0.2 mmol) and **2a** (49.6 mg, 0.4 mmol). Purification by column chromatography on silica gel (*n*-Hexane/EtOAc 1:1) yielded **3qa** (50.7 mg, 59%) as a colourless oil. ^{1}H-NMR (400 MHz, $CDCl_3$): δ = 7.56 (s, 1H), 7.41 – 7.37 (m, 3H), 7.31 – 7.28 (m, 3H), 7.16 – 7.14 (m, 2H), 6.50 (bs, 1H), 5.53 (s, 2H), 5.47 – 5.41 (m, 2H), 4.66 (d, *J* = 5.7 Hz, 2H), 3.51 – 3.48 (m, 2H), 2.31 (s, 3H), 2.13 – 2.07 (m, 2H), 1.37 – 1.27 (m, 8H), 0.94 – 0.87 (m, 3H). ^{13}C-NMR (101 MHz, $CDCl_3$): δ = 170.1 (C_q), 145.0 (C_q), 136.3 (C_q), 135.7 (C_q), 135.5 (C_q), 134.5 (C_q), 131.2 (CH), 131.0 (CH), 129.9 (CH), 129.2 (CH), 128.9 (CH), 128.1 (CH), 128.0 (CH), 127.6 (CH), 122.2 (CH), 54.3 (CH_2), 35.4 (CH_2), 31.8 (CH_2), 30.5 (CH_2), 29.6 (CH_2), 29.1 (CH_2), 27.3 (CH_2), 22.7 (CH_2), 20.8 (CH_3), 14.1 (CH_3). MS (ESI) *m/z* (relative intensity): 453 (56) $[M+Na]^+$, 431 (100) $[M+H]^+$. HR-MS (ESI) *m/z* calcd for $C_{27}H_{35}N_4O$ $[M+H]^+$ 431.2805, found 431.2814.

(*Z*)-*N*-[(1-Benzyl-1*H*-1,2,3-triazol-4-yl)methyl]-5-methoxy-2-(non-2-en-1-yl)benzamide (3ra)

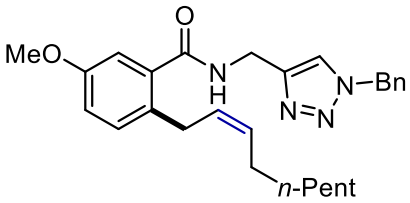

The representative procedure was followed using **1r** (64.5 mg, 0.2 mmol) and **2a** (49.6 mg, 0.4 mmol). Purification by column chromatography on silica gel (*n*-hexane/EtOAc 1:1) yielded **3ra** (44.6 mg, 50%) as a colourless oil. ^{1}H-NMR (400 MHz, $CDCl_3$): δ = 7.55 (s, 1H), 7.41 – 7.37 (m, 3H), 7.30 (d, *J* = 3.2 Hz, 2H), 7.18 – 7.13 (m, 1H), 6.92 – 6.87 (m, 2H), 6.46 (bs, 1H), 5.53 (d, *J* = 1.4 Hz, 2H), 5.43 (p, *J* = 5.3 Hz, 2H), 4.67 (dd, *J* = 5.7, 1.6 Hz, 2H), 3.79 (s, 3H), 3.45 (d, *J* = 5.4 Hz, 2H), 2.09 (q, *J* = 6.5 Hz, 2H), 1.37 – 1.26 (m, 8H), 0.90 (t, *J* = 6.7 Hz, 3H). ^{13}C-NMR (101 MHz, $CDCl_3$): δ = 169.8 (C_q), 157.6 (C_q), 144.9 (C_q), 136.5 (C_q), 134.5 (C_q), 131.2 (CH), 131.1 (C_q), 131.1 (CH), 129.2 (CH), 128.9 (CH), 128.1 (CH), 128.1 (CH), 122.2 (CH), 116.0 (CH), 112.4 (CH), 55.5 (CH_3), 54.3 (CH_2), 35.4 (CH_2), 31.8 (CH_2), 30.2 (CH_2), 29.6 (CH_2), 29.1 (CH_2), 27.3 (CH_2), 22.7 (CH_2), 14.1 (CH_3). MS (ESI) *m/z* (relative intensity): 469 (60) $[M+Na]^+$, 447 (100) $[M+H]^+$. HR-MS (ESI) *m/z* calcd for $C_{27}H_{35}N_4O_2$ $[M+H]^+$ 447.2755, found 447.2759.

(*Z*)-*N*-[(1-benzyl-1H-1,2,3-triazol-4-yl)methyl]-2-(non-2-en-1-yl)-5-(trifluoromethyl)benzamide (3sa)

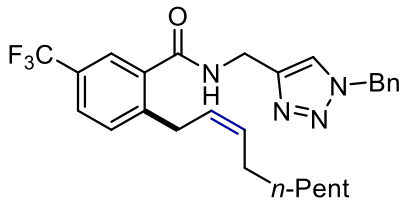

The representative procedure was followed using **1s** (73.2 mg, 0.2 mmol) and **2a** (49.6 mg, 0.4 mmol). Purification by column chromatography on silica gel (*n*-Hexane/EtOAc 1:1) yielded **3sa** (51.0 mg, 52%) as a colourless oil. ^{1}H-NMR (400 MHz, $CDCl_3$): δ = 7.60 – 7.59 (m, 2H), 7.56 (s, 1H), 7.41 – 7.38 (m, 4H), 7.31 (d, *J* = 2.7 Hz, 2H), 6.65 (bs, 1H), 5.56 – 5.49 (m, 3H), 5.47 – 5.38 (m, 1H), 4.69 (d, *J* = 5.6 Hz, 2H), 3.58 (d, *J* = 7.0 Hz, 2H), 2.14 – 2.07 (m, 2H), 1.37 – 1.26 (m, 8H), 0.95 – 0.86 (m, 3H). ^{13}C-NMR (101 MHz, $CDCl_3$): δ = 168.6 (C_q), 144.5 (C_q), 143.6 (C_q), 136.3 (C_q), 134.4 (C_q), 132.50 (CH), 130.45 (CH), 129.21 (CH), 128.92 (CH), 128.5 (q, $^{2}J_{C\text{-}F}$ = 33 Hz C_q), 128.14 (CH), 126.8 (q, $^{4}J_{C\text{-}F}$ = 4 Hz, CH), 126.4 (CH), 124.0 (q, $^{3}J_{C\text{-}F}$ = 4 Hz, CH), 123.8 (q, $^{1}J_{C\text{-}F}$ = 272 Hz, C_q), 122.1 (CH), 54.3 (CH_2), 35.5 (CH_2), 31.8 (CH_2), 30.9 (CH_2), 29.5 (CH_2), 29.0 (CH_2), 27.4 (CH_2), 22.7 (CH_2), 14.1 (CH_3). ^{19}F-NMR (565 MHz, $CDCl_3$): δ = -62.4 (s). MS (ESI) *m/z* (relative intensity): 507 (100) $[M+Na]^+$. HR-MS (ESI) *m/z* calcd for $C_{27}H_{32}F_3N_4O$ $[M+H]^+$ 485.2523, found 485.2526.

(*Z*)-*N*-[(1-Benzyl-1*H*-1,2,3-triazol-4-yl)methyl]-3-(non-2-en-1-yl)-2-naphthamide (3ta)

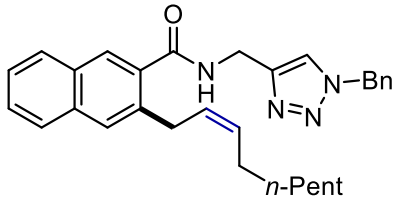

The representative procedure was followed using **1t** (68.4 mg, 0.2 mmol) and **2a** (49.6 mg, 0.4 mmol). Purification by column chromatography on silica gel (*n*-Hexane/EtOAc 1:1) yielded **3txa** (84.9 mg, 91%) as a white waxy solid. ^{1}H-NMR (400 MHz, $CDCl_3$): δ = 7.86 (s, 1H), 7.79 (m, 2H), 7.68 (s, 1H), 7.59 (s, 1H), 7.51 (m, 1H), 7.46 (m, 1H), 7.41 – 7.37 (m, 3H), 7.30 (dd, *J* = 7.4, 2.3 Hz, 2H), 6.71 (t, *J* = 5.7 Hz, 1H), 5.59 – 5.48 (m, 4H), 4.72 (d, *J* = 5.7 Hz, 2H), 3.71 (d, *J* = 5.5 Hz, 2H), 2.15 (q, *J* = 6.8 Hz, 2H), 1.40 – 1.26 (m, 8H), 0.92 – 0.86 (m, 3H). ^{13}C-NMR (101 MHz, $CDCl_3$): δ = 170.0 (C_q), 144.9 (C_q), 136.4 (C_q), 134.5 (C_q), 134.4 (C_q), 134.1 (C_q), 131.8 (CH), 131.1 (C_q), 129.2 (CH), 128.9 (CH), 128.3 (CH), 128.1 (CH), 127.9 (CH), 127.5 (CH), 127.3 (2 x CH), 127.0 (CH), 126.0 (CH), 122.2 (CH), 54.3 (CH_2), 35.5 (CH_2), 31.8 (CH_2), 31.0 (CH_2), 29.7 (CH_2), 29.1 (CH_2), 27.4 (CH_2), 22.7 (CH_2), 14.1 (CH_3). MS (ESI) *m/z* (relative intensity): 489 (100) $[M+Na]^+$. HR-MS (ESI) *m/z* calcd for $C_{30}H_{35}N_4O$ $[M+H]^+$ 467.2805, found 467.2814.

(*Z*)-*N*-[(1-Benzyl-1*H*-1,2,3-triazol-4-yl)methyl]-3-(non-2-en-1-yl)benzo[*b*]thiophene-2-carboxamide (3ua)

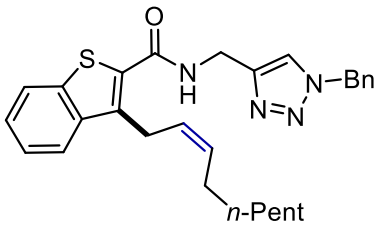

The representative procedure was followed using **1u** (69.7 mg, 0.2 mmol), dppen (12.0 mg, 0.03 mmol) and **2a** (49.6 mg, 0.4 mmol). Purification by column chromatography on silica gel (*n*-Hexane/EtOAc 1:1) yielded **3ua** (59.8 mg, 70%) as a colourless oil. ^{1}H-NMR (400 MHz, $CDCl_3$). δ = 7.82 – 7.79 (m, 2H), 7.58 (s, 1H), 7.44 – 7.36 (m, 5H), 7.30 – 7.28 (m, 2H), 6.80 (t, *J* = 5.7 Hz, 1H), 5.52 (s, 2H), 5.50 – 5.40 (m, 2H), 4.69 (d, *J* = 5.7 Hz, 2H), 3.95 (d, *J* = 6.1 Hz, 2H), 2.25 (q, *J* = 6.9 Hz, 2H), 1.44 – 1.32 (m, 8H), 0.97 – 0.89 (m, 3H). ^{13}C-NMR (101 MHz, $CDCl_3$): δ = 163.4 (C_q), 144.9 (C_q), 139.8 (C_q), 139.0 (2 x C_q), 134.5 (C_q), 131.8 (CH), 130.9 (C_q), 129.2 (CH), 128.8 (CH), 128.1 (CH), 126.5 (CH), 126.4 (CH), 124.6 (CH), 123.5 (CH), 122.7 (CH), 122.4 (CH), 54.3 (CH_2), 35.7 (CH_2), 31.8 (CH_2), 29.5 (CH_2), 29.1 (CH_2), 27.7 (CH_2), 25.7 (CH_2), 22.7 (CH_2), 14.2 (CH_3). MS (ESI) *m/z* (relative intensity): 495 (100) $[M+Na]^+$, 473 (27) $[M+H]^+$. HR-MS (ESI) *m/z* calcd for $C_{28}H_{33}N_4OS$ $[M+H]^+$ 473.2370, found 473.2373.

(*Z*)-*N*-[(1-Benzyl-1*H*-1,2,3-triazol-4-yl)methyl]-1-methyl-3-(non-2-en-1-yl)-1*H*-indole-2-carboxamide (3va)

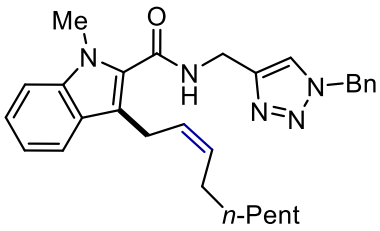

The representative procedure was followed using **1v** (69.1 mg, 0.2 mmol), dppen (12.0 mg, 0.03 mmol) and **2a** (49.6 mg, 0.4 mmol). Purification by column chromatography on silica gel (*n*-Hexane/EtOAc 1:1) yielded **3va** (49.8 mg, 53%) as a pale-yellow oil. ^{1}H-NMR (400 MHz, $CDCl_3$): δ = 7.62 (d, *J* = 8.1 Hz, 1H), 7.58 (s, 1H), 7.38 (dd, *J* = 5.2, 1.9 Hz, 3H), 7.34 – 7.31 (m, 2H), 7.31 – 7.27 (m, 2H), 7.17 – 7.13 (m, 1H), 6.77 (bs, 1H), 5.52 (s, 2H), 5.51 – 5.40 (m, 2H), 4.71 (d, *J* = 5.4 Hz, 2H), 3.85 (s, 3H), 3.65 (d, *J* = 5.0 Hz, 2H), 2.15 (q, *J* = 6.7 Hz, 2H), 1.44 – 1.31 (m, 8H), 0.97 – 0.89 (m, 3H). ^{13}C-NMR (101 MHz, $CDCl_3$): δ = 163.0 (C_q), 138.0 (C_q), 134.6 (C_q), 131.4 (CH), 129.8 (C_q), 129.2 (CH), 128.8 (CH), 128.2 (CH), 128.1 (2 x CH), 126.5 (2 x C_q), 124.2 (CH), 120.1 (CH), 119.8 (CH), 116.3 (C_q), 109.9 (CH), 54.3 (CH_2), 35.5 (CH_2), 31.8 (CH_2), 31.3 (CH_3), 29.5 (CH_2), 29.1 (CH_2), 27.5 (CH_2), 23.1 (CH_2), 22.7 (CH_2), 14.2 (CH_3). MS (ESI) *m/z* (relative intensity): 961 (33) $[2M+Na]^+$, 492 (100) $[M+Na]^+$, 470 (68) $[M+H]^+$. HR-MS (ESI) *m/z* calcd for $C_{29}H_{36}N_5O$ $[M+H]^+$ 470.2914, found 470.2918.

(*Z*)-*N*-[(1-Benzyl-1*H*-1,2,3-triazol-4-yl)methyl]-3-(non-2-en-1-yl)thiophene-2-carboxamide (3wa)

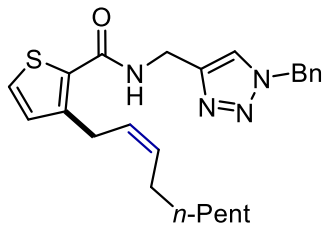

The representative procedure was followed using **1w** (59.7 mg, 0.2 mmol) and **2a** (49.6 mg, 0.4 mmol). Purification by column chromatography on silica gel (*n*-Hexane/EtOAc 1:1) yielded **3wa** (54.1 mg, 64%) as a colourless oil. ^{1}H-NMR (400 MHz, $CDCl_3$): δ = 7.55 (s, 1H), 7.41 – 7.36 (m, 3H), 7.31 – 7.26 (m, 3H), 6.94 (d, *J* = 5.0 Hz, 1H), 6.58 (t, *J* = 5.7 Hz, 1H), 5.57 – 5.46 (m, 4H), 4.65 (d, *J* = 5.7 Hz, 2H), 3.70 (d, *J* = 5.6 Hz, 2H), 2.16 – 2.08 (m, 2H), 1.39 – 1.27 (m, 8H), 0.93 – 0.86 (m, 3H). ^{13}C-NMR (101 MHz, $CDCl_3$): δ = 163.0 (C_q), 145.0 (C_q), 144.9 (C_q), 134.5 (C_q), 132.0 (CH), 130.8 (CH), 130.5 (C_q), 129.2 (CH), 128.8 (CH), 128.1 (CH), 127.0 (CH), 126.7 (CH), 122.4 (CH), 54.3 (CH_2), 35.4 (CH_2), 31.8 (CH_2), 29.5 (CH_2), 29.0 (CH_2), 27.6 (CH_2), 27.3 (CH_2), 22.7 (CH_2), 14.1 (CH_3). MS (ESI) *m/z* (relative intensity): 423 (100) $[M+H]^+$. HR-MS (ESI) *m/z* calcd for $C_{24}H_{31}N_4OS$ $[M+H]^+$ 423.2213, found 423.2217.

(*Z*)-*N*-[(1-Benzyl-1*H*-1,2,3-triazol-4-yl)methyl]-2-methyl-6-(non-2-en-1-yl)benzamide (3xa)

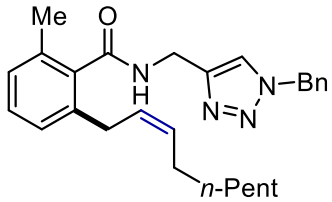

The representative procedure was followed using **1x** (61.2 mg, 0.2 mmol) and **2a** (49.6 mg, 0.4 mmol). Purification by column chromatography on silica gel (*n*-Hexane/EtOAc 1:1) yielded **3xa** (19.8 mg, 23%) as a colourless oil. ^{1}H-NMR (400 MHz, $CDCl_3$): δ = 7.59 (s, 1H), 7.39 (dd, *J* = 5.2, 1.9 Hz, 3H), 7.27 (dd, *J* = 4.9, 1.8 Hz, 2H), 7.19 (t, *J* = 7.7 Hz, 1H), 7.02 (dd, *J* = 13.4, 7.6 Hz, 2H), 6.36 (t, *J* = 5.8 Hz, 1H), 5.54 (s, 2H), 5.52 – 5.39 (m, 2H), 4.69 (d, *J* = 5.7 Hz, 2H), 3.33 (d, *J* = 6.1 Hz, 2H), 2.17 (s, 3H), 2.12 – 2.04 (m, 2H), 1.35 – 1.27 (m, 8H), 0.90 (t, *J* = 7.0 Hz 3H). ^{13}C-NMR (101 MHz, $CDCl_3$): δ = 170.2 (C_q), 144.8 (C_q), 137.6 (C_q), 136.6 (C_q), 134.5 (C_q), 134.3 (C_q), 131.3 (CH), 129.2 (CH), 129.1 (CH), 128.8 (CH), 128.0 (CH), 127.8 (CH), 127.5 (CH), 126.5 (CH), 122.2 (CH), 54.3 (CH_2), 35.2 (CH_2), 31.8 (CH_2), 30.8 (CH_2), 29.6 (CH_2), 29.1 (CH_2), 27.3 (CH_2), 22.7 (CH_2), 19.1 (CH_3), 14.1 (CH_3). MS (ESI) *m/z* (relative intensity): 453 (100) $[M+Na]^+$. HR-MS (ESI) *m/z* calcd for $C_{27}H_{35}N_4O$ $[M+H]^+$ 431.2805, found 431.2809.

(*Z*)-*N*-[(1-Benzyl-1*H*-1,2,3-triazol-4-yl)methyl]-2-(oct-1-en-1-yl)benzamide (3ab)

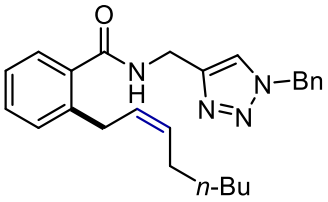

The representative procedure was followed using **1a** (58.5 mg, 0.2 mmol) and **2b** (44.0 mg, 0.4 mmol). Purification by column chromatography on silica gel (*n*-Hexane/EtOAc 1:1) yielded **3ab** (59.8 mg, 76%) as a colourless oil. ^{1}H-NMR (400 MHz, $CDCl_3$): δ = 7.57 (s, 1H), 7.41 – 7.31 (m, 5H), 7.30 – 7.23 (m, 3H), 7.19 (td, *J* = 7.5, 1.3 Hz, 1H), 6.63 (t, *J* = 5.4 Hz, 1H), 5.52 (s, 2H), 5.49 – 5.43 (m, 2H), 4.66 (d, *J* = 5.4 Hz, 2H), 3.58 – 3.49 (m, 2H), 2.15 – 2.07 (m, 2H), 1.40 – 1.28 (m, 6H), 0.90 (t, *J* = 6.8 Hz, 3H). ^{13}C-NMR (101 MHz, $CDCl_3$): δ = 170.0 (C_q), 139.5 (2 x C_q), 135.7 (C_q), 134.5 (C_q), 131.4 (CH), 130.2 (CH), 129.9 (CH), 129.2 (CH), 128.8 (CH), 128.1 (2 x CH), 127.7 (CH), 127.0 (CH), 126.0 (CH), 54.3 (CH_2), 35.4 (CH_2), 31.6 (CH_2), 30.9 (CH_2), 29.3 (CH_2), 27.3 (CH_2), 22.6 (CH_2), 14.1 (CH_3). MS (ESI) *m/z* (relative intensity): 425 (100) $[M+Na]^+$, 403 (71) $[M+H]^+$. HR-MS (ESI) *m/z* calcd for $C_{25}H_{31}N_4O$ $[M+H]^+$ 403.2492, found 403.2498.

(*Z*)-*N*-[(1-Benzyl-1*H*-1,2,3-triazol-4-yl)methyl]-2-(undec-2-en-1-yl)benzamide (3ac)

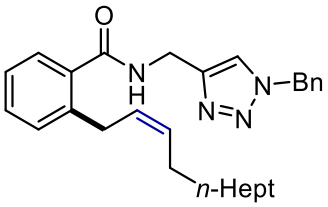

The representative procedure was followed using **1a** (58.5 mg, 0.2 mmol) and **2c** (60.9 mg, 0.4 mmol). Purification by column chromatography on silica gel (*n*-Hexane/EtOAc 1:1) yielded **3ac** (66.7 mg, 75%) as a colourless oil. ^{1}H-NMR (400 MHz, $CDCl_3$): δ = 7.56 (s, 1H), 7.40 – 7.33 (m, 4H), 7.30 – 7.24 (m, 4H), 7.20 (td, *J* = 7.5, 1.3 Hz, 1H), 6.55 (bs, 1H), 5.53 (s, 2H), 5.50 – 5.41 (m, 2H), 4.67 (d, *J* = 5.7 Hz, 2H), 3.54 (d, *J* = 5.8 Hz, 2H), 2.10 (q, *J* = 6.7 Hz, 2H), 1.38 – 1.24 (m, 12H), 0.90 (t, *J* = 6.8 Hz, 3H). ^{13}C-NMR (101 MHz, $CDCl_3$): δ = 170.0 (C_q), 145.0 (C_q), 139.5 (C_q), 135.7 (C_q), 134.5 (C_q), 131.5 (CH), 130.2 (CH), 130.0 (CH), 129.2 (CH), 128.9 (CH), 128.1 (CH), 127.6 (CH), 127.0 (CH), 126.0 (CH), 122.2 (CH), 54.3 (CH_2), 35.4 (CH_2), 31.9 (CH_2), 30.9 (CH_2), 29.7 (CH_2), 29.6 (CH_2), 29.4 (CH_2), 29.3 (CH_2), 27.3 (CH_2), 22.7 (CH_2), 14.1 (CH_3). MS (ESI) *m/z* (relative intensity): 467 (100) $[M+Na]^+$, 445 (35) $[M+H]^+$. MS (ESI) *m/z* (relative intensity): 425 (100) $[M+Na]^+$, 403 (71) $[M+H]^+$. HR-MS (ESI) *m/z* calcd for $C_{28}H_{37}N_4O$ $[M+H]^+$ 445.2962, found 445.2967.

(*Z*)-*N*-[(1-Benzyl-1*H*-1,2,3-triazol-4-yl)methyl]-2-(4-phenylbut-2-en-1-yl)benzamide (3ad)

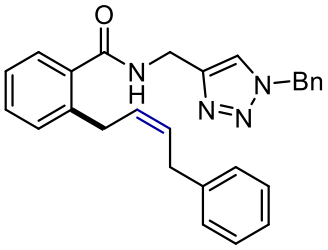

The representative procedure was followed using **1a** (58.5 mg, 0.2 mmol) and **2d** (52.0 mg, 0.4 mmol). Purification by column chromatography on silica gel (*n*-Hexane/EtOAc 1:1) yielded **3ad** (69.3 mg, 82%) as a white waxy solid. ^{1}H-NMR (400 MHz, $CDCl_3$): δ = 7.51 (s, 1H), 7.39 – 7.34 (m, 5H), 7.33 – 7.29 (m, 2H), 7.27 – 7.19 (m, 7H), 6.61 (t, *J* = 5.7 Hz, 1H), 5.68 – 5.56 (m, 2H), 5.46 (s, 2H), 4.64 (d, *J* = 5.7 Hz, 2H), 3.68 (d, *J* = 5.8 Hz, 2H), 3.47 (d, *J* = 5.7 Hz, 2H). ^{13}C-NMR (101 MHz, $CDCl_3$): δ = 170.0 (C_q), 144.9 (C_q), 140.8 (C_q), 139.2 (C_q), 135.7 (C_q), 134.5 (C_q), 130.3 (CH), 130.1 (CH), 129.4 (CH), 129.2 (CH), 128.8 (2 x CH), 128.5 (2 x CH), 128.1 (CH), 127.1 (CH), 126.2 (CH), 126.0 (CH), 122.2 (CH), 54.2 (CH_2), 35.4 (CH_2), 33.5 (CH_2), 31.0 (CH_2). MS (ESI) *m/z* (relative intensity): 445 (100) $[M+Na]^+$. HR-MS (ESI) *m/z* calcd for $C_{27}H_{27}N_4O$ $[M+H]^+$ 423.2179, found 423.2174.

(*Z*)-*N*-[(1-Benzyl-1*H*-1,2,3-triazol-4-yl)methyl]-2-(7-phenoxyhept-2-en-1-yl)benzamide (3ae)

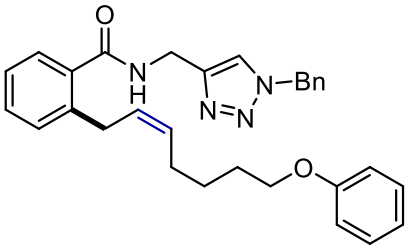

The representative procedure was followed using **1a** (58.5 mg, 0.2 mmol) and **2e** (75.2 mg, 0.4 mmol). Purification by column chromatography on silica gel (*n*-Hexane/EtOAc 1:1) yielded **3ae** (73.1 mg, 76%) as a pale-yellow oil. ^{1}H-NMR (400 MHz, $CDCl_3$): δ = 7.55 (s, 1H), 7.39 – 7.31 (m, 7H), 7.27 – 7.24 (m, 3H), 7.20 (td, *J* = 7.6, 1.3 Hz, 1H), 6.95 (d, *J* = 7.4 Hz, 1H), 6.93 – 6.88 (m, 2H), 6.61 (t, *J* = 5.5 Hz, 1H), 5.52 – 5.45 (m, 4H), 4.66 (d, *J* = 5.7 Hz, 2H), 3.97 (t, *J* = 6.4 Hz, 2H), 3.56 (d, *J* = 5.5 Hz, 2H), 2.21 – 2.16 (m, 2H), 1.85 – 1.79 (m, 2H), 1.60 – 1.53 (m, 2H). ^{13}C-NMR (101 MHz, $CDCl_3$): δ = 170.0 (C_q), 159.1 (C_q), 144.9 (C_q), 139.4 (C_q), 135.6 (C_q), 134.5 (C_q), 130.8 (CH), 130.3 (CH), 129.9 (CH), 129.4 (CH), 129.2 (CH), 128.8 (CH), 128.2 (CH), 128.1 (CH), 127.1 (CH), 126.1 (CH), 122.2 (CH), 120.5 (CH), 114.5 (CH), 67.7 (CH_2), 54.2 (CH_2), 35.4 (CH_2), 31.0 (CH_2), 28.9 (CH_2), 27.0 (CH_2), 26.1 (CH_2). MS (ESI) *m/z* (relative intensity): 503 (100) $[M+Na]^+$. HR-MS (ESI) *m/z* calcd for $C_{30}H_{33}N_4O_2$ $[M+H]^+$ 481.2598, found 481.2596.

(*Z*)-*N*-[(1-Benzyl-1*H*-1,2,3-triazol-4-yl)methyl]-2-(7-(phenylthio)hept-2-en-1-yl)benzamide (3af)

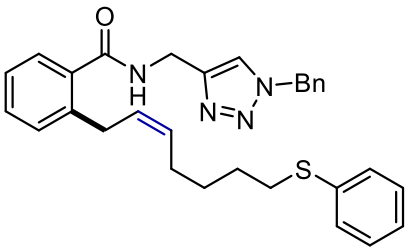

The representative procedure was followed using **1a** (58.5 mg, 0.2 mmol) and **2f** (82.1 mg, 0.4 mmol). Purification by column chromatography on silica gel (*n*-Hexane/EtOAc 1:1) yielded **3af** (54.6 mg, 55%) as a pale-yellow oil. ^{1}H-NMR (400 MHz, $CDCl_3$): δ = 7.54 (s, 1H), 7.38 – 7.31 (m, 7H), 7.31 – 7.26 (m, 3H), 7.25 – 7.16 (m, 4H), 6.59 (t, *J* = 5.9 Hz, 1H), 5.51 (s, 2H), 5.50 – 5.39 (m, 2H), 4.65 (d, *J* = 5.7 Hz, 2H), 3.53 (d, *J* = 6.4 Hz, 2H), 2.93 (t, *J* = 7.3 Hz, 2H), 2.12 (q, *J* = 7.0 Hz, 2H), 1.68 (dq, *J* = 8.7, 7.0 Hz, 2H), 1.57 – 1.47 (m, 2H). ^{13}C-NMR (101 MHz, $CDCl_3$): δ = 170.0 (C_q), 144.9 (C_q), 139.3 (C_q), 136.9 (C_q), 135.6 (C_q), 134.5 (C_q), 130.6 (CH), 130.3 (CH), 129.9 (CH), 129.2 (CH), 128.9 (CH), 128.9 (CH), 128.8 (CH), 128.3 (CH), 128.1 (CH), 127.1 (CH), 126.1 (CH), 125.7 (CH), 122.2 (CH), 54.3 (CH_2), 35.4 (CH_2), 33.5 (CH_2), 30.9 (CH_2), 28.7 (CH_2), 28.7 (CH_2), 26.8 (CH_2). MS (ESI) *m/z* (relative intensity): 519 (100) $[M+Na]^+$. HR-MS (ESI) *m/z* calcd for $C_{30}H_{33}N_4OS$ $[M+H]^+$ 497.2370, found 497.2374.

(*Z*)-2-[7-(9*H*-Carbazol-9-yl)hept-2-en-1-yl]-*N*-[(1-benzyl-1*H*-1,2,3-triazol-4-yl)methyl] benzamide (3ag)

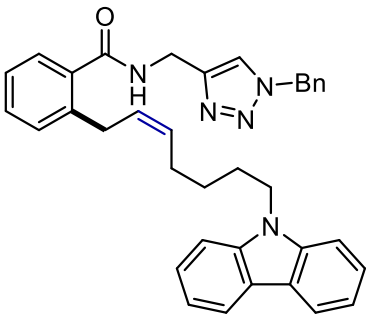

The representative procedure was followed using **1a** (58.5 mg, 0.2 mmol) and **2g** (86.6 mg, 0.4 mmol). Purification by column chromatography on silica gel (*n*-Hexane/EtOAc 1:1) yielded **3ag** (68.7 mg, 62%) as a pale-yellow solid. M.p. = 110-112 °C. ^{1}H-NMR (400 MHz, $CDCl_3$): δ = 8.12 (dd, *J* = 7.7, 1.0 Hz, 2H), 7.50 – 7.46 (m, 2H), 7.44 – 7.40 (m, 3H), 7.36 – 7.33 (m, 3H), 7.30 – 7.26 (m, 3H), 7.25 – 7.22 (m, 3H), 7.19 (dd, *J* = 8.0, 1.3 Hz, 1H), 7.14 (td, *J* = 7.4, 1.3 Hz, 1H), 6.39 (t, *J* = 5.7 Hz, 1H), 5.51 – 5.42 (m, 3H), 5.42 – 5.32 (m, 1H), 4.60 (d, *J* = 5.6 Hz, 2H), 4.32 (t, *J* = 7.1 Hz, 2H), 3.51 (dd, *J* = 7.1, 1.5 Hz, 2H), 2.12 (qd, *J* = 7.3, 1.4 Hz, 2H), 1.87 (dt, *J* = 15.2, 7.2 Hz, 2H), 1.50 – 1.40 (m, 2H). ^{13}C-NMR (101 MHz, $CDCl_3$): δ = 169.9 (C_q), 140.4 (C_q), 139.4 (2 x C_q), 135.5 (C_q), 134.4 (C_q), 130.5 (CH), 130.2 (CH), 129.9 (CH), 129.1 (CH), 128.8 (CH), 128.4 (CH), 128.1 (CH), 127.0 (CH), 126.0 (CH), 125.6 (CH), 122.8 (C_q), 122.2 (CH), 120.4 (CH), 118.8 (CH), 108.7 (CH), 54.2 (CH_2), 43.0 (CH_2), 35.3 (CH_2), 31.0 (CH_2), 28.7 (CH_2), 27.2 (CH_2), 27.0 (CH_2). MS (ESI) *m/z* (relative

intensity): 576 (78) $[M+Na]^+$, 554 (100) $[M+H]^+$. HR-MS (ESI) *m/z* calcd for $C_{36}H_{36}N_5O$ $[M+H]^+$ 554.2914, found 554.2919.

(*Z*)-*N*-[(1-Benzyl-1*H*-1,2,3-triazol-4-yl)methyl]-2-(7-hydroxyhept-2-en-1-yl)benzamide (3ah)

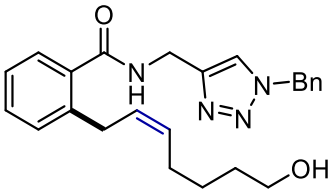

The representative procedure was followed using **1a** (58.5 mg, 0.2 mmol) and **2h** (90.4 mg, 0.4 mmol). Purification by column chromatography on silica gel (*n*-Hexane/EtOAc 1:1) yielded **3ah** (50.1 mg, 62%) as a colourless oil. ^{1}H-NMR (400 MHz, $CDCl_3$): δ = 7.59 (s, 1H), 7.38 – 7.30 (m, 5H), 7.28 – 7.22 (m, 3H), 7.19 – 7.15 (m, 1H), 6.87 (t, *J* = 5.7 Hz, 1H), 5.50 (s, 2H), 5.48 – 5.38 (m, 2H), 4.63 (d, *J* = 5.7 Hz, 2H), 3.61 (t, *J* = 6.4 Hz, 2H), 3.52 (d, *J* = 6.0 Hz, 2H), 2.09 (q, *J* = 7.0 Hz, 2H), 1.54 (dt, *J* = 8.3, 6.4 Hz, 2H), 1.41 (qd, *J* = 9.3, 8.6, 6.1 Hz, 2H), 1.27 (bs, 1H). ^{13}C-NMR (101 MHz, $CDCl_3$): δ = 170.1 (C_q), 144.9 (C_q), 139.4 (C_q), 135.6 (C_q), 134.5 (C_q), 131.0 (CH), 130.2 (CH), 129.9 (CH), 129.2 (CH), 128.8 (CH), 128.1 (CH), 128.0 (CH), 127.2 (CH), 126.0 (CH), 122.4 (CH), 62.3 (CH_2), 54.2 (CH_2), 35.3 (CH_2), 32.2 (CH_2), 30.9 (CH_2), 26.9 (CH_2), 25.6 (CH_2). MS (ESI) *m/z* (relative intensity): 427 (100) $[M+Na]^+$, 405 (21) $[M+H]^+$. HR-MS (ESI) *m/z* calcd for $C_{24}H_{29}N_4O_2$ $[M+H]^+$ 405.2285, found 405.2288.

(*Z*)-*N*-[(1-Benzyl-1*H*-1,2,3-triazol-4-yl)methyl]-2-(7-chlorohept-1-en-1-yl)benzamide (3ai)

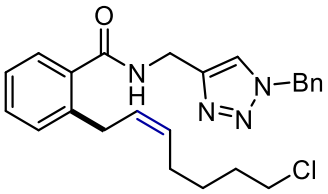

The representative procedure was followed using **1a** (58.5 mg, 0.2 mmol) and **2i** (52.0 mg, 0.4 mmol). Purification by column chromatography on silica gel (*n*-Hexane/EtOAc 1:1) yielded **3ai** (52.4 mg, 62%) as a colourless oil. ^{1}H-NMR (400 MHz, $CDCl_3$): δ = 7.56 (s, 1H), 7.40 – 7.32 (m, 5H), 7.31 – 7.27 (m, 2H), 7.26 – 7.22 (m, 1H), 7.19 (td, *J* = 7.4, 1.3 Hz, 1H), 6.64 (t, *J* = 5.7 Hz, 1H), 5.52 (s, 2H), 5.51 – 5.39 (m, 2H), 4.65 (d, *J* = 5.7 Hz, 2H), 3.58 – 3.50 (m, 4H), 2.14 (q, *J* = 7.0 Hz, 2H), 1.82 – 1.75 (m, 2H), 1.57 – 1.47 (m, 2H). ^{13}C-NMR (101 MHz, $CDCl_3$): δ = 170.0 (C_q), 144.9 (C_q), 139.3 (C_q), 135.6 (C_q), 134.5 (C_q), 130.4 (CH), 130.3 (CH), 129.9 (CH), 129.2 (CH), 128.8 (CH), 128.5 (CH), 128.1 (CH), 127.1 (CH), 126.1 (CH), 122.2 (CH), 54.3 (CH_2), 45.0 (CH_2), 35.4 (CH_2), 32.2 (CH_2), 30.9 (CH_2), 26.8 (CH_2), 26.5 (CH_2). MS (ESI) *m/z* (relative intensity): 445 (100) $[M+Na]^+$. HR-MS (ESI) *m/z* calcd for $C_{24}H_{28}ClN_4O$ $[M+H]^+$ 423.1946, found 423.1943.

Methyl (*Z*)-12-{2-[((1-benzyl-1*H*-1,2,3-triazol-4-yl)methyl)carbamoyl]phenyl}dodec-11-enoate (3aj)

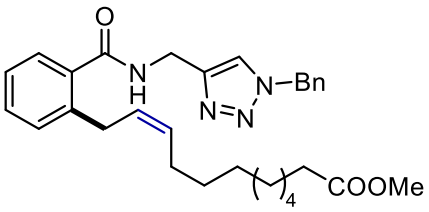

The representative procedure was followed using **1a** (58.5 mg, 0.2 mmol) and **2j** (84.1 mg, 0.4 mmol). Purification by column chromatography on silica gel (*n*-Hexane/EtOAc 1:1) yielded **3aj** (53.2 mg, 53%) as a colourless oil. ^{1}H-NMR (400 MHz, $CDCl_3$): δ = 7.56 (s, 1H), 7.40 – 7.32 (m, 5H), 7.31 – 7.25 (m, 2H), 7.22 (dd, *J* = 10.4, 1.4 Hz, 1H), 7.18 (dd, *J* = 7.5, 1.3 Hz, 1H), 6.60 (t, *J* = 5.7 Hz, 1H), 5.52 (s, 2H), 5.49 – 5.43 (m, 2H), 4.66 (d, *J* = 5.6 Hz, 2H), 3.67 (s, 3H), 3.53 (d, *J* = 4.9 Hz, 2H), 2.31 (t, *J* = 7.5 Hz, 2H), 2.13 – 2.06 (m, 2H), 1.64 – 1.59 (m, 2H), 1.36 – 1.25 (m, *J* = 11.6, 7.2 Hz, 10H). ^{13}C-NMR (101 MHz, $CDCl_3$): δ = 174.4 (C_q), 170.0 (C_q), 145.0 (C_q), 139.4 (C_q), 135.7 (C_q), 134.5 (C_q), 131.4 (CH), 130.2 (CH) , 129.9 (CH), 129.2 (CH), 128.8 (CH), 128.1 (CH), 127.7 (CH), 127.0 (CH), 126.0 (CH), 122.2 (CH), 54.3 (CH_2), 51.5 (CH_3), 35.4 (CH_2), 34.1 (CH_2), 30.9 (CH_2), 29.6 (CH_2), 29.3 (CH_2), 29.3 (CH_2), 29.2 (CH_2), 29.1 (CH_2), 27.3 (CH_2), 25.0 (CH_2). MS (ESI) *m/z* (relative intensity): 525 (78) $[M+Na]^+$, 503 (100) $[M+H]^+$. HR-MS (ESI) *m/z* calcd for $C_{30}H_{39}N_4O_3$ $[M+H]^+$ 503.3017, found 503.3012.

(*Z*)-7-{2-[((1-Benzyl-1*H*-1,2,3-triazol-4-yl)methyl)carbamoyl]phenyl}hept-5-en-1-yl benzoate (3ak)

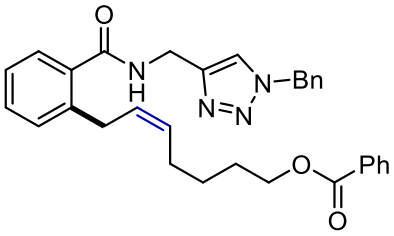

The representative procedure was followed using **1a** (58.5 mg, 0.2 mmol) and **2k** (86.1 mg, 0.4 mmol). Purification by column chromatography on silica gel (*n*-Hexane/EtOAc 1:1) yielded **3ak** (57.2 mg, 56%) as a colourless oil. ^{1}H-NMR (400 MHz, $CDCl_3$): δ = 8.08 – 8.03 (m, 2H), 7.60 – 7.54 (m, 2H), 7.45 (t, *J* = 7.7 Hz, 2H), 7.40 – 7.33 (m, 6H), 7.31 – 7.24 (m, 2H), 7.19 (td, *J* = 7.4, 1.4 Hz, 1H), 6.58 (s, 1H), 5.56 – 5.43 (m, 4H), 4.67 (d, *J* = 5.6 Hz, 2H), 4.32 (t, *J* = 6.6 Hz, 2H), 3.56 (d, *J* = 6.4 Hz, 2H), 2.19 (q, *J* = 7.1 Hz, 2H), 1.79 (dt, *J* = 15.2, 6.7 Hz, 2H), 1.58 – 1.49 (m, 2H). ^{13}C-NMR (101 MHz, $CDCl_3$): δ = 170.0 (C_q), 166.7 (C_q), 144.9 (C_q), 139.3 (C_q), 135.6 (C_q), 134.5 (C_q), 132.9 (CH), 130.6 (CH), 130.4 (C_q), 130.3 (CH), 129.9 (CH), 129.6 (CH), 129.2 (CH), 128.8 (CH), 128.4 (2 x CH), 128.1 (CH), 127.0 (CH), 126.1 (CH), 122.2 (CH), 64.9 (CH_2), 54.3 (CH_2), 35.4 (CH_2), 30.9 (CH_2), 28.4 (CH_2), 26.9 (CH_2), 26.0 (CH_2). MS (ESI) *m/z* (relative intensity): 531 (100) $[M+Na]^+$, 509 (12) $[M+H]^+$. HR-MS (ESI) *m/z* calcd for $C_{31}H_{33}N_4O_3$ $[M+H]^+$ 509.2547, found 509.2555.

_N_-[(1-Benzyl-1_H_-1,2,3-triazol-4-yl)methyl)-2-[(_Z_)-7-(((1_R_,2_S_,5_R_)-2-isopropyl-5-methylcyclohexyl)oxy)hept-2-en-1-yl]benzamide (3al)

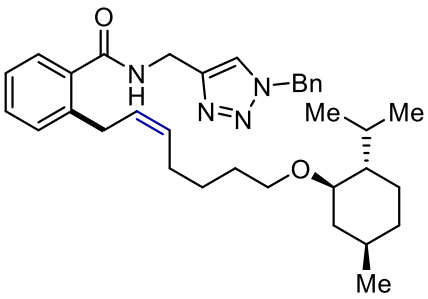

The representative procedure was followed using **1a** (58.5 mg, 0.2 mmol) and **2l** (106.5 mg, 0.4 mmol). Purification by column chromatography on silica gel (*n*-Hexane/EtOAc 1:1) yielded **3ax** (71.6 mg, 66%) as a colourless oil. ^{1}H-NMR (400 MHz, $CDCl_3$): δ = 7.56 (s, 1H), 7.38 – 7.31 (m, 5H), 7.28 – 7.26 (m, 2H), 7.24 (dd, *J* = 8.1, 1.3 Hz, 1H), 7.18 (td, *J* = 7.5, 1.4 Hz, 1H), 6.65 (t, *J* = 5.6 Hz, 1H), 5.51 (s, 2H), 5.48 – 5.43 (m, 2H), 4.65 (d, *J* = 5.7 Hz, 2H), 3.62 (dt, *J* = 9.1, 6.2 Hz, 1H), 3.53 (d, *J* = 4.9 Hz, 2H), 3.28 (dt, *J* = 9.1, 6.6 Hz, 1H), 3.00 (td, *J* = 10.6, 4.1 Hz, 1H), 2.27 – 2.19 (m, 1H), 2.15 – 2.07 (m, 3H), 1.68 – 1.53 (m, 4H), 1.49 – 1.42 (m, 2H), 1.39 – 1.26 (m, 1H), 1.25 – 1.18 (m, 1H), 1.03 – 0.95 (m, 1H), 0.93 – 0.89 (m, 6H), 0.86 – 0.82 (m, 2H), 0.78 (d, *J* = 7.0 Hz, 3H). ^{13}C-NMR (101 MHz, $CDCl_3$): δ = 170.0 (C_q), 139.4 (2 x C_q), 135.7 (C_q), 134.5 (C_q), 131.1 (CH), 130.2 (CH), 129.9 (CH), 129.2 (CH), 128.8 (CH), 128.1 (CH), 127.9 (CH), 127.0 (CH), 126.0 (CH), 122.2 (CH), 79.2 (CH), 68.4 (CH_2), 54.2 (CH_2), 48.3 (CH), 40.5 (CH_2), 35.4 (CH_2), 34.6 (CH_2), 31.6 (CH), 30.9 (CH_2), 30.0 (CH_2), 27.1 (CH_2), 26.4 (CH_2), 25.6 (CH), 23.4 (CH_2), 22.4 (CH_3), 21.0 (CH_3), 16.3 (CH_3). MS (ESI) *m/z* (relative intensity): 565 (100) $[M+Na]^+$. HR-MS (ESI) *m/z* calcd for $C_{34}H_{47}N_4O_2$ $[M+H]^+$ 543.3694, found 543.3699.

(3R,8R,9R,10S,13S,14R,17S)-10,13-Dimethyl-17-[(S)-6-methylheptan-2-yl]-2,3,4,7,8,9,10,11,12,13,14,15,16,17-tetradecahydro-1_H_-cyclopenta[_a_]phenanthren-3-yl (_Z_)-6-{2-[((1-benzyl-1_H_-1,2,3-triazol-4-yl)methyl)carbamoyl]phenyl}hex-4-enoate (3am)

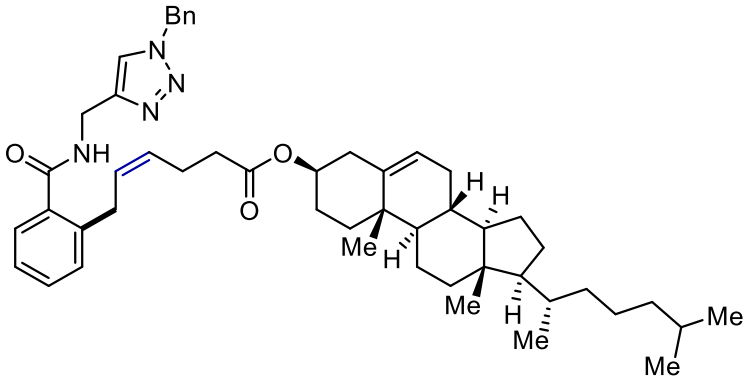

The representative procedure was followed using **1a** (58.5 mg, 0.2 mmol) and **2m** (192.3 mg, 0.4 mmol). Purification by column chromatography on silica gel (*n*-Hexane/EtOAc 1:1) yielded **3am**

(74.2 mg, 48%) as a pale-yellow waxy solid. ^{1}H-NMR (400 MHz, $CDCl_3$): δ = 7.60 (s, 1H), 7.40 – 7.32 (m, 5H), 7.30 – 7.27 (m, 2H), 7.24 (d, *J* = 7.9 Hz, 1H), 7.22 – 7.17 (m, 1H), 6.66 (bs, 1H), 5.56 – 5.48 (m, 3H), 5.46 – 5.35 (m, 2H), 4.69 – 4.57 (m, 3H), 3.55 (d, *J* = 7.1 Hz, 2H), 2.42 – 2.39 (m, 2H), 2.37 – 2.29 (m, 4H), 2.06 – 1.95 (m, 2H), 1.90 – 1.81 (m, 4H), 1.64 – 1.44 (m, 7H), 1.42 – 1.26 (m, 4H), 1.22 – 1.07 (m, 5H), 1.05 – 0.98 (m, 7H), 0.93 (d, *J* = 6.5 Hz, 3H), 0.89 – 0.87 (m, 6H), 0.70 (s, 3H). ^{13}C-NMR (101 MHz, $CDCl_3$): δ = 172.6 (C_q), 170.0 (C_q), 139.7 (2 x C_q), 139.1 (C_q), 135.7 (C_q), 134.5 (C_q), 130.3 (CH), 130.0 (CH), 129.2 (2 x CH), 128.9 (CH), 128.8 (CH), 128.1 (CH), 127.0 (CH), 126.1 (CH), 122.7 (2 x CH), 74.0 (CH), 56.7 (CH), 56.1 (CH), 54.3 (CH_2), 50.0 (CH), 42.3 (C_q), 39.7 (CH_2), 39.5 (CH_2), 38.2 (CH_2), 37.0 (CH_2), 36.6 (C_q), 36.2 (CH_2), 35.8 (CH), 35.4 (CH_2), 34.5 (CH_2), 31.9 (CH_2), 31.9 (CH), 30.9 (CH_2), 28.2 (CH_2), 28.0 (CH), 27.8 (CH_2), 24.3 (CH_2), 23.8 (CH_2), 22.9 (CH_2), 22.8 (CH_3), 22.6 (CH_3), 21.0 (CH_2), 19.3 (CH_3), 18.7 (CH_3), 11.9 (CH_3). MS (ESI) *m/z* (relative intensity): 795 (100) $[M+Na]^+$, 773 (69) $[M+H]^+$. HR-MS (ESI) *m/z* calcd for $C_{50}H_{69}N_4O_3$ $[M+H]^+$ 773.5364, found 773.5366.

(3a*R*,6*S*,6a*R*)-6-[(*S*)-2,2-Dimethyl-1,3-dioxolan-4-yl]-2,2-dimethyltetrahydrofuro[3,4-*d*][1,3]dioxol-4-yl (*Z*)-6-{2-[((1-benzyl-1*H*-1,2,3-triazol-4-yl)methyl)carbamoyl)phenyl}hex-4-enoate (3an)

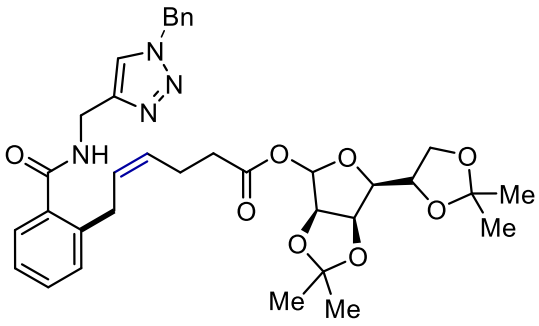

The representative procedure was followed using **1a** (58.5 mg, 0.2 mmol) and **2n** (141.7 mg, 0.4 mmol). Purification by column chromatography on silica gel (*n*-Hexane/EtOAc 1:1) yielded **3an** (32.3 mg, 25%) as a colourless oil. ^{1}H-NMR (400 MHz, $CDCl_3$): δ = 7.59 (s, 1H), 7.41 – 7.32 (m, 4H), 7.30 – 7.26 (m, 2H), 7.26 – 7.17 (m, 3H), 6.67 (bs, 1H), 6.13 (s, 1H), 5.59 – 5.49 (m, 3H), 5.43 – 5.33 (m, 1H), 4.86 (dd, *J* = 5.9, 3.6 Hz, 1H), 4.70 (d, *J* = 5.9 Hz, 1H), 4.66 (d, *J* = 5.7 Hz, 2H), 4.44 – 4.38 (m, 1H), 4.11 – 3.99 (m, 3H), 3.55 (dd, *J* = 7.3, 1.6 Hz, 2H), 2.44 – 2.33 (m, 4H), 1.50 (s, 3H), 1.45 (s, 3H), 1.38 (s, 3H), 1.35 (s, 3H). ^{13}C-NMR (101 MHz, $CDCl_3$): δ = 171.6 (C_q), 170.0 (C_q), 144.9 (C_q), 139.0 (C_q), 135.7 (C_q), 134.6 (C_q), 130.3 (CH), 129.9 (CH), 129.7 (CH), 129.1 (CH), 128.8 (CH), 128.3 (CH), 128.1 (CH), 127.1 (CH), 126.1 (CH), 122.3 (CH), 113.2 (C_q), 109.3 (C_q), 100.8 (CH), 85.1 (CH), 82.3 (CH), 79.3 (CH), 72.9 (CH), 66.8 (CH_2), 54.2 (CH_2), 35.3 (CH_2), 34.0 (CH_2), 30.9 (CH_2), 27.0 (CH_3), 26.0 (CH_3), 25.2 (CH_3), 24.7 (CH_3), 22.5 (CH_2). MS (ESI) *m/z* (relative intensity): 669 (100) $[M+Na]^+$. HR-MS (ESI) *m/z* calcd for $C_{35}H_{43}N_4O_8$ $[M+H]^+$ 647.3075, found 647.3080.

(*Z*)-7-{2-[((1-Benzyl-1*H*-1,2,3-triazol-4-yl)methyl)carbamoyl]phenyl}hept-5-en-1-yl pyrene-1-carboxylate (3ao)

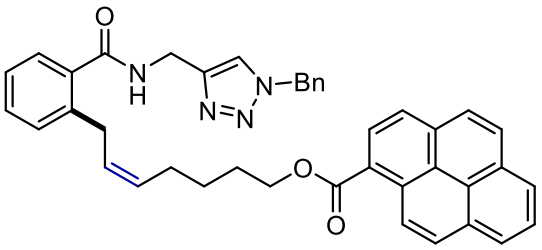

The representative procedure was followed using **1a** (58.5 mg, 0.2 mmol) and **2o** (136.2 mg, 0.4 mmol). Purification by column chromatography on silica gel (*n*-hexane/EtOAc 1:1) yielded **3ao** (79.7 mg, 63%) as a yellow oil. ^{1}H-NMR (400 MHz, $CDCl_3$): δ = 9.28 (d, *J* = 9.4 Hz, 1H), 8.64 (d, *J* = 8.1 Hz, 1H), 8.31 – 8.23 (m, 3H), 8.19 (t, *J* = 8.1 Hz, 2H), 8.13 – 8.06 (m, 2H), 7.51 (s, 1H), 7.38 – 7.29 (m, 5H), 7.28 – 7.21 (m, 3H), 7.16 (t, *J* = 7.4 Hz, 1H), 6.56 (t, *J* = 5.7 Hz, 1H), 5.59 – 5.48 (m, 2H), 5.47 (s, 2H), 4.66 (d, *J* = 5.6 Hz, 2H), 4.52 (t, *J* = 6.6 Hz, 2H), 3.59 (d, *J* = 5.5 Hz, 2H), 2.26 (q, *J* = 6.9 Hz, 2H), 1.98 – 1.88 (m, 2H), 1.70 – 1.61 (m, 2H). ^{13}C-NMR (101 MHz, $CDCl_3$): δ = 170.0 (C_q), 168.2 (C_q), 144.9 (C_q), 139.3 (C_q), 135.6 (C_q), 134.4 (C_q), 134.3 (C_q), 131.1 (C_q), 131.0 (C_q), 130.7 (CH), 130.4 (C_q), 130.3 (CH), 129.9 (CH), 129.6 (CH), 129.4 (CH), 129.1 (CH), 128.8 (CH), 128.4 (2 x CH), 128.1 (CH), 127.2 (CH), 127.0 (CH), 126.3 (2 x CH), 126.2 (CH), 126.0 (CH), 124.9 (CH), 124.9 (C_q), 124.2 (CH), 124.2 (C_q), 123.9 (C_q), 122.1 (CH), 65.2 (CH_2), 54.2 (CH_2), 35.4 (CH_2), 31.0 (CH_2), 28.5 (CH_2), 26.9 (CH_2), 26.2 (CH_2). MS (ESI) *m/z* (relative intensity): 655 (100) $[M+Na]^+$. HR-MS (ESI) *m/z* calcd for $C_{41}H_{37}N_4O_3$ $[M+H]^+$ 633.2860, found 633.2863.

(*Z*)-*N*-[(1-Benzyl-1*H*-1,2,3-triazol-4-yl)methyl]-2-{7-[(12,32,52,72-tetrapropoxy-1,3,5,7(1,3)-tetrabenzenacyclooctaphane-15-yl)oxy]hept-2-en-1-yl}benzamide (3ap)

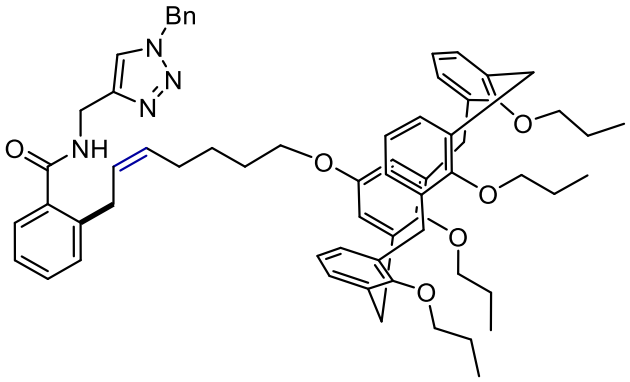

The representative procedure was followed using **1a** (29.3 mg, 0.1 mmol) and **2p** (77.3 mg, 0.11 mmol). Purification by column chromatography on silica gel (*n*-Hexane/EtOAc 1:1) yielded **3ap** (45.8 mg, 46%) as a colourless oil.^{1}H-NMR (400 MHz, $CDCl_3$): δ = 7.55 (s, 1H), 7.41 – 7.33 (m, 5H), 7.31 – 7.24 (m, 3H), 7.24 – 7.19 (m, 1H), 6.73 – 6.68 (m, 4H), 6.63 (t, *J* = 7.4 Hz, 2H), 6.56

– 6.45 (m, 4H), 6.06 (s, 2H), 5.52 (s, 2H), 5.50 – 5.43 (m, 2H), 4.67 (d, *J* = 5.6 Hz, 2H), 4.46 (t, *J* = 13.5 Hz, 4H), 3.90 – 3.82 (m, 6H), 3.78 (t, *J* = 7.3 Hz, 2H), 3.63 (t, *J* = 6.4 Hz, 2H), 3.56 (d, *J* = 5.6 Hz, 2H), 3.17 (d, J = 13.4 Hz, 2H), 3.11 (d, J = 13.4 Hz, 2H), 2.15 (q, *J* = 6.9 Hz, 2H), 1.96 – 1.89 (m, 8H), 1.70 – 1.63 (m, 2H), 1.51 – 1.44 (m, 2H), 1.06 – 0.96 (m, 12H). ^{13}C-NMR (101 MHz, $CDCl_3$): δ = 170.0 (C_q), 156.9 (C_q), 156.5 (C_q), 153.5 (C_q), 150.4 (C_q), 144.9 (C_q), 139.4 (C_q), 135.7 (C_q), 135.5 (2 x C_q), 135.3 (C_q), 134.9 (C_q), 134.5 (C_q), 130.9 (CH), 130.3 (CH), 130.0 (CH), 129.2 (CH), 128.8 (CH), 128.3 (CH), 128.2 (2 x CH), 128.1 (CH), 128.0 (CH), 127.0 (CH), 126.1 (CH), 122.2 (CH), 121.9 (CH), 121.7 (CH), 113.7 (CH), 76.8 (CH_2), 76.7 (CH_2), 76.7 (CH_2), 67.6 (CH_2), 54.3 (CH_2), 35.4 (CH_2), 31.2 (CH_2), 31.0 (2 x CH_2), 29.1 (CH_2), 27.1 (CH_2), 26.2 (CH_2), 23.3 (CH_2), 23.2 (CH_2), 23.2 (CH_2), 10.5 (CH_3), 10.4 (CH_3), 10.3 (CH_3). MS (ESI) *m/z* (relative intensity): 1018 (46) $[M+Na]^+$, 996 (100) $[M+H]^+$. HR-MS (ESI) *m/z* calcd for $C_{64}H_{75}N_4O_6$ $[M+H]^+$ 995.5681, found 995.5681.

_N_-[(1-Benzyl-1_H_-1,2,3-triazol-4-yl)methyl]-2-(3-pentyloct-2-en-1-yl)benzamide (3aq)

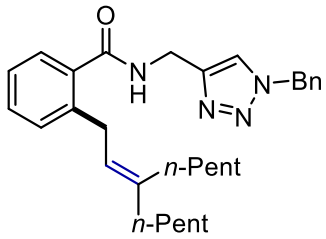

The representative procedure was followed using **1a** (58.5 mg, 0.2 mmol) and **2q** (72.1 mg, 0.4 mmol). Purification by column chromatography on silica gel (*n*-Hexane/EtOAc 1:1) yielded **3aq** (79.3 mg, 84%) as a colourless oil. ^{1}H-NMR (400 MHz, $CDCl_3$): δ = 7.56 (s, 1H), 7.42 – 7.31 (m, 5H), 7.31 – 7.26 (m, 2H), 7.26 – 7.23 (m, 1H), 7.19 (t, *J* = 7.4, 1H), 6.56 (t, *J* = 5.4 Hz, 1H), 5.52 (s, 2H), 5.22 (t, *J* = 7.1 Hz, 1H), 4.66 (d, *J* = 5.6 Hz, 2H), 3.50 (d, *J* = 7.1 Hz, 2H), 2.12 – 2.03 (m, 2H), 1.99 (t, *J* = 7.7 Hz, 2H), 1.42 – 1.22 (m, 12H), 0.92 – 0.87 (m, 6H). ^{13}C-NMR (101 MHz, $CDCl_3$): δ = 170.1 (C_q), 145.0 (C_q), 141.7 (C_q), 140.1 (C_q), 135.7 (C_q), 134.5 (C_q), 130.2 (CH), 129.9 (CH), 129.2 (CH), 128.8 (CH), 128.1 (CH), 127.1 (CH), 125.9 (CH), 122.4 (CH), 122.2 (CH), 54.2 (CH_2), 36.9 (CH_2), 35.5 (CH_2), 32.1 (CH_2), 31.8 (CH_2), 31.3 (CH_2), 30.2 (CH_2), 28.1 (CH_2), 28.0 (CH_2), 22.6 (2 x CH_2), 14.1 (2 x CH_3). MS (ESI) *m/z* (relative intensity): 495 (100) $[M+Na]^+$. HR-MS (ESI) *m/z* calcd for $C_{30}H_{41}N_4O$ $[M+H]^+$ 473.3275, found 473.3277.

(*Z*)-*N*-[(1-Benzyl-1*H*-1,2,3-triazol-4-yl)methyl]-2-(3-phenylbut-2-en-1-yl)benzamide (3ar)

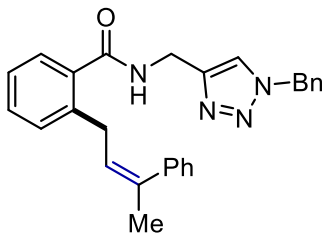

The representative procedure was followed using **1a** (58.5 mg, 0.2 mmol) and **2r** (52.0 mg, 0.4 mmol). Purification by column chromatography on silica gel (*n*-Hexane/EtOAc 1:1) yielded **3ar** (71.8 mg, 85%) as a colourless oil. ^{1}H-NMR (400 MHz, $CDCl_3$): δ = 7.52 (s, 1H), 7.39 – 7.36 (m, 3H), 7.36 – 7.30 (m, 4H), 7.28 – 7.24 (m, 3H), 7.24 – 7.20 (m, 2H), 7.20 – 7.15 (m, 2H), 6.58 (s, 1H), 5.61 (t, *J* = 7.3, 1H), 5.50 (s, 2H), 4.57 (d, *J* = 5.7 Hz, 2H), 3.47 (d, *J* = 7.2 Hz, 2H), 2.06 (s, 3H). ^{13}C-NMR (101 MHz, $CDCl_3$): δ = 169.9 (C_q), 145.0 (C_q), 141.6 (C_q), 139.6 (C_q), 137.6 (C_q), 135.5 (C_q), 134.5 (C_q), 130.2 (CH), 130.0 (CH), 129.2 (CH), 128.8 (CH), 128.2 (CH), 128.1 (CH), 128.0 (CH), 127.1 (CH), 126.8 (CH), 126.0 (CH), 125.6 (CH), 122.2 (CH), 54.2 (CH_2), 35.3 (CH_2), 32.7 (CH_2), 25.7 (CH_3). MS (ESI) *m/z* (relative intensity): 445 (100) $[M+Na]^+$. HR-MS (ESI) *m/z* calcd for $C_{27}H_{27}N_4O$ $[M+H]^+$ 423.2179, found 423.2186.

(*Z*)-*N*-[(1-Benzyl-1*H*-1,2,3-triazol-4-yl)methyl]-2-(3-methyloct-2-en-1-yl)benzamide (3as)

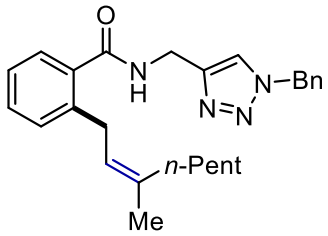

The representative procedure was followed using **1a** (58.5 mg, 0.2 mmol) and **2s** (49.7 mg, 0.4 mmol). Purification by column chromatography on silica gel (*n*-Hexane/EtOAc 1:1) yielded **3as** (50.0 mg, 60%) as a colourless oil.^{1}H-NMR (400 MHz, $CDCl_3$): δ = 7.56 (s, 1H), 7.39 – 7.31 (m, 5H), 7.28 (dd, *J* = 7.6, 2.1 Hz, 2H), 7.23 (d, *J* = 7.2 Hz, 1H), 7.21 (td, *J* = 7.5, 1.3 Hz, 1H), 6.64 (t, *J* = 5.7 Hz, 1H), 5.51 (s, 2H), 5.21 (td, *J* = 7.3, 1.7 Hz, 1H), 4.65 (d, *J* = 5.7 Hz, 2H), 3.48 (d, *J* = 7.1 Hz, 2H), 2.11 – 2.02 (m, 2H), 1.68 (d, *J* = 1.5 Hz, 3H), 1.44 – 1.23 (m, 6H), 0.90 (t, *J* = 6.9 Hz, 3H). ^{13}C-NMR (101 MHz, $CDCl_3$): δ = 170.1 (C_q), 145.0 (C_q), 140.0 (C_q), 137.3 (C_q), 135.6 (C_q), 134.5 (C_q), 130.2 (CH), 130.0 (CH), 129.2 (CH), 128.8 (CH), 128.1 (CH), 127.1 (CH), 125.9 (CH), 123.1 (CH), 122.2 (CH), 54.2 (CH_2), 35.4 (CH_2), 31.9 (2 x CH_2), 31.5 (CH_2), 27.7 (CH_2), 23.5 (CH_3), 22.6 (CH_2), 14.1 (CH_2). MS (ESI) *m/z* (relative intensity): 439 (100) $[M+Na]^+$, 417 (37) $[M+H]^+$. HR-MS (ESI) *m/z* calcd for $C_{26}H_{33}N_4O$ $[M+H]^+$ 417.2649, found 417.2645.

_N_-[(1-Benzyl-1_H_-1,2,3-triazol-4-yl)methyl]-2-(3-phenylhex-2-en-1-yl)benzamide (3at)

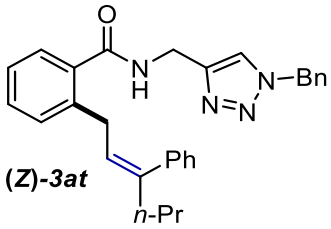

(*Z*)-*3at*

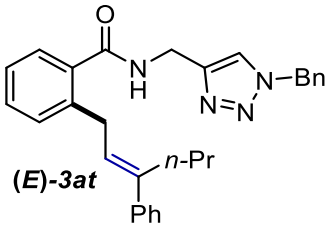

(*E*)-*3at*

The representative procedure was followed using **1a** (58.5 mg, 0.2 mmol) and **2t** (52.0 mg, 0.4 mmol). Purification by column chromatography on silica gel (*n*-Hexane/EtOAc 1:1) yielded **3at** (75.7 mg, 84%, **(*Z*)-3at**/**(*E*)-3at**: 13:1) as a colourless oil.

Characterization data for major isomer **(*Z*)-3at**:

^{1}H-NMR (400 MHz, $CDCl_3$): δ = 7.52 (s, 1H), 7.40 – 7.22 (m, 10H), 7.19 – 7.15 (m, 4H), 6.57 (bs, 1H), 5.60 (t, *J* = 7.3 Hz, 1H), 5.50 (s, 2H), 4.57 (d, *J* = 5.7 Hz, 2H), 3.43 (d, *J* = 7.3 Hz, 2H), 2.34 (t, *J* = 7.5 Hz, 2H), 1.34 (q, *J* = 7.4 Hz, 2H), 0.88 (t, *J* = 7.3 Hz, 3H). ^{13}C-NMR (101 MHz, $CDCl_3$): δ = 170.0 (C_q), 145.0 (C_q), 142.4 (C_q), 140.8 (C_q), 139.7 (C_q), 135.5 (C_q), 134.5 (C_q), 130.2 (CH), 129.9 (CH), 129.2 (CH), 128.8 (CH), 128.4 (CH), 128.1 (2 x CH), 127.0 (CH), 126.6 (CH), 125.9 (CH), 125.1 (CH), 122.2 (CH), 54.2 (CH_2), 41.4 (CH_2), 35.3 (CH_2), 32.4 (CH_2), 21.2 (CH_2), 13.7 (CH_3). MS (ESI) *m/z* (relative intensity): 473 (100) $[M+Na]^+$. HR-MS (ESI) *m/z* calcd for $C_{29}H_{31}N_4O$ $[M+H]^+$ 451.2492, found 451.2497.

(*Z*)-N-[(1-Benzyl-1_H_-1,2,3-triazol-4-yl)methyl]-2-(4-phenylnon-3-en-2-yl)benzamide (3au)

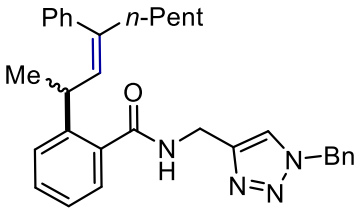

The representative procedure was followed using **1a** (58.5 mg, 0.2 mmol) and **2u** (80.0 mg, 0.4 mmol). Purification by column chromatography on silica gel (*n*-Hexane/EtOAc 1:1) yielded **3au** (30.1 mg, 30 %) a colourless oil. ^{1}H NMR (400 MHz, $CDCl_3$): δ = 7.47 – 7.35 (m, 6H), 7.32 – 7.25 (m, 2H), 7.22 – 7.14 (m, 5H), 6.93 – 6.87 (m, 2H), 5.84 (t, *J* = 5.8 Hz, 1H), 5.73 (d, *J* = 9.3 Hz, 1H), 5.59 – 5.42 (m, 2H), 4.44 (dd, *J* = 15.2, 6.3 Hz, 1H), 4.20 – 4.09 (m, 1H), 3.69 (dq, *J* = 9.3, 6.9 Hz, 1H), 2.28 (t, *J* = 6.9 Hz, 2H), 1.28 – 1.25 (m, 9H), 0.86 (t, *J* = 7.0 Hz, 3H). ^{13}C NMR (101 MHz, $CDCl_3$): δ = 170.1 (C_q), 145.6 (2 x C_q), 141.4 (2 x C_q), 135.2 (C_q), 134.0 (C_q), 131.3 (CH), 130.1 (CH), 129.2 (CH), 128.9 (CH), 128.2 (CH), 128.1 (2 x CH), 127.4 (CH), 126.8 (CH), 126.5 (CH), 125.6 (CH), 122.4 (CH), 54.4 (CH_2), 39.4 (CH_2), 35.2 (CH), 35.1 (CH_2), 31.4 (CH_2), 27.6 (CH_2), 24.6 (CH_3),

22.5 (CH_2), 14.1 (CH_3). MS (ESI) *m/z* (relative intensity): 515 (100) $[M+Na]^+$. HR-MS (ESI) *m/z* calcd for $C_{32}H_{37}N_4O$ $[M+H]^+$ 493.2962, found 493.2965.

4.4.8 Key mechanistic findings

Intermolecular KIE

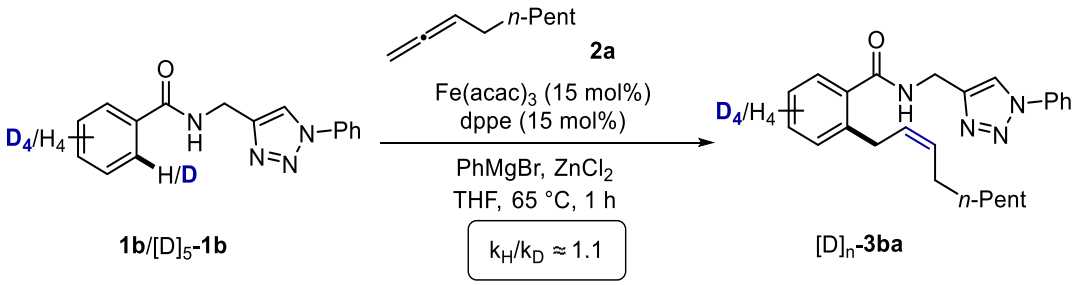

To a stirred solution of Fe(acac)3 (10.6 mg, 0.03 mmol), dppe (12.0 mg, 0.03 mmol), zinc chloride (1.0 M in THF, 400 µL, 0.4 mmol), **1b** (27.8 mg, 0.10 mmol) and [D]5-**1b** (28.3 mg, 0.10 mmol) in THF(200 µL) under N2 atmosphere, PhMgBr (1.0 M in THF, 600 µL, 0.60 mmol) was added in a single portion. Then, **2a** (49.6 mg, 0.4 mmol) was added and the mixture was placed in a pre-heated oil bath at 65 °C. After stirring for 30 min, the reaction was cooled to room temperature and quenched by the addition of an aqueous solution of HCl (1.0 M, 5.0 mL). The reaction was extracted with CH2Cl2 (3x10 mL), and the combined organic extracts were dried over Na2SO4, filtered and concentrated. The crude product was purified by column chromatography (*n*-Hexane/EtOAc). The mixture was analysed by 400 MHz ^{1}H-NMR spectroscopy to determine the ratio of **3ba**/[D]4-**3ba** [(0.53/0.47) = 1.13].

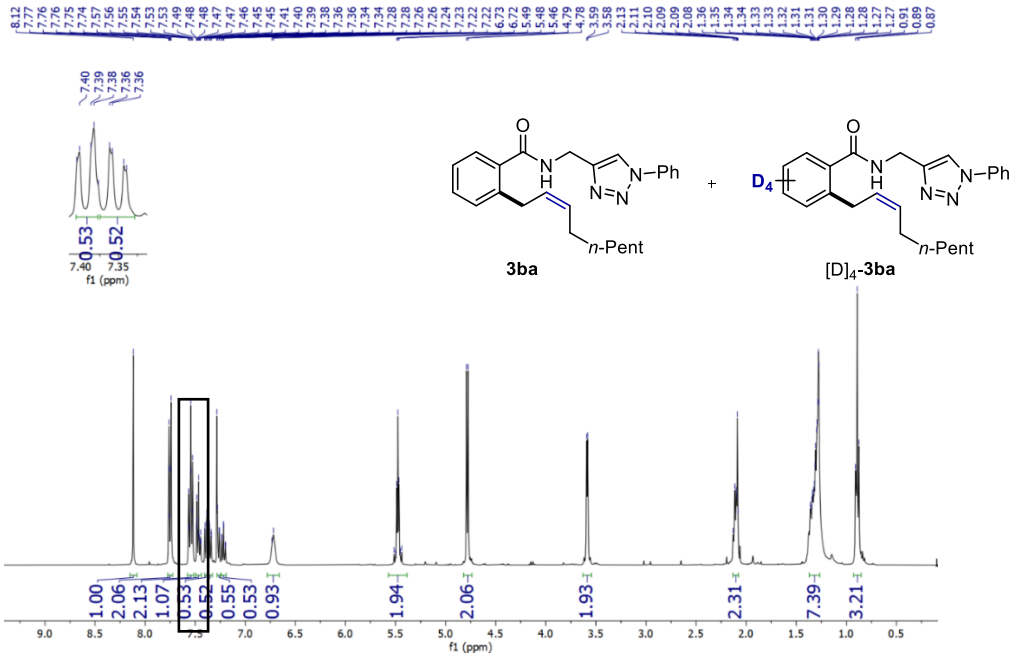

Intramolecular KIE

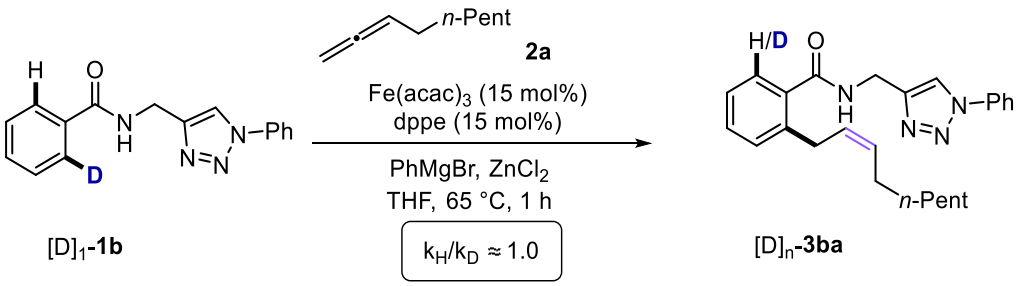

To a stirred solution of $Fe(acac)_3$ (10.6 mg, 0.03 mmol), dppe (12.0 mg, 0.03 mmol), zinc chloride (1.0 M in THF, 400 µL, 0.4 mmol) and $[D]_1$-**1b** (55.9 mg, 0.20 mmol) in THF (200 µL) under N_2 atmosphere, PhMgBr (1.0 M in THF, 600 µL, 0.60 mmol) was added in a single portion. Then, **2a** (49.6 mg, 0.20 mmol) was added and the mixture was placed in a pre-heated oil bath at 65 °C. After stirring for 30 min, the reaction was cooled to room temperature and quenched by the addition of an aqueous solution of HCl (1.0 M, 5.0 mL). The reaction was extracted with CH_2Cl_2 (3x10 mL), and the combined organic extracts were dried over Na_2SO_4, filtered and concentrated. The crude product was purified by column chromatography (*n*-Hexane/EtOAc). The mixture was analysed by 400 MHz ^{1}H-NMR spectroscopy to determine the ratio of **3ba**/$[D]_1$-**3ba** [(1.0-0.50/0.50) = 1.0].

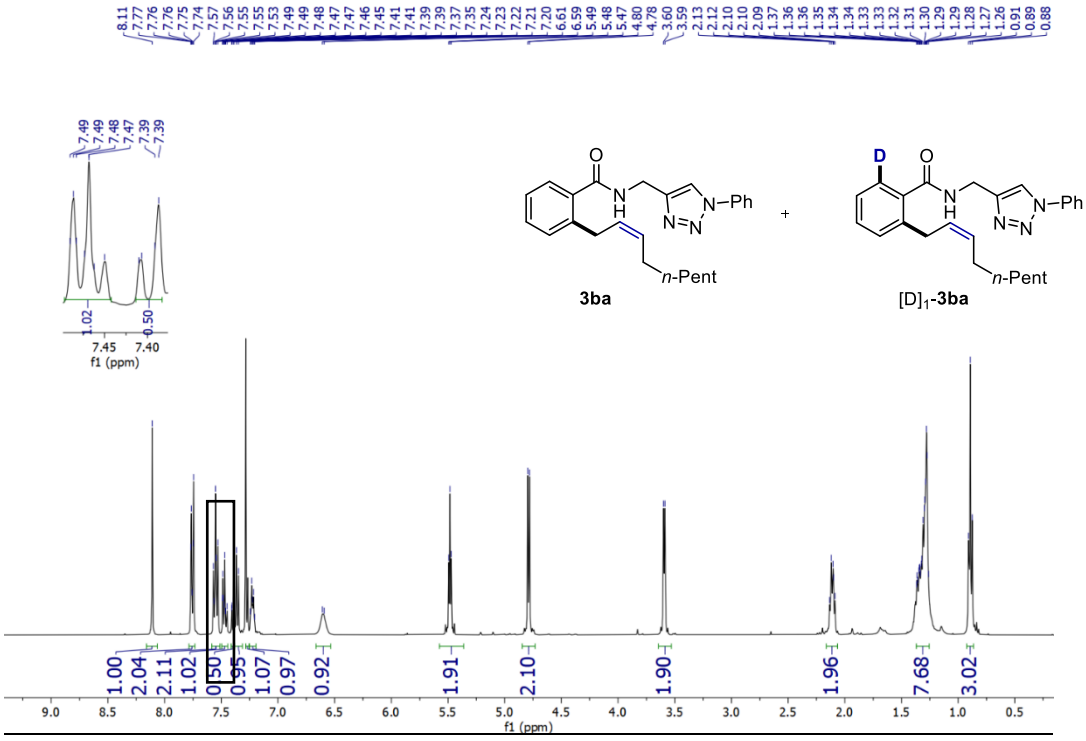

Competition Experiments

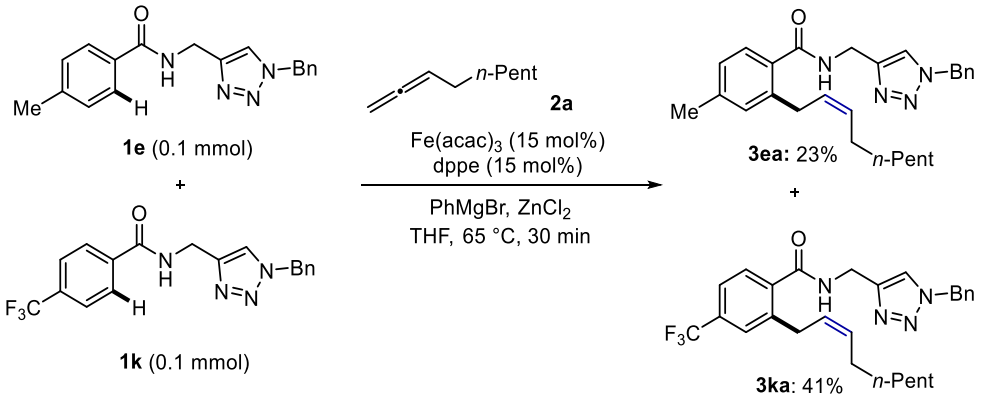

To a stirred solution of $Fe(acac)_3$ (10.6 mg, 0.03 mmol), dppe (12.0 mg, 0.03 mmol), zinc chloride (1.0 M in THF, 400 µL, 0.4 mmol), **1e** (30.6 mg, 0.10 mmol) and **1k** (36.6 mg, 0.10 mmol) in THF (200 µL) under N_2 atmosphere, PhMgBr (1.0 M in THF, 600 µL, 0.60 mmol) was added in a single portion. Then, **2a** (49.6 mg, 0.4 mmol) was added and the mixture was placed in a pre-heated oil bath at 65 °C. After stirring for 30 minutes, the reaction was cooled to room temperature and quenched by the addition of an aqueous solution of HCl (1.0 M, 5.0 mL). The reaction was extracted with CH_2Cl_2 (3x10 ml), and the combined organic extracts were dried over Na_2SO_4, filtered and concentrated. The residue was purified by column chromatography (*n*-Hexane/EtOAc) affording a mixture of **3ea** and **3ka** (30.0 mg). ^{1}H-NMR analysis showed that the ratio between **3ea** and **3ka** was 1/1.81. Accordingly, the yields of **3ea** and **3ka** were calculated to be 23% and 41%, respectively.

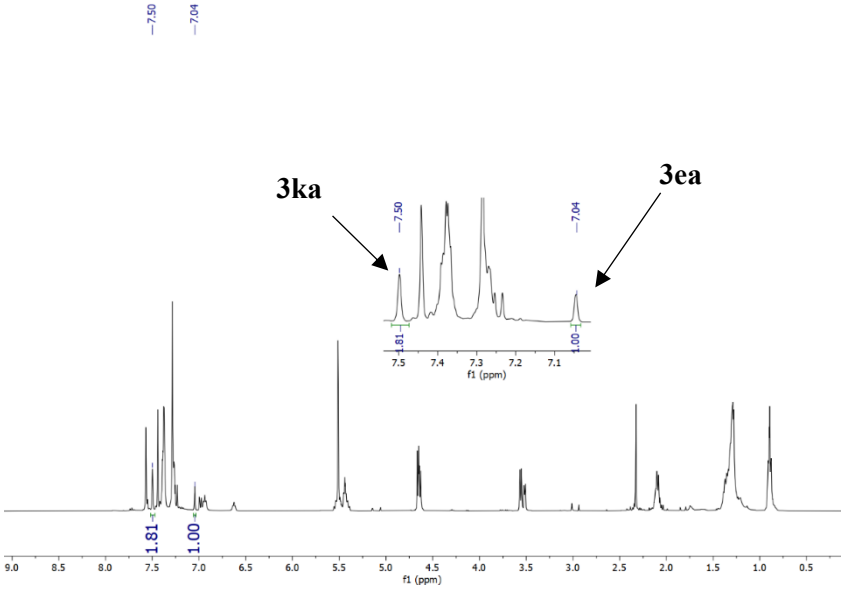

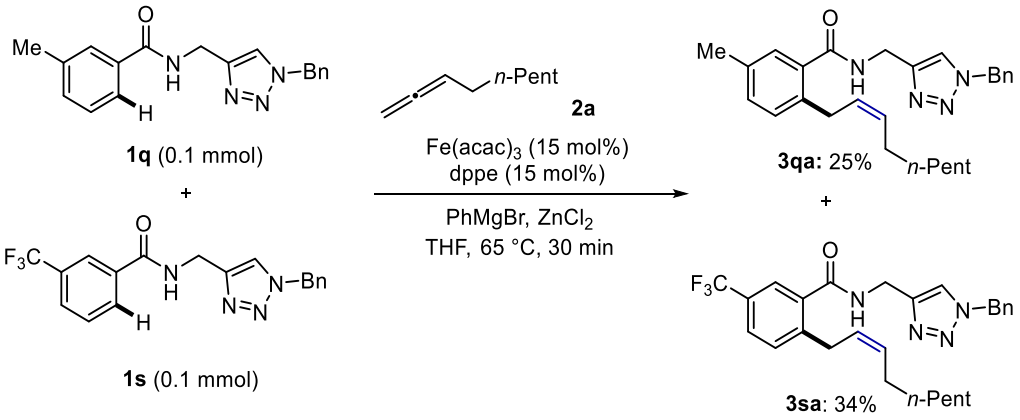

To a stirred solution of Fe(acac)3 (10.6 mg, 0.03 mmol), dppe (12.0 mg, 0.03 mmol), zinc chloride (1.0 M in THF, 400 µL, 0.4 mmol), **1q** (30.6 mg, 0.10 mmol) and **1s** (36.6 mg, 0.10 mmol) in THF (200 µL) under N2 atmosphere, PhMgBr (1.0 M in THF, 600 µL, 0.60 mmol) was added in a single portion. Then, **2a** (49.6 mg, 0.4 mmol) was added and the mixture was placed in a pre-heated oil bath at 65 °C. After stirring for 30 minutes, the reaction was cooled to room temperature and quenched by the addition of an aqueous solution of HCl (1.0 M, 5.0 mL). The reaction was extracted with CH2Cl2 (3x10 mL), and the combined organic extracts were dried over Na2SO4, filtered and concentrated. The crude mixture was analyzed by ^{1}H-NMR spectroscopy using 1,3,5-trimethoxybenzene as the internal standard affording a product ratio between **3qa** and **3sa** of 1/1.36.

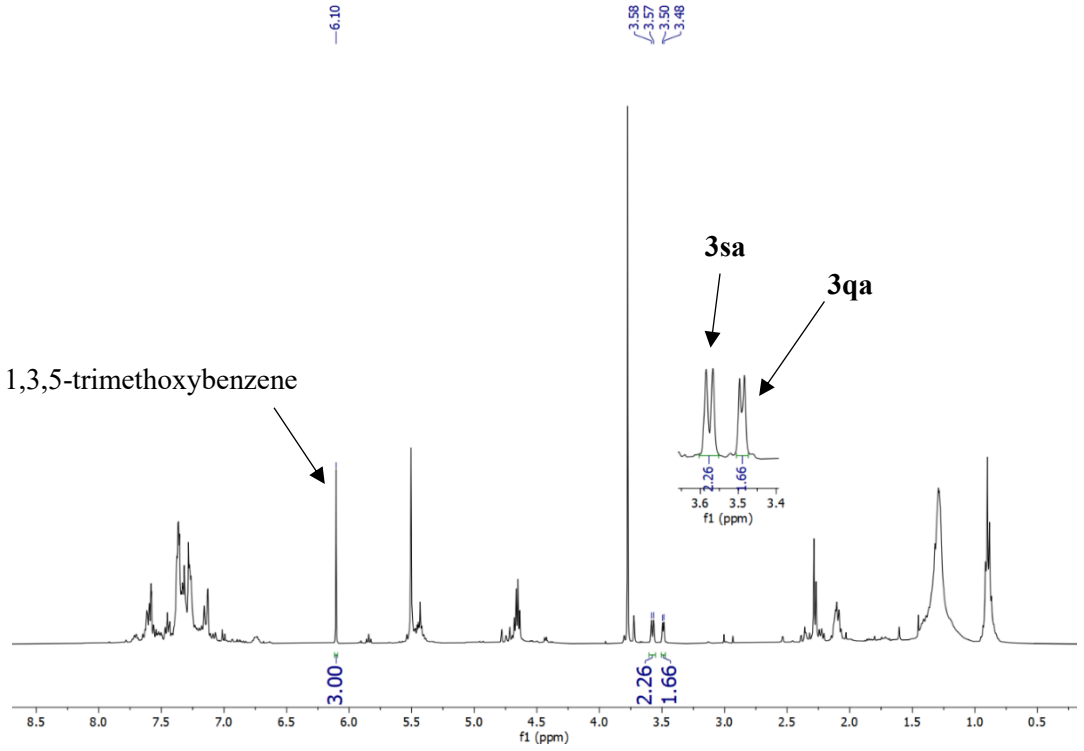

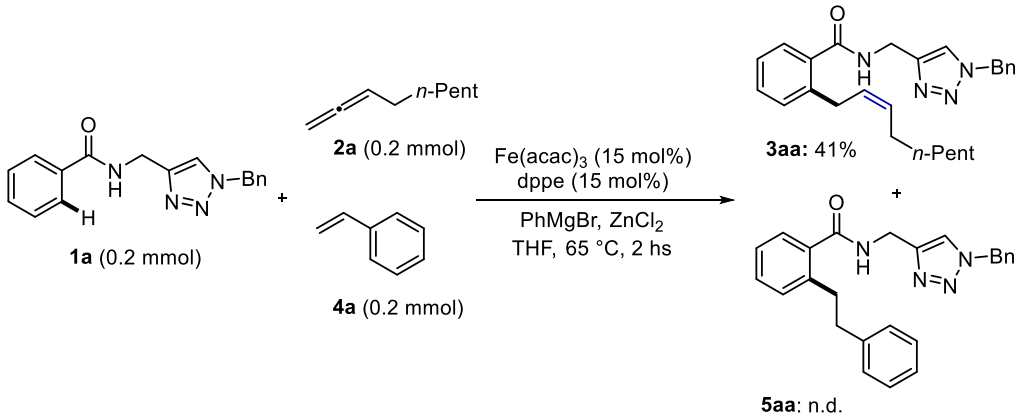

To a stirred solution of Fe(acac)3 (10.6 mg, 0.03 mmol), dppe (12.0 mg, 0.03 mmol), zinc chloride (1.0 M in THF, 400 µL, 0.4 mmol), **1a** (58.4 mg, 0.20 mmol) in THF (200 µL) under N2 atmosphere, PhMgBr (1.0 M in THF, 600 µL, 0.60 mmol) was added in a single portion. Then, **2a** (24.8 mg, 0.2 mmol) and **4a** (20.8 mg, 0.2 mmol) were added and the mixture was placed in a pre-heated oil bath at 65 °C. After stirring for 1 h, the reaction was cooled to room temperature and quenched by the addition of an aqueous solution of HCl (1.0 M, 5.0 mL). The reaction was extracted with CH2Cl2 (3x10 mL), and the combined organic extracts were dried over Na2SO4, filtered and concentrated. Crude ^{1}H-NMR analysis of the reaction mixture showed no formation of product **5aa**. The NMR yield of product **3aa** was calculated to be 41% using 1,3,5-trimethoxybenzene as the internal standard.

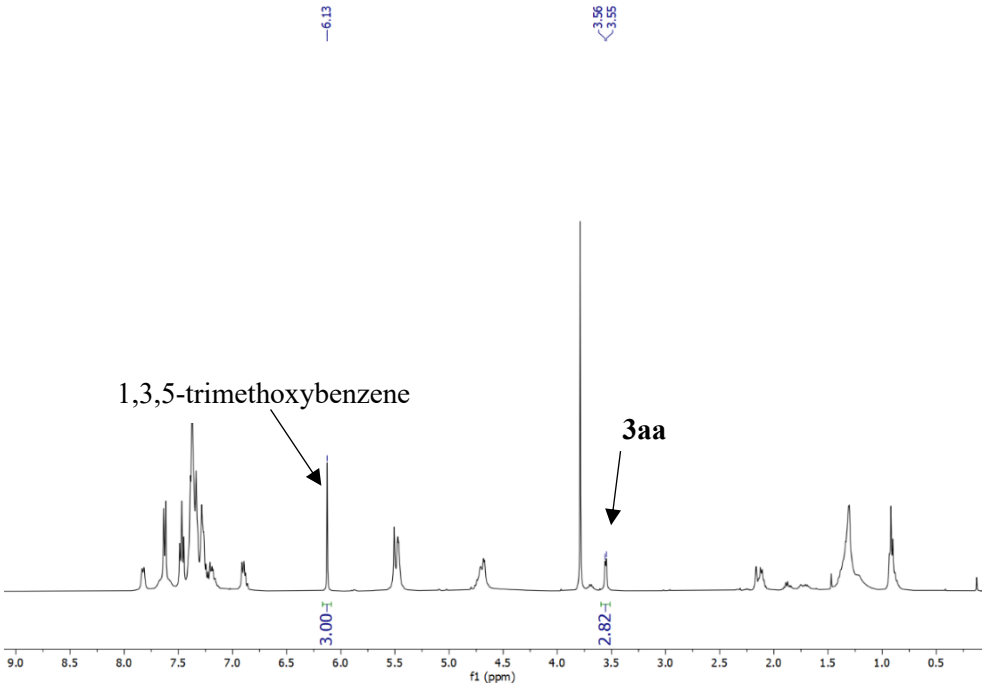

Reaction with Isotopically-labelled Substrates

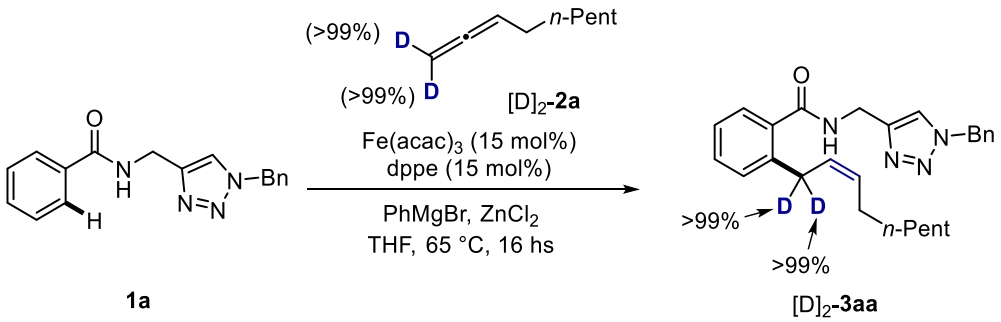

To a stirred solution of $Fe(acac)_3$ (10.6 mg, 0.03 mmol), dppe (12.0 mg, 0.03 mmol), zinc chloride (1.0 M in THF, 400 µL, 0.4 mmol) and **1a** (58.5 mg, 0.20 mmol) in THF (200 µL) under N_2 atmosphere, PhMgBr (1.0 M in THF, 600 µL, 0.60 mmol) was added in a single portion. Then, $[D]_2$-**2a** (50.4 mg, 0.40 mmol) was added and the mixture was placed in a pre-heated oil bath at 65 °C. After stirring for 16 hs, the reaction was cooled to room temperature and quenched by the addition of an aqueous solution of HCl (1.0 M, 5.0 mL). The reaction was extracted with CH_2Cl_2 (3x10 mL) and the combined organic extracts were dried over Na_2SO_4, filtered and concentrated. Purification by column chromatography on silica gel (*n*-Hexane/EtOAc 1:1) yielded $[D]_2$-**3aa** (62.7 mg, 75%) as a colourless oil.

$[D]_2$-**3aa** (400 MHz, $CDCl_3$)

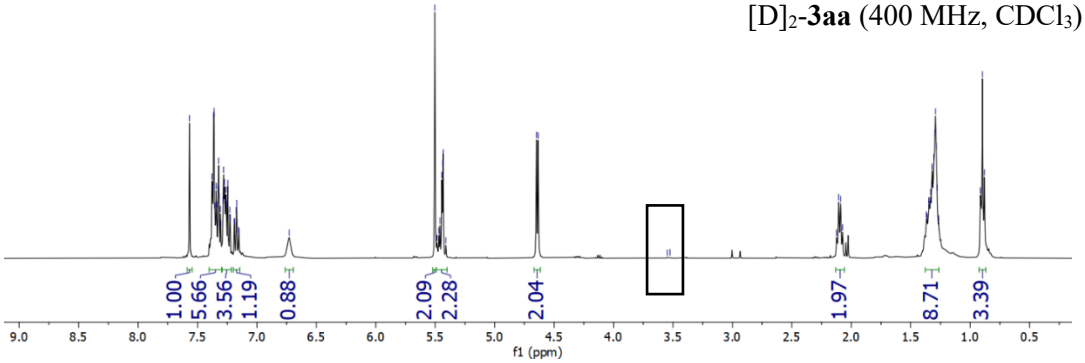

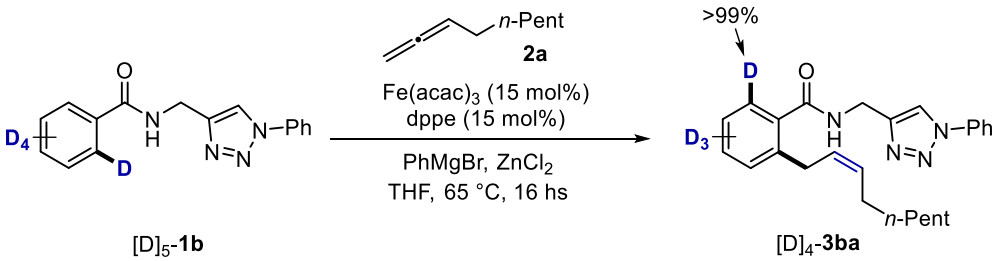

[D]$_5$-**1b** [D]$_4$-**3ba**

To a stirred solution of Fe(acac)$_3$ (10.6 mg, 0.03 mmol), dppe (12.0 mg, 0.03 mmol), zinc chloride (1.0 M in THF, 400 µL, 0.4 mmol) and **1b** (56.6 mg, 0.20 mmol) in THF (200 µL) under N_2 atmosphere, PhMgBr (1.0 M in THF, 600 µL, 0.60 mmol) was added in a single portion. Then, **2a** (46.5 mg, 0.40 mmol) was added and the mixture was placed in a pre-heated oil bath at 65 °C. After stirring for 16 hs, the reaction was cooled to room temperature and quenched by the addition of an aqueous solution of HCl (1.0 M, 5.0 mL). The reaction was extracted with CH_2Cl_2 (3x10 mL) and the combined organic extracts were dried over Na_2SO_4, filtered and concentrated. Purification by column chromatography on silica gel (*n*-Hexane/EtOAc 1:1) yielded [D]$_4$-**3ba** (62.7 mg, 48%) as a colourless oil.

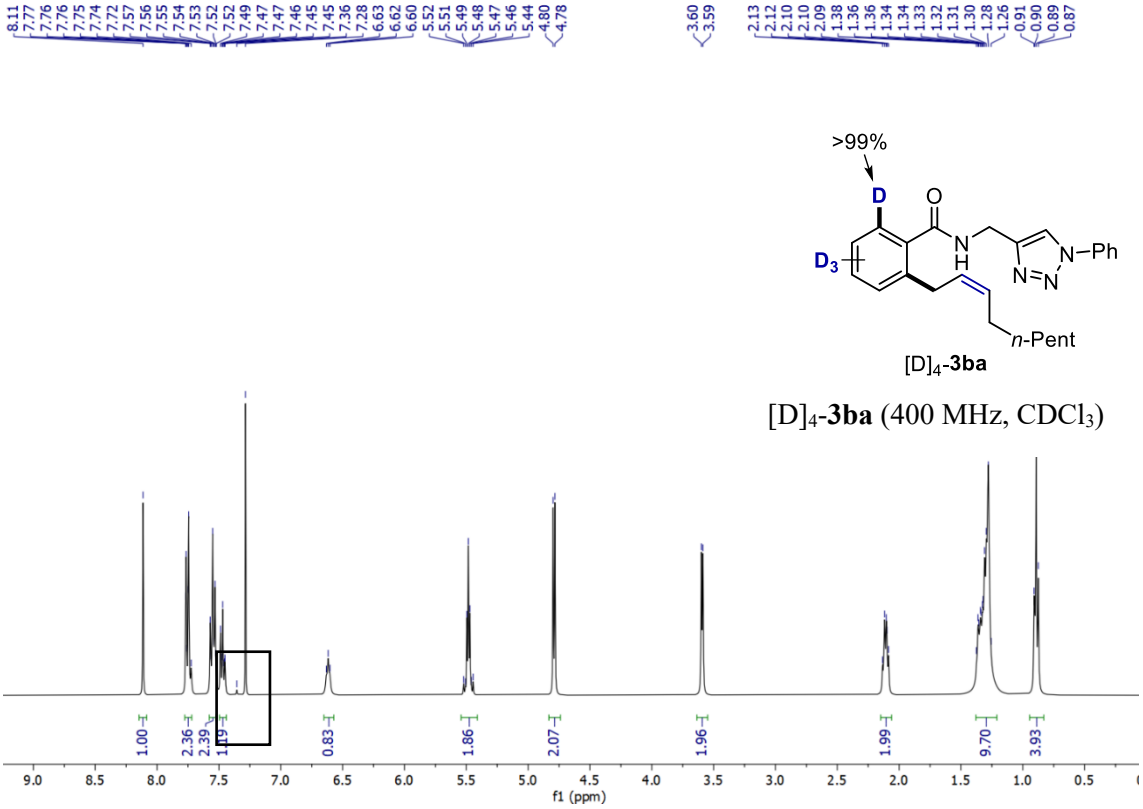

[D]$_4$-**3ba**

[D]$_4$-**3ba** (400 MHz, $CDCl_3$)

4.4.9 Late-stage synthetic manipulations

(*Z*)-3-(Non-2-en-1-yl)-2-naphthoic acid (6ra)

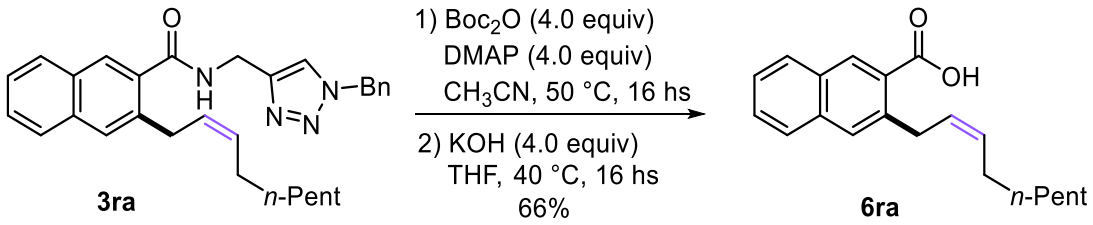

Step 1. To a solution of **3ra** (93.0 mg, 0.2 mmol) in dry CH_3CN (5 mL), Boc_2O (174 mg, 0.8 mmol, 4.0 equiv.) and DMAP (97.1 mg, 0.8 mmol, 4.0 equiv.) were added. The resulting solution was stirred at 50 °C for 16 hs. Then, the reaction mixture was diluted with water (15 mL) and extracted with CH_2Cl_2 (2 x 10 mL). The combined organic extracts were dried over Na_2SO_4, and the filtrate was concentrated under reduced pressure delivering the desired product which was used in the next step without further purification.

Step 2. To a solution of Boc-protected benzamide in THF (2 mL), KOH (45.0 mg, 0.8 mmol, 4.0 equiv.) was added. The resulting mixture was stirred at 40 °C for 16 hs. Afterwards, the reaction was diluted with CH_2Cl_2 (10 mL) and washed with HCl (1.0 M, 10 mL). The organic layer was dried over Na_2SO_4 and concentrated under reduced pressure. Purification by column chromatography on silica gel (*n*-Hexane/EtOAc 7:3) yielded **6ra** (39.1 mg, 66%, over two steps) as a white solid. M.p. = 84-85 °C. ^{1}H-NMR (400 MHz, $CDCl_3$): δ = 8.69 (s, 1H), 7.94 (d, *J* = 8.1 Hz, 1H), 7.85 – 7.81 (m, 1H), 7.78 (s, 1H), 7.60 (dd, *J* = 8.2, 6.8 Hz, 1H), 7.52 (dd, *J* = 8.1, 6.8 Hz, 1H), 5.73 – 5.58 (m, 2H), 4.01 (d, *J* = 6.8 Hz, 2H), 2.24 (q, *J* = 7.1 Hz, 2H), 1.48 – 1.27 (m, 8H), 0.92 – 0.87 (m, 3H). ^{13}C-NMR (101 MHz, $CDCl_3$): δ = 173.1 (C_q), 138.9 (C_q), 135.6 (C_q), 133.5 (CH), 131.7 (CH), 131.0 (C_q), 128.9 (2 x CH), 128.6 (CH), 127.7 (CH), 127.2 (CH), 126.7 (C_q), 126.1 (CH), 32.2 (CH_2), 31.8 (CH_2), 29.7 (CH_2), 29.1 (CH_2), 27.5 (CH_2), 22.7 (CH_2), 14.1 (CH_3). The proton of the carboxylic acid was not detected due to the excessive broadening under the experimental conditions. MS (ESI) *m/z* (relative intensity): 319 (100) $[M+Na]^+$. HR-MS (ESI) *m/z* calcd for $C_{20}H_{25}O_2$ $[M+H]^+$ 297.1849, found 297.1847.

(*Z*)-(2-(Non-2-en-1-yl)phenyl)(phenyl)methanone (7aa)

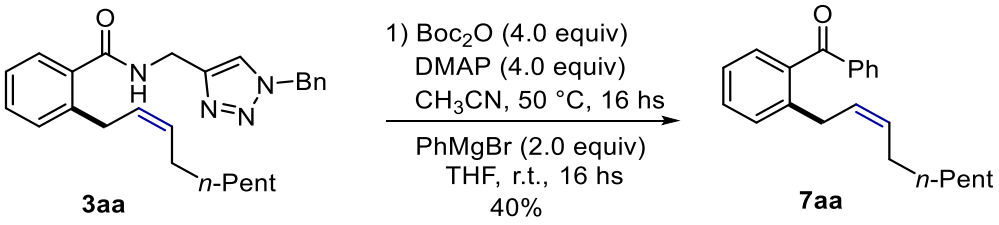

Step 1: To a solution of **3aa** (62.5 mg, 0.15 mmol) in dry CH_3CN (5 mL), Boc_2O (174 mg, 0.8 mmol, 4.0 equiv.) and DMAP (97.1 mg, 0.8 mmol, 4.0 equiv.) were added. The resulting solution was stirred at 50 °C for 16 hs. Then, the reaction mixture was diluted with water (15 mL) and extracted with CH_2Cl_2 (2 x 10 mL). The combined organic extracts were dried over Na_2SO_4, and the filtrate was concentrated under reduced pressure delivering the desired product which was used in the next step without further purification.

Step 2: Modifying a literature procedure[18], to a solution of Boc-protected benzamide in THF (2 mL), PhMgBr (1.0 M in THF, 2.0 equiv.) was added dropwise at 0 °C. The mixture was initially stirred at the same temperature and then at ambient temperature for 16 hs. Afterwards, the reaction was quenched by the addition of an aqueous solution of HCl (1.0 M, 5.0 mL). The reaction was extracted with CH_2Cl_2 (3x10 mL) and the combined organic extracts were dried over Na_2SO_4, filtered and concentrated. Purification by column chromatography on silica gel (*n*-Hexane/EtOAc 95:5) yielded **7aa** (21.6 mg, 47%, over two steps) as a colourless oil. ^{1}H-NMR (400 MHz, $CDCl_3$): δ = 7.86 – 7.80 (m, 2H), 7.63 – 7.57 (m, 1H), 7.51 – 7.42 (m, 3H), 7.36 (d, *J* = 7.7 Hz, 1H), 7.33 – 7.25 (m, 2H), 5.48 – 5.36 (m, 2H), 3.45 (d, *J* = 6.0 Hz, 2H), 1.99 (q, *J* = 6.6 Hz, 2H), 1.32 – 1.22 (m, 8H), 0.89 (t, *J* = 6.8 Hz, 3H). ^{13}C-NMR (101 MHz, $CDCl_3$): δ = 198.6 (C_q), 140.1 (C_q), 138.7 (C_q), 137.8 (C_q), 133.2 (CH), 131.5 (CH), 130.3 (CH), 130.2 (CH), 129.9 (CH), 128.4 (2 x CH), 127.4 (CH), 125.4 (CH), 31.7 (CH_2), 31.0 (CH_2), 29.5 (CH_2), 29.0 (CH_2), 27.2 (CH_2), 22.6 (CH_2), 14.1 (CH_3). MS (ESI) *m/z* (relative intensity): 329 (100) $[M+Na]^+$. HR-MS (ESI) *m/z* calcd for $C_{22}H_{27}O$ $[M+H]^+$ 307.2056, found 307.2050.

3-(1-Hydroxyhexyl)isochroman-1-one (8ab)

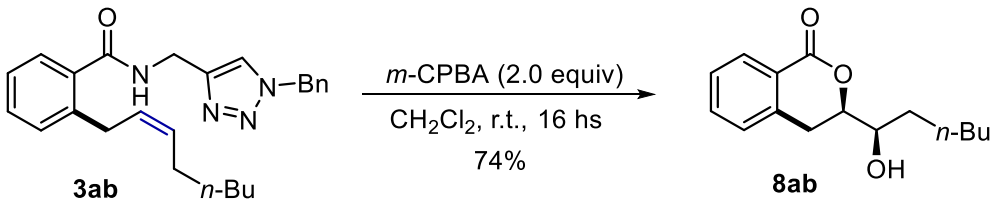

To a solution of **3ab** (66.0 mg, 0.16 mmol) in CH_2Cl_2 (2.0 mL), *m*-CPBA (55.2 mg, 0.32 mmol, 2.0 equiv.) were added. The resulting solution was stirred at room temperature for 16 hs. Then, the reaction mixture was diluted with water (5.0 mL) and extracted with CH_2Cl_2 (2x50 mL). The combined organic extracts were dried over Na_2SO_4, and the filtrate was concentrated under reduced pressure. Purification by column chromatography on silica gel (*n*-Hexane/EtOAc 1:1) yielded **8ab**(29.4 mg, 74%) as a colourless oil. ^{1}H-NMR (400 MHz, $CDCl_3$): δ = 8.11 (dd, *J* = 7.8, 1.4 Hz, 1H), 7.57 (td, *J* = 7.5, 1.4 Hz, 1H), 7.42 (t, *J* = 7.6 Hz, 1H), 7.30 (d, *J* = 8.7 Hz, 1H), 4.48 – 4.43 (m, , 1H), 3.80 – 3.75 (m, 1H), 3.28 (dd, *J* = 16.3, 12.7 Hz, 1H), 2.86 (dd, *J* = 16.4, 3.0 Hz, 1H), 1.73 – 1.64 (m, 2H), 1.62 – 1.52 (m, 1H), 1.52 – 1.42 (m, 1H), 1.40 – 1.32 (m, 4H), 0.92 (t, *J* = 6.9 Hz, 3H). ^{13}C-NMR (101 MHz, $CDCl_3$): δ = 165.2 (C_q), 139.1 (C_q), 134.0 (CH), 130.4 (CH), 127.7 (CH), 127.6 (CH), 124.8 (C_q), 81.3 (CH), 72.9 (CH), 32.7 (CH_2), 31.8 (CH_2), 29.8 (CH_2), 25.2 (CH_2), 22.6 (CH_2), 14.0 (CH_3). MS (ESI) *m/z* (relative intensity): 287 (45) $[M+K]^+$, 271 (100) $[M+Na]^+$. HR-MS (ESI) *m/z* calcd for $C_{15}H_{21}O_3$ $[M+H]^+$ 249.1485, found 249.1489.

3-Heptylisochroman-1-one (9aa)

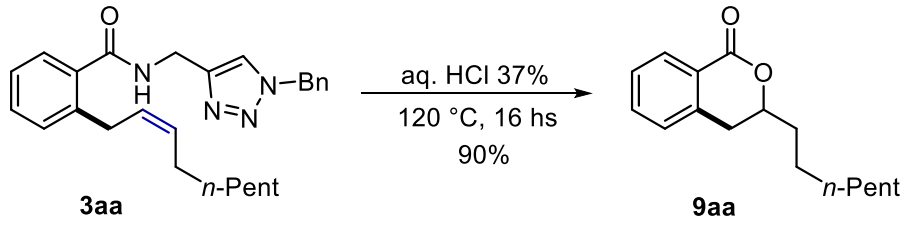

A solution of **3aa** (41.7 mg, 0.10 mmol) in aqueous HCl (2.0 mL, 37% w/w) was stirred at 120 °C for 24 hs. Then, the reaction mixture was diluted with water (15 mL) and extracted with CH_2Cl_2 (3x5 mL). The combined organic extracts were dried over Na_2SO_4, and the filtrate was concentrated under reduced pressure. Purification by column chromatography on silica gel (*n*-Hexane/EtOAc 1:1) yielded **9aa** (22.0 mg, 90%) as a colourless oil. ^{1}H-NMR (400 MHz, $CDCl_3$): δ = 8.11 (dd, *J* = 7.8, 1.4 Hz, 1H), 7.54 (td, *J* = 7.5, 1.4 Hz, 1H), 7.40 (t, *J* = 7.6 Hz, 1H), 7.26 (d,

J = 7.6 Hz, 1H), 4.57 – 4.50 (m, 1H), 3.04 – 2.88 (m, 2H), 1.95 – 1.86 (m, 1H), 1.78 – 1.69 (m, 1H), 1.62 – 1.55 (m, 1H), 1.52 – 1.44 (m, 1H), 1.37 – 1.27 (m, 8H), 0.90 (t, *J* = 6.8 Hz, 3H). ^{13}C-NMR (101 MHz, $CDCl_3$): δ = 165.7 (C_q), 139.3 (C_q), 133.6 (CH), 130.3 (CH), 127.6 (CH), 127.4 (CH), 125.3 (C_q), 78.8 (CH), 35.0 (CH_2), 33.2 (CH_2), 31.8 (CH_2), 29.4 (CH_2), 29.2 (CH_2), 24.9 (CH_2), 22.6 (CH_2), 14.1 (CH_3). MS (ESI) *m/z* (relative intensity): 269 (100) $[M+Na]^+$, 247 (15) $[M+H]^+$. HR-MS (ESI) *m/z* calcd for $C_{16}H_{23}O_2$ $[M+H]^+$ 247.1693, found 247.1699.

4.4.10 Additional References

[1] S. Cattani, A. Secchi, L. Ackermann, G. Cera, *Org. Biomol. Chem.* **2023**, *21*, 1264-1269.

[2] S. Cattani, N. K. Pandit, M. Buccio, D. Balestri, L. Ackermann, G. Cera, *Angew. Chem. Int. Ed.* **2024**, e202404319.

[3] B. Wrackmeyer, Carbon-13 NMR spectroscopy of boron compounds. *Prog. Nucl. Magn. Reson. Spectrosc.* **1979**, *12*, 227−259.

[4] J. Kuang, S. Ma, *J. Org. Chem.* **2009**, *74*, 1763–1765.

[5] A. Köpfer, B. Breit, *Angew.Chem. Int.Ed.* **2015**, *54*, 6913–6917.

[6] Y. Kim, H. Lee, S. Park, Y. Lee, *Org. Lett.* **2018**, *20*, 17, 5478–5481.

[7] D. Berthold, B. Breit, *Org. Lett.* **2020**, *22*, 2, 565–568.

[8] M.-H. Lin, W.-S. Tsai, L.-Z. Lin, S.-F. Hung, T.-H. Chuang, Y.-J. Su, *J. Org. Chem.* **2011**, *76*, 20, 8518–8523.

[9] Y. Zhong, I. Douair, T. Wang, C. Wu, L. Maron, D. Cui, *Angew. Chem. Int. Ed.* **2020**, *59*, 4947 –4952.

[10] S. Arai, A. Izaki, Y. Amako, M. Nakajima, M. Uchiyama, A. Nishida, *Adv. Synth. Catal.* **2019**, *361*, 4882– 4887.

[11] R. E. Kinder, Z. Zhang, R. A. Widenhoefer, *Org. Lett.* **2008**, *10*, 14, 3157–3159.

[12] *Beilstein J. Org. Chem.* **2011**, *7*, 596-600.

[13] G. Giovanardi, S. Cattani, D. Balestri, A. Secchi, G. Cera, *J. Org. Chem.* **2024**, *89*, 12, 8486–8499.

[14] N. Nishina, Y. Yamamoto, *Angew. Chem. Int. Ed.* **2006**, *45*, 3314 –3317.

[15] H. Clavier, K. L. Jeune, I. de Riggi, A. Tenaglia, G. Buono, *Org. Lett.* **2011**, *13*, 2, 308–311.

[16] S. Yamazaki, Y. Yamamoto, Y. Fukushima, M. Takebayashi, T. Ukai, Y. Mikata, *J. Org. Chem.* **2010**, *75*, 15, 5216–5222.

[17] Q. Jiang, H. Li, X. Zhao, *Org. Lett.* **2021**, *23*, 8777−8782.

[18] P. Sureshbabu, S. Azeez, N. Muniyappan, S. Sabiah, J. Kandasamy, *J. Org. Chem.* **2019**, *84*, 11823−11838.

5. Iron(0)-NHC Complexes for C–H Activation Reactions without Grignard Reagents

The research presented in this chapter was conducted during a visiting stay in the Ackermann Group at the Georg-August-Universität in Göttingen.

From this chapter:

Z.-J. Zhang, S. Golling, S. Cattani, X. Chen, L. Ackermann**,** *J. Am. Chem. Soc.* ***2025****, 147,* 8, 6897–6904.

5.1 Introduction

Many efforts have been directed towards developing metal-catalyzed activation of C–H bonds with non-toxic, abundant, and cost-effective 3d transition metals, particularly iron.[1] However, despite the clear benefits of iron catalysis, the advancement of iron-catalyzed C–H activations remains considerably underdeveloped with respect to the use of other 3d-transition metals.[2] In particular, iron-catalyzed C–H activations conducted without additives and Grignard reagents under mild conditions are still rare.[3]

Although there are numerous powerful iron-catalyzed C–H activation methods involving Grignard reagents that enable the formation of new C–C and C-heteroatom bonds (See Introduction for more details), the use of these reactants presents several disadvantages. Firstly, they are sensitive to oxygen and moisture, so their use typically necessitates rigorously dried, aprotic, toxic, and volatile organic solvents and an inert atmosphere.[4] Moreover, they are frequently incompatible with reactive functional groups, which often limits the applicability of the methods in terms of substrate scope. Additionally, from a sustainability perspective, Grignard reagents contribute to the production of waste products that must be removed from the reaction environment, leading to processes with a low atom economy.

5.1.1 Phosphine- and Carbonyl-based Systems

To address the limitations related to the use of Grignard reagents, C–H bond functionalizations using weakly-coordinating, monodentate directing groups have emerged as a complementary approach to bidentate-assisted, iron-catalyzed C–H bond activations. These systems typically require an iron(0) complex as catalytic active species to promote the desired transformation. Following pioneering studies that demonstrated the catalytic activity of iron(0) complexes,[5] the Kakiuchi group presented the first example of iron-catalyzed *ortho* C–H homoallylation of aromatic ketones **I** with methylenecyclopropanes **II** (MCPs) (Scheme 5.1).[3b] This transformation is enabled by the weak coordination of the ketone to the iron(0) catalyst. The model reaction is carried out in cyclohexane with just 5 mol % of $Fe(PMe_3)_4$ catalyst under very mild reaction conditions, demonstrating a broad substate scope and functional group tolerance.

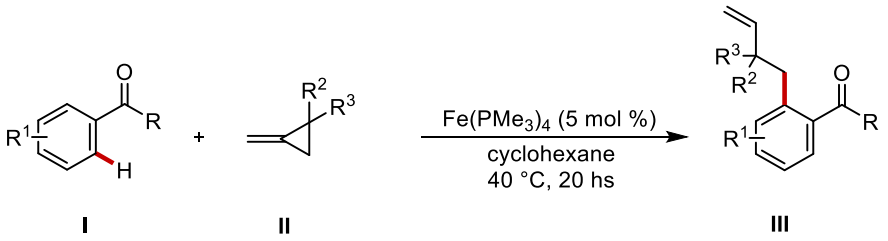

Scheme 5.1 Iron-catalyzed C–H homoallylation of ketones with methylenecyclopropanes **II**.

Following their initial studies, the same group applied the previously developed $Fe(PMe_3)_4$ catalytic system for the *ortho* C–H alkenylation of aromatic ketones with internal alkynes **IV** (Scheme 5.2).[6] A key feature of this method is its complete regio- and stereoselectivity in C–H alkenylation, resulting in the formation of a single isomer. Various aryl(silyl)acetylenes were subjected to C–H alkenylation with *para*-trifluoromethylpivalophenone, yielding the desired products **V** in good to excellent yields. Regarding the scope for aromatic ketones, the *p*-CF_3 substitution was crucial for the reaction's success, in fact although other electron-withdrawing groups in the *para* position were tolerated, the products were obtained in lower yields.

This approach was also exploited by the Ackermann group which in 2020 reported the iron(0) catalyzed C–H hydroarylation of ketones with allenes (See Chapter 4, section 4.1.2 for more details).[3d]

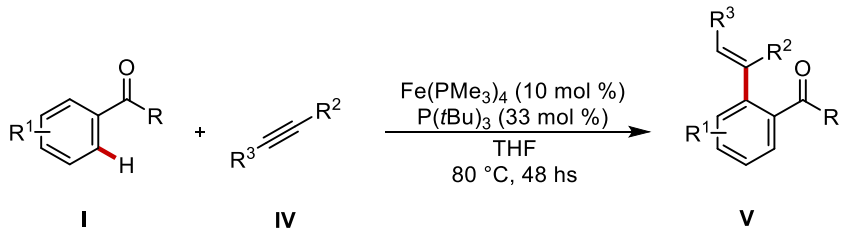

Scheme 5.2 Iron-catalyzed C–H alkenylation of ketones with alkynes **IV**.

In 1965, Pauson reported the stoichiometric C–H bond activation of arenes mediated by iron(0) carbonyl complex such as $[Fe_2(CO)_9]$ and $[Fe_3(CO)_{12}]$.[7] Thus, based on this stoichiometric reaction, Wang and co-workers described an iron-catalyzed redox-neutral [4 + 2] cyclization reaction between internal alkynes and aromatic imines **VI** to deliver *cis*-3,4-dihydroisoquinolines **VII** (Scheme 5.3).[3a] However, a limitation of this protocol relies in its harsh reaction conditions and the necessity to perform the reactions in pressurized vessels.

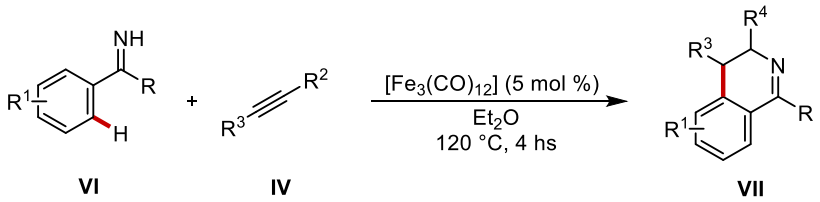

Scheme 5.3 Iron-carbonyl-catalyzed annulation of N–H imines with internal alkynes.

To address the limitations discussed so far, the Ackermann group recently reported a chelation-assisted, photo-promoted iron-catalyzed C–H activation of aromatic imines with internal alkynes. (Scheme 5.4).[8] Notably, the reaction proceeds at room temperature without the need of Grignard reagents, using the *cis*-[Fe(H)$_2$(dppe)$_2$] complex as the precatalyst and mild visible light. The absence of Grignard additives allows for high functional group tolerance, mild reaction conditions, and full atom economy. After a deep investigation of the reaction mechanism, the authors propose that the light is required to reduce iron dihydride complex *cis*-[Fe(H)$_2$(dppe)$_2$] to its active iron(0) form [Fe(dppe)$_2$] and at the same time to generate an empty coordination site for the alkyne through the photodissociation of the dppe ligand.

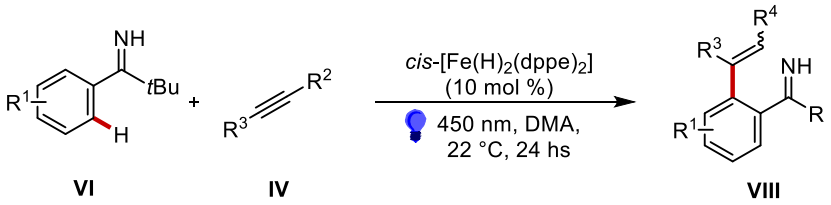

Scheme 5.4 Photo-promoted, Grignard free, iron catalyzed C–H alkenylation of aromatic imines.

5.1.2 *N*-Heterocyclic Carbene-based Systems

Most of the examples presented so far utilize iron(0)-based systems in combination with mono- or bidentate phosphine ligands, which have proven to be highly effective in facilitating alkenylation reactions under mild conditions, notably avoiding the use of Grignard reagents. However, bidentate phosphine ligands are not easy to synthesize, nor its easy to vary their steric and electronic properties. Furthermore, the use of iron-phosphine systems is still closely tied to the development of racemic reactions.

N-heterocyclic carbenes (NHCs) have gained significant interest as ligands for transition metals.[9] Similar to phosphines, they function as 2-electron donor ligands. However, NHCs are distinguished by their stronger σ-donating and weaker π-accepting properties.[10] The use of easily accessible chiral NHC ligands can pave the way for the development of iron-catalyzed enantioselective C–H functionalization reactions, which are unfortunately still scarce. In this context, the literature so far reports only one example where chiral phosphines have been used to achieve iron-catalyzed enantioselective C–H functionalization reactions. In 2017 Butenschön and Schmiel reported an iron-catalyzed *ortho*-alkylation and arylation of ferroceneamides (Scheme 5.5).[11] After a screening of commercially available chiral *P*,*P*-ligands, they identified (*R*,*R*)-Chiraphos as a promising ligand for controlling the enantioselective arylation process. Despite the moderate enantioselectivity, this study represents the first example of enantioselective iron-catalyzed C–H activation controlled by chiral phosphine ligands, with bidentate directing groups.

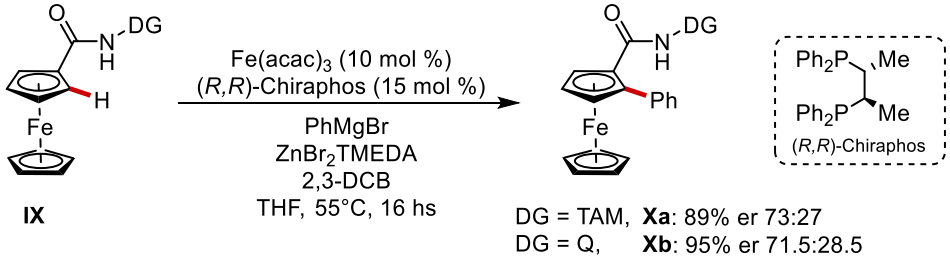

Scheme 5.5 Enantioselective iron-catalyzed C–H arylation of ferrocenes with chiral phosphine ligand.

In contrast, Ackermann's group achieved a highly enantioselective iron-catalyzed C–H alkylation of indoles using easily accessible chiral NHC ligands (Scheme 5.6).[12] Inspired by Yoshikai's previous racemic report on imine-directed indole C–H alkylation,[13] the authors developed a catalytic system that requires an iron(III) precatalyst, a chiral NHC ligand and a Grignard reagent (CyMgCl) in combination with TMEDA. The key to their success was the development of novel *meta*-decorated NHC ligands, with the best stereoselectivity results obtained using bulky *meta*-1-adamantyl substituents represented in Scheme 5.6. This C–H alkylation method proved effective for a wide range of indoles and azaindoles, utilizing variously substituted styrenes and

alkenylmetallocenes. Notably, this study represents the first and highly enantioselective transformation *via* inner-sphere iron-catalyzed C–H activation.

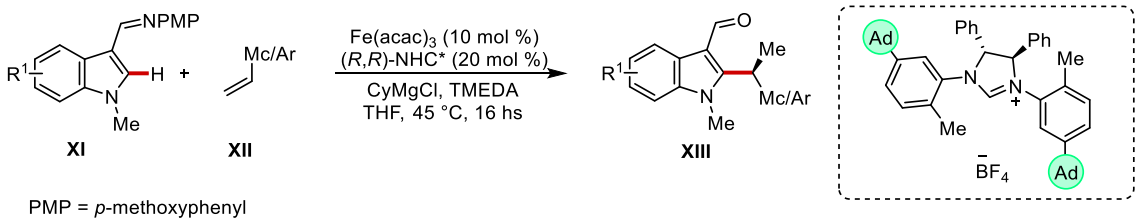

Scheme 5.6 Asymmetric iron-catalyzed C–H Alkylation with alkenylmetallocenes and styrenes.

The major limitation associated with this methodology lies in the narrow substrate scope, particularly regarding the use of electron-withdrawing or Grignard-sensitive functional groups. As shown in Scheme 5.7, substitution on both the aromatic ring of the indole and the styrenes used as reaction partners is limited mainly to alkyl (**XIIIc-d**, **j**), aryl (**XIIIg**), and ether groups (**XIIIa, i**). Halogens, except for fluorine (**XIIIb**, **f**), esters, and nitriles are absent, making this methodology, although excellent in terms of enantioselectivity, very limited in terms of applicability.

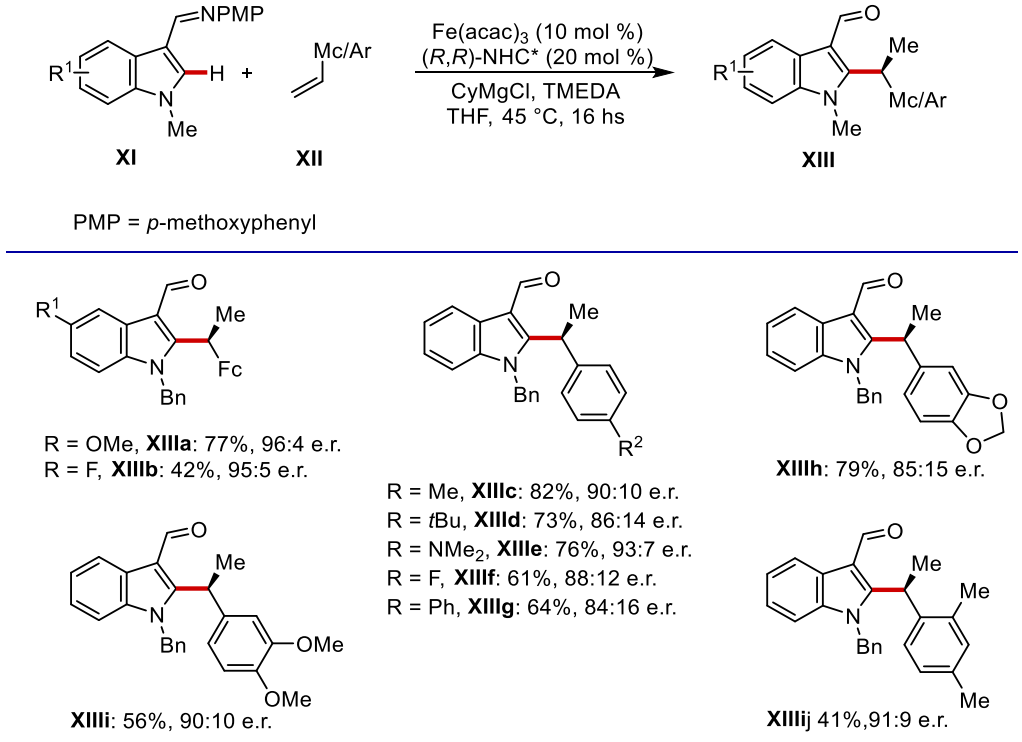

Scheme 5.7 Selected substrate scope for asymmetric iron-catalyzed C–H Alkylation.

Very recently, the same group further exploited the iron-NHC system to achieve the simultaneous construction of C–N axial chirality and central chirality (Scheme 5.8).[14] In this context, the high

diastereo- and enantioselectivity is primarily determined by the design of the NHC salt preligand utilized in the reaction (**NHC***). In particular, the *meta* substitution that provides steric hindrance (Adamantyl group) and the *ortho* substitution with a methoxy group that is responsible of noncovalent interactions, facilitating the simultaneous generation of C–N axial chirality and a C-stereogenic center. Computational studies revealed that the coordination of the methoxy group to the iron center stabilizes the transition state for the major product. Additionally, non-covalent interactions such as the CH–π interaction between this group and the indole substate are responsible for determining the axial chirality. Moreover, the π-π stacking interaction between the indole and the phenyl group of the styrene determines the central chirality.

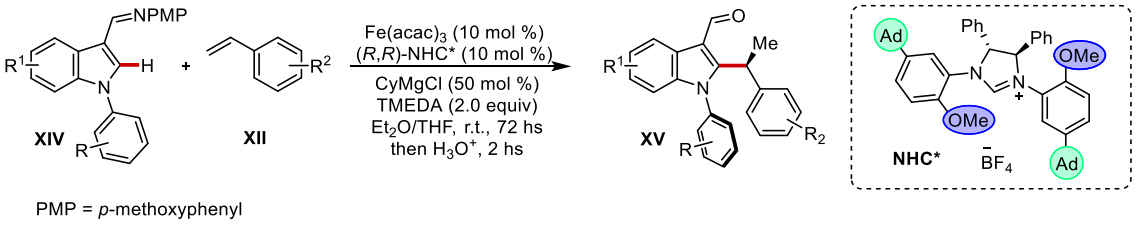

PMP = *p*-methoxyphenyl

Scheme 5.8 Asymmetric iron-catalyzed C–H alkylation for simultaneous construction of C–N axial and C-central chirality.

To gain insights into the working mode of the iron catalyst, the authors conducted a series of mechanistic experiments. Their aim was to define the potential reactive iron-NHC species responsible for C–H activation and obtain molecular-level insight into the role of the TMEDA additive in catalysis. In this context, a recent study from the Neidig group revealed the formation of a low-valent Fe-styrene species under similar reaction conditions,[15] which may act as a precursor to a catalytic active low-valent Fe-NHC complex.

In line with this hypothesis, they synthesized the Fe(0) species [Fe(Cy)(η^2-styrene)$_3$][MgCl(THF)$_5$] (**A**), starting from the Fe(acac)$_3$ pre-catalyst, TMEDA, styrene and cyclohexyl Grignard reagent (CyMgCl). The iron complex **A** was then treated with an excess of CyMgCl in the presence of the chiral NHC ligand, resulting in the formation of a new iron species (Scheme 5.9, a). This species was identified by in situ freeze-trapped 80 K ^{57}Fe Mössbauer spectroscopy (Scheme 5.9, b). The authors propose that this new iron species is the low-valent Fe(NHC*)(η^2-styrene)$_2$ complex (**B**), as similar compounds have been documented in the literature. These studies were further extended to evaluate the *in situ* iron speciation during catalysis. Freeze-trapped ^{57}Fe Mössbauer spectroscopy at 360 minutes into the C–H alkylation reaction revealed the presence of a single major iron species with parameters comparable to **B** (Scheme 5.9, c).

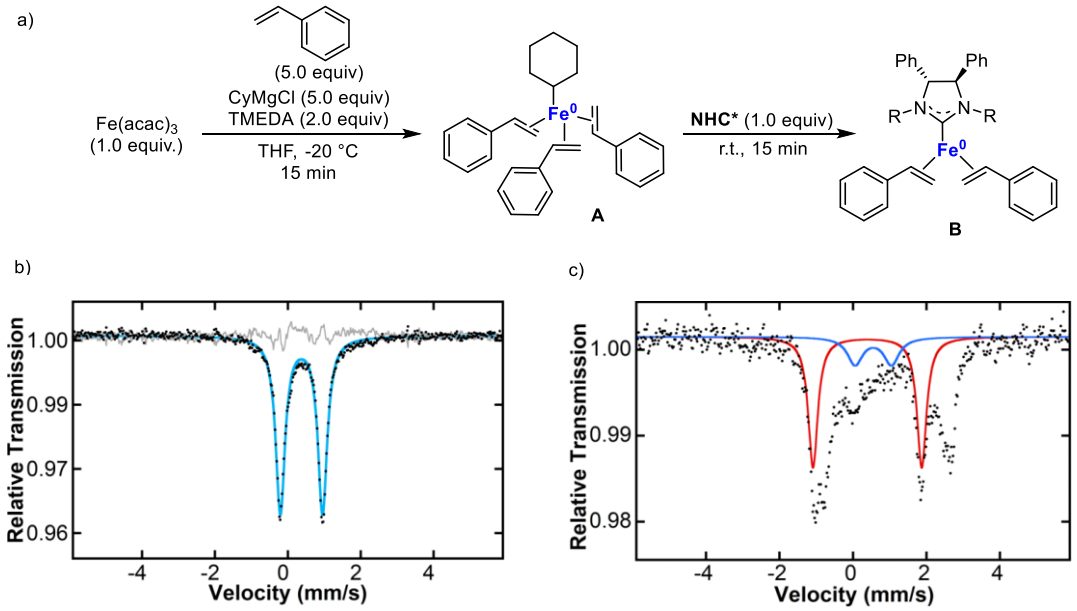

Scheme 5.9 a) Synthesis of low-valent iron species; b) ^{57}Fe Mössbauer spectra of **A** with δ = 0.37 mm/s and $|\Delta EQ|$ = 1.16 mm/s (100%); c) ^{57}Fe Mössbauer spectra of the reaction between Fe(Cy)(η^2-styrene)$_3$ (**A**) and a solution of NHC* (1.5 equiv.) for 2 min. The red species with δ = 0.39 mm/s and $|EQ|$ = 2.84 mm/s is the dominant species (37%) likely corresponding to **B**. The blue species correspond to a small amount of unreacted **A** (16% of total iron).

Efforts to isolate iron complexes with chiral carbene were unsatisfactory, likely due to the highly lipophilic nature of the carbene ligand, which hindered crystallization, combined with the air-sensitive nature of the target complexes. For these reasons, the chiral carbene was replaced with the achiral surrogate SIMes•HCl, which has a saturated backbone like NHC*. This ligand allowed the formation of the iron(0) complex Fe(S-IMes)(η^2-styrene)$_2$ (**B'**) which showed a ^{57}Fe Mössbauer spectra similar to the one obtained for **B**, confirming its identification as Fe(NHC*)(η^2-styrene)$_2$ (Scheme 5.10, a). Moreover, this complex was generated and reacted *in situ* with indole substrate **XIV**, delivering the C–H alkylated product (*rac*)-3 in 54% yield (Scheme 5.10, b). These findings support that Fe(NHC*)(η^2-styrene)$_2$ species are likely the active iron species in the catalytic system.

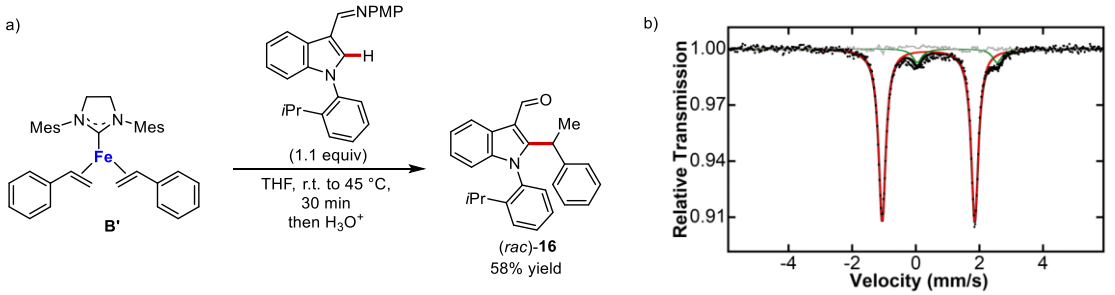

Scheme 5.10 a) Reaction of in situ generated **B'** with indole substrate to generate C−H alkylated product; b) 80 K 57Fe Mössbauer spectra of B* with δ = 0.39 mm/s and |ΔEQ| = 2.92 mm/s.

Further DFT calculations showed that starting from the iron(0) complex **B**, which is coordinated by a chiral NHC and two styrenes, a ligand exchange occurs, forming the substrate-coordinated intermediate **Int1**. The classic oxidative addition of the indole C−H bond to the iron center is feasible; however the calculation showed that the competing ligand-to-ligand hydrogen transfer (LLHT) pathway from **Int1** directly to **Int2** is more favourable, followed by olefin insertion into the Fe−H bond. The resulting **Int3** then undergoes reductive elimination to regenerate the active iron species **B** and delivering the C−H alkylation product (Scheme 5.11). Thus, the authors demonstrated through detailed mechanistic studies involving experiments, Mössbauer spectroscopy, and computational analysis, that an iron(0)-NHC complex serves as the catalytic active species.

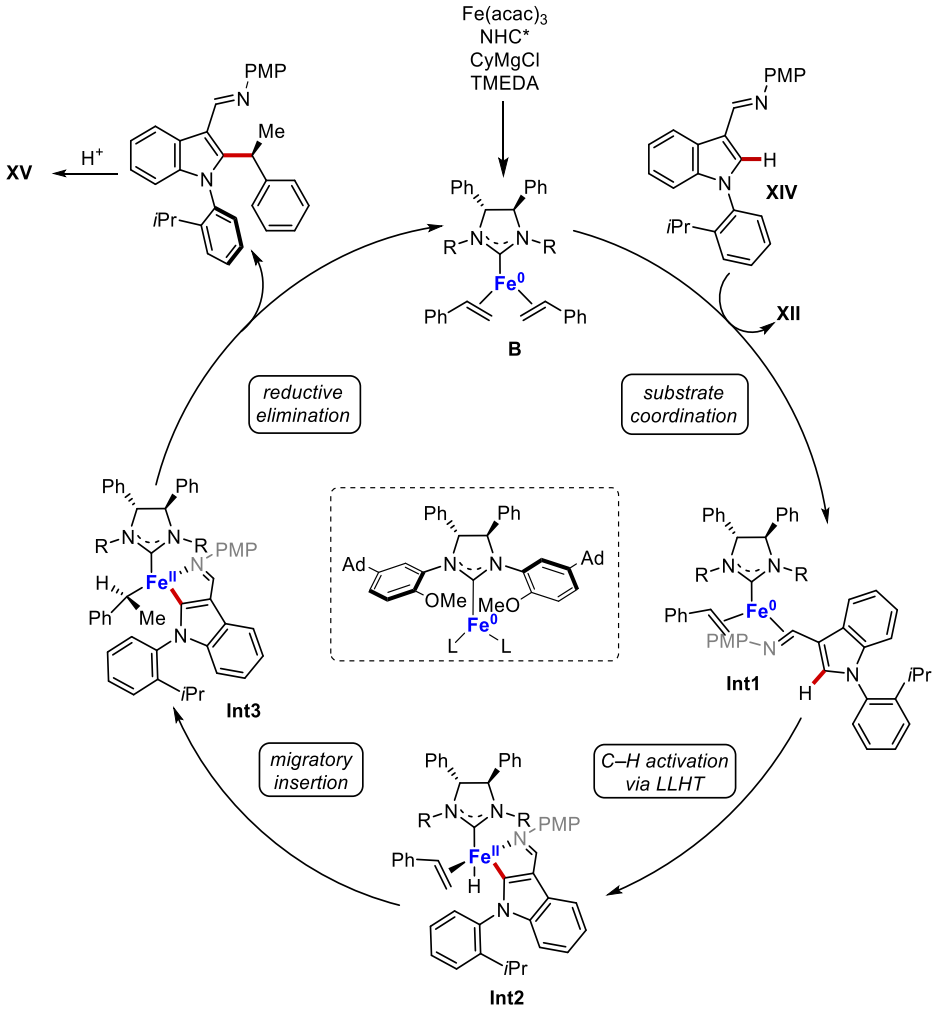

Scheme 5.11 Proposed catalytic cycle for iron(0)-catalyzed asymmetric C–H alkylation.

5.2 Results and Discussion

Iron-NHC complexes have been reported to be useful in various types of reactions, including C–C[16] and C–Het[17] bond formation, reduction reactions,[18] cyclizations[19] and polymerizations.[20] This derives from their powerful versatility in accessing diverse structural motifs with varying oxidation states, diverse coordination geometries, and different substitution patterns of *N*-heterocyclic carbene ligands.

However, the scenario of C–H functionalizations catalyzed by iron-NHC complexes is still quite restricted. For this reason, the research project commenced in Ackermann's group in collaboration with Dr. Zi-Jing Zhang, aimed to synthesize iron(0) complexes with NHC ligands and test their catalytic activity. The objective was to extend the reactivity of this system to new types of substrates and develop C–H functionalization methods that avoid the use of Grignard reagents, as the active iron(0) species would be already present in the reaction, eliminating the need for *in situ* reduction of the precatalyst. Moreover, this approach could also be beneficial in terms of the applicability of the methods, as it would provide a more tolerant system towards sensitive and potentially reactive functional groups, thereby increasing the chemoselectivity of the reaction.

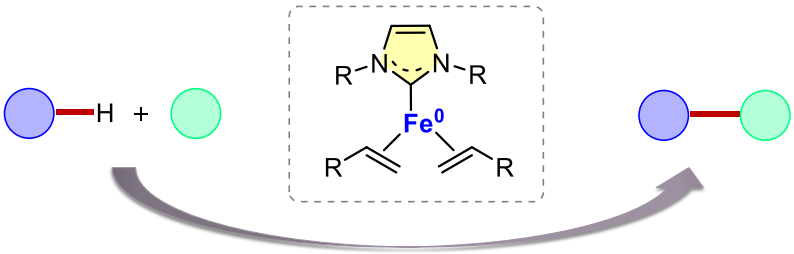

Scheme 5.12 Iron(0)-NHC complex for C–H functionalizations.

5.2.1 Synthesis of Iron(0)-NHC Complexes

The investigation began with the synthesis of a family of iron(0) complexes featuring differently substituted carbene ligands to evaluate their influence on catalytic activity in terms of electronic and steric effects. Thus, at first we synthesized the *N*-heterocyclic carbene (NHC) ligands following a straightforward method reported in the literature. Starting with commercially available glyoxal and anilines, the reaction of glyoxal with two equivalents of the desired aniline produces diazabutadienes (**3a**-**b**). These are then converted into NHC salts using a slight excess of paraformaldehyde and hydrochloric acid (Scheme 5.13).

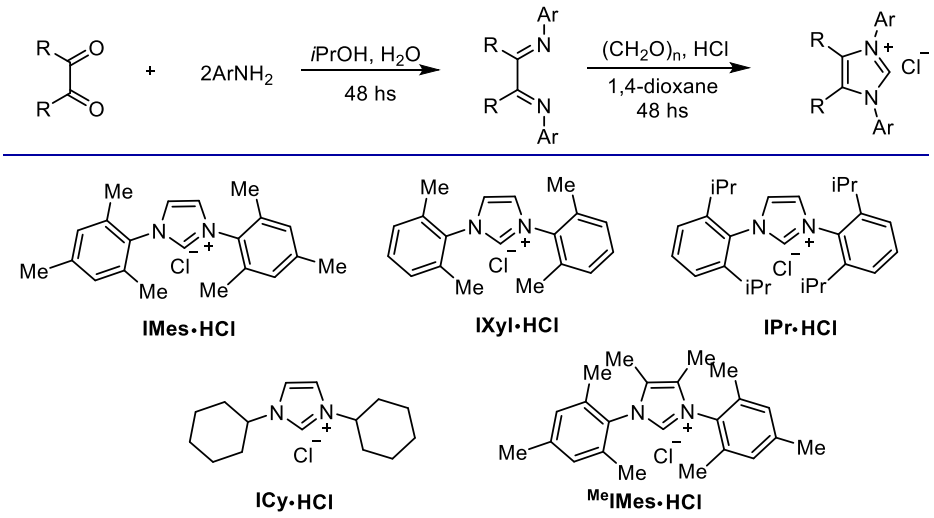

Scheme 5.13 General procedure for the synthesis of NHC salts pre-ligands.

The final deprotonation step, conducted in a nitrogen-filled glove-box with 1.2 equivalents of sodium hydride and a catalytic amount of potassium *tert*-butoxide (KO*t*Bu) in tetrahydrofuran, led to the synthesis of the corresponding free NHCs (Scheme 5.14). The pure ligands were obtained by precipitation from *n*-pentane, after filtering the insoluble solids from the reaction mixture and concentrating the residual solvent. Notably, no special precautions are required for the synthesis of the salt precursors while the final deprotonation step and isolation need to be conducted under an inert atmosphere. Unfortunately, we failed to obtain the free ICy carbene as the final deprotonation led to the partial decomposition of the starting material.

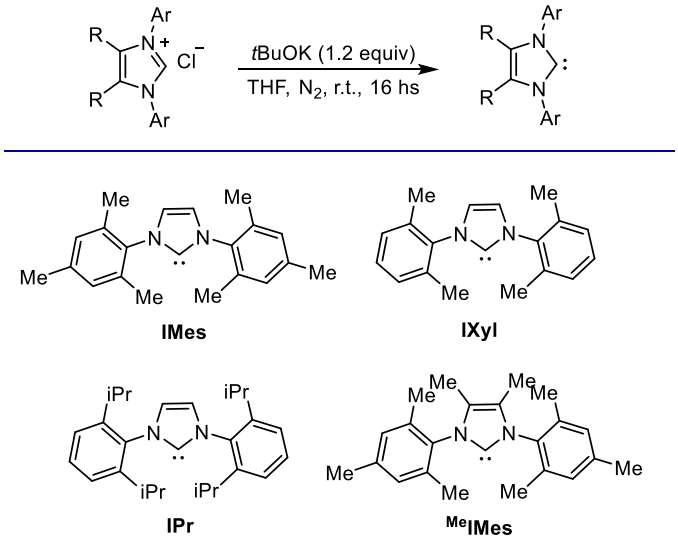

Scheme 5.14 General procedure for the synthesis of free NHC ligands.

Lastly, the free NHC ligands were utilized for the synthesis of a family of three-coordinate low-valent iron(0) complexes stabilized with two units of styrene as additional ligands.[21] These iron complexes were synthesize using a one-pot reaction protocol were an initial mixture of $FeCl_2$ and 1.0 equivalent of free NHC is stirred in THF at room temperature for several hours, until clear solutions are formed. Subsequently, 2.0 equivalents of styrene and potassium graphite (KC_8) are added to these solutions. The reaction mixtures are then stirred at room temperature for an additional 16 hours. Afterwards, the complexes are isolated through workup of the reaction mixture and precipitation from *n*-pentane. Complexes are air- and moisture-sensitive, so the synthesis and every operation conducted during the workup and isolation needs to be performed in a strictly controlled environment.

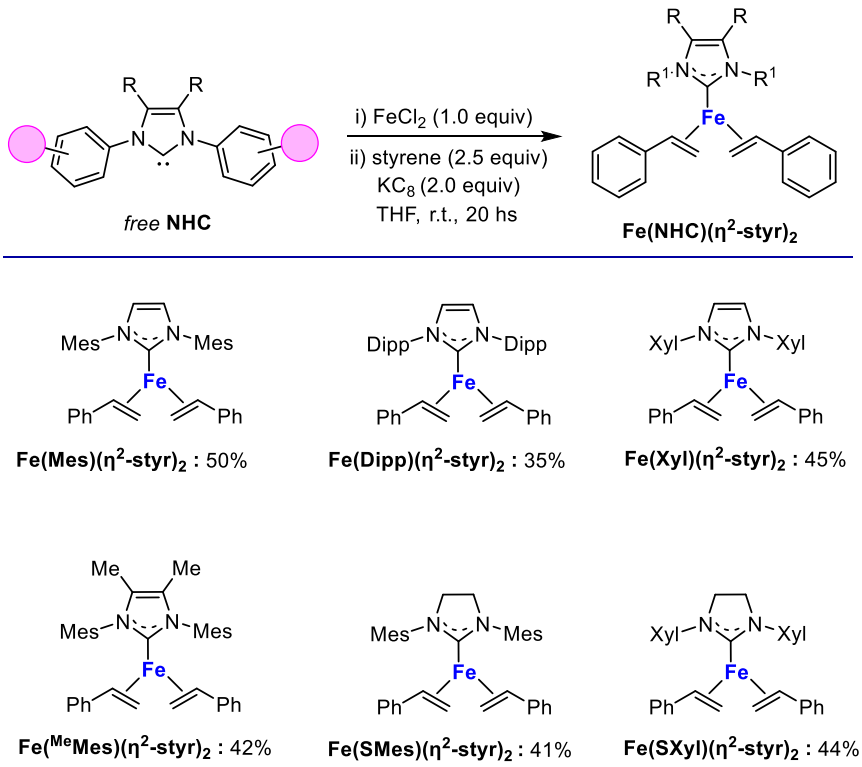

Scheme 5.15 General procedure for the synthesis of iron(0)-NHC-styrene complexes.

In addition to styrene-coordinate Fe(0) complexes, a three-coordinate complex with persistent carbene and vinylsiloxane ligand was synthesized. The synthesis was performed following the same procedure employed before, using divinyltetramethyldisiloxane (dvtms) as the stabilizing ligand.

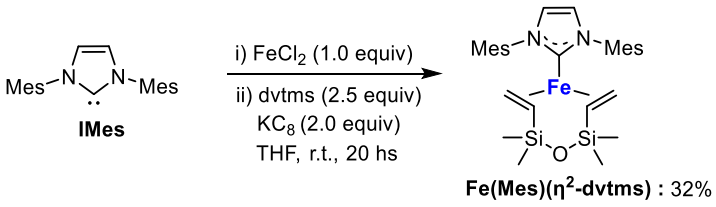

Scheme 5.16 Synthesis of iron(0)-NHC-dvtms complex.

5.2.2 Catalytic Activity of Iron(0)-NHC Complexes

Once the family of Fe(0)-based complexes was synthesized, their catalytic activity was tested using the imine-directed indole C–H alkylation with styrene as the model reaction (Scheme 5.17). Specifically, *N*-methyl indole substrate **1a** was reacted with 1.5 equivalents of styrene **2a** using a 10 mol % of different iron(0)-NHC complexes, under mild reaction conditions at room temperature and without the presence of a Grignard reagent.

A depicted in Scheme 5.17, the iron complex that exhibited the highest catalytic activity is **Fe(Mes)(η^2-styr)$_2$**, which features an NHC ligand decorated with mesitylene substituents (Mes). The desired alkylated indole **3aa** was obtained in 80% yield with complete Markovnikov selectivity when using **Fe(Mes)(η^2-styr)$_2$** as catalyst. An increase in the steric hindrance of the *ortho* substituents of the aromatic rings in the NHC ligand led to an inhibition of the catalytic activity. Thus, complex **Fe(Dipp)(η^2-styr)$_2$**, that features two isopropyl groups on the carbene moiety, led to the formation of the desired product only in traces. Removing the substituent from the *para* position of the aromatics as in complex **Fe(Xyl)(η^2-styr)$_2$**, decorated with a xylene group, did not impact greatly on the outcome of the reaction, with formation of product **3aa** in slightly diminished yield. Introducing substituents on the backbone of the NHC ligand, as in **Fe(^{Me}Mes)(η^2-styr)$_2$**, significantly reduced the yield of the reaction, with product **3aa** obtained only in 38% yield. The use of NHC ligands with saturated backbones, **Fe(SMes)(η^2-styr)$_2$** and **Fe(SXyl)(η^2-styr)$_2$**, resulted in a slight decrease in the yield of the reaction. When the reaction was performed employing the low-valent Fe(0) complex stabilized with a vinylsiloxane ligand **Fe(Mes)(dvtms)** the reaction was completely shut down without formation of any product, but only recovery of the unreacted starting material. This is accounted for the strong coordination of the ligand that prevents the coordination of **1a**.

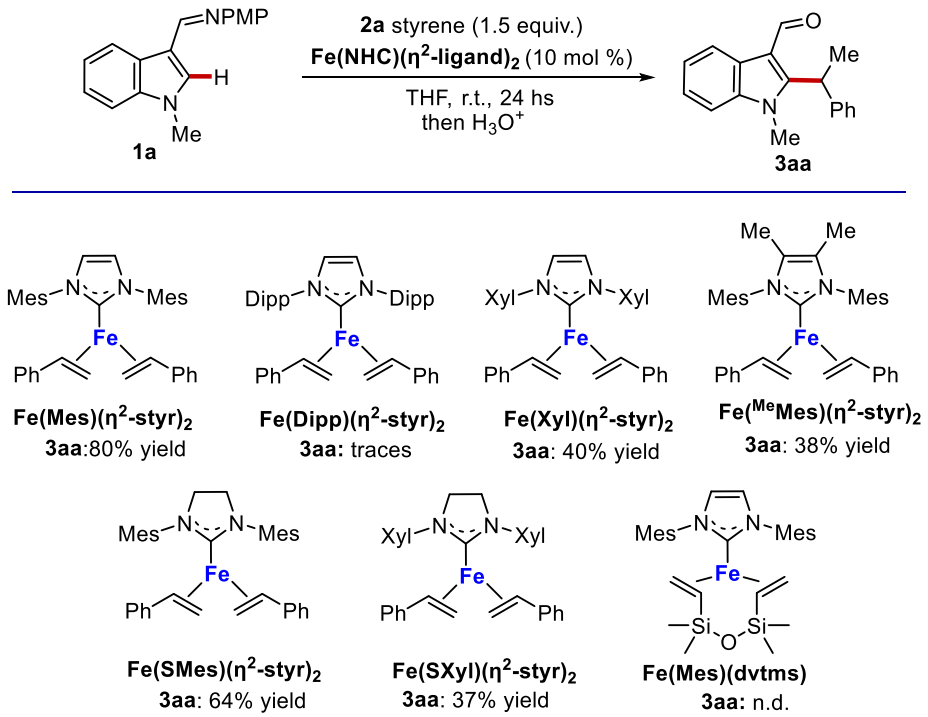

Scheme 5.17 Indole C–H alkylation with iron(0)-NHC complexes.

Complex **Fe(Mes)(η²-styr)₂**, which showed the best catalytic activity, was subsequently employed in the reaction between styrene and *N*-aryl indole **1b**, decorated with an isopropyl substituent at the *ortho* position of the aromatic ring (Scheme 5.18). The desired racemic product **3ba** was obtained in 50 % yield after chromatographic purification, demonstrating once again the feasibility of this catalytic system that allows to obtain the desired alkylation product at room temperature and without the aid of a Grignard reagent.

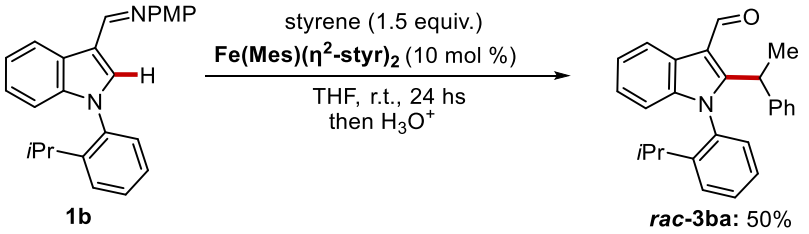

Scheme 5.18 Indole C–H alkylation catalyzed by **Fe(Mes)(η²-styr)₂**.

With the aim of extending the reactivity of the Fe(0)-NHC system to new types of substrates and developing C−H functionalization methods that avoid the use of Grignard reagents, the reactivity of **Fe(Mes)(η²-styr)₂** complex was further investigated by varying the directing group on the indole substrate. Specifically, the reaction was attempted with C3-ketone decorated indole **4** and *N*-quinoline alkylated substrate **6**; however, neither conducting the reaction at room temperature nor heating it at 60 °C resulted in the formation of the desired product. Additionally, the

intramolecular reaction of the imine-directed indole **1d**, functionalized with an olefin-terminal alkyl chain on the nitrogen atom, also failed to yield the target product.

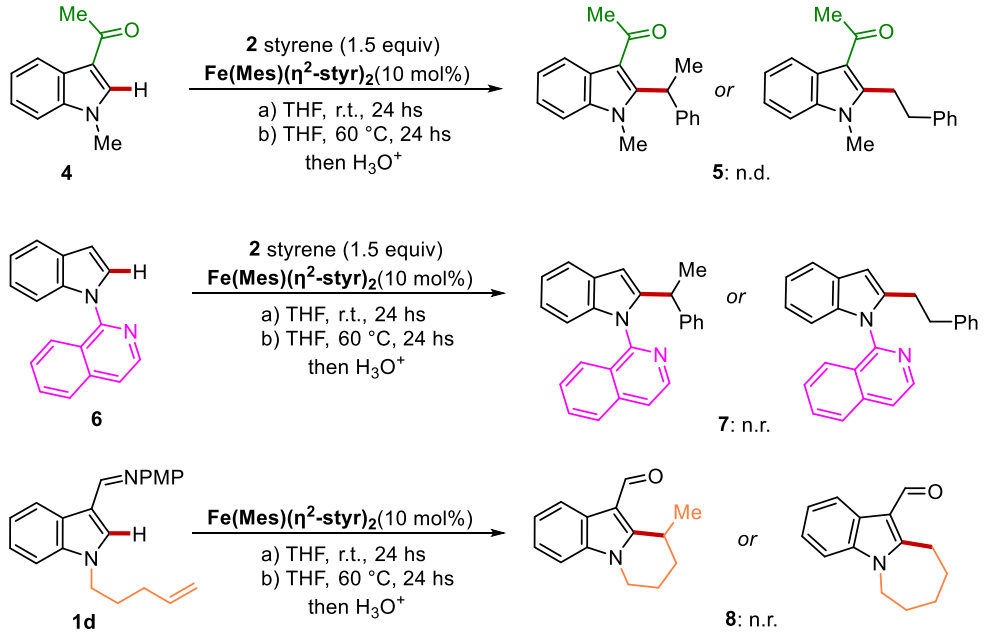

Scheme 5.19 Survey on different indole substrates.

Furthermore, other substrates were evaluated, including an aromatic imine **12**, pivaloyl phenone **13** and ferrocene derivatives with different directing groups (Scheme 5.20). Despite the efforts, all the substrates proved to be unreactive under the various reaction conditions (Conditions a) and b), Scheme 5.20). Additionally, both benzothiazole and benzimidazole substrates also failed in the reaction, with complete recovery of the unreacted starting material. Therefore, at present, the system remains limited to the use of imine-directed indoles as substrates.

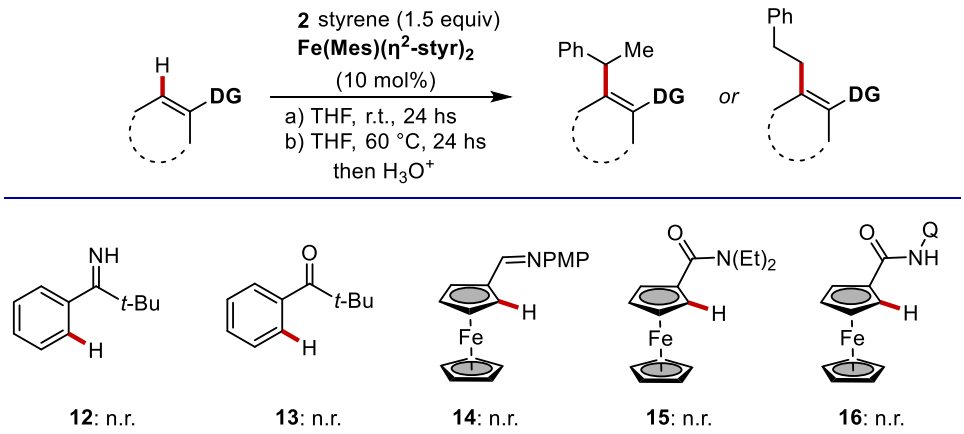

Scheme 5.20 Survey on different types of substrates.

Next, we investigated the reactivity of the model indole substrate **1** utilizing different reaction partners (Scheme 5.21). Unactivated alkenes like 1-hexene (**2b**) did not undergo any reaction both at room temperature (Condition a) and at 60 °C (Condition b). Similarly, disubstituted alkenes, such as *trans*-*β*-methyl styrene, and allyl benzene were incompatible under the devised reaction conditions. Moreover, other types of unsaturated compounds such as terminal alkyne and allenes failed to deliver any desired product.

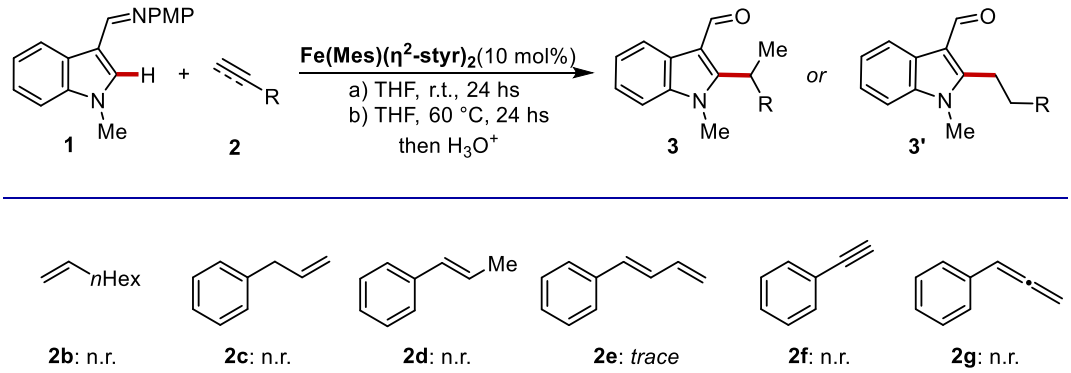

Scheme 5.21 Survey on different types of unsaturated compounds.

Lastly, we evaluated vinylsilanes **9** as the alkene motif in the Fe(0)-NHC catalyzed C−H alkylation of *N*-methyl indole **1a**. Interestingly, when we used a trisubstituted(vinyl)silane as substrate, the alkylated indole was obtained with complete anti-Markovnikov selectivity. Although the reaction performed with triphenyl vinylsilane **9a** at room temperature led to the formation of the product only in very low yield, carrying out the reaction at higher temperature allowed for the isolation of the desired product **10aa** in 76% yield with high linear selectivity (> 20:1). In sharp contrast, styrene derivatives typically yield the thermodynamically favoured Markovnikov branch products with complete selectivity. Thus, the generation of complementary linear alkylated products under the present iron(0)-NHC catalysis is especially significant.

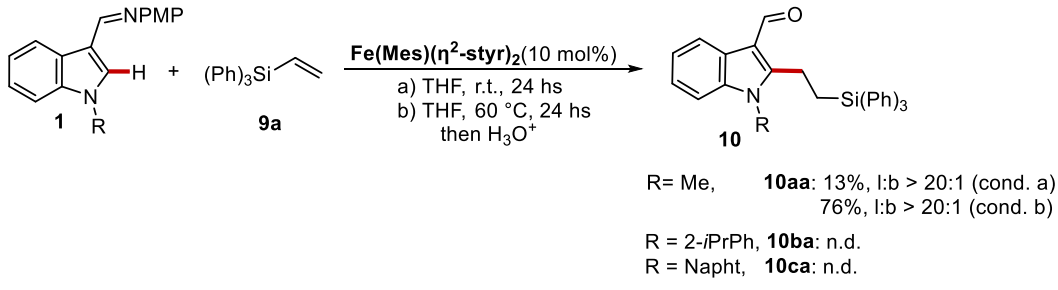

Scheme 5.22 C–H alkylation of indoles with vinylsilanes catalyzed by **Fe(Mes)(η²-styr)₂**.

5.2.3 Functional Group Tolerance of Iron(0)-NHC System

Further, we aimed to investigate whether the **Fe(Mes)(η²-styr)₂** complex could catalyze the alkylation reaction using substrates decorated with sensitive functional groups, which are typically not tolerated in systems that require the use of a Grignard reagent. Therefore, styrenes substituted at the *para* positions with sensitive functional groups such as bromo, chloro, and methyl ester, which failed to yield the desired products in the presence of the Grignard reagent (Scheme 5.23, condition **b**), were subjected to the reaction using only the iron(0)-NHC complex **Fe(Mes)(η²-styr)₂** (Scheme 5.23, condition **a**). However, even under these conditions, the alkylated products **3ab**-**3ad** were not detected at either room temperature or elevated temperatures (60 °C for 24 hs). Additionally, substituted indoles were synthesized to compare the reactivity in both systems. Indole substituted at the 6 position with a chlorine (**3e**) showed an improved reactivity when the reaction was conducted using the **Fe(Mes)(η²-styr)₂** complex as the catalyst, with product **3ea** recovered in 71% yield (34% yield with Grignard system). A 6-substituted methyl ester indole **3f** failed to deliver the desired product with both the Grignard system and the pre-formed iron(0) complex. However, cyano group (**3g**), which was incompatible with the Grignard reagent system, was well tolerated in the reaction performed with **Fe(Mes)(η²-styr)₂** complex, indicating that this reaction has an improved functional group compatibility.

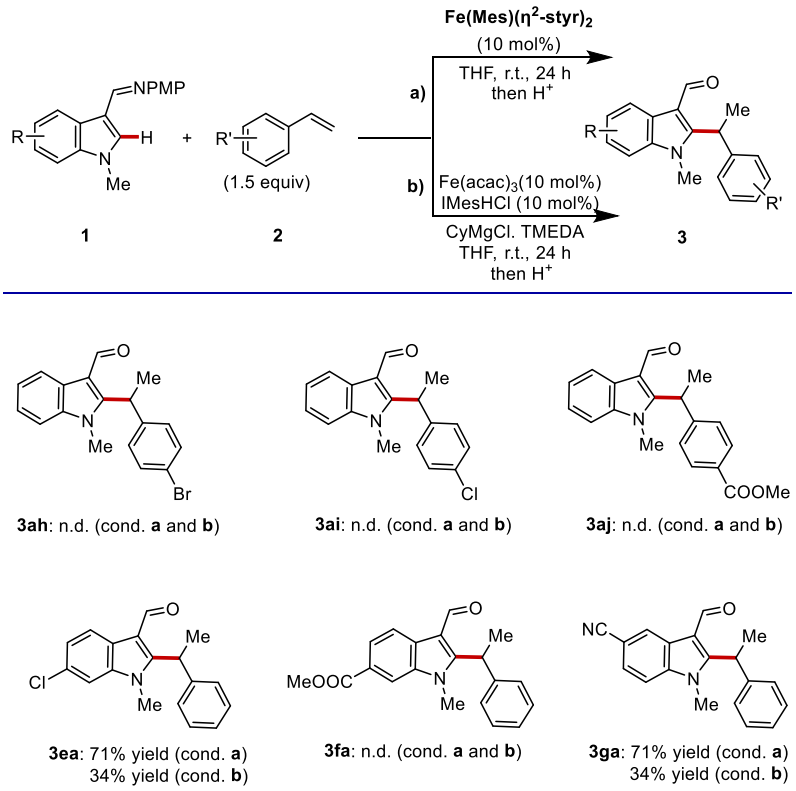

Scheme 5.23 Functional group tolerance in indole C–H alkylation.

5.3 Conclusions

In summary, we have synthesized a family of three-coordinate iron(0) complexes stabilized with *N*-heterocyclic carbene ligands (NHCs). The straightforward synthesis of these ligands has facilitated the effective modification of their properties. In particular, we changed the steric hindrance and electronic properties of the aromatic substituents on the NHC ligands to evaluate how it would affect the catalytic activity of the iron(0) complexes in the imine-directed indole C–H alkylation with olefins. We discovered that the iron complex that exhibited the highest catalytic activity is **Fe(Mes)(η^2-styr)$_2$**, which was efficiently employed for the regioselective C–H alkylation that proceeds under mild conditions without Grignard reagent and additional additives. The regioselectivity of the C–H alkylation is affected by the nature of the alkene substrate (styrenes or vinylsilanes), resulting in alkylated indoles with Markovnikov or anti-Markovnikov selectivity. Moreover, this approach was also beneficial in terms of the applicability of the method, as sensitive and potentially reactive functional groups were tolerated. However, despite several attempts, this system remains limited to the use of imine-directed indoles, as different substrates were not reactive under the devised **Fe(Mes)(η^2-styr)$_2$** catalytic system.

5.4 References

[1] P. Gandeepan, T. Müller, D. Zell, G. Cera, S. Warratz, L. Ackermann, *Chem. Rev*. **2019**, *119*, 2192–2452.

[2] a) R. Shang, L. Ilies, E. Nakamura, *Chem. Rev.* **2017**, *117*, 9086–9139; b) G. Cera, L. Ackermann, *Top. Curr. Chem.* **2016***,* 57, 374.

[3] a) T. Jia, C. Zhao, R. He, H. Chen, C. Wang, *Angew. Chem. Int. Ed.* **2016**, *55*, 5268–5271; b) N. Kimura, T. Kochi, F. Kakiuchi, *J. Am. Chem. Soc.* **2017**, *139*, 14849–14852; c) N. Kimura, T. Kochi, F. Kakiuchi, *Asian J. Org. Chem*. **2019**, *8*, 1115–1117; d) A. M. Messinis, L. H. Finger, L. Hu, L. Ackermann, *J. Am. Chem. Soc*. **2020**, *142*, 13102–13111; e) A. M. Messinis, J. C. A. Oliveira, A. C. Stückl, L. Ackermann, *ACS Catal.* **2022**, *12*, 4947–4960; f) N. Kimura, S. Katta, Y. Kitazawa, T. Kochi, F. Kakiuchi, *J. Am. Chem. Soc.* **2021**, *143*, 4543–4549.

[4] For selected reviews/books about organomagnesium chemistry, see: a) J. F. Garst, M. P. Soriaga, *Coordination Chemistry Reviews,* **2004***, 248, 623–652*; b) The Chemistry of Organomagnesium Compounds, ed. Z. Rappoport and I. Marek, Patai Series, Wiley, Chichester, **2008**; c) D. Seyferth, *Organometallics* **2009**, *28*, 6, 1598–1605.

[5] a) M. M. Bagga, P. L. Pauson, F. J. Preston, R. I. Reed, *Chem. Commun.* **1965**, 543–544; b) G. Hata, H. Kondo, A. Miyake, *J. Am. Chem. Soc*. **1968**, *90*, 9,2278–2281; c) C. A. Tolman, S. D. Ittel, A. D. English, J. P. Jesson, *J. Am. Chem. Soc.* **1979**, *101*, 7, 1742–1751; d) M. V. Baker, L. D. Field, *J. Am. Chem. Soc*. **1986**, *108,* 23, 7433–7434; e) H.-F. Klein, S. Camadanli, R. Beck, D. Leukel, U. Flörke, *Angew. Chem. Int. Ed*. **2005**, *44*, 6, 975–977; f) S. Camadanli, R. Beck, U. Flörke, H.-F. Klein, *Organometallics* **2009**, *28*, 7, 2300–2310; g) L. Wang, H. Sun, X. Li, O. Fuhr, D. Fenske, *Dalton Trans*. **2016**, *45*, 18133–18141.

[6] Y. Kitazawa, T. Kochi, F. Kakiuchi, *J. Org. Chem*. **2023**, *88*, 3, 1890–1897.

[7] For selected examples: a) P. E. Baikie, O. S. Mills, *Chem. Commun*. **1966**, 707–708; b) M. M. Bagga, W. T. Flannigan, G. R. Knox, P. L. Pauson, F. J. Preston, R. I. Reed, *J. Chem. Soc. C* **1968**, 36–40; d) W. T. Flannigan, G. R.Knox, P. L. Pauson, *J. Chem. Soc. C* **1969**, 2077–2080.

[8] A. M. Messinis, T. von Münchow, M. Surke, L. Ackermann, *Nat. Catal*. **2024**, *7*, 273–284.

[9] For selected examples, see: a) D. Bourissou, O. Guerret, F. P. Gabbai, G. Bertrand, *Chem. Rev*. **2000**, *100*, 39–92; b) W. A. Herrmann, *Angew. Chem. Int. Ed.* **2002**, *41*, 1290–1309; c) X. Hu, Y. Tang, P. Gantzel, K. Meyer, *Organometallics* **2003**, *22*, 612–614; d) L. Cavallo, A. Correa, C.

Costabile, H. J. Jacobsen, *Organomet. Chem.* **2005**, *690*, 5407–5413; e) S. P. Nolan, N-Heterocyclic Carbenes in Synthesis; Wiley-VCH: Weinheim, Germany, **2006**; f) F. Glorius, N-Heterocyclic Carbenes in Transition-Metal Catalysis; Springer: New York, **2007**; Topics in Organometallic Chemistry 21; g) J. A. Mata, M. Poyatos, E. Peris, *Coord. Chem. Rev*. **2007**, *251*, 841–859; h) S. Dìez-Gonzalez, S. P. Nolan, *Coord. Chem. Rev*. **2007**, *251*, 874–883; i) E. A. B. Kantchev, C. J. O'Brien, M. G. Organ, *Angew. Chem. Int. Ed.* **2007**, *46*, 2768–2813; j) F. E. Hahn, M. C. Jahnke, *Angew. Chem., Int. Ed.* **2008**, *47*, 3122–3172; k) S. Würtz, F. Glorius, *Acc. Chem. Res.* **2008**, *41*, 1523–1533; l) H. Jacobsen, A. Correa, A. Poater, C. Costabile, L. Cavallo, *Coord. Chem. Rev*. **2009**, *253*, 687–703; m) S. Dìez-Gonzalez, N. Marion, S. P. Nolan, *Chem. Rev*. **2009**, *109*, 3612–3676; n) D. G. Gusev, *Organometallics* **2009**, 28, 6458–6461; o) H. Clavier, S. P. Nolan, *Chem. Commun*. **2010**, 841–861; p) T. Dröge, F. Glorius, *Angew. Chem. Int. Ed*. **2010**, *49*, 6940–6952.

[10] a) X. Hu, Y.J. Tang, P. Gantzel, K. Meyer, *Organometallics* **2003**, *22*, 612−614; b) X. Hu, I. Castro Rodriguez, K. Olsen, K. Meyer, *Organometallics* **2004**, *23*, 755− 764.

[11] D. Schmiel, H. Butenschön, *Organometallics* **2017**, *36*, 4979−4989.

[12] J. Loup, D. Zell, J. C. A. Oliveira, H. Keil, D. Stalke, L. Ackermann, *Angew. Chem. Int. Ed*. **2017**, *56*, 14197–14201.

[13] M.Y. Wong, T. Yamakawa, N. Yoshikai, *Org. Lett*. **2015**, *17*, 3, 442–445.

[14] Z.-J. Zhang, N. Jacob, S., Bhatia, P. Boos, X. Chen, J. C. DeMuth, A. M. Messinis, B. Bongsuiru Jei, J. C. A. Oliveira, A. Radović, M. L. Neidig, J. Wencel-Delord, L. Ackermann, *Nat. Commun*. **2024**, *15*, 3503.

[15] P. G. N. Neate, M. D. Greenhalgh, W. W. Brennessel, S. P. Thomas, M. L. Neidig, *Angew. Chem. Int. Ed*. **2020**, *59*, 17070–17076.

[16] R. B. Bedford, M. Betham, D. W. Bruce, A. A. Danopoulos, R. M. Frost, M. Hird, *J. Org. Chem.*, **2006**, *71*, 1104–1110.

[17] S. A. Cramer, D. M. Jenkins, *J. Am. Chem. Soc.* **2011**, *133*, 19342–19345.

[18] V. V. K. M. Kandepi, J. M. S. Cardoso, E. Peris, B. Royo, *Organometallics*, **2010**, *29*, 2777–2782.

[19] G. Hilt, P. Bolze, I. Kieltsch, *Chem. Comm*. **2005**, 1996–1998.

[20] J. Louie, R. H. Grubbs, *Chem. Comm.* **2000**, *16*, 1479–1480.

[21] W. Chen, Q. Chen, Y. Ma, X. Leng, S.-D. Bai, L. Deng, *Chin. Chem. Lett.* **2020**, *31*, 1342–1344.

5.5 Experimental Part

5.5.1 General remarks

Methods

All operations were conducted under an atmosphere of dry nitrogen using standard Schlenk techniques or in an MBraun nitrogen-filled glove box unless otherwise stated. Solvents used in catalysis and for synthesising organometallic reagents were dried using a solvent purification system (SPS) from Inert and degassed before use. All reactions were carried out in Schlenk tubes in a nitrogen-filled glove box, using pre-dried glassware. Column chromatography was performed on silica gel 60 (40-63 mesh). Melting points were measured with an Electrothermal apparatus and are uncorrected. NMR spectra were recorded on a Bruker 300 MHz or 400 MHz using solvents as internal standards (7.26 ppm for ^{1}H-NMR and 77.00 ppm for ^{13}C-NMR for $CDCl_3$). The terms m, s, d, t, q, and quint represent multiplet, singlet, doublet, triplet, quadruplet, and quintuplet respectively, and the term bs means a broad signal. Mass spectra were recorded in the ESI mode. Exact masses were recorded on a LTQ ORBITRAP XL Thermo Mass Spectrometer (ESI source).

Materials

All starting materials, reagents and solvents were purchased from commercial suppliers (Aldrich, Alfa, TCI, etc.) and used as supplied unless otherwise stated. Substrates **12,**[1] **14**,[2] **15** and **16**[3] were synthetized according to previously described methods. Tetrahydrofuran was dried over Na and distilled prior to use.

5.5.2 Synthesis of N-heterocyclic carbene ligands (NHCs)

General procedure A

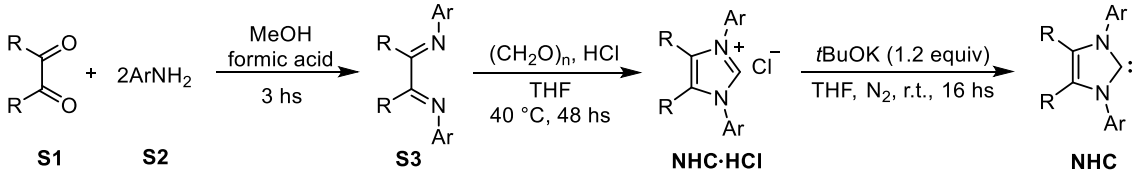

Step 1: **S1** (10 mmol, 1.0 equiv.) was added to a stirring solution of the appropriate aniline (2.0 equiv.) in methanol (1.2 M) at room temperature. Formic acid (5 drops) was then added, and the solution was stirred at room temperature for 3 hours. The resulting yellow precipitate was collected by filtration and washed with methanol (3×20 mL) and dried under vacuum to give the desired diazabutadienes **S3** as a solid. The product was used directly in the following step without further purification.

Step 2**:** Hydrochloric acid (4M in dioxane, 1.4 equiv.) and paraformaldehyde (1.0 equiv.) were stirred until complete dissolution of the white solid. THF (1 M) followed by **S3** (1.0 equiv.) were added slowly. The resulting solution was stirred at 40°C for 2 days. Then the suspension was cooled to room temperature and the white precipitate was collected by filtration, washed with THF and diethyl ether to afford **NHC•HCl**. The product was used directly in the following step without further purification.

Step 3: Into a nitrogen-filled glovebox, the corresponding **NHC•HCl** (1.0 equiv.) was loaded in a 10 mL vial and dissolved in anhydrous THF (0.1 M). To this solution was added *t*BuOK (1.2 equiv.) and the reaction was left to stir overnight at room temperature. The solution was then filtered through a celite pad into a Schlenk flask. The solvent was removed in vacuum until a solid appeared. The solid was transferred to a glass frit and washed with hexanes (3 x 10 mL) until the wash turned clear. The product was then dried in vacuo overnight to afford the desired free **NHC**.

1,3-Bis(2,4,6-trimethylphenyl)-1,3-dihydro-2*H*-imidazol-2-ylidene (IMes)

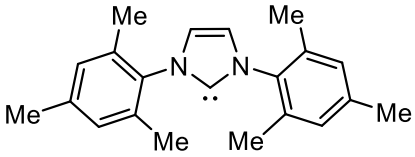

The title compound was obtained following general procedure **A**, starting from glyoxal and 1,3,5-trimethyl aniline. **IMes** carbene was obtained as an off-white solid (1.31 g, 43% yield). ^{1}H-NMR (400 MHz, C_6D_6): δ = 6.81 (s, 4H), 6.48 (s, 2H), 2.16 (s, 12H), 2.15 (s, 6H).

The spectroscopic data are in accordance with those reported in the literature.[4]

1,3-Bis-(2,6-diisopropylphenyl) 1,3-dihydro-2*H*-imidazol-2-ylidene (IPr)

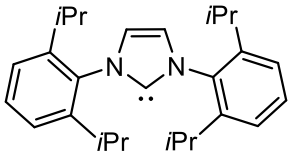

The title compound was obtained following general procedure **A**, starting from glyoxal and 1,5-diisopropyl aniline. **IPr** carbene was obtained as an off-white solid (3.36 g, 87%). ^{1}H-NMR (400 MHz, C_6D_6): δ = 7.40 (t, *J* = 7.6 Hz, 2H), 7.29 (d, *J* = 7.6 Hz, 4H), 6.71 (s, 2H), 3.06 (sept, *J* = 6.8 Hz, 4H), 1.41 (d, *J* = 6.8 Hz, 12H), 1.30 (d, *J* = 6.8 Hz, 12H).

The spectroscopic data are in accordance with those reported in the literature.[4]

1,3-Bis-(2,6-dimethylphenyl) 1,3-dihydro-2*H*-imidazol-2-ylidene (IXy)

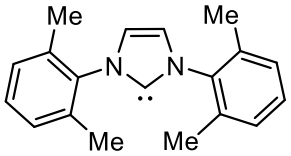

The title compound was obtained following general procedure **A**, starting from glyoxal and 1,5-dimethyl aniline. **IXy** carbene was obtained as an off-white solid (1.85 g, 67%). ^{1}H-NMR (400 MHz, C_6D_6): δ = 7.07 (m, 2H), 7.00 (d, *J* = 7.6 Hz, 4H), 6.46 (s, 2H), 2.07 (s, 12H).

The spectroscopic data are in accordance with those reported in the literature.[4]

1,3-di(2',4',6'-trimethylphenyl)-4,5-dimethyl-imidazol-2-ylidene

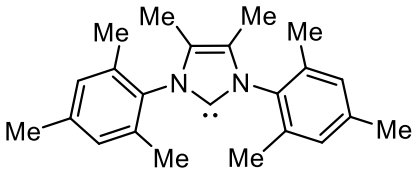

The title compound was obtained following general procedure **A**, starting from biacetyl and 1,3,5-trimethyl aniline. **^{Me}Mes** carbene was obtained as an off-white solid (1.91 g, 58% yield). ^{1}H-NMR (400 MHz, C_6D_6): δ = 6.84 (s, 4H), 2.18 (s, 6H), 2.15 (s, 12H), 1.65 (2, 6H).

The spectroscopic data are in accordance with those reported in literature.[5]

5.4.3 Synthesis of Iron(0)-NHC complexes

Fe(Mes)(η²-styr)₂

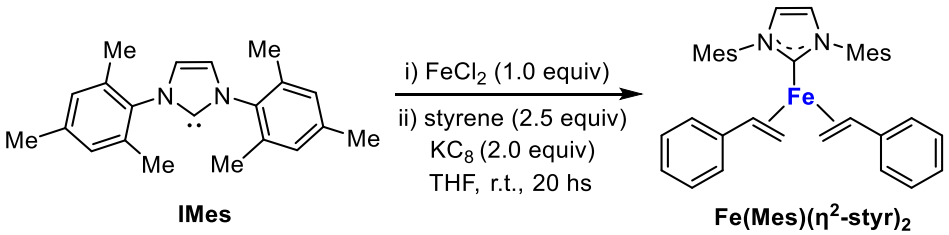

In a nitrogen-filled glove box, a 10 mL vial was loaded with a PTFE-coated stir bar and IMes (1.0 mmol, 304.4 mg). THF (5 mL) was added, followed by the addition of $FeCl_2$ (1.0 mmol, 126.7 mg) at room temperature. The reaction mixture was stirred at room temperature for 4 hs, and then styrene (2.5 mmol, 287 µL) and KC_8 (2.0 mmol, 270.3 mg) were added subsequently. After stirring at room temperature for 16 hs, the mixture was filtered on a celite pad to give a dark green solution. The solvent was removed in vacuum and the resultant dark green residue was suspended in *n*-pentane (10 mL). The solid was filtered, washed with fresh *n*-pentane (2 x 3 mL) and dried under vacuum. **Fe(Mes)(η²-styr)₂** was obtained as a dark green solid (273.1 mg, 48% yield). The analytical data are in accordance with those reported in literature.[6]

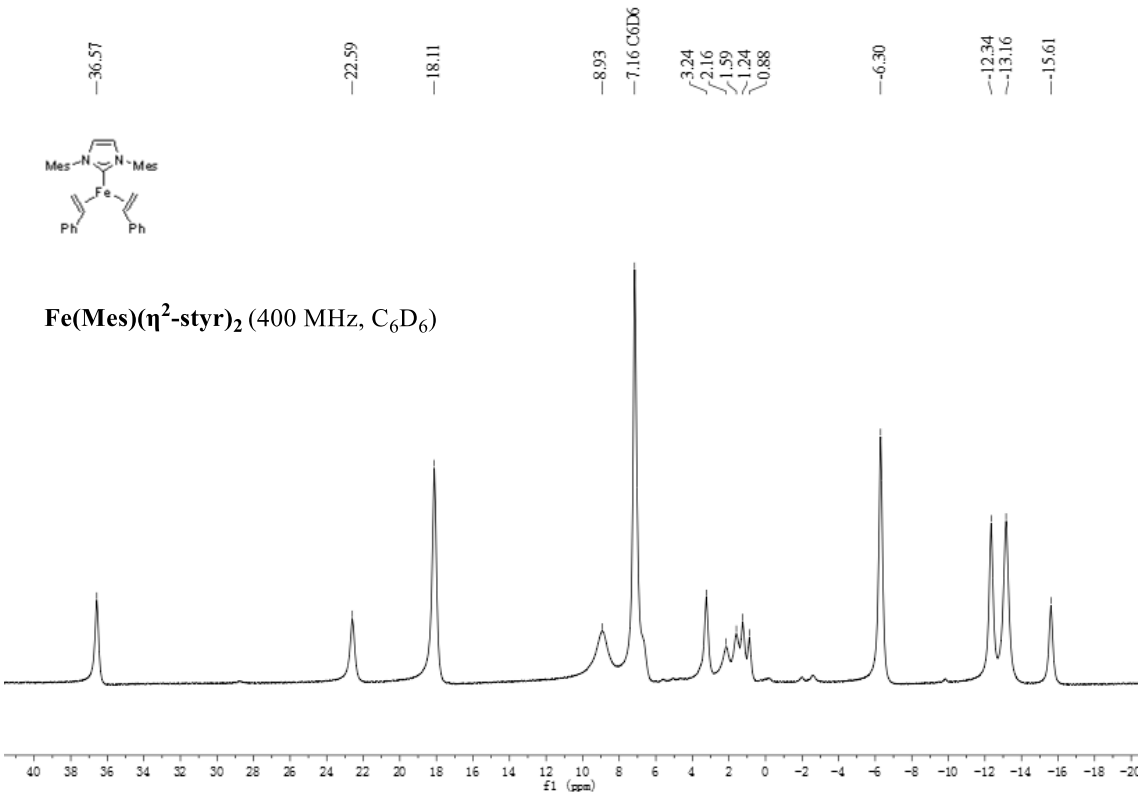

Fe(Mes)(η²-styr)₂ (400 MHz, C_6D_6)

Fe(Dipp)(η²-styr)₂

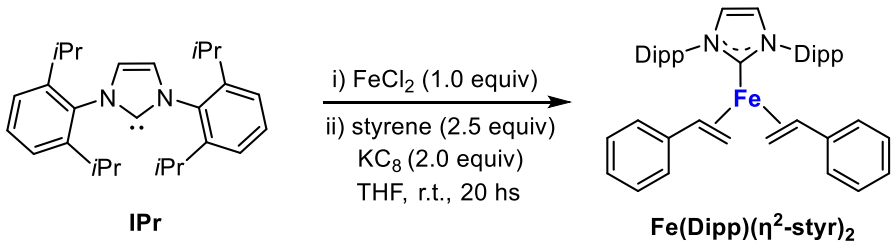

IPr **Fe(Dipp)(η²-styr)₂**

In a nitrogen-filled glove box, a 10 mL vial was loaded with a PTFE-coated stir bar and IPr (1.0 mmol, 388.6 mg). THF (5 mL) was added, followed by the addition of $FeCl_2$ (1.0 mmol, 126.7 mg) at room temperature. The reaction mixture was stirred at room temperature for 4 hs, and then styrene (2.5 mmol, 287 µL) and KC_8 (2.0 mmol, 270.3 mg) were added subsequently. After stirring at room temperature for 16 hs, the mixture was filtered on a celite pad to give a dark green solution. The solvent was removed in vacuum and the resultant dark green residue was suspended in *n*-pentane (10 mL). The solid was filtered, washed with fresh *n*-pentane (2 x 3 mL) and dried under vacuum. **Fe(Dipp)(η²-styr)₂** was obtained as a yellow-green solid (280.9 mg, 43% yield). The analytical data are in accordance with those reported in literature.[6]

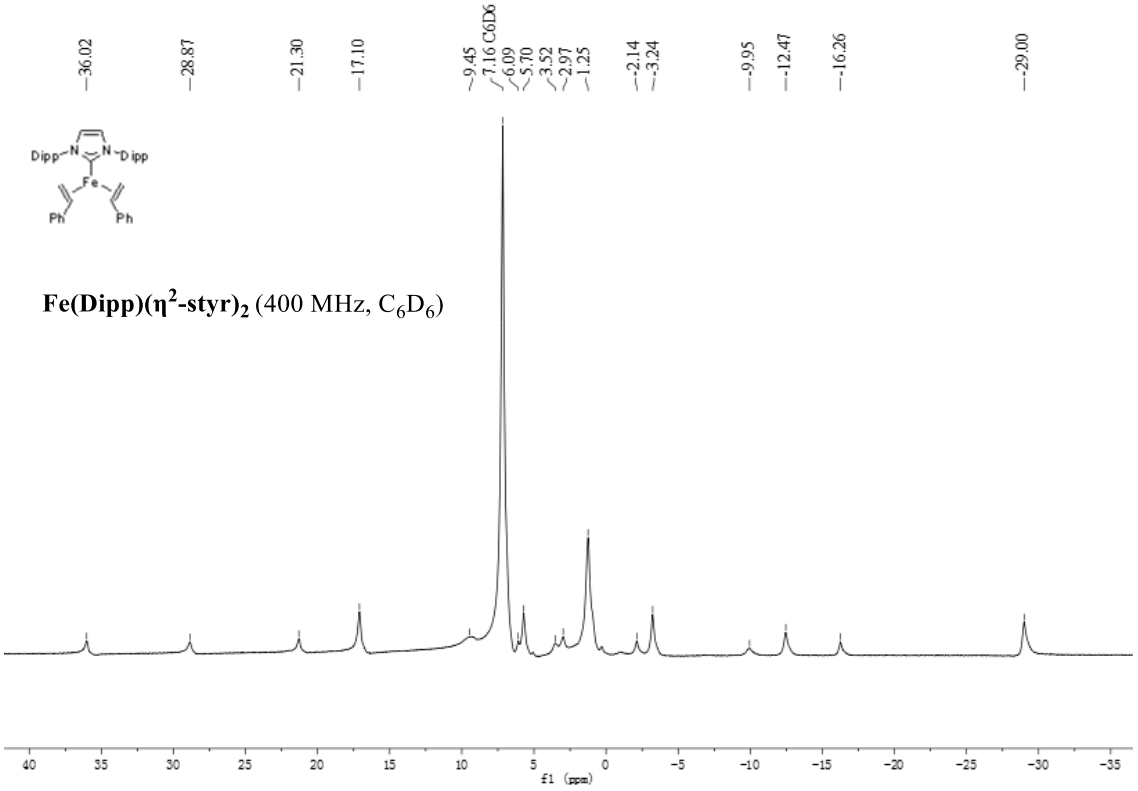

Fe(Dipp)(η²-styr)₂ (400 MHz, C_6D_6)

Fe(Xyl)(η²-styr)₂

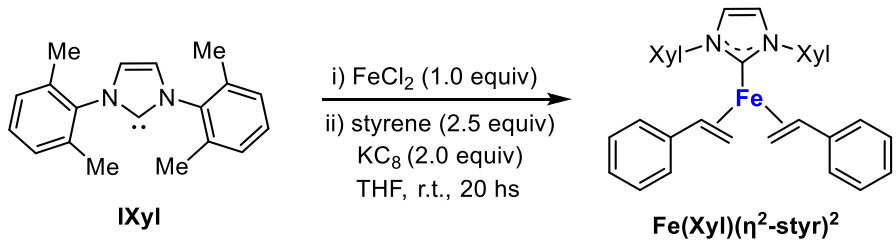

In a nitrogen-filled glove box, a 10 mL vial was loaded with a PTFE-coated stir bar and IXyl (1.0 mmol, 276.4 mg). THF (5 mL) was added, followed by the addition of $FeCl_2$ (1.0 mmol, 126.7 mg) at room temperature. The reaction mixture was stirred at room temperature for 4 hs, and then styrene (2.5 mmol, 287 µL) and KC_8 (2.0 mmol, 270.3 mg) were added subsequently. After stirring at room temperature for 16 hs, the mixture was filtered on a celite pad to give a dark green solution. The solvent was removed in vacuum and the resultant dark green residue was suspended in *n*-pentane (10 mL). The solid was filtered, washed with fresh *n*-pentane (2 x 3 mL) and dried under vacuum. **Fe(Xyl)(η²-styr)₂** was obtained as a dark green solid (298.7 mg, 55% yield).
The analytical data are in accordance with those reported in literature.[6]

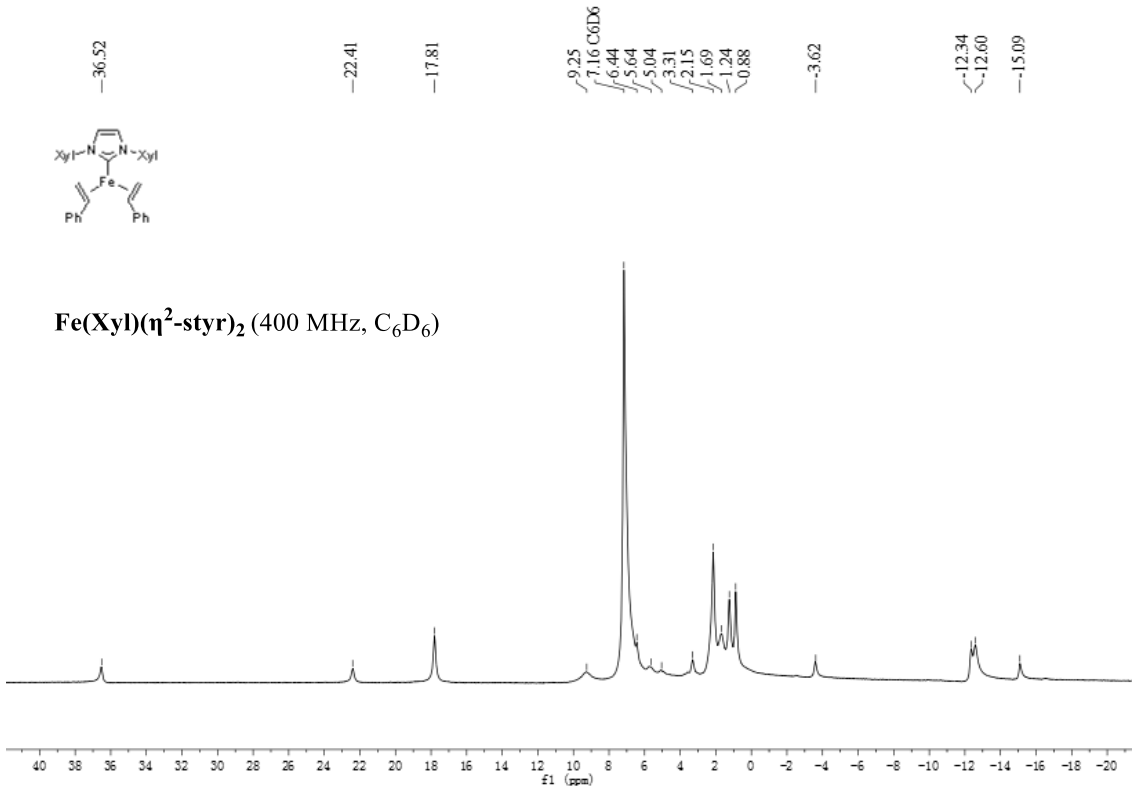

Fe(Xyl)(η²-styr)₂ (400 MHz, C_6D_6)

Fe(^{Me}Mes)(η^2-styr)$_2$

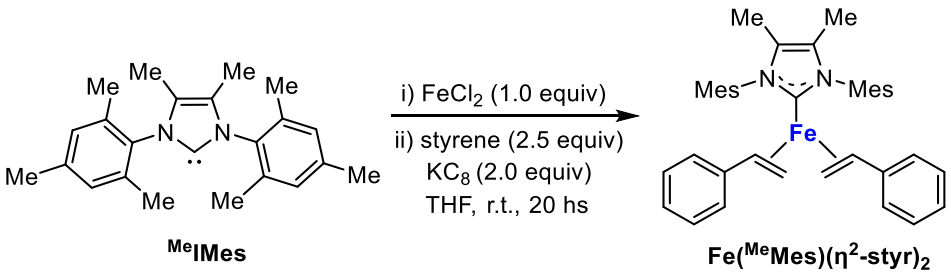

^{Me}IMes — Fe(^{Me}Mes)(η^2-styr)$_2$

In a nitrogen-filled glove box, a 10 mL vial was loaded with a PTFE-coated stir bar and IMes^{Me} (1.0 mmol, 332.5 mg). THF (5 mL) was added, followed by the addition of $FeCl_2$ (1.0 mmol, 126.7 mg) at room temperature. The reaction mixture was stirred at room temperature for 4 hs, and then styrene (2.5 mmol, 287 µL) and KC_8 (2.0 mmol, 270.3 mg) were added subsequently. After stirring at room temperature for 16 hs, the mixture was filtered on a celite pad to give a dark green solution. The solvent was removed in vacuum and the resultant dark green residue was suspended in *n*-pentane (10 mL). The solid was filtered, washed with fresh *n*-pentane (2 x 3 mL) and dried under vacuum. **Fe(^{Me}Mes)(η^2-styr)$_2$** was obtained as a brown solid (341.2 mg, 57% yield).

The analytical data are in accordance with those reported in literature.[6]

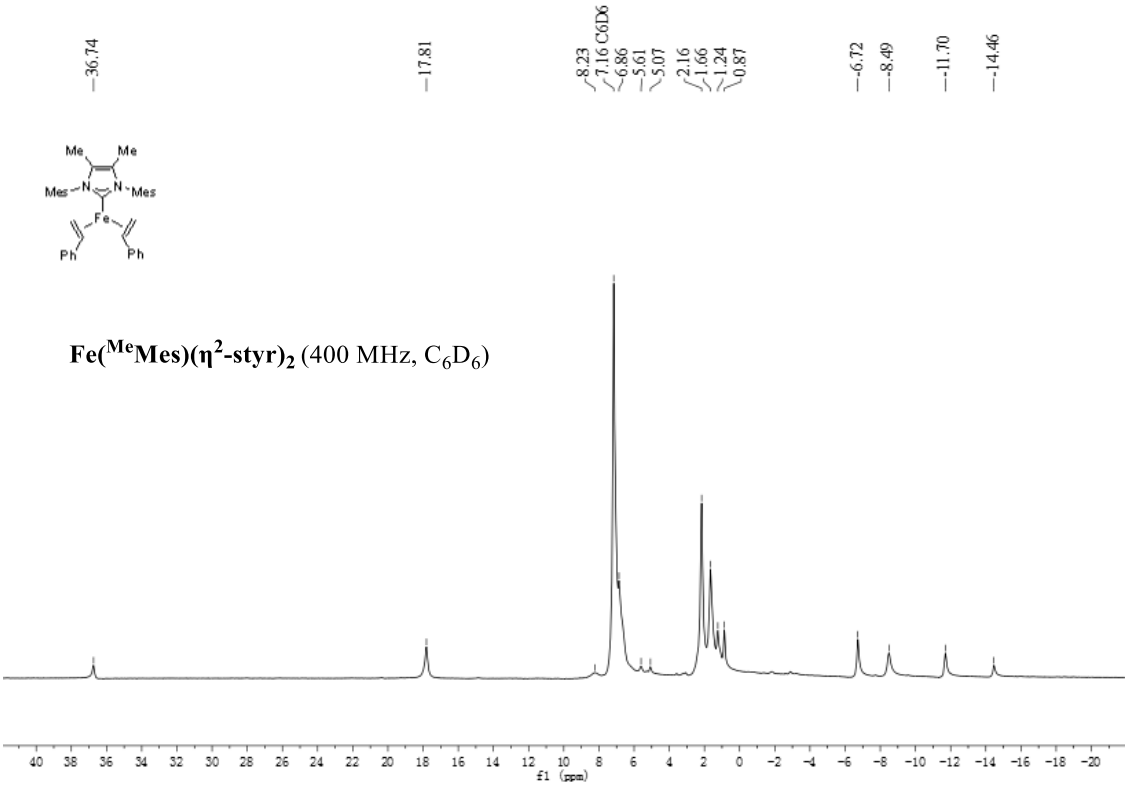

Fe(^{Me}Mes)(η^2-styr)$_2$ (400 MHz, C_6D_6)

Fe(SXyl)(η^2-styr)$_2$

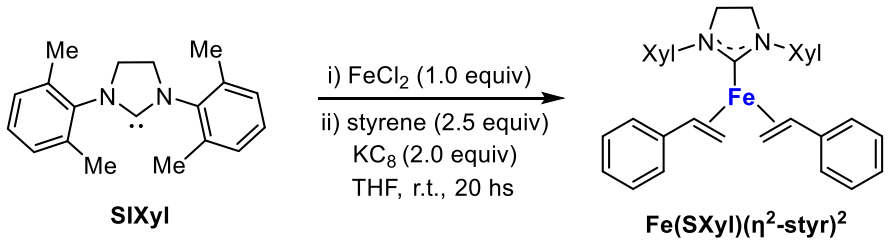

In a nitrogen-filled glove box, a 10 mL vial was loaded with a PTFE-coated stir bar and SIXyl (1.0 mmol, 278.4 mg). THF (5 mL) was added, followed by the addition of $FeCl_2$ (1.0 mmol, 126.7 mg) at room temperature. The reaction mixture was stirred at room temperature for 4 hs, and then styrene (2.5 mmol, 287 µL) and KC_8 (2.0 mmol, 270.3 mg) were added subsequently. After stirring at room temperature for 16 hs, the mixture was filtered on a celite pad to give a dark green solution. The solvent was removed in vacuum and the resultant dark green residue was suspended in *n*-pentane (10 mL). The solid was filtered, washed with fresh *n*-pentane (2 x 3 mL) and dried under vacuum. **Fe(SXyl)(η^2-styr)$_2$** was obtained as a dark green solid (240.3 mg, 44% yield).

The analytical data are in accordance with those reported in literature.[6]

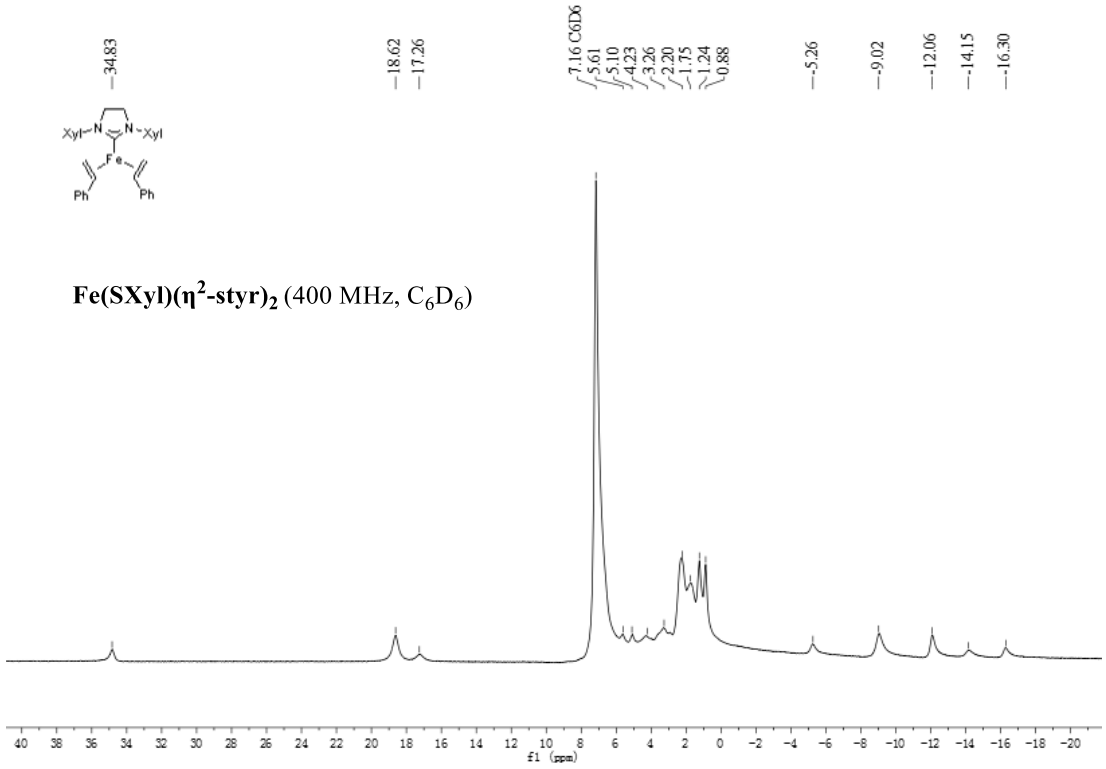

Fe(SXyl)(η^2-styr)$_2$ (400 MHz, C_6D_6)

Fe(SMes)(η^2-styr)$_2$

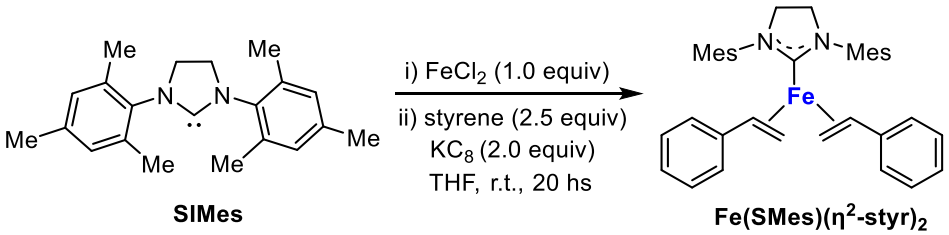

In a nitrogen-filled glove box, a 10 mL vial was loaded with a PTFE-coated stir bar and SIMes (1.0 mmol, 306.5 mg). THF (5 mL) was added, followed by the addition of $FeCl_2$ (1.0 mmol, 126.7 mg) at room temperature. The reaction mixture was stirred at room temperature for 4 hs, and then styrene (2.5 mmol, 287 µL) and KC_8 (2.0 mmol, 270.3 mg) were added subsequently. After stirring at room temperature for 16 hs, the mixture was filtered on a celite pad to give a dark green solution. The solvent was removed in vacuum and the resultant dark green residue was suspended in *n*-pentane (10 mL). The solid was filtered, washed with fresh *n*-pentane (2 x 3 mL) and dried under vacuum. **Fe(SXyl)(η^2-styr)$_2$** was obtained as a dark green solid (233.1 mg, 41% yield).

The analytical data are in accordance with those reported in literature.[6]

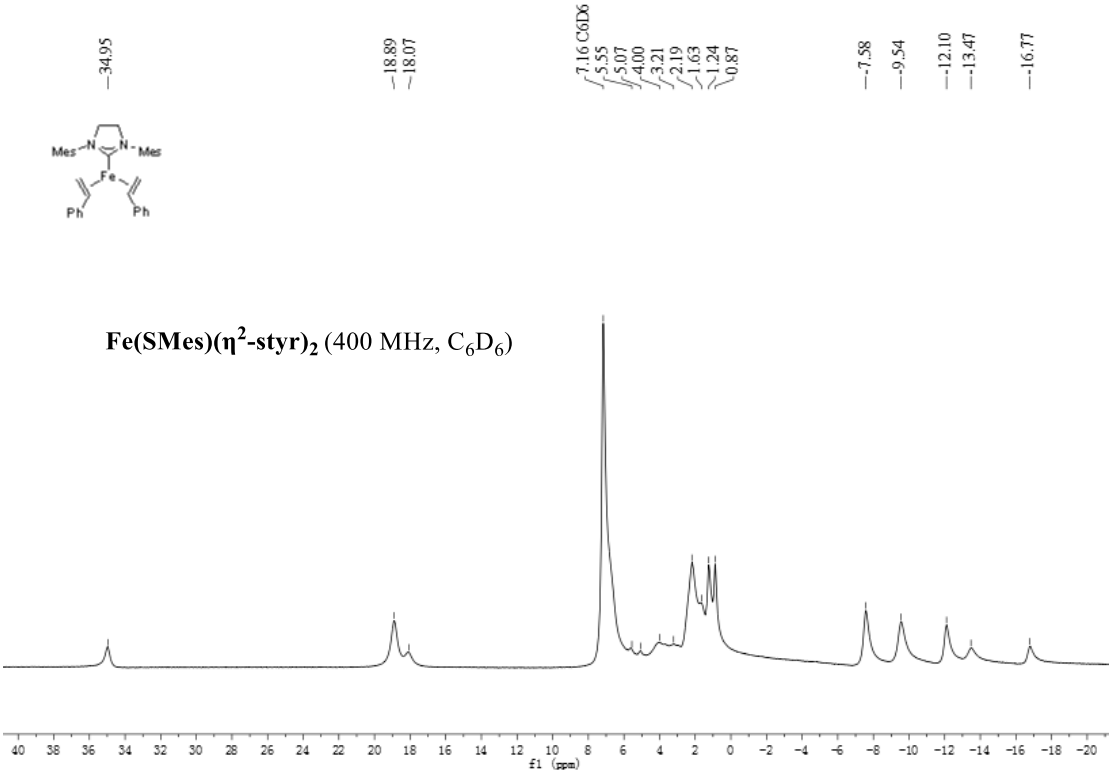

Fe(Mes)(dvtms)

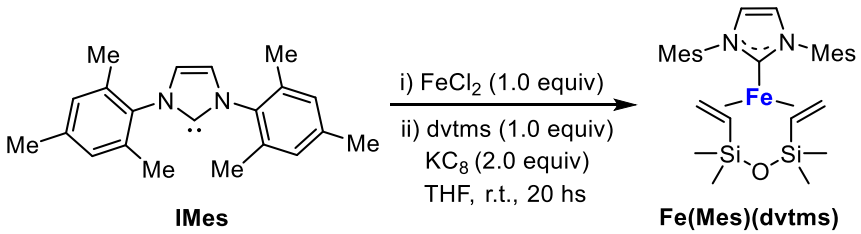

In a nitrogen-filled glove box, a 10 mL vial was loaded with a PTFE-coated stir bar and IMes (1.0 mmol, 304.4 mg). THF (5 mL) was added, followed by the addition of $FeCl_2$ (1.0 mmol, 126.7 mg) at room temperature. The reaction mixture was stirred at room temperature for 4 hs, and then 1,1,3,3-tetramethyl-1,3-divinyldisiloxane (1.0 mmol, 230 µL) and KC_8 (2.0 mmol, 270.3 mg) were added subsequently. After stirring at room temperature for 16 hs, the mixture was filtered on a celite pad to give a dark green solution. The solvent was removed in vacuum and the resultant dark green residue was suspended in *n*-pentane (10 mL). The solid was filtered, washed with fresh *n*-pentane (2 x 3 mL) and dried under vacuum. **Fe(Mes)(dvtms)** was obtained as a dark green solid (431.6 mg, 79% yield).

The analytical data are in accordance with those reported in literature.[7]

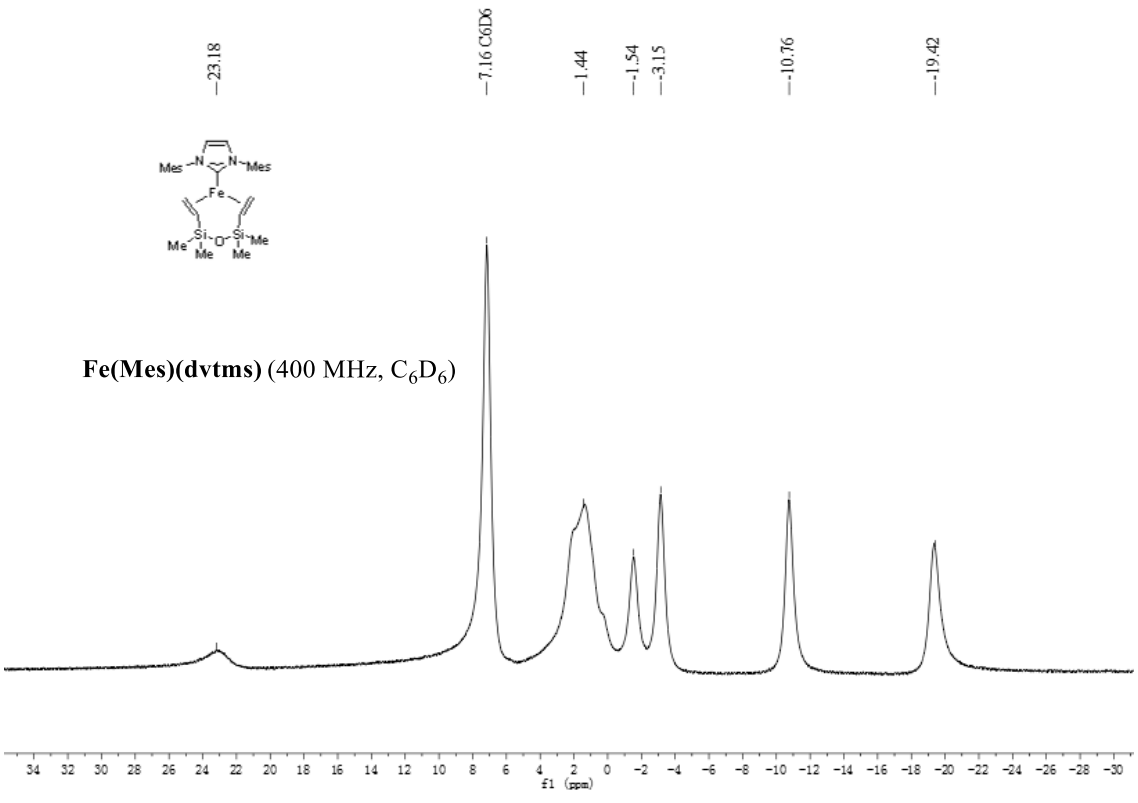

5.5.4 Synthesis and Characterization of Indole substrates

General procedure B

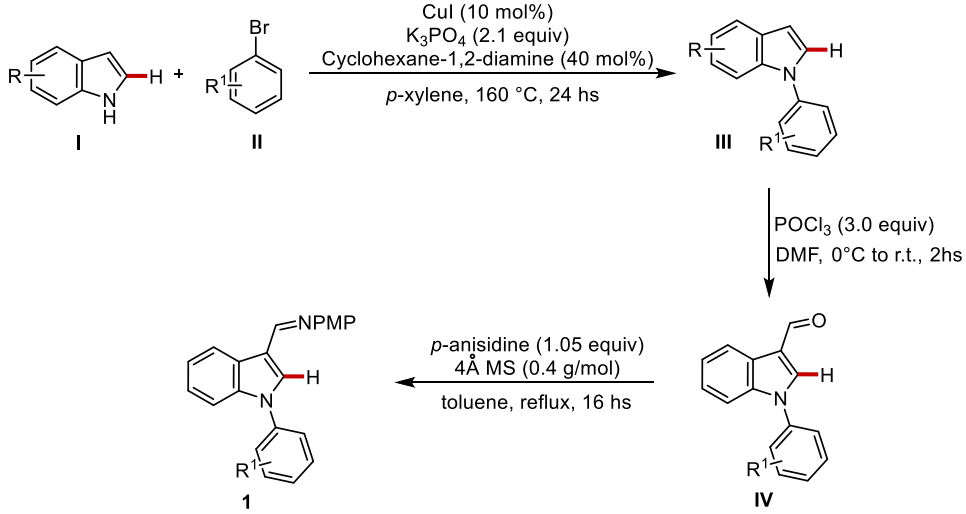

Step 1: To a Schlenk flask indole derivative **I** (1.0 equiv., 10.0 mmol), CuI (10 mol%., 1.0 mmol, 189.8 mg) and potassium phosphate (2.1 equiv., 21.0 mmol, 4.45 g) were added. The flask was evacuated and refilled with nitrogen three times. Subsequently, the corresponding aryl bromide **II** (1.5 equiv., 15.0 mmol), cyclohexane-1,2-diamine (40 mol%, 4.0 mmol) and *p*-xylene (0.8 M, 12.5 mL) were added. The mixture was heated to 160 °C and stirred for 24 hours. After cooling to room temperature, the mixture was quenched with saturated NH_4Cl aqueous solution. The resulting solution was extracted with ethyl acetate (2x50 mL) and the combined organic layers were dried over Na_2SO_4, filtered and concentrated under reduced pressure. The residue was purified by column chromatography on silica gel (*n*-hexane/dichloromethane) to afford the desired product **III**.

Step 2: To a stirred solution of indole derivative **III** in DMF (0.1 M) was added $POCl_3$ (3.0 equiv., 30.0 mmol) dropwise at 0 °C. The resulting mixture was stirred for 2 hours at room temperature. After completion, the reaction mixture was carefully quenched with a mixture of ice and water. Then, NaOH pellets were added until reaching pH 8-9. Et_2O was added and the phases were separated. The aqueous phase was extracted (3x50 mL) with Et_2O and the combined organic layers were washed with water (4x50 mL), dried over Na_2SO_4, filtered and concentrated under reduced pressure. The crude aldehyde **IV** was directly used in the next step without further purification.

Step 3: In a flame-dried round bottom flask under nitrogen, were added aldehyde **IV**, *p*-anisidine (1.05 equiv., 10.5 mmol) and 4Å molecular sieves (0.4 g/mmol). Then, dry toluene (0.5 M) was added and the reaction mixture was refluxed for 16 hours. After completion of the reaction, the

reaction mixture was cooled to room temperature, filtered through a celite pad (eluted with EtOAc) and concentrated under reduced pressure. The residue was purified by recrystallization (*n*-hexane/EtOAc) or flash chromatography on silica gel (*n*-hexane/EtOAc = 10:1 with 0.5 v% NEt_3) to afford desired product **1**.

General procedure C

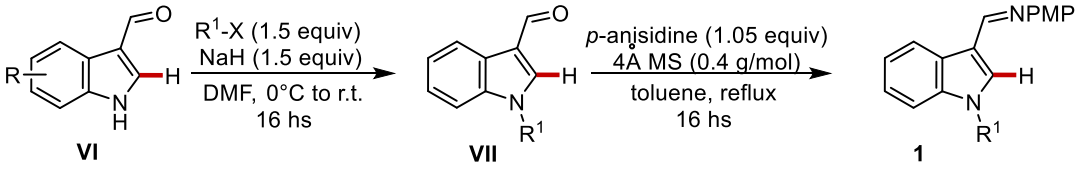

Step 1: In a flame-dried round bottom flask under nitrogen, sodium hydride (1.5 equiv.) was added to a solution of 1*H*-indole-3-carbaldehyde **VI** (10 mmol, 1.0 equiv.) in DMF (1.2 M) at 0 °C. The corresponding alkyl halyde R^1-X (1.5 equiv.) was then added dropwise and the resulting mixture was stirred at room temperature for 12 hs. The reaction was quenched by the addition of water at 0 °C, and the resulting mixture was extracted with EtOAc (3 x 20 mL). The combined organic layer were dried over Na_2SO_4 and concentrated under reduced pressure. Purification of the crude product by silica gel chromatography (hexane/EtOAc) afforded the desired compound **VII**.

Step 1: In a flame-dried round bottom flask under nitrogen, were added aldehyde **VII**, *p*-anisidine (1.05 equiv.) and 4Å molecular sieves (0.4 g/mmol). Then, dry toluene (0.5 M) was added, and the reaction mixture was refluxed for 16 hours. After completion of the reaction, the reaction mixture was cooled to room temperature, filtered through a celite pad (eluted with EtOAc) and concentrated under reduced pressure. The residue was purified by recrystallization (*n*-hexane/ EtOAc) or flash chromatography on silica gel (*n*-hexane/EtOAc = 10:1 with 0.5 v% NEt_3) to afford desired product **1**.

(*E*)-1-[1-(2-Isopropylphenyl)-1*H*-indol-3-yl]-*N*-(4-methoxyphenyl)methanimine (1b)

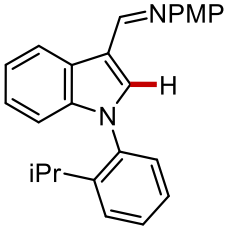

The general procedure **B** was followed using 1*H*-indole (10.0 mmol, 1.17 g) and 1-bromo-2-isopropylbenzene (15.0 mmol, 2.97 g) to afford **1b** (2.14 g, 58% yield over 3 steps) as a white solid. ^{1}H-NMR (300 MHz, $CDCl_3$): δ = 8.75 (s, 1H), 8.57 (d, *J* = 7.7 Hz, 1H), 7.58 (s, 1H), 7.55 – 7.43 (m, 2H), 7.39 – 7.20 (m, 6H), 7.04 (d, *J* = 7.9 Hz, 1H), 6.96 (d, *J* = 8.8 Hz, 2H), 3.83 (s, 3H), 2.70 (hept, *J* = 6.9 Hz, 1H), 1.14 (d, *J* = 6.9 Hz, 3H), 1.11 (d, *J* = 6.9 Hz, 3H).

The spectroscopic data are in accordance with those reported in literature.[8]

(*E*)-*N*-(4-Methoxyphenyl)-1-(1-(naphthalen-1-yl)-1*H*-indol-3-yl)methanimine (1c)

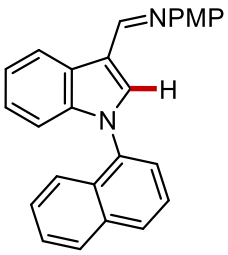

The general procedure **B** was followed using 1*H*-indole (10.0 mmol, 1.17 g) and 1bromonaphthalene (15.0 mmol, 3.09 g) to afford 1g (2.82 g, 75% yield over 3 steps) as a white solid. ^{1}H-NMR (400 MHz, $CDCl_3$) δ 8.73 (s, 1H), 8.65 (d, J = 7.9 Hz, 1H), 7.96 (t, J = 7.3 Hz, 2H), 7.71 (s, 1H), 7.61 – 7.49 (m, 3H), 7.46 – 7.36 (m, 2H), 7.32 (ddd, J = 8.1, 7.0, 1.0 Hz, 1H), 7.27 (d, J = 8.8 Hz, 2H), 7.24 – 7.15 (m, 1H), 6.99 (d, J = 8.2 Hz, 1H), 6.94 (d, J = 8.8 Hz, 2H), 3.81 (s, 3H).

The NMR data are consistent with the reported literatures.[8]

(E)-N-((1-(but-3-en-1-yl)-1H-indol-3-yl)methylene)-4- methoxyaniline (1d).

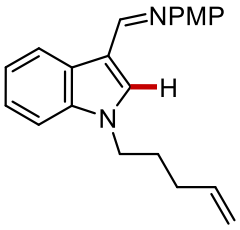

The general procedure **C** was followed using 1*H*-indole-3-carbaldehyde (10.0 mmol, 1.45 g) and 5-bromo-1-butene (15.0 mmol, 2.0 g) to afford **1b** (2.67 g, 84% yield over 2 steps) as a yellow oil. ^{1}H-NMR (400 MHz, $CDCl_3$): δ = 8.64 (s, 1 H), 8.47-8.45 (m, 1 H), 7.55 (s, 1 H), 7.37-7.35 (m, 1 H), 7.32-7.27 (m, 2 H), 7.22 (app. d, J = 8.8 Hz, 2 H), 6.93 (app. d, J = 8.9 Hz, 2 H), 5.83-5.77 (m, 1 H), 5.08-5.03 (m, 2 H), 4.16 (t, J = 7.0 Hz, 2 H), 3.83 (s, 3 H), 2.13-2.07 (m, 2 H), 2.02-1.96 (m, 2 H).

The NMR data are consistent with the reported literatures.[9]

1-(1H-indol-1-yl)isoquinoline (6)

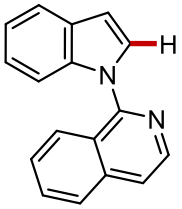

The general procedure **B** *Step 1* was followed using 1*H*-indole (10.0 mmol, 1.17 g) and 1-bromoisoquinoline (15.0 mmol, 3.12 g) to afford 1g (2.00 g, 82%) as a yellow solid. ^{1}H-NMR (400 MHz, $CDCl_3$) δ 8.51 (d, J = 5.3 Hz, 1H), 7.94 (d, J = 8.0 Hz, 2H), 7.79–7.47 (m, 5H), 7.36 (s, 1H), 7.24–7.14 (m, 2H), 6.80 (s, 1H).

The NMR data are consistent with the reported literatures.[10]

(*E*)-1-(6-Chloro-1-methyl-1*H*-indol-3-yl)-*N*-(4- methoxyphenyl)methanimine (1e)

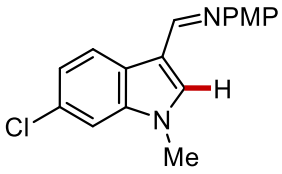

The general procedure **B** was followed using 6-chloro-1*H*-indole-3-carbaldehyde (10.0 mmol, 1.79 g) and iodomethane (15.0 mmol, 2.12 g) to afford **1e** (2.00 g, 67% yield over 2 steps) as a yellow solid. ^{1}H-NMR (400 MHz, $CDCl_3$) δ = 8.60 (s, 1H), 8.45 (dd, *J* = 8.5, 0.5 Hz, 1H), 7.45 (s, 1H), 7.35 (dd, *J* = 1.8, 0.6 Hz, 1H), 7.29 – 7.27 (m, 1H), 7.26 – 7.22 (m, 2H), 6.98 – 6.93 (m, 2H), 3.86 (s, 3H), 3.80 (s, 3H).

The spectroscopic data are in accordance with those reported in literature.[11]

Methyl (*E*)-3-[((4-methoxyphenyl)imino)methyl]-1-methyl-1*H*-indole-6-carboxylate (1f)

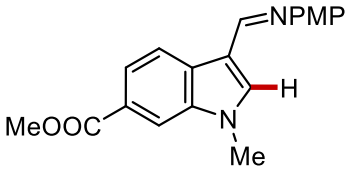

The general procedure **B** was followed using 3-formyl-1*H*-indole-6-carboxylic acid (10.0 mmol, 1.8 g) and iodomethane (15.0 mmol, 2.12 g) to afford **1e** (1.74 g, 54% yield over 2 steps) as a white solid. ^{1}H-NMR (400 MHz, $CDCl_3$) δ = 8.67 (s, 1H), 8.50 (dd, *J* = 8.4, 0.7 Hz, 1H), 8.15 (dd, *J* = 1.5, 0.7 Hz, 1H), 7.99 (dd, *J* = 8.4, 1.4 Hz, 1H), 7.70 (s, 1H), 7.29 – 7.23 (m, 2H), 7.00 – 6.91 (m, 2H), 3.99 (s, 3H), 3.94 (s, 3H), 3.86 (s, 3H).

The spectroscopic data are in accordance with those reported in literature.[11]

(*E*)-1-(5-Isocyano-1-methyl-1*H*-indol-3-yl)-N-(4-methoxyphenyl)methanimine (1g)

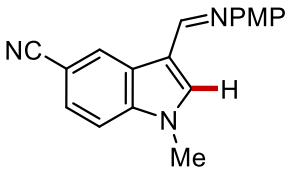

The general procedure **B** was followed using 3-formyl-1*H*-indole-5-carbonitrile (10.0 mmol, 1.70 g) and iodomethane (15.0 mmol, 2.12 g) to afford **1g** (1.85 g, 64% yield over 2 steps) as a pale-yellow solid. ^{1}H-NMR (400 MHz, $CDCl_3$) δ = 8.96 (dd, *J* = 1.6, 0.7 Hz, 1H), 8.63 (s, 1H), 7.63 – 7.51 (m, 2H), 7.41 (dd, *J* = 8.6, 0.7 Hz, 1H), 7.31 – 7.20 (m, 2H), 7.05 – 6.92 (m, 2H), 3.90 (s, 3H), 3.87 (s, 3H).

The spectroscopic data are in accordance with those reported in literature.[11]

5.5.5 Three-coordinate iron(0) complex-catalyzed regioselective C–H alkylation of indole derivatives with aryl alkenes

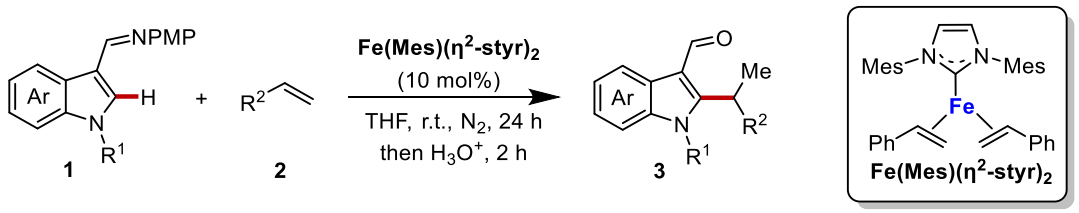

To a flame-dried and N2-purged Schlenk tube were added indole substrate **1** (0.1 mmol) and **Fe(Mes)(η^2-styr)$_2$** (10 mol%, 0.01 mmol, 5.7 mg) in the glove box. Alkene substrate **2** (0.15 mmol) and tetrahydrofuran (0.3 mL) were added *via* syringe. The Schlenk tube was taken out of the glove box and the resulting mixture was stirred at room temperature for 24 hours. Then, the reaction mixture was diluted with tetrahydrofuran (2.0 mL) and quenched with HCl aqueous solution (1 M, 1.0 mL). The resulting mixture was stirred at room temperature for 2 hours. The phases were then separated, the aqueous layer was extracted with ethyl acetate (5.0 mL ×3). The combined organic layer was washed with brine, dried over Na_2SO_4, filtered and concentrated *in vacuo*. The linear and branch ratio was determined by ^{1}H-NMR analysis of the crude reaction mixture. The residue was purified by column chromatography on silica gel (*n*-hexane: ethyl acetate = 5:1) to afford the desired product **3**.

5.5.6 Three-coordinate iron(0) complex-catalyzed regioselective C–H alkylation of indole derivatives with vinyl silanes

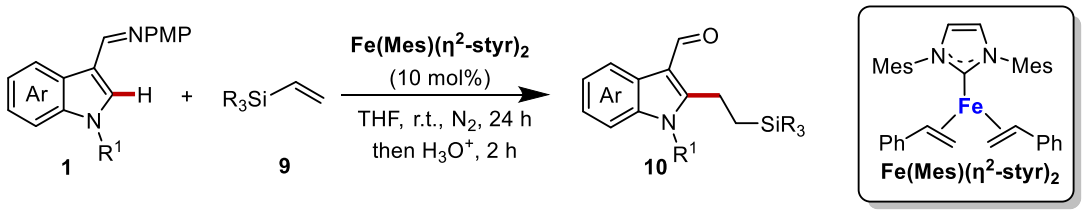

To a flame-dried and N2-purged Schlenk tube were added indole substrate **1** (0.1 mmol) and **Fe(Mes)(η^2-styr)$_2$** (10 mol%, 0.01 mmol, 5.7 mg) in the glove box. Vinyl silane **9** (0.15 mmol) and tetrahydrofuran (0.3 mL) were added *via* syringe. The Schlenk tube was taken out of the glove box and the resulting mixture was stirred at 60 °C for 24 hours. Then, the reaction mixture was diluted with tetrahydrofuran (2.0 mL) and quenched with HCl aqueous solution (1 M, 1.0 mL). The resulting mixture was stirred at room temperature for 2 hours. The phases were then separated, the aqueous layer was extracted with ethyl acetate (5.0 mL ×3). The combined organic layer was washed with brine, dried over Na_2SO_4, filtered and concentrated *in vacuo*. The linear and branch ratio was determined by ^{1}H-NMR analysis of the crude reaction mixture. The residue was purified by column chromatography on silica gel (*n*-hexane: ethyl acetate = 10:1) to afford the desired product **10**.

5.5.7 Characterization Data of Products

1-Methyl-2-(1-phenylethyl)-1*H*-indole-3-carbaldehyde (3aa)

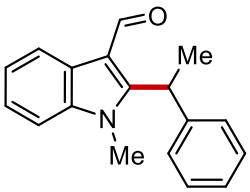

The general procedure was followed using indole substrate **1a** (0.1 mmol, 26.4 mg) and styrene **2a** (0.15 mmol, 17 µL). Purification by column chromatography on silica gel (n-hexane/EtOAc 5:1) yielded **3aa** as a pale-yellow solid (21.1 mg, 80% yield). M.p.: 94-96 °C. ^{1}H-NMR (300 MHz, $CDCl_3$): δ = 10.26 (s, 1H), 8.47 – 8.26 (m, 1H), 7.39 – 7.15 (m, 8H), 5.21 (q, *J* = 7.4 Hz, 1H), 3.44 (s, 3H), 1.87 (d, *J* = 7.4 Hz, 3H). ^{13}C-NMR (75 MHz, $CDCl_3$): δ = 184.9 (CH), 153.6 (C_q), 141.1 (C_q), 137.5 (C_q), 129.0 (CH), 127.1 (CH), 127.0 (CH), 125.9 (C_q), 123.5 (CH), 123.1 (CH), 121.5 (CH), 114.7 (C_q), 109.4 (CH), 34.6 (CH_3), 31.3 (CH), 18.7 (CH_3). HRMS (ESI) m/z calcd for $C_{18}H_{18}NO$ $[M+H]^+$ 264.1383, found: 264.1383.

The analytical data are in accordance with those reported in literature.[12]

(2-Isopropylphenyl)-2-(1-phenylethyl)-1H-indole-3-carbaldehyde (3ba)

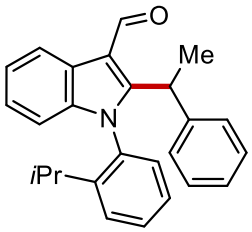

The general procedure **1** was followed using indole substrate **1b** (0.1 mmol, 36.8 mg) and styrene **2a** (0.15 mmol, 17 µL). Purification by column chromatography on silica gel (n-hexane/EtOAc 5:1) yielded **3ba** (18.4 mg, 50% yield, >95:5 d.r.) as a white solid. M.p.: 137-139 °C. ^{1}H-NMR (400 MHz, $CDCl_3$): δ = 10.25 (s, 1H), 8.43 (d, J = 7.9 Hz, 1H), 7.66 – 7.49 (m, 2H), 7.39 – 7.14 (m, 8H), 7.06 (d, J = 7.8 Hz, 1H), 6.80 (d, J = 8.1 Hz, 1H), 4.20 (q, J = 7.4 Hz, 1H), 2.47 (hept, J = 6.9 Hz, 1H), 1.88 (d, J = 7.4 Hz, 3H), 1.21 (d, J = 6.9 Hz, 3H), 1.06 (d, J = 6.8 Hz, 3H). ^{13}C-NMR (101 MHz, $CDCl_3$): δ = 186.4 (CH), 154.9 (C_q), 148.0 (C_q), 142.9 (C_q), 138.4 (C_q), 133.3 (C_q), 130.6 (CH), 129.5 (CH), 128.8 (CH), 127.5 (CH), 127.3 (CH), 127.2 (CH), 126.9 (CH), 126.0 (C_q), 123.8 (CH), 123.6 (CH), 122.2 (CH), 114.9 (C_q), 111.3 (CH), 37.1 (CH), 28.0 (CH), 24.8 (CH_3), 23.8 (CH_3), 22.7 (CH_3).

The NMR data are consistent with the reported literatures.[8]

1-Methyl-2-(2-(triphenylsilyl)ethyl)-1*H*-indole-3-carbaldehyde (10aa)

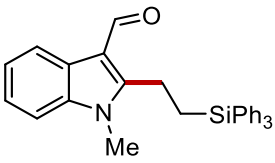

The general procedure **2** was followed using indole substrate **1a** (0.1 mmol, 26.4 mg) and triphenyl(vinyl)silane (**9a**) (0.15 mmol, 43.0 mL). Purification by column chromatography on silica gel (n-hexane/EtOAc 5:1) yielded **10aa** (28.9 mg, 65% yield) as a white solid. M.p.: 180-182 °C. ^{1}H-NMR (300 MHz, $CDCl_3$): δ = 10.01 (s, 1H), 8.30 – 8.17 (m, 1H), 7.70 – 7.53 (m, 6H), 7.51 – 7.33 (m, 9H), 7.31 – 7.16 (m, 3H), 3.51 (s, 3H), 3.19 – 3.08 (m, 2H), 1.82 – 1.64 (m, 2H). ^{13}C-NMR (75 MHz, $CDCl_3$): δ = 184.0 (CH), 153.9 (C_q), 137.2 (C_q), 135.7 (CH), 133.9 (C_q), 130.1 (CH), 128.4 (CH), 125.9 (C_q), 123.3 (CH), 123.0 (CH), 121.2 (CH), 113.1 (C_q), 109.4 (CH), 29.6 (CH_3), 19.2 (CH_2), 15.2 (CH_2). HRMS (ESI) m/z calcd for $C_{30}H_{28}NOSi$ $[M+H]^+$ 446.1935, found: 446.1931.

6-Chloro-1-methyl-2-(1-phenylethyl)-1*H*-indole-3-carbaldehyde (3ea)

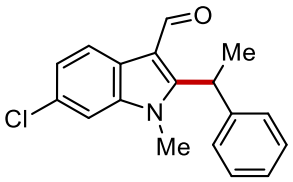

The general procedure **1** was followed using indole substrate **1e** (0.1 mmol, 29.8 mg) and styrene **2a** (0.15 mmol, 17 µL). Purification by column chromatography on silica gel (n-hexane/EtOAc 5:1) yielded **3ea** (21.2 mg, 71% yield) as a colourless oil. ^{1}H-NMR (300 MHz, $CDCl_3$); δ = 10.23 (s, 1H), 8.29 (d, *J* = 8.9 Hz, 1H), 7.39 – 7.22 (m, 7H), 5.17 (q, *J* = 7.4 Hz, 1H), 3.42 (s, 3H), 1.89 (d, *J* = 7.4 Hz, 3H). ^{13}C-NMR (75 MHz, $CDCl_3$): δ = 184.8 (CH), 154.2 (C_q), 140.8 (C_q), 138.1 (C_q), 129.6 (C_q), 129.1 (CH), 127.2 (CH), 127.1 (CH), 124.3 (C_q), 123.7 (CH), 122.6 (CH), 114.7 (C_q), 109.7 (CH), 34.7 (CH_3), 31.4 (CH), 18.8 (CH_3). HRMS (ESI) m/z calcd for $C_{18}H_{17}ClNO$ $[M+H]^+$ 298.0993, found: 298.0996.

3-Formyl-1-methyl-2-(1-phenylethyl)-1*H*-indole-5-carbonitrile (3ga)

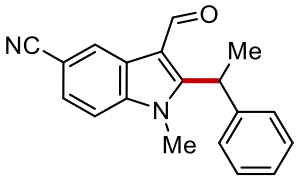

The general procedure **1** was followed using indole substrate **1g** (0.1 mmol, 28.9 mg) and styrene **2a** (0.15 mmol, 17 µL). Purification by column chromatography on silica gel (n-hexane/EtOAc 5:1) yielded **3ga** (15.5 mg, 54% yield) as a pale-yellow solid. M.p.: 130-132 °C. ^{1}H-NMR (300 MHz, $CDCl_3$): δ = 10.25 (s, 1H), 8.74 (dd, *J* = 1.7, 0.7 Hz, 1H), 7.53 (dd, *J* = 8.5, 1.6 Hz, 1H), 7.39 – 7.31 (m, 3H), 7.31 – 7.27 (m, 1H), 7.24 (d, *J* = 6.8 Hz, 2H), 5.17 (q, *J* = 7.4 Hz, 1H), 3.51 (s, 3H), 1.91 (d, *J* = 7.4 Hz, 3H). ^{13}C-NMR (75 MHz, $CDCl_3$): δ = 184.8 (CH), 155.6 (C_q), 140.4 (C_q), 139.1 (C_q), 129.2 (CH), 127.4 (CH), 127.1 (CH), 127.0 (CH), 126.8 (CH), 125.7 (C_q), 120.1 (C_q), 114.9 (C_q), 110.4 (CH), 106.4 (C_q), 34.9 (CH_3), 31.6 (CH), 18.9 (CH_3). HRMS (ESI) m/z calcd for $C_{19}H_{17}N_2O$ $[M+H]^+$ 289.1335, found: 289.1340.

5.5.8 Additional References

[1] R. A. Laskar, N. Yoshikai, *J. Org. Chem*. **2019**, *84*, 13172-13178.

[2] G. Valero, A.-N. Balaguer, A. Moyano, R. Rios, *Tetrahedron Letters* **2008,** 49, 6559–6562.

[3] Schmiel, H. Butenschön, *Organometallics* **2017**, *36*, 4979−4989.

[4] L. D. Pham, R. O. Smith-Sweetser, B. Krupinsky, C. E. Dewey, J. R. Lamb, *Angew. Chem. Int. Ed.* **2023**, *62*, e202314376.

[5] H. Kinuta, M. Tobisu, N. Chatani, *J. Am. Chem. Soc*. **2015**, *137*, 4, 1593–1600.

[6] W. Chen, Q. Chen, Y. Ma, X. Leng, S.-D. Bai, L. Deng, *Chin. Chem. Lett.* 2020, *31*, 1342–1344.

[7] H. Zhang, Z. Ouyang, Y. Liu, Q. Zhang, L. Wang, L. Deng, *Angew. Chem. Int. Ed.* 2014, *53*, 8432–8436.

[8] Z.-J. Zhang, N. Jacob, S., Bhatia, P. Boos, X. Chen, J. C. DeMuth, A. M. Messinis, B. Bongsuiru Jei, J. C. A. Oliveira, A. Radović, M. L. Neidig, J. Wencel-Delord, L. Ackermann, *Nat. Commun*. **2024**, *15*, 3503.

[9] Z. Ding, N. Yoshikai, *Angew. Chem. Int. Ed.* **2013**, *52*, 33, 8574-8578.

[10] C. Zhou, Q.-C. Gan, T.-P. Zhou, T. Lei, C. Ye, X.-J. He, B. Chen, H. Lu, Q. Wan, R.-Z. Liao, C.-H. Tung, L.-Z. Wu, *Angew. Chem. Int. Ed*. **2022**, *61*, e202116421.

[11] B. J. Fallon, E. Derat, M. Amatore, C.Aubert, F. Chemla, F. Ferreira, A. Perez-Luna, M. Petit, *Org. Lett.* **2016**, *18*, 9, 2292–2295.

[12] M. Y. Wong, T. Yamakawa, N. Yoshikai, *Org. Lett.* **2015**, *17*, 442–445.

6. Nickel-Catalyzed Atroposelective C–H Alkylation Enabled by Bimetallic Catalysis with Air-Stable Heteroatom-Substituted Secondary Phosphine Oxide Preligands

The research presented in this chapter was conducted during a visiting stay in the Ackermann Group at the Georg-August-Universität in Göttingen.

From this chapter:

Z.-J. Zhang, M. M. Simon, S. Yu, S.-W. Li, X. Chen, S. Cattani, X. Hong*, L. Ackermann*, *J. Am. Chem. Soc.* **2024***, 146,* 13, 9172–9180.

6.1 Introduction

6.1.1 Ni–Al Bimetallic Catalysis for C–H Bond Activation

In recent decades, late and noble transition metal catalysts have been widely utilized for C–H bond functionalizations due to their straightforward application in organic synthesis. Interest in developing C–H bond activation catalyzed by first-row transition metals has only recently increased.[1] Among 3d metal catalysts, nickel-catalyzed C–H activation has attracted significant attention due to its low cost, easy availability, and unique catalytic properties.[2] Nickel's ability to exist in various oxidation states allows for diverse redox pathways during reactions, enabling access to various types of reactivity and transformations.[3] The first example of Ni-mediated aromatic C–H bond activation was documented by Kleiman and Dubeck in 1963 (Scheme 6.1).[4] They found that heating nickelocene **I** with diazobenzene **II** produced an organo-nickel complex (**III**) that derives from the C–H nickelation of **II**.

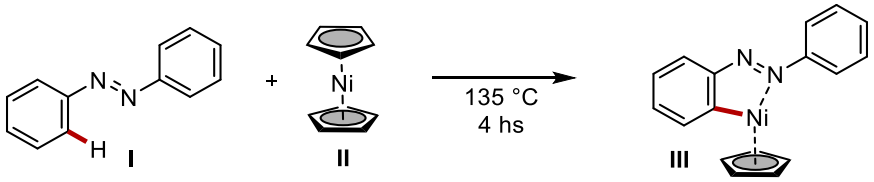

Scheme 6.1 Early example of C−H cyclometallation with nickel complexes.

However, compared to other transition metals, Ni-catalyzed C–H bond activation has remained relatively underexplored. The combination of strongly coordinating bidentate directing groups (DGs) with nickel catalysts has proven to be the most effective for nickel-catalyzed C–H functionalizations.[5] Although reactions using non-directing-group strategies have been less explored compared to directing-group strategies, they have been extensively employed to access enantioselective transformations, among others.[6] In fact, the presence of strong bidentate DGs can interfere with the coordination of sterically hindered chiral ligands to the metal center, thus preventing the development of enantioselective C–H functionalizations.

Despite the power of transition metal catalyzed C–H functionalization methodologies, sometimes mono-metallic catalysts struggle to promote more difficult reactions, particularly those involving unreactive bond transformations. Introducing an extra transition metal or main-group element to enhance catalytic synergism can help to overcome these limitations, not only in boosting reactivity and selectivity, but also in improving the tunability of catalytic systems. In recent years, nickel has been successfully employed in bimetallic catalysis, mainly with aluminum (Al) as a suitable coordinating metal. To effectively pair these two metals, the use of appropriate

bifunctional ligands is often crucial. So far, three types of bifunctional ligands have been identified as particularly effective in coordinating both Ni and Al: secondary phosphine oxide (SPO) ligands, hydroxyl-functionalized *N*-heterocyclic carbene (NHC-OH) ligands, and *in situ*-formed phosphine ligands.[7]

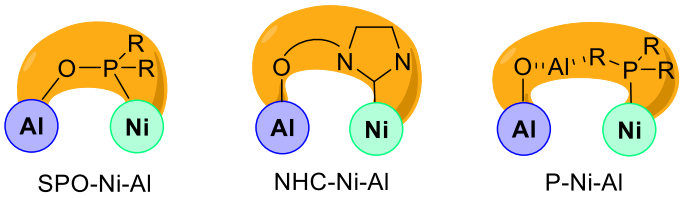

Scheme 6.2 Schematic representation of bifunctional ligands coordination modes.

6.1.2 Secondary Phosphine Oxide (SPO)-ligated Ni–Al Enantioselective Bimetallic Catalysis

Among the bifunctional ligand utilized in ligand-ligated Ni–Al bimetallic catalysis, secondary phosphine oxide (SPO) are the most important ones. SPOs are air-stable preligand that represent a robust alternative to traditional phosphine ligands in transition metal catalysis.[8] In solution, SPOs exist in equilibrium between penta- and trivalent phosphorus tautomeric species (Scheme 6.3, a).[9] At room temperature, the pentavalent phosphorus form predominates, which contributes to the overall air stability of SPOs. Thus, secondary phosphine oxides have been found to be excellent chiral ligands in Ni–Al bimetallic catalytic systems. In the coordination mode of SPOs, the oxygen atom of the trivalent phosphorous tautomer coordinates with the Al-Lewis acid, while the soft P atom preferentially binds to the low-valent transition metal. Since the coordination of Al-Lewis acid to the substrate plays a crucial role in reactivity, it's important that the substrate contains an anchoring site, typically ah heteroatom (Scheme 6.3, b).

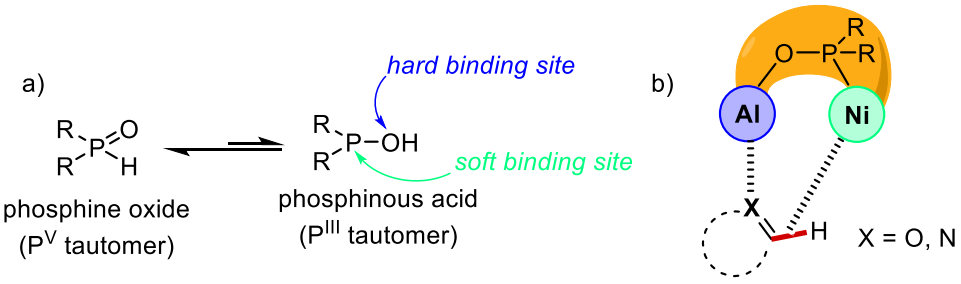

Scheme 6.3 a) Tautomerization of SPOs, b) Coordination mode of the SPO-ligated Ni–Al catalyst.

In 2013, the Cramer group developed an asymmetric nickel-catalyzed intramolecular hydrocarbamoylation of homoallylic formamides with unreactive alkenes.[10] The reaction is promoted by the chiral heteroatom-substituted secondary phosphine oxide (HASPO) **A** preligand through a heterobimetallic activation mechanism. The protocol allowed for the synthesis of a wide range of chiral γ-lactam derivatives, achieving up to 98% yield and 95% enantiomeric excess (Scheme 6.4). Although a nickel catalyst derived solely from the chiral HASPO exhibited limited activity, the inclusion of a co-catalytic amount of PPh_3 significantly enhanced its performance. This is likely due to PPh_3 displacement of the cyclooctadiene (cod) ligand from the nickel precatalyst.

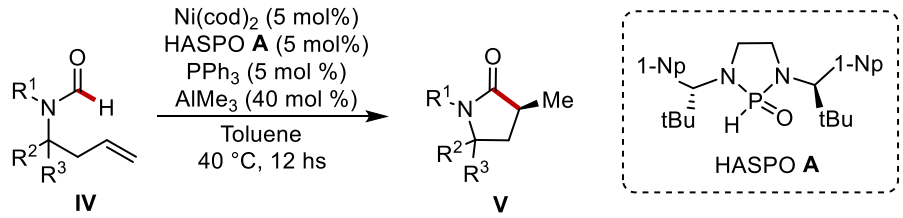

Scheme 6.4 Asymmetric Ni–Al-catalyzed intramolecular hydrocarbamoylation of formamides.

The authors propose a plausible catalytic cycle that starts with the formation of the Lewis acid/HASPO adduct **A-Al** (Scheme 6.5). This bifunctional ligand features an aluminum center that retains its Lewis acidity, while the Lewis basic phosphorus atom coordinates to $Ni(cod)_2$ (**Int1**). The Lewis acidic aluminum center then activates the carbonyl group of **IV**, producing intermediate **Int2**. Following this, the nickel center undergoes oxidative insertion into the C–H bond, forming a six-membered hetero-bimetallacycle **Int3**. Migratory insertion leads to **Int4**, and reductive elimination releases product **V** while regenerating the heterobimetallic catalyst **Int1**.

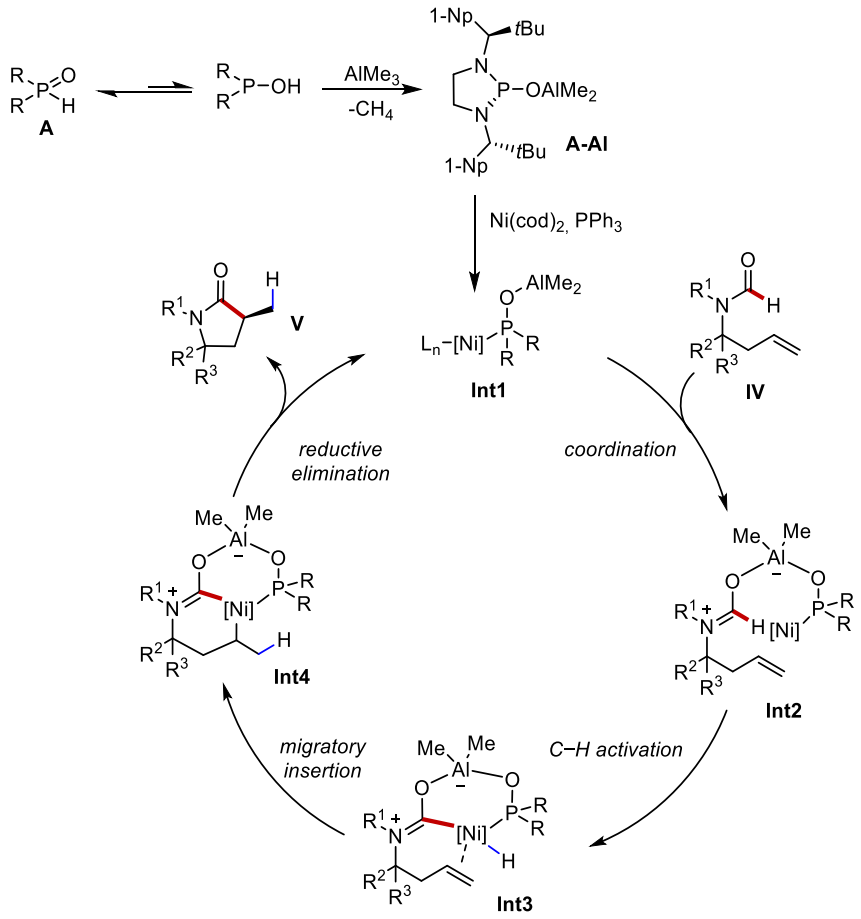

Scheme 6.5 Proposed catalytic cycle for asymmetric nickel-catalyzed intramolecular hydrocarbamoylation of **IV**.

In 2020, Ye and coworkers employed SPO–Ni–Al bimetallic catalysts to develop an asymmetric two-fold oxidative C(sp²)–H annulation of ferrocene-based formamides (**VI**) and alkynes (**VII**).[11] A BINOL-derived chiral SPO ligand (**B**) was found to be optimal for delivering planar chiral ferrocene amide derivatives with both high yields and enantioselectivities (Scheme 6.6). Notably, The SPO–Ni–Al bimetallic catalyst effectively activated both the formyl C–H bond and the aryl C–H bond, eliminating the need for additional directing groups.

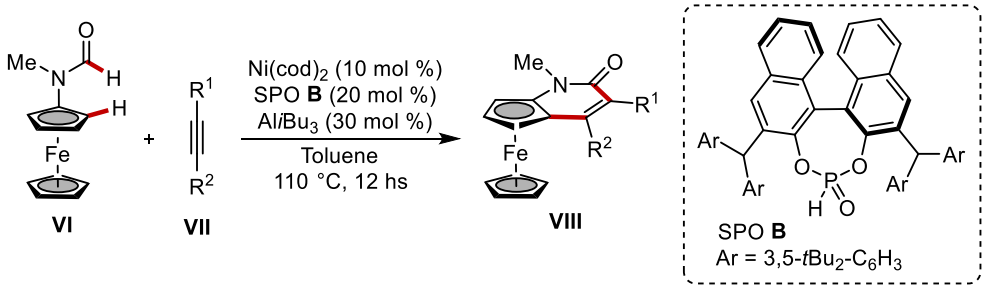

Scheme 6.6 Asymmetric Ni–Al-catalyzed C(sp²)–H annulation of ferrocene formamides.

Very recently, the Ye group reported the first example of enantioselective nickel-catalyzed aliphatic C(sp³)–H bond activation of formamides.[12] They employed heteroatom substituted secondary phosphine oxide-ligated Ni–Al bimetallic catalyst to enable the annulation of formamides (**IX**) with alkynes (**VII**). The reaction is compatible with several dialkyl, diaryl and alkylaryl alkynes, in combination with primary and secondary C(sp³)–H bonds. The newly designed HASPO preligand **C,** that features a partially hydrogenated binaphthyl backbone, allowed to access high levels of ee and yields. The authors propose that the partial hydrogenation of the naphthyl rings increases steric hindrance resulting in a larger dihedral angle at the phosphorus center, thereby facilitating a better interaction between the substrate and the catalyst.

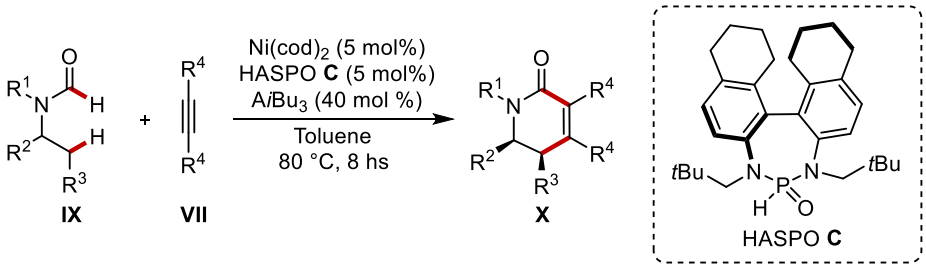

Scheme 6.7 Asymmetric Ni–Al-catalyzed aliphatic C(sp³)–H bond annulation of formamides.

In 2018 Ye and coworkers reported the first example of Ni–Al catalyzed enantioselective *exo*-selective C−H cyclization of (benzo)imidazole with alkenes.[13] Inspired by Cavell's study, where a mild *exo*-selective cyclization was achieved using imidazole salts as substrates and nickel(0) as

the catalyst,[14] the authors submitted a homoallylic tethered benzoimidazole **XI** to the Ni–Al bimetallic system in the presence of the Taddol-derived SPO chiral preligand **D**. The synergy between SPO ligand, Ni, and Al offers an effective approach for controlling enantioselectivity, resulting in the synthesis of various bi- and polycyclic imidazoles with challenging *β*-stereocenters in high yields and excellent ee.

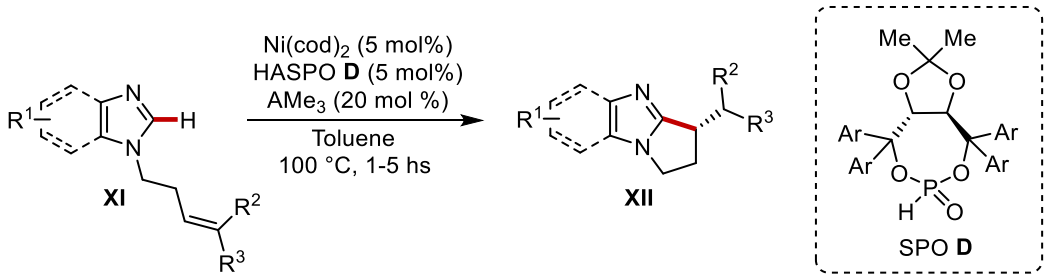

Scheme 6.8 Ni–Al catalyzed enantioselective *exo*-selective C−H cyclization of (benzo)imidazoles.

The plausible mechanism starts with the formation of the Lewis acid/SPO adduct **D-Al**. This intermediate can then coordinate with the nickel precatalyst to generate complex **Int1**. In a heterobimetallic activation mode, the Lewis acidic aluminum center coordinates one of the nitrogen atoms of (benzo)imidazole **XI** (anchoring site), while the nickel center binds to the olefin group, forming **Int5**. Based on experimental evidence, the authors proposed that the C−H cleavage step to form **Int7** could proceed directly from **Int5** through a direct ligand-to-ligand hydrogen transfer (LLHT) from the imidazole to the alkene. However, they acknowledged that an oxidative addition pathway (**Int6**) followed by a migratory insertion could not be entirely excluded. A final reductive elimination releases product **XI** while regenerating the heterobimetallic catalyst **Int1**.

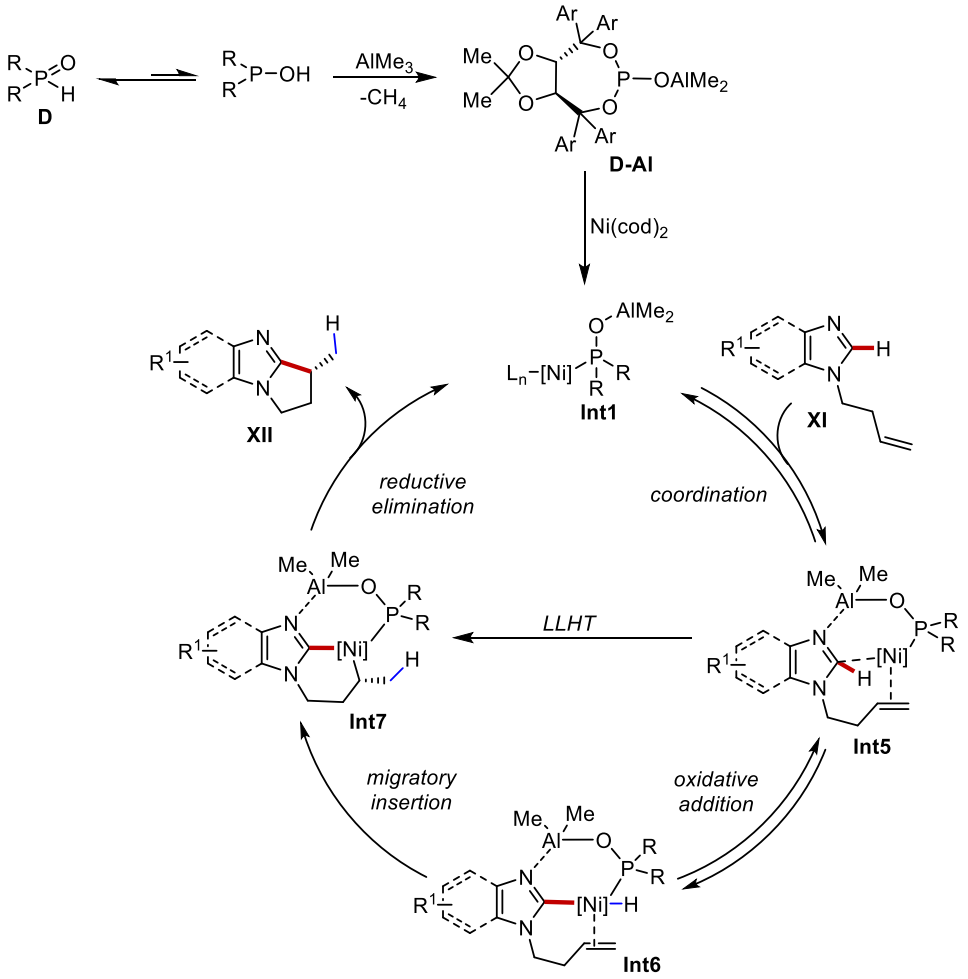

Scheme 6.9 Proposed catalytic cycle for Ni–Al catalyzed enantioselective *exo*-selective C−H cyclization of (benzo)imidazoles.

All the example presented so far exploit the synergy of Ni–Al bimetallic catalysis to achieve enantioselective transformations of unreactive bonds. The drawback associated with this approach relies in the indispensable necessity of using pyrophoric and reactive organoaluminum reagents as additives. Not only these reagents are harmful to handle but they can also impact on the functional group tolerance of the transformation. To overcome this limitation, Ackermann and colleagues recently introduced an innovative approach involving the intramolecular, aluminum-free, nickel-catalyzed enantioselective *endo*-hydroarylation of (benzo)imidazoles thetered alkenes **XIII** (Scheme 6.10).[15] The key to obtain high yields and enantioselectivities relies in the use of a JoSPOphos-type ligand **E**, whose applications had previously been limited only to rhodium(I)-catalyzed hydrofunctionalizations.[16] The Al-free reaction conditions greatly impact on the applicability of the reaction with complete tolerance of sensitive functional groups, such as amines, chlorine, and methyl ester.

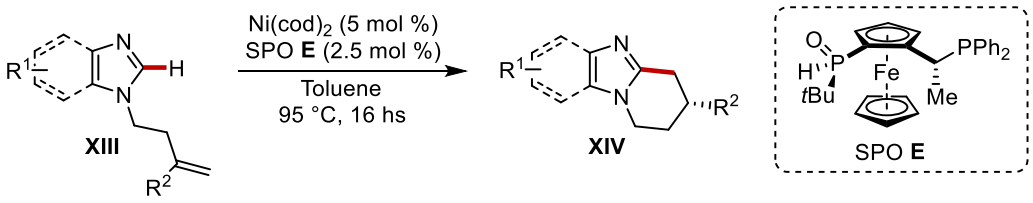

Scheme 6.10 Ni–Al-catalyzed enantioselective *endo*-hydroarylation of (benzo)imidazoles.

In 2022, the Ye group introduced a new class of chiral HASPO preligands featuring a central chiral 1,2-diphenyl ethylenediamine backbone with non-symmetrical side chains.[17] When a 2-methyl naphthyl group and a 3,5-di-*tert*-butyl group were introduced as non-symmetrical side chains, the phosphine oxide ligand existed as two separable isomers. Both isomers were able to promote the reaction, yielding similar enantiomeric excesses (95% vs. 91%) but with opposite stereoconfiguration. In contrast, when the two isomers were mixed, the reaction resulted in poor enantioselectivity, indicating that the chiral P center of these isomers played a crucial role in determining the enantioselectivity of the reaction. Thus, the best isomer HASPO **F** was efficiently employed in the enantioselective Ni–Al bimetallic-catalyzed C2−H alkylation of pyridines (**XV**) with 1,3-dienes (**XVI**) (Scheme 6.11). The method enabled the enantioselective C2 alkylation of unsubstituted pyridine, C3, C4, or C2-substituted pyridines, as well as complex pyridine-containing bioactive molecules.

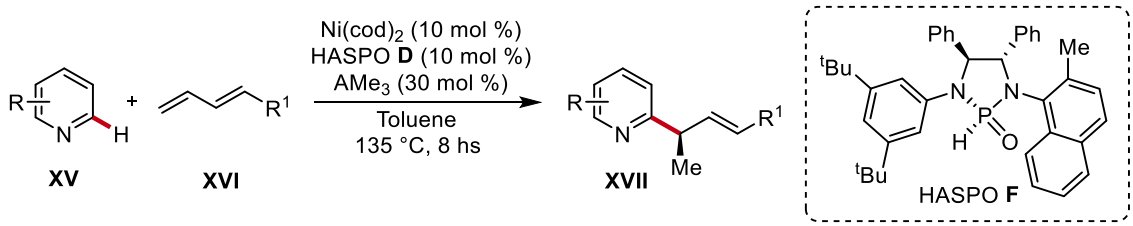

Scheme 6.11 Ni–Al-catalyzed C2−H alkylation of pyridines with 1,3-dienes.

The authors conducted a series of mechanistic experiments and density functional theory calculation to shed light on the mechanism of the reaction. They propose that the C–H activation step from **Int9** to **Int10** proceeds *via* a reversible LLHT pathway. Then, the isomerization of η^1 to η^3 allylic nickel complex delivers **Int11**. This intermediate undergoes enantiodetermining reductive elimination to generate **Int12**, which upon release of product **XVII** and pyridine coordination, regenerates the catalytic active species **Int8**.

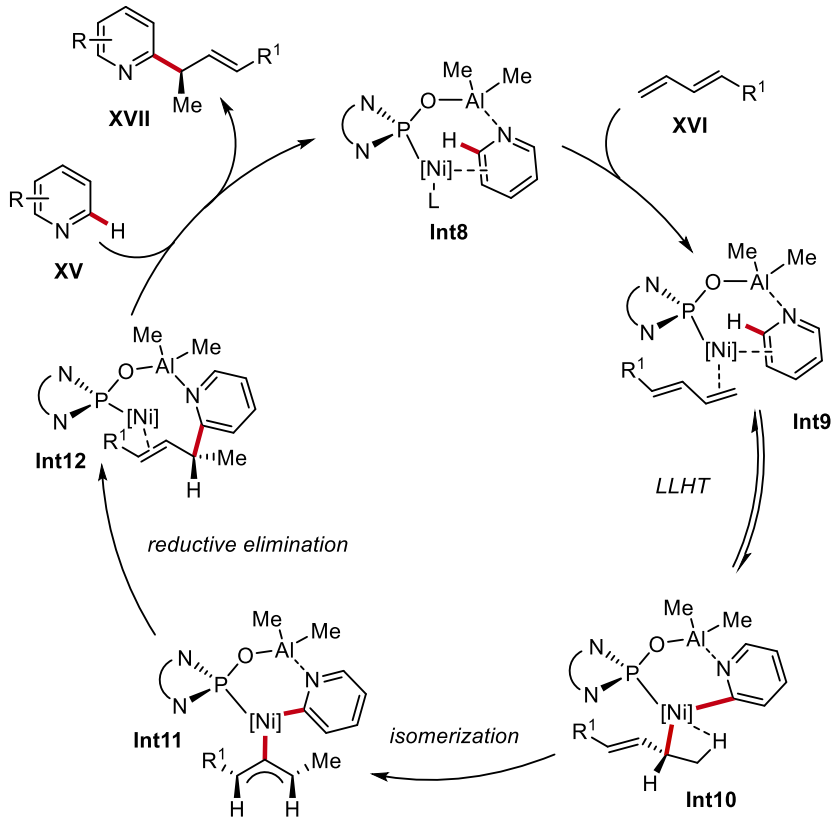

Scheme 6.12 Proposed catalytic cycle for Ni–Al-catalyzed C2−H alkylation of pyridines.

6.2 Results and Discussion

During the six-months visiting stay in Ackermann's group my research work was also related to an ongoing project developed by Dr. Z.-J. Zhang and M. M. Simon focused on the development of nickel-catalyzed atroposelective C−H alkylation of benzimidazole substrates with olefins for the construction of C−N axially chiral compounds. Despite the several enantioselective transformations promoted by secondary phosphine oxide (SPO)-ligated Ni–Al bimetallic catalysis, the exploration of this system for achieving atroposelective C−H functionalization has yet to be investigated. In this project, the design of new heteroatom-substituted secondary phosphine oxide (HASPO) as highly effective chiral preligands was crucial for achieving C−N axially chiral benzimidazole derivatives with high enantioselectivities utilizing a Ni–Al bimetallic system. A diverse array of alkenes, both terminal and internal, were highly compatible with the reaction, resulting in the formation of the desired alkylation products with excellent yields and enantioselectivities.

In the following sections will be presented all the results obtained in this project, providing a comprehensive overview of the Ni–Al catalyzed atroposelective C−H alkylation method enabled by HASPO preligands.

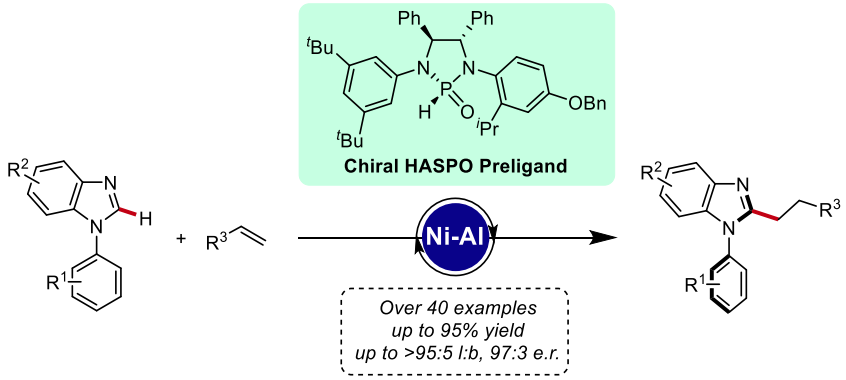

Scheme 6.13 Nickel-catalyzed atroposelective C−H alkylation enabled by bimetallic catalysis with HASPO preligands.

6.2.1 Optimization Studies

The study commenced with the synthesis and subsequent evaluation of the catalytic activity of various HASPO preligands in the atroposelective C−H alkylation of model benzimidazole **1** with styrene **2**, utilizing Ni−Al bimetallic catalysis. Initial attempts using chiral Taddol- (**L1**-**L3**), diamine- (**L4**, **L5**), BINOL-derived (**L6**), and bidentate JoSPOphos-derived (**L7**, **L8**) HASPO preligands resulted in the formation of the linear alkylated product with low yields and poor enantioselectivity. Next, the focus shifted to chiral diamine-derived HASPO preligands, allowing for the exploration of a broader range of structural modifications. Only moderate stereoselectivity was observed when the preligand featured identical *N*-substituted aromatic rings (**L9**-**L11**). However, when the two aromatic rings displayed different substitution patterns (**L12**-**L14**), the formation of a more effectively structured chiral pocket resulted in improved stereoselectivity. For this reason, various asymmetric HASPO preligands were synthetized (**L12**-**L23**) and among these, **L22** was found the best in promoting the envisioned transformation. It features an aromatic ring with an isopropyl group at the *ortho*-position and an additional benzyloxy group at the *para*-position. These structural modifications result in a more effective chiral pocket, which significantly enhances both the enantioselectivity and yield of the reaction. Notably, when the reaction was conducted employing the diastereomer **L22-isomer**, which has the opposite P-centered chirality compared to **L22**, the alkylation proceeded with almost no stereoselectivity. Additionally, the 2-methyl naphthyl-substituted HASPO preligands (**L24**-**L26**) that were successfully employed by Ye in the enantioselective C–H alkylation of pyridines,[17] were found to be less effective than the newly designed preligand **L22**.

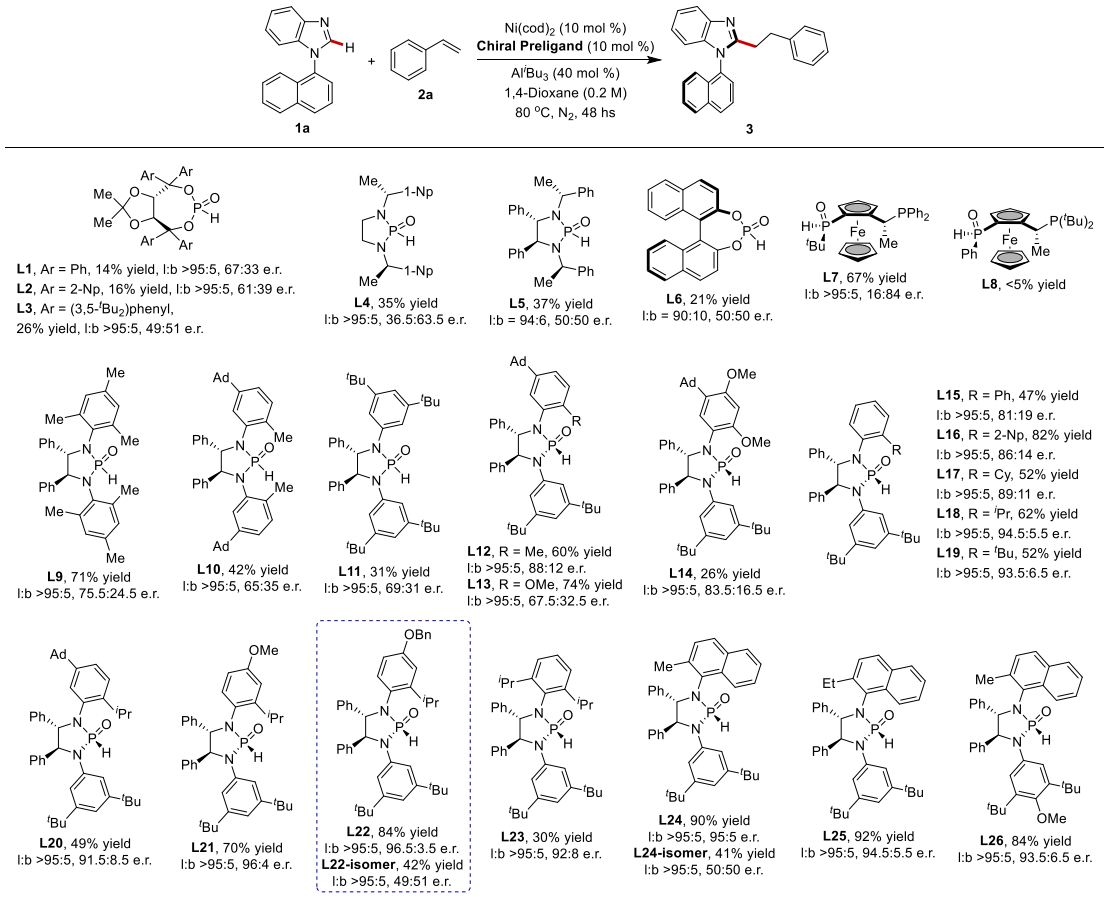

Scheme 6.14 Ligand optimization for Ni–Al-catalyzed atroposelective C−H alkylation.

The synthesis of all the novel chiral HASPOs was achieved following a three-step procedure starting from the commercially available (1*S*,2*S*)-1,2-diphenylethane-1,2-diamine (**S1**). For ligands with different *N*-substituted aromatic rings, in the first step, the chiral diamine is reacted with a substituted aryl bromide (**S2**, 0.7 equiv.) via a traditional Buchwald-Hartwig amination protocol to deliver the monofunctionalized intermediate **S3**, which is then reacted with a different bromide (**S4**) to obtain the asymmetric intermediate **S5**. In the third step, intermediate **S5** is reacted with PCl_3 to obtain the corresponding phosphorchloridite (air- and moisture-sensitive), which, after hydrolysis and subsequent workup, delivered the desired heteroatom-substituted secondary phosphine oxides preligand.

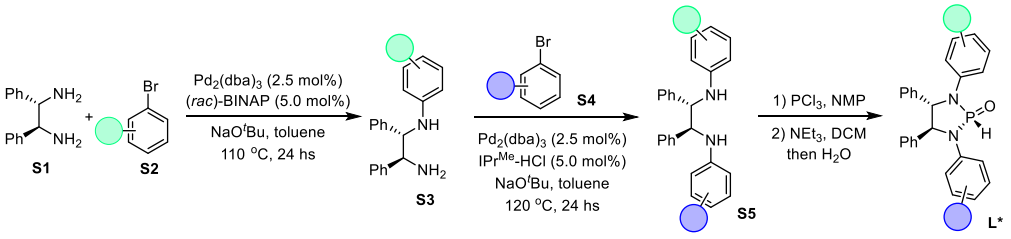

Scheme 6.15 General scheme for asymmetric HASPO preligands synthesis.

Further optimization led to the identification of the best reaction conditions that involve the use of $Ni(cod)_2$ as the catalyst in combination with Al^iBu_3 as the Al-based Lewis acid, in 1,4-dioxane at 80 °C for 48 hours. Other aluminum Lewis acid such as $AlMe_3$ or $AlEt_3$ led to diminished enantioselectivity and yields (entries 1-2) as well as the use of other solvents (entries 6-9). The presence of the Al^iBu_3 was also evaluated fundamental for the reaction to enable the reactivity of the nickel catalyst (entry 16).

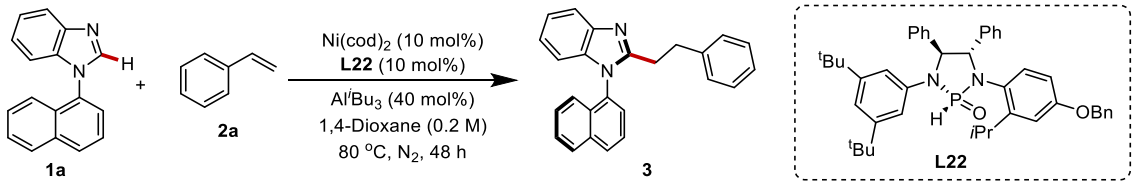

Entry[a]	Deviation from standard conditions	Yield (%)	l:b	e.r.
1	none	84 (82)	>95:5	96.5:3.5
2	$AlMe_3$ (40 mol%) instead of Al^iBu_3	90	>95:5	92:8
3	$AlEt_3$ (40 mol%) instead of Al^iBu_3	68	>95:5	95.5:4.5
6	Toluene (0.2 M) instead of 1,4-dioxane	62	>95:5	96.5:3.5
7	THF (0.2 M) instead of 1,4-dioxane	70	>95:5	96:4
8	Cyclohexane (0.2 M) instead of 1,4-dioxane	92	>95:5	94:6
9	PhOMe (0.2 M) instead of 1,4-dioxane	54	>95:5	96:4
12	$Pd(dba)_2$ (10 mol%) instead of $Ni(cod)_2$	n.d.	-	-
14	Without $Ni(cod)_2$	n.d.	-	-
15	Without **L22**	16	>95:5	50:50
16	Without Al^iBu_3	n.d.	-	-

[a] Reaction conditions: **1a** (0.1 mmol), **2a** (0.15 mmol), $Ni(cod)_2$ (10 mol%), **L22** (10 mol%), Al^iBu_3 (1.1 M in toluene, 40 mol%), 1,4-dioxane (0.5 mL), 80 °C, 48 hs, N_2 atmosphere. The yield was determined by ^1H NMR spectroscopy using 1,3,5-trimethoxybenzene as the internal standard. The enantiomeric ratio (e.r.) was determined by HPLC.

Table 6.1 Optimization of Ni–Al-catalyzed atroposelective C−H alkylation.

6.2.2 Substrate Scope

With the optimal HASPO preligand (**L22**), the substrate scope was evaluated under the optimized reaction conditions (Scheme 6.16). A series of benzimidazoles **1** with various *N*-aryl substituents was tested and only a minor impact on the enantioselectivity was observed with the variation of the steric hindrance of the *ortho*-substituents (**3**-**7**). Additionally, a family of substituted benzimidazole was synthesized with both electron-withdrawing and electron-donating groups that were well tolerated under the optimized reaction conditions, yielding the desired products in moderate to good yields with high enantioselectivities (**8**-**14**). Further, single-crystal X-ray diffraction analysis of product **14** allowed for the assignment of the absolute configuration of the products.

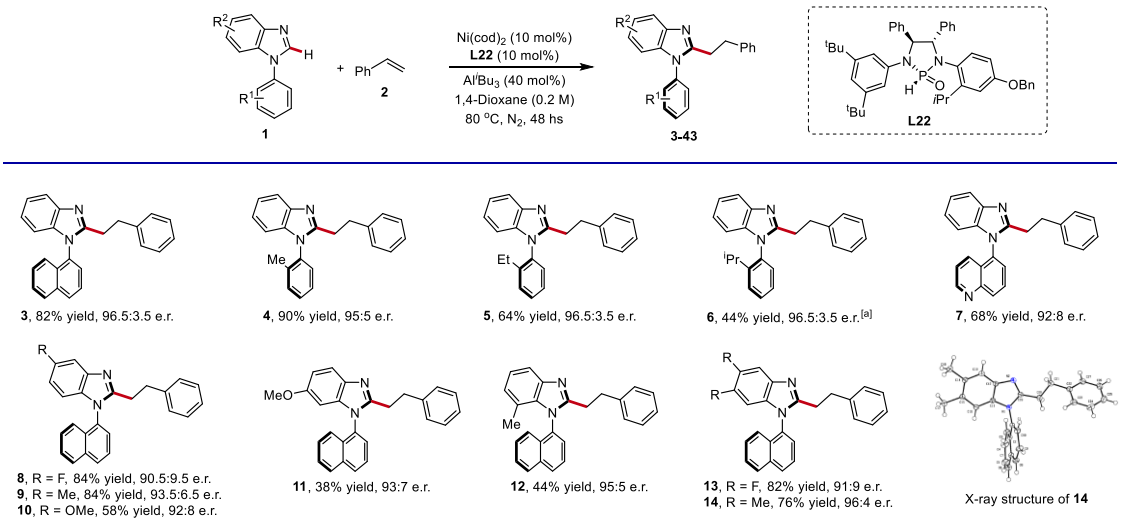

Scheme 6.16 Substrate scope of benzimidazoles **1**.

The reaction scope was also extended to differently substituted styrene derivatives (Scheme 6.17). Substrates containing either electron-withdrawing or donating groups at the *para*-, *meta*-, or *ortho*-positions of the aromatic ring, performed effectively, yielding the corresponding products (**15**-**29**) in high yields and excellent enantioselectivities. Both 2-vinylnaphthalene and vinylferrocene were also compatible, providing the target products **30** and **31**, respectively.

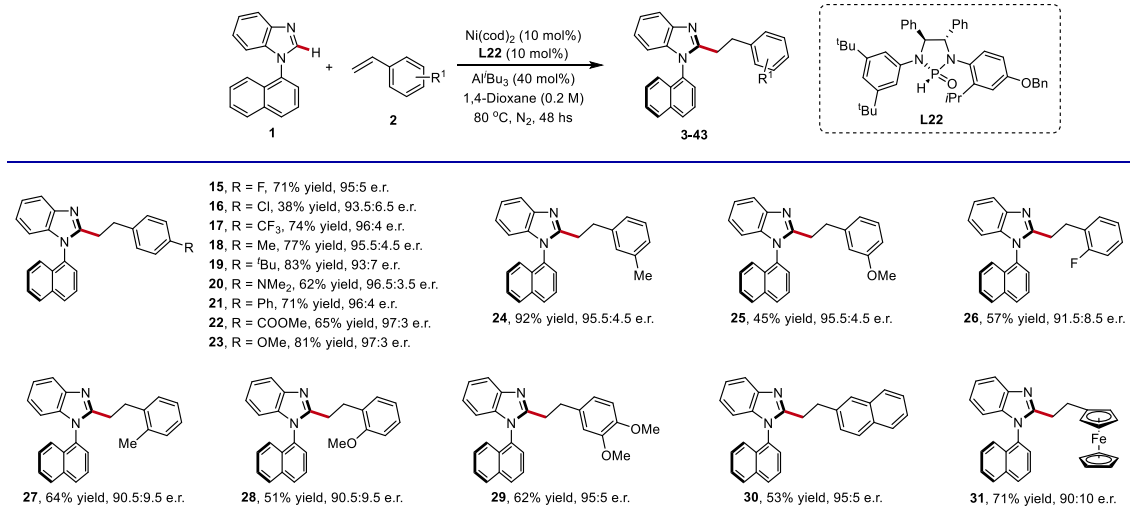

Scheme 6.17 Substrate scope of styrenes **2**.

One of the key features of the developed protocol is that its applicability is not restricted only to styrene derivatives but also to unactivated alkenes, such as allylbenzenes, vinyl silanes, and 1-octene. These reacted efficiently under the Ni–Al bimetallic catalysis, delivering the desired linear products **32**–**41** with moderate to good enantioselectivities (Scheme 6.18). Additionally, alkenes derived from natural products like eugenol and δ-tocopherol were submitted to the devised protocol, yielding products **42** and **43** in good yields with high stereoselectivities.

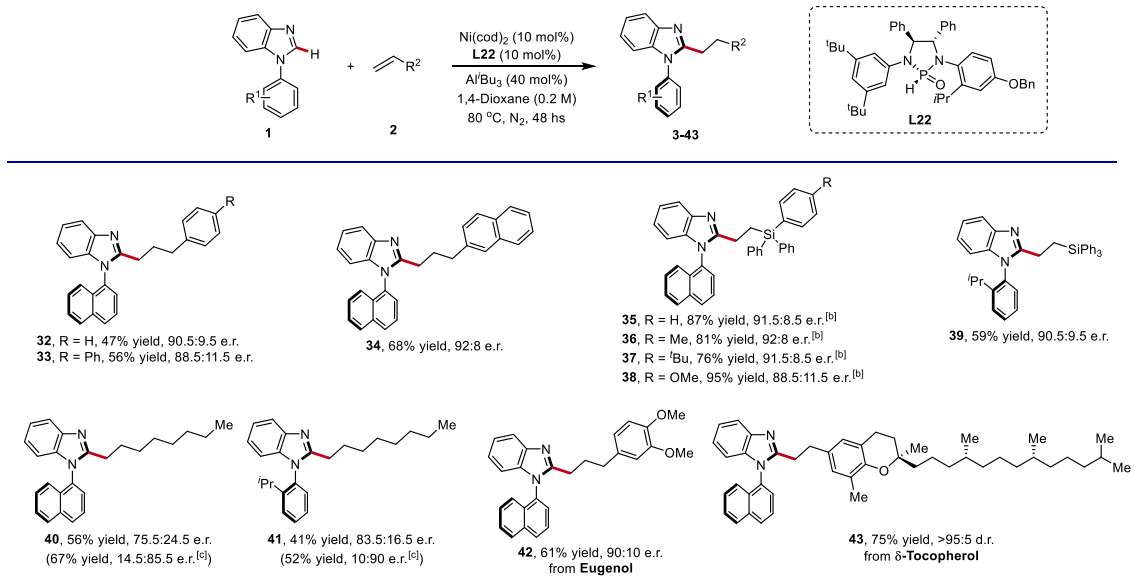

Scheme 6.18 Substrate scope of unactivated alkenes.

The substrate scope was then extended with internal alkenes and 1,3-dienes as substrates (Scheme 6.19). When *trans*-*β*-substituted styrenes (**44** and **45**) were used, linear-selective products (**32** and **46**) were obtained in high yields and enantioselectivities (Scheme 6.19, a). This outcome is attributed to the chain-walking process of the nickel(II) intermediate, which undergoes iterative *β*-hydride elimination and migratory insertion, converting an internal alkene into a terminal alkene, and ultimately forming the desired product. Next, the reaction was conducted with phenyl 1,3-diene **47** which allowed to obtain branch-selective products (**48** and **49**) with high regio- and stereoselectivities (Scheme 6.19, b).

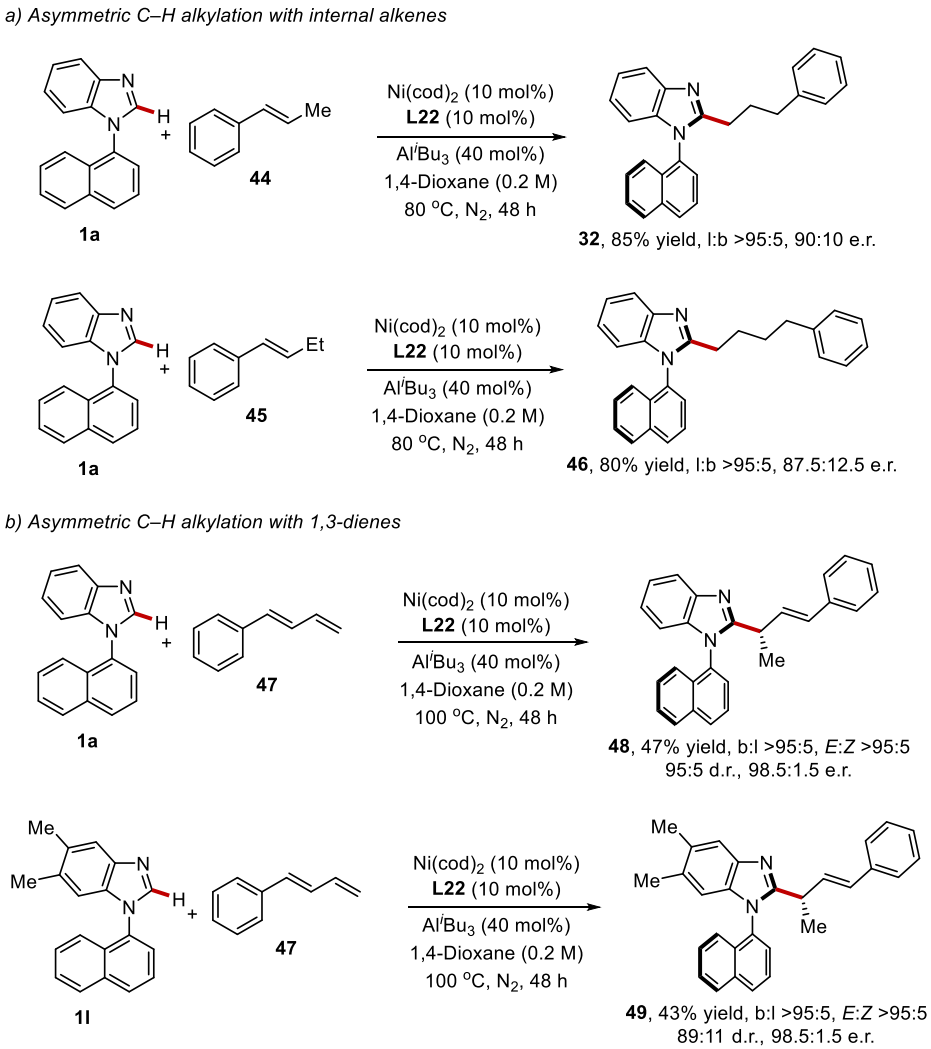

Scheme 6.19 Asymmetric C–H alkylation with internal alkenes and 1,3-dienes.

6.2.3 Mechanistic Investigation

To gain a deeper understanding of the reaction mechanism, a series of mechanistic experiments were conducted (Scheme 6.20). The reaction of the C2-deuterated benzimidazole substrate [D]$_1$-**1a** with styrene **2a** resulted in the formation of product [D]$_1$-**3**, with transfer of the C2-deuterium from the benzimidazole to the two methylene groups (Scheme 6.20, a). This is attributed to the iterative *β*-hydride elimination and migratory insertion process of the nickel(II) intermediate that caused deuterium scrambling between the two methylene groups. Furthermore, 23% of the benzimidazole substrate remained unreacted and was isolated as a 42:58 mixture of [D]$_1$-**1a** and **1a**. Next, a deuterium scrambling experiment was conducted using a 1:1 mixture of substrates [D]$_1$-**1a** and **1h** under standard reaction conditions (Scheme 6.20, b). The minor H/D crossover observed in the products suggests that the formation of the alkyl-nickel species may be a reversible process.

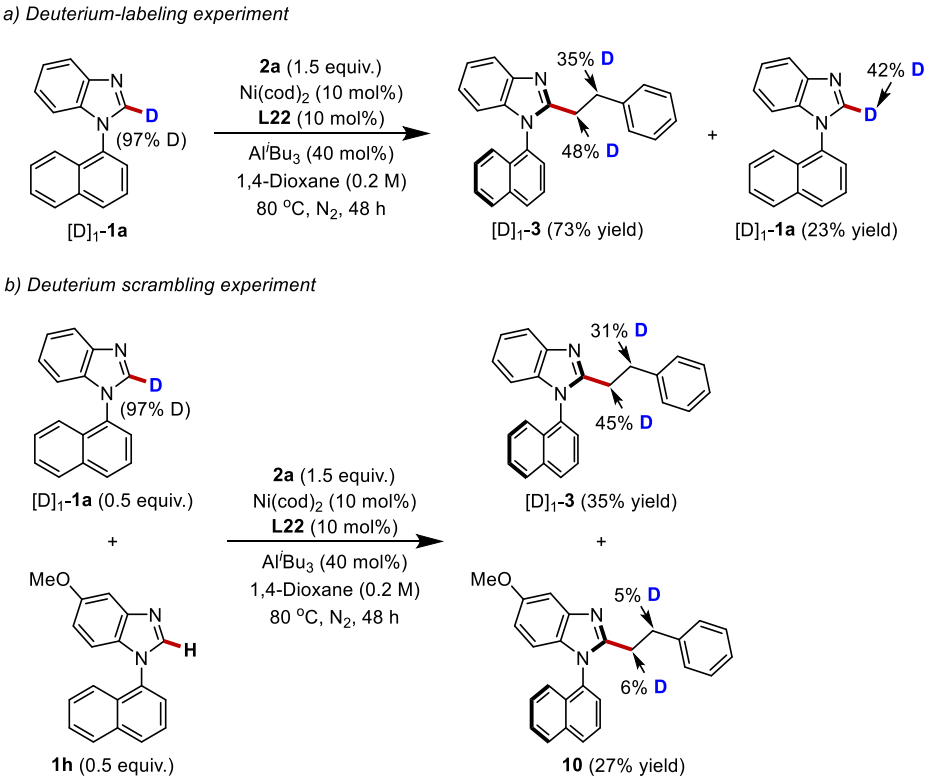

Scheme 6.20 Deuterium-labelling and deuterium scrambling experiments.

6.2.4 Proposed Catalytic Cycle

The study of the reaction mechanism was also performed by means of DFT calculations which showed a barrierless ligand-to-ligand hydrogen transfer (LLHT) that generates alkyl-nickel(II) species **IntIII**. The competing oxidative addition of the C−H bond to the nickel center was calculated to be unfavorable, requiring a much higher energy barrier. The subsequent reductive elimination of the alkyl-nickel(II) species **IntIII** to form **IntIV** is the rate- and stereodetermining step. The non-C2 symmetry characteristic of ligand **L22** plays a crucial role in determining the stereoselectivity control. Furthermore, a comprehensive data science analysis of the structure−enantioselectivity relationship of the HASPO preligand revealed the critical characteristics of bulkiness and geometric shape of the chiral preligands in governing the enantioselectivity. Based on mechanistic studies and previous reports, a plausible catalytic cycle is proposed (Scheme 6.21). The chiral HASPO-ligated Ni−Al bimetallic catalyst **IntI** initially coordinates with the benzimidazole substrate **1a** and styrene **2a**, forming **IntII**. This is followed by the C−H activation step that occurs via direct ligand-to-ligand hydrogen transfer pathway, leading to the formation of intermediate **IntIII**. Finally, **IntIII** undergoes an irreversible reductive elimination, releasing the desired product **3** and simultaneously regenerating the catalytically active HASPO−Ni−Al intermediate **IntI**.

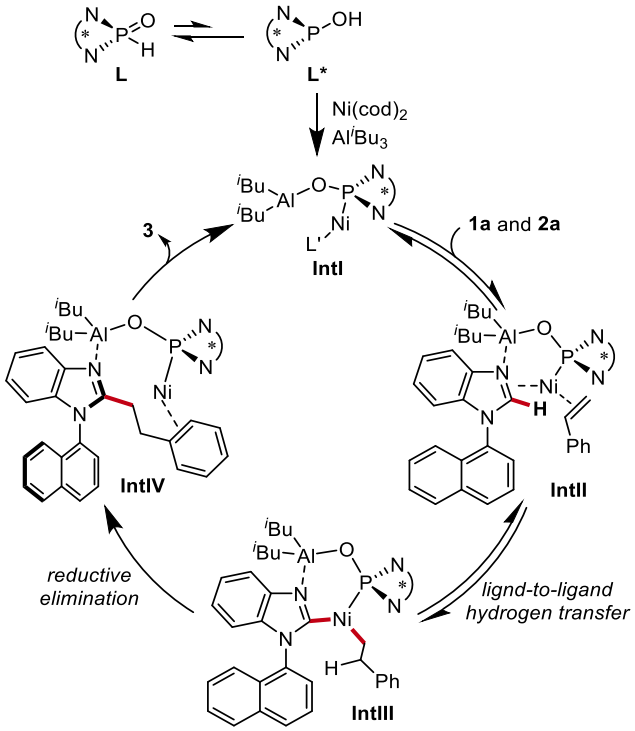

Scheme 6.21 Proposed mechanism.

6.3 Conclusions

In conclusion, the first nickel-catalyzed atroposelective C−H alkylation of benzimidazoles through bimetallic catalysis using a novel air-stable HASPO preligand was developed. This method enabled the effective construction of axially chiral C−N atropisomers with high yields and enantioselectivities. The reaction demonstrates remarkable versatility, showing compatibility with a wide range of alkenes, including aryl alkenes, alkyl alkenes, internal alkenes, and 1,3-dienes. Mechanistic experiments and density functional theory calculations shed light on the catalyst's mode of action, while an extensive data science analysis identified the key characteristics of the chiral preligands that govern the enantioselectivity.

6.4 References

[1] P. Gandeepan, T. Müller, D. Zell, G. Cera, S. Warratz, L. Ackermann, *Chem. Rev*. **2019**, *119*, 2192−2452.

[2] K. S. Egorova, V. P. Ananikov, *Angew. Chem., Int. Ed*. **2016**, *55*, 12150−12162.

[3] a) S. Z. Tasker, E. A. Standley, T. F. Jamison, *Nature* **2014**, *509*, 299–309; b) Y. Nakao, *Chem. Rec*. **2011**, *11*, 242–251; c) Y. Tamaru, Modern organonickel chemistry, Wiley-VCH, Weinheim, **2005**.

[4] J. P. Kleiman, M. Dubeck, *J. Am. Chem. Soc.* **1963**, *85*, 1544–1545.

[5] a) S. M. Khake, N. Chatani, *Trends Chem*. **2019**, *1*, 524–539; b) Y.-H. Liu, Y.-N. Xia, B.-F. Shi*, Chin. J. Chem*. **2020**, *38*, 635－662.

[6] a) J. Loup, U. Dhawa, F. Pesciaioli, J. Wencel-Delord, L. Ackermann, *Angew. Chem., Int. Ed*. **2019**, *58*, 12803−12818; b) Ł.Woźniak, N. Cramer, *Trends Chem.* **2019**, *1*, 471−484.

[7] Y.-X. Luan, M. Ye, *Chem. Commun*. **2022**, *58*, 12260–12273.

[8] L. Ackermann, *Isr. J. Chem*. **2010**, *50*, 652–663.

[9] L. D. Quin, A Guide to Organophosphorus Chemistry, Wiley-Interscience, New York, **2000**.

[10] P. A. Donets, N. Cramer, *J. Am. Chem. Soc.* **2013**, *135*, 32, 11772–11775.

[11] H. Chen, Y. X. Wang, Y. X. Luan, M. Ye, *Angew. Chem., Int. Ed*., **2020**, *132*, 9528–9532.

[12] Y.-X. Wang, F.-P. Zhang, H. Chen, Y. Li, J.-F. Li, M. Ye, *Angew. Chem., Int. Ed*. **2022**, e202209625.

[13] Y.-X. Wang, S.-L. Qi, Y.-X. Luan, X.-W. Han, S. Wang, H. Chen, M. Ye, *J. Am. Chem. Soc.* **2018**, *140*, 16, 5360–5364.

[14] a) N. D. Clement, K. J. Cavell, *Angew. Chem. Int. Ed*. **2004**, *43*, 3845–3847; b) A. T. Normand, S. K. Yen, H. V. Huynh, T. S. A. Hor, K. J. Cavell, *Organometallics* **2008**, *27*, 13, 3153–3160.

[15] J. Loup, V. Müller, D. Ghorai, L. Ackermann, *Angew. Chem. Int. Ed*. **2019**, 58, 1749–1753.

[16] For relevant examples, see: a) D. Berthold, B. Breit, *Org. Lett*. **2018**, *20*, 598–601; b) X. Wu, Z. Chen, Y.-B. Bai, V. M. Dong, *J. Am. Chem. Soc*. **2016**, *138*, 12013–12016; c) A. M. Haydl, L. J. Hilpert, B. Breit, *Chem. Eur. J.* **2016**, *22*, 6547–6551; d) A. M. Haydl, K. Xu, B. Breit, *Angew. Chem. Int. Ed*. **2015**, *54*, 7149–7153; e) K. Xu, N. Thieme, B. Breit, *Angew. Chem. Int. Ed*. **2014**, *53*, 7268–7271.

[17] J.-F. Li, D. Pan, H.-R. Wang, T. Zhang, Y. Li, G. Huang, M. Ye, *J. Am. Chem. Soc*. **2022**, *144*, 41, 18810–18816.

6.5 Experimental Section

For the complete experimental part please refer to the Supporting Information file of the following publication:

Z.-J. Zhang, M. M. Simon, S. Yu, S.-W. Li, X. Chen, S. Cattani, X. Hong*, L. Ackermann*, *J. Am. Chem. Soc.* **2024***, 146,* 13, 9172–9180.

https://doi.org/10.1021/jacs.3c1460

UNIONE EUROPEA
Fondo Sociale Europeo
Ministero dell'Università e della Ricerca
PON RICERCA E INNOVAZIONE 2014 - 2020
REACT EU
UNIVERSITÀ DI PARMA

La borsa di dottorato è stata cofinanziata con risorse del
Programma Operativo Nazionale Ricerca e Innovazione 2014-2020, risorse FSE REACT-EU
Azione IV.4 “Dottorati e contratti di ricerca su tematiche dell’innovazione”
e Azione IV.5 “Dottorati su tematiche Green”.